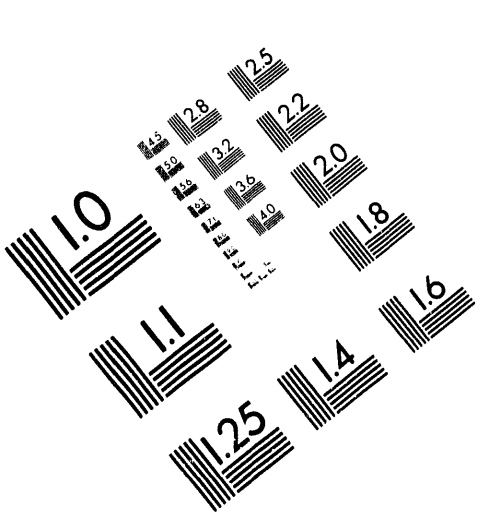

Association for Information and Image Management

1100 Wayne Avenue, Suite 1100
Silver Spring, Maryland 20910

301/587-8202

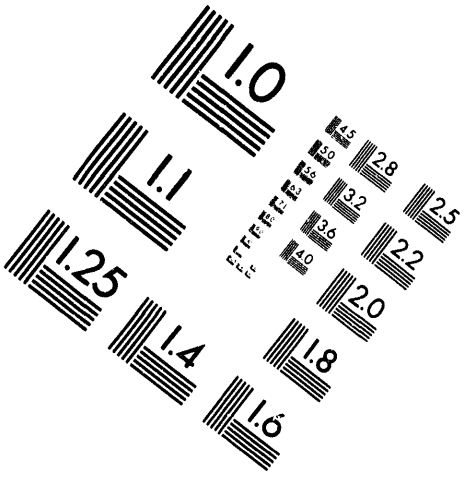

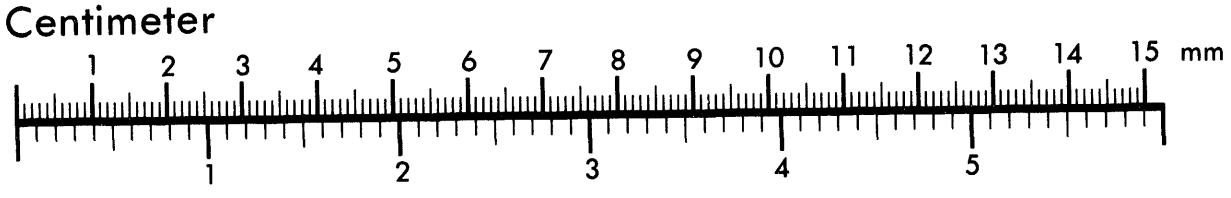

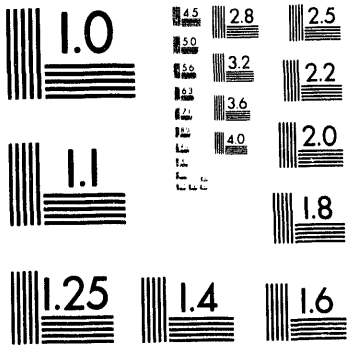

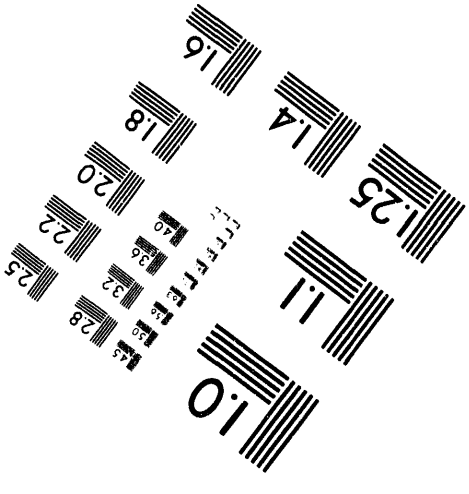

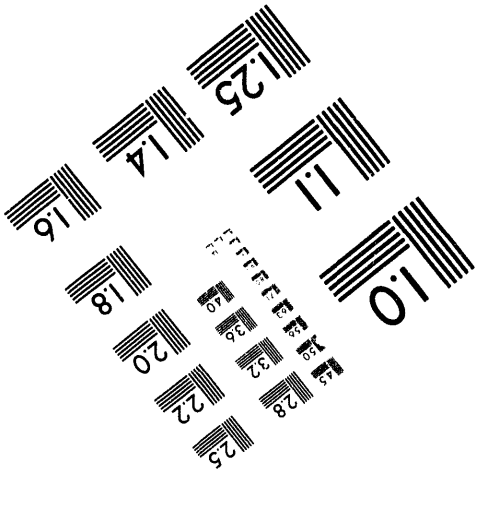

MANUFACTURED TO AIIM STANDARDS
BY APPLIED IMAGE, INC.

1 of 4

Distribution Category
Nuclear Energy (UC-940)

ANL/RERTR/TM-19
CONF-9209266

ARGONNE NATIONAL LABORATORY
9700 South Cass Avenue
Argonne, Illinois 60439

Proceedings of the
1992 International Meeting on

REDUCED ENRICHMENT FOR RESEARCH AND TEST REACTORS

Roskilde, Denmark
September 27-October 1, 1992

Karsten Haack
Program Chairman

Administrative Arrangements

Grethe Christiansen
Anni Lambæk Hansen

July 1993

The previous Reduced Enrichment for Research and Test Reactor meetings were held at:

Argonne National Laboratory - November 1978

Saclay, France - December 1979

Argonne National Laboratory - November 1980

Juelich, FRG - September 1981

Argonne National Laboratory - November 1982

Tokai, Japan - October 1983

Argonne National Laboratory - October 1984

Petten, The Netherlands - October 1985

Gatlinburg, Tennessee - November 1986

Buenos Aires, Argentina - September 1987

San Diego, California - September 1988

Berlin, Germany - September 1989

Newport, Rhode Island - September 1990

Jakarta, Indonesia - November, 1991

Roskilde, Denmark - September, 1992

PREFACE

The 15th annual RERTR international meeting was organized by Risø National Laboratory in cooperation with the International Atomic Energy Agency and Argonne National Laboratory.

Although odd-numbered RERTR international meetings are usually hosted by the U.S., conducting the meeting in Denmark provided the participants with an unique opportunity to visit the DR3 research reactor. In operation since completion of the 1990 conversion, the DR3 reactor has been operating at 10 MW with a full core of low enriched uranium silicide fuel elements. In addition, RERTR Program participants toured the local fuel element production plant. This plant has supplied the DR3 reactor with HEU, MEU, and a multitude of other LEU fuel elements for more than 20 years.

The topics of the meeting were the following: National Programs, Fuel Fabrication, Licensing Aspects, States of Conversion, Fuel Testing, and Fuel Cycle. The meeting was terminated by a Round Table Discussion.

The meeting included an address to the U.S. Secretary of Energy, Admiral James D. Watkins. Expressing a deep concern stemming from the situation involving the back-end of the fuel cycle, the non-U.S. participants agreed that such an speech was necessary. Many of the participants in the RERTR program had no means to complete their Fuel Cycle after the December 31, 1992 expiration of the U.S. Department of Energy's program for the reprocessing of foreign research and test reactor spent fuel. Luckily, the March 3, 1993 response from the USDOE was encouraging in that the USDOE now proposes to renew its reprocessing policy.

An additional letter was sent to the IAEA Deputy Director General, Dr. Sueo Machi. This letter suggested that the IAEA take over RERTR responsibilities on a global scale in order to minimize the use of HEU in the world's research reactors.

The welcome address was given by Risø's Scientific Director, Dr. Jørgen Kjems.

The after-dinner speech at the Wednesday, September 30, 1992 evening banquet was given by Professor Dr. Alan R. Mackintosh.

I would like to acknowledge the support and cooperation of the Argonne National Laboratory RERTR program members in helping to not only prepare for and execute the meeting, but also ultimately publish the proceedings.

I would also like to acknowledge the competent work of the organizing committee members whose coordinated efforts contributed to the successful nature of the 1992 RERTR international meeting.

Karsten Haack
Program Chairman

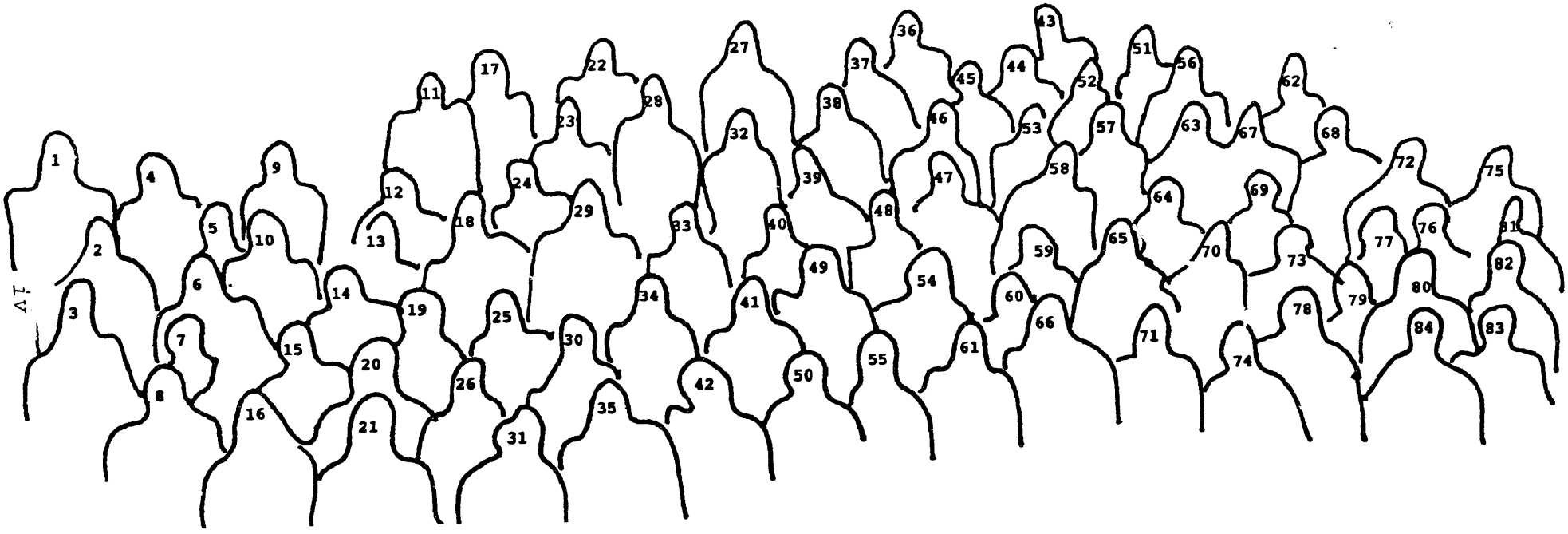

1. J. Borring, Risø Nat. Lab., Denmark
2. J. Pauty, COGEMA/BE, France
3. S. Palleck, AECL-CRNL, Canada
4. H. Preble, B&W, U.S.
5. H. Ichikawa, JAERI, Japan
6. K. Parker, AEA Technology, U.K.
7. D. Thom, AEA-Fuel Services, U.K.
8. J. Matos, ANL, U.S.
9. N. Peasor, B&W, U.S.
10. F. Wijtsma, ECN Petten, The Netherlands
11. W. Bollerts, Nissho Iwai Deutschland GmbH, Germany
12. S. Bouchardy, COGEMA/BE, France
13. J. Poupard, CERCA, France
14. B. Thurgood, GA, U.S.
15. A. Spin, Instituto de Asuntos Nucleares, Colombia
16. P. Karam, GA Tech., U.S.
17. V. Downs, B&W, U.S.
18. M. Kobayashi, Pechiney, Japan
19. J. Mota, Euratom Supply Agency, Belgium
20. S. Fukushima, Nissho Iwai Corp., Japan
21. Y. Futamura, JAERI, Japan
22. T. Michaels, NRC, U.S.
23. H. Hassel, CECCN, Germany
24. C. Zerri, COGEMA/BR, France
25. H. Buchholz, Hahn-Meitner Institut Berlin GmbH, Germany
26. Y. Komori, JAERI, Japan
27. W. Knop, GKSS Forschungszentrum, Germany
28. G. Harbonnier, CERCA, France
29. S.E. Jensen, Risø Nat. Lab., Denmark
30. P. Fuse, NUKEM GmbH, Germany
31. K. Kanda, Research Reactor Institute, Kyoto University, Japan
32. P. Vanluchene, CECCN, Germany
33. G. Copeland, ORNL, U.S.
34. A. Gevers, JPC Petten, The Netherlands
35. H. Müller, NUKEM GmbH, Germany
36. K. Singer, Risø Nat. Lab., Denmark
37. R. Dagan, Soreq Nuclear Research Center, Israel
38. C. Bonnery, COGEMA/BR, France
39. N. Tsuchida, JAERI, Japan
40. T. Nilsson, Risø Nat. Lab., Denmark
41. J. Guineux, COGEMA/DC, France
42. H. Floto, Risø Nat. Lab., Denmark
43. E. Listik, Nuclear Res. Institute, Czech.
44. B. Lelievre, CERCA, France
45. C. Rebreyend, CERCA, France
46. B. Bartoli, Commissariat à l'Energie Atomique, France
47. T. Nakajima, JAERI, Japan
48. W. Woodruff, ANL, U.S.
49. K. Haack, Risø Nat. Lab., Denmark
50. J. De Vries, IRI, The Netherlands
51. J. Beylot, Commissariat à l'Energie Atomique, France
52. A. Beeckmans, Centre d'etude de L'Energie Nucleaire, Belgium
53. J. Paillere, Commissariat à l'Energie Atomique, France
54. T. Schmidt, Nuclear Cargo & Service, Germany
55. G. Gruber, NUKEM GmbH, Germany
56. E. Adolph, Risø Nat. Lab., Denmark
57. D. Goutx, COGEMA, France
58. A. Sameh, Nuclear Research Center, Germany
59. J. Snelgrove, ANL, U.S.
60. K. Kobayashi, Res. React. Inst., Kyoto Univ., Japan
61. A. Travelli, ANL, U.S.
62. H. Tschiesche, Nuclear Cargo & Service, Germany
63. G. Hofman, ANL, U.S.
64. W. Hwang, KAERI, Korea
65. R. Rydin, Univ. of Va., U.S.
66. G. Thamm, Forschungszentrum Jülich, Germany
67. E. Jonsson, Studsvik, Sweden
68. K. Håkansson, Studsvik, Sweden
69. C. Kim, KAERI, Korea
70. C. Papastergiou, Inst. of Nuclear Tech., Greece
71. K. Akhtar, IAEA, Austria
72. A. Ballagny, Comm. a l'Energie Atomique, France
73. J. Deen, ANL, U.S.
74. W. Kruil, GKSS Research Center, Germany
75. P. Romand, CERCA, France
76. J. Schreader, Atomic Energy of Canada Res., Canada
77. D. Sears, AECL-CRNL, Canada
78. J. Kysavy, Nuclear Res. Institute, Czechoslovakia
79. M. McClary, DOE, U.S.
80. P. Porte, Cerca, France
81. C. McColm, AEA Tech., U.K.
82. J. Durand, CERCA, France
83. N. Pavenscrott, Edlow Int. Co., U.S.
84. Y. Fanjas, CERCA, France

WELCOME ADDRESS TO PARTICIPANTS TO THE 15. RERTR-CONFERENCE REDUCED ENRICHMENT FOR RESEARCH AND TEST REACTORS

Jørgen Kjems
Risø Naticnal Laboratory
DK-4000 Roskilde, Denmark

Ladies and Gentlemen,

On behalf of Risø National Laboratory I should like to welcome you all to Roskilde and to the 15th meeting on the program for the use of Reduced Enrichment for Research and Test Reactors, for which you use the acronym RERTR - impossible to pronounce!

We are happy to see that so many of our colleagues have been able to attend the meeting. I am told that 18 nations are represented covering more than 40 organizations and agencies.

In particular we welcome the new attendees to these meetings from the eastern european nations and from the developing countries.

The meeting has been organized in cooperatic:n with the International Atomic Energy Agency and I should like to thank both the agency and the other collaborators for their efforts in the support and planning of this meeting.

Let me quickly introduce myself, I am a solid state physicist by training, and - up until a few years ago- I have devoted my scientific career to the use of neutron scattering to solve problems in solid state physics, chemistry and biology.

I can therefore appreciate the importance of the scientific contributions that flow from the continued use of research and test reactors around the globe.

Many of these installations have reached a mature age - our own reactor DR 3 is still going strong in its 33rd year of operations. But - despite their age - they remain much needed tools for the advancement of both science and technology.

This has recently been illustrated to us by the fact that the DR 3 reactor has been selected for the European program for common use of Large Scientific Installations. Under this program some 50 European scientific user groups will gain access to the neutron beam facilities at the DR 3 reactor.

Isotope production, silicon transmutation and activation analysis are other important uses we make of the DR 3 reactor.

This illustrates the use of the DR 3 reactor. The research and test reactors in your countries have similar tasks, which - I am sure - are performed with similar professional pride and care.

Common for all is the desireand requirement for safe and reliable operation of these facilities, including all aspects of the fuel cycle.

This brings me to the issue of non-proliferation, and to the RERTR-program, which I see as a significant contribution to the global control of fissile material.

Early on, Risø National Laboratory has adapted the RERTR-program strategy for our own fuel cycle, and at this meeting you will hear reports that summarizes our experiences, including:

- the development the LEU-elements and of our production capability,

- the production of the LEU-elements for the DR 3 reactor and others,

- the process of converting the DR 3 reactor for LEU-operation. This was completed in december of 1990 - and we were proud to be among the first in the world to achieve this milestone,

- the collaboration through IAEA on guidebooks for the technical conversion and for the approval procedures to be used by the authorities.

But alas - even though all of these achievements represent significant steps in the right direction - one cannot claim that the fuel cycle situation for research reactors is fully satisfactory.

On the global scale we have to recognize the political changes that have occurred in eastern europe and elsewhere.

These have changed the basis for the recommendations that came out of the 1978-1980 International Nuclear Fuel Cycle Evaluation and for the RERTR-program.

It is appropriate to reassess these recommendations in the light of our present situation.

Here I should like to point once again to the International Atomic Energy Agency, and ask that the promotion, review and monitoring of the RERTR-program is given sufficient priority among all the other important tasks of the agency - connected with the Non-Proliferation Treaty.

As I mentioned earlier, the IAEA has played an important role in the planning of this meeting, and I hope that it can be extended to future meetings and to the time in between.

This is on way in which the IAEA can contribute to the continued success of the RERTR-program.

Another outstanding issue of immediate concern is the completion of the fuel cycle. Here I refer to the handling, reprocessing and storage of the spent fuel and associated waste.

In this area we need increased international collaboration on a bilateral as well as a regional basis, - and also between continents.

Denmark - like several other nations - have chosen not to use nuclear power for electricity production. Hence we will probably not develop capabilities in these areas - in foreseeable future.

Presently, we are dependent on the solutions and opportunities other nations can offer within the scope of collaborative agreements.

I hope that this meeting also can be used to discuss these issues and that we can develop ideas for workable common solutions, that serves everybody's interests.

These are tough issues with both political and technical ramifications. The only way to make progress is through dialogue.

In this respect, these meetings offer unique occasions for fruitful discussions between reactor operators, reactor users, fuel manufacturers, fuel and waste handlers and transporters as well as representatives from licensing and other authorities.

I trust that you will use this occasion where you can exchange views and experiences gained around the globe.

This will allow each of us to continue improving our daily performance and to make new contributions to the safe and reliable operation of research and test reactors.

In this spirit I welcome all of you to Roskilde and wish you a successful meeting.

*****

THE CROCODILE AND THE ELEPHANT

Rutherford, Bohr and Quantum Physics

Professor Allan R. Mackintosh
University of Copenhagen
Copenhagen, Denmark

In 1907, Ernest Rutherford (later named "The Crocodile" by Peter Kapitza), who was then 36 years old and already a world-famous physicist, moved from McGill University in Montreal to the University of Manchester. In the same year, Niels Bohr (later known by some as "The Elephant" - he was one of very few non-royal recipients of the Order of the Elephant), a young student of 22 at the University of Copenhagen, received the Gold Medal of the Royal Danish Academy for his first research project, and experimental and theoretical study of water jets. During the next 30 years, until the death of Rutherford in 1937, these two great scientists dominated quantum physics. Rutherford was the father of nuclear physics, together they founded atomic physics and, with their students and colleagues, they were responsible for the great majority of the decisive advances made in the inter-war years. In this lecture, the story of this development is told, and some comparisons are made between Bohr and Rutherford, as men and scientists, drawing especially on the extensive correspondence between them from 1912 to 1937, the material which Bohr gathered together in connection with the publication in 1961 of his Rutherford Memorial Lecture, the interviews which he gave right before his death in 1962, and other published and unpublished material from the Niels Bohr Archive in Copenhagen.

In Canada, Rutherford had placed the study of radioactivity on a quantitative basis by establishing, with Frederick Soddy, the transformation theory which, for the first time, described a quantum statistical process. It was for this work that he received the Nobel Prize in Chemistry in 1908, being transformed instantly from a physicist to a chemist, as he remarked in his speech at the banquet. Starting in Cambridge during his research student period, he had also discovered, named, and determined the properties of the α-particle. Soon he demonstrated unambiguously that it is a doubly-charged helium atom, later shown to be identical with the helium nucleus. During the rest of his life, he was to use the α-particle with amazing virtuosity to uncover the secrets of nature. As he later wrote to Bohr: "I always felt that it had within its structure a large part of the problems of modern physics." Soon after arriving in Manchester, he asked Hans Geiger and Ernest Marsden to investigate α-particle scattering by thin foils and, as a result of their surprising observation of scattering through large angles, he developed his nuclear model of the atom, showing by his own calculations that it accounted accurately for the experiment's results. He first presented his theory at a meeting of the Manchester Literary and Philosophical Society in 1911. Thus was a discovery of transcendent importance introduced to the world.

In the meantime, Niels Bohr had received his doctorate in Copenhagen for a thesis on the electron theory of metals, and obtained a scholarship to study in Cambridge, in the hope of interesting J.J. Thompson, the discoverer of the electron, in his work. Failing to accomplish this, he moved to Manchester early in 1912, with the

intention of learning the techniques of radioactivity from Rutherford. He rapidly became fully convinced of the validity and significance of the Rutherford atom, more so perhaps than even Rutherford himself, and began to try and explain its stability and properties on the basis of Max Planck's quantum of action. On returning to Denmark and learning of Balmer's formula for the frequencies of the spectral lines in Hydrogen, he postulated in 1913 his atomic model, with quantum rules determining stationary states, whose energy differences govern the spectral frequencies through Planck's constant. These fundamental concepts still lie at the basis of our understanding of atomic structure. Bohr's model was given decisive support by the brilliant experiments of Henry Mosely, soon thereafter tragically killed in the First World War, who used X-ray spectra to determine the atomic number, the electric charge on the nuclei of the atoms.

Bohr returned to Manchester as a Reader in 1914, at the beginning of the war, to teach and develop his atomic theory, but went home to Denmark in 1916 to become Professor of Theoretical Physics at the University of Copenhagen. Under extremely difficult conditions, Rutherford managed to continue a little research during the war and in a letter to Bohr at the end of 1917 announced "results which, I think, will ultimately prove of great importance." By bombarding nitrogen with α-particles, he carried out the first controlled transformation of a nucleus, creating protons and, as was later proved by Patrick Blackett, oxygen nuclei. In 1919, he moved to Cavendish Laboratory, Cambridge, where he and his colleagues, particularly James Chadwick and Charles Ellis, continued to explore the nucleus. Many nuclear transmutations were produced by bombardment with α-particles, and their anomalous scattering led to the discovery of the strong nuclear force. Just before the war, Chadwick had shown that the electrons emitted in radioactive ß-decay do not have a unique energy, but rather a continuous distribution. This surprising result was confirmed by Ellis who, in a series of elegant experiments in the 1920's, explored thoroughly the nature of ß-and γ-emission and laid the foundations of nuclear spectroscopy. The continuous ß-spectrum required a radical explanation; either energy is not conserved in the nuclear process, a hypothesis favored for a while by Bohr, or it is carried away by another, elusive particle, Wolfgang Pauli's neutrino, which was indeed later proved to exist.

After his return to Denmark, Bohr was for a number of years occupied with using the quantum theory and his correspondence principle to explain the structure of atoms and the periodic table of the elements, thus providing the basis for quantum chemistry. This work culminated at about the time he received the Nobel Prize in 1922, simultaneously with the discovery of the element hafnium, whose properties he had predicted, by his colleagues Dirk Costerr and George Hevesy. He had first met the latter in Rutherford's laboratory in Manchester in 1912, and they remained close friends for the rest of their lives. Thereafter the inadequacies of the old quantum theory became increasingly apparant, until the deepening crisis of atomic physics was resolved through the discovery of quantum mechanics by Wernwer Heisenberg, Bohr's young associate. As it is apparant from his letters, Bohr's relationship with Heisenberg was reminiscent of that of Rutherford to himself in earlier years; he described him, for example, as "an ingenious (sic) and sympathetic young man indeed." Their later partial estrangement due to events during the Second War was therefore particularly painful for both of them. Bohr played

little direct part in the establishment of quantum mechanics, though he took a keen interest in the revolutionary advances made by his younger colleagues, particularly Heisenberg and Paul Dirac. However, he became increasingly interested in the philosophical foundations of the theory, and his principle of complementarily formed the basis for the "Copenhagen interpretation" which is generally accepted today. It was not however accepted by a number of the distinguished pioneers of the quantum theory, notably Albert Einstein, with whom Bohr conducted a dialogue, based on deep disagreement and an equally deep mutual respect, until Einstein's death.

The research on nuclear physics in the Cavendish Laboratory culminated in the annus mirabilis of 1932, when Chadwick discovered the neutron , John Cockcroft and Ernest Walton carried out the first transmutation of nuclei by artificially accelerated particles, producing α-particles from lithium by bombardment with protons, and Blackett and Occhialini observed the electron-positron pairs which had been predicted by Dirac. Rutherford's willingness to countenance the construction of the Cockcroft-Walton accelerator, which was terribly expensive by his standards, was strongly influenced by the arguments of George Gamov, who came on a visit from Copenhagen at the suggestion of Bohr. Gamov had shown that particle of even moderate energy should be able to induce nuclear transmutations by quantum mechanical tunneling. These and subsequent developments showed that quantum mechanics could indeed be applied to the nucleus, after all, and Bohr rapidly showed an interest in doing so. His scientific contracts to Rutherford, which had been relatively sparse during the 1920's because of divergent interests, were thereby again intensified. He used his early experience with liquids to develop the liquid-drop model of the nucleus, and explained nuclear reactions as proceeding via the formation of a compound nucleus. It was on this subject that he gave his last course of lectures in Cambridge at the invitation of Rutherford in 1936.

After the momentous events of 1932, nuclear physics of the highest quality continued to be performed in the Cavendish Laboratory. In 1934, for example, Rutherford made his last great discovery, with Marcus Oliphant and Paul Harteck, of the fusion of the nuclei of heavy hydrogen - deuterons - to yield the new isotopes tritium and helium-3, plus the energy which may power electricity stations in the future. Whereas, before this time, almost every significant advance in nuclear physics had been made either by Rutherford or his colleagues, the center of activity diffused away from Cambridge thereafter. Artificial radioactivity was discovered by Irene Curie and Frederic Joliot in Paris, Ernest Lawrence's cyclotron in Berkeley pointed the way towards the future of nuclear and particle physics, and Enrico Fermi in Rome used slow-neutron capture to produce a variety of nuclear reactions, including the synthesis of radioactive isotopes of many elements, and fission, although he did not identify it as such. In the middle 1930's, most of Rutherford's younger colleagues left to establish their own departments and, at his untimely death in 1937, the Cavendish Laboratory began to look for new fields to conquer. Rutherford just failed to experience the discovery of fission, when his former student Otto Hahn and Fritz Strassman identified Barium as a product of the bombardment of uranium with neutrons, and Lise Meitner and Otto Frisch, colleagues of Hahn and Bohr respectively, showed that its presence was due to the disintegration of the uranium nucleus. Bohr and John Wheeler developed a theory of fission based on

the compound-nucleus model, just before the outbreak of war brought to a close this most remarkable era in the history of physics.

After the war, Bohr performed little physics, but played an extremely important role, nationally and internationally as an elder statesman of science. He and Rutherford, who had already established such a position at the time of his death, would have made as formidable a combination in science policy as they had earlier in research. Bohr attempted to curb the menace of nuclear weapons by his Open Letter to the United Nations, which had rather little political influence at the time, but which contains many useful lessons for the present period of East-West rapprochement. He worked actively and effectively for the establishment of CERN in Geneva, and the Risø National Laboratory and NORDITA, the Nordic Institute for Theoretical Physics, in Denmark. He presided over the change in the generations at his own institute. Under the leadership of his son, Aage, and Ben Mottelson, supported by many distinguished colleagues, the Niels Bohr institute maintained its position as a world leader in nuclear physics. By the time of Niels Bohr's death in 1962, Danish physics was on the path to new successes, with a quality and breadth unusual for such a small country.

The backgrounds, personalities, and styles of these two scientific giants afford interesting comparisons and contrasts. They were both born in small countries, almost diametrically opposite on the globe, but their attitudes towards their homelands were quite different. Rutherford realized early in his career that it would be necessary to travel in order to be at the center of scientific activity, and he never seriously considered a permanent return to New Zealand. Bohr, on the other hand, was only really at home in Denmark and never seriously considered emigration, despite many attractive offers. He responded for example to Rutherford's offer of a Chair in Manchester by writing: "The fact is that I feel that I have morally pledged myself to do what I can to help in the development of the scientific physical research here in Denmark." Bohr's background was in the comfortable, academic middle-class while Rutherford was a member of a large pioneering family, whose survival and modest prosperity was based on extremely hard work. Their differences created no barriers between them, however, nor did they shown any signs of class-consciousness in their dealings with others. They both had excellent, though dissimilar educations. Their wives, who were very different, provided an essential practical and emotional support from the beginning of their careers. They both survived their husbands by many years. The letters written from England by the two young scientists to their fiances provides a rich source of information on their early struggles and successes.

At first sight, there could hardly have been a stronger contrast between their personalties. Bohr was soft in voice and manner, while Rutherford was loud. Beneath the surface, however, they were quite similar. Chadwick's description of Rutherford applied to both of them:

> He knew his worth, but he was and remained, amidst his many honors, innately modest. Pomposity and humbug he disliked, and he himself never presumed on his reputation or position. He treated his students, even the most junior, as brother workers in the same field.

Their point of greatest similarity lay, however, in their uncompromising determination to solve the scientific problems which they set themselves. Combined with a prodigious capacity for work and an exceptional insight into the workings of nature, this unswerving devotion to their craft resulted in remarkable achievements. Their scientific styles were characterized by an unerring instinct for the important problems, and the simplicity of the means by which they obtained results of the greatest originality and significance. As Bohr put it, in a speech of thanks to Rutherford in Copenhagen, "If a single word could be used to describe so vigorous and many-sided a personality, it would certainly be 'simplicity'." Rutherford discovered, explored, and transformed the nucleus with the α-particle and little more, and was not very enthusiastic about complex equipment, while Bohr founded atomic physics using Planck's quantum combined with subtle and powerful arguments, rather than elaborate mathematics. Although they never published a joint paper, the collaboration between them was one of the most important in the history of science. Not since the time of Tycho Brahe and Kepler had a young disciple taken the observations of a master and used them to transform our understanding of the universe.

Rutherford and Bohr were among the greatest of scientific teachers. Many of their students became eminent in their own right and, with very few exceptions, all the most distinguished physicists of the first half of the century were decisively influenced by contacts with them. Chadwick wrote of Rutherford after his death, "he came to regard the training of students in methods of research as of almost equal importance to the advancement of knowledge." There is no doubt that Bohr's style of intense but informal discussions with his students and colleagues owed a great deal to his observations of Rutherford in Manchester in his own student days. They were both memorable lecturers but, whereas Rutherford impressed by his clarity and enthusiasm, Bohr inspired by his manifest searching after the truth, despite a frequently impenetrable obscurity. Both were scientific leaders of the greatest importance, being at the centers of great schools of physics. Surprisingly, Rutherford, the experimentalist, was much less adept at obtaining financial support than was Bohr, the theoretician. He had a preference for uncomplicated equipment and had difficulty in sympathizing with or supporting those with more elaborate ambitions. It was this trait which caused the disagreement with Chadwick, a nuclear physicist second to only Rutherford himself, which caused the former reluctantly to leave Cambridge. Bohr, on the other hand, played the fund-raising game with consummate skill and was able to not only construct and man his own institute, and equip it with the most modern apparatus (including the first operating cyclotron in Europe), but also to make a major contribution to the establishment of other institutions and activities, including the first school of radiobiology under Hevesy. Through these initiatives, his influence on science in Denmark and in the world was incalculable.

The voluminous literature about Rutherford and Bohr, and particularly the testimony of those that knew them, provides convincing evidence that they were not only great scientists, but also great men. Their correspondence is full of examples of their generosity towards others, and they both made major, demanding, and successful efforts to assist the victims of Nazism. This should not, of course, be taken as implying that they were saints. They surely

had the same human weaknesses as the rest of mankind, but were more successful than most in overcoming them. Their tremendous scientific authority could, however, have an intimidating effect on their younger colleagues. At the beginning of their long association, Rutherford discouraged Bohr from publishing his, perfectly correct and important, conclusions of the radioactive displacement laws and isotopes. There are a number of later examples where both, from the best of motives, inhibited the publication of important results or speculations. Nevertheless, their colleagues or pupils spoke of them with the greatest respect and affection. Notwithstanding his disenchantment with Rutherford's autocratic and penny-pinching attitude, Chadwick concluded his obituary:

> All over the world, workers in radioactivity, nuclear physics, and allied subjects regarded Rutherford as the great authority and paid him tribute of high admiration; but we, his students, bore him also a very deep affection. The world mourns the death of a great scientist, but we have lost our friend, our counsellor, our staff, and our leader.

All scientists can derive inspiration from their example; devotion to the highest ideals of science may also lead to humanity and wisdom. The lives of both Ernest Rutherford and Niels Bohr may be fittingly characterized by Bohr's last recorded words, "it is a very beautiful story, because he took things very seriously."

SESSION I

September 28, 1992

PROGRESS REPORTS ON NATIONAL PROGRAMMES
Chairman: H. Floto (Risø National Laboratory, Denmark)

Page

THE RERTR PROGRAM: A STATUS REPORT
A. Travelli, ANL 3

STATUS OF REDUCED ENRICHMENT PROGRAMS FOR RESEARCH REACTORS IN JAPAN
K. Kanda and H. Nishihara, KURRI
Y. Futamura, E. Shirai, and T. Asaoka, JAERI 14

STATUS OF CANADIAN LOW-ENRICHED URANIUM CONVERSION PROGRAM
J.W. Schreader, S.J. Palleck, D.F. Sears, and P.M. Brewster, AECL Research 24

SESSION II

September 28, 1992

FUEL DEVELOPMENT AND FABRICATION
Chairman: A. Travelli (Argonne National Laboratory, USA)

OPTIMIZATION OF SILICIDE FUEL ELEMENTS
A. Ballagny, J.P. Beylot, and J. Paillere, CEA Saclay
J.P. Durand, Y. Fanjas, and A. Tissier, CERCA 31

DEVELOPMENT OF HIGHER DENSITY FUEL AT CERCA
J.P. Durand, Y. Fanjas, and A. Tissier, CERCA 50

CERCA IS CHANGING ITS SHAREHOLDING
J.P. Durand, CERCA 62

QUALITY ASSURANCE AND ULTRASONIC INSPECTION STUDIES IN LEU FUEL PRODUCTION
P. Toft, J. Borring, E. Adolph, and T.M. Nilsson, Risø National Laboratory 63

CHARACTERIZATION OF ATOMIZED U_3Si_2 POWDER FOR RESEARCH REACTORS
C.K. Kim, K.H. Kim, S.J. Jang, H.D. Jo, and I.H. Kuk, KAERI 76

A NEW X-RAY INSPECTION OF FUEL PLATES
J.F. Poupard and A. Tissier, CERCA 85

CHARACTERIZATION OF COMMERCIALLY PURE ALUMINUM POWDER FOR RESARCH REACTOR FUEL PLATES
V.D. Downs, B&W
T.C. Wiencek, ANL 92

SESSION III

September 28, 1992

LICENSING ASPECTS
Chairman: H. Buchholz (Hahn-Meitner-Institut, Germany)

HEU-LEU CONVERSION OF NON-POWER REACTORS LICENSED BY THE NUCLEAR REGULATORY COMMISSION
T. Michaels, NRC 105

SESSION IV

September 28, 1992

REACTORS DURING AND AFTER CONVERSION TO LEU
Chairman: Y. Futamura (JAERI, Japan)

CONTINUED CONVERSION OF THE R2 REACTOR TO LEU FUEL
E. Jonsson and R. Håkansson,
Studsvik Nuclear AB 113

STATUS OF THE UNIVERSITY OF VIRGINIA REACTOR LEU CONVERSION
R.A. Rydin, University of Virginia 119

COMPLETION OF THE OSURR FUEL CONVERSION AND POWER UPGRADE
J.W. Talnagi and T. Aldemir, The Ohio State University . . 128

SESSION V

September 30, 1992

FUEL TESTING AND EVALUATION
Chairman: Y. Fanjas (CERCA, France)

ANALYTICAL ANALYSES OF STARTUP MEASUREMENTS ASSOCIATED WITH THE FIRST USE OF LEU FUEL IN ROMANIA'S 14-MW TRIGA REACTOR
M.M. Bretscher, J.L. Snelgrove, ANL, and M. Ciocanescu, INR 141

MEASUREMENTS AND COMPUTATIONS FOR NEUTRON FLUX IN THE ROMANIAN TRIGA STEADY STATE REACTOR HEU CORE WITH FOUR EXPERIMENTAL LEU FUEL CLUSTERS
C. Toma, D. Barbos, M. Ciocanescu, and P. Busuioc, INR
W. Whittemore, General Atomics
J. Snelgrove, ANL 152

PROGRESS OF TRANSIENT IRRADIATION TESTS WITH
LEU SILICIDE FUEL
H. Ichikawa, T. Kodaira, K. Yanagisawa,
and T. Fujishiro, JAERI 165

A SWELLING MODEL OF LEU SILICIDE FUEL FOR KMRR
W. Hwang, B.G. Kim, K.S. Sim, Y.H. Heo,
and H.C. Suk, KAERI 174

A NEW SWELLING MODEL AND ITS APPLICATION TO
URANIUM SILICIDE RESEARCH REACTOR FUEL
G.L. Hofman, J. Rest, and J.L. Snelgrove, ANL 186

SESSION VI

September 30, 1992

HEU AND LEU FUEL CYCLE
Chairman: J. Mota (Euratom Supply Agency, Belgium)

EXTERNAL RESEARCH REACTOR FUEL CYCLE: BACK-END OPTIONS
G.J. Gruber, NUKEM GmbH 199

THE RE-USE OF HIGHLY ENRICHED URANIUM (HEU)
REPROCESSED IN EUROPE
H. Müller, NUKEM GmbH 204

RECYCLING OF REPROCESSED URANIUM FROM RESEARCH REACTORS
S. Bouchardy and J.F. Pauty, COGEMA 210

INTERMEDIATE FUEL ELEMENT STORAGE FACILITY AT REACTOR DR 3
J. Qvist, Reactor DR 3
E. Nonbøl, Risø National Laboratory 220

SESSION VII

September 30, 1992

SAFETY TESTS AND EVALUATIONS
Chairman: K. Kanda (KURRI, Japan)

LONG TERM STORAGE/DIRECT DISPOSAL V REPROCESSING -
A COMPARISON OF THE COSTS FOR RESEARCH AND
TEST REACTOR OPERATORS
C. McColm, AEA Fuel Services 231

ANALYSES FOR CONVERSION OF THE GEORGIA TECH RESEARCH
REACTOR FROM HEU TO LEU FUEL
J.E. Matos, S.C. Mo, and W.L. Woodruff, ANL 239

SAFETY ANALYSIS OF THE JMTR WITH LEU FUEL
Y. Komori, F. Sakurai, E. Ishitsuka,
T. Sato, M. Saito, and Y. Futamura, JAERI 251

DOSE ANALYSIS IN SAFETY AND SITE EVALUATION FOR THE JMTR CORE CONVERSION TO LEU FUEL
N. Tsuchida, T. Shiraishi, Y. Takahashi, S. Inada, K. Kitano, M. Saito, and Y. Futamura, JAERI 259

EARLY DETECTION OF COOLANT BOILING IN RESEARCH REACTORS WITH MTR-TYPE FUEL
R. Kozma, E. Türkcan, and J.P. Verhoef, Netherlands Energy Research Foundation 267

A COMPARISON OF WIMS-D4 AND WIMS-D4m GENERATED CROSS-SECTION DATA WITH MONTE CARLO
W.L. Woodruff and J.R. Deen, ANL
C.I. Costescu, University of Illinois 277

SESSION VIII

September 30, 1992

CORE CONVERSION STUDIES
Chairman: G. Thamm (KFA, Germany)

CORE CONVERSION OF IAN-R1 REACTOR
A. Spin Ramirez, Instituto de Asuntos Nucleares 289

STATUS OF THE BER II
A. Axmann, H. Buchholz, C.O. Fischer, and H. Krohn, Hahn-Meitner-Institut 294

GREEK RESEARCH REACTOR PERFORMANCE CHARACTERISTICS AFTER ADDITION OF BERYLLIUM REFLECTOR AND LEU FUEL
J.R. Deen and J.L. Snelgrove, ANL
C. Papastergiou, National Center for Scientific Research 301

SESSION IX

October 1, 1992

UTILIZATION OF CONVERTED REACTORS
Chairman: J.W. Schreader (AECL Research, Canada)

HEU AND LEU MTR FUEL ELEMENTS AS TARGET MATERIALS FOR THE PRODUCTION OF FISSION MOLYBDENUM
A.A. Sameh and A. Bertram-Berg, Nuclear Research Center Karlsruhe 313

EPI-THERMAL NEUTRON SPECTRA FROM LOW AND HIGH ENRICHMENT URANIUM FUELS AT THE GEORGIA TECH RESEARCH REACTOR FOR BORON NEUTRON CAPTURE THERAPY
K.A. Klee and R.A. Karam, Georgia Institute of Technology 334

CONTRIBUTED PAPERS

CHILEAN FUEL ELEMENTS FABRICATION PROGRESS REPORT
J. Baeza, H. Contreras, J. Chàvez, J. Klein, R. Mansilla, J. Marin, and R. Medina, CCHEN 347

Letter From Mr. Sun Rongxian, Nuclear Power Institute of China 357

Final List of Attendees 359

S E S S I O N I

September 28, 1992

PROGRESS REPORTS ON NATIONAL PROGRAMMES

Chairman:

H. Floto
(Risø National Laboratory, Denmark)

THE RERTR PROGRAM: A STATUS REPORT*

A. Travelli
Argonne National Laboratory
Argonne, Illinois, USA

ABSTRACT

The progress of the Reduced Enrichment Research and Test Reactor (RERTR) Program is described. The major events, findings, and activities of 1991 are reviewed after a brief summary of the results which the RERTR Program had achieved by the end of 1991 in collaboration with its many international partners.

The disappearance of the Soviet Union, the cooperative attitude of the republics which have taken its place, and the end of the Cold War have affected the RERTR program in several ways. The program is now managed by the DOE Office of Arms Control and Nonproliferation, which directs all arms control and nonproliferation activities within DOE, and is part of the ANL Arms Control and Nonproliferation Program, which directs all corresponding activities at Argonne National Laboratory.

The program would welcome the opportunity of cooperating with the CIS republics towards the elimination of Russian-origin HEU from international commerce. With renewed interest in nonproliferation, Congress came very close to funding resumption of RERTR fuel development and promised to reconsider the issue.

The technical efforts of the RERTR Program were concentrated on technology transfer and implementation activities, consistent with DOE guidance. Existing fuel data were analyzed and interpreted to derive a better understanding of the behavior of dispersion fuels under irradiation. Computer codes were modified and upgraded for the analysis of research reactors operating with LEU fuels. In particular, the WIMS-D4 code was benchmarked by comparison with a Monte Carlo code. Analyses, calculations, and safety evaluations were conducted to support LEU conversions of both US and foreign research reactors.

One more U.S. university reactor has been converted to LEU fuel, bringing the total to six converted U. S. reactors. An approximate quantitative evaluation of the overall LEU conversion progress shows that about 57% of the work required to eliminate the need for further HEU exports has been accomplished.

The major current program goal is to work closely with the various reactor and fuel fabrication organizations that are pursuing LEU conversions, so that their objective can be attained at the earliest possible date. International cooperation continues to be essential to the achievement of this goal.

---

*As revised on October 2, 1992.

INTRODUCTION

Very few years, in the history of mankind, will be remembered as having brought more change to the way we live and interact with the rest of the world than the past twelve months. The Soviet Union has disappeared, fifteen new republics have emerged in its place, and these republics have repudiated communism and established friendly and cooperative relations with the West: in short, the Cold War is over. The single, powerful, dangerous adversary which the West has opposed at great cost for nearly half a century no longer exists. In its place, the major current threat to international stability comes from many smaller countries where nationalistic, ethnic, or religious motives may encourage the development and use of weapons of mass destruction.

Much of the attention and resources that used to be dedicated to waging the Cold War are now turning to nonproliferation. Elimination of the international traffic in weapons-grade materials is viewed as an essential step in hindering proliferation of nuclear weapons, and the Reduced Enrichment Research and Test Reactor (RERTR) Program and the international organizations associated with it find themselves squarely in the focus of this effort.

The RERTR Program was established in 1978 by the Department of Energy (DOE), which continues to fund and manage the program in coordination with the Arms Control and Disarmament Agency (ACDA), the Department of State (DOS), and the Nuclear Regulatory Commission (NRC). The primary objective of the program is to develop the technology needed to use Low-Enrichment Uranium (LEU) instead of High-Enrichment Uranium (HEU) in the research and test reactors whose fuel requirements cause most of the HEU traffic, and to do so without significant penalties in experiment performance, economics, or safety aspects of the reactors.

Close cooperation with the many international organizations represented at this meeting has been the cornerstone of the RERTR Program since its beginning and since its first international meeting fourteen years ago. This cooperation and the high quality of the technical contributions which many partners have brought to the overall effort are to be credited for much of the progress which the program has achieved to date.

Cooperation between the RERTR Program and RISØ began in 1980, when the International Atomic Energy Agency assembled a team of experts to assess the feasibility of converting heavy-water moderated research reactors to the use of LEU fuels. Dr. Haack was there to represent the DR-3 reactor. That was the beginning of a long and fruitful interaction centering on the performance, safety, and fabrication of the new silicide fuels that Argonne was developing. Two RISØ scientists visited ANL in 1984 to learn about the fabrication process, and ANL personnel returned the visit in 1985. It was a resounding success for all of us when, at the 1990 meeting in Newport, Dr. Haack announced that the DR-3 had become the first European research reactor to convert to LEU silicide fuel, and that it had done so with indigenously fabricated fuel.

It gives me a special pleasure to take part in this International RERTR Meeting in Denmark, in close proximity to the RISØ National Laboratory and its DR-3 reactor. As you know, a long-standing tradition of the RERTR meetings is that even-year meetings are held in the United States, but the accomplishments that our RISØ colleagues had to report were

so exceptional that the U.S. RERTR Program decided to yield the site of this meeting to RISØ. From the interest that this meeting has aroused, as evidenced by the preliminary list of attendees, we know that our decision was right. We look forward to an excellent program, to interesting technical exchanges, to touring the converted DR-3 reactor and the fuel fabrication facilities, to visiting with old friends, and to the traditional hospitality of this beautiful country.

OVERVIEW OF THE SEPTEMBER 1991 PROGRAM STATUS

By September 1991, when the last International RERTR Meeting was held[1], the main results achieved in the fuel development area were:

(a) The qualified uranium densities of the three main fuels which were in operation with HEU in research reactors when the program began (UAl_x-Al with up to 1.7 g U/cm^3; U_3O_8-Al with up to 1.3 g U/cm^3; and $UZrH_x$ with 0.5 g U/cm^3) had been increased significantly. The new uranium densities extended up to 2.3 g U/cm^3 for UAl_x-Al, 3.2 g U/cm^3 for U_3O_8-Al, and 3.7 g U/cm^3 for $UZrH_x$. Each fuel had been tested extensively up to these densities and, in some cases, beyond them. All the data needed to qualify these fuel types with LEU and with the higher uranium densities had been collected.

(b) For U_3Si_2-Al, after reviewing the data collected by the program, the U.S. Nuclear Regulatory Commission (NRC) had issued a formal and generic approval[2] of the use of U_3Si_2-Al fuel in research and test reactors, with uranium densities up to 4.8 g/cm^3. A whole-core demonstration using this fuel had been successfully completed in the ORR using a mixed-core approach.

(c) For U_3Si-Al, miniplates with up to 6.1 g U/cm^3 had been fabricated by ANL and the CNEA, and irradiated to 84-96% in the Oak Ridge Research Reactor (ORR). PIE of these miniplates had given good results, but had shown that some burnup limits might need to be imposed for the higher densities. Four full-size plates fabricated by CERCA with up to 6.0 g U/cm^3 had been successfully irradiated to 53-54% burnup in SILOE, and a full-size U_3Si-Al (6.0 g U/cm^3) element, also fabricated by CERCA, had been successfully irradiated in SILOE to 55% burnup. However, conclusive evidence indicating that U_3Si became amorphous under irradiation had convinced the RERTR Program that this material as then developed could not be used safely beyond the limits established by the SILOE irradiations.

(d) Two concepts based on hot-isostatic pressing (HIP) procedures had been developed for LEU silicide fuels with the potential of holding effective uranium densities much greater than 4.8 g U/cm^3. One of the concepts was based on a composite structure of U_3Si wires and aluminum (up to 12.9 g U/cm^3), while the other was based on a U_3Si_2-Al dispersion structure (up to 10.2 g U/cm^3). Sample miniplates had been produced for both concepts.

In other important program areas, reprocessing studies at the Savannah River Laboratory had concluded that the RERTR fuels could be successfully reprocessed at the Savannah River Plant and DOE had defined the terms and conditions under which these fuels will be accepted for reprocessing.

A new analytical/experimental program had begun to determine the feasibility of using LEU instead of HEU in fission targets dedicated to the production of ^{99}Mo for medical applications. A procedure for basic dissolution and processing of LEU silicide targets had been developed and was ready for demonstration on a full-size target with prototypic burnup.

Extensive studies had been conducted, with favorable results, on the performance, safety, and economic characteristics of LEU conversions. These studies included many joint study programs, which were in progress for about 28 reactors from 17 different countries.

Coordination of the safety calculations and evaluations was continuing for the US university reactors planning to convert to LEU as required by the 1986 NRC rule. Five of these reactors had already been converted, two other safety evaluations had been completed, and calculations for five more reactors were in progress.

DOE guidance received at the beginning of 1990 had redirected the efforts of the US RERTR Program away from the development of new and better fuels, toward the transfer of already developed fuel technologies, and toward providing assistance to reactors undergoing conversion.

PROGRESS OF THE RERTR PROGRAM IN 1992

The historical events which have occurred during the past twelve months and which were mentioned in the introduction have affected the RERTR Program in several ways.

At the beginning of 1992, shortly after the USSR flag was hauled down at the Kremlin, DOE announced a reorganization which concentrated all DOE activities related to arms control and nonproliferation within the Office of Arms Control and Nonproliferation (OAN), reporting directly to the Secretary of Energy. Since then, management of the RERTR program has been assumed by DOE/OAN, which appears to be particularly well suited to supporting and managing the program.

Shortly after DOE's action, Argonne National Laboratory also consolidated all its activities related to arms control and nonproliferation in a single office, the ANL Arms Control and Nonproliferation (ACNP) Program, of which the RERTR program became an important component. The net result is that the RERTR program now has access to enhanced resources and personnel.

Since its inception, the RERTR program has limited its efforts to eliminating the international traffic in HEU *of U.S. or other Western origin*. This qualifier was required not by any intrinsic safety of the HEU produced in the Soviet Union, but by our admitted inability to influence that country's policies. The end of the Cold War and the new friendly relations with the republics which have replaced the Soviet Union have made that qualifier unnecessary. We would welcome the establishment of a CIS RERTR program and stand ready to cooperate with it to the fullest extent. We would also encourage all our many international partners to join us in this effort, to eliminate the dangers of HEU traffic from those parts of the world which were closed to us while the Cold War was being waged.

A plan to resume development of LEU fuels with uranium densities higher than the currently qualified 4.8 g/cm^3 was prepared by the RERTR program and submitted to DOE. Acting independently from this submittal, last summer the U.S. House of Representatives voted to allocate enough funds to the RERTR program to resume its fuel development effort. The allocation was rescinded in mid-September in conference with the Senate, but the final bill requested DOE to provide Congress with a detailed description of the progress of the RERTR program and of the costs involved in resuming development of new fuels. Such development, of course, would greatly facilitate collaboration with a CIS RERTR program.

With the disappearance of the USSR, the smaller number of nuclear weapons needed to defend the U.S. against a potential attack, and the large number of weapons that must be destroyed according to arms control treaties, operation of expensive production reactors and related reprocessing plants became unnecessary. In 1992, DOE announced that the reprocessing plants at Savannah River and at the Idaho National Engineering Laboratory would be permanently shut down in the near future. While logical and probably unavoidable, this decision had important repercussions for the research reactors whose fuel was normally reprocessed at those plants. All the work that the RERTR program and Savannah River personnel had accomplished to ensure that RERTR fuels could be reprocessed within the normal envelope of the Savannah River flowsheets became suddenly useless. We have a keen interest in the reprocessing solutions that are being pursued by reactor operators and potential reprocessors other than DOE, and we intend to cooperate as much as possible to ensure that a viable solution for reprocessing LEU fuels is found.

Consistent with DOE guidance, during the past year the RERTR Program has focused on the conversion of research reactors using the low-enrichment fuels which the program had already developed, and has concentrated its efforts on technology transfer and analytical assistance related to such conversions.

The main technical accomplishments of the program during 1992 are listed below.

1. The results of postirradiation examinations of dispersion fuels were further studied to derive a better understanding of the irradiation behavior, safety characteristics, and applicability of these fuels.[3]. Whenever needed, the results were transmitted to the operators of reactors preparing for conversion, so that they could be taken into account in the required safety evaluations.

2. Several computer codes have been modified and upgraded to improve our capability to analyze the performance and safety characteristics of research reactors operating with LEU fuels. In particular, a modified version of the WIMS-D4 code has been prepared which provides improved data in formats that can interface with U. S. diffusion and burnup codes. Qualification of the code has included detailed comparisons with the VIM Monte Carlo code.[4]

3. Analyses, calculations, and safety evaluations were performed for reactors undergoing or considering conversions outside the US, within the joint study agreements which are in effect between the RERTR Program and several international research reactor organizations. Contribution of the RERTR Program of special significance in this area concern the SSR reactor in Romania[5,6] and the GRR-1 reactor in Greece.[7]

4. Analyses, calculations, and safety evaluations were also conducted to support US research reactors in their efforts to convert to LEU fuels as required by the US Nuclear Regulatory Commission. Some results of this work, concerning the Georgia Tech Reactor, are included in one of the papers presented at this meeting[8].

I reported last year[1] on the overall progress toward conversion which had been achieved by the end of 1991 toward the conversion to LEU fuels of all the research reactors which required HEU exports when the program began, and which were still in operation without imminent plans of being shut down. It is of interest to revisit the situation of these reactors today, and to see how much new progress has been accomplished during the intervening year.

The research reactors of interest for this review are the forty-two research reactors with power of at least one megawatt which used to import HEU either from the United States or from other Western sources. Listed below are the accomplishments of which we have become aware since the previous report was prepared. I hope that additional progress will be reported at this meeting.

1. The SSR reactor (14 MW), at INR in Pitesti, Romania, began the conversion to LEU TRIGA fuel with 45 wt% uranium in February 1992. Four LEU elements were successfully used to bring the reactor to power, and fourteen more LEU elements are expected to enter into use beginning next year.

2. The R-2 reactor (50 MW), at Studsvik, Sweden, continued its successful conversion effort to LEU silicide fuel. This conversion is expected to be complete by the end of 1992.

3. The KUR reactor (5 MW), at Kyoto University in Kyoto, Japan, began irradiation of two prototype LEU silicide elements in February 1992.

4. The NRU reactor (125 MW), at Chalk River, Canada, began the conversion to LEU silicide fuel during 1992.

The list of the fully-converted reactors, which includes nine reactors (OSIRIS, THOR, PRR-1, DR-3, RA-3, FRG-1, ASTRA, NRCRR, and PARR), has not changed since last year, but several reactors have made significant advances towards conversion.

To assess the overall conversion progress, six important steps which most reactors are expected to take on their way toward conversion have been defined as detailed in Ref. 1:

1. Determine feasibility of conversion.

2. Develop conversion plan.

3. Begin irradiation of prototype elements.

4. Order LEU elements for conversion.

5. Load first LEU elements in the core.

6. Unload last HEU elements from the core.

The forty-two operating reactors which required HEU exports when the RERTR Program began can be subdivided in seven categories according to the most advanced step which they have achieved. The two graphs of Fig. 1 illustrate the distributions of the numbers of the reactors, and of the average number of kilograms of ^{235}U yearly exported for use in their fuels, among the various categories. Both diagrams would be blank if no progress toward reduction of HEU exports had been achieved, and fully shadowed if total success had been achieved and no further HEU exports were to be required. The percentages of accomplished work are now 55.6% for the number of reactors and 57.7% for the yearly ^{235}U exports, while they were 54.9% and 54.8%, respectively, last year. The incremental conversion progress recorded during the past year was not as remarkable as that recorded in 1991, but still points to an excellent overall conversion accomplishment. It must be recalled in this connection that, unless RERTR fuel development is resumed, four of the reactors considered in the diagrams cannot be converted: therefore, the highest fractions which are theoretically achievable are 90.5% and 79.2%.

Comparable progress has been attained also by the U.S. university reactors, which are considered separately because they do not require HEU exports. The University of Missouri at Rolla Reactor was successfully converted to LEU silicide fuel, bringing the total number of U. S. converted reactors to six. Safety documentation was completed for one reactor and is nearly complete for five others. In addition, work was initiated for four TRIGA reactors using HEU fuel. The LEU conversion progress of the U. S. research reactors licensed by the U. S. Nuclear Regulatory Commission is discussed in Ref. 9.

PLANNED ACTIVITIES

The future activities which the RERTR Program plans to undertake are consistent with the recent DOE guidance and with the plan outlined at last year's international meeting. The major elements of this plan are described below.

1. Complete testing, analysis, and documentation of the fuels which have already been developed, and support their implementation.

2. Transfer LEU fuel fabrication technology to countries and organizations which require such assistance.

3. Perform calculations and evaluations for reactors planning to undergo conversion, to assist in improving performance and in resolving safety issues.

4. Within the available budget, develop a viable process, based on LEU, for the production of fission ^{99}Mo in research reactors.

SUMMARY AND CONCLUSION

The disappearance of the Soviet Union and the end of the Cold War have brought significant changes for the RERTR program. The new DOE Office of Arms Control and Nonproliferation is now responsible for all DOE arms control and nonproliferation activities, and has assumed management of the RERTR program. Similarly, the RERTR program is now an important component of the ANL Arms Control and Nonproliferation program. The program would welcome the opportunity to cooperate with the CIS republics towards the elimination of the international traffic in Russian-supplied HEU.

The new emphasis on nonproliferation has caused renewed interest in the program's accomplishments and goals. Congress came very close to funding resumption of fuel development within the program, and asked for more information on the subject.

The Secretary of Energy announced that the reprocessing plants at Savannah River and at the Idaho National Engineering Laboratory will be shut down in the near future. The RERTR program intends to cooperate to the fullest extent with reactor operators and potential commercial reprocessors to ensure that a viable solution for reprocessing LEU fuel is found.

Consistent with DOE guidance and with a reduced but stable budget projection, the RERTR Program has concentrated its efforts on technology transfer and analytical assistance related to conversion utilizing already developed fuels. The conversion progress achieved to date corresponds to approximately 57% of what would be needed to convert all the reactors which used to import HEU from the West.

The RERTR Program intends to continue to participate in cooperative efforts to facilitate and accelerate as much as possible the process of eliminating HEU from international commerce.

REFERENCES

1. Travelli, A., "Progress of the RERTR Program in 1990," Proceedings of the XIV International Meeting on Reduced Enrichment for Research and Test Reactors, Jakarta, Indonesia, 4-7 November 1991 (to be published).

2. U.S. Nuclear Regulatory Commission: "Safety Evaluation Report Related to the Evaluation of Low-Enriched Uranium Silicide-Aluminum Dispersion Fuel for Use in Non-Power Reactors," U.S. Nuclear Regulatory Commission Report NUREG-1313 (July 1988).

3. Hofman, G. L., Rest, J., and Snelgrove, J. L., "A New Swelling Model and its Application to Aluminum Silicide Research Reactor Fuels," (these proceedings).

4. Woodruff, W. L., Deen, J. R., and Costescu, C. I., "A Comparison of WIMS-D4M Generated Cross-section Data with Monte Carlo," (these proceedings).

5. Bretscher, M. M., Snelgrove, J. L., and Ciocanescu, M., "Analytical Analysis of Startup Measurements Associated with the First Use of LEU Fuel in Romania's 14-MW TRIGA Reactor," (these proceedings).

6. Toma, C., Barbos, D., Ciocanescu, M., Busuioc, P., Whittamore, W., and Snelgrove, J. L., "Measurement and Computations for Neutron Flux in TRIGA HEU Core with Four Experimental LEU Fuel Clusters," (these proceedings).

7. Deen, J. R., Snelgrove J. L., and Papastergiou, C., "Greek Research Reactor Performance Characteristics after Addition of Beryllium Reflector and LEU Fuel," (these proceedings).

8. Matos, J. E., "Analysis for Conversion of the Georgia Tech Research Reactor to LEU Fuel," (these proceedings).

9. Michaels, T., "Status of HEU-LEU Conversions for Non-power Reactors Licensed by the U.S. Nuclear Regulatory Commission," (these proceedings).

Fig.1 PROGRESS TOWARD CONVERSION OF RESEARCH REACTORS REQUIRING HEU EXPORTS

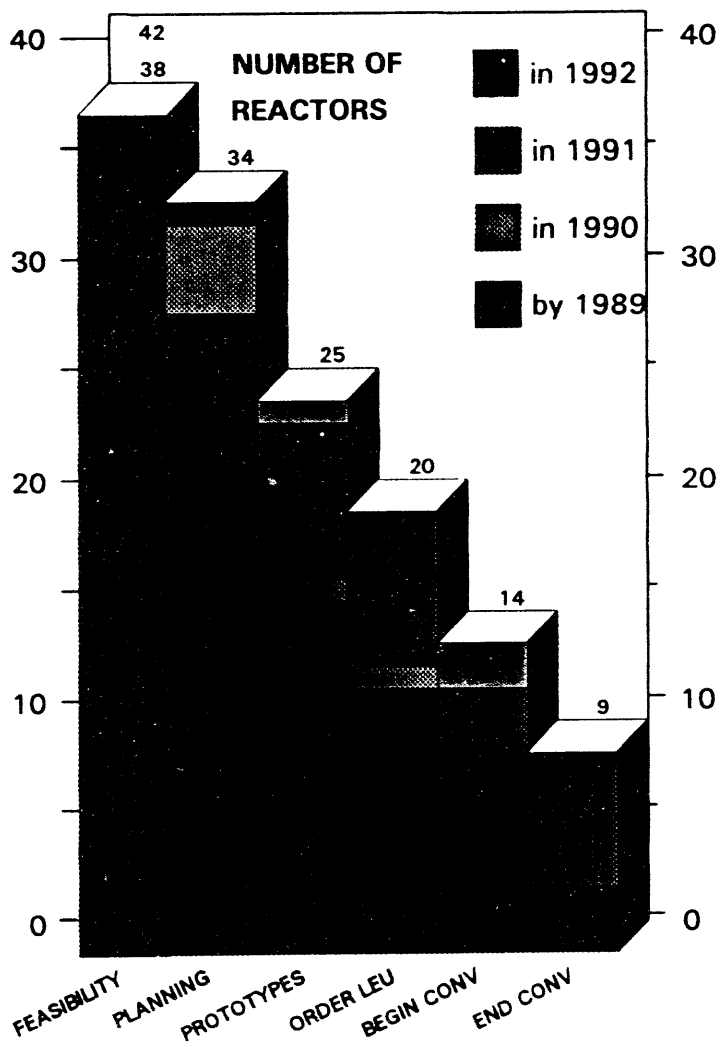

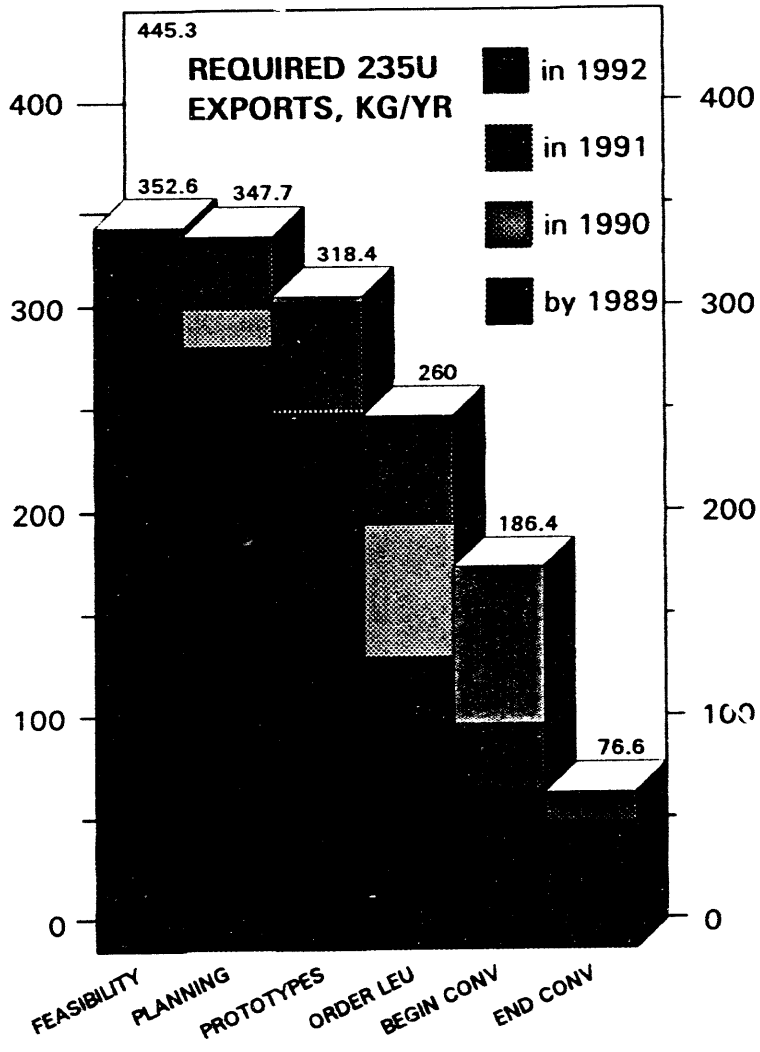

STATUS OF REDUCED ENRICHMENT PROGRAMS FOR RESEARCH REACTORS IN JAPAN

Keiji Kanda, Hideaki Nishihara

Research Reactor Institute, Kyoto University
Kumatori-cho, Sennan-gun, Osaka 590-04, Japan

and

Yoshiaki Futamura, Eiji Shirai and Takumi Asaoka

Japan Atomic Energy Research Institute
Uchisaiwai-cho, Chiyoda-ku, Tokyo 100, Japan

ABSTRACT

The reduced enrichment programs for the JRR-2, JRR-3, JRR-4 and JMTR of Japan Atomic Energy Research Institute (JAERI), and the KUR of Kyoto University Research Reactor Institute (KURRI) have been partially completed and are mostly still in progress under the Joint Study Programs with Argonne National Laboratory (ANL).

The JMTR and JRR-2 have been already converted to use MEU aluminide fuels in 1986 and 1987, respectively. The operation of the upgraded JRR-3 was started in March 1990 with the LEU aluminide fuels.

The safety review application for two LEU silicide elements in the KUR was approved in May 1991 and the two elements have been inserted to the core in May 1992. The safety review application for the full core conversion to use LEU silicide in the JMTR was approved in February 1992 and the conversion is scheduled in November 1993. The Japanese Government approved a cancellation of the KUHFR Project in February 1991, and the related fuel problem is under discussion.

INTRODUCTION

Among eighteen research reactors and critical assemblies in Japan (Tables 1 and 2), those which are relevant to the RERTR program are the JRR-2, JRR-3, JRR-4 and JMTR of JAERI and the KUR of KURRI (Table 3). The RERTR program in Japan has been pursued extensively under the direction of the Five Agency Committee on Highly Enriched

Uranium, which consists of the Science and Technology Agency, the Ministry of Education, Science and Culture, the Ministry of Foreign Affairs, JAERI and KURRI, which is held every three months. It has played a remarkable role in deciding policies related to the program, and the 62nd Committee was held on July 6, 1992, where Babcock & Wilcox was authorized as a fabricator of LEU silicide fuel for Japanese research reactors as well as CERCA. Recently, reprocessing of spent fuel has been mainly discussed.

The program in JAERI for the first step, in which the JRR-2 and JMTR were to be converted to use 45% enriched uranium (MEU) aluminide fuels and the JRR-3 to use 20% enriched uranium (LEU) aluminide fuels, has been completed. The first criticality of the new JRR-3 was achieved in March 1990. After that, the reactor power was increased step by step to high power level and the maximum power to 20 MW was established.

Further core conversion of the JMTR for use of LEU silicide fuel with burnable absorber has been studied since 1984 in accordance with the Joint Study with ANL. The safety review application of the conversion was approved in February 1992, and the conversion is scheduled in November 1993. Studies on silicide fuel plate behavior under accidental conditions are progressing by utilizing the NSRR. The JRR-2 has been remodeled to realize the neutron field for the boron neutron capture therapy, and seven patients were treated since August 1990.

On the other hand, in KURRI the same efforts as in JAERI to reduce the enrichment of the KUR are in progress. The safety review application for two LEU silicide elements in the KUR was approved in May 1991 and the two elements have been inserted to the core in May 1992. The application of safety review of the full core conversion to use LEU silicide fuel will follow. Since February 1990, 21 patients were treated with the boron neutron capture therapy.

JAERI

JRR-2

The fuel of JRR-2 was converted from 93% high enriched uranium (HEU) to 45% medium enriched uranium (MEU) in 1987. JRR-2 has been subsequently operated for 39 operation cycles (12 days / cycle) of more than 96,000 MWh.

After completion of the JRR-3 upgrading program, reactor utilization such as a neutron beam experiment gradually decreases in JRR-2. On the other hand, Boron Neutron Capture Therapy (BNCT) has been actively done in this reactor, and seven patients have been successfully treated since August 1990. A trouble of the main cooling pump was occurred in July, 1991 and the repair works were followed for almost one year. The reactor has been smoothly operated after the restart at the end of July 1992.

JRR-2 has been operated more than 30 years and its retirement might come near future.

JRR-3M

The upgrading work for JRR-3 was started in August 1985 and the first criticality of the new JRR-3 (JRR-3M) was achieved in March 1990, using LEU aluminum fuels (2.2 gU/cc). The JRR-3M began to operate for capsule irradiation, beam experiments and so on at the reactor power of 20 MWt in November 1990. One operational cycle consists of four weeks for operation and one week for shut down work. No evidence of fuel failure has been observed.

Neutron fluxes at beam experimental holes in JRR-3M are quite satisfactory and the cold neutron source has been also operated successfully.

The equilibrium core was attained in May 1991, and fourteen operation cycles have been subsequently achieved with the integral output of ~150,000 MWh as of beginning of July 1992.

JRR-4

It is expected that the reactor operation with HEU fuels continues up to the middle of 1994, when almost all the HEU fuels will be consumed in JRR-4. Then, the conversion works of the reactor core to LEU fuels might follow for about two years. JRR-4 is planned to resume its operation in 1997.

The core design with LEU fuels is now under way. Seismic analyses of the reactor building, accident analyses of fuel element and so on are carrying out for the safety evaluation. The upgrade of utilization facilities is also under consideration.

JMTR

The conversion of the JMTR core from MEU fuel to LEU fuel is scheduled to be made in November 1993. The LEU fuel for the JMTR is the silicide (U_3Si_2) fuel with 4.8gU/cc, and burnable absorbers of cadmium wires are placed in each side plate. The use of the silicide fuel allows the JMTR to operate 26 consecutive days without refueling, which is presently carried out after 12 days' operation. Operating characteristics of the JMTR remain unchanged.

For the safety analysis of the JMTR LEU core, many R&D works on silicide fuel have been successfully conducted such as fission product release measurement, hydraulic tests with dummy fuel elements and measurements of thermal conductivity. Inpile experiments have been progressing in the NSRR to study the silicide fuel behavior under reactivity insertion accident condition.

The safety review was finished and the license on the use of the silicide fuel was issued in February 1992. As a result of the safety analysis based on the latest knowledge, the emergency cooling system, the emergency power system and the safety protection system were decided to be partly upgraded. Approval on design and construction procedures of these upgradings by the Science and Technology Agency has been obtained, and the installation work is to be carried out in the next reactor overhaul period (from August to October of 1993).

KURRI

The Kyoto University Research Reactor (KUR, 5MW) has been operated since 1964 using HEU fuel. The operation time has been shortened from 2,000 hr to 1,500 hr per year since 1991 to save uranium consumption. The existing HEU fuel can be used until March 1995. In May 1995, the KUR is scheduled to convert to use LEU silicide fuel. The KUR has been still utilized for boron neutron capture therapy. Since February 1990, 21 patients of cancer were treated by six chief medical doctors.

Prior to the full conversion, a demonstration to use two fuel elements (U_3Si_2-Al, 3.2 gU/cc) in the core had been planned. The safety review was completed and approved in May 1991, and fuels were fabricated by CERCA in November 1992. After some improvement e.g. to install a new CVCF electricity equipment to avoid a flow reverse of primary coolant, the two fuel elements have been inserted to the core in May 1992.

On the other hand, according to the suggestion of the government, the cancellation of the KUHFR (30MW) Project was applied to the government in December 1990 and approved in February 1991. The handling of HEU received for the KUHFR is under discussion with the US Government.

R&D WORKS FOR LEU FUELS

Pulse Irradiation of Silicide Fuels in the NSRR

Inpile experiments are progressing in the NSRR to study the silicide fuel behavior under accidental conditions. Thermal and mechanical response, fuel failure initiation and fuel fragmentation are being investigated by subjecting the silicide test fuel plates to pulse irradiation.

So far, ten experiments have been conducted with mini-plate type, low enriched (19.89%) and high density (4.8g/cc) fresh silicide fuels cooled by stagnant water at room temperature and at atmospheric pressure in the test capsule. The energy deposited in the fuel ranged from 62 to 164 cal/g fuel and the maximum cladding temperature rises were 200°C to 970°C depending on the energy depositions.

In this test period, fuel behavior at lower energy depositions has been studied in details. It has newly observed that cracks on the solid cladding are formed, most probably at quenching from film boiling, at around 100 cal/g fuel at which energy deposition cladding temperature increases beyond the departure from nucleate boiling (DNB) condition but the peak temperature is still much lower than the melting point of the cladding.

Development of High Uranium Density Fuels

Uranium silicides (U_3Si_2, U_3Si) and U_6Me (Me = Fe, Mn, Ni) have been examined to clarify their irradiation performance and metallurgical behaviors with emphasis on the

latter because of higher uranium density.

Specimens were fabricated and subjected to the neutron irradiation in the JMTR. Post-irradiation examinations of the first capsule are now under way. Irradiation of the second capsule containing U_6Me-type miniplates is in progress.

REFERENCES

1. K. Kanda, "Reducing Enrichment Program for Research Reactors in Japan", in *Proceedings of the International Meeting of Research and Test Core Conversion from HEU to LEU Fuels*, Argonne, USA, November 8-10, ANL/RERTR/TM-4 CONF-**821155**, pp.24-32 (September 1983).

2. K. Sato, "Opening Statement to the International Meeting on Reduced Enrichment for Research and Test Reactors", in *Proceedings of the International Meeting on Reduced Enrichment for Research and Test Reactors*, Tokai, Japan, October 24-27, 1983, JAERI-M **84-073**, pp.8-10 (May 1984).

3. K. Kanda, T. Shibata, I. Miyanaga, H. Sakurai and M. Kanbara, "Status of Reduced Enrichment Program for Research Reactor Fuels in Japan", in *Proceedings of International Meeting of Reduced Enrichment of Research and Test Reactors*, Argonne, USA, October 15-18, 1984, ANL/RERTR/TM-6 CONF-**8410173**, pp.11-20 (July 1985).

4. I. Miyanaga, K. Kamei, K. Kanda and T. Shibata, "Present Status of Reduced Enrichment Program for Research and Test Reactor Fuels in Japan", in *Reduced Enrichment for Research and Test Reactors*, Proceedings of an International Meeting, Petten, The Netherlands, October 14-16, 1985, D. Reidel Publishing Company, Dordrecht/Boston/Lancaster/Tokyo, pp.21-32 (March, 1986).

5. K. Kanda, T. Shibata, Y. Iso, H. Sakurai and Y. Okamoto, "Status of Reduced Enrichment Program for Research and Test Reactor Fuels in Japan", in *Proceedings of the 1986 International Meeting on Reduced Enrichment for Research and Test Reactors*, Gatlinburg, USA, November 3-6, 1986, ANL/RERTR/TM-9 CONF-**861185**, pp.14-22.

6. Y. Futamura, H. Sakurai, Y. Iso, K. Kanda and I. Kimura, "Status of Reduced Enrichment Program for Research and Test Reactor Fuels in Japan", in *Proceedings of the 10th RERTR Meeting*, Buenos Aires, Argentina, September 28- October 1, 1987, in press.

7. K. Kanda, H. Nishihara, Y. Futamura, H. Sakurai and Y. Iso, "Status of Reduced Enrichment Program for Research Reactors in Japan", in *Proceedings of the 11th RERTR Meeting*, San Diego, USA, September 19-22, 1988, in press.

8. Y. Futamura, M. Kawasaki, Y. Iso, K. Kanda and M. Utsuro, "Status of Reduced Enrichment Program for Research and Test Reactor Fuels in Japan", in *Proceedings of the 12th RERTR Meeting*, West Berlin, FGR, September 11-13, 1989, in press.

9. K. Kanda, H. Nishihara, Y. Futamura, M. Kawasaki and T. Asaoka, "Status of Reduced Enrichment Program for Research Reactors in Japan", in *Proceedings of the 13th RERTR Meeting*, Newport, USA, September 23-27, 1990, in press.

10. Y. Futamura, M. Kawasaki, T. Asaoka, K. Kanda and H. Nishihara, "Status of Reduced Enrichment Program for Research Reactors in Japan", in *Proceedings of the 14th RERTR Meeting*, Jakarta, Indonesia, November 4-7, 1991, in press.

Table 1. Japanese Research Reactors in Operation

Name	Owner	Site	Type and	enrichment		Max. Power	Start-up date
JRR-2	JAERI	Tokai	D_2O(CP-5)	U-Al	93%	10 MW	1960.10
				UAl_x	45%	10 MW	1987.11
UTR-KINKI	Kinki Univ.	Higashi-osaka	H_2O(UTR)	U-Al	90%	1 W	1961.11
TRIGA-II	Rikkyo Univ.	Yokosuka	H_2O(TRIGA)	U-ZrH	20%	100 kW	1961.12
TTR	Toshiba	Yokosuka	H_2O(pool)	U-Al	20%	100 kW	1962. 3
JRR-3	JAERI	Tokai	D_2O(tank)	NU		10 MW	1962. 9
				UO_2	1.5%		
			H_2O(pool)	UAl_x-Al	20%	20 MW	1990. 3
TRIGA-II MUSASHI	Musashi Inst. Tech.	Kawasaki	H_2O(TRIGA)	U-ZrH	20%	100 kW	1963. 3
KUR	KURRI	Kumatori	H_2O(tank)	U-Al	93%	5 MW	1964. 6
JRR-4	JAERI	Tokai	H_2O(pool)	U-Al	93%	3.5 MW	1965. 1
JMTR	JAERI	Oarai	H_2O(MTR)	U-Al	93%	50 MW	1968. 3
				UAl_x	45%	50 MW	1986. 8
YAYOI	Univ. of Tokyo	Tokai	fast (horizontally movable)	U	93%	2 kW	1971. 4
NSRR	JAERI	Tokai	H_2O(TRIGA)	U-ZrH	20%	300 kW	1975. 6

Table 2. Japanese Critical Assemblies in Operation

Name	Owner	Site	Type and enrichment			Max. power	Start-up date
VHTRC	JAERI	Tokai	Graphite horizontally split	U	20%	10 W	1961. 1
TCA	JAERI	Tokai	H_2O(tank)	UO_2 UO_2-PuO_2	2.6% 2.6%	200 W	1962. 8
NCA	NAIG	Kawasaki	H_2O(tank)	UO_2	1-4.9%	200 W	1963.12
JMTRC	JAERI	Oarai	H_2O(pool)	U-Al UAl	93% 45%	100 W	1965.10 1983. 8
FCA	JAERI	Tokai	fast horizontally split	U U Pu	93% 20%	2 kW	1967. 4
DCA	PNC	Oarai	D_2O(tank)	UO_2 UO_2-PuO_2	0.22% 1.5%	1 kW	1969.12
KUCA	KURRI	Kumatori	various multi-core	U-Al UAl_x	93% 45%	100 W 1 kW (short time)	1974. 8 1981. 5

Table 3. Research Reactor Relevant to RERTR in Japan

Name	Power (MW)	First Critical	Fuel Enrichment	Conversion
KUR (KURRI)	5	1964	HEU → LEU	1995
KUHFR (KURRI)	30	canceled		
JRR-2 (JAERI)	10	1960	HEU → MEU	1987
JRR-3 (JAERI)	20	1962	LEU → LEU	1990
JRR-4 (JAERI)	3.5	1965	HEU → LEU	1997
JMTR (JAERI)	50	1968	MEU → LEU	1993
Related Critical Assemblies				
KUCA (KURRI)	0.0001	1974	HEU → MEU	1981
JMTRC (JAERI)	0.0001	1965	HEU → MEU	1983

Table 4. History of Reduced Enrichment Program for Research and Test Reactor in Japan

1977.11.	Japanese Committee on INFCE WC-8 was started.
1977.11.	Joint Study Program was proposed at the time of the application of export license of HEU for the KUHFR.
1978. 5.	ANL-KURRI Joint Study Phase A was Started.
1978. 6.	Five Agency Committee on Highly Enriched Uranium was organized.
1978. 2.	ANL-KURRI Joint Study Phase A was completed.
1979. 5.	Project team for RERTR was formed in JAERI.
1979. 7.	ANL-KURRI Joint Study Phase B was started.
1980. 1.	ANL-JAERI Joint Study Phase A was started.
1980. 8.	ANL-JAERI Joint Study Phase A was completed.
1980. 9.	ANL-JAERI Joint Study Phase B was started.
1981. 5.	MEU UAl_x-Al full core experiment was started in the KUCA.
1983. 3.	ANL-KURRI Phase B was completed.
1983. 8.	MEU UAl_x-Al full core experiment in the JMTRC was started.
1983.11.	ANL-KURRI Phase C was started.
1984. 3.	ANL-JAERI Phase B was complete.
1984. 4.	ANL-JAERI Phase C was started.
1984. 4.	MEU-HEU mixed core experiment in the KUCA was started.
1984. 9.	Irradiation of 2 MEU and 1 LEU UAl_x-Al full size elements in the JRR-2 was started.
1984.10.	Irradiation of LEU UAl_x-Al full size elements in the JRR-4 was started.
1984.11.	Thermal-hydraulic calculations for the KUR core conversion from HEU to LEU was performed.
1985. 1.	Irradiation of MEU UAl_x-Al full size elements in the JMTR was started.
1985. 3.	Irradiation of MEU UAl_x-Al full size elements in the JMTR was completed. Irradiation of LEU U_xSi_y-Al miniplates in the JMTR was started.
1985. 6.	Irradiation of LEU U_xSi_y-Al miniplates in the JMTR was completed.
1985.10.	Neutronics calculations for the KUR core conversion from HEU to LEU was performed.
1986. 1.	Irradiation of MEU UAl_x-Al full size elements in the JRR-2 was completed.
1986. 5.	Irradiation of MEU UAl_x-Al full size elements in the JRR-2 was completed.
1986. 8.	The JMTR was fully converted from HEU to MEU fuels.
1987.11.	MEU UAl_x-Al full core in the JRR-2 was started.
1988. 7.	PIE of MEU, LEU UAl_x-Al full size elements in the JRR-2 was completed.
1988.12.	Irradiation of a LEU UAl_x-Al full size elements in the JRR-4 was completed.
1990. 3.	LEU UAl_x-Al full core test in the new JRR-3 (JRR-3M) was started.
1990.11.	Full power operation of 20 MW in the JRR-3M was started.
1992. 5.	Two LEU U_3Si_2 elements were inserted into the KUR core.

STATUS OF CANADIAN LOW-ENRICHED URANIUM CONVERSION PROGRAM

J.W. Schreader, S.J. Palleck, D.F. Sears, P.M. Brewster
AECL Research, Chalk River Laboratories
Chalk River, Ontario, Canada KOJ 1JO

ABSTRACT

The Canadian low-enriched uranium (LEU) conversion program has centered around the conversion of AECL Research's NRU reactor. The Conversion will soon be completed. Over half the reactor core now contains LEU fuel rods. Current reactor loading schedules should see a complete LEU core by the end of 1992 or early in 1993. This is a major accomplishment for the Canadian program and certainly complementary to the RERTR program.

The Nuclear Fuel Fabrication Facility, built to house fabrication equipment for new LEU fuel, is now licensed and production is exceeding NRU reactor requirements. Complete results of a test irradiation of Al-U_3Si_2 have been delayed due to a reactor shutdown in 1991.

INTRODUCTION

As part of an international effort to reduce the use of highly enriched uranium (HEU, 93 wt% U-235) in research reactors, Chalk River Laboratories has developed low-enriched uranium (LEU, < 20 wt% U-235) fuels for the conversion of the NRU reactor. LEU fuel will also be used in the new MAPLE-type research reactors being developed by AECL. The 10 MW prototype, MAPLE-X10, is currently under construction at Chalk River. The LEU fuel is manufactured in a new fuel-fabrication facility, built at Chalk River.

This paper presents the progress made in converting the NRU reactor from a HEU-fueled reactor to a LEU-fueled reactor. The status of manufacturing in the new fuel-fabrication facility at Chalk River is discussed. A report on the status in the test irradiation of three fuel-sized NRU fuel rods containing Al-U_3Si_2 dispersion fuel is included. A brief update on AECL's plans for closing the fuel cycle for Mo-99 production is also provided.

CONVERSION OF NRU TO AL-U_3Si DISPERSION FUEL

A significant milestone in the LEU conversion program was achieved in 1991 November, when the Canadian Atomic Energy Control Board granted license approval for the operation of the NRU reactor with a low-enriched Al-U_3Si dispersion fuel. As noted in the previous presentations, a 31-fuel-rod demonstration (representative of 1/3 of the reactor core) was successfully completed in 1990 January.

In 1992 January, the first LEU rods of the full-scale conversion effort were inserted into the reactor. For the first four months, reactor loadings were both HEU and LEU rods. Since that time, only LEU fuel has been loaded into the reactor, and at the end of 1992 August the core consisted of 40 HEU rods and 50 LEU rods. At the current loading schedule, by year end or early in 1993, the entire NRU core will be made up of LEU fuel. This will complete the conversion of the NRU reactor from a HEU (93 wt% U-235) -fuelled reactor to a LEU-reactor (19.75 wt% U-235).

With over half the reactor conversion complete, there is nothing to indicate that this target will not be met. This will mark the culmination of a tremendous effort, which has seen AECL not only develop a new fuel, but also new fabrication processes and facilitates to fabricate the fuel. It has also led to the development of the LEU-fuelled MAPLE-X reactor. Assuming the conversion of NRU reactor remains trouble-free, fuel wise, the need for HEU to fuel this reactor will no longer exist. For the RERTR program, this effectively reduces the export of HEU from the USA by 66.4 kg/a and is a milestone for the program.

NRU-EXPERIENCE WITH LEU DRIVER FUEL RODS

From the reactor operations point of view, there are a few differences between the HEU and LEU driver fuel rods.

The U-235 content of both rod types is specified to be the same, 0.49 kg. The shape and size of the 12 elements are indistinguishable. The basic difference between the rods is that the LEU 'meat' contains 0.3 kg less aluminum, 0.1 kg more silicon, and 2.0 kg more U-238 than the HEU 'meat.'

The additional mass of the rod assemblies does not affect the usual fuel handling.

The additional U-238 is a reactivity load; however, the effect is partially offset by the reactivity gain due to the production of plutonium. From the fuel management point of view, the two rod types are equivalent, except for the extra plutonium in spent LEU rods. A greater energy output [MWd] is required from the LEU rods to keep the fissile content of spent rods below 130 g. This limit is imposed to minimize the cost of interim storage of spent rods.

To achieve this greater burnup, the core loading of the reactor is being modified as more and more sites contain LEU rods. Two actions can increase the exit burnup: Providing additional fuel rod sites or removing a neutron absorber. To increase the number of fuel rod sites, a peripheral moderator site may be converted to a site for an old fuel rod. To reduce neutron absorption, and isotope production rod, such as an alumina nitride rod for the production of Carbon-14 from Nitrogen-14, may be removed from the core and used as a moderator site or as an additional fuel-rod site. Since NRU is a large reactor with a lattice of 227 positions, there are many options for rearranging the core.

The effects of converting the core from HEU to LEU driver fuel rods were surveyed in 1984. This predicted that the exit burnup would be reduced by 5% is five additional fuel-rod sites were used without changing the number of absorber rods. Although it is really too early to either confirm or deny our predictions, it appears the impact on our core loading will be smaller than predicted.

NUCLEAR FUEL FABRICATION UPDATE - LEU PRODUCTION

Since the last update was given in 1990, the LEU Nuclear Fuel Fabrication Facility (NFFF) at Chalk River has achieved one of its major goals in developing the fabrication process. It has been licensed to operate with no limitation on quantities processed within the maximum amounts allowed criticality approval. Prior to this, the facility was licensed to process only a fixed small quantity of fuel at a time.

The major challenge is realizing the full capability of the production equipment has not been technological, but to learn what it takes to comply to modern regulatory requirements.

The NFFF has been operating since 1990 June, fabricating LEU fuel for the NRU research reactor. Conditions in licensing permitted only small quantities of fuel processing, until satisfactory training and quality programs could be demonstrated. While developing these programs, the regulatory requirements changed. By the time an acceptable quality program was developed, what was initially acceptable as a training program was no longer valid: The regulators in Canada were indeed raising their standards and the NFFF, as a new facility, provided an opportunity for them to set an example for other upcoming projects.

The NFFF is currently in a position to fully meet all production requirements. Customers in 1993 include NRU operating full time, NRX part-time, first charge and replacement charge fuel for MAPLE-X10 at Chalk River, first charge and replacement charge fuel for South Korea's MAPLE research reactor, and supporting the isotope production business. We have also acquired new electron beam welding equipment for welding fuel elements and flow tubes, and real-time X-ray for improved fuel inspection.

The LEU fuel presently being produced is based on Al-U_3Si. However, a new glovebox line has been designed for Al-U_3Si_2-based LEU fuel. From a fuel-fabrication perspective, our interest in changing to U_3Si_2 is improved efficiency to the fuel fabrication process. Once the results of the test irradiations of the three full-size Al-U_3Si_2 fuel rods are known, and assuming they are positive, we will proceed with the procurement and set-up of this new line. Some changes to our operating license will be required, but these will likely be minimal.

AL-U_3Si_2 FUEL DEVELOPMENT AND IRRADIATION TESTING

As reported previously, Al-U_3Si_2 fuel-fabrication technology has been developed at Chalk River to complement our Al-U_3Si capability. The irradiation of 12 mini-elements containing Al-64 wt% U_3Si_2 was completed successfully in 1989 December, and the results were shared at the RERTR Conferences in both Newport and Jakarta.

A demonstration irradiation of three prototype full-length Al-U_3Si_2 fuel rods has just been completed. The three fuel-rod length rods were inserted in NRU in 1990 August. However, with the shutdown of NRU for most of 1991, completion of the full test-irradiation was delayed until this year. The three test fuel rods were removed from the reactor during the first week of 1992 September. We have completed visual examinations of the high-burnup rods and the elements appear to be in excellent condition. However, there has been insufficient time for detailed post-irradiation examination. Therefore, we are not able to report the final results of irradiation at this meeting, but do look forward to sharing those results at the next RERTR meeting.

TARGETS FOR ISOTOPE PRODUCTION

One of the long-term objectives of the radioisotopes operation at Chalk River has been to close the fuel cycle for Mo-99 production. The needed steps include recovering the enriched uranium inventory from previous Mo-99 target dissolution, recycling the material, and further depleting it. The program, of course, will have to satisfy both environmental and safeguards criteria and regulations.

Consequently, preliminary studies on recovering the uranium from Mo-99 target dissolutions are continuing. In parallel, a project on the development and qualification of a new target, based on recovered enriched uranium (REU), as well as LEU, is underway. Both metal and oxide target designs are being pursued at present. We anticipate irradiation testing is approximately 1-2 years away.

CONCLUSIONS

1. The LEU fuel-fabrication facility at Chalk River has overcome the major obstacle to full-capacity production. Programs have been developed to satisfy modern regulatory requirements, and the facility is well positioned to achieve full efficiency and maintain the high standards of quality and safety experienced at Chalk River.

The NFFF is also fully capable of meeting all its customers' demands while considering opportunities for new commercial fuel contracts, as well as commercial electron beam welding and the specialized applications for real-time X-ray inspections.

2. The conversion of the NRU reactor from HEU to LEU will soon be completed. From the reactor operators' point of view, the conversion to date has been uneventful. Fuel failures have not occurred and no fission-product contamination has been detected in the coolant.

3. Assuming that the current fueling schedule of NRU with LEU fuel rods remains trouble-free, NRU's conversion to LEU will be complete by the end of 1992 or early in 1993. This effectively reduces the quantity of HEU exported from the USA by 66.4 kg/a. This is a major achievement for Canada and the RERTR program.

REFERENCES

1. Sears, D.F.: "Development and Irradiation Testing of Al-U_3Si_2 Fuel at Chalk River Laboratories," Proceedings of the International RERTR Meeting, Jakarta, Indonesia, 1991 November 4-7 (to be published).

2. Sears, D.F.: "Status of LEU Fuel Development and Testing at CRNL," Proceedings of the International RERTR Meeting, Newport, Rhode Island, USA, 1990 September 23-27 (to be published).

3. Sears, D.F.: "Status of LEU Fuel Development and Conversion of NRU," Proceedings of the International RERTR Meeting, West Berlin, FRG, 1989 September 10-14, Published 1991.

4. Schreader, J.W., Kennedy, I.C., and Sears, D.F.: "Status of Canadian Low-Enriched Uranium Conversion Program," Proceedings of International RERTR Meeting, San Diego, USA, 1988 September 19-22 (to be published).

S E S S I O N II

September 28, 1992

FUEL DEVELOPMENT AND FABRICATION

Chairman:

A. Travelli
(Argonne National Laboratory, USA)

OPTIMIZATION OF SILICIDE FUEL ELEMENTS

A. BALLAGNY - J-P. BEYLOT - J. PAILLERE
CEA SACLAY
91191 GIF-SUR-YVETTE CEDEX, FRANCE

J-P. DURAND - Y. FANJAS - A. TISSIER
CERCA ROMANS
BP 1114
26104 ROMANS-SUR-ISERE, FRANCE

ABSTRACT

The purpose of this paper is to show that it is possible to increase the U-235 loading per fuel element without exceeding the universally qualified maximum uranium density of 4.8 g/cm3 or modifying the fuel element geometry. The corresponding R & D work includes both safety aspects and industrial production requirements.

INTRODUCTION

Most of the reactor operators who have decided to use silicide fuels for core conversion have chosen the U3Si2 fuel, with a maximum density of 4.8 g/cm3.
This choice stems from the need of the best balance between the following requirements :

- high U-235 loading
- easy fuel manufacturing technique
- good behaviour under irradiation.

All qualification programs have been concentrated on this product.
However, in the past two years, the picture has been profoundly modified.
Although the reactor operators had been implicitly led to the conviction that the DOE would be willing to reprocess this type of fuel, to day it is no longer the case.

Only two solutions could be considered for LEU fuels (slide 1) :

. Either fuel reprocessing in Europe but this is not truly realistic, taken into account the fact that even reprocessing of HEU seems to meet so many obstacles.
. Or direct disposal, which could not be operational before 10 to 20 years.

Given these conditions, the priority must be given to the end cycle. In other terms, the reduction of the number of fuel elements which are burnt in each reactor becomes the main concern, as it will be necessary to keep them in storage for many years.

To be significant, this reduction should amount to around 20 %. The problem is threefold :

- keep the qualification parameters unchanged,
- keep the fuel element geometry unchanged (as well as the core volume),
- allow only those minor modifications, the scope of which stays within the limits set by the Safety Authority.

I- POINT OF VIEW OF THE REACTOR OPERATOR

I.1- Reduction of the consumption of fuel

Reducing the number of fuel elements which are burnt per year leads to extending the life of these elements, by extending their specific energy content and consequently their uranium loading.

For a given enrichment, and a given burn up

$$W_{MWd/cm^3} = [aB + (B, e_0)]\, m_{05}$$

The specific energy is a linear function (for a given enrichment e_0 and a given burn up B) of the initial fuel loading m_{05}, "a" being a constant.
Parametric studies have shown that, for a given density, the gain in reactivity, as a function of the fuel loading, increases to a maximum and then decreases.

I.2- The possible ways of increasing the initial fuel loading

Slide 2 shows a schematic view of the fuel plates bundle in a fuel element. From the geometry of this sketch, slide 3 shows how to write the uranium loading per fuel element.

Based on the following two assumptions that :

- on the one hand, the total fuel element volume is kept unchanged (so that the element can fit on the reactor grid),
- on the other hand, the total water volume in the fuel plates bundle is kept constant (in order to minimize the variations of the moderating factor and of the cooling capacity) the uranium loading per element can be written as a function of four parameters :

$$M = \rho \frac{u}{v_m}(K - k.n.e_c) = n.v_m.d$$

where :
ρ is the uranium weight per unit volume of uranium phase
$\frac{u}{v_m}$, volume fraction of dispersed uranium phase in the plate meat

n, number of fuel plates per element
e_c, cladding thickness,
K and k being constants.

In these conditions the obvious choices for increasing the uranium core loading (keeping the element volume, V, constant) are summarized by the graph below :

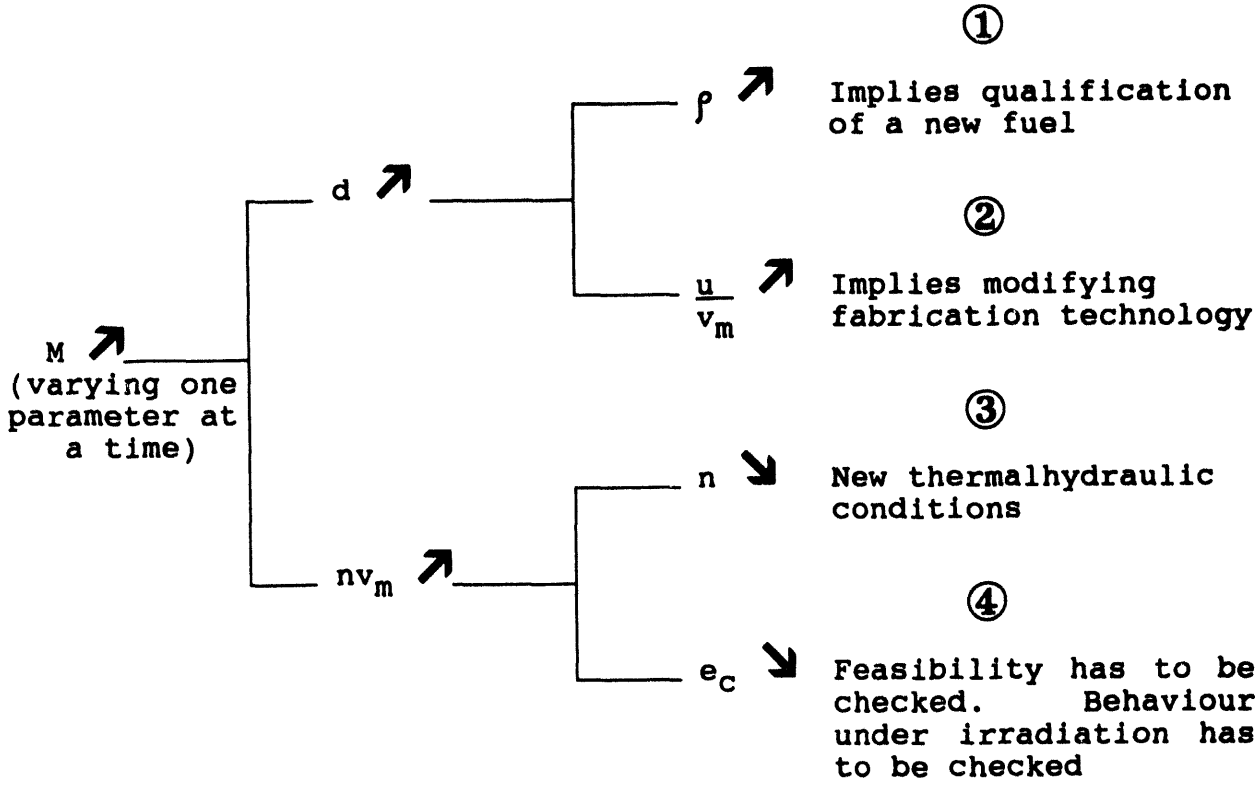

I.2.1- Discussion

- Branch ① : Increase of ρ : involves developing a denser qualified compound. So far the U3Six fuel has been successfully tested.
However, the qualification of this type of fuel could take some time.
It is the subject of various studies which will not be discussed here.

- Branch ② : Increasing the ratio :

$$\frac{\text{volume of uranium dispersed phase}}{\text{volume of meat}}$$

means going beyond the present fabrication limits in order to be able to produce U3Si2-Al plates loaded at more than 5 g/cm^3.

- Branch ③ : The decrease of the number of plates leads to a smaller overall exchange surface area and to a different element pressure drop. This choice would imply changing the thermalhydraulic conditions of the core.

- Branch ④ : The diminution of the cladding thickness allows an increase of the meat volume without modifying the number of plates or their overall thickness. This solution seems interesting, provided manufacturing difficulties can be tackled.

I.2.2- Limitations and prospects

A Δe_{clad} reduction in the cladding thickness leads to a meat thickness increase $2 \Delta e_{clad}$, if the overall plate thickness is kept constant.

A reasonable compromise could be to reduce the cladding thickness from 0.38 mm to 0.34 mm (about 10 % reduction) leading to a core thickness increase from 0.51 mm to 0.59 mm (about 15 % increase) corresponding - at constant density - to a 15 % core loading increase (to achieve the same uranium loading increase, without modifying the cladding thickness, would require to increase the density from 4.8 g/cm^3 to $4.8 \text{ g/cm}^3 \times \frac{0.59}{0.51} = 5.55$ g/cm^3)

For the OSIRIS reactor,this 15 % uranium loading increase would correspond to the burning of 60 elements per year instead of 70 per year.

Cladding thickness of current fabrications is 0.38 mm with local absolute minimum fixed at 0.25 mm.
Assuming the local meat thickness variations are independant from the average cladding thickness, the reduction of the average cladding from 0.38 to 0.34 mm requires a corresponding reduction of the local minimum cladding. The allowable cladding reduction as well as the acceptable surface defects depth will be determined by irradiation experiments.

II- SAFETY ANALYSIS

From the above considerations it follows that the qualification of fuel elements with increased core thickness will rely essentially upon the behaviour under irradiation. Consequently a dedicated program has been set up, the purpose of which is to irradiate full size plates with local minimum cladding thickness reaching 0.2 mm.
The experimental irradiation will take place in the SILOE reactor.

Description of the IRIS irradiation test device (slide 4)

IRIS "Installation d'Irradiation et du Suivi d'épaisseur" is the experiment set up at the reactor SILOE in GRENOBLE for the above purpose.

It consists of an irradiation box located at the periphery of the reactor core, with a capacity for 8 full size plates.
Four of them are inert and have an overall thickness of 1.27 mm and the other four ones are fuel plates with the same overall thickness, the former ones insuring the correct water distribution.

The fuel plates are removable. At the end of each fuel cycle, they are taken out of the irradiation box and placed on a specially designed measuring bench.

Swelling under irradiation is monitored along 5 vertical tracks. Thickness variations are automatically recorded (slide 5).

III- POINT OF VIEW OF THE FUEL MANUFACTURER

III.1- Technical aspects

Slide 6 shows the comparison between the present OSIRIS fuel plate and the new plate type considered above.
The present OSIRIS plate corresponds to the standard silicide plate : classical dimensions for the cladding (0.38 mm), the meat (0.51 mm) and the plate (1.27 mm) and standard uranium density of 4.8 g/cm^3 with the U3Si2 dispersion fuel.

With respect to this classical plate (later referred to as standard plate in this paper), the new type (later referred to as thick core plate) is characterized by the following modifications:

- a 10 % decrease in the average cladding thickness
- a 20 % decrease in the cladding local minimum
- and a 15 % increase in the meat thickness.

Other characteristics such as overall plate thickness and uranium density remain unchanged.

Above modifications may give rise to some consequences on the manufacturing and the quality of fuel plates. As far as manufacturing is concerned, the manufacturer has to check the rolling behaviour of the product. As far as quality is concerned, one must make sure that the specified criteria can be reliably met on large scale production. Practically, the following criteria are of concern :

- the local minimum cladding in the current part of the meat and in the dog-bone area.
- the maximum permissible surface defect depth which will be all the smaller as the absolute minimum cladding will be reduced.
- besides, the increased meat thickness influence on the uranium distribution homogeneity in the fuel plate has to be checked.

III.2- Preliminary tests

In order to check the technical feasibility of plates with thicker meat and reduced cladding, 16 full size depleted fuel plates were produced. Due to the previously explained particularities of the product, the fabrication parameters were adjusted and the necessary manufacturing precautions taken.
For purpose of comparison, standard plates were simultaneously produced as a reference.
The test results are described herebelow.

III.2.1- Cladding and meat thicknesses

5 of the 16 thick core and 1 of the 6 standard plates were cut for micrographic inspection. Two sections were made in the dog-bone area (one at each core end) and one in the current part of the meat.

The corresponding results are summarized in slide 7.
The range of results obtained for the plates is reported in the column "measurements result".
For each variable, the measured data stand within a narrow range, which is an indication of the good reproducibility of results.

For both types of plates, the average cladding and meat thicknesses comply with the expected values : respectively 0.38 and 0.34-0.35 mm for the cladding, 0.51 and 0.58-0.59 mm for the meat.

In any case, the minimum cladding remains significantly above the specification. With respect to the standard plate, it is decreased by 0.04-0.05 mm which is consistent with the average cladding thickness reduction.
Examination of the micrographic pictures (slide 8) does not indicate noticeable differences between the two types of plates. Both present a normal morphology and a sound interface between meat and cladding.

III.2.2- Uranium distribution homogeneity

Specially designed X-ray scanning machines are used to control quantitatively the homogeneity of uranium distribution in fuel plates. A focused X-ray beam goes through the plate. By measuring the absorption of the beam across the plate, the uranium density variations are determi ed.
The whole plate surface is inspected by successive scans along its core length. Slide 9 shows a representative record along one scanning line of each plate type.
As can be seen on the slide, both records look alike. In each case the uranium distribution easily stands within the specified limits. The similar aspects of the profiles indicate that the change in meat thickness does not significantly modify the fuel core homogeneity.

III.3- Influence on the fabrication yield

The preliminary tests show the feasibility of reduced cladding fuel plates. All the manufactured plates have successfully passed the usual inspections and the dispersion of corresponding results is small.

Nevertheless, as for any new product and in particular in this case since we stand outside the standard manufacturing conditions, large scale reproducibility tests must be carried out to make sure that the fabrication yield remains high enough so that economic conditions can be achieved.
In this respect, the maximum allowable surface defect depth is of special importance due to the reduced cladding thickness : it will be determined by the test under irradiation of plates bearing calibrated grooves machined on their surfaces.

IV- IRRADIATION TEST PROGRAM

IV.1- Irradiation testing

Although the fuel meat in pile behaviour does not need to be proven anymore, it is necessary to irradiate test plates to check the reduced cladding resistance to corrosion and fission products release. In particular, the cladding thickness absolute minimum, which results from a combination of local meat thickness variations and surface defects, will be decided from the test results. Therefore, the following three-phase irradiation program has been set up :
- Irradiation of 4 full size plates in the SILOE reactor using the IRIS device : one standard (for purpose of comparison) and 3 thick core plates will be irradiated. One of the three thick core plates will present a defectless surface. The other two will bear calibrated machined defects which will locally reduce the cladding thickness to less than 0.2 mm.

- Fission product release :
  As part of a more general program to study the fission product release of silicide fuels, thick core mini plates will be tested to compare their behaviour with standard mini plates. These tests will be carried out in an irradiation loop of the SILOE reactor.

- Prototype elements irradiation :
  The third phase corresponds to the official in pile qualification of fuel elements made with thick core plates. For this purpose two prototype elements will be irradiated in the OSIRIS reactor.

IV.2- Irradiation program schedule (slide 10)

The optimization phase consisting of design calculations and fabrication feasibility has been completed as previously presented. Irradiation testing is under preparation. The 4 plates to be tested in SILOE are under fabrication at CERCA.
Their irradiation will take place in 1993. As far as the fission product release experiment is concerned, the test plates will be manufactured in 1993 and irradiated in 1993-1994. The two OSIRIS prototype elements will be produced in 1993 for irradiation in the OSIRIS reactor in 1994.

CONCLUSION

The concept of thicker meat and constant plate thickness allows to increase significantly the uranium loading per fuel element without changing the type of fuel, the fuel density or the thermalhydraulic conditions. Therefore it is a valuable and relatively easy way to extend the fuel element core lifetime.
The preliminary manufacturing tests demonstrated the feasibility of the thick core plates. A specific program aiming at qualifying them under irradiation is underway which will be completed by the end of 1994.

CEA

CERCA

END OF CYCLE ALTERNATIVES

LEU FUEL REPROCESSING IN EUROPE - UNLIKELY

DIRECT DISPOSAL - NOT BEFORE 10 TO 20 YEARS (IF PERMITTED SOME DAY)

INTERIM PALLIATIVE

REDUCTION OF THE NUMBER OF FUEL ELEMENTS BURNT EACH YEAR THROUGH SIGNIFICANT (15 %) FUEL LOADING INCREASE.

CEA CERCA

FUEL PLATE AND FUEL ELEMENT SECTION SCHEMATIC DESIGN

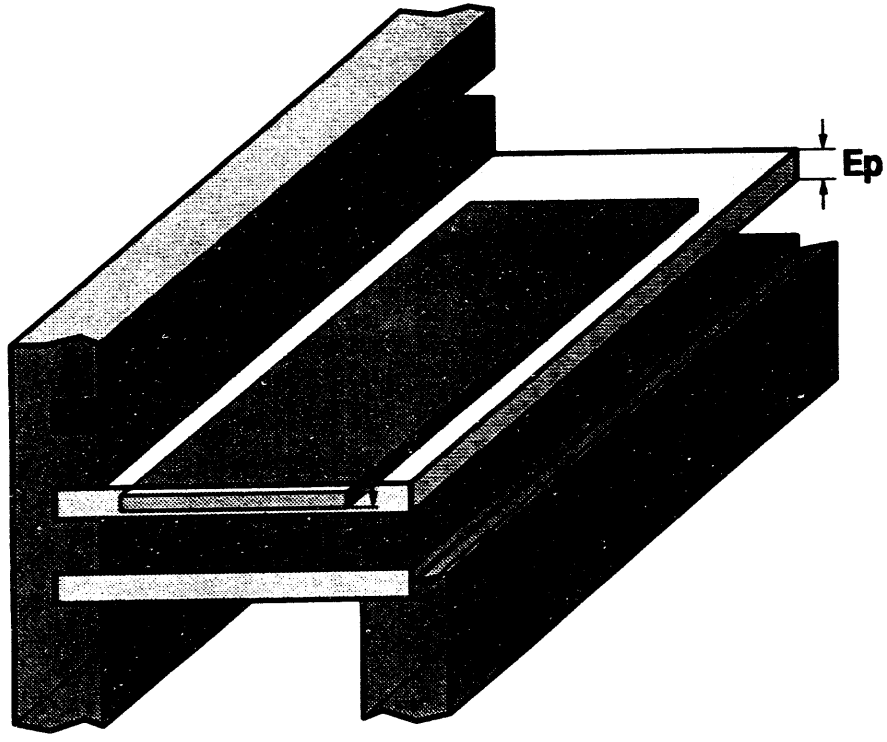

Slide 2

CEA

CERCA

FUEL ELEMENT URANIUM LOADING

$$M = m \cdot n = d \cdot v_m \cdot n$$

$$d = \rho \frac{u}{V_m}$$

$$v_m = S\,(e_p - 2e_c)$$

$$M = \rho \frac{u}{V_m} \cdot S\,(e_p - 2e_c) \cdot n$$

$$\left.\begin{array}{l} n\,S\,e_p = V_{met} \\ V = V_w + V_{met} \end{array}\right\} \Rightarrow n\,S\,e_p = cst = K$$

(V: cst; V_w: cst)

$$M = \rho \frac{u}{V_m} \cdot (K - k.n.e_c)$$

M	= U mass/element
m	= U mass/plate
n	= Nbr. of plates/element
d	= U density in meat
v_m	= meat volume/plate
ρ	= U mass/unit vol. of fuel phase
u	= fuel dispersion vol. per fuel plate
S	= plate meat area
e_p	= plate thickness
e_c	= cladding thickness
V	= total vol. of fuel bundle
V_w	= water vol. in fuel bundle
V_{met}	= metal vol. in fuel bundle

CEA CERCA

IRIS

Installation d'Irradiation et de Suivi d'Epaisseur de Plaques combustibles à SILOE

COEUR DE SILOE :

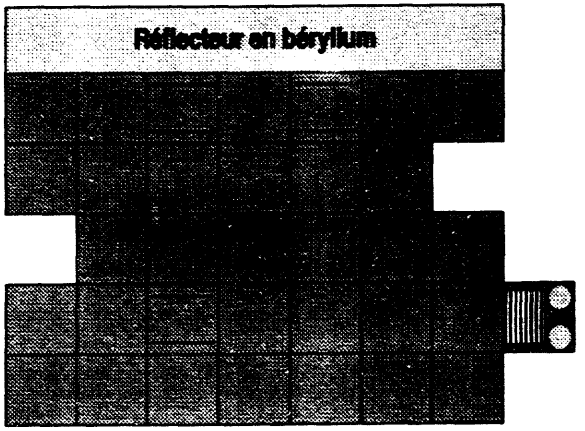

PLAQUE COMBUSTIBLE

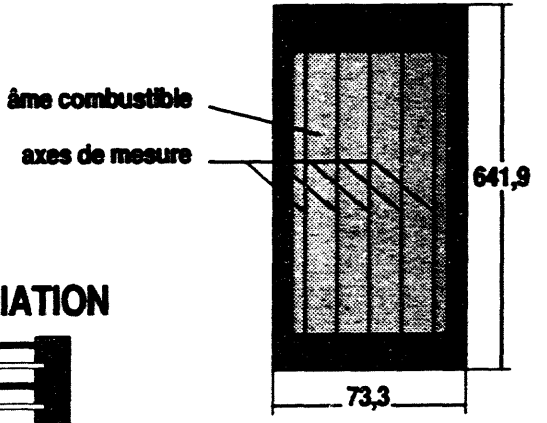

BOITIER D'IRRADIATION

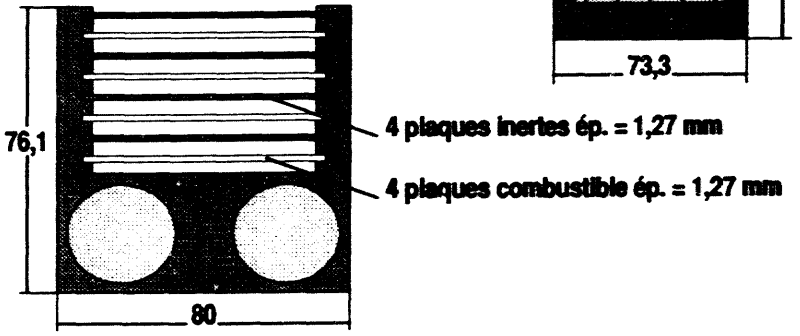

Slide 4

CEA CERCA

IRIS

Installation d'Irradiation et de Suivi d'Epaisseur de Plaques combustibles à SILOE

IRIS : Fuel plate # SAZE05, thickness evolution : central vertical scan, after irradiation in SILOE at 35MW

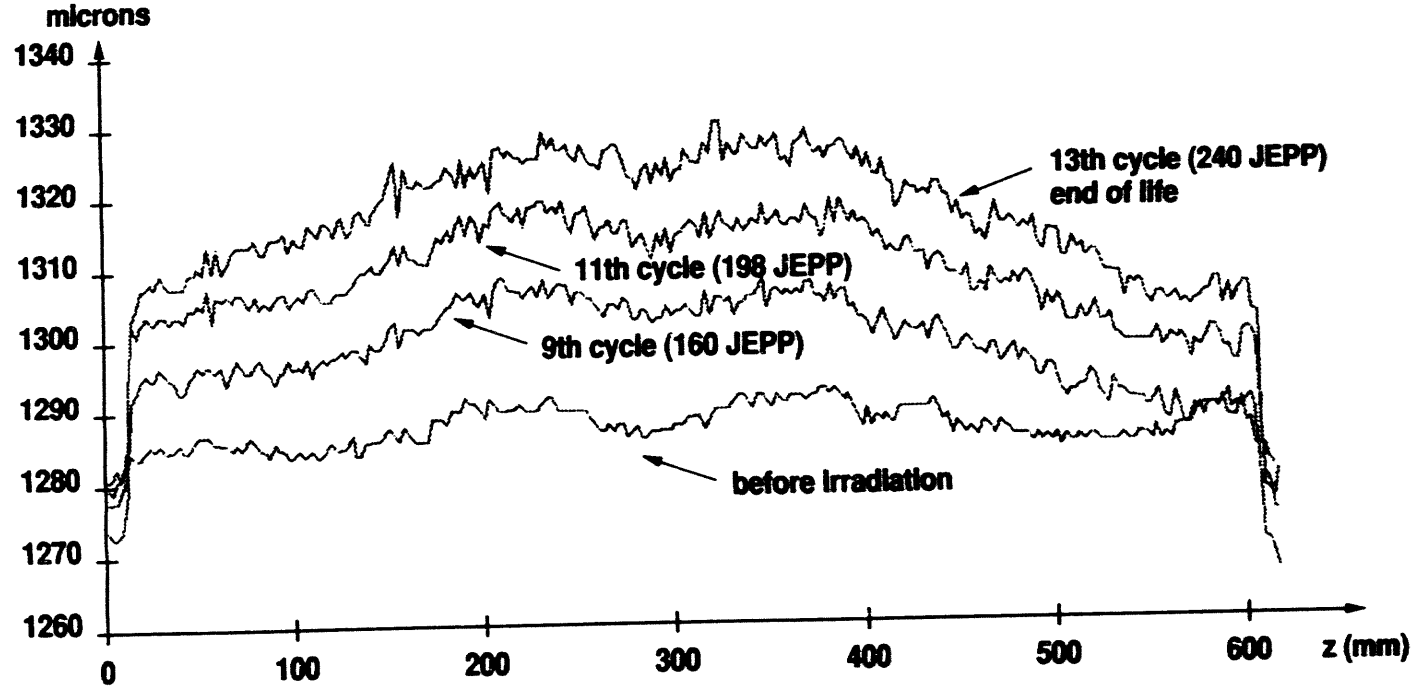

Slide 5

CEA

CERCA

COMPARISON OF OSIRIS STANDARD AND THICK CORE PLATE TYPES

CHARACTERISTICS	STANDARD		THICK CORE		DESIGN VARIATIONS (%)
	DESIGN	MEASUREMENTS RESULT	DESIGN	MEASUREMENTS RESULT	
CLADDING THICKNESS (mm)					
Average	0.38		0.34		-10
Mini current part	0.25		0.20		-20
Mini Dog. Bone	0.25		0.20		-20
MEAT THICKNESS (mm)	0.51		0.59		+15
PLATE THICKNESS (mm)	1.27		1.27		-
FUEL	U_3Si_2		U_3Si_2		-
URANIUM DENSITY (g/cm^3)	4.8		4.8		-

Slide 6

CEA CERCA

COMPARISON OF OSIRIS STANDARD AND THICK CORE PLATE TYPES

CHARACTERISTICS	STANDARD		THICK CORE		DESIGN VARIATIONS (%)
	DESIGN	MEASUREMENTS RESULT	DESIGN	MEASUREMENTS RESULT	
CLADDING THICKNESS (mm)					
Average	0.38	0.38	0.34	0.34 - 0.35	-10
Mini current part	0.25	0.29	0.20	0.24	-20
Mini Dog. Bone	0.25	0.27	0.20	0.23	-20
MEAT THICKNESS (mm)	0.51	0.51	0.59	0.58 - 0.59	+15
PLATE THICKNESS (mm)	1.27	1.27	1.27	1.25 - 1.27	-
FUEL	U_3Si_2		U_3Si_2		-
URANIUM DENSITY (g/cm^3)	4.8		4.8		-

CEA

CERCA

MICROGRAPHIC INSPECTION

OSIRIS STANDARD PLATE (0.51 mm meat)

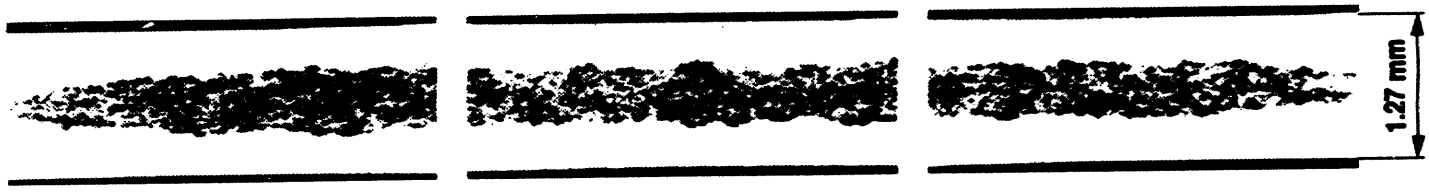

OSIRIS THICK CORE PLATE (0.59 mm meat)

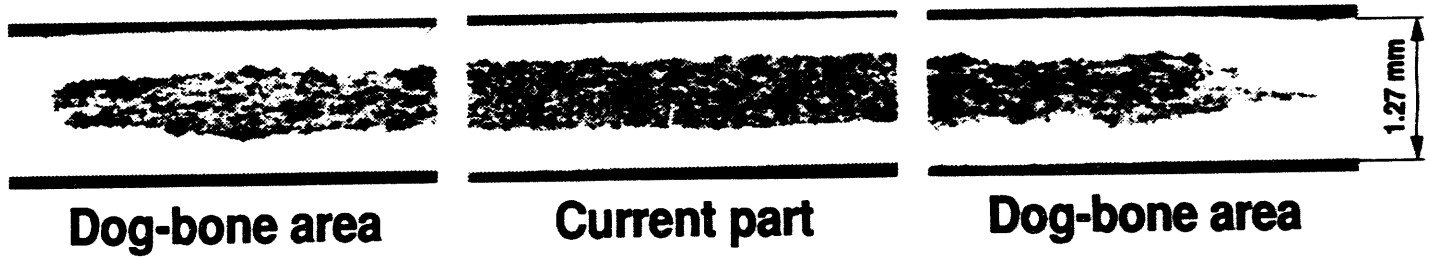

CEA

CERCA

U DISTRIBUTION HOMOGENEITY ALONG OSIRIS STANDARD AND THICK CORE PLATES

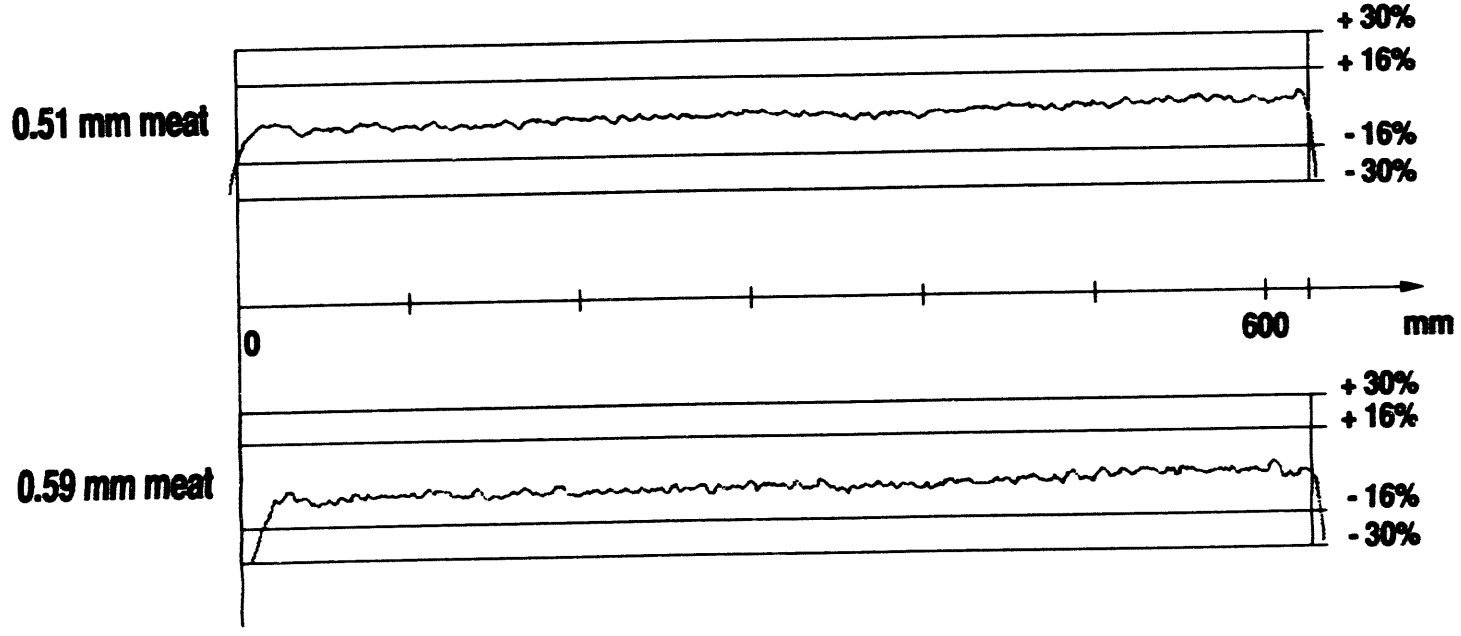

Slide 9

CEA

CERCA

SCHEDULE

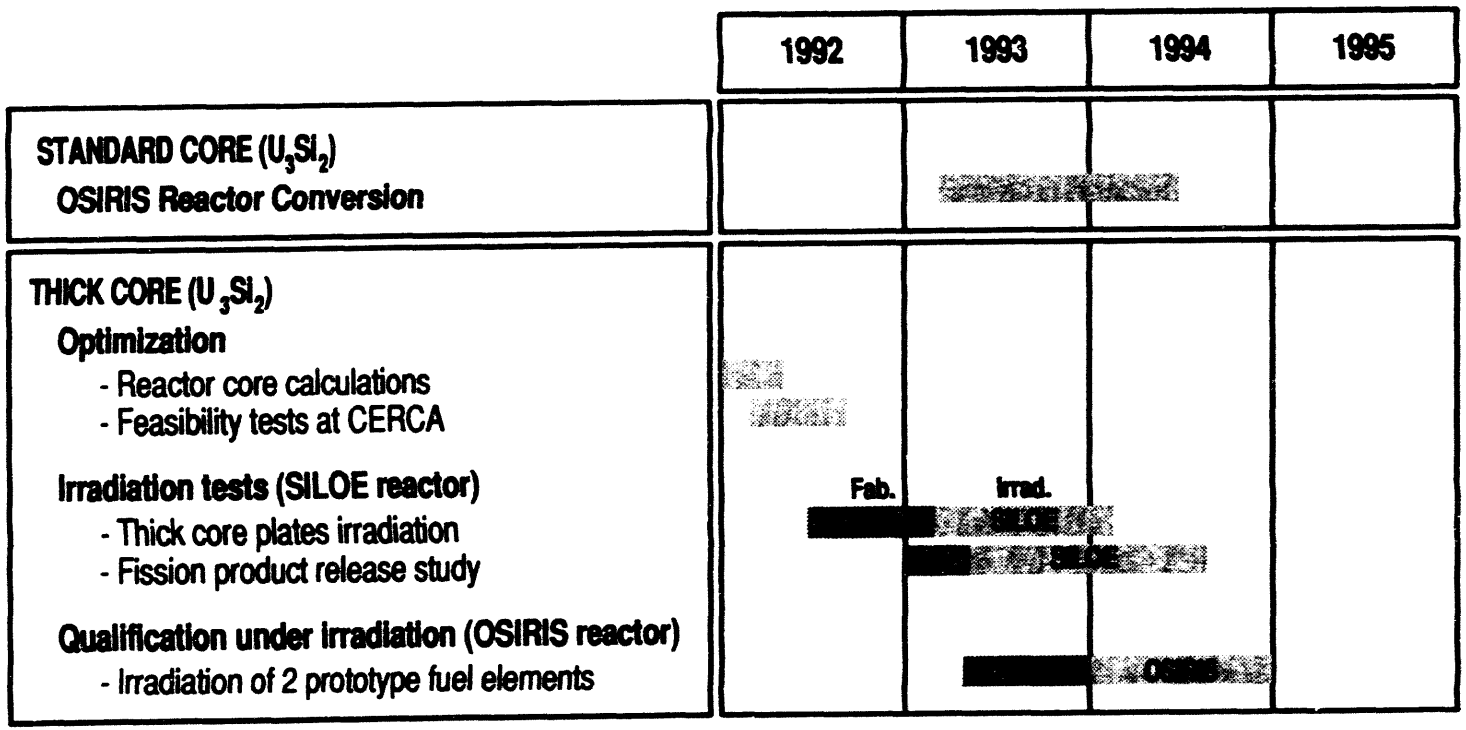

Slide 10

DEVELOPMENT OF HIGHER DENSITY FUEL AT CERCA
Status as of Nov.92

JP. DURAND - Y. FANJAS - A. TISSIER
CERCA
Les Bérauds - BP 1114
26104 Romans-Sur Isère, France

ABSTRACT

CERCA has initiated a fundamental research program for better understanding the behaviour of materials during the fuel plate manufacturing process. Thanks to a major breakthrough and a careful and systematic experimental validation of fabrication parameters, CERCA succeeded to set up an advanced production process adapted to high densities up to 6 g U_T/cm^3. The fabrication test was carried out on full size plates with pure U_3Si_2 in industrial conditions (on 50 plates). Next development steps include checking the stability of obtained results on large scale production and evaluating the cost increase due to the use of advanced process. Furthermore irradiation tests are necessary to qualify the 6 g density in reactor.

---

1. INTRODUCTION

During the last RERTR meeting, several customers have expressed their wish for a Uranium density increase above the presently qualified limit of 4,8 g U_T/cm^3 LEU fuel.

Aiming at further improving the quality of its products, CERCA had initiated a fundamental research program for a better understanding of the materials behaviour during the fuel plate manufacturing process.

Taking into account its customer's request, CERCA reoriented this program to reach, in a first step, a significantly higher uranium density.

As shown in the common presentation [1] of CERCA - CEA, there are four ways to increase the uranium loading per fuel element :

- Using a denser fuel
- increasing the volumic fraction of Uranium in the meat
- changing the external geometry of fuel plates (plate thickness, number of plates...)
- reducing the cladding thickness leading to a thicker meat.

The first and fourth ways have already been explored by Cerca and results previously presented [1-2]. The third way implies thermalhydraulic modifications that must be avoided as far as possible.

The purpose of this paper is to present the work done on the second way. This corresponds to an increase in the volumic fraction of the uranium phase in the meat to reach at least 6 g U_T/cm^3 with the U_3Si_2 fuel.

In its first part, this paper presents a comparison between 4,8 g U_T/cm^3 and 6 g U_T/cm^3 fuel meat characteristics and problems which could occur in the 6 g U_T/cm^3 plates production.

In the second part, this paper describes the main results that CERCA obtained on 6 g U_T/cm^3 plates after having optimized the production parameters, thanks to a fundamental research on the manufacturing process.

As a conclusion, the opportunities that this research program opens for future work will be presented.

2. COMPARISON BETWEEN 4,8 g U_T/cm^3 and 6 g U_T/cm^3

2.1. Fuel meat characteristics

	4,8 g U_T/cm^3	6 g U_T/cm^3
FUEL	U_3Si_2	U_3Si_2
Increase in U loading	0	+ 25 %
Volumic fraction of U_3Si_2 in the meat	43,5 %	54,4 %

To reach 6 g U_T/cm^3 implies a 25 % increase in uranium loading, keeping the plate geometry unchanged.

The volumic ratio of the fuel phase increases by about 10 % only, leading to a corresponding decrease in aluminium.

2.2. Technical problems of production

Increasing the fuel density above 4,8 g U_T/cm^3 with the usual standard manufacturing process leads to the occurence of the following specific defects :

- inhomogeneity of uranium distribution
- a too important dog bone effect that leads to a very thin cladding
- higher number of stray particles out of the meat area.

To illustrate those defects, Figure 1 shows micrographs of 4,8 g U_T/cm^3 and 6 g U_T/cm^3 fuel plate manufactured with the same standard production process.

The dog bone effect on the 6 g U_T/cm^3 is important and meat thickness is not regular at all.

The standard manufacturing conditions are definitely not appropriate to 6 g U_T/cm^3 plates.

Therefore CERCA focused its development effort on the optimization of its production process and fabrication parameters.

3. RESULTS OF THE OPTIMIZATION OF PRODUCTION PARAMETERS TO REACH HIGH DENSITY 6 g U_T/cm^3

Thanks to a major breakthrough in understanding the manufacturing process and with a careful and systematic experimental validation of the fabrication parameters, an advanced production process adapted to high densities was successfully set up.

The following results were achieved on 6 g U_T/cm^3 density plates. They were obtained on 50 full size plates in industrial conditions.

As a comparison basis we will present simultaneously the results obtained with the standard process on 4,8 g U_T/cm^3 and the results obtained on 6 g U_T/cm^3 plate with the advanced production process.

3.1. Micrographic results

Figure 2 shows micrographs of 4,8 U_T/cm^3 plates in current part and dog bone areas. The dog bone effect of the 6 g U_T/cm^3 plate is maintained at a lower level than the 4,8 g plate. Meat thickness of the 6 g plate is remarkably regular all along its length as compared to the 4,8 g U_T/cm^3 plate.

3.2. Bonding quality

As can be seen on micrographs (Figure 3), the bond between cladding and meat is sound. Blister test and UT inspection results confirm this observation.

Within the meat, despite the lower aluminium volumic fraction, fuel particles are still well dispersed in the matrix which allows keeping a good cohesion between aluminium matrix and particles.

3.3. Radiographic inspection

Radiographic films were taken for all the 6 g fuel plates. The results show :

- a good homogeneity of the meat
- a good geometry of the meat
- no increase in the number of remote islands out of the meat with respect to the reference plates.

3.4. Homogeneity of uranium distribution

Figure 4 shows X-ray scanning measurements on 4,8 and 6 g U_T/cm^3 fuel plates.

The X-ray scanning machine measures quantitatively the homogeneity of uranium distribution. A focused beam of X-ray goes through the thickness of the plate. By measuring the absorption of the beam across the plate, the uranium density variations are determined.

For the 4,8 U_T/cm^3 plates obtained with the standard process the homogeneity diagram stands within the allowed limits all along the plates length. That means that 4,8 g U_T/cm^3 plate is conform to commonly used specification for this kind of uranium loading.

On the 6 g U_T/cm^3 plates obtained with the optimized process we can see an even more regular and homogeneous distribution of uranium with a minimum level of variation. All along the plate length the X-ray diagram stands very easily between the allowed limits.

3.5. Conclusions on results about 6 g U_T/cm^3 plate

The previous results show that very sound fuel plate loaded to 6 g U_T/cm^3 can be produced with the optimized process.

Using this density, we decided to further increase the uranium content per plate.

4. FURTHER INCREASE IN THE URANIUM LOADING

We carried out an additional test on a few plates combining the following two ways :

- density higher than 4,8 g U_T/cm^3
- a reduced cladding thickness that implies a thick meat of 0,59 mm instead of 0,51 mm.[1]

U loading of 6 g U_T/cm^3 plate with thick meat of 0,59 mm equals, on the point of view of U loading, to a plate of 6,94 g U_T/cm^3 with standard meat thickness 0,51 mm.

Micrographs of Figure 5 show a 4,8 g plate with standard meat thickness of 0,51 mm produced with the usual standard process and a 6 g plate with thick meat of 0,59 mm produced with the optimized process. As expected, we obtain an average cladding thickness which is reduced but it can be noticed that the dog bone effect remains very low and acceptable.

5.FUTURE WORKS

If the results presented today receive a positive answer from research reactors, the next development steps should include checking the stability of obtained results on large scale production and evaluating the cost increase due to the use of this advanced process.

Irradiation tests on 6 g U_T/cm^3 fuel plate will be necessary to qualify this density in reactor.

From our past experience, this work including the post irradiation examination should take around 3 to 4 years from now on, depending on the irradiation programm.

6.CONCLUSION

We have been able to optimize production parameters in order to reach 6 g U_T/cm^3 with pure U_3Si_2.

6 g U_T/cm^3 fuel plate test production with standard meat thickness (0,51 mm) was carried out in industrial conditions on 50 plates. A few 6 g U_T/cm^3 plates with thick meat (0,59 mm) were also successfully manufactured. Those tests were sufficient to demonstrate the feasibility of good plates loaded to 6 g U_T/cm^3.

The advanced process is more sophisticated and requires a careful control of production parameters and much more on line measurements.

We are ready to go on with a large scale production test as long as this appears to be of interest to our customers.

REFERENCES

1. "OPTIMIZATION OF SILICIDE FUEL ELEMENTS "
   A. BALLAGNY - JP. BEYLOT - J. PAILLERE - (CEA)
   JP. DURAND - Y. FANJAS - A. TISSIER - (CERCA)
   Proceedings of the RERTR meeting in ROSKILDE - 1992

2. "LEU FUELS AT CERCA"
   Status as of Nov. 91
   Y. FANJAS
   Proceedings of the RERTR meeting in JAKARTA-INDONESIA - 1991

CERCA

FIGURE 1

RESULTS OBTAINED WITH STANDARD PROCESS

4,8 g U_T / cm^3 STANDARD PROCESS

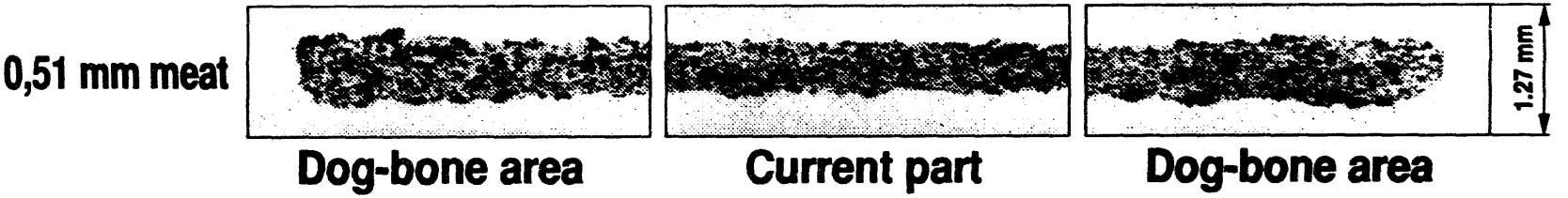

6 g U_T / cm^3 STANDARD PROCESS

CERCA

FIGURE 2

COMPARISON BETWEEN STANDARD AND ADVANCED PROCESSES

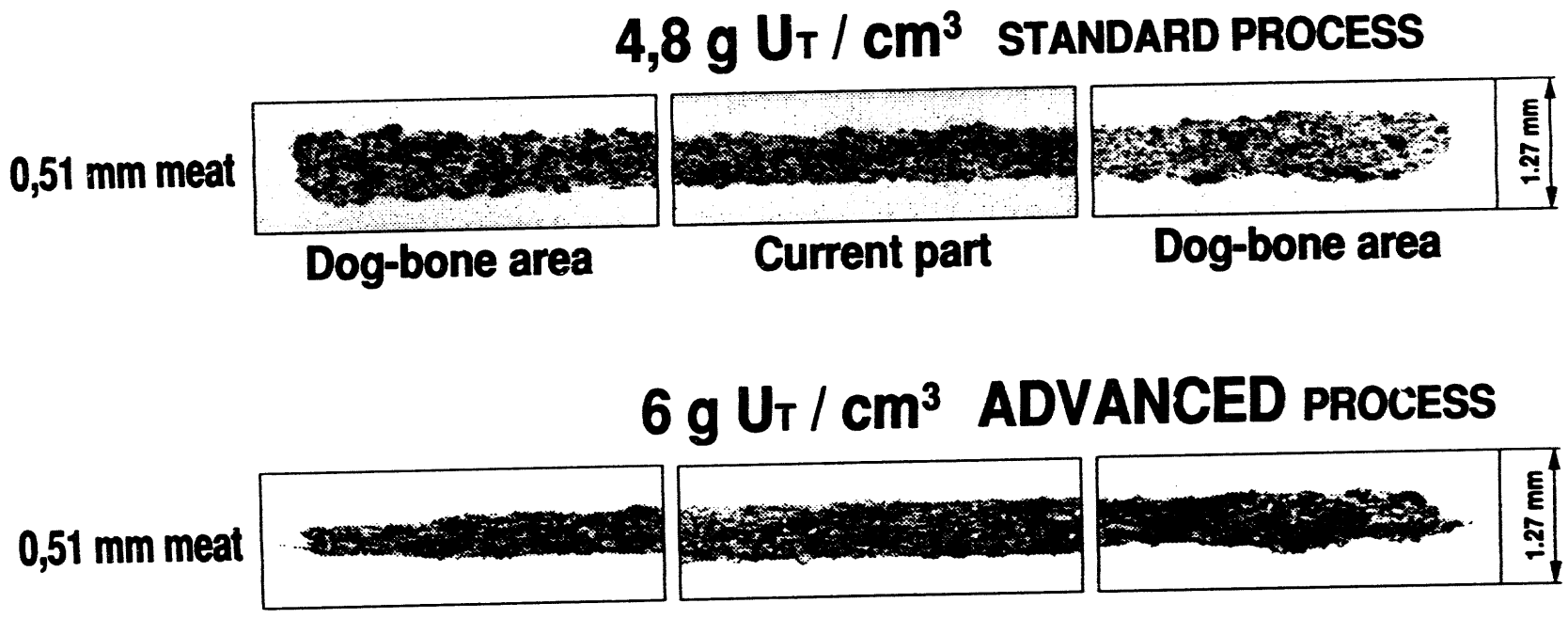

CERCA

FIGURE 3

BONDING QUALITY

100 µm

4,8 g U_T / cm^3 STANDARD PROCESS

Within the meat

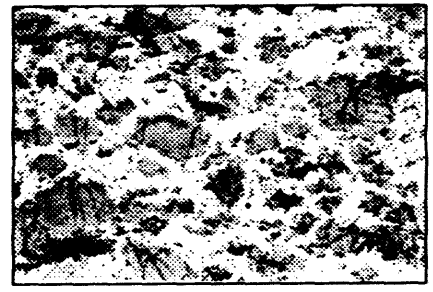

Between meat and cladding

6 g U_T / cm^3 ADVANCED PROCESS

Within the meat

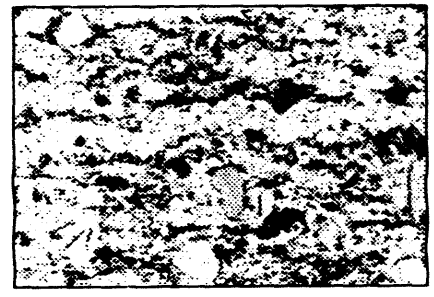

Between meat and cladding

CERCA

FIGURE 4

X RAY HOMOGENEITY

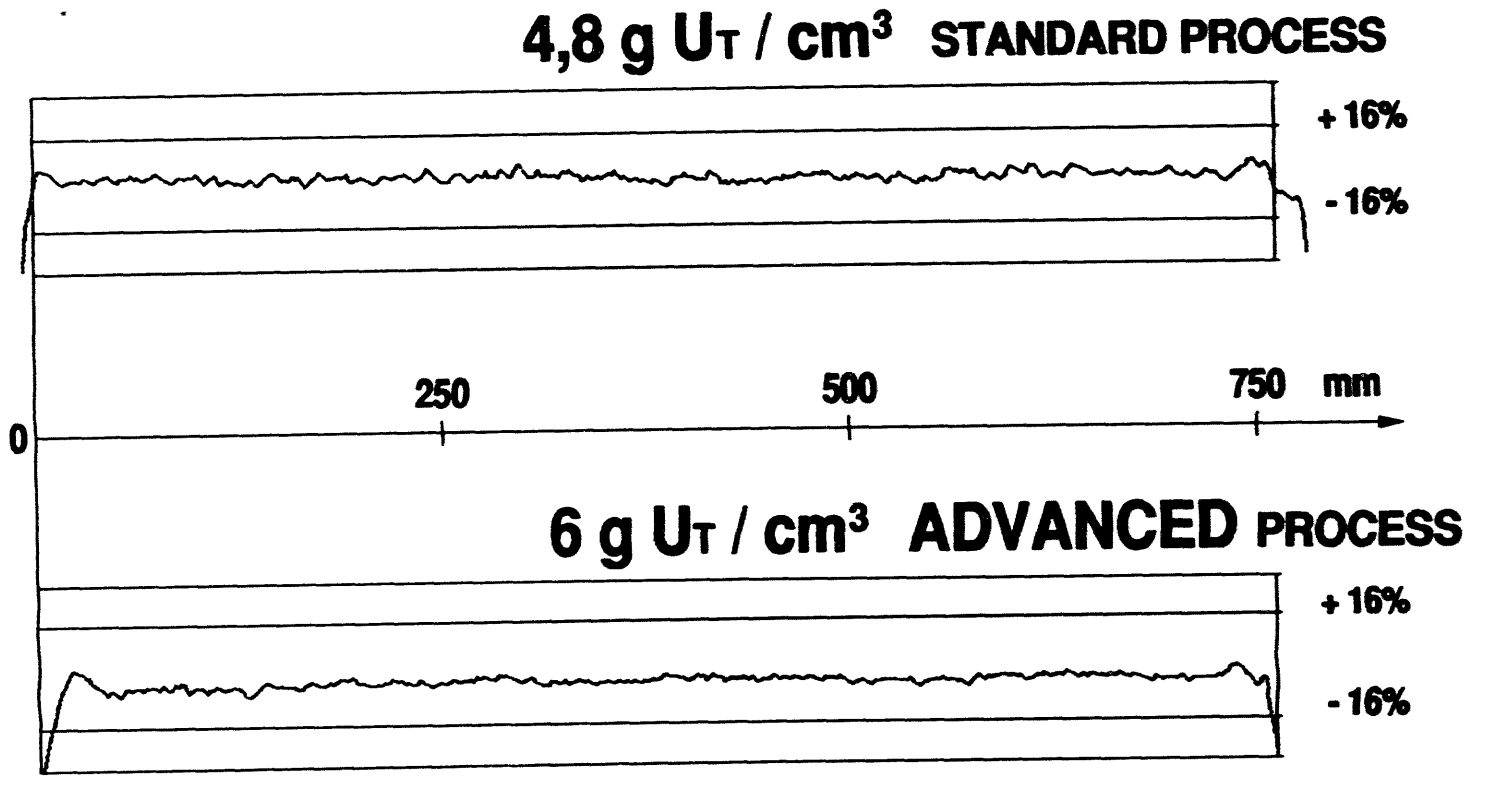

CERCA

FIGURE 5

COMBINATION OF INCREASED DENSITY AND INCREASED MEAT THICKNESS

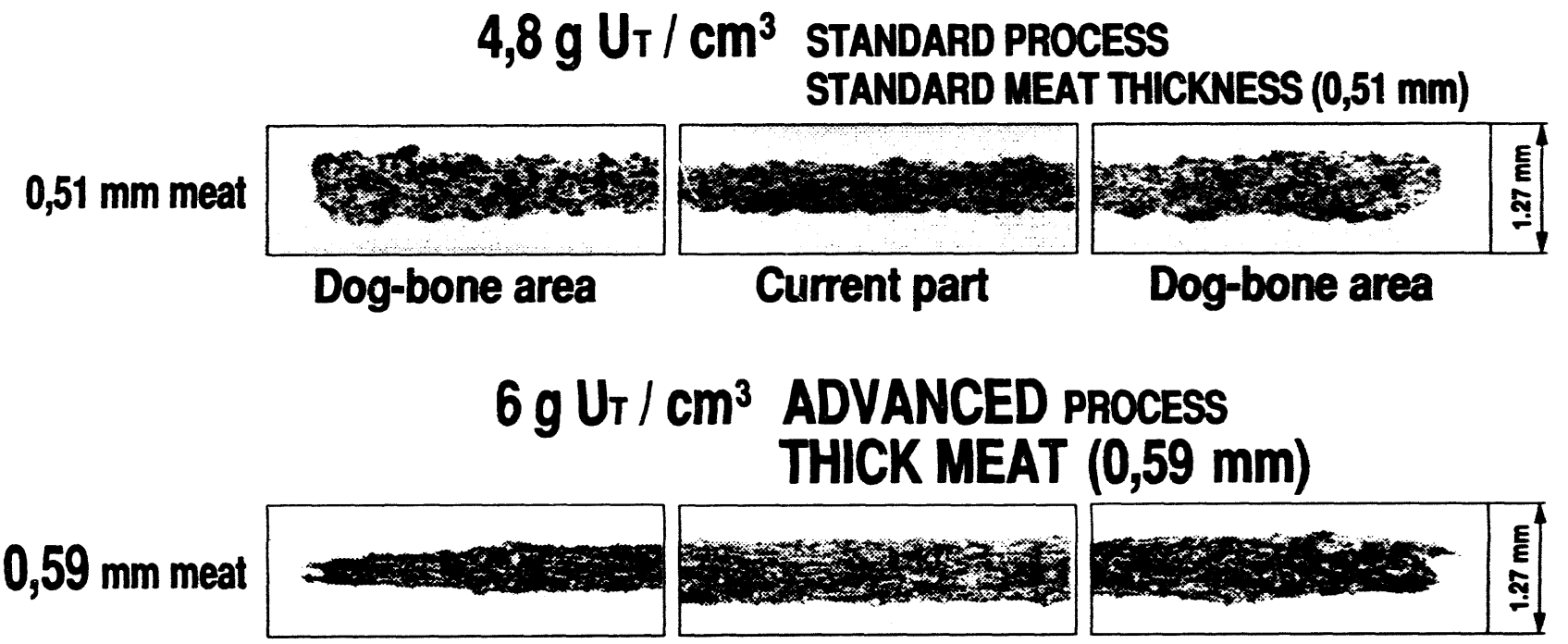

CERCA IS CHANGING ITS SHAREHOLDING

JP. Durand
CERCA

The shareholding of CERCA, previously 50% Framatome and 50% Pechiney is becoming 51% Framatome and 49% Cogema. This new distribution of the shares offers Framatome the position of major shareholder. This evolution strengthens the position of CERCA in the French nuclear industry while maintaining its specificity as a manufacturer of nuclear fuel assemblies and special equipments for research reactors, as well as a designer and manufacturer of complex mechanisms for use in large equipments for physics of particles and fundamental research.

Three main advantages should be underlined in this change:

1. Continuity in the company as regards persons, plants, commercial network and R & D programs. CERCA is keeping its organization and its operational fabrication and sales structure. In particular, the R & D programs are carried on to serve customers. Moreover, CERCA maintains its commercial network in order to continue to offer customers competent, flexible, and quick service.

2. Synergy and logistical support which CERCA will receive from its shareholders. Framatome is equipped with specialized means in the following fields:
   - engineering and calculation departments
   - specialized studies: Such as resistance of materials, modelization, safety studies, support in metallurgy and in assembling techniques.

Framatome Engineering services are most adequate to study, on behalf of CERCA's customers, design modification, or new projects interesting research reactor operators.

Cogema supports Cerca in certain services related to the fissile material: As an example, CERCA signed with Cogema an agreement which allows Cerca, in addition to its own means of scraps recycling, to subcontract special uranium recycling operations to Cogema's chemical facilities. Moreover, Cogema can, on demand, ensure supply of fissile material.

3. At last especially the service to customers in a spirit of independence and technical progress. It has to be underlined that Cerca, a humanly dimensioned company specialized in the field of research reactors ensures its customers the independent services they may wish, adapted to their specific needs. In the frame of international rules, Cerca guarantees confidentiality and safety to its customers.

QUALITY ASSURANCE AND ULTRASONIC INSPECTION STUDIES IN LEU FUEL PRODUCTION

P. Toft, J. Borring, E. Adolph, T.M. Nilsson
Risø National Laboratory, Denmark

ABSTRACT

In connection with the efforts to market Low Enriched Uranium Fuel Elements internationally, a Quality Assurance System for the production at Risø National Laboratory, Materials Department is described. The department has established a Quality Assurance program to comply with the applicable clauses and elements of the ISO 9002 standard. As a special feature, the development of Ultrasonic Scanning Techniques for detection of blisters and measuring layer thicknesses are described.

INTRODUCTION

Fabrication of fuel elements for test reactors was started at Risø National Laboratory in 1965. In 1988, the production of LEU fuel elements based on U_3Si_2, began in the Materials Department. At present, 200 LEU fuel elements have been produced, of which about 100 have now completed irradiation in the Danish test reactor, DR3, all of them successfully.

The LEU fuel elements which are produced at Risø are made in accordance with the recommendations given in the IAEA guidebook TECDOC-467: "Standardization of Specifications and Inspection Procedures for LEU Plate Type Research Reactor Fuels." Our Quality Control and Quality Assurance procedures comprise a well functioning system, which in all major parts complies with the requirements in the ISO 9002 Standard.

This paper provides a brief presentation of our QA system and an Ultrasonic Scanning Technique for detection of blisters and measuring of layer thicknesses in fuel plates.

QUALITY SYSTEM

The system consists of a QA handbook which refers to a number of quality inspection manuals.

The handbook contains a description of overall policy, management, organization, and a brief presentation of the quality inspection manuals.

The inspection manuals contain a detailed description of the various activities which are used in order to ensure production of fuel elements according to specifications and of high and uniform quality. The figure below shows an overview of the system.

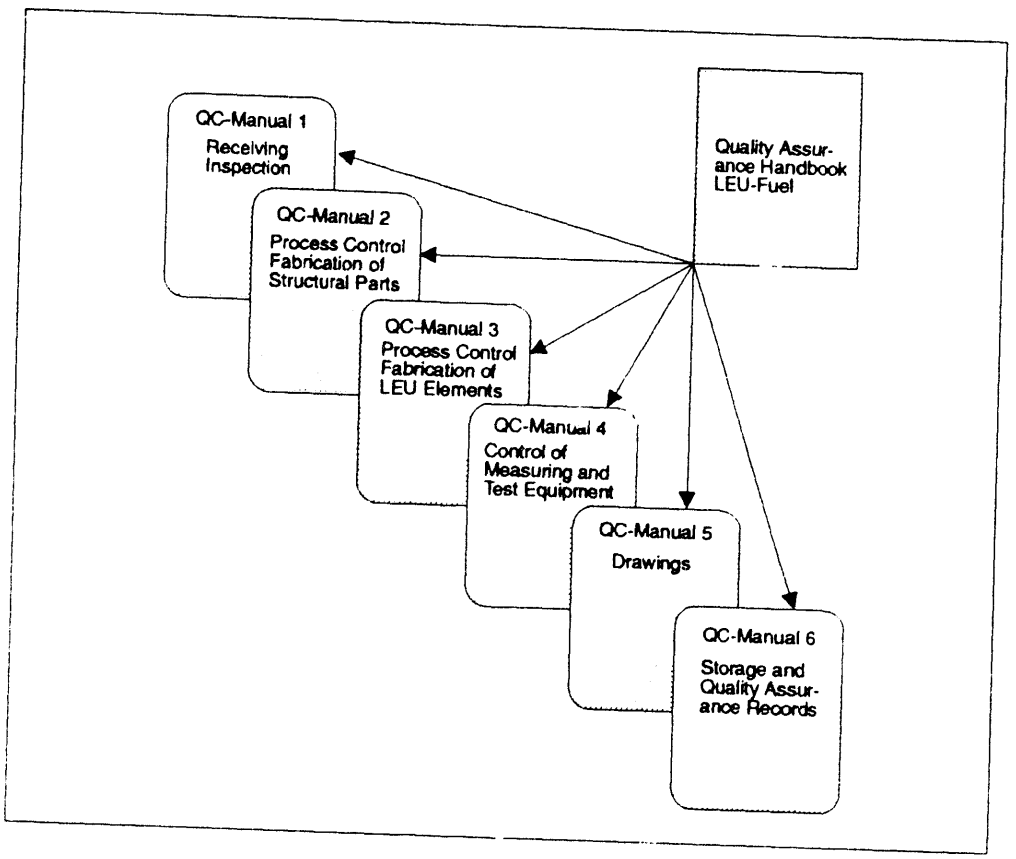

Figure 1: Quality System

QUALITY POLICY

The quality policy of the Materials Department has been to establish and thereafter maintain a quality assurance system which ensures that all the relevant activities of the department are carried out according to prearranged procedures and specifications. This is achieved with the optimal use of QA activities, using both preventative and surveillance QA methods.

ORGANIZATION

A documented organizational structure, which defines functional responsibilities and levels of authority, has been established. The flow chart given below shows how the QA function refers directly to the department management.

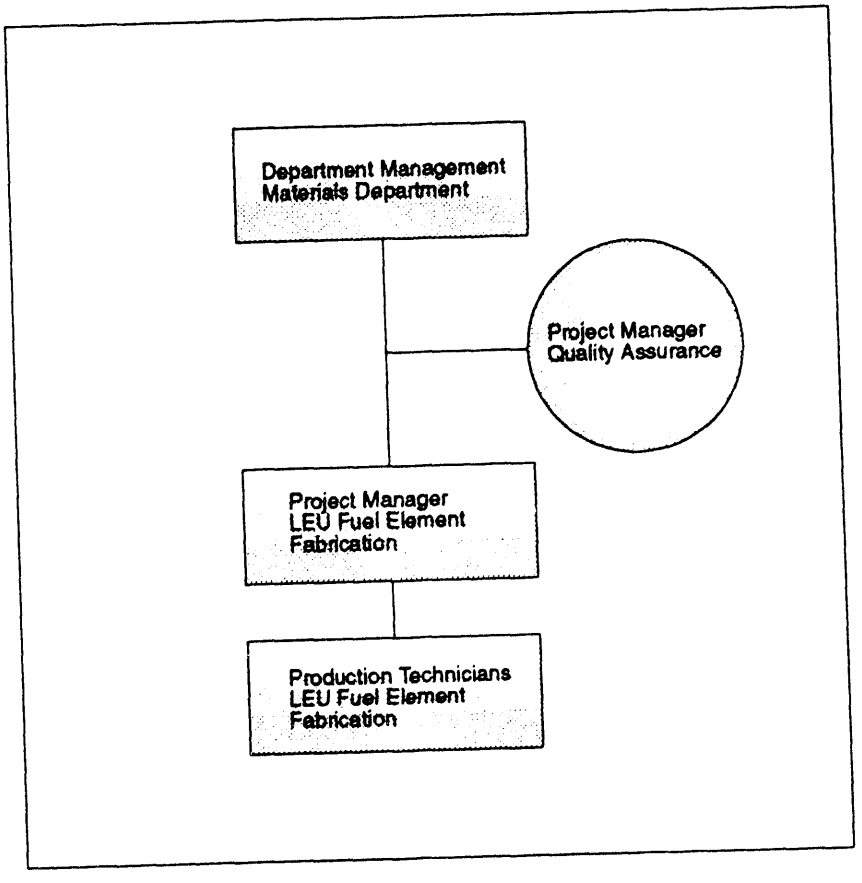

Figure 2: Organization

MANUFACTURING QUALITY CONTROL

Quality Assurance begins, of course, with the production process itself and the people who are directly involved. Our production technicians are apprenticed craftsmen and have many years of experience in the development and fabrication of fuel plates and elements.

To assure that the manufacturing process runs optimally and according to the requirements, a detailed description of all production steps, cleaning procedures, and heat treatments, etc. is followed by the technicians.

This "Process Specification" is not a direct part of the QA system, but is strongly connected to it by the use of special QA cards. These QA-cards are designed to be used both as a check list for vital process variables and as cards where actual results achieved during the process are documented by the technicians ore inspectors.

The flow chart shown below illustrates the complete set of QA-cards used during the fabrication of LEU fuel elements.

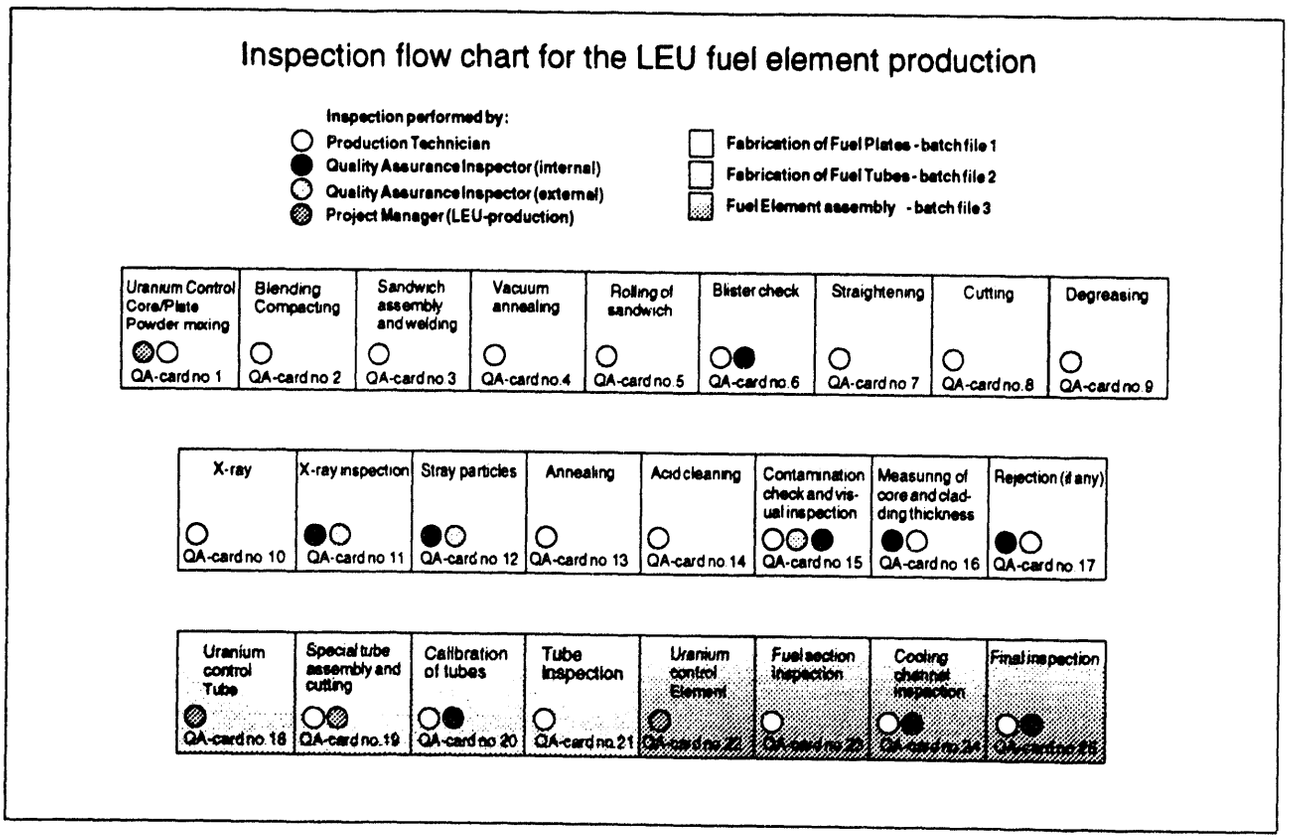

Figure 3: Inspection flow chart for the LEU fuel element fabrication process

From the key in the upper left corner of the chart it can be seen that we use different levels of inspection. Some points are checked only by the technicians, others by an internal inspector and some may also be checked by an external inspector (buyer).

For practical reasons, we have divided the fuel element fabrication into three main parts:

1. Fuel Plate fabrication (QA-cards nos. 1-17)
2. Fuel Tube fabrication (QA-cards nos. 18-21)
3. Fuel Element assembly (QA-cards nos. 22-25)

Criticality avoidance demands that we only handle a certain number of each of these parts in a batch. Such a batch is given its own identification code and followed by a batch file containing the actual QA-cards and Safeguard Identification cards.

An example of a QA-card is shown in figure 4. In this particular card, the location of possible blisters are documented, both by a technician and by a QA-inspector after a blister test is performed.

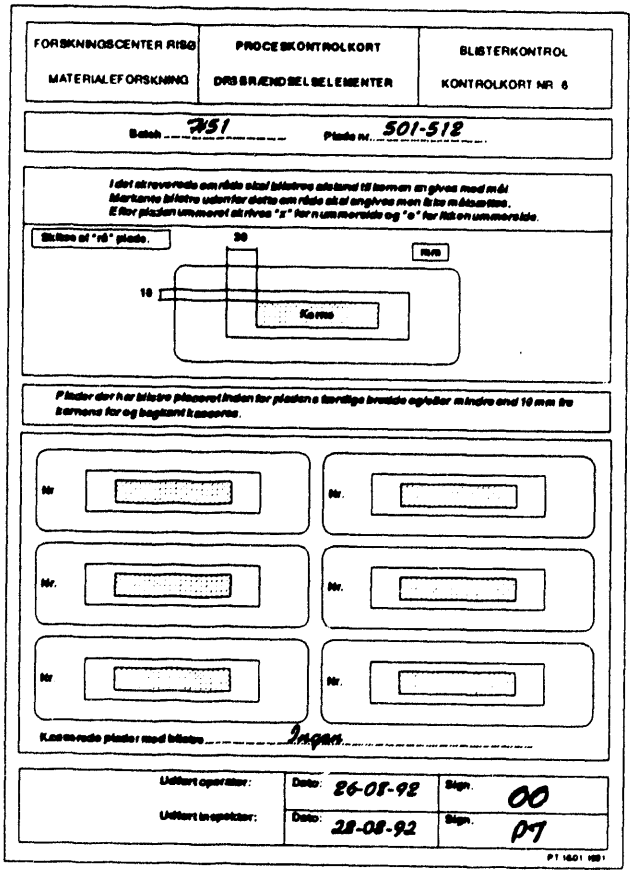

Figure 4: QA Card - Blister Inspection.

Rejected Fuel Plates are documented in a special QA-card at the time they are rejected. To ensure full traceability, all parts and batches are uniquely marked and documented in the QA-cards or directly in the form of printouts, x-ray film, etc. All relevant data on annealing and thermal treatments during the fabrication are documented as printed graphs. After passing the final inspection, the elements in a batch are provided with a certificate. This certificate consists partly of a number of QA-cards from the fuel fabrication. Each certificate therefore documents all important factors, with a detailed description of each fuel element and fuel tube together with uranium content and the results of final inspection and metallographical examinations.

Procedures are established for additional examinations, if such are necessary, of fuel plates, fuel tubes, or fuel elements. Typical examinations would be of microstructural characteristics obtained by using Scanning Electron Microscopy, Transmission Electron Microscopy, or Optical Microscopy. The results of these examinations are documented in spacial QA-cards.

AUDITS

A system of documented internal audits has been established to ensure that the implemented QA system is, at all times, in compliance with the Materials Department's quality policy.

All audits are performed in accordance with check lists, and cover all activities affecting quality.

The results of these audits are documented in the form of an audit report. This report is distributed to the departments and the project management.

Follow-up actions (if any) are taken immediately after issuing the audit report.

IMPROVING TEST METHODS

As an integral part of the Materials Department, the fuel fabrication group has the possibility to utilize the departments advanced characterization and testing equipment as well as its wide experience for special examinations or for trying out new test methods.

An example of the latter is an ongoing feasibility study in order to investigate the possibility of using ultrasonic measurements of fuel plates for the location of non-bonded area and the determination of cladding thickness.

At present, the bonding between layers is verified visually in a "blister test" and the determination of core and cladding thickness is made destructively, i.e., specimens are punched from fuel plates and examined metallographically.

In an effort to improve the detection of non-bonded area and to measure core and cladding thicknesses non-destructively, a program of ultrasonic scanning measurements has been initiated with the aim of establishing an inspection technique which could be used in the future as a standard check of the fuel plates.

Figure 5 shows our precision ultrasonic scanning equipment in use for the scanning of a fuel plate in water. Advanced software enables on-line graphical display of scanned plates.

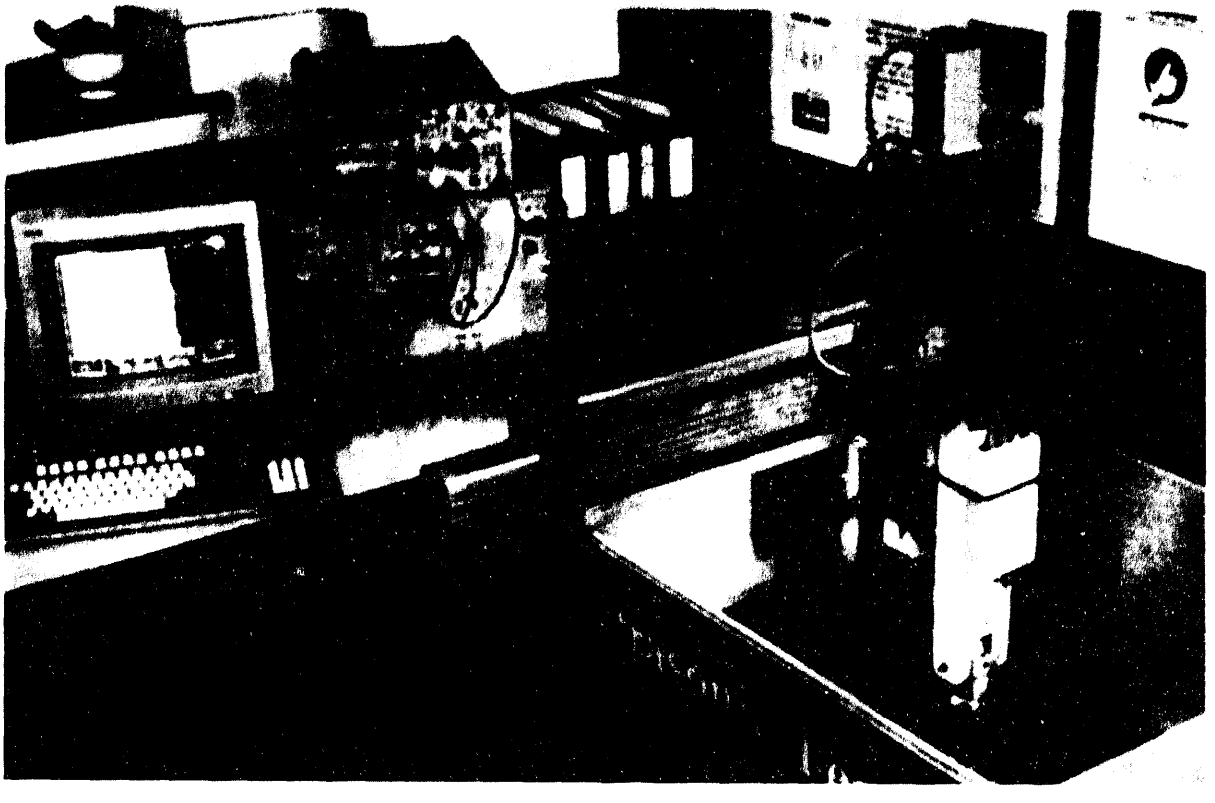

Figure 5.: Precision Ultrasonic Scanning Equipment

Figure 6 shows schematically the ultrasonic echo patterns from a fuel plate. The figure indicates an echo pattern at three different locations on the fuel plate. A: Outside the core, and B: Outside the core with a blister in the first cladding layer, and C: Over the core. The signal waveform shows echoes from the core or blisters. It is possible to obtain a scanning resolution of only 10 μm between the measuring points in both directions.

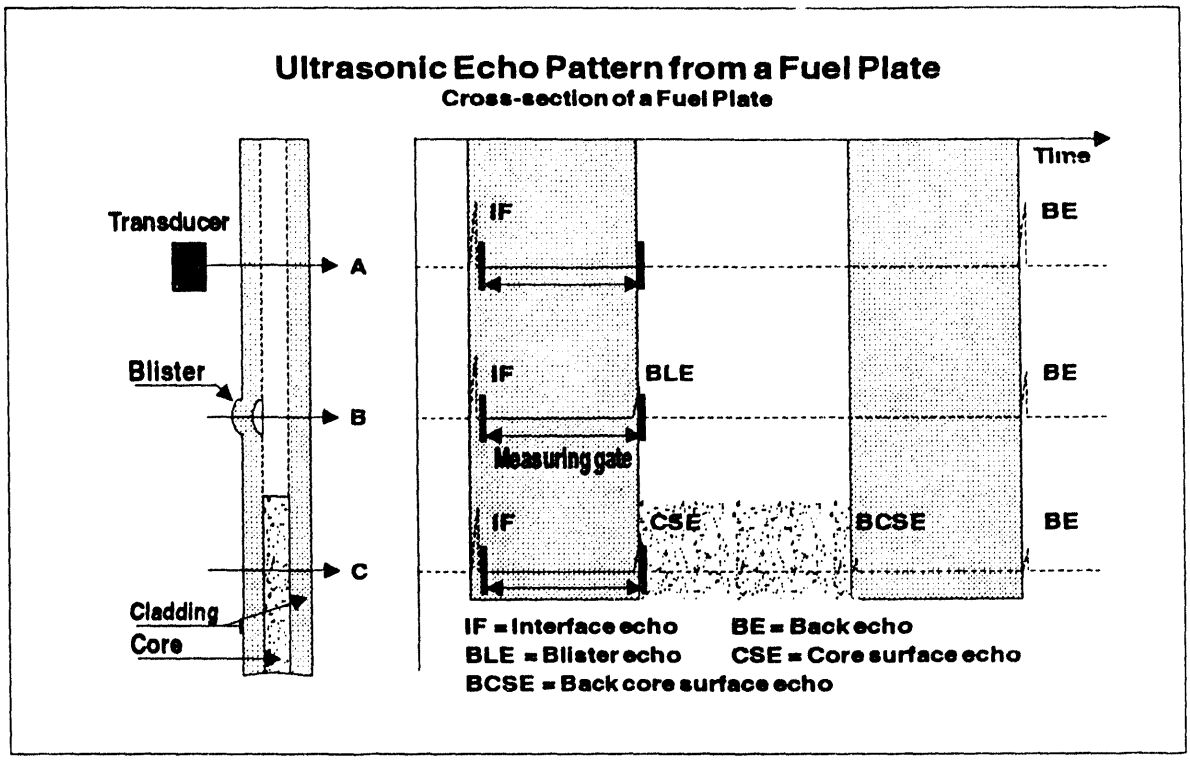

Figure 6: Left: Cross section of a fuel plate. Right: Ultrasonic echo pattern from the plate.

Figure 7 shows, in color, the echo height from a test fuel plate with a blister outside the core. Only echoes from within a depth (see figure 6) ranging from just below the fuel plate surface to approximately 1/3 of the fuel ,plate thicknesses are recorded. The different colors indicates differences in echo heights. For non-bonded area (blisters) the echoes are high. The color scale is logarithmic (-dB). Therefore, high echoes are to the left (yellow) and small echoes to the right (green).

The time of flight between the echo reflected from the interface (IF) and the echo from the "defect" can easily be converted into a distance, knowing the sound velocity in aluminum.

The system can, in one scanning measurement, store the echo heights together with the time of flight measurements.

In figure 8, the distance plot recording obtained during the scanning is shown. Here, the colors indicate differences in depth to the "defects" generating the echoes.

It can be seen that the blister is located at the same level (green) as the core - i.e. between the frame and the upper coverplate. For the core itself, a small amount of "dogboning" can be observed.

CONCLUSION

At present, the Materials Department has produced nearly 1000 fuel elements, of which 200 are of the LEU type. These fuel elements have been produced by using a comprehensive Quality Assurance system that has been developed during the last 25 years of fuel fabrication.

As reported at the last RERTR-meeting in Jakarta, Risø is now marketing LEU-fuel elements internationally.

In this connection, we found that it was important to have our complete Quality Assurance System evaluated by auditors in Quality Management from the Danish Technological Institute. These experts concluded in a report that all the important requirements in the ISA 9002 standard were fulfilled and we are now, after some minor system modifications, ready to apply for an approval.

The Ultrasonic Scanning Technique has not yet been implemented as a standard procedure, but the Materials Department is however equipped to offer the measuring technique to comply with customers' demands, if so specified.

ACKNOWLEDGEMENT

The authors wish to thank Hans Erik Gundtoft, Kaj Kvisgaard Borum, and Ole Kjær Jepsen for their invaluable contribution to the ultrasonic scanning measurements and evaluations.

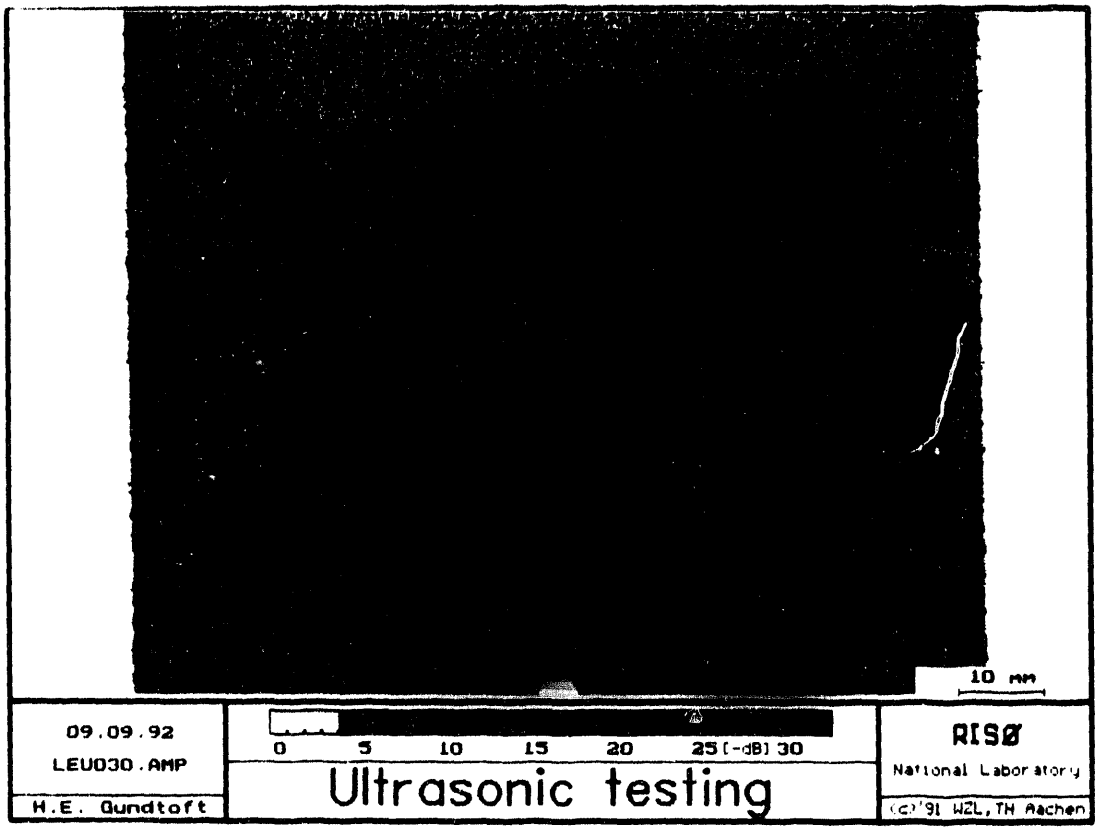

Figure 7: Echo plot of fuel plate end with core (blue/purple) and a blister (brown/yellow).

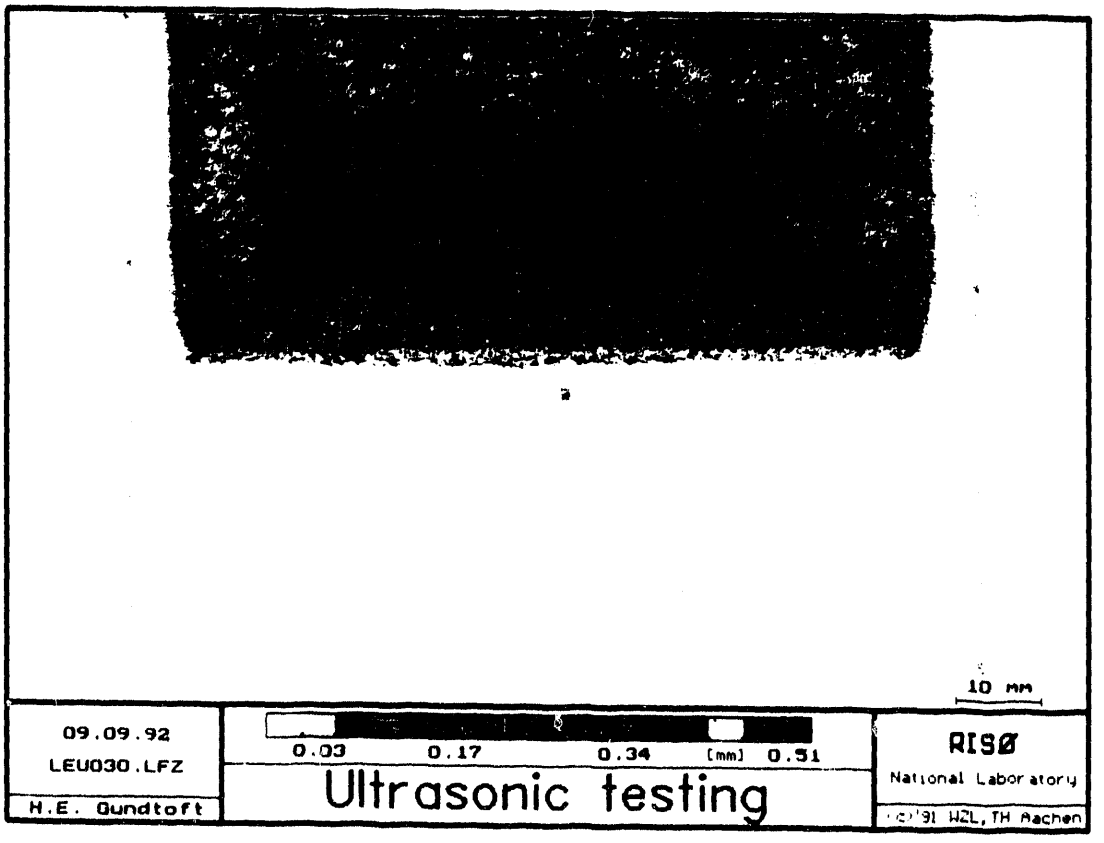

Figure 8: Distance plot of figure 7.

Figure 9 shows another distance plot from a fuel plate end, but now the main scanning direction was longitudinal (right angled to the direction shown in figure 7 and 8) and the resolution was approx. 10 times higher than in figure 8.

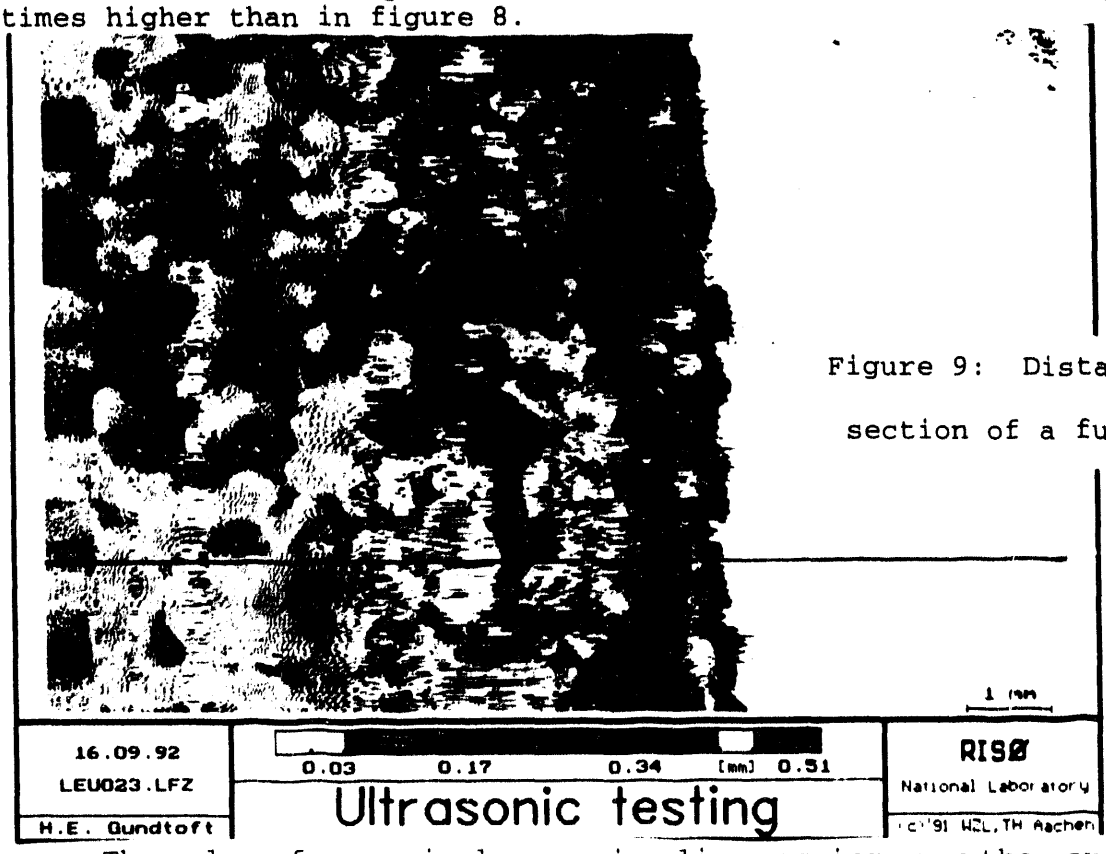

Figure 9: Distance plot of a section of a fuel plate end.

The values from a single scanning line passing over the core end are shown in figure 10. The figure gives an indication of the fuel core surface, and thus the cladding thickness, along the specific scanning line.

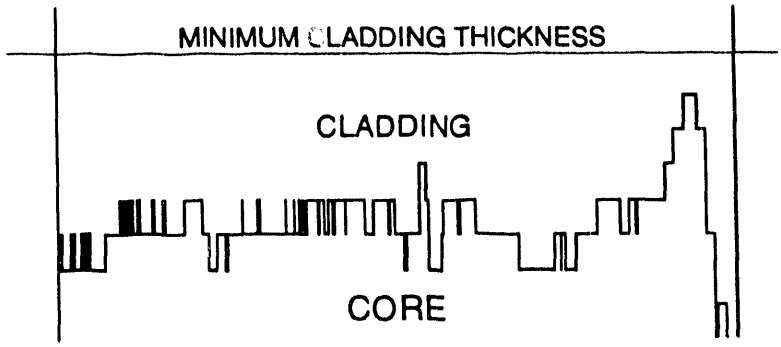

Figure 10: Values from a scanning line passing over the core end.

A dogboning effect at the end of the core can be clearly seen. With a line across the plot locating the minimum specified cladding thickness, it can be concluded that the cladding thickness is within the specified limit.

If the purpose of the distance scanning is only to check that the cladding thickness is greater than the specified minimum, a presentation of the results could be drawn as shown in figure 11. Here only areas/points having the minimum measured cladding distance will appear in the corresponding color.

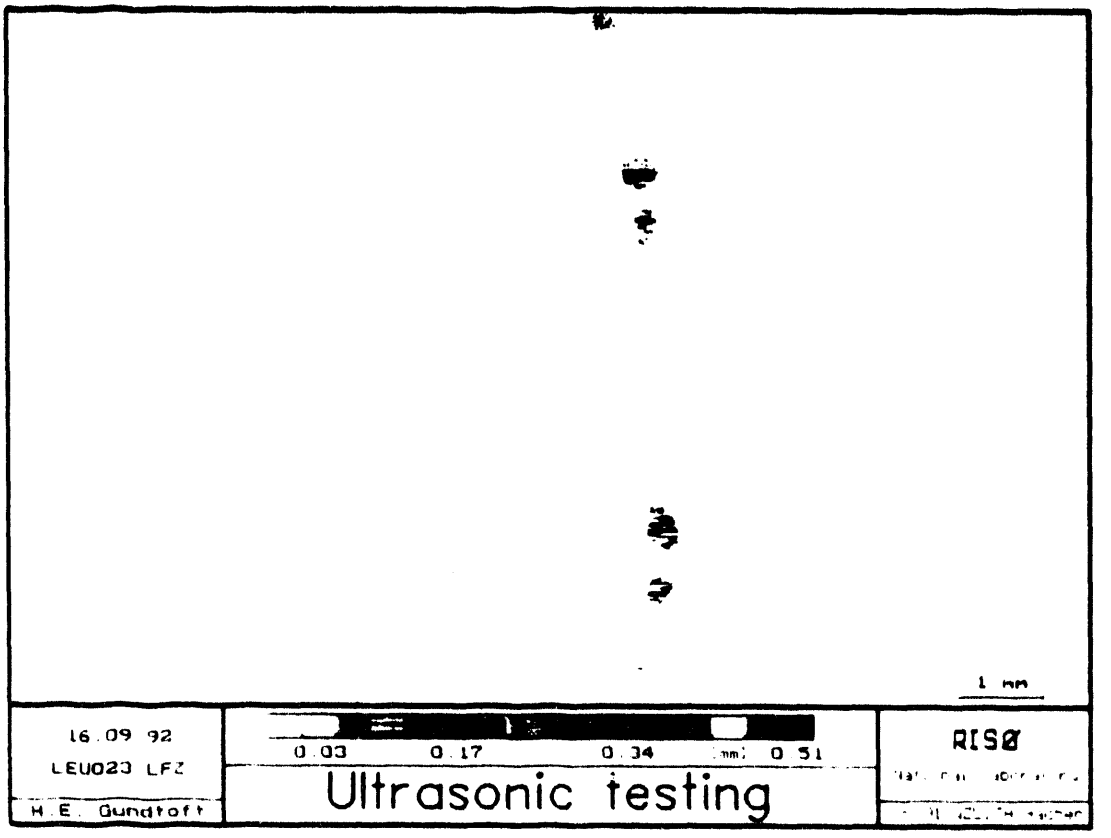

Figure 11: Example of data processing

The above illustration is only one way to present the data, because once measured, it is a matter of system capacity and software handling as to how the results are presented.

With the described Ultrasonic Scanning Technique, it has been made possible to check fuel plates over the whole surface for non bonded areas and the minimum cladding thickness requirement.

CHARACTERIZATION OF ATOMIZED U_3Si_2 POWDER FOR RESEARCH REACTOR

C.K.Kim, K.H.Kim, S.J.Jang. H.D.Jo, I.H.Kuk
Korea Atomic Energy Research Institute
Daeduk-Danji, Taejon, Korea,

ABSTRACT

Atomization technique was developed to produce U_3Si_2 powder using rotating disk. It was found that the atomized U_3Si_2 powder has spherical shape and smooth surface. Surface area of atomized powder is smaller by about 30% than that of comminuted powder. Only U_3Si_2 peaks appear on X-ray diffraction of atomized powder and the second phase exists with a small fraction and thin width on microstructure observation. It is also noticed that the atomized U_3Si_2 powder has homogeneous U_3Si_2 phase. Characteristics of atomized U_3Si_2 powder, i.e., spherical shape, smooth surface and homogeneous phase formation, are expected to give improvements in fabrication and to the properties of research reactor fuel.

INTRODUCTION

Rotating disk atomizing technique was applied to the fabrication of KMRR fuel in order to overcome the difficulties in comminuting tough U_3Si billet, to eliminate the impurities and to obtain rapidly solidified spherical powder. As a result, fabrication process can be economized and the properties of the fuel can be improved. [1),2)]

In fabrication of fuel plate where U_3Si_2 is dispersed in aluminum matrix, the spherical shaped U_3Si_2 powder can give desirable effects of improving plastic formability and homogenous dispersion. The dog boning can be eliminated in rolling the fuel plate. Additionally, the surface area of U_3Si_2 particle is smaller than the irregular comminuted particle, so that the reaction swelling is expected to decrease.

U_3Si atomization was presented in the last meeting. For the general application, U_3Si_2 is atomized in this year. U_3Si_2 alloy is melted at much higher temperature than U_3Si alloy. The liquid phase forms directly to the fine solid particle without passing through the two phase region of solid/liquid at 1665℃. The atomizing equipment was

adapted as before, but some modifications were needed needed with parts of high-temperature resistant materials in accordance with the liquid properties of U_3Si_2 alloy.

In this paper, atomized U_3Si_2 powder is characterized in respect to the fuel property in comparison with the comminuted powder.

EXPERIMENTS

Atomizing equipment was modified with parts of high-temperature resistant materials. In order to obtain the suitable size distribution of atomized U_3Si_2 powder, operating parameters, such as feeding rate of melt, superheating and rotating speed of disk, were adjusted. For raw materials, uranium as shown in table 1 and metal

Table 1. Chemical composition of uranium

(impurities in ppm)

U (wt%)	C	Fe	Si	Ni	Cu	H	C	Mg
99,5	20	54	10	37	27	7	2	12

silicon with purity 99.999% were used. Loading composition of raw materials to induction furnace was DU-7.4wt%Si, which was slightly higher in silicon than nominal composition. The alloying elements were loaded in a graphite crucible coated with high temperature resistant ceramics. Molten alloy was fed onto the rotating disk and was atomized by centrifugal force.

Powder size was measured by sieve analysis and light diffraction method. Glycerine 50 % solution was used for dispersion. The powder of different size group was observed under the optical microscope and the scanning electron microscope. The phases of the microstructure were analyzed by EDX and X-ray diffraction. The rapid cooling effect was investigated in respect to the particle size. Some powder was found to contain internal pore. It was found that the number and size of the internal pore increases with the particle size. Area fraction of the internal pore was measured by the image analyzer under the microscope in relation with the particle size.

The atomized powder is generally spherical and the surface is smooth, whereas the powder comminuted from ingot is irregular in shape and the surface is very rough. This implies that the specific surface area of the atomized powder is smaller

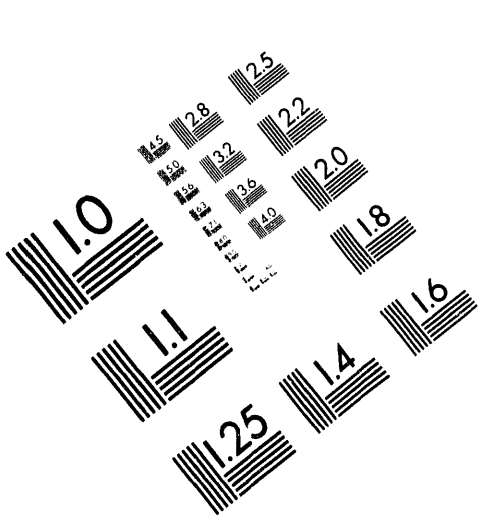

Association for Information and Image Management
1100 Wayne Avenue, Suite 1100
Silver Spring, Maryland 20910
301/587-8202

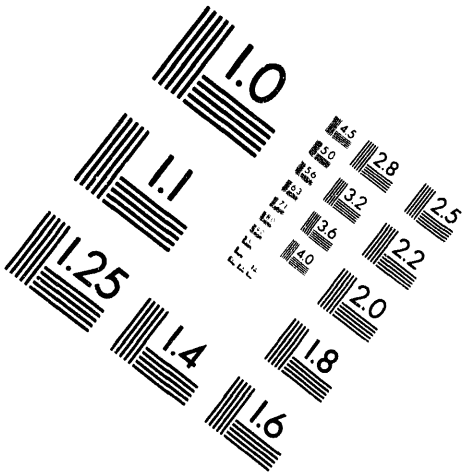

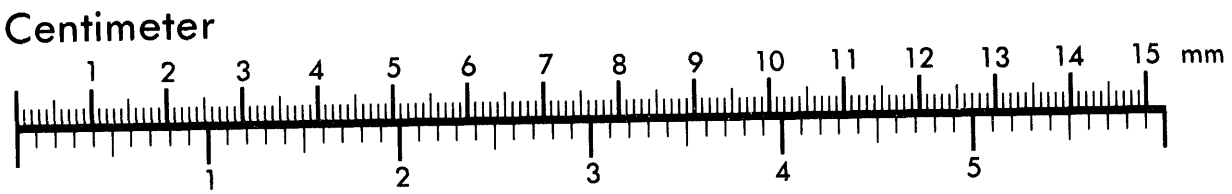

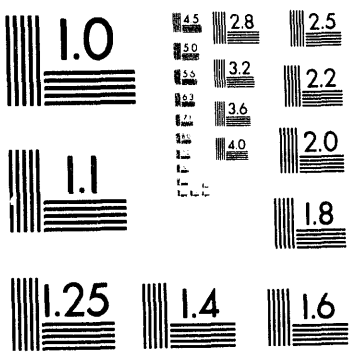

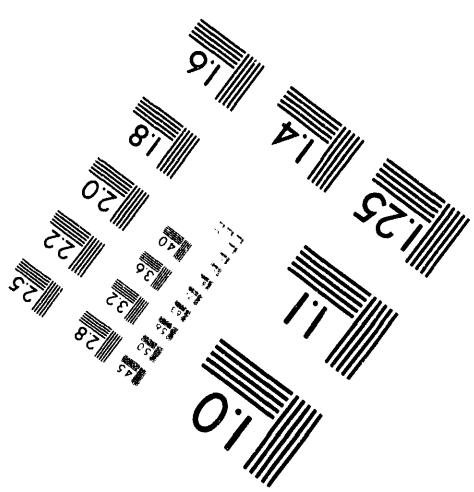

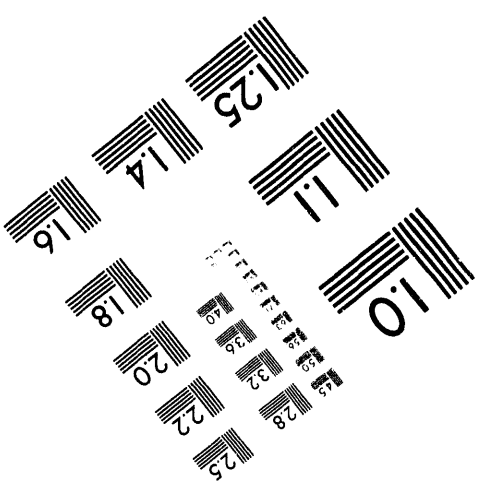

MANUFACTURED TO AIIM STANDARDS
BY APPLIED IMAGE, INC.

2 of 4

than that of comminuted powder. Gas absorption method was used in measuring specific surface area.

RESULTS AND DISCUSSION

Particle shape

Figure 1 shows the typical shape of U_3Si_2 powder dispersed. Most of the particles

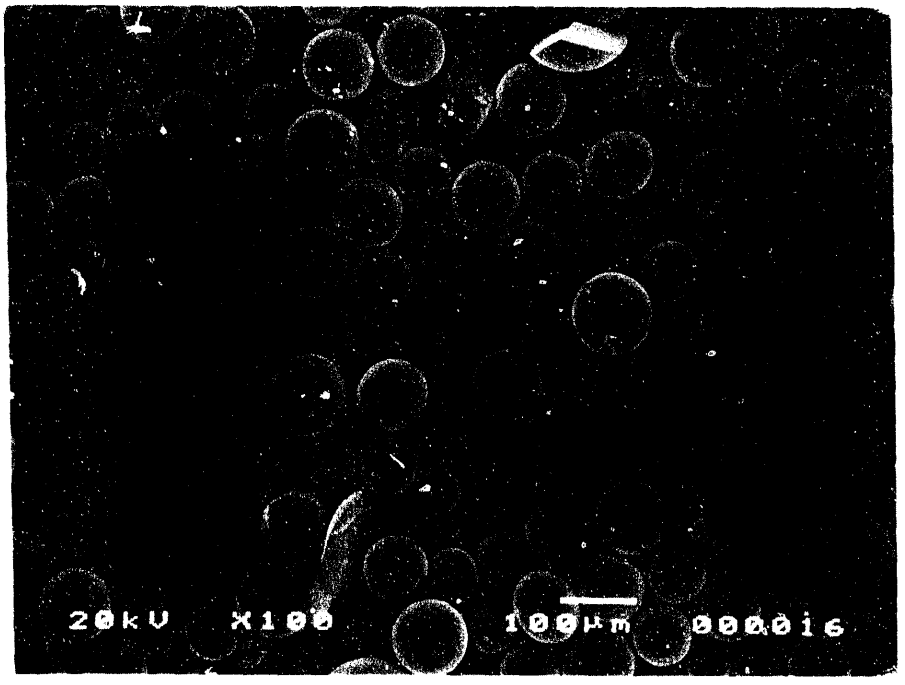

Fig. 1. Photograph of atomized U_3Si_2 powder illustrating particle shape

are spherical but some are not. As was mentioned above, U_3Si_2 melting point is much higher than that of U_3Si. Some amount of melt has already solidified and adhered to the rotating disk surface before it leaves the disk. Small irregular shape is produced by tearing forcefully the partly solidified particles from the edge of the disk. Irregular particles with sharp edges seem to be fragments of a big particle broken into pieces when the flying droplets hit onto the tank wall. Teardrop shape particles are assumed to form from the secondary droplet. When the surface tension of the melt droplet is smaller than the viscosity, this type of powder is formed. Ellipsoidal or bar-shape particle is all in this category and is produced by the so called ligament droplet formation mechanism. This is typical phenomenon happened when the feed rate of the melt is relatively high.

Particle size distribution

Size distribution of atomized U_3Si_2 powder was obtained as figure 2. The mean

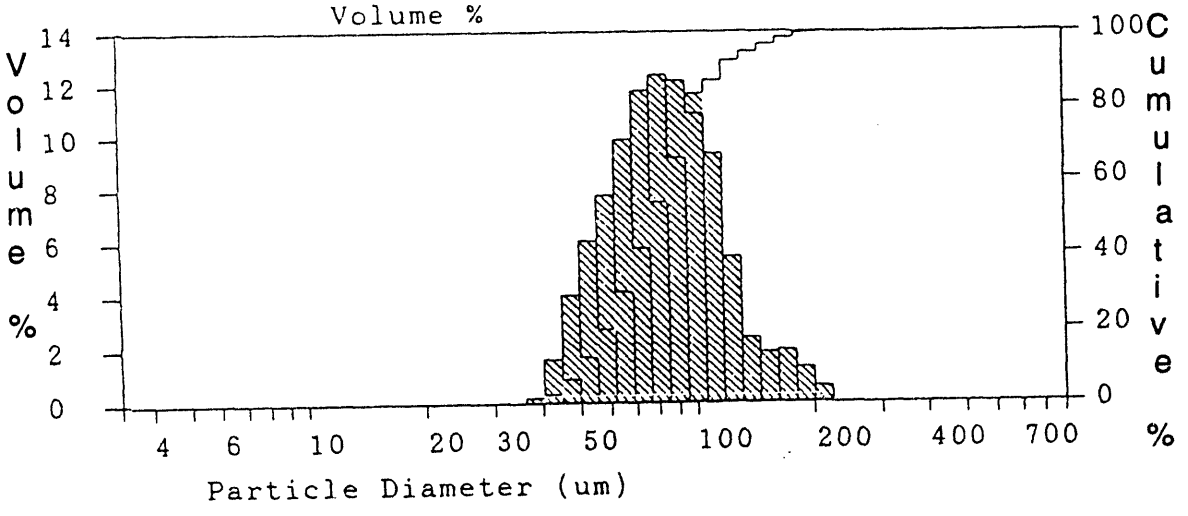

Fig. 2. Particle size distribution of atomized U_3Si_2 powder by light scattering method

size is 87.8 ㎛. Particle size varies with atomizing parameters such as the rotating speed, disk diameter, feeding rate of the melt and the degree of the superheat. They follow the relation proposed by Champagne et al.[3)]

$$d \propto \frac{1}{\omega^{0.98}} \cdot \frac{1}{D^{0.64}} \cdot \left(\frac{\gamma}{\rho}\right)^{0.43} \cdot Q^{0.12}$$

d : The particle diameter of atomized powder
ω : The angular speed of rotating disk
D : The diameter of disk
γ : The viscosity of melt
ρ : The density of melt
Q : The feed rate of melt

Here it shows that the particle size decreases with increasing the rotating speed, disk diameter and degree of superheating and with decreasing the feeding rate of the melt.

It is seen that the size distribution is mono-modal. In general, atomized powder is spherical and the size distribution is bimodal when the feeding rate of the melt is relatively low. It is explained by the direct droplet formation mechanism. Large particle is separated from the head and small one is separated from the neck in equal number. From the fact that most of the atomized U_3Si_2 particles are spherical, they are assumed to be produced mainly by the direct droplet mechanism. In the middle of the experiment it was found that the feeding nozzle was enlarged with time. This changes the feeding rate and results in the change of the particle size with time. Mono-modal size distribution is attributed to the enlargement of the feeding nozzle.

Surface morphology

The surface morphologies of the atomized powder and the comminuted powder are shown in figure 3. It is seen that the surface of the atomized particle is much smoother than the surface of the comminuted particle. Comminuted powder has many edges and cleavage surfaces, while atomized powder has smooth surface with a few small winkles and pin holes.

Results of surface area analyzed by gas absorption method show that the surface area of atomized powder is smaller by about 30% than that of comminuted powder as shown in table 2. In atomizing process the powder surface is formed as minimizing

Table 2. Surface area of atomized powder measured by gas absorption method

	BET surface area (sq. m/g)	Langmuir surface area (sq. m/g)	Single point surface area (sq. m/g)
Atomized powder	0.0694	0.1559	0.042
Arc-melted powder	0.1091	0.2164	0.700

liquid/gas interface energy, whereas in pulverizing process the surface is formed as cleaving along the crack.

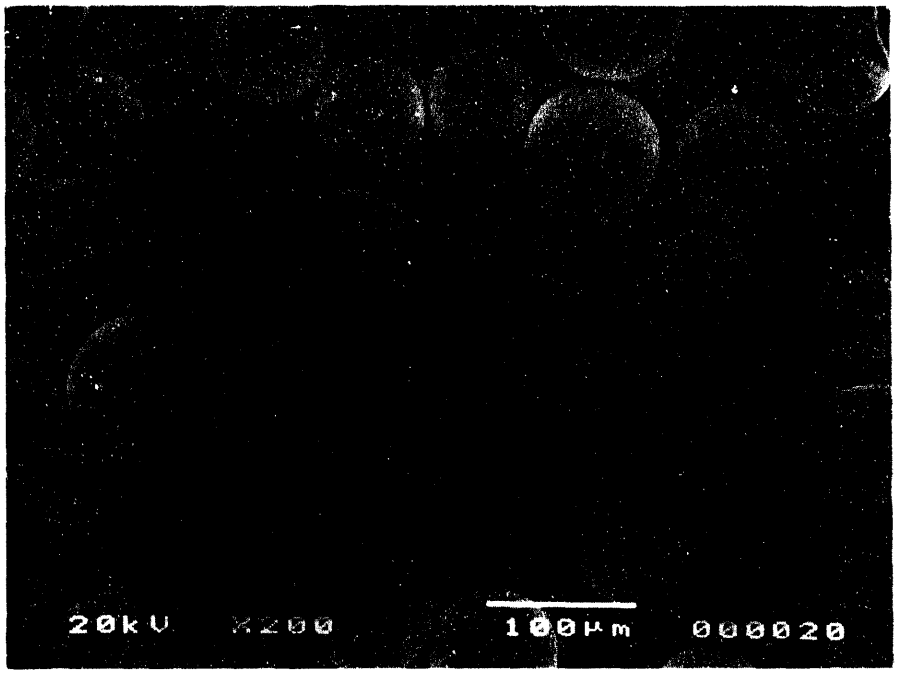

a) Atomized U_3Si_2 powder

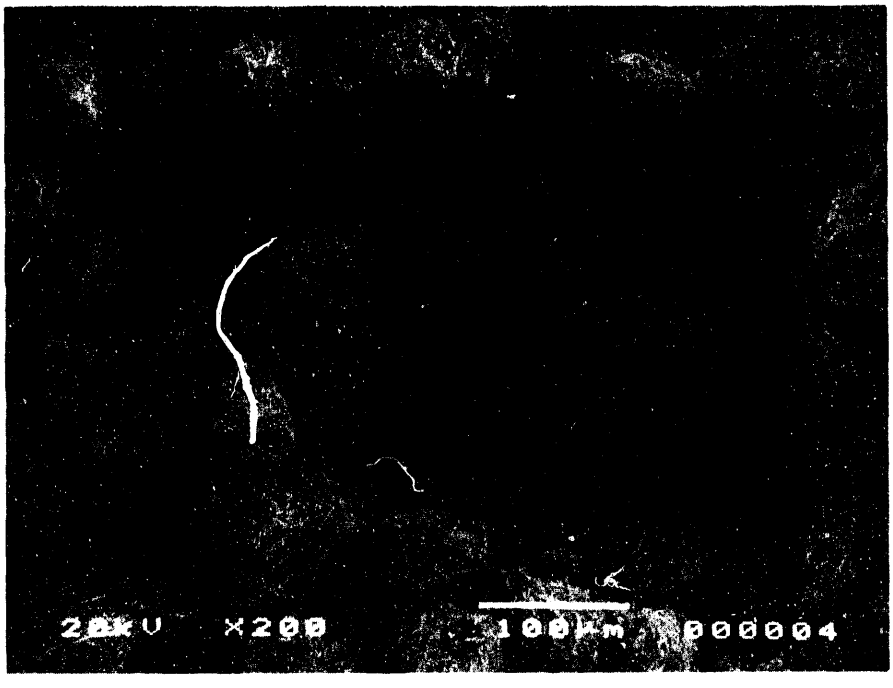

b) Comminuted powder

Fig. 3. Comparison of surface morphology between atomized powder and comminuted powder

Microstructure

The microstructure of atomized powder is shown in figure 4. Main phase of atomized particle is found to be U_3Si_2 by x-ray diffraction analysis as is shown in figure 5. Second phase which exists in network or in dendrite is turned out to be silicon-rich

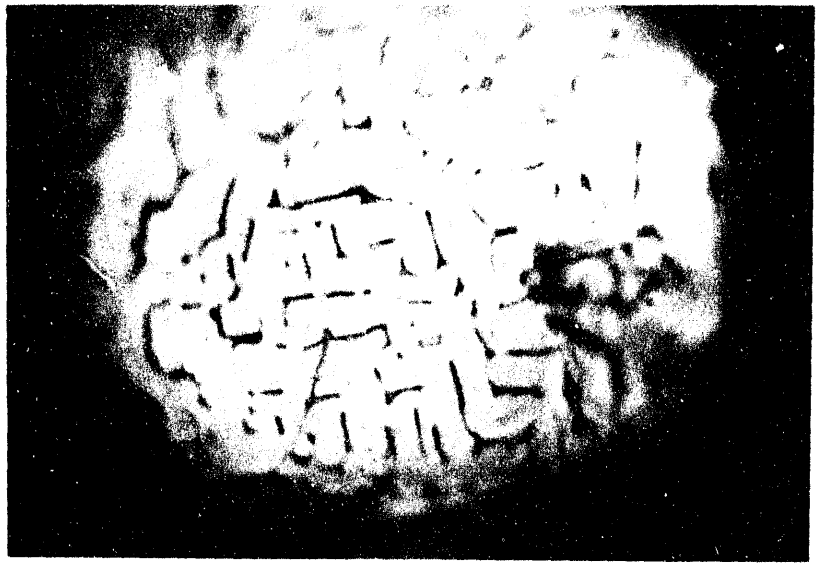

Fig. 4 . Typical microstructure of atomized U_3Si_2 particles

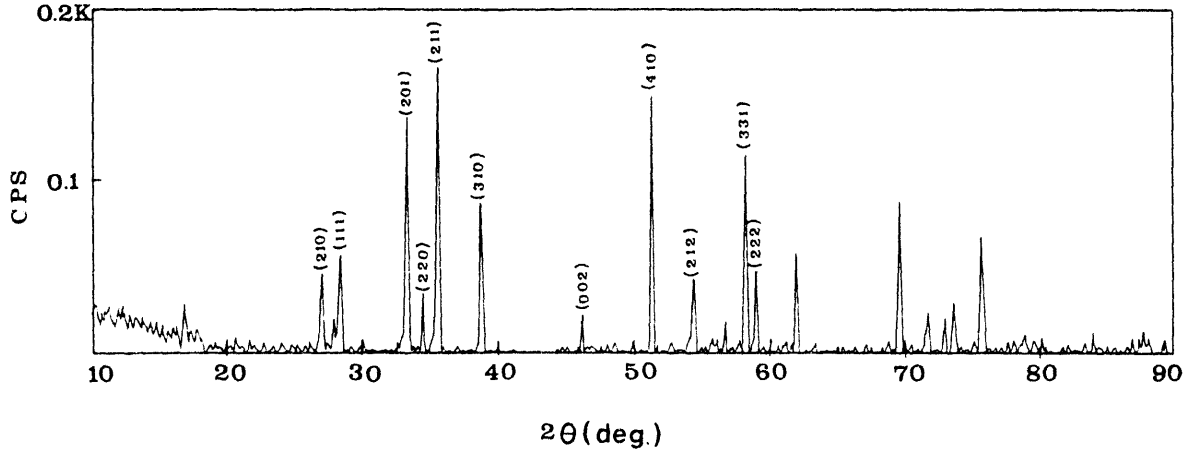

Fig. 5. X-ray diffraction results of atomized U_3Si_2 powder

phase such as USi or $U_2Si_{7.5}$ by EDX analysis. On the X-ray diffraction analysis some weak peaks of silicon-rich phases are detected in arc-melted U_3Si_2 button but are not detected in the atomized U_3Si_2 powder. It is assumed that homogenization is achieved in the melt by magnetic stirring effect of induction melting.

The grain refinement in U_3Si_2 is not as great as in U_3Si. In U_3Si atomization, grains are getting smaller as powder size gets smaller. However, this phenomenon does not appear remarkably in U_3Si_2 as in U_3Si. This is attributed to the fact that U_3Si_2 forms directly from the liquid phase without solute diffusion. Also, the silicon-rich second phase is found to have thin width.

Some atomized U_3Si_2 powder has internal pore as found in U_3Si. The area fraction of internal pores and the frequency increase with powder size as shown figure 6. This results explain that the large droplet has low surface tension and has large chance for cooling gas to be trapped while it is separated from the disk. [4)]

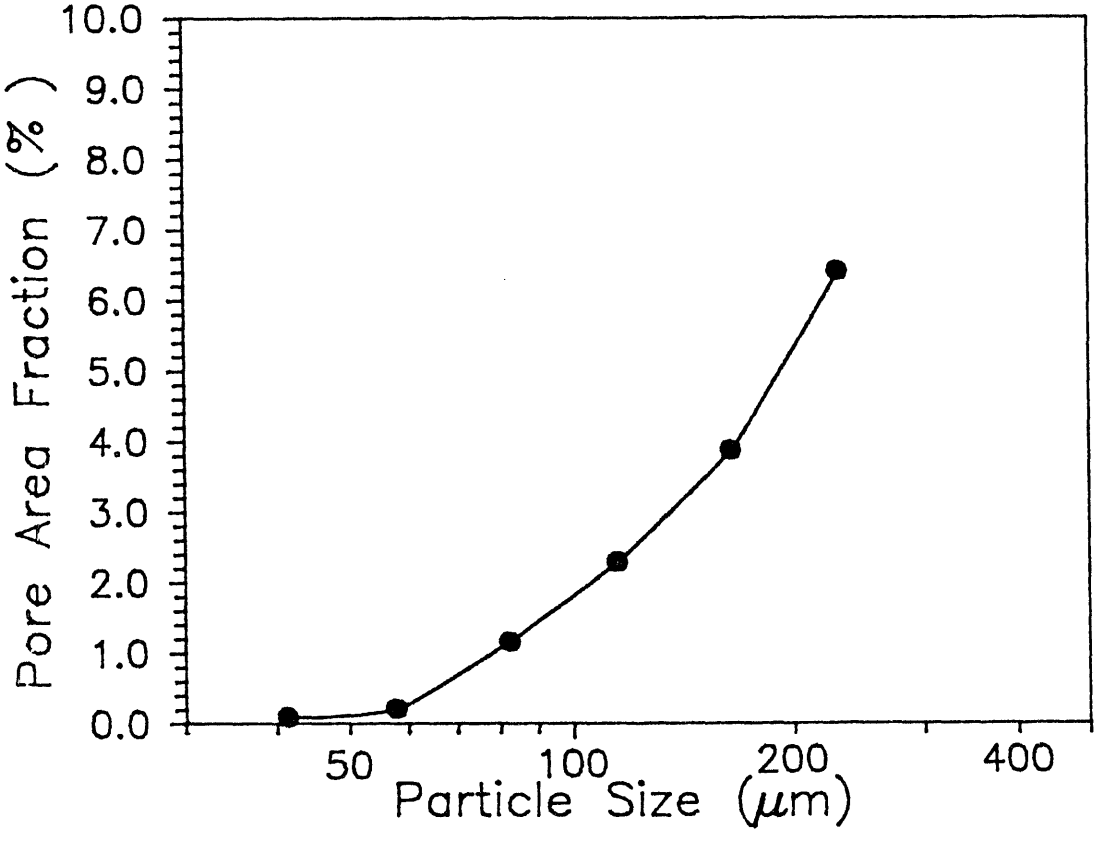

Fig, 6. Variation of the pore area fraction in microstructure observation with various particle sizes

CONCLUSION

A technique was developed to produce U_3Si_2 powder using rotating disk atomizer, following U_3Si atomization last year. It is found that the atomized U_3Si_2 powder has spherical shape and smooth surface as U_3Si. Grain refinement is not as great as in U_3Si. However, homogeneous phase is found to be formed in the resultant atomized particle. Some powder contains internal pores as U_3Si and the frequency increases with particle size.

Characteristics of the atomized U_3Si_2 powder, i.e., spherical shape, smooth surface and homogeneity are expected to give some improving effects on fabrication and reactor performance of the research reactor fuel.

REFERENCE

1. I. H. KuK, "Atomization of U_3Si Nuclear Fuel", Proceedings of the International Meeting on Reduced Enrichment for Research and Test Reactor, Rhode Island, U.S.A., September, 1990

2. C. K. Kim, "Atomization of U_3Si for research reactor fuel", Proceedings of the international Meeting on Reduced Enrichment for Research and Test Reactor, Jakarta, Indonesia, November, 1991

3. B. Champagne, R. Angers, " Fabrication of Powder by the Rotating Electrode Process", The international Journal of Powder Metallurgy & Powder technology, 16(1980)359-367

4. L. L'Estrade. H. Hallen and R. Ljunggren, "Internal Porosity of Gas & Atomized Powders", HOGANAS, Sweden

A NEW X-RAY INSPECTION OF FUEL PLATES

JF. POUPARD - A TISSIER
CERCA
Les Bérauds - BP 1114
26104 Romans-Sur Isère, France

ABSTRACT

A new X-Ray Inspection Machine based on directly numerized signals has been developed by CERCA. For U-distribution check, this machine presents specific advantages with respect to the previously used equipments. It also allows image processing for further developments.

INTRODUCTION

As the silicide fuel plates production increased at CERCA, the inspection methods have been adapted to these new products. New equipments have been developed for U-235 content in fuel cores and for ultrasonic inspection of fuel plates. As the MTR activities increased very quickly, CERCA has defined a R&D program to improve the services we offer to our customers. Within this R&D program, CERCA has developed a machine for X-Ray inspection based on image processing.

GENERAL SCOPE

The machine has to achieve the following three inspections :

- to check dimensions, geometry and positioning of the meat in the fuel plates : fluoroscopy;
- to detect, to locate and to measure possible inclusions in the meat and stray particles ("remote islands") outside the meat : X-Ray films examination;
- to verify the homogeneity of the uranium distribution in the meat : uranium distribution

The principles of the machine are as follows :

1/ the fuel plate is submitted to an X-Ray exposure;
2/ the fuel plate is placed in a steady mechanical device between the X-Ray source and the detector;
3/ the detector is placed on the other side of the fuel plate to convert the X-Ray flux transmitted through the fuel plate into numerical signals;

See Appendix 1, for schematic principles.

All the numerical data (in grey levels) given by the detector are transmitted to a computer to give a real-time image of the fuel plate. This image is processed in order to give an evaluation of :

- U density in fuel plates on a given reference surface (usually 10 x 10 mm);
- dimensions and locations of defects giving a contrast exceeding a given level ("black" or "white" spots);
- meat dimensions to be compared automatically to dimensions and locations defined by the specifications.

All the results may be stored on a mass memory system (optical numerical disk).

SCHEDULE

The schedule of development of this machine is given in Appendix 2. The equipment is installed in the MTR workshop at the Romans plant since beginning of July 1992.

Evaluation tests have started now for U distribution and for image processing as presented here below.

FIRST STEP : URANIUM DISTRIBUTION

Principles :

The same basic principle has been chosen for inspection. It is based on X-Ray absorption and comparison to an aluminium standard of an equivalent thickness. The X-Ray station works in the same energy range . The machine issues the same reports and same charts than the previous equipment and the machine is able to perform the inspection with the spot size or surface defined in the specifications.

Basically the most important is that this equipment can perform the inspection for uranium distribution in respect with all the existing specifications, as required under CERCA Quality Assurance procedures.

Advantages :

- the inspection time per fuel plate is strongly reduced;
- it is very easy to choose scanning of the whole surface or scanning of one or two lines;
- the mechanics used is more modern and more precise;
- flexibility is increased : it is possible to choose inspection compared to nominal value of U-density or compared to mean value of U-density of the fuel plate;
- inspection may be performed on fuel plates before cutting to size (short delay between manufacturing and inspection which permits quick feedback for process control).

Results :

Comparison has been done with the results given by the previous equipments. Both totally agree.

Of course, we are very open to cooperate with every interested customer.

SECOND STEP : IMAGE PROCESSING

Principles :

In fact U distribution inspection results from a treatment of numerical data given by the equipment. Those data could also be used to give an image of the fuel plate (meat and aluminium sides and ends). This image can be used to evaluate dimensions of meat (including lack of uranium, horn, overlength) accordingly to computerized customer's specification. Moreover the image processing allows to detect, locate and measure inclusions on the meat and stray particles outside the meat.

Advantages :

- a near real time imaging equipment allowing very quick feedback to manufacturing process;
- no variability due to film processing or operator interpretation;

- storage and archive of data on optical numerical disk easier to handle and to store than films (specially for long time storage);
- reliability of automatic interpretation by computer system increased compared to human interpretation;
- quantified values of defects given directly by image processing and used for building a data base useful for process improvement.
- easier surveillance inspection performed by customers without difficult interpretation of X-ray films.

Preliminary results :

Tests have been performed to verify that the equipment is able to conduct inspection according to the existing specification.

Images of fuel plates could be presented with the different types of defects.

We have the intent to go further on the definition of this inspection, and of course, for that, we have to cooperate with all our customers.

CONCLUSION

A new equipment for X-Ray inspection of fuel plates has been developed by CERCA. We wanted to have an equipment able to be used on an industrial scale for U distribution test. It is planned to use new advantages of this machine, due to its flexibility, to perform a complete X-Ray inspection. This step is planned in accordance with the general goals for quality within the company.

To improve quality CERCA will strongly try :

- to reduce times between manufacturing and inspection operations in order to provide quick feedback to the manufacturing process;

- to give, as far as possible, numerical values and data of defects, in order to provide a complete data base on process capability.

The new equipment was designed in respect to these general goals.

Now, to perform a complete X-Ray inspection with this machine we have to follow the very fast evolution of related new techniques.

In order to satisfy really the needs and requirements of our customers an additional work has to be done in cooperation with them. Such points as recording means, documentation of results, archive methods have to be defined with the customers.

This is the challenge for the coming years.

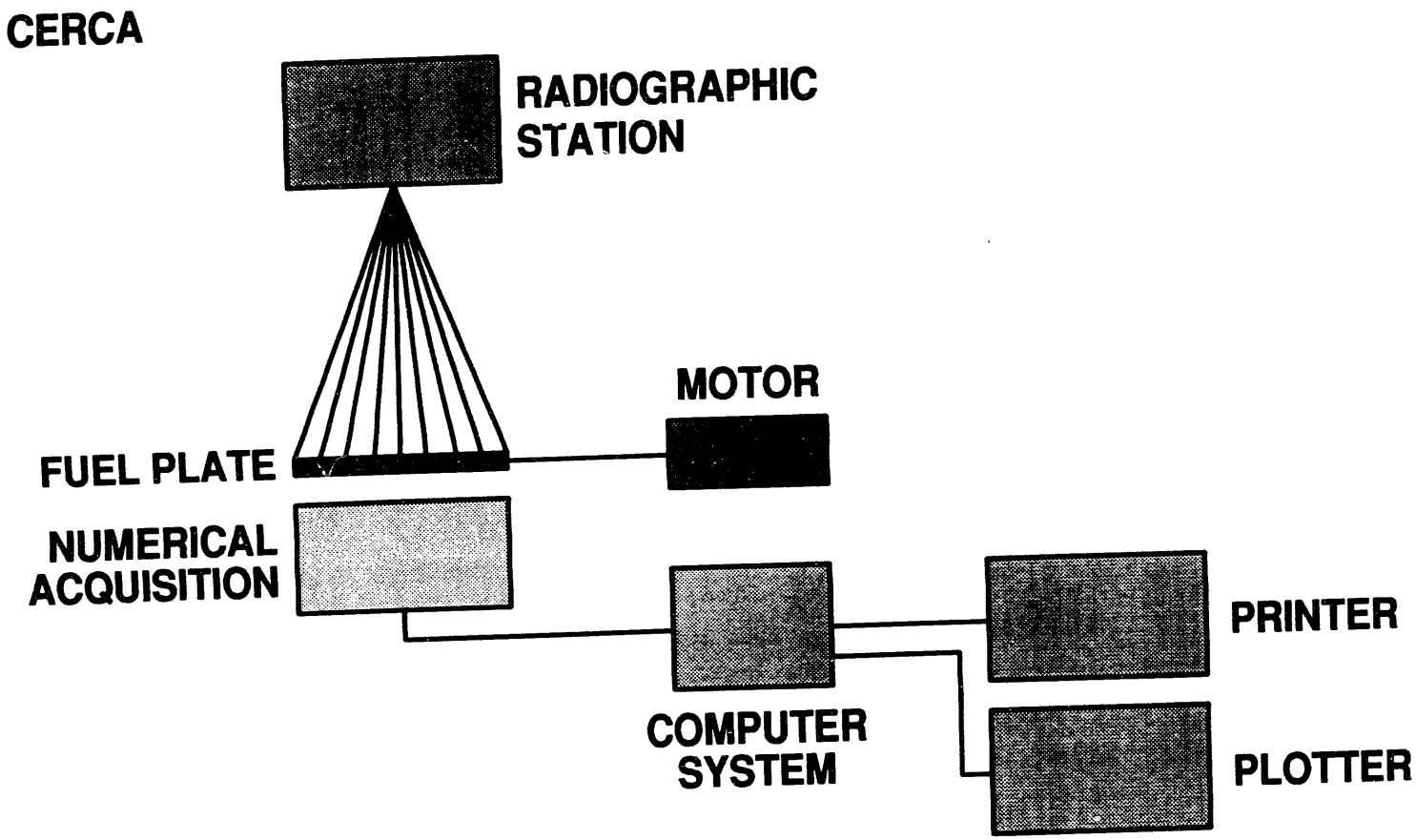
CERCA
RADIOGRAPHIC STATION
MOTOR
FUEL PLATE
NUMERICAL ACQUISITION
PRINTER
COMPUTER SYSTEM
PLOTTER

APPENDIX 1

CERCA

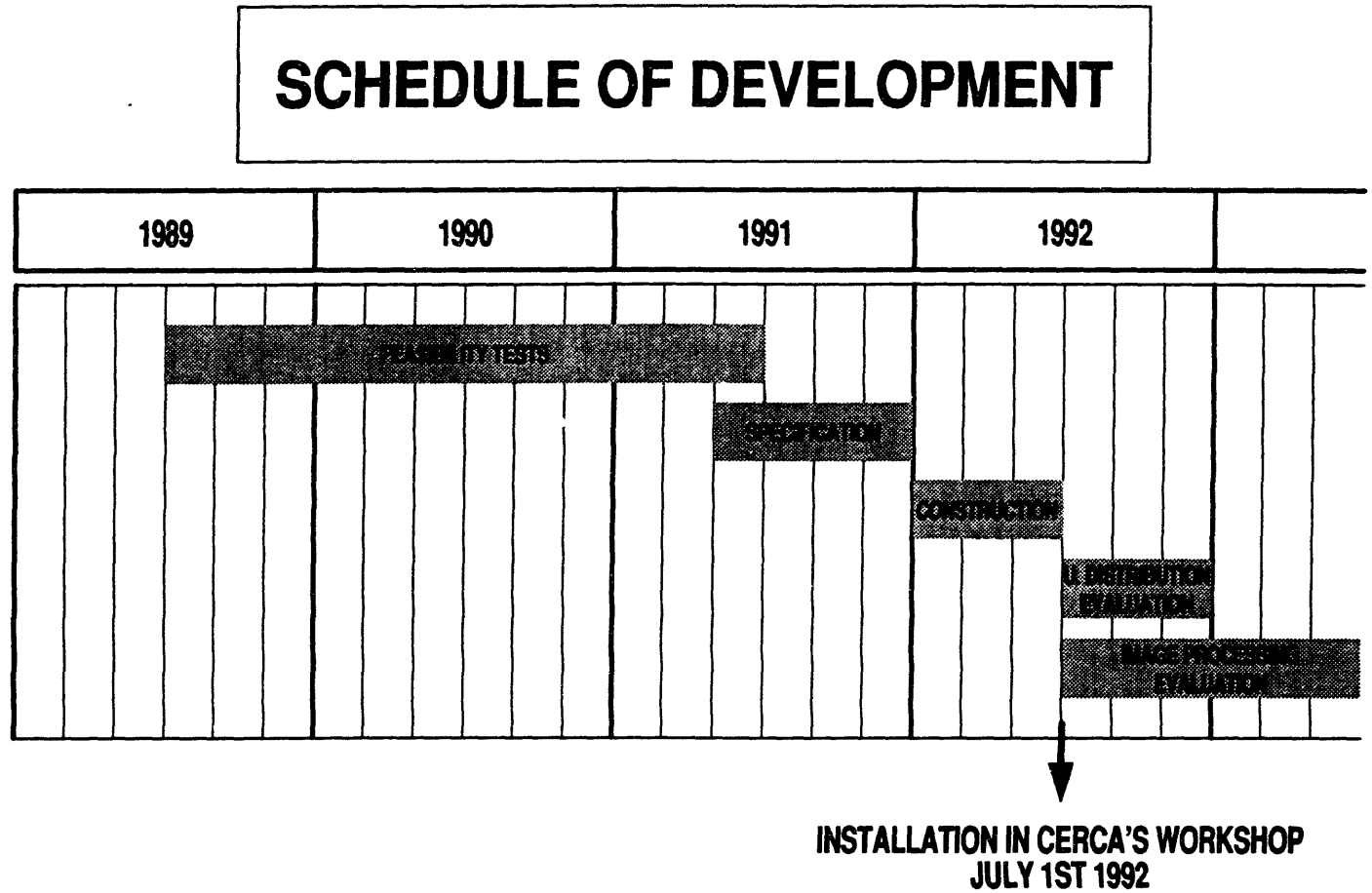

APPENDIX 2

CHARACTERIZATION OF COMMERCIALLY PURE ALUMINUM POWDER FOR RESEARCH REACTOR FUEL PLATES*

V. D. Downs
Babcock & Wilcox
Lynchburg, VA USA

and

T. C. Wiencek
Argonne National Laboratory
Argonne, IL USA

ABSTRACT

Aluminum powder is used as the matrix material in the production of uranium aluminide, oxide, and silicide dispersion fuel plates for research and test reactors. Variability in the characteristics of the aluminum powder, such as moisture content and particle-size distribution, influences blending and compacting of the aluminum/fuel powder.

A detailed study was performed to characterize the physical properties of three aluminum powder lots. An angle-of-shear test was devised to characterize the cohesiveness of the aluminum powder. Flow-rate measurements, apparent density determination, subsieve analysis, surface area measurements, and scanning electron microscopy were also used in the study.

It was found that because of the various types of commercially available powders, proper specification of powder variables will ensure the receipt of consistent raw materials. Improved control of the initial powder will reduce the variability of fuel-plate production and will improve overall plate reproducibility. It is recommended that a standard specification be written for the aluminum powder and silicide fuel.

1 INTRODUCTION

The success of fuel-plate production depends to a great extent on the characterization and control of the initial raw materials. Reproducibility of the fabrication processes is best achieved by the use of consistent raw materials. Often the problem is not so much how to control the raw material, but rather knowing what to control. Powders have many characteristics, some interrelated, that must be considered. Among these are shape, surface area, particle structure, composition, bulk density, apparent density, size

*Work supported by the U.S. Department of Energy, Office of International Affairs and Energy Emergencies, under Contract No. W-31-109-ENG-38

distribution, compressibility, flow-rate, and average size. Only a few may be critical for a given application, but the final selection can be made only if all of the major characteristics are understood. Standard testing methods allow the quantitative measurement of certain of these physical properties; some of these methods are reviewed in this paper and, in addition, nonstandard test methods are also presented.

The properties of powders can change over time between manufacture and actual use. The powders studied were stored in "sealed" (not airtight) containers that either contained air or were under a vacuum. Specific trends due to age of the powder were not considered unless powder conditions, such as "degassed and 24 hr exposure to air", were specified. Due to differences in production facilities, a comprehensive study of powder characteristics under all environmental conditions was not possible. Therefore, the goal of this paper is to show general trends in powder characteristics.

2 BACKGROUND

Aluminum powder, in particular Alcan 101, is used extensively in the Research and Test Reactor program. Aluminum powder is the matrix material used in the picture-frame method for manufacturing aluminum fuel plates. In this process, aluminum powder is blended with fuel particles, the mixture is poured into a die cavity and pressed to form a compact, and the compact and aluminum alloy frame is assembled and then hot rolled into a fuel plate.

Discussions with one major powder supplier, Alcan Toyo America, Inc., revealed two classifications of aluminum powder: conventional and spherical. Conventional is molten aluminum atomized in air; the result is a globular powder form. This powder's nonspherical shape is due to the formation, during cooling, of surface oxide films that distort the internal liquid aluminum as it solidifies. Alcan lists 13 types of conventional powders, with percentage of powder passing through a 325-mesh (44 μm) sieve ranging from 35-99%. Spherical powder is produced by atomization in an argon atmosphere containing 3-4% oxygen for controlled oxidation. This powder is used primarily for armament. The heat generated by the powerful exothermic reaction of oxidizing aluminum, combined with an explosive, has a devastating effect. The low percentage of oxygen produces a thin protective oxide layer that permits safe handling of the powder when exposed to atmosphere. Alcan lists 14 different types of spherical powder, with the average particle size ranging from 3 to 35 μm. Particle-size distributions for selected types are plotted in Figures 1 and 2. The graphs show particle-size distribution based on the percentage that is finer than a certain size. For instance, in Figure 1, approximately 90% of the Type 101 particles are smaller than 82 μm. For spherical powder, however (Figure 2), 90% of the type X-86 particles are smaller than 65 μm.

3 SAMPLING

Given the large population of particles in most powdered metals, a sampling method must be used to achieve statistically meaningful results. Careful attention must be given to collecting unbiased samples. Recommended techniques[1] provide samples that are representative of the total powder population. However, the science of sampling is beyond the scope of this paper. The key here is the use of a good sampling method.

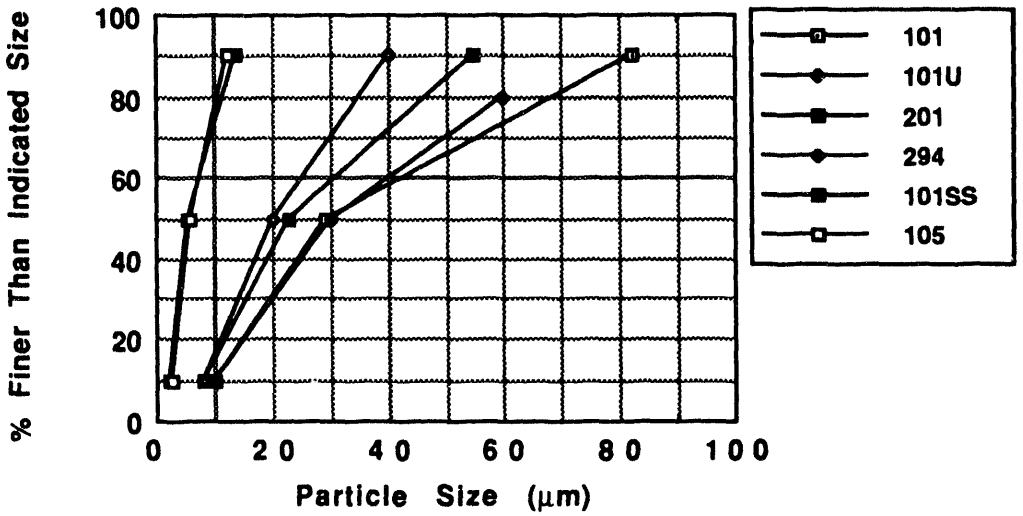

Figure 1. Particle-Size Distributions of Conventional Aluminum Powders

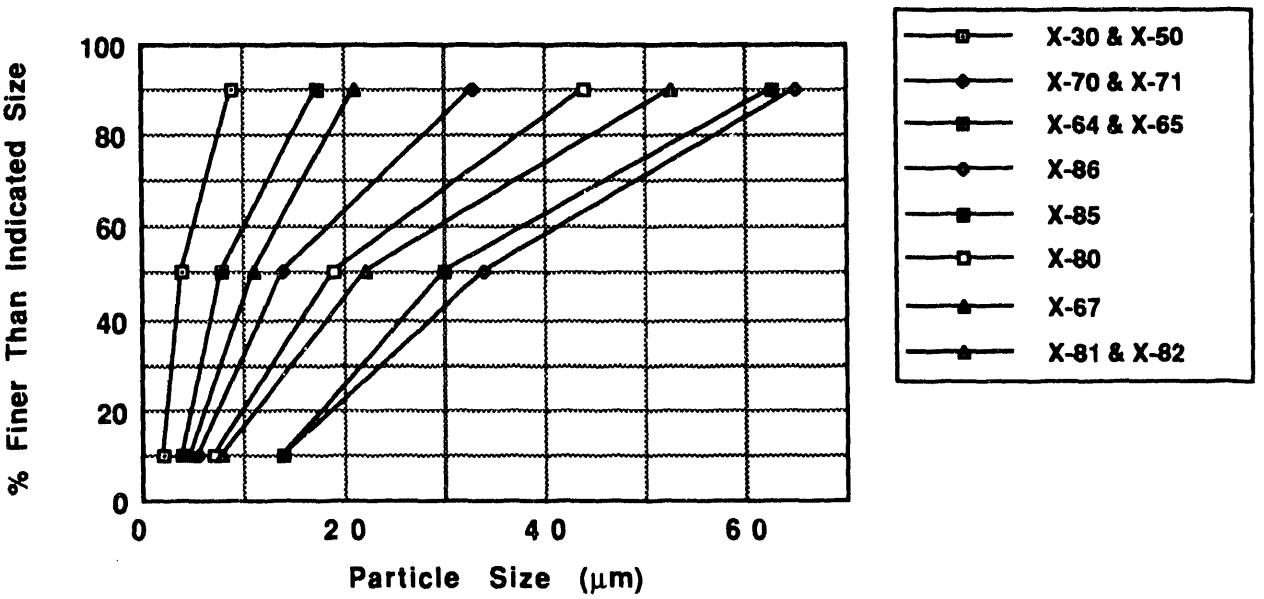

Figure 2. Particle-Size Distributions of Spherical Aluminum Powders

4 CHARACTERISTICS OF STANDARD POWDERED METAL

4.1 Analysis of Powder Size by Sieve Tests

Particle-size analysis[2] is a common, rapid, and easy test for powdered metals. Data are usually generated by sieving the material through a series of screens. Results are given by the weight percentage of material above a certain diameter that will not pass through the screen. The screens range from large >0.3 cm (6-mesh) to the smallest commonly used standard sieve size of 37 μm (400-mesh).

The majority of the aluminum powder used for fuel plate production is smaller than 44 μm. A common powder is Alcan Type 101. This powder has a range of 75-85 wt.% <44 μm particles. Thus, a common specification is the requirement of a minimum amount of <44 μm-size powder. However, this can be a misleading specification because sieve-test results are greatly influenced by the time of sieving and the intensity of vibration. Sieve tests are only valid if the forces that tend to agglomerate powders are overcome by the mechanical action of the sieve shaker. Forces that bind particles together result from (a) friction due to the physical shape of particles, (b) Van der Waals forces acting on the powder itself, and (c) adsorbed surface-water molecules.

Small particles are more influenced by Van der Waals forces than are larger particles due to the smaller mass per surface area. This force is further enhanced by water molecules attached to small particles. To prevent these forces from influencing powder-particle-size determination, wet sieving is recommended. A low-viscosity liquid, (e.g., acetone) can be used as a carrier vehicle to counteract the forces acting on the dry powder. This general test is very useful for describing aluminum powder, but should not be the sole specification for production powder.

Three lots of aluminum powder were extensively studied in this review. Table 1 summarizes analytical results of the as-certified Alcan powder.

Powders from the three different batches of as-received aluminum powder were individually blended and then dry sieved at Argonne National Laboratory (ANL) for comparison with the manufacturer's data. The results are given in Figure 3 for the coarse (>44 μm) particles. The fines (<44 μm)) were 78, 84, and 77% for Lots 10003, 1770 and CO-713, respectively. The data agree well with those in Table 1. Two characteristics are of major concern in controlling the feedstock powder. First, a significant amount of powder is present in the 53-125 μm sizes. Control of this powder distribution may be necessary to improve fuel core reproducibility. Second, the range of allowable <44 μm powder for Alcan 101 aluminum is 75-85%. Although all three lots fall within this range, the differences between lots are significant and may affect the final powder properties. Overall, Figure 3 shows significant differences in powder-size distributions. These differences may lead to variance in final fuel-plate homogeneity.

Table 1. Manufacturer's Certified Analytical Results for the Three Lots of Alcan Type 101 Aluminum Powder

Characteristic	Lot 10003	Lot 1770	Lot CO-713
Free Aluminum (wt.%)	99.5	99.3	99.4
Volatiles (wt.%)	0.01	0.03	0.02
Oil and Grease (wt.%)	0.01	0.10	0.01
Screen Analysis			
-100 Mesh (<150 μm, %)	100	100	100
-200 Mesh (<74 μm, %)	94.0	96.8	94.8
-325 Mesh (<44 μm, %)	81.8	85.0	77.0
+325 Mesh (>44 μm, %)	18.2	15.0	23.0

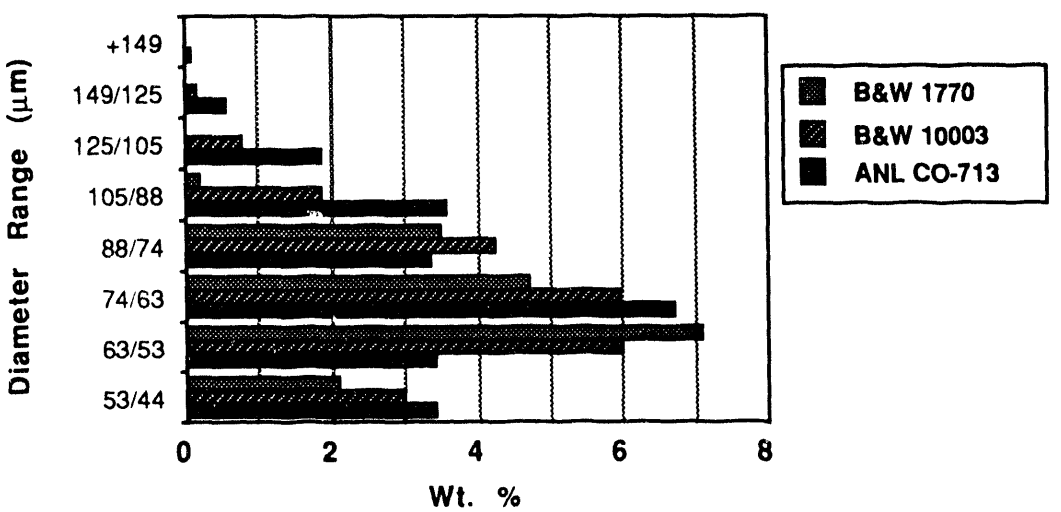

Figure 3. Distribution of 149-44 μm As-received, Blended Powder from Lots 1770, 10003, and CO-713 (B&W = Babcock & Wilcox)

Another related powder specification is average particle diameter. This value is not very informative without any knowledge of the specific particle size distribution. Specifying both a minimum of <44 μm percentage and an average particle diameter is recommended as a method to decrease powder variability.

4.2 Analysis of Subsieve Particle Size

Because the majority of the aluminum powder is <44 μm (-325 mesh), a technique other than standard mesh sieving must be used. Various methods can be used to determine the distribution of subsieve-size particles in a metal powder.[3,4] Results were generated on a Leeds and Northrup Microtrac particle-size analyzer, which can analyze powder distributions with sizes <44 μm. This machine uses a laser beam to measure 0.2 to 42 μm particles dispersed in water. Figure 4 gives the results of these tests for Lots 10003 and 1770.

4.3 Measurement of Apparent Density

Standard devices are readily available for determining the flow-rate and apparent density of free-flowing and non-free-flowing powders.[5-7] The most commonly used instrument, the Hall flowmeter, is an accurately machined funnel. For non-free-flowing powders, a Carney flowmeter (a larger-hole version of the Hall flowmeter) is used. The time required for a weighed sample of powder (usually 50 g) to flow from the funnel into a cup is determined and the flow rate is expressed in seconds, or g/min if a nonstandard weight of the sample is used.

The Hall flowmeter can also be used to measure another commonly reported characteristic for metal powders, i.e., apparent density. The powder is allowed to flow through the flowmeter into a container of known volume (usually 25 cm^3). After the powder is struck level, it is weighed and the result is given in g/cm^3.

The three as-received lots of aluminum powder were sampled at the top, center, and bottom of the shipping container and the results are given in Figure 5. Significant differences between the three lots were measured. Apparent density decreased from the top to the bottom of the can, possibly because of segregation of the powder during shipping and handling. The effect of particle size on apparent density was also measured. In general, coarser particles led to reduced apparent densities.

Due to poor flow of the powders, no Hall or Carney flow times were measured on the three lots of powder. It is recommended that flow time not be used as an aluminum powder specification.

Another related characteristic is tap density, a measure of the density of a powder sample after a specified number of taps or controlled vibrations. Because there are no established standards, this method was not used during the characterization and is mentioned here only to make others aware of it.

4.4 Measurement of Surface Area

A standard method used to determine the surface area of powders is the Brunnauer, Emmett, and Teller (BET) test. This nondestructive test determines

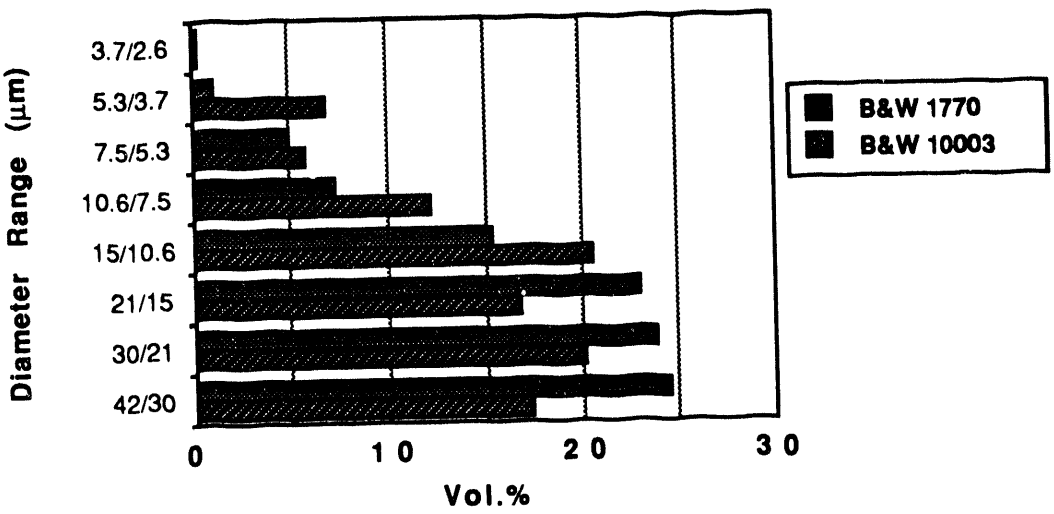

Figure 4. Results of Subsieve Analysis

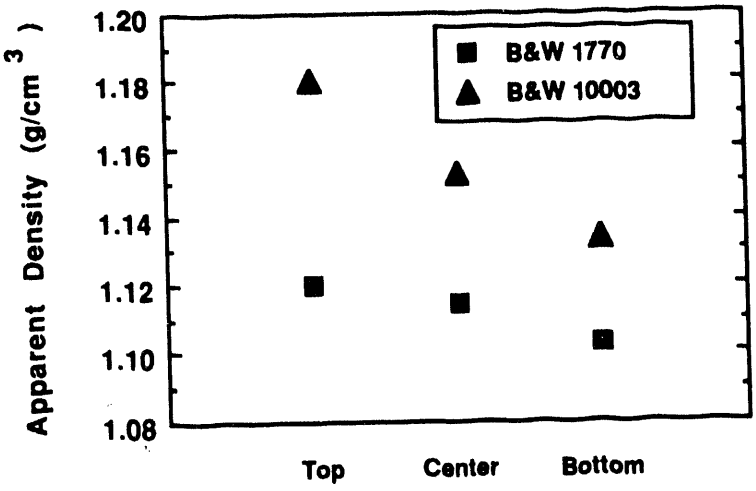

Figure 5. Comparison of Apparent Density of B&W Aluminum Powders

the surface area by measuring the amount of absorbed gas on a known weight of powder. This sorption method relies on the fact that under certain circumstances molecules may be adsorbed onto the surface of powder particles to form monomolecular layers. To obtain accurate results from the standardized methods[8] that have been developed, the proper gas must be used.

Surface areas in the range of 0.02 to 5.0 m^2/g area (111-0.44 μm average particle size) are measured with krypton gas as the adsorbate. In the range from 3 to 100 m^2/g (0.74-0.02 μm average particle size), nitrogen gas is used.

For surface-area measurements, a Micromeritics Instrument Corporation FlowSorb II 2300 was available. However, due to scheduling and equipment problems only limited measurements were taken. Because of the preliminary nature of the information, the results are not included in this report.

5 NONSTANDARD TESTS FOR POWDER METAL CHARACTERISTICS

5.1 Angle of Shear

Cohesive strength is a critical parameter in predicting blending and die-loading characteristics of powders. Both blending and die loading directly affect the homogeneity of the final fuel core. The angle of shear (which is similar to angle of repose) determines the relative cohesive strength of the aluminum powder. No simple and inexpensive standardized test was found that could provide the necessary information. A simple test was developed that uses a bottom-sieve testing catch pan. A fine-grit abrasive paper was placed in the bottom of the pan to ensure that the relative shear forces within the powder will be determined, rather than sliding friction between powder and pan. Powder was shaken onto the abrasive paper to form a rectangular section. One edge of the pan was placed against a reference mark, while the opposite edge was slowly tilted upward alongside a vertical ruler. When the powder moved, trigonometric principles were used to calculate the angle of shear. Results of testing at ANL and B&W are shown in Table 2.

Annealed powder was maintained in vacuum storage until needed. The tests at ANL were performed in the winter with typically 25-35% relative humidity. Testing at B&W took place during the summer in a humidity-controlled room with less than 64% relative humidity. Humidity was found to be an important factor in determining angle of shear. The powder adsorbed moisture immediately upon exposure to air. Moisture adsorption continued to affect the angle of shear until, in the case of Lot 10003, the pan was raised to the maximum possible angle vertically and the powder remained intact as a pile. It has not been determined why one powder lot was affected more by moisture than the others.

5.2 Surface Morphology

Three center samples were examined by scanning electron microscopy (SEM). Two different size ranges, >63 μm (+230 mesh) and <44 μm (-325 mesh), from each lot were studied. No significant differences in shape or surface were noted after visual inspection at magnifications of 75 to 800X for all six samples. All three lots were granular or complex-nodular (not spherical), which is characteristic of air-atomized powder. A typical SEM photograph of the aluminum powder is shown in Figure 6. For production-powder analysis, an imaging program such as Image 1.44 from the USA National Institutes for Health could be used to analyze for the average particle size and distribution.

Table 2. Comparison of Angle of Shear for B&W and ANL Aluminum Powder

Sample	B&W Lot 10003	B&W Lot 1770	ANL Lot CO-713
ANL Tests			
Top[1]	45°	45°	Not Measured
Center[1]	45° (46.0°)[2]	48°	45°
Bottom[1]	44°	47°	Not Measured
B&W Tests			
Center[1]	71°	49°	Not Measured
Center[2]	72°	46°	Not Measured
Center[3]	85°+	59°	Not Measured

[1]As-received powder.
[2]As-degassed powder.
[3]After 10-day exposure to room air.

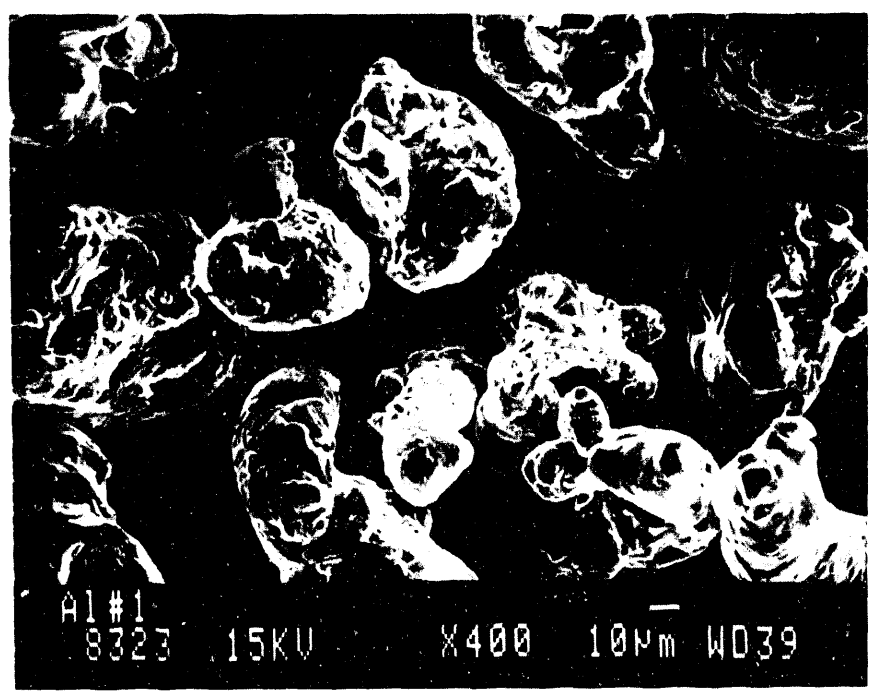

Figure 6. SEM Photomicrograph of >63 µm Lot CO-713 Aluminum Powder

6 SUMMARY AND RECOMMENDATIONS

A precise aluminum powder specification is a key step in consistently manufacturing acceptable powder-metallurgy-type fuel plates. ANL and B&W are working jointly (in conjunction with Oak Ridge National Laboratory and EG&G Idaho National Engineering Laboratory) to establish a standard specification for aluminum powder. It may be beneficial to the Research and Test Reactor Fuel Elements (RTRFE) community to establish an international standard for: powder type (atomized, flake, or granule), particle shape (globular, spherical, acicular, irregular, etc.), range limits for average particle size, particle size distribution, and surface area. An international standard would ensure uniformity in the materials used to manufacture fuel plates.

Receipt inspection and testing of aluminum powder lots are necessary before releasing the powder to the fabrication process. Because the original powder costs make up only a low percentage of the final finished fuel-plate cost, any lot not meeting the desired specifications should be rejected. In addition, a standard specification such as that for plutonium dioxide powder[9] may also need to be developed for the fuel powder.

REFERENCES

1. Standard Test Methods of Sampling Finished Lots of Metal Powders, American Society for Testing and Materials, Standard No. B 215, Vol. 02.05, 1982.

2. Standard Test Method for Sieve Analysis of Granular Metal Powders, American Society for Testing and Materials, Standard No. B 214, Vol. 02.05, 1986.

3. Standard Test Method for Average Particle Size of Powders of Refractory Metals and Their Compounds By the Fisher Sub-Sieve Sizer, American Society for Testing and Materials, Standard No. B 330, Vol. 02.05, 1982.

4. Standard Test Method for Particle Size Distribution of Refractory Metal-Type Powders by Turbidimetry, American Society for Testing and Materials, Standard No. B 430, Vol. 02.05, 1984.

5. Standard Test Method for Apparent Density of Free-Flowing Metal Powders, American Society for Testing and Materials, Standard No. B 212, Vol. 02.05, 1982.

6. Standard Test Method for Flow Rate of Metal Powders, American Society for Testing and Materials, Standard Number B 213, Volume 02.05, 1990.

7. Standard Test Method for Apparent Density of Non-Flowing Metal Powders, American Society for Testing and Materials, Standard No. B 417, Vol. 02.05, 1989.

8 Standard Methods for Chemical, Mass Spectrometric and Spectrochemical Analysis of Nuclear-Grade Uranium Dioxide Powders and Pellets, American Society for Testing and Materials, Standard No. C 696, Vol. 12.01, 1980.

9. Standard Specification for Nuclear-Grade Plutonium Dioxide Powder, Sinterable, American Society for Testing and Materials, Standard No. C 757, Vol. 12.01, 1983.

S E S S I O N III

September 28, 1992

LICENSING ASPECTS

Chairman:

H. Buchholz
(Hahn-Meitner-Institut, Germany)

HEU-LEU CONVERSION OF NON-POWER REACTORS LICENSED BY THE NUCLEAR REGULATORY COMMISSION

Theodore S. Michaels
U.S. Nuclear Regulatory Commisssion

NRC REGULATION ON HEU TO LEU CONVERSION FOR NON-POWER REACTORS - 10 CFR 50.64:

- Regulation became effective March 27, 1986
- No construction permits for HEU unless unique purpose
  - Experiments or long term goals that can use LEU and serve the national interest
  - Reactor physics or development based on HEU
  - Projects based on flux levels or neutron spectra requiring HEU
  - Reactor core whose design will not work without HEU
- All licenses with HEU prepare proposal for conversion to LEU
- Conversion to HEU contingent on:
  - Availability of government funds
  - Availability of suitable fuel
  - Unique purpose

STATUS OF NRC HEU-LEU CONVERSIONS AS OF 09/92

- 25 reactors with HEU in 1986
- 1 license terminated (Westinghouse Zion 10/88)
- 2 decommisioning orders, HEU fuel removed (Cintichem 11/91, Va. Cavalier 02/92)
- 1 planning to decommission, HEU fuel removed (Univ. of Washington)

The follwing 6 reactors have converted:

Rensselaer Polytechnic Inst.	100W	09/87
Ohio State University	500 kW	12/88
Worcester Polyrechnic Inst.	10 kW	12/88
Iowa State University	10 kW	08/91
Manhattan College	0.1 W	03/92
U. of Missouri Rolla	250 kW	07/92

- 15 reactors still have HEU
- 9 reactors have funding from DOE for safety analysis
- 1 will have funding from DOE safety analysis in FY-93
- 3 no funding or unsuitable fuel (General Atomic, General Electric has no funds, Mass. Inst. of Technology has unsuitable fuel)
- 2 requests for unique purpose exemption (National Inst. of Standards and Technology, U. of Missouri, Columbia)

STATUS OF FUNDED FACILITIES

FACILITY	SAR SUBMITTAL	FUEL AVAILABLE	REMARKS
Virginia	11/89	12/92	Safety analysis (SA) under review
Rhode Island	11/91	6/93	SA under review
Lowell	12/92	6/93	Argonne is doing transient analysis
Purdue	12/92	10/93	analysis in house with help from Argonne
Florida	12/92	9/93	Analysis in house
Georgia T.	12/92	12/93	Analysis in house with help from Argonne
Oregon St.	9/93	94	Minimal assistance (MA) from Argonne
U. of Wisc.	12/93	94	MA from Argonne
Wash. State	6/94	95	Considerable assistance (CA) from Argonne

FUELS APPROVED BY THE NRC

- Uranium Silicide in aluminum dispersion plate-type fuels, U_3Si_2-Al, NUREG-1313 reactors with this fuel - OSU, Iowa, Manhattan, U. of Mo. Rolla
- Triga - high-uranium content, low-enriched uranium-zirconium hydride fuels, NUREG-1282

- SPERT (Special Power Excursion Reactor Test), stainless-steel-clad uranium oxide (UO_2) fuel pins Nureg-1282, RPI has this fuel

- Uranium aluminide in aluminum was used at Worcester Poly. Inst.

CONTENTS OF APPLICATION TO NRC FOR AUTHORIZATION TO CONVERT TO LEU

- SAR - description and analysis of all safety factors affected by change from HEU to LEU (see graph on SAR details)

- Proposed changes in license, including tech specs

- Proposed quantities and duration of possessing both HEU and LEU

- Proposed changes in other license-related programs (plans) - if there are no changes provide statement to this effect with explanation

    - Physical security
    - Emergency planning
    - Operator re-training and/or requalification
      Outline of plan for retraining operators an how and when effectiveness will be verified

- Fuel load plan and reactor calibrations (before startup)
  Include fuel loading scenario, approach to critical, reactor startup, power, reactivity, and control rod calibrations and experience history of involved personnel

SAR DETAILS

Discuss the following for both HEU and LEU

- Fuel construction and geometry
  Composition and placement of fuel elements/rods

    - Grams U-235 per plate/rod
    - Number of elements/rods, partial elements/rods
    - fuel element/rod configuration

- Fuel storage

    - Storage of HEU and LEU
    - New fuel racks

. Critical operating masses of U-235

- Critical operating mass
- Sensitivity calculations of reactivity for different core configurations
- Comparison of prompt neutron lifetime and effective delayed neutron fraction

. Hydraulics and thermal-hydraulics
Maximum fuel temperatures

. Power density and power peaking
- Power distribution among fuel elements
- Power densities in fuel plates/rods
- Over power condition at which onset of nucleate boiling occurs

. Control rod worths for each rod

. Shutdown margin

. Excess reactivity

. Temperature, void, and doppler feedback coefficients

. Fission product inventory and fuel cladding thickness

. Potential accident scenarios
Discuss accident scenarios in original license or renewal applications affected by conversion from HEU to LEU

. Describe related facility changes, if any

OUTLINE OF REACTOR START-UP REPORT AND COMPARISON WITH CALCULATIONS

. Measure the following for HEU and LEU and compare with calculations for HEU and LEU

- Critical mass
- Excess (operational) reactivity
- Control and regulating rod calibrations
Measurements of differential and total rod worths
- Shutdown margin
- Thermal neutron flux distributions

. Reactor Power Calibration
Methods and Measurements that assure operation within the license limit, comparison between HEU and LEU nuclear instrumentation set points, detector positions and detector output

. Partial fuel element worths for LEU
Measured for different numbers of plates for which the fuel is capable; comparison with calculations

- Discuss how compliance with void and temperature coefficient values in tech specs is to be assured. Compare with any calculations

- Explain any significant differences in the values previously measured or calculated which have an impact on both the normal operation and potential accidents with the reactor

- Measurements made during initial loading of the LEU fuel, presenting subcritical multiplication measurements, predictions of multiplication for next fuel additions, and prediction and verification of final criticality conditions

S E S S I O N IV

September 28, 1992

REACTORS DURING AND AFTER CONVERSION TO LEU

Chairman:

Y. Futamura
(JAERI, Japan)

CONTINUED CONVERSION OF THE R2 REACTOR TO LEU FUEL

Erik B Jonsson and Rune Håkansson
Studsvik Nuclear AB

ABSTRACT

A gradual conversion of the R2 reactor in Sweden started in January 1991. This transient conversion, which was optimized to utilize all the HEU fuel, have proceeded according to plans and the change is expected to be completed at the end of 1992. The first LEU elements were loaded in January 1991 and since then 80 LEU elements have been used in 29 different core layouts.

The change to LEU has been quite undramatic as the LEU fuel design was chosen rather conservative. Apart from some power peaking problems in the beginning the conversion has not created any serious problem.

The initial large power peaking in fresh LEU bundles adjacent to the high burned HEU control rod followers required some precaution and was solved by a premature loading of LEU control rod followers.

Irradiation of seven LEU lead elements started in 1987 and they have now been exposed to high burnups. Weighing has shown that the swelling of the fuel plates is less than 2% even at fission densities of 1.8E21 fissions/cm3.

BACKGROUND

The Swedish R2 reactor has since the beginning of 1991 gradually been changing to LEU operation by inserting 4 to 8 fresh LEU bundles for each three week cycle. This transient conversion was necessary from the fuel economy point of view with a large stock of partly burnt HEU fuel available.

Paper to be presented at the 15th International Meeting on Reduced Enrichment for Research and Test Reactors in Roskilde, September 1992.

TRANSITION CORES

In 1991 and 1992 the R2 reactor has operated with 29 different loading patterns and with an increasing number of LEU fuel elements. No fresh HEU fuel has been added during this period. However, there are still some 40 HEU elements that are not fully burnt and the cores contain 10 to 20 % of HEU elements.

During this period the number of fuel elements in the core has varied between 47 and 49 plus 6 control rods with 9 to 11 irradiation positions in the 8x8 core matrix.

The gradual increase of LEU elements in the core is shown graphically in figure 1.

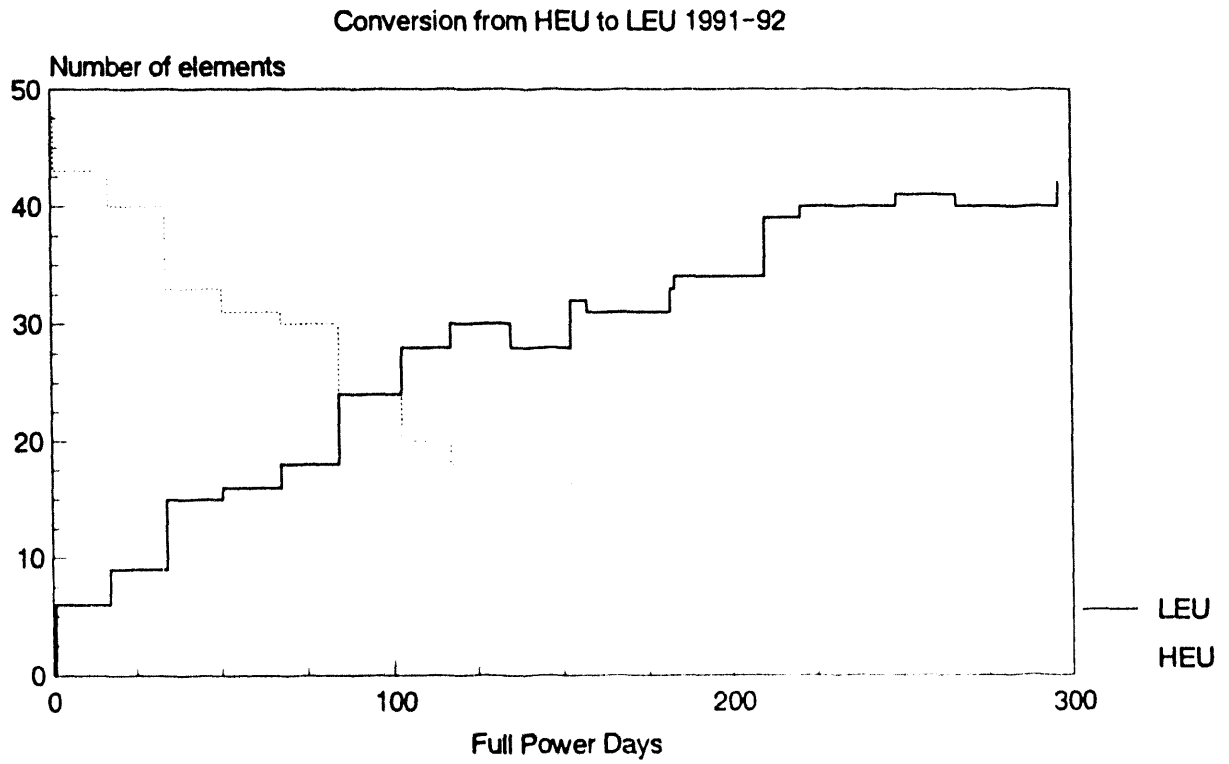

Figure 1. HEU and LEU Fuel Element Loadings 1991-92

The loading principles for the cores have been rather pragmatic with the requirements of the different experimental positions guiding the loading.

SWELLING MEASUREMENTS ON LEU LEAD ELEMENTS

In the framework of the RERTR program an agreement between Studsvik and ANL irradiation of 7 LEU lead elements were started in 1987. The program has been described in earlier RERTR meetings [2].

The test elements were divided into two groups, one group with conservative 323 g U235 per element and one group with 490 g U235 per element. A summary of the irradiation history for all 7 elements up to August 1992 is given in Table 1.

Table 1. Irradiation data for LEU demo elements

Element Name	Initial U235 (g)	Reactor Days	Fissions *E21/cm3	Burnup U235 (%)
CA011	490	358	1.58	79
NM021	490	333	1.65	79
BW 01	325	239	0.93	68
BW 02	325	217	0.98	71
BW 03	325	188	0.90	65
BW 04	490	325	1.61	78
BW 05	490	311	1.31	63

According to the irradiation plan the elements were to be weighed in the pool at intervals to monitor the swelling of the plates. The first results [2] were confusing and inconsistent so we had to reconsider the methodology. The formation of aluminumoxide on the surfaces was found to be an important part of the change in weight. We found that a 10 micron oxide layer formed for each 4000 h power operation [3]. No provision was taken for formation of oxide during the shut down periods.

After correction for increase of weight due to the oxide growth and for loss of neutron mass the swelling was calculated from the change in weight. The results are shown in figures 2 to 4. Five of the elements increase in plate volume by about 1 % per 1.E21 fissions/cm3, but 2 of the elements BW 04 and BW 05 are decreasing in volume. We have not a good explanation for this behavior, it could be caused by a much faster oxide layer formation on these elements.

Our conclusions from these tests are that the weighing method could give a rough estimate of the swelling behavior for specific fuel element constructions and operation conditions. The results suggest that the R2 fuel loading of 400 g U235 is conservative as a maximum of 2.2E21 fissions/cm3 achievable. (For the safety evaluations it ought however be complemented with channel width measurements.)

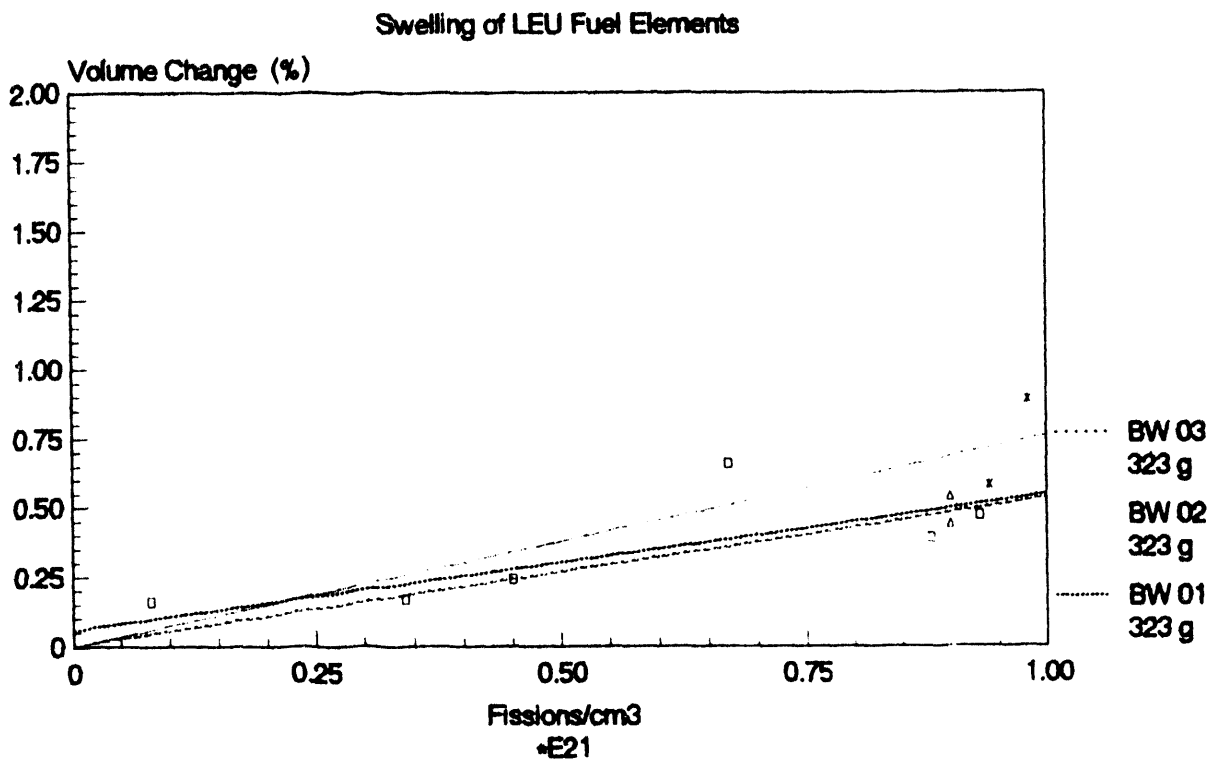

Figure 2. Estimated fuel plate swelling of test LEU elements BW 01, BW 02 and BW 03.

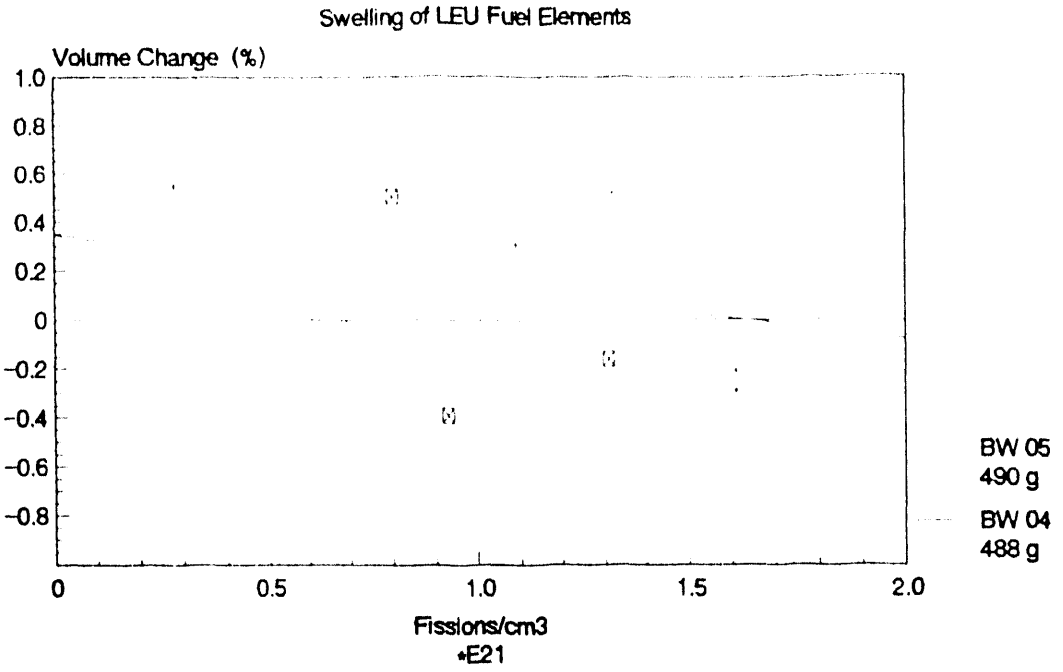

Figure 3. Estimated fuel plate swelling of test LEU elements BW 04 and BW 05.

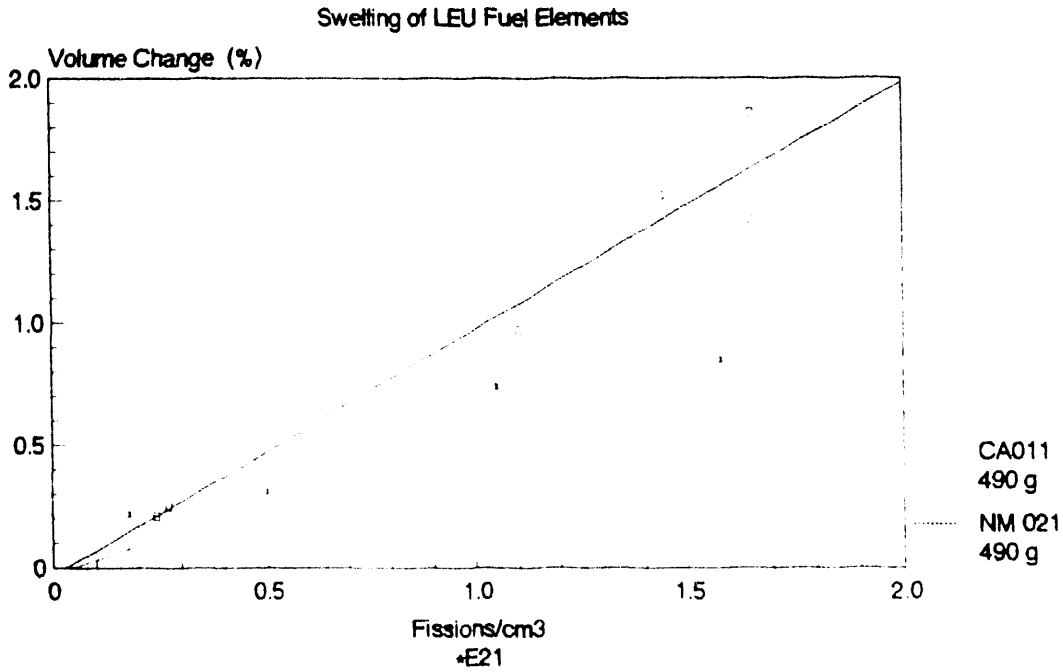

Figure 4. Estimated fuel plate swelling of test LEU elements CA 011 and NM 021.

POWER PEAKING

The low enriched LEU fuel in HEU cores created power mismatch problems due to the large difference in absorption cross section for the new fuel compared to the highly burnt HEU fuel. This problem was accentuated around the HEU control rod followers, which are normally burnt to more than 90% burnup.

The detailed calculations on this problem were reported in last RERTR-meeting [1]. To solve the problem permanently the HEU control rod followers were replaced in advance and only the fine control rod were kept as a HEU element.

CALCULATIONAL METHOD

The flux and power mismatch between HEU and LEU fuel assemblies has been studied with the CASMO-3 code. CASMO is a two-dimensional, multigroup transport code for the calculation of the eigenvalue, flux and power distribution as function of depletion in pin cells and on LWR fuel assemblies. The code is capable of handling fuel rods, absorbing rods and absorbing slabs. The feature of the code is the ability to perform detailed transport theory calculations in 70 groups with standard cross section library based on ENDF/B V.

The CASMO code is normally used to produce burnup dependent, homogenized, two group cross sections for 3-D nodal or diffusion core analysis codes. The code has no option for plate type fuel, so the LEU (or HEU) plates have to be modeled as equivalent fuel rods. Each type of fuel element is thus modeled and depleted to give the burnup dependent cross sections and isotopic compositions.

REFERENCES

1. E. B. Jonsson, "Importance of Power and Flux Mismatch Between HEU and LEU Elements During a Gradual Conversion" Proceedings from the 14th International Meeting on Reduced Enrichment for Research and Test Reactors in Jakarta, November 1991.

2. I Pazsit, K. Saltvedt, "Experience with the RE Fuel Transition at the Studsvik R2 Rector," Proceedings from 12th International Meeting on Reduced Enrichment for Research and Test Reactors in Berlin, September 1989.

3. Report from the Advanced Neutron Source (ANS) Aluminium Cladding Corrosion Workshop 21(5), 20451 INIS

STATUS OF THE UNIVERSITY OF VIRGINIA REACTOR LEU CONVERSION

R.A. Rydin
Department of Mechanical, Aerospace and Nuclear Engineering
University of Virginia
Charlottesville, Virginia, USA

ABSTRACT

The University of Virginia began working on converting the CAVALIER and UVAR reactors to LEU fuel in the Spring of 1986. Early in 1987, based on reactor use considerations, a decision was made to shut down the CAVALIER. A decommissioning plan was submitted to the NRC, and the decommissioning order was issued in early 1992. There is now a tentative agreement to donate the CAVALIER equipment without fuel to the University of North Texas. Design calculations for the UVAR were completed, and the Safety Analysis Report was submitted to the NRC in late 1989. The DOE/EG&G order to manufacture UVAR fuel was placed at B&W in March 1992, and conversion is expected to take place early in 1993.

DESCRIPTION OF THE UVAR FACILITY

The UVAR is a 2 MWT swimming pool-type research reactor. It is made up of plate-type MTR fuel elements mounted on an 8-by-8 grid plate that is suspended from a movable bridge above a large, open pool of water. The reactor can be moved to either end of the pool while the other pool half is drained for maintenance purposes. However, the core can only be operated at full power when it is mounted at the South end of the pool, directly above a coolant funnel that provides forced down-flow circulation. This position is shown in Figure 1, which also shows the location of the experimental beam ports.

The original UVAR design was done by J.L. Meem [1] et al., circa 1960, using analytical two-group theory. The Technical Specifications (TS) require maintenance of a minimum shut-down margin of 0.4% $\Delta k/k$ with the largest worth shim rod fully withdrawn, and a maximum excess reactivity of 5% $\Delta k/k$. Any core arrangement that will fit on the grid plate and that meets this TS can be used, providing that the control rods are experimentally recalibrated each time a new core arrangement, not previously tried, is assembled. The UVAR has been operated for more than twenty five years using experimental techniques to determine TS compliance. During this time, both 12-flat-plate fuel elements and 18-curved-plate HEU fuel elements have been used in separate cores, and arrangements having anywhere from 16 to 27 fuel elements have been operated. Some cores have been entirely water reflected, and others graphite reflected, while most cores have had water on some sides and graphite on the others.

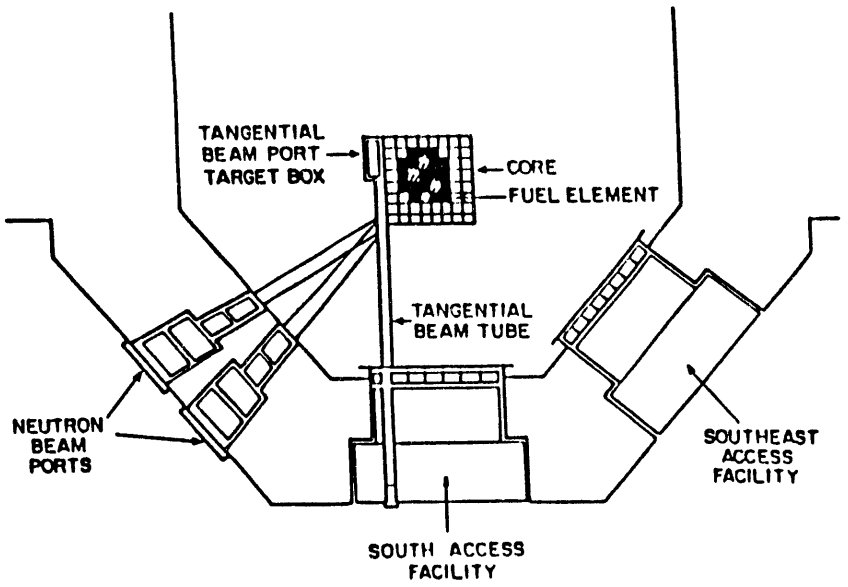

Figure 1. Sketch of UVAR Pool Showing 8-by-8 Grid Plate

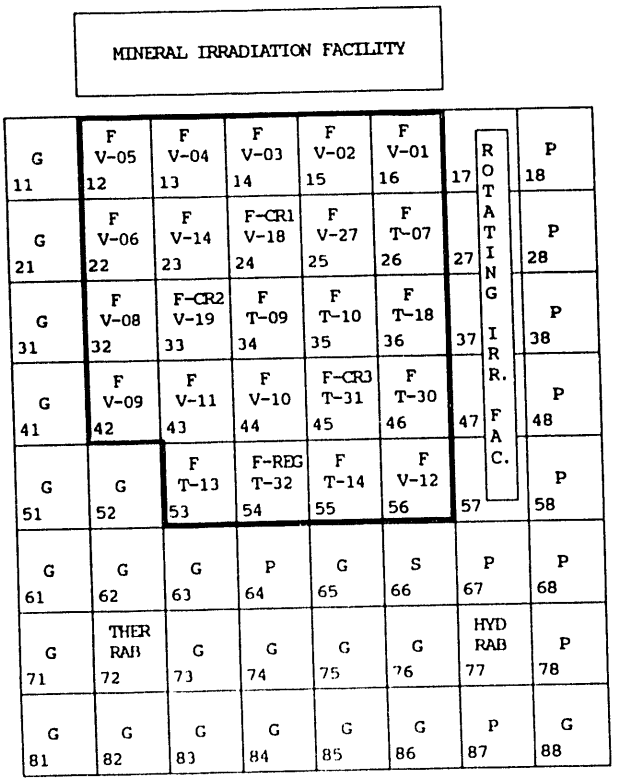

Figure 2. Recent 24-Element UVAR Fuel Loading, Showing Experimental Facilities

A recent 24-fuel-element HEU core loading diagram of the UVAR is shown in Figure 2, which illustrates the positions of our Epithermal Mineral Irradiation Facility, used for color enhancement of topaz, and our Rotating Irradiation Facility, used for activating Iridium seeds for brachytherapy. Thermal neutrons extracted from the Southeast corner of the core through a beam tube are used for Neutron Radiography experiments. We are now beginning to examine the feasibility of using the Southwest Access Port for Boron Neutron Capture Therapy work, either for melanoma treatments (thermal neutrons) or brain tumor therapy (epithermal neutrons).

LEU DESIGN STUDIES

In order to make the LEU design problem tractable, we picked three fixed core arrays (4-by-4, 4-by-5 and 5-by-5) as the bases of comparison, and did core-life calculations with HEU-18-plate fuel and LEU-18 and LEU-22-plate replacement fuel [2]. All LEU cores start out with a somewhat lower k_{eff} than the corresponding HEU cores because they have a harder neutron spectrum and a consequently greater leakage. The burnup curves for LEU are less steep than for HEU, and therefore the excess reactivity curves eventually cross as depletion increases. However, for the 4-by-4 core, the lower initial k_{eff} of LEU-18 fuel cannot be overcome by the decreased burnup slope before the excess reactivity crosses zero, and therefore LEU-18 fuel will not last as long as HEU-18 fuel. On the other hand, LEU-22 fuel will have comparable performance to HEU-18 fuel.

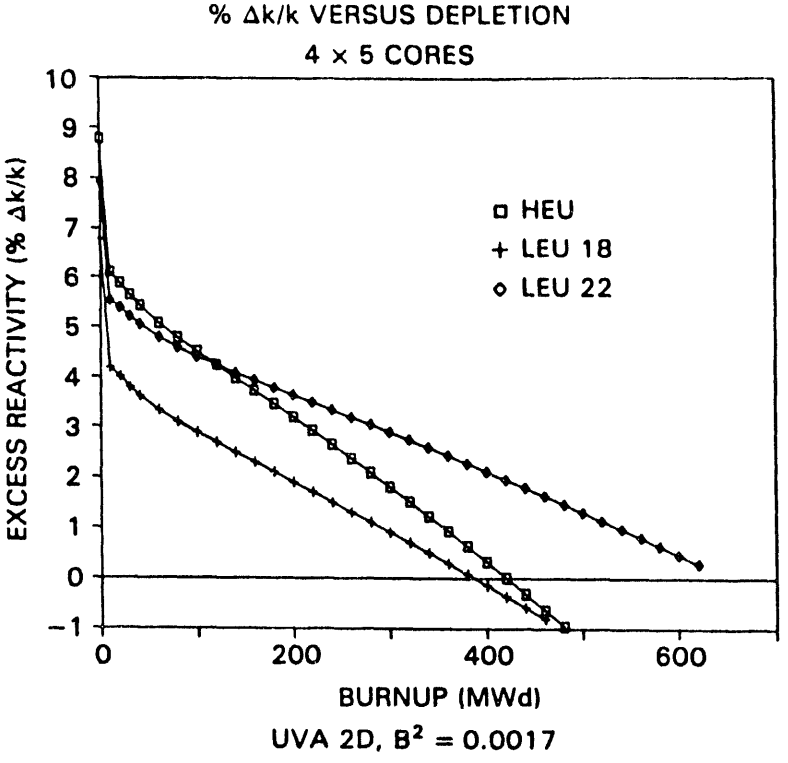

Figure 3. Unshuffled 4-by-5 Array, Depletion of HEU and LEU Cores Using 2DBUM

For a 4-by-5 array, as seen in Figure 3, one finds that both the LEU-18 and HEU-18 fuel reach an asymptotic behavior, and these cores attain essentially equal burnup at the same point in life where the excess reactivity crosses zero. On the same basis, LEU-22 fuel lasts about 50% longer than LEU-18 fuel, even though the uranium loading is only 20% greater.

A similar behavior is seen for the 5-by-5 core models. Again, the HEU-18 and LEU-18 cores have essentially the same endpoint, while the LEU-22 core lasts about 50% longer. But the most interesting result is that the LEU-22 core in a 4-by-5 array lasts almost as long as an LEU-18 core in a 5-by-5 array. This means that an LEU-22 core can be kept in a 4-by-5 configuration, with attendant higher average thermal flux for experimental purposes, and still operate almost as long as our previous larger cores.

The best replacement option for the UVAR appears to be the use of 22-plate LEU fuel assemblies in a fixed 4-by-5 core array. We will seriously consider the adoption of a shuffle pattern recommended by ANL. On the other hand, it is to our advantage to retain the flexibility of loading UVAR cores to meet experimental needs.

THERMAL HYDRAULIC ANALYSIS

The UVAR thermal hydraulic analysis makes use of three basic computer code packages, PARET, THERHYD and NATCON. The PARET code from ANL was used to calculate an envelope of maximum achievable power transients, based upon pump coastdown and period trips, all accompanied by Scram. The net result of all of the PARET analyses is the finding that the control rod release and insertion times are the limiting factors for the UVAR, and that temperature feedback plays only a minor role. The responses for both HEU and LEU cores are quite similar. Transients not accompanied by Scram are argued to fall within the SPERT Experiment envelope.

The NATCON code from ANL was used to calculate the limits of core performance under natural convection conditions. The primary results are that adequate natural convection cooling exists for LEU-22 cores that are operated beneath our allowable TS limit of 200 kW. The use of additional fuel plates in our fuel elements increases the amount of natural convection cooling available.

The main tool for our thermal hydraulic analysis is the THERHYD code [3], developed at UVA in 1967. This code is used to calculate limiting-power versus system-flow envelopes for the UVAR, below which all PARET transients must lie. The code handles forced convection down-flow, using an axial power distribution fit and planar peaking factors from 2DBUM. The limiting condition is given using a burnout ratio of 1.49 (99% confidence that burnout will not occur) and taking into account channel and loading tolerances and bypass flow.

The peaking factors obtained from 2DBUM are shown in Table 1 for all of the cores that have been analyzed [2]. Also shown is an older experimental measurement [4,5], scaled up to an 18-plate HEU fuel element. In general, the calculated peaking factors are a bit larger than the measured value, but lie within the experimental uncertainty.

Table 1. Planar Power Peaking Factors

CORE CONFIGURATION	CALCULATED	EXPERIMENTAL*
HEU-18 4-BY-4	1.59	1.45 ± 0.15
LEU-18 4-BY-4	1.64	
LEU-22 4-BY-4	1.69	
LEU-18 4-BY-5	1.73	
LEU-22 4-BY-5	1.78	

*Scaled From 12-Plate Measurement

When these data were employed in THERHYD, we obtained limiting-power versus system-flow curves. The overall conclusion is that for forced convection the LEU fuel is only slightly worse than HEU fuel from a thermal hydraulic standpoint. This result will require a small revision in the minimum safety system settings for the UVAR when it is converted. Otherwise, the small 4-by-4 core is more limiting than the larger 4-by-5 core (due to a higher average heat flux), and the 22-plate fuel element is more limiting than the 18-plate fuel element (due to manufacturing tolerances).

In more recent work, the flow coastdown characteristics of our present coolant pump were measured in order to compare it to the old pump data used in the previously-reported analysis. The new data are plotted in Figure 4, where it is seen that we actually have more initial flow and a longer flow coastdown time than was assumed earlier. Hence, we have a considerably greater margin of safety than was previously reported.

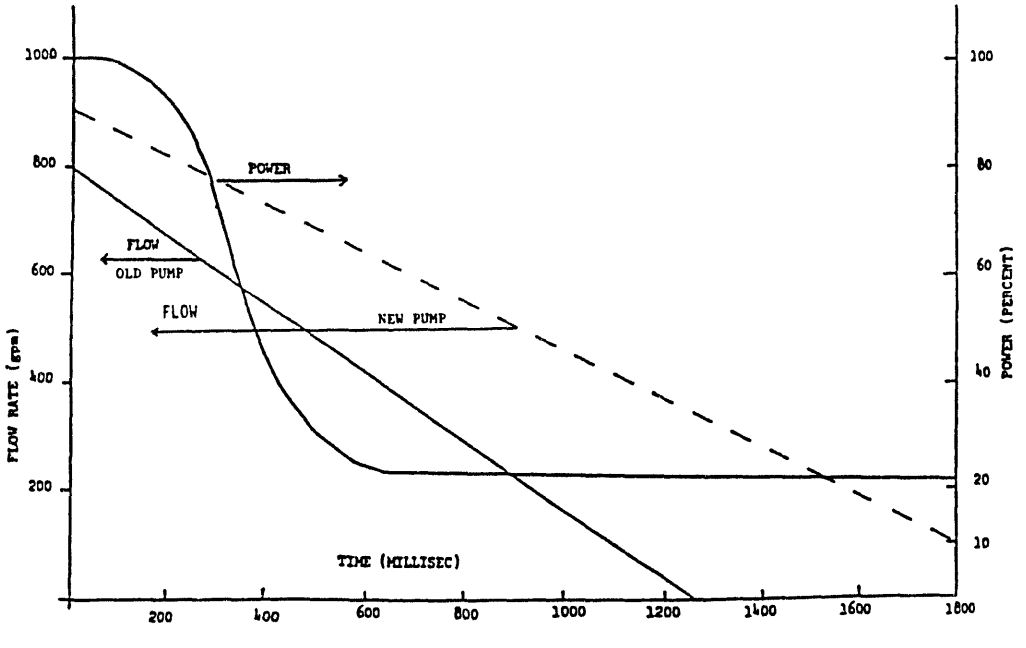

Figure 4. Comparison of Flow Coastdown Curves for the Old and New Pumps.

UNIVERSITY OF VIRGINIA REACTOR CORE LOADING DIAGRAM

Proposed

CORE LOADING LEU- 1 SHUTDOWN MARGIN ____ % delta k/k

DATE ____ EXCESS REACTIVITY ____ % delta k/k

U-235 ____ GRAMS ____ EXPERIMENT WORTH ____ % delta k/k

F - Normal Fuel Element
PF - Partial Fuel Element
CR - Control Rod Fuel Element
G - Graphite Element
S - Graphite Source Element
REG - Control Rod Fuel Element with Regulating Rod
P - Grid Plate Plug
HYD RAB - Hydraulic Rabbit
THER RAB - Thermal Pneumatic Rabbit
EPI RAB - Epithermal Pneumatic Rabbit
RB - Radiation Basket

Rod Worths #1 - ____ % #2 - ____ % #3 - ____ % Reg - ____ %

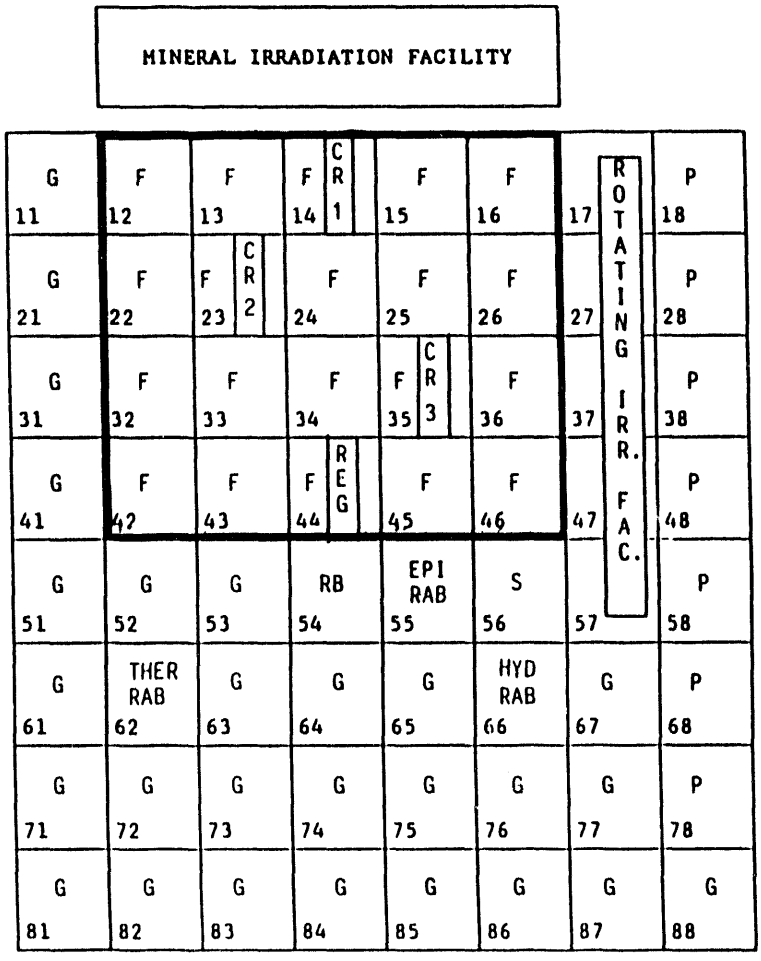

Figure 5. Proposed loading Diagram for Core LEU-1

TESTING PLAN FOR UVAR LEU CORES

A Safety Analysis Report (SAR), based upon information reported at the 12th RERTR meeting in Berlin [2], was submitted to the Nuclear Regulatory Commission (NRC) in November 1989. A series of questions were asked by NRC in November 1990; primarily, we were requested to prepare a detailed plan to test the new LEU core, and to supply an analysis of fission product inventories in our new core. Our response was submitted to NRC in February of 1991 and included revised thermal hydraulics data, based upon the use of an "aluminum softening" criterion as reported at the 13th RERTR meeting in Newport, RI, [6]. We also included the revised pump data shown in Figure 4.

Specifically, we propose to test both a 4-by-4 LEU core array, and the 4-by-5 core array shown in Figure 5. Our measurements will include control rod worths, shutdown margin, excess reactivity and pressure drop. We will then do flux measurements to determine if the peaking factors are consistent with those reported in Table 1, and assess the impact of this information on our Thermal Hydraulic Analysis. Eventually, we will also do temperature coefficient and void coefficient measurements.

FISSION PRODUCT INVENTORIES

Using Sandia-ORIGEN, a well-documented code which calculates detailed isotopic compositions as a function of time in nuclear reactor fuel irradiation problems, uranium fuel concentrations, power, and time were input to determine the nuclide concentrations due to irradiation of the UVAR fuel.

The code is a point code (no spatial dependence) and therefore, the core geometry is not a factor in the calculation. The calculations were done using the fuel concentration per element and an average power per element based on a total core power of 2 MW. (The core is assumed to contain 16 normal elements and 4 control rod elements). Two irradiation times (120 days and 720 days, both 2 MW, 24 hr/day) were used for comparing the LEU and HEU cores. Also a 1440 day cycle (24 hr/day, 2 MW), far exceeding the length of time an element would be in the core, was used for evaluating the maximum fission product build-up in the LEU core.

The results of the code showed that fission product inventories, excluding actinides, were similar (within grams) between HEU and LEU cores. When activities of fission product elements (708 nuclides are listed in the code output, comprising 41 elements) are compared, following a 120 day decay period less than a 10% difference is noted and the activity of the LEU core is less than the HEU core. U235 burn-up amounts and core flux levels fell within 10% of the expected or known values.

The major actinide produced is plutonium which constitutes about 90% of the actinide concentration. This is expected because of the large increase in U238 when going from HEU (12 g/elem.) to LEU (1100 g/elem.). However, even after a 1440 day continuous run at 2 MW, the Pu concentration in LEU fuel is less than 15 grams/elem. This is still not a significant amount, representing $< 2\%$ of the Uranium inventory. Only plutonium deviates > 0.1 g/element between HEU and LEU cores.

Table 2. UVAR Radioisotope Inventories

INVENTORY PER ELEMENT	120 DAY HEU	120 DAY LEU	720 DAY HEU	720 DAY LEU	1440 DAY LEU
FISSION PRODUCT ACTIVITIES	5.23E5 Ci	5.26E5 Ci	4.86E5 Ci	4.89E5 Ci	4.96E5 Ci
FISSION PRODUCT ACTIVITY: (Irrad. + 120 day decay)	8.53E3 Ci	8.52E3 Ci	1.65E4 Ci	1.62E4 Ci	1.93E4 Ci
Pu. + FISSION PRODUCTS:	14.04 g	14.93 g	82.68 g	89.20 g	117.6 g
TOTAL PLUTONIUM:	0.09 g	0.93 g	0.35 g	5.53 g	11.9 g
TOTAL URANIUM:	164.7 g	1377.0 g	95.07 g	1302.0 g	1212.0 g

HISTORY OF THE CAVALIER REACTOR

The CAVALIER 100 watt training reactor went into operation in 1974 when the University of Virginia had a large undergraduate Nuclear Engineering program. Despite a significant reduction in the undergraduate population during the late 1970s, the CAVALIER was extensively used in the early 1980s while the UVAR was being operated around-the-clock for EPRI-sponsored pressure vessel steel radiation damage studies. However, when the EPRI program terminated, use of the CAVALIER almost stopped, although regulatory surveillance requirements continued.

Our original intention in 1986 was to convert both the UVAR and the CAVALIER reactors to LEU fuel. However, the significant Staff effort needed to maintain the CAVALIER license could no longer be justified, and a decision was made early in 1987 to shut the CAVALIER down. At first we asked the NRC for permission to dismantle the CAVALIER and retain a possession-only license. The NRC preferred that we decommission the reactor. The reactor was defueled in March 1988, and TS surveillance requirements were then simplified.

A decommissioning plan was submitted to the NRC early in 1990, and an NRC order to dismantle and dispose of the component parts was issued in February 1992. As a result of a contact at a TRTR meeting in 1991, the University of North Texas at Denton had earlier expressed an interest in acquiring UVa's subcritical facility. In July of 1992, a donation transfer agreement was being processed for both the subcritical facility and for all CAVALIER components except the fuel and core tank. If these arrangements are consummated, the CAVALIER will eventually be relicensed in Texas as an LEU reactor.

CONCLUSION

The order for new LEU fuel for the UVAR reactor was placed by DOE/EG&G

at Babcock and Wilcox in March 1992. We will receive a minimum core load plus enough extra fuel for around-the-clock operation for a year. This constitutes 26 full fuel elements, 5 control elements, 2 partial elements and 2 dummy elements. The estimated replacement cost per element is approximately $20,000, making the total order worth approximately $600,000. The dummy elements are expected to be available for trial fitting in the core grid plate in late September, and the first LEU core is expected in December 1992. Conversion will tentatively take place early in 1993, subject to availability of a spent-fuel shipping cask and acceptance of spent HEU fuel at a government facility.

The total amount of money supplied to UVa by DOE for design studies amounted to $120,000. This financed 3 Master of Science theses [7,8,9], plus partial support of several other students. Unreimbursed costs to the University amount to about $40,000, with further Faculty and Staff costs expected during the LEU first-core testing phase. Over the long term, the use of the longer-life 22-plate fuel elements will produce savings in staff time for refuelling activities, require fewer spent fuel shipments, and reduce the cost to DOE of resupplying fuel for the UVAR.

REFERENCES

1. J.L. Meem, Two Group Reactor Theory, Appendix A, Gordon and Breach Science Publishers, New York, N.Y., 1964.

2. R.A. Rydin, D.W. Freeman, B. Hosticka and R.U. Mulder, "Safety Analysis for the University of Virginia Reactor LEU Conversion", Proceedings of the XIIth International Meeting, Reduced Enrichment for Research and Test Reactors, Berlin, FRG, 10-14 September 1989, pp 211-226.

3. J.A. Dahlheimer, "Thermal-Hydraulic Safety Analysis of a Pool Reactor", M.S. Thesis, University of Virginia, 1967.

4. W.K. Brunot, "An Analysis of Fuel Element Surface Temperature and Coolant Flow Rate in the University of Virginia Reactor," M.S. Thesis, University of Virginia, 1961.

5. R.L.J. McGuiness, "Thermal-Hydraulic Safety Analysis of 18-Plate Reactor Fuel Elements", B.S. Thesis, University of Virginia, 1973.

6. B. Hosticka, C. Mora and R.A. Rydin, "State of the LEU Conversion Effort at the University of Virginia Reactor, Proceedings of the XIIIth International meeting, Reduced Enrichment for Research and Test Reactors, Newport, RI, 23-27 September 1990.

7. M.K. Fehr, "Design Optimization of a Low Enrichment University of Virginia Nuclear Reactor," M.S. Thesis, University of Virginia, January 1989.

8. S. Wasserman, "Effective Diffusion Theory Cross Sections for UVAR Control Rods," M.S. Thesis, University of Virginia, January 1990.

9. D.W. Freeman, "Neutronic Analysis for the UVAR Reactor HEU to LEU Conversion Project," M.S. Thesis, University of Virginia, January 1990.

COMPLETION OF THE OSURR FUEL CONVERSION AND POWER UPGRADE

J. W. Talnagi* and T. Aldemir**

*The Ohio State University Nuclear Reactor Laboratory
1298 Kinnear Road, Columbus, Ohio 43212 U.S.A.

**The Ohio State University, Nuclear Engineering Program
206 West 18th Avenue, Columbus, Ohio 43210 U.S.A.

ABSTRACT

The 10 kW Ohio State University Research Reactor (OSURR) went critical with the standardized 20% enrichment U_3Si_2 – Al fuel elements on 15 December 1988 and has been operating at power levels up to 500 kW since 19 December 1991 with natural convection core cooling. The computational and engineering work related to the conversion/upgrade process is described.

INTRODUCTION

Conversion of The Ohio State University Research Reactor (OSURR) began in August, 1985, with the award of a DOE grant, matched in part with University funds, for a program to convert the OSURR fuel from 93% enrichment UAl fuel to a nominal 20% enrichment U_3Si_2 – Al fuel, and in the process increase the operating power from 10 to 500 kW steady-state thermal output. The program consisted of three phases: analyses of the low- enrichment uranium (LEU) fueled OSURR core under various operating conditions, licensing activities including the submission of a Safety Analysis Report (SAR) for the upgraded, LEU fueled OSURR, and facility engineering related to both LEU conversion and power upgrade.

This paper will provide a summary of the overall program, including discussion of the conversion/upgrade program history, results obtained and experience gained and an evaluation of the program benefits to the OSURR.

BACKGROUND

OSURR Operational History

In many ways, the history of the OSURR facility is typical of university- based research reactors in the United States. Initial construction funds were provided in part by the Atomic Energy Commission, the predecessor agency of the U.S. Department of Energy (DOE), with the intent of providing a research and educational facility for The Ohio State University and other educational institutions. Construction began in 1960, with completion and initial operation of the reactor in 1961. The design chosen was based on the original MTR design, and construction patterned after the Bulk Shielding Reactor (BSR) at Oak Ridge National Laboratory. The Nuclear Products Division of the Lockheed Georgia Company was the reactor system supplier.

Operating power was deliberately restricted to 10 kW steady-state thermal output for several reasons. First, it was thought that for a facility whose primary mission was to be instruction and education, the ability to perform precise, repeatable core physics experiments would be of primary importance. Second, because of the geographical proximity of the Battelle Memorial Institute's research reactor (a 2 MW facility), a high-flux reactor would be available and relatively affordable for researchers desiring higher flux levels. Also, the University did not wish to engage in the relatively complex operations of fuel management and offsite shipment of irradiated fuel, as is required for higher power reactors. Finally, it was thought that adequate University funding would be made available to the OSURR to continue its operation as a primarily instructional facility for the lifetime of the reactor.

System Description

As noted above, the OSURR is patterned after the MTR/BSR designs, featuring an open reactor pool containing a light-water moderated reactor core, with a total of four control rods. Initial core loading was with high-enrichment uranium (HEU) fuel elements of the flat-plate, picture frame type, with a nominal 3-inch by 3-inch cross-section. The HEU fuel elements also had a cylindrical lower end box which allowed insertion into a grid plate having a 5 x 6 array of possible fuel positions, thus allowing up to 30 elements to be placed on the grid plate. Experimental facilities included an air-filled central irradiation tube (denoted the CIF, for Central Irradiation Facility), a set of graphite-bearing isotope irradiation elements (GIIEs), a pneumatic transfer system (Rabbit), and two 6-inch inner-diameter beam ports located along one edge of the core. The OSURR core is reflected on two sides by graphite slabs forming the end extensions of graphite-loaded thermal columns.

OSURR control rods consist of three shim safety rods and a single regulating rod. The shim safety rods are grooved stainless steel, oval-shaped solid rods having a nominal 1.5%-weight natural boron concentration, while the regulating rod is solid, ungrooved stainless steel. The poison section length of the shim safety rods is a nominal 61 centimeters.

The OSURR reactor pool is 20 feet deep, with a minimum depth of 15 feet above the core, and contains 5800 gallons of demineralized, filtered light water. The core is cooled by natural convection, with the bulk pool temperature at near room temperature and the pool surface at atmospheric pressure.

Operation of the HEU-fueled OSURR at 10 kW required loading of a core with a 5 x 5 fuel element array, with the CIF occupying the central grid position, and the control rods positioned symmetrically within this array. A row of graphite- bearing elements was loaded in the remaining 5 x 1 row of grid plate positions. This arrangement, denoted as Standard Core I, was the nominal OSURR core configuration, utilizing the original HEU fuel elements, for over 25 years. During this time, which included regular fuel element inspections and pool water radionuclide assays, no abnormal fuel element behavior was noted.

Facility Utilization

OSURR utilization is typical of that for low and intermediate power research reactors in university settings. Instructional utilization accounts for about one-half of all operational hours, with various experiments and research use accounting for the remainder of operating hours. Instructional utilization includes various student laboratory exercises such as subcritical multiplication and approach to critical experiments, flux mapping, control rod worth measurements, reactor transfer function determination, void coefficient measurement, and analysis of delayed neutron parameters. Research use includes material irradiation, neutron activation analysis, neutron radiography, neutron spectral measurement, and boron neutron capture therapy. Typical OSURR energy output when licensed for 10 kW maximum power was about 2000 kW-hours per year.

Conversion/Upgrade Program

Initial consideration of converting the OSURR to LEU fuel began in 1984, when it became clear that the U.S Nuclear Regulatory Commission (NRC) would likely pass a rule requiring the use of LEU, where feasible, in domestic, non- power research reactors falling under the NRC's jurisdiction. In March, 1985, a proposal was submitted to DOE to provide funds, to be matched in part by the University, for LEU conversion and power uprating of the OSURR. Ideally, DOE funds would be directed towards fuel conversion activities, while University funds would support the power upgrade effort. The DOE award was made in July, 1985, with work beginning in August, 1985.

The overall purpose of the program was to accomplish fuel conversion to DOE- standard U_3Si_2 – Al LEU fuel while concurrently increasing the OSURR operating power from 10 to 500 kW steady-state thermal power. Towards these ends, the following goals were established:

1. Complete removal of the original HEU fuel, with eventual shipment to DOE's Savannah River Plant for reprocessing, and replacement with DOE-standard U_3Si_2 – Al LEU fuel.
2. Restoration of OSURR operations at power levels up to 10 kW using an LEU core, measurement of safety-related core parameters.
3. Concurrent facility engineering activities directed towards installation of a heat removal system to allow power operations above 10 kW.
4. A stepwise increase in OSURR operating power, ultimately reaching 500 KW, with various engineering measurements performed at each chosen operating power level step.

The overall motivation for undertaking this program was twofold. First, fuel conversion would meet the impending NRC requirement and provide a "test case" for the planned licensing process. Second, the operational situation had changed from that which was present when the OSURR was initially planned as a low-

power instructional facility. The Battelle Research Reactor was decommissioned in mid-1970's. This made a high flux facility relatively diffucult to access conveniently. Also, university support for the OSURR operations was substantially reduced in the early 1980's and it became necessary to generate a substantial part of the facility budget from outside funding. To do this, it was necessary to broaden the potential user base which would be facilitated by having higher fluxes available to the users. A 500 kW power level was chosen since it would provide a central core flux at about 10^{13} neutrons/cm^2.s and allow various material irradiation experiments while maintaining natural convection as the primary heat removal mechanism.

The program was organized into two working groups: the analytical and computational personnel, and the licensing and engineering group. Naturally, close communication between the two groups was established since the work of one would necessarily affect that of the other. It turned out that the majority of personnel assigned to the analytical group consisted of Nuclear Engineering Program graduate students and faculty, while the engineering group was composed largely of OSURR operating staff, supplemented by private consultants and engineering firms, when necessary.

Program progress and results to date have been largely reported in previous publications and presentations.[1-10] Briefly, the overall program started in August, 1985, with the computational and analytical studies taking approximately two years to complete. These studies are summarized in the following section. Results of the analytical and computational work were used to write a Safety Analysis Report (SAR) for the OSURR fueled with LEU, and operating at power levels up to 500 kW. The SAR was submitted to the NRC in October, 1987. After resolution of NRC's questions and points of contention, an Order from the NRC requiring LEU conversion of the OSURR was issued on 27 September 1988. This Order appeared in the Federal Register (FR) on 4 October 1988, and, allowing that there were no petitions for leave to intervene filed within the required 30-day period from the appearance of the Order in the FR, the Order became effective on 3 November 1988. Since the LEU fuel had arrived at the OSURR facility on 8 November 1988, HEU core unloading began essentially immediately, with the complete unloading being completed by late November 1988. LEU fuel elements were loaded starting on 7 December 1988, with attainment of a critical geometry on 15 December 1988. Routine OSURR operations at power levels up to 10 kW were resumed in January, 1989. Concurrent licensing activities and facility engineering work continued during the following months directed towards increased operating power.

Licensing issues related to increased operating power were resolved between the NRC and OSURR by 30 April 1990. The NRC issued revised OSURR Technical Specifications for operating power levels up to 500 kW on 14 November, 1990. Facility engineering work allowing operating power up to 100 kW were completed by 11 September, 1991. Testing at 50 kW and 100 kW was completed on 18 September, 1991 and 17 October, 1991, respectively. Further engineering work necessary for operation up to 500 kW was completed by 30 November, 1992, with testing at 250 kW and 500 kW completed on 18 December, 1992 and 19 December, 1992, respectively. Routine operations of the OSURR at power levels up to 500 kW have been conducted since.

ANALYTICAL PROGRAM

The main objective of the analytical program were to identify core and pool configurations which would satisfy the following criteria:

1. The cold, clean core must have sufficient excess reactivity to compensate for experiment worth (0.7% $\Delta k/k$), temperature and xenon feedback at full power (500 kW) and other burnup effects (>0.5% $\Delta k/k$) while maintaining a minimum of 1.5% $\Delta k/k$ shutdown margin with the highest worth rod stuck out.
2. The margin to onset of nucleate boiling (ONB) in the hot channel should be a minimum of 20% at full power.
3. The thermal neutron flux levels at the CIF and the beam tube positions should not be less than 1×10^{13} and 7×10^{12}n/cm^{2}s, respectively.
4. The pool configuration should lead to as low as reasonable achievable pool top ^{16}N activity and also maximize the inlet water temperature to the primary side of the pool heat removal system (PHRS) to improve heat exchanger efficiency.

The related neutronic and thermal-hydraulic work has been described in detail in previous presentations and publications.[4,5,7-10] The LEU fuel elements were chosen to have the same outer dimensions the as the HEU elements (i.e. 7.62 x 7.62 cm in cross-section), with the standard elements (SEs) consisting of 18 1.27 mm thick plates 16 of which had U_3Si_2 – Al meat containing 12.5 g of ^{235}U per plate. The remaining two plates are pure Al and placed on the outside for mechanical protection. The control elements has 10 fueled and 2 pure Al plates with the same dimensions as the standard fuel element plates. The non-fueled plates serve as guide plates for the control rods.

The analytical program was able to identify two 18 SE and one 17 SE core configurations that satisfy the above criteria. In addition, another 16 SE core configuration was identified with 1.5% $\Delta k/k$ excess reactivity for the initial conversion and testing phase at 10 kW. The computational work indicated that Criterion #4 above would be achieved if the core were contained in a shroud with a 75 cm chimney, with the water to the primary side of the PHRS drawn from the chimney and passed through an insulated decay tank placed in the reactor pool before entering PHRS main heat exchanger.[2,6,9]

FUEL CONVERSION ACTIVITIES

HEU Removal

Removal of the HEU fuel from the OSURR core, which had hitherto composed the only operational core ever used in the history of the OSURR, was a key milestone of the overall program. Prior to the actual HEU removal, a series of preliminary activities were planned and completed. Lacking immediate access to an approved fuel transport cask, plans were made for temporary onsite storage of the HEU fuel, pending ultimate shipment to Savannah River. The logical storage location was the Bulk Shielding Facility (BSF) pool, located immediately adjacent to the OSURR pool, but having a separate water cleanup system, and having sufficient volume and depth for storage of irradiated but unusable HEU fuel elements.

The NRC approval for this storage plan was sought and ultimately obtained. Facility modifications to store the HEU fuel included installation of security systems in and around the BSF pool, design, analysis, and fabrication of criticality-safe storage racks for the fuel elements, and design and construction of a transfer cask to move the irradiated fuel elements from the reactor pool to the BSF pool.

The transfer cask was necessitated by the lack of a direct portal (canal) between the two pools, and the need to keep doses to personnel as low as reasonably achievable. Design constraints on the cask included reducing near- surface doses rates to as low a value as possible for the most highly-irradiated fuel element, while allowing the cask to be lifted using the 3-ton bridge crane available in the OSURR facility. These constraints resulted in the design and construction of a cask having an 8-inch thick wall, shaped into a cylinder with an outer jacket of mild steel, a removal lid, and a cavity volume sufficient to accommodate a single HEU fuel element.

Two storage racks were fabricated, each capable of holding 16 fuel elements in a 2 x 8 array. These racks, fabricated from sheet and angle aluminum components, were analyzed for criticality safety assuming the two fully-loaded racks were placed adjacent to each other and submersed in purified, demineralized light water. Criticality safety was assured by specifying the pitch of the fuel elements sufficient to produce a multiplication factor of an infinite array of the OSURR HEU fuel elements of less than one. Other features included a wide base to prevent tipping, and spacers to prevent adjacent placement of the racks.

Administrative activities necessary for HEU removal included development and approval of rack placement and transfer cask handling procedures, post-removal fuel inspection and monitoring activities, and ongoing surveillance of BSF pool water purity and radionuclide content. To the extent possible, all administrative and procedure development work was completed prior to beginning fuel removal.

A decay period of about 3 days was allowed between the last operation of the OSURR and the beginning of fuel removal. Actual fuel removal took about one week to complete, including various dose rate surveys and inspections of the removed elements that might not have been strictly required. The highest near-contact dose rate measured for the removed elements was approximately 120 R/hr in air, detected with a remotely-operated ionization chamber. No measurable personnel doses were recorded for the entire HEU removal operation, which demonstrated the effectiveness of the handling procedures and techniques.

LEU Core Installation

LEU core loading was accomplished using procedures and tools used for standard HEU fuel handling, since the design of the LEU fuel elements specified physical compatibility with the existing OSURR grid plate and fuel handling tools. Fuel loading order was dictated by the approved OSURR operating procedure for conducting a critical experiment. Actual loading time was about one week, allowing time for data collection and analysis preceding and following each incremental loading.

Results of the initial core loading experiments yielded data on a minimum critical loading, and a subsequent configuration suitable for operations up to 10 kW power. Comparisons were made with predicted results.

OSURR operations at 10 kW were conducted for the following year, with further LEU core loading activity beginning on 7 July, 1991, related to higher-power operations. Core geometry was changed to increase excess reactivity to allow for temperature feedback and xenon poisoning, based on predicted core behavior. A final core configuration suitable for power operations up to 500 kW was attained on 16 July, 1991.

PREDICTIONS, MEASUREMENTS, AND COMPARISONS FOR LEU-FUELED OSURR OPERATIONS

Initial Criticality: Minimum Core Size

Initial criticality was attained with a core geometry shown in Fig.1(a). This geometry provided only a minimum core size estimate and was not practical for routine operations because of its very low excess reactivity and the need to operate with the control rods at very near their fully withdrawn positions. However, this core provided a useful measurement in that minimum core size was estimated and compared to that predicted. The actual value of 3,497 grams of ^{235}U compares well with the minimum predicted value of 3,570 grams.

Low Power Operations

For routine OSURR operations, the core geometry shown in Fig.1(b) was used. This core configuration, denoted as LEU-2, provided excess reactivity and control rod positions allowing operation of the reactor up to 10 kW. Note that the element in position 5B is a partially loaded element with a ^{235}U loading of a nominal 125 grams. Initially, this geometry was tested with a fully loaded element at this position, but the excess reactivity and shutdown margins were close to the Technical Specifications limit for OSURR operations at or below 10 kW. Thus, a partially fueled element was placed at this position, which is a relatively low-worth position on the grid plate for the near-symmetric core loading shown in the Figure.

Table 1 shows comparisons between predicted and measured values for various core parameters, as well as comparison with values obtained for the standard HEU core, where available. In general, measured and predicted values agree reasonably well. The changes resulting from conversion to LEU also follow predictable trends, with the primary differences being in temperature feedback coefficient of reactivity, and prompt neutron lifetime.

Table 1
Comparison of Predicted and Measured Values For OSURR HEU and LEU-2 Cores

Parameter Description	LEU-2 Core Predicted Value	LEU-2 Core Measured Value	HEU Core Measured value
Excess Reactivity (%Δk/k)	1.5	1.5	0.67
Void Coefficient (%Δk/k/%void)	- 0.32	- 0.79	- 0.28
Temperature Coefficient (%Δk/k/°C)	- 0.0079	- 0.0069	- 0.002
Safety Rod 1 Worth (%Δk/k)	2.70	2.56	2.86
Safety Rod 2 Worth (%Δk/k)	2.47	2.20	2.05
Safety Rod 3 Worth (%Δk/k)	2.16	1.93	1.85
Regulating Rod Worth (%Δk/k)	0.48	0.54	0.56
Minimum Shutdown Margin (%Δk/k)	3.23	2.63	3.30
Prompt Neutron Lifetime (μsec)	66	68	89
CIF Total Neutron Flux At 10 kW For 0.001 eV - 10 MeV Range (neutrons/cm^{2}s)	5.5×10^{11}	7.5×10^{11}	6.8×10^{11}
Rabbit Total Neutron Flux At 10 kW For 0.001 eV - 10 MeV Range (neutrons/cm^{2}s)	N.A.	6.2×10^{11}	6.3×10^{11}

The core denoted as LEU-2 operated from 23 December 1988 to 31 May 1991, at various power levels up to and including 10 kW steady-state thermal power. The core was immersed in the reactor pool water at all times, with fuel elements being visually inspected twice during this time. Core temperatures were at or near ambient for most of the operating period. Pool water radionuclide assays taken regularly during this period

showed no detectable quantities of water-soluble fission products, and random air sampling using both continuous air monitors and activated charcoal filters showed no airborne radionuclides except the ^{41}Ar routinely detected during OSURR operations. Fuel performance was thus judged to be entirely satisfactory during this operating cycle.

POWER INCREASE ACTIVITIES

OSURR System Modifications

The planned power increase from 10 to 500 kW required a number of reactor system changes. Since the original OSURR design allowed sufficient pool wall thickness for operations up to 1 MW, additional shielding was unnecessary. Natural convection cooling would remain the primary mechanism for heat removal from the core, thus avoiding installation of high-capacity pumps and piping. Further, the natural convective cooling mode would result in relatively high core outlet water temperature, thus allowing a somewhat large temperature difference across the heat removal system heat exchangers. This allowed consideration of alternatives to the traditional wet cooling tower design system.

The final design of the heat removal system featured a primary- secondary loop using plate-frame heat exchangers, and a fan-forced dry air cooler for ultimate heat rejection to the ambient air. The dry cooler design, sometimes called an air blast heat exchanger, is a reasonable alternative to a cooling tower if the inlet temperature to the heat exchanger is relatively high. The primary loop fluid is the purified, demineralized light water from the reactor pool, while the secondary loop uses an ethylene glycol and water mixture to allow operation when the outdoor air temperature is low.

Cooling system capacity was specified such that the entire 500 kW heat load can be rejected to the outside air if the ambient temperature is below 73°F, with the primary and secondary flow rates set at maximum. For those days when the outdoor temperature exceeds this limit, added heat rejection capacity can be obtained from an auxiliary heat exchanger using city water as the heat sink in a once-through flow path.

Primary and secondary loop flow rates can be adjusted by means of throttle valves and the use of a variable displacement pump in the secondary loop. City water flow rate through the auxiliary heat exchanger can also be adjusted. The secondary loop features a bypass flow loop which allows varying amounts of the total secondary fluid flow to be directed through the outdoor cooling unit. In this way, total system heat rejection capacity can be adjusted when the outdoor air temperature is very low.

Cooling system inlet suction is drawn from the top of the core, through a manifold built into a core shroud assembly which is placed over and around the core. The shroud serves to minimize bypass flow and direct the bulk of the heated pool water directly into the cooling system. Primary loop flow rate is adjusted so that natural convective flow through the core is not severely disturbed. That is, the cooling system does not "draw" water through the core.

Instrumentation changes required for the power increase included extending the range of various power monitoring channels, changing alarm and trip setpoints, and adding various alarms and trips related to cooling system operation and reactor core inlet temperature. The cooling system control panel was interfaced to existing alarm and scram buses through isolated, redundant alarm modules. Power monitoring channels utilizing compensated and uncompensated ion chambers were adjusted to the new operating power by movement of the detectors and, where necessary, extending the dynamic range of the signal conditioning circuits. Cooling system data acquisition and display was facilitated by the addition of a computer-based data collection and logging system. However, the computer has no direct safety-related function, such as actuating trip systems or prompting operator action.

Various OSURR operating procedures were modified to allow for higher power operation. These included both the pre-startup and post- shutdown checklists, initial power ascension and power change procedures, and radiation safety protocols. OSURR system maintenance procedures were expanded to account for cooling system maintenance requirements, and the need for the additional monitoring instrumentation. Operator training sessions were held to acquaint licensed operators with cooling system operation and monitoring, the effects of changing from HEU to LEU, and procedural and administrative changes.

LEU Core Reconfiguration

Prior to starting the phased power change program, the OSURR core geometry was changed to account for the stronger feedback effects expected at higher operating powers. Specifically, negative reactivity feedback from higher average core temperature and the buildup of xenon during extended operation at higher power had to compensated by a higher excess reactivity, in addition to maintaining adequate reactivity to allow for

experiment installation and the need to generate reasonable reactor periods during startup. The excess reactivity was increased by increasing the ^{235}U loading. The core configuration shown in Fig.1(c), denoted as core LEU-3, was loaded on 16 July, 1991. This geometry was selected because it provided an excess reactivity adequate to meet operational needs, while allowing reasonably conservative margins for shutdown margin and overall core reactivity.

Table 2 shows comparisons between measured values and those predicted for a as close a core geometry to that chosen as was available from the analytical studies. In general, agreement is good between predicted and measured results.

Table 2
Comparison of Predicted and Measured Values
For OSURR LEU-3 Core (Loading 3,821.65 g ^{235}U)

Parameter	Predicted Value	Measured Value
Excess Reactivity (%Δk/k)	2.08	2.34
Safety Rod 1 Worth (%Δk/k)	2.69	2.95
Safety Rod 2 Worth (%Δk/k)	3.01	2.49
Safety Rod 3 Worth (%Δk/k)	2.58	2.30
Regulating Rod Worth (%Δk/k)	N.A.	0.53

High-Power Operation

The OSURR power increase was planned as a stepwise ascension in power, with planned "hold" points at various power levels to perform measurements and assess system performance. Measurements were planned at 50, 100, 250, and the final operating power of 500 kW. Safety- related core parameters measured included excess reactivity, control rod worths and minimum shutdown margin, and reactivity coefficients for void formation, and prompt (Doppler) and delayed (moderator heating) temperature feedback. In addition, other measurements made included various health physics tests such as dose rate measurements at various locations around the reactor building, ^{41}Ar concentration measurements for various operating times and at several building locations, and, when possible, core physics tests to determine the reactor transfer function, prompt neutron lifetime, and neutron flux magnitudes and energy spectra.

Most of the changes observed as a result of higher-power operation follow the expected patterns. The magnitude of the neutron flux is significantly increased in various experimental facilities, as listed in Tables 3(a) and 3(b). The neutron energy spectra show measurable shifts towards higher energies, with a small loss in thermal flux when compared with the HEU core.[1]

Table 3(a)
Neutron Fluxes in the CIF

Flux Type	HEU Core at 10 kW		LEU-2 Core at 10 kW		LEU-3 Core at 500 kW	
	Predicted Value	Measured Value	Predicted Value	Measured Value	Predicted Value	Measured Value
Total Neutron Flux For 0.001 eV - 18 MeV (neutrons/cm^{2}s)	5.4×10^{11}	6.6×10^{11}	5.5×10^{11}	7.5×10^{11}	2.46×10^{13}	3.0×10^{13}
Thermal Neutron Flux For 0.001 eV - 0.2 eV[a] (neutrons/cm^{2}s)	3.3×10^{11}	4.3×10^{11}	3.2×10^{11}	4.2×10^{11}	1.30×10^{13}	1.53×10^{13}
Epithermal Neutron Flux For 0.2 eV - 18 Mev[b] (neutrons/cm^{2}s)	2.1×10^{11}	2.3×10^{11}	2.3×10^{11}	3.3×10^{11}	1.16×10^{13}	1.47×10^{13}

[a]Predicted values are for the 0.001 eV - 0.414 eV range
[b]Predicted values are for the 0.414 eV - 10 MeV range

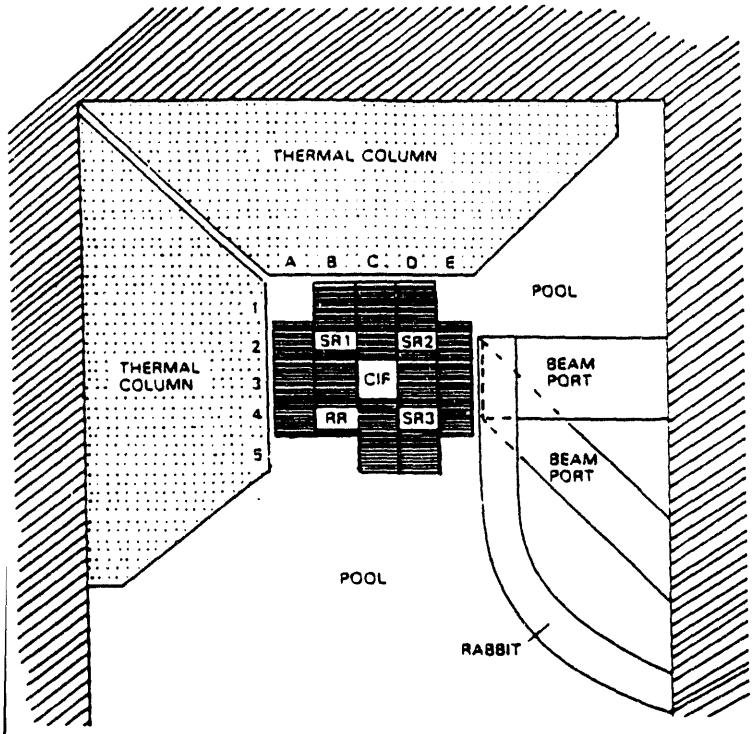

(a) Initial Critical Geometry With LEU Fuel

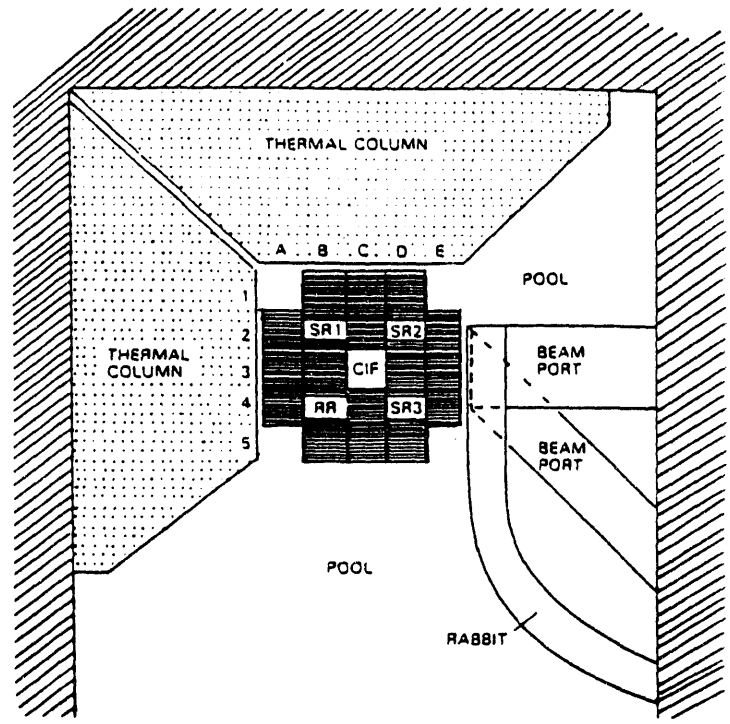

(b) LEU-2 Core*

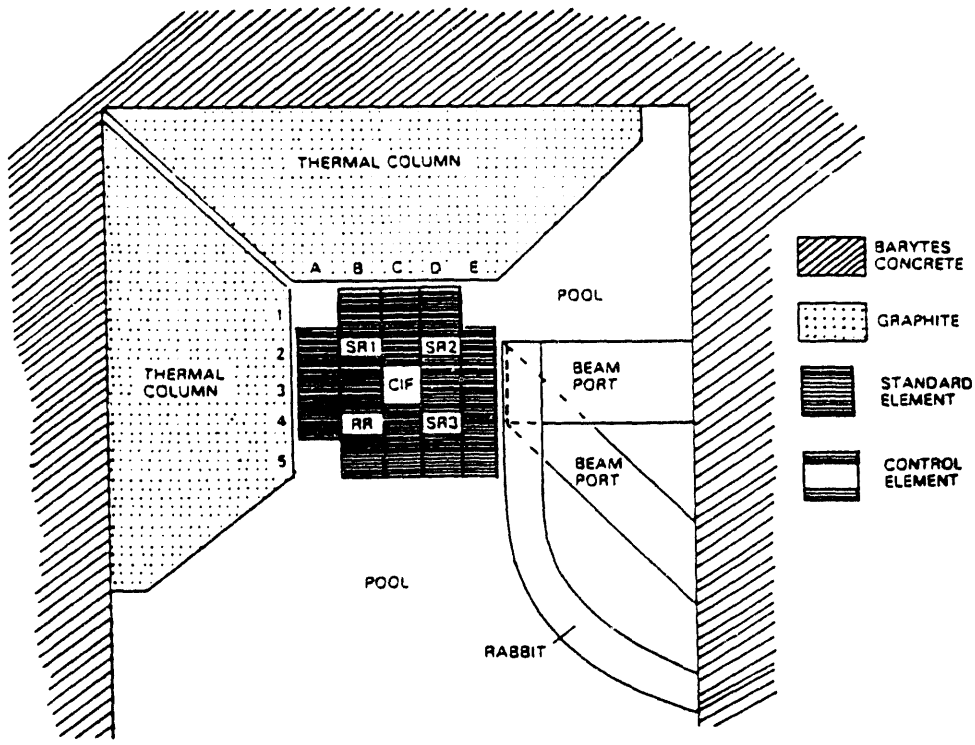

(c) LEU-3 Core*

*Position B-5 is a Partial Element (125 g ^{235}U)

Figure 1: Various OSURR Core Configurations With LEU Fuel (SR: Safety Rod, RR: Regulating Rod).

Table 3(b)
Measured Neutron Fluxes in the Rabbit

	HEU Core at 10 kW	LEU-2 Core at 10 kW	LEU-3 Core at 500 kW
Total Neutron Flux For 0.001 eV - 18 MeV (neutrons/cm^{2}s)	6.4×10^{10}	6.2×10^{10}	2.7×10^{12}
Thermal Neutron Flux For 0.001 eV - 0.2 eV (neutrons/cm^{2}s)	4.5×10^{10}	4.4×10^{10}	1.8×10^{12}
Epithermal Neutron Flux For 0.2 eV - 18 MeV (neutrons/cm^{2}s)	1.9×10^{10}	1.8×10^{10}	9.0×10^{11}

Operations at higher power result in measurable temperature feedback during operation and, for longer run times, xenon feedback. The additional excess reactivity for core LEU-3 has proven adequate to compensate for these feedback effects. Previous operations at lower power did not produce measurable effects, thus allowing lower excess reactivity.

As expected, higher dose rates and increased ^{41}Ar concentrations were measured at various locations around the reactor building. However, nothing has been detected that would indicate the potential for violation of regulations, or the ALARA guidelines followed at the OSURR. The highest measured dose rates are at the pool surface directly above the reactor core. At full power, the surface dose rate is on the order of 70 mr/hr. However, this position, located over the surface of the pool, is not considered to be a routinely accessible location. At the edge of the pool, which is the nearest accessible area to this location, dose rates on the order of 40 mr/hr have been measured. During full power operations, access to this area is limited by administrative procedures.

After nearly one year of operation at higher power levels, LEU fuel performance has been entirely satisfactory. Regular radionuclide assay of the pool water has not detected any trace of fission products, and visual inspection of the fuel elements has not revealed any abnormal behavior. Because of the somewhat limited duty cycle to this time, fuel replacement as a result of burnup has not been necessary.

SUMMARY AND CONCLUSIONS

OSURR fuel conversion and power upgrade has been successfully completed. The analytical program provided accurate predictions of the LEU-fueled OSURR characteristics when operating at various power levels. This allowed preparation of an SAR adequate for relicensing of the reactor for LEU fuel use at higher operating power. Facility engineering to add a heat removal system and upgrade instrumentation was completed, and higher power operation was attained within a reasonable time. LEU fuel performance has been completely satisfactory. The changes resulting from LEU conversion have not had a severe adverse impact on OSURR operations as a general-purpose research reactor. Indeed, when coupled with a power increase effort, LEU conversion can provide an opportunity for low and intermediate power research reactors to significantly enhance their potential utilization. In this context, the experience can only be viewed as a positive one for the OSURR.

REFERENCES

1. J. W. Talnagi, L. A. Heimberger, T. Aldemir, "Prediction and Measurement of the Neutron Environment in OSURR Experimental Facilities Following Conversion to LEU", to appear in the Proceedings of the 1990 International Meeting on Reduced Enrichment for Research and Test Reactors, Newport, Rhode Island (Sept. 24-27, 1990)
2. T. Aldemir, J. W. Talnagi, D. W. Miller, "Analytical, Engineering and Licensing Aspects of the OSURR LEU Conversion/Upgrade", to appear in the Proceedings of the 1988 International RERTR Meeting, San Diego, California (Sept. 18-22, 1988)
3. J. W. Talnagi, T. Aldemir, "Initial Testing of The Ohio State University Research Reactor LEU Core", *Proc. XIIth International Meeting on Reduced Enrichment for Research and Test Reactors*, G. Thamm, M. Brandt (Eds.), 303-311, Konferenzen des Forschungszentrums Julich, Band 4, KFA Julich, Germany (1991)

4. T. Aldemir, J. W. Talnagi, D. W. Miller, "Low Enriched Uranium Conversion/Upgrade of The Ohio State University Research Reactor", *Nucl. Technol., 86*, 248-263 (September 1989).

5. M. Belhadj, T. Aldemir, R. N. Christensen, "Onset of Nucleate Boiling in Thin Rectangular Channels Under Low-Velocity, Upward-Flow Conditions", *Nucl. Technol., 82*, 330-340 (September 1988)

6. T. Aldemir, J. W. Talnagi, D. W. Miller, "System Design For the Low Enriched Uranium Conversion/Power Upgrade of a Natural Convection Cooled Research Reactor", *50 Years With Nuclear Fission*, 767-774, American Nuclear Society, LaGrange Park, IL (1989)

7. H. S. Aybar, T. Aldemir, "An Investigation of the Effect of Partially Inserted Rods on Power Peaking and Rod Worth for the LEU Conversion Upgrade of OSURR", *Proc. 1988 Int. Reactor Physics Conf., II*, 453-462, American Nuclear Society, LaGrange Park, IL (1988)

8. T. Aldemir, "Neutronic/Thermal-Hydraulic Studies for the LEU Conversion/Upgrade of OSURR", Trans. Am. Nucl. Soc. 56, 572-573 (June 1988) (invited paper)

9. J.J. Ha, T. Aldemir, "Pool Dynamics of Natural Convection Cooled Research Reactors", *Nucl. Technol.,79*, 297-310 (December 1987)

10. M. Caner, T. Aldemir, "Preliminary Neutronics Calculations For the OSURR LEU Conversion/Upgrade Program", *Reduced Enrichment For Research and Test Reactors*, P. von der Hardt, A. Travelli (Eds.), D. Reidel Publishing Co., 273-285 (1986)

S E S S I O N V

September 30, 1992

FUEL TESTING AND EVALUATION

Chairman:

Y. Fanjas
(CERCA, France)

ANALYTICAL ANALYSES OF STARTUP MEASUREMENTS ASSOCIATED WITH THE FIRST USE OF LEU FUEL IN ROMANIA'S 14-MW TRIGA REACTOR

M. M. Bretscher and J. L. Snelgrove
Argonne National Laboratory
Argonne, Illinois 60439 USA

and

M. Ciocanescu
Institute for Nuclear Research
Pitesti, Romania

ABSTRACT

The 14-MW TRIGA steady state reactor (SSR) is located in Pitesti, Romania. Beginning with an HEU core (10 wt% U), the reactor first went critical in November 1979 but was shut down ten years later because of insufficient excess reactivity. Last November the Institute for Nuclear Research (INR), which operates the SSR, received from the ANL RERTR program a shipment of 125 LEU pins fabricated by General Atomics and of the same geometry as the original fuel but with an enrichment of 19.7% ^{235}U and a loading of 45 wt% U. Using 100 of these pins, four LEU clusters, each containing a 5 x 5 square array of fuel rods, were assembled. These four LEU clusters replaced the four most highly burned HEU elements in the SSR. The reactor resumed operations last February with a 35-element mixed HEU/LEU core configuration.

In preparation for full power operation of the SSR with this mixed HEU/LEU core, a number of measurements were made. These included control rod calibrations, excess reactivity determinations, worths of experiment facilities, reaction rate distributions, and themocouple measurements of fuel temperatures as a function of reactor power. This paper deals with a comparison of some of these measured reactor parameters with corresponding analytical calculations.

INTRODUCTION

The 14-MW TRIGA Steady State Reactor (SSR) is located in Pitesti, Romania, and is operated by the Institute for Nuclear Research. Initially, the beryllium-reflected core contained 29 HEU fuel clusters each consisting of a square 5x5 array of Incoloy-clad uranium-zirconium hydride-erbium fuel pins enclosed within an aluminum shroud. As burnup proceeded, the core size increased until the complete inventory of 35 fuel clusters was in use. After about 13,600 MWD's of operation, the SSR was shut down in 1990 because of insufficient excess reactivity.

At the time of the 1991 International RERTR Meeting in Jakarta, Indonesia, the Institute for Nuclear Research received a shipment of 125 LEU TRIGA pins from the ANL RERTR program for use

in the SSR. These pins are of identical geometry as the original HEU fuel. After a detailed series of inspections and measurements performed by SSR personnel, four LEU fuel clusters were assembled.

In preparation for full-power operation of the SSR with a mixed HEU/LEU core consisting of 31 burned HEU and 4 fresh LEU elements, a series of measurements was undertaken last February at which time the ANL authors of this paper were present. This paper deals with a comparison of some of these measured reactor parameters with corresponding analytical calculations.

The first set of measurements was made in the 35-cluster HEU core shown in Fig. 1. Based on ^{137}Cs gamma-scanning measurements of the irradiated fuel pins together with an absolute ^{137}Cs standard, cluster-averaged burnups had been assigned to each fuel element. Table 1 summarizes these results. This tables differs somewhat from that given in Ref. [1] because of the rearrangement of some fuel pins so as to maximize the burnup of those clusters which were to be replaced with four fresh LEU fuel elements.

Experiment loops are normally located in grid positions G7 (A Loop), D6+E6 (C1 Capsule), and E4 and E9 (standard natural uranium experiments) and may be replaced with water. These loops are described in Ref. [2]. The A Loop includes six zircaloy-clad CANDU type UO_2 rods with 5% enrichment while the C1 Capsule is loaded with a single 5% enriched UO_2 rod. The standard experiments in E4 and E9 each contain three natural uranium UO_2 rods.

The methods used to determine atom densities in fresh HEU and LEU fuel as well as burnup- and axially-dependent atom densities for the fuel described in Table 1 are discussed in detail in Ref. [1]. This reference also describes the structure of the 8-group cross section sets used in this study and the modeling methods needed for diffusion and burnup calculations.

EXCESS REACTIVITIES FOR 13 SSR CORE CONFIGURATIONS WITH FRESH HEU FUEL

It is useful to test multigroup cross sections, modeling procedures, and computational methods by comparing calculated and measured excess reactivities for relatively simple core configurations. The initial approach-to-critical measurements in the SSR and the cluster-by-cluster expansion from the just critical 17-element fresh HEU core configuration to the 29-element standard core provides a very useful set of data for testing computational techniques. A reactivity computer was used to measure the excess reactivity of each of these 13 core configurations. The results of these measurements, including control rod elevations at critical, are recorded in the SSR logbook [4].

The reactivity computer determines the excess reactivity by analyzing the shape of the time-dependent amplitude of a detector signal, proportional to the instantaneous reactor power, during a small positive reactivity transient. Table 2 lists the kinetic parameters used by the reactivity computer (see Ref. 3, p. 17). They are based on the properties of fresh HEU fuel. For comparison, Table 2 includes a calculated set of delayed neutron parameters for the 35-cluster core with 31 burned HEU fuel elements and 4 fresh LEU clusters. The loading sequence for expanding the fresh core from 17 to 29 fuel clusters is shown in Fig. 2.

Table 3 summarizes the results of measured and calculated excess reactivities for each of the 13 HEU core configurations. This table also shows that both measurements and calculations indicate that the 16-cluster assembly is subcritical. For these measurements all eight control rods were banked together and operated as a unit. Fully inserted and fully withdrawn control rods correspond to 100 and 900 units of withdrawal, respectively, which represents a total rod displacement equal to the height of the fuel column (55.88 cm). The intermediate rod bank positions shown in Table 3 are the experimentally

SSR 35 HEU CLUSTER CORE CONFIGURATION
(with experiment loops)

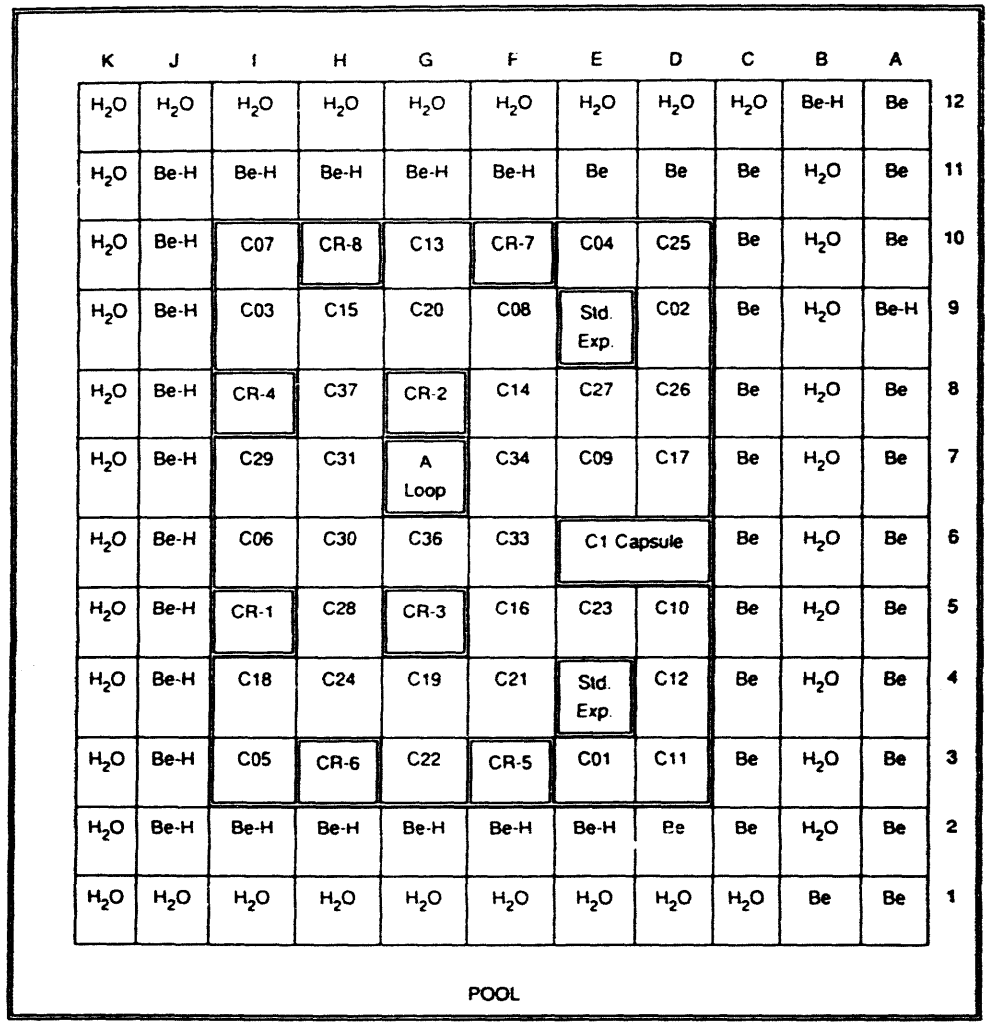

Be-H = Beryllium reflector element with central water hole

FIGURE 1

TABLE 1
SSR HEU FUEL CLUSTER EXPOSURES AND ^{235}U BURNUPS
(Based on Gamma-Scanning Measurements)

Fuel Cluster	MWD's Exposure	% ^{235}U Burnup
C11	498	62.7
C05	487	61.4
C04	485	61.2
C25	482	60.8
C01	475	59.9
C23	448	56.6
C22	447	56.5
C21	444	56.2
C02	440	55.6
C12	436	55.1
C18	433	54.8
C24	433	54.7
C26	431	54.6
C03	431	54.5
C07	430	54.3
C13	429	54.2
C17	428	54.1
C27	427	54.0
C29	426	53.9
C19	426	53.8
C08	425	53.8
C15	422	53.4
C10	421	53.2
C20	418	52.9
C28	416	52.7
C06	411	52.0
C09	402	51.0
C16	399	50.5
C14	393	49.8
C31	246	31.4
C34	245	31.3
C33	195	24.9
C37	35	4.5
C30	33	4.2
C36	29	3.7

TABLE 2
SSR DELAYED NEUTRON PARAMETERS FOR THE 29-CLUSTER FRESH HEU CORE AND FOR THE 35-CLUSTER BURNED HEU/LEU MIXED CORE

	29-Cluster Fresh HEU Core*				35-Cluster Burned HEU/LEU Mixed Core**			
Group	$\lambda_i(sec^{-1})$	β_i	a_i	ℓ_p-μs	$\lambda_i(sec^{-1})$	β_i	a_i	ℓ_p-μs
1	1.244-2	2.31-4	0.033		1.2722-2	2.7961-4	0.038241	
2	3.051-2	1.533-3	0.219		3.1737-2	1.5497-3	0.21195	
3	1.114-1	1.372-3	0.196		1.1617-1	1.3732-3	0.18780	
4	3.013-1	2.765-3	0.395		3.1137-1	2.9748-3	0.40684	
5	1.1362	8.05-4	0.115		1.4001	9.4171-4	0.12879	
6	3.0135	2.94-4	0.042		3.8706	1.9297-4	0.026390	
TOTAL		7.00-3	1.000	22.0***		7.3120-3	1.0000	27.90

* See Ref. 3, p. 17.

**These parameters were generated using ENDF/B-V delayed neutron data.

***This value was obtained from Ref. 5, p. 2-224.

SSR GRID LOCATIONS FOR THE INITIAL CORE LOADING SEQUENCE

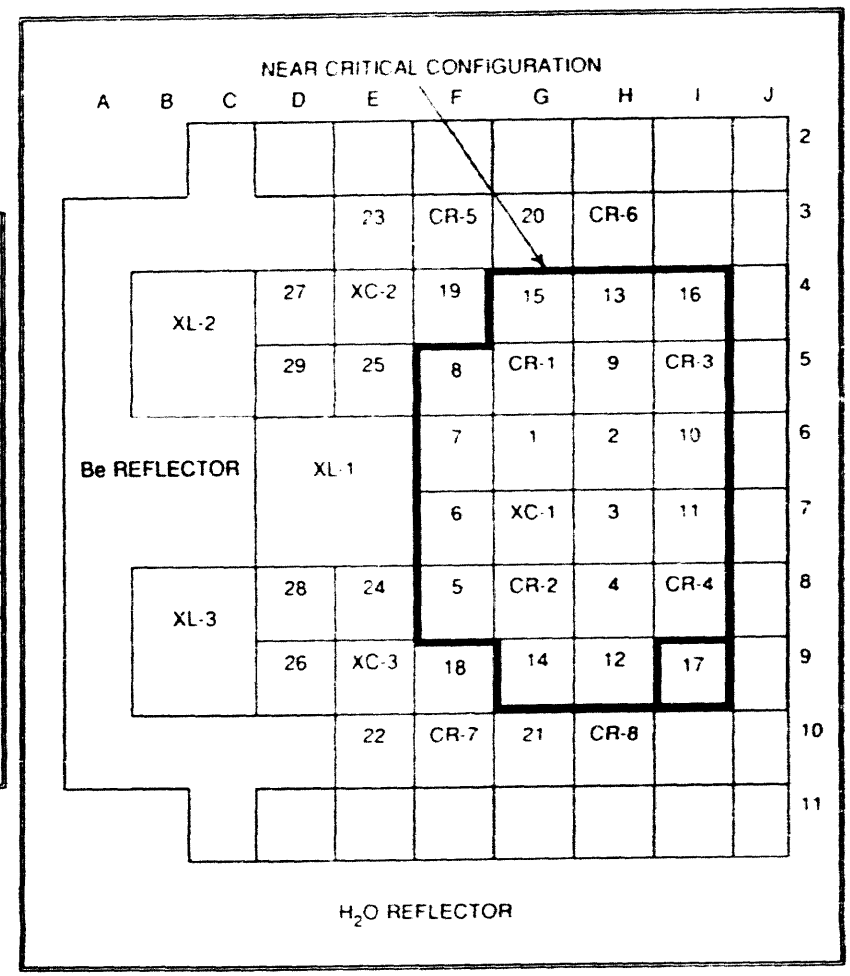

ALL EXPERIMENT LOCATIONS (XL-1, 2, 3; XC-1, 2, 3; AND THE HOLES IN THE BERYLLIUM REFLECTOR) ARE FILLED WITH WATER

FIGURE 2

TABLE 3
ROOM TEMPERATURE EXCESS REACTIVITIES FOR 13 SSR CORE CONFIGURATIONS WITH FRESH HEU FUEL

No. of Clusters	Rod Bank Units	$K_{eff}(C)$	$K_{eff}(E)$	$\rho_{ex}(C)$ $	$\rho_{ex}(E)$ $	C/E
16	900	0.9975				
17	900	1.0097	1.0101			
	775	1.0010	1.0000	1.23	1.43	0.86
18	900	1.0137	1.0133			
	748	1.0026	1.0000	1.56	1.88	0.83
19	900	1.0201	1.0188			
	708	1.0014	1.0000	2.62	2.64	0.99
20	900	1.0299	1.0266			
	664	1.0021	1.0000	3.84	3.70	1.04
21	900	1.0347	1.0303			
	647	1.0052	1.0000	4.05	4.20	0.96
22	900	1.0369	1.0317			
	640	1.0045	1.0000	4.45	4.39	1.01
23	900	1.0403	1.0339			
	631	1.0033	1.0000	5.06	4.69	1.08
24	900	1.0444	1.0386			
	610	1.0032	1.0000	5.62	5.31	1.06
25	900	1.0509	1.0458			
	581	1.0044	1.0000	6.30	6.26	1.01
26	900	1.0525	1.0476			
	575	1.0026	1.0000	6.75	6.49	1.04
27	900	1.0548	1.0503			
	565	1.0015	1.0000	7.20	6.84	1.05
28	900	1.0563	1.0532			
	555	1.0010	1.0000	7.46	7.21	1.03
29	900	1.0585	1.0576			
	539	1.0004	1.0000	7.84	7.78	1.01

SSR RHO–EXCESS IN DOLLARS FOR FRESH HEU CLUSTERS

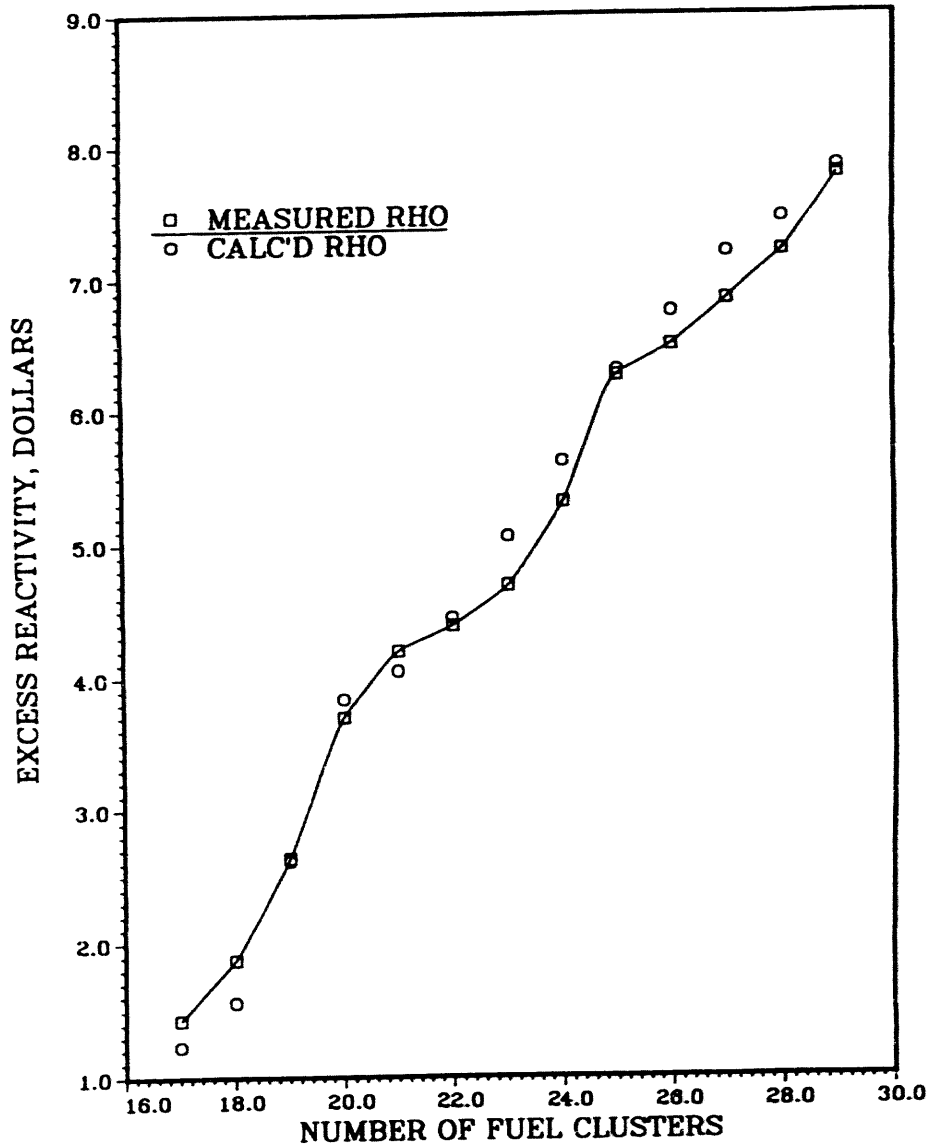

FIGURE 3

determined elevations for which the reactor cores are critical. A total delayed neutron fraction of 0.0070 (Table 2) was used to convert excess reactivities from absolute units to dollars and vice versa. The calculated-to-experiment (C/E) ratios given in Table 3 show that the analytical results are in reasonable agreement with the measured values, which lends credence to the computational methods used in this study. Note too the good agreement between the calculated value of k_{eff} for the critical rod positions and unity. For the 13 cores at critical the average calculated eigenvalue is 1.0026 ± 0.0015. Figure 3 provides a graphical display of this data.

EXCESS REACTIVITIES FOR THE SSR CORE WITH 35 BURNED HEU FUEL CLUSTERS

The purpose of this set of measurements was to determine the reactivity worth of each of the experiment loops relative to water as well as that for a fresh LEU fuel element and a near-fresh HEU cluster. Figure 1 shows the core configuration used for these determinations. Before beginning these measurements, the reactivity computer was used to calibrate each of the control rods. Excess reactivities were obtained from the observed control rod elevations at critical and the rod calibration data. Since the measurements were made at low power (about 500 W), the analytical results are based on cross sections generated at 296K. As before, a value of $\beta_{eff} = 0.0070$ was used to compare measured and calculated excess reactivities.

The results of these measurements are summarized in Table 4. The calculated k_{eff}'s for the critical rod positions are consistent but below unity (0.9929 ± 0.0020). Improved modeling of the experiment loops may reduce some of the C/E ratios for the excess reactivities. Particularly disturbing is the large C/E ratio (1.48) for the case where the C36 HEU cluster (3.7% burnup) in grid location G6 was replaced with water. The consistency of the calculated critical k_{eff}'s for the three experiments involving the G6 location suggests that the banked rod position is correct in each case. One suspects that the discrepancy might be due to inaccuracies in the rod calibration curves, especially near the upper ends of travel. No errors in the measurements or in the calculations have been identified.

EXCESS REACTIVITIES FOR THE 35-CLUSTER SSR CORE WITH FOUR FRESH LEU ELEMENTS REPLACING FOUR HIGHLY BURNED HEU ELEMENTS

In preparation for the first use of LEU fuel in the SSR, some of the HEU clusters in Fig. 1 were relocated while all the experiment loops were removed and replaced with water. This modified core configuration is shown in Fig. 4. The highly burned fuel clusters C25, C01, C11, and C05 (see Table 1) were replaced, one at a time, with the fresh LEU clusters C42, C40, C38, and C39, respectively. With each fuel cluster replacement the control rod bank elevation at critical was determined. With the four LEU clusters in place at the end of these measurements, the control rods were recalibrated again making use of the reactivity computer. This calibration data was used to evaluate the measured excess reactivities. Later, the C1 Capsule was placed in grid positions D6+E6, the standard natural uranium experiments in E4 and E9, and a 5x5 stainless steel (SS) shim bundle in G7.

Table 5 summarizes the results of these measurements and the corresponding calculations. Except for the first case, measured and calculated excess reactivities are in good agreement. As in the last section, all these measurements were carried out at low power and so the analytical results are based on 296K cross sections. Also, a value of $\beta_{eff} = 0.0070$ was used.

TABLE 4

EXCESS REACTIVITIES FOR THE SSR FIGURE 1 CORES

Deviation from Fig. 1 Core	Rod Bank Units	$K_{eff}(C)$	$K_{eff}(E)$	$\rho_{ex}(C)$ $	$\rho_{ex}(E)$ $	C/E
None	900	1.03885	1.04570	6.436	6.243	1.03
	545	0.99240	1.00000			
G6: C36→H_2O	900	1.00880	1.01153	2.417	1.629	1.48
	728	0.99187	1.00000			
G6: C36→C38 (LEU)	900	1.04360	1.05226	7.039	7.095	0.99
	517	0.99256	1.00000			
D6+E6: C1→H_2O	900	1.03442	1.04045	6.205	5.554	1.12
	568	0.98994	1.00000			
G7: A Loop→H_2O	900	1.03214	1.03606	5.098	4.972	1.03
	588	0.99547	1.00000			
G7: A Loop→H_2O D6+E6: C1→H_2O E4, E9: Std Exp's→H_2O	900	1.03114	1.03349	4.997	4.629	1.08
	600	0.99538	1.00000			
G7: A Loop→H_2O D6+E6: C1→H_2O	900	1.02756	1.03101	4.805	4.297	1.13
	612	0.99281	1.00000			

SSR 35 HEU CLUSTER CORE CONFIGURATION
BEFORE THE ADDITION OF FOUR FRESH LEU ELEMENTS

K	J	I	H	G	F	E	D	C	B	A	
H_2O	H_2O	H_2O	H_2O	H_2O	H_2O	H_2O	H_2O	H_2O	Be-H	Be	12
H_2O	Be-H	Be-H	Be-H	Be-H	Be-H	Be	Be	Be	H_2O	Be	11
H_2O	Be-H	C02	CR-8	C15	CR-7	C18	C07	Be	H_2O	Be	10
H_2O	Be-H	C19	C24	C28	C06	H_2O	C12	Be	H_2O	Be-H	9
H_2O	Be-H	CR-4	C37	CR-2	C25	C09	C20	Be	H_2O	Be	8
H_2O	Be-H	C11	C31	H_2O	C34	C23	C10	Be	H_2O	Be	7
H_2O	Be-H	C05	C30	C36	C33	H_2O		Be	H_2O	Be	6
H_2O	Be-H	CR-1	C29	CR-3	C01	C27	C08	Be	H_2O	Be	5
H_2O	Be-H	C21	C17	C16	C14	H_2O	C26	Be	H_2O	Be	4
H_2O	Be-H	C22	CR-6	C04	CR-5	C03	C13	Be	H_2O	Be	3
H_2O	Be-H	Be-H	Be-H	Be-H	Be-H	Be-H	Be	Be	H_2O	Be	2
H_2O	H_2O	H_2O	H_2O	H_2O	H_2O	H_2O	H_2O	H_2O	Be	Be	1

POOL

Be-H = Beryllium reflector element with central water hole

FIGURE 4

TABLE 5
EXCESS REACTIVITIES FOR THE SSR FIGURE 4 CORES

Deviation from Fig. 4 Core	Rod Bank Units	$K_{eff}(C)$	$K_{eff}(E)$	$\rho_{ex}(C)$ $	$\rho_{ex}(E)$ $	C/E
None	900	1.02196	1.02598			
	636	0.99116	1.00000	4.344	3.618	1.20
F8: C25→C42 (LEU)	900	1.03204	1.03282			
	602	0.99814	1.00000	4.701	4.539	1.04
F8: C25→C42 (LEU)	900	1.03975	1.03933			
F5: C01→C40 (LEU)	572	1.00100	1.00000	5.319	5.406	0.98
F8: C25→C42 (LEU)	900	1.04603	1.04621			
F5: C01→C40 (LEU)	542	1.00124	1.00000	6.110	6.310	0.97
I7: C11→C38 (LEU)						
F8: C25→C42 (LEU)	900	1.05298	1.05214			
F5: C01→C40 (LEU)	517	1.00119	1.00000	7.018	7.079	0.99
I7: C11→C38 (LEU)						
I6: C5→C39 (LEU)						
F8: C25→C42 (LEU)	900	1.04769	1.04000			
F5: C01→C40 (LEU)	569	1.00641	1.00000	5.593	5.494	1.02
I7: C11→C38 (LEU)						
I6: C5→C39 (LEU)						
D6+E6: H_2O→C1 Capsule						
E4, E9: H_2O→Std. Nat. U Exp.						
G7: H_2O→SS Shim Bundle						

INTEGRAL CONTROL ROD WORTHS FOR THE SSR 35-CLUSTER CORE WITH FOUR FRESH LEU FUEL ELEMENTS

This core configuration is shown in Fig. 4 but with the highly burned HEU fuel clusters in grid locations F5, F8, I6, and I7 replaced with fresh LEU fuel elements. Each control rod was calibrated using the reactivity computer [3] to measure the reactivity worth associated with small outward displacements of the control rod assembly. Measurements covered the full range of control rod motion from the fully inserted to the fully withdrawn position. The integral worth is the sum of the measured worths for each segment of rod withdrawal.

SSR control rod assemblies consist of an upper poison section and a lower aluminum follower section. The poison section (Ref. 5, p. 2-127) consists of a 58.42 cm stack of pressed B_4C (natural boron) pellets in the form of a square annulus with water at the center. For some initial diffusion calculations the poison section of the control rod was represented by a set of group-dependent internal boundary conditions (current-to-flux ratios) applied at the surface of the B_4C absorber and calculated by the methods described in Ref. [6]. It was soon learned, however, that nearly the same results for control rod worths are obtained by using normal diffusion theory with cross sections homogenized over the entire control rod cell. This more approximate method has the advantage of significantly reducing the number of mesh intervals needed. Use of the internal boundary conditions increases the calculated rod worth by about 0.3%.

The output from the reactivity computer is based on the delayed neutron parameters for fresh HEU fuel shown in Table 2. Probably a better set of parameters for this particular core is the second set also listed in Table 2. An estimate of the reactivity computer's response based on this second set of parameters resulted in a correction which tends to reduce the experimental results by about 1% or less. Because of uncertainties in this calculation, this small correction was not applied to the experimental data.

Table 6 compares the measured and calculated integral control rod worths. The calculations are based on the eigenvalues obtained for the fully withdrawn rod (900 units) and the fully inserted rod (100 units). For these calculations the remaining 7 rods are banked together and withdrawn to the position where the reactor was observed to be critical for the the rod in question located at its mid withdrawal point (500 units). As before, a value of $\beta_{eff} = 0.0070$ (Table 2) was used to convert absolute worths to dollars.

Table 6 shows that the calculations and measurements are in satisfactory agreement for the relatively high worth rods (rods 1-4), but that the low worth rods (5-8) are significantly under-calculated. These low worth rods are located adjacent to the beryllium reflector and perhaps a different set of cross sections are needed for the evaluation of their worths. Since eigenvalue changes of only about 0.0004 would bring these calculated results into reasonable harmony with the measurements, the diffusion calculations require the eigenvalues to converge to within 1.0E-5. Figure 5 displays these results by showing the C/E ratio for each control rod and the % ^{235}U burnup for each fuel cluster.

CONCLUSION

The 14-MW TRIGA research reactor in Pitesti, Romania, was shut down in 1990 because the fuel was too highly burned to continue operations. Last November they received a shipment of 125 unirradiated LEU fuel pins from the ANL RERTR program. After a number of preliminary measurements, the SSR resumed operations last February with a mixed 31 HEU/4 LEU core. Our calculations indicate that the SSR should be able to operate for about 2450 MWD's with this core configuration. Based on current operating schedules, this will allow the SSR to continue running until

TABLE 6
CONTROL ROD WORTHS FOR THE SSR 31 HEU/4 LEU CORE CONFIGURATION
(without experiment loops)

Control Rod	Units of Elevation		K_{eff}(C)	W(C)	W_c(C)*	W(E)	C/E
	Rod	Bank		$	$	$	
1	900	519	1.00766				
	100	519	0.99612	1.642	1.648	1.798	0.92
2	900	523	1.01529				
	100	523	0.98757	3.949	3.962	3.851	1.03
3	900	525	1.01810				
	100	525	0.98610	4.553	4.568	4.803	0.95
4	900	519	1.00786				
	100	519	0.99598	1.691	1.696	1.664	1.02
5	900	505	1.00258				
	100	505	0.99861	0.566	0.568	0.782	0.73
6	900	518	1.00395				
	100	518	1.00105	0.412	0.414	0.566	0.73
7	900	517	1.00572				
	100	517	1.00011	0.797	0.799	1.018	0.79
8	900	519	1.00398				
	100	519	1.00064	0.475	0.476	0.535	0.89

*Based on the use of internal boundary conditions for the B_4C.

$W_c(C) = 1.003175\ W(C)$.

CONTROL ROD WORTH C E RATIOS AND % U-235 BURNUPS
FOR THE SSR 31 HEU/4 LEU CORE CONFIGURATION

K	J	I	H	G	F	E	D	C	B	A	
H_2O	H_2O	H_2O	H_2O	H_2O	H_2O	H_2O	H_2O	H_2O	Be-H	Be	12
H_2O	Be-H	Be-H	Be-H	Be-H	Be-H	Be	Be	Be	H_2O	Be	11
H_2O	Be-H	C02 55.6	CR-8 0.89	C15 53.4	CR-7 0.79	C18 54.8	C07 54.3	Be	H_2O	Be	10
H_2O	Be-H	C19 53.8	C24 54.7	C28 52.7	C06 52.0	H_2O	C12 55.1	Be	H_2O	Be-H	9
H_2O	Be-H	CR-4 1.02	C37 4.5	CR-2 1.03	C42 0.0	C09 51.0	C20 56.5	Be	H_2O	Be	8
H_2O	Be-H	C38 0.0	C31 31.4	H_2O	C34 31.3	C23 56.6	C10 53.2	Be	H_2O	Be	7
H_2O	Be-H	C39 0.0	C30 4.2	C36 3.7	C33 24.9	H_2O		Be	H_2O	Be	6
H_2O	Be-H	CR-1 0.92	C29 53.9	CR-3 0.95	C40 0.0	C27 54.0	C08 53.8	Be	H_2O	Be	5
H_2O	Be-H	C21 56.2	C17 54.1	C16 50.5	C14 49.8	H_2O	C26 54.6	Be	H_2O	Be	4
H_2O	Be-H	C22 56.6	CR-6 0.73	C04 61.2	CR-5 0.73	C03 54.5	C13 54.2	Be	H_2O	Be	3
H_2O	Be-H	Be-H	Be-H	Be-H	Be-H	Be-H	Be	Be	H_2O	Be	2
H_2O	H_2O	H_2O	H_2O	H_2O	H_2O	H_2O	H_2O	H_2O	Be	Be	1

POOL

Be-H = Beryllium reflector element with central water hole

FIGURE 5

they receive a shipment of LEU fuel pins, now being fabricated by General Atomics, for 14 fresh fuel clusters.

To test ANL's analytical methods, a series of 13 fresh HEU core configurations was analyzed and excess reactivities were compared with directly measured values. Calculated results were found to be in good agreement with the measured ones.

In preparation for full power operation of the SSR with a mixed HEU/LEU core, a number of low power measurements were undertaken last February. Many of these measured values have been compared with calculated results. Generally speaking, the calculations agree rather well with the corresponding measurements. However, there are some notable exceptions. For the core shown in Fig. 1 the worth of the C36 fuel cluster, relative to water, is significantly overpredicted. The integral worths of the low worth control rods (rods 5-8) in the 31 HEU/4 LEU mixed core are underpredicted by 11 to 27%. These differences are being investigated, but no completely satisfactory explanation is currently available.

LEU fuel pins, sufficient in number for 14 additional clusters, are being fabricated by General Atomics. These pins are expected to be available for use in the SSR before the end of life of the current 31 HEU/4 LEU mixed core.

REFERENCES

1. M. M. Bretscher and J. L. Snelgrove, "Transition From HEU To LEU Fuel In Romania's 14-MW TRIGA Reactor," 14th International RERTR Meeting, Jakarta, Indonesia, November 4-7, 1991.

2. C. Iorgulis and C. Costescu, "Tridimensional Neutronic Calculation Methods Used In Romanian 14 MW TRIGA-SSR Fuel Management and Irradiation Experiments Evaluation," Eleventh European TRIGA Users Conference, Heidelberg, Germany, September 11-13, 1990, GA TOC-22.

3. "R-20A Reactivity Computer Operation and Maintenance Manual ELE 313-0000-2," General Atomic Company, E-115-569, February 1976.

4. The measured excess reactivities and critical control rod elevations for the fresh HEU core configurations were recorded in the SSR logbook on December 12, 1979.

5. "Safety Analysis Report of the TRIGA Steady-State Research/Materials and Testing Reactor for the Institute of Nuclear Technologies, Bucharest, Romania," General Atomic Company, E-117-323, Vol. II, February 1974.

6. M. M. Bretscher, "Blackness Coefficients, Effective Diffusion Parameters, and Control Rod Worths for Thermal Reactors," ANL/RERTR/TM-5 September 1984.

MEASUREMENTS AND COMPUTATIONS FOR NEUTRON FLUX IN THE ROMANIAN TRIGA STEADY STATE REACTOR HEU CORE WITH FOUR EXPERIMENTAL LEU FUEL CLUSTERS

by

Constantin Toma, Dumitru Barbos, Marin Ciocanescu, and Petre Busuioc

Institute for Nuclear Research
Pitesti, Romania

William Whittemore

General Atomics
San Diego, California, U.S.A.

James Snelgrove

Argonne National Laboratory
Argonne, Illinois, U.S.A.

ABSTRACT

The four HEU fuel clusters with the highest ^{235}U burnups were removed from the highly burned 14-MW steady state Romanian TRIGA reactor and replaced with four fresh LEU fuel clusters. The fuel rods in these new clusters contained 45 wt% uranium enriched to about 19.75% ^{235}U with erbium as a burnable poison.

A series of measurements was conducted to characterize the neutronic behavior of the new core configuration and to compare with calculated parameters. The neutron flux level and spectrum were measured in an in-core experimental region using the method of activated foils and the SAND II computer code. Additionally, the silver reaction rate distribution was determined using self-powered neutron detectors positioned in a number of fuel rod locations.

Separate measurements were made for the gamma rays from the ^{235}U distributed in 15 of the unirradiated fuel rods. The results of careful axial gamma-ray scans of the rods yielded results in agreement with manufacturing records for the ^{235}U distribution.

The operational experience for the new core configuration including reactivity values and fuel temperatures will be reported in other papers.

INTRODUCTION

Gradual conversion of the core of the Romanian 14-MW TRIGA steady state reactor (SSR) to an LEU fuel cycle began in February 1992. In the first stage of the conversion the four HEU fuel clusters having the highest ^{235}U burnups (~60% average and ~80% peak) were removed from the reactor core and replaced with four fresh LEU fuel clusters. The fresh LEU fuel contains 45 wt% U and ~1.1 wt% Er (~1345 g ^{235}U/25-rod cluster), and the HEU fuel contained 10 wt% U and 2.8 wt% Er (~1035 g ^{235}U/25-rod cluster) when fresh. Before the LEU fuel was loaded into the reactor, the uniformity of the ^{235}U distribution in the fuel rods was characterized by gamma scanning 15 fresh rods. After LEU fuel loading, reaction rate measurements were made to obtain neutron fluxes in the mixed HEU-LEU configuration in order to provide an experimental baseline and to allow comparison with computed values. In addition, the reactivities of fuel elements and experimental devices with respect to other fuel elements and/or to water were measured. The results of the measurements using neutron activation detectors and self-powered neutron detectors are presented in this paper. The results of many of the reactivity measurements are presented in [1].

UNIFORMITY OF ^{235}U LOADING IN FRESH LEU FUEL

An apparatus was set up to perform an axial gamma-ray scan of selected TRIGA LEU fuel rods. The 185.6 keV photopeak of ^{235}U was recorded using a traveling slit manipulated in an automatic handling system. Each rod was counted at 142 points spaced 4 mm apart, covering the 558.8-mm (22-in.) length of the fuel. About 2.75 days was required to scan a single rod with sufficient statistical accuracy (1700 s at each point).

Fifteen rods were scanned, but only the results for the ten fuel rods for which there was no evidence of scanning equipment malfunction will be reported. The axial distribution of gamma-ray counts from rod No. 2047 is shown in Fig. 1. The uniformity of the ^{235}U loading of each of these ten fuel rods is consistent with its manufacturing records.

An average of 411,649 total counts (0.16% accuracy) was obtained for each rod. A statistical analysis of the ten gamma-ray scans showed a standard deviation of 0.42%, which corresponds to 0.226 g of ^{235}U in a TRIGA LEU rod having an average loading of 53.81 g of ^{235}U. The distribution of total gamma-ray counts for the ten rods, normalized to a nominal 53.81-g ^{235}U loading per rod, is presented in the histogram in Fig. 2. The nominal uranium loading of these TRIGA LEU rods is 45 wt% (~20 vol%). The measured standard deviation of 0.226 g of ^{235}U in 53.81 g of ^{235}U corresponds to about 45 ± 0.19 wt% U, well within the manufacturing specification of 45 ± 0.5 wt% U.

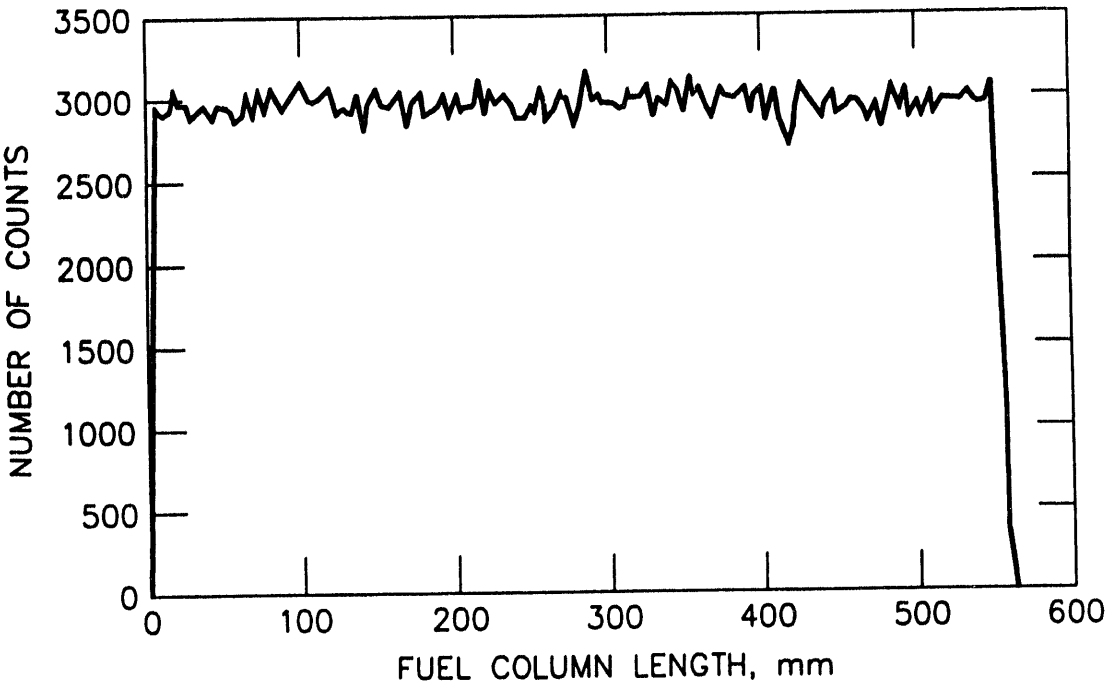

Fig. 1. Axial Distribution of Gamma-Ray Counts from Fuel Rod No. 2047.

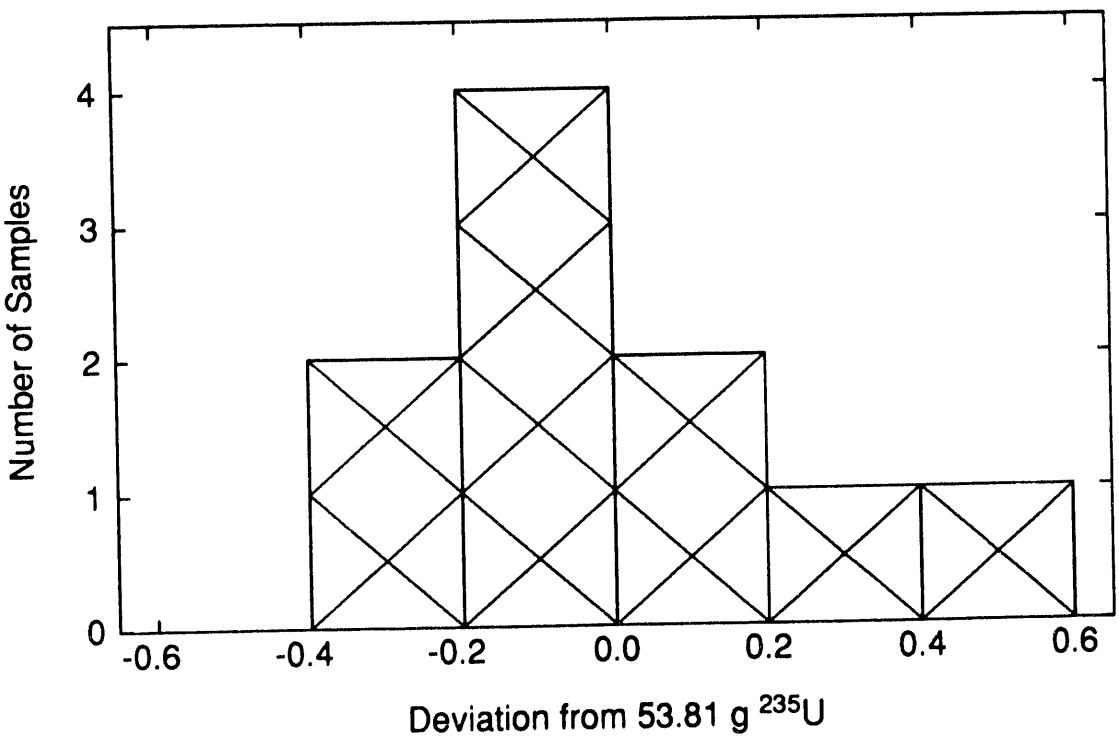

Fig. 2. Distribution of Deviations Around the Average ^{235}U Content (53.81 g) for the Ten Measured Fuel Rods; $\sigma = 0.226$ g.

NEUTRON FLUX SPECTRUM MEASUREMENTS BY FOIL ACTIVATION DETECTORS AND FISSION DETECTORS

Reaction Rate Measurements

The neutron flux spectrum was measured in the water-filled XC1 channel, located in position G-7, as shown in Fig. 3, utilizing procedures and data from [2,3,4,5]. Nine foil activation detectors and two fission detectors were selected to cover the complete neutron spectrum energy range of zero to 14 MeV.

Table 1 contains a listing of the detectors used, the reactions of interest, the cover used during irradiation, and the measured reaction rate. Three detectors (Au, ^{235}U, and ^{239}Pu) were irradiated in 1-mm-thick cadmium covers in order to separate the epithermal and thermal components of the reactions. The detectors were placed in an aluminum cylinder for transfer in and out of the reactor core through the pneumatic transfer system. During irradiation the foils were located 28 cm above the plug surface (Fig. 4).

The reactor was nearly Xe-free and operated at a power of 3 MW. Control rods Nos. 1, 4, 5, 6, 7, and 8 were fully inserted; rod No. 2 was fully withdrawn; and rod No. 3 was at an index position of 690. A fully inserted rod is at an index position of 100, and a fully withdrawn rod is at an index position of 900.

Table 1. Foils Used and Reaction Rates Determined During Measurements in Water-Filled Channel XC1

No.	Sample	Reaction of Interest	Cover	Reaction Rate (disint./nucl.·s)
1	Gold	$^{197}Au(n,\gamma)^{198}Au$	Al	5.079×10^{-9}
2	Gold	$^{197}Au(n,\gamma)^{198}Au$	Cd	1.841×10^{-9}
3	Uranium	$^{235}U(n,f)F.P.$	Al	1.949×10^{-8}
4	Uranium	$^{235}U(n,f)F.P.$	Cd	4.250×10^{-10}
5	Plutonium	$^{239}Pu(n,f)F.P.$	Al	2.914×10^{-8}
6	Plutonium	$^{239}Pu(n,f)F.P.$	Cd	4.598×10^{-10}
7	Nickel	$^{58}Ni(n,p)^{58}Co$	Al	9.654×10^{-13}
8	Iron	$^{58}Fe(n,\gamma)^{59}Fe$	Al	4.605×10^{-11}
9	Iron	$^{54}Fe(n,p)^{54}Mn$	Al	4.028×10^{-12}
10	Lutetium	$^{176}Lu(n,\gamma)^{177}Lu$	Al	1.397×10^{-7}
11	Aluminum	$^{27}Al(n,\alpha)^{24}Na$	Al	7.155×10^{-15}
12	Indium	$^{115}In(n,n')^{115m}In$	Al	2.045×10^{-12}
13	Tungsten	$^{186}W(n,\gamma)^{187}W$	Al	1.953×10^{-9}
14	Dysprosium	$^{164}Dy(n,\gamma)^{165}Dy$	Al	1.035×10^{-7}
15	Manganese	$^{55}Mn(n,\gamma)^{56}Mn$	Al	4.570×10^{-10}

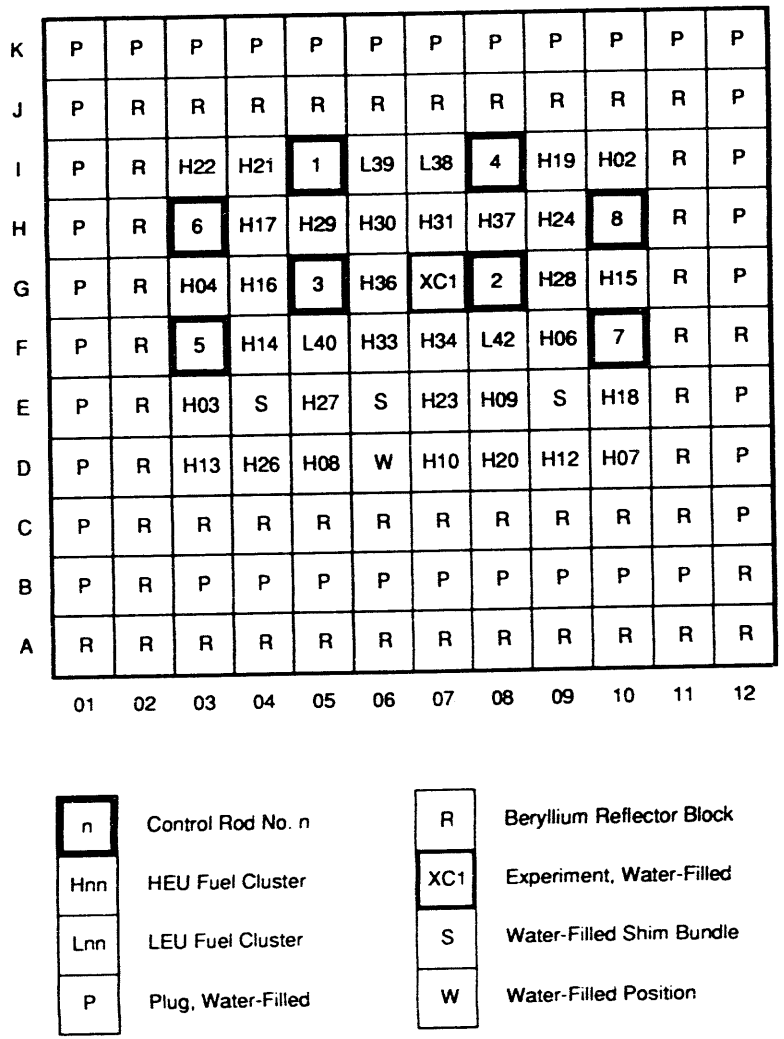

Fig. 3. SSR Configuration with Four LEU Fuel Clusters (February 24, 1992).

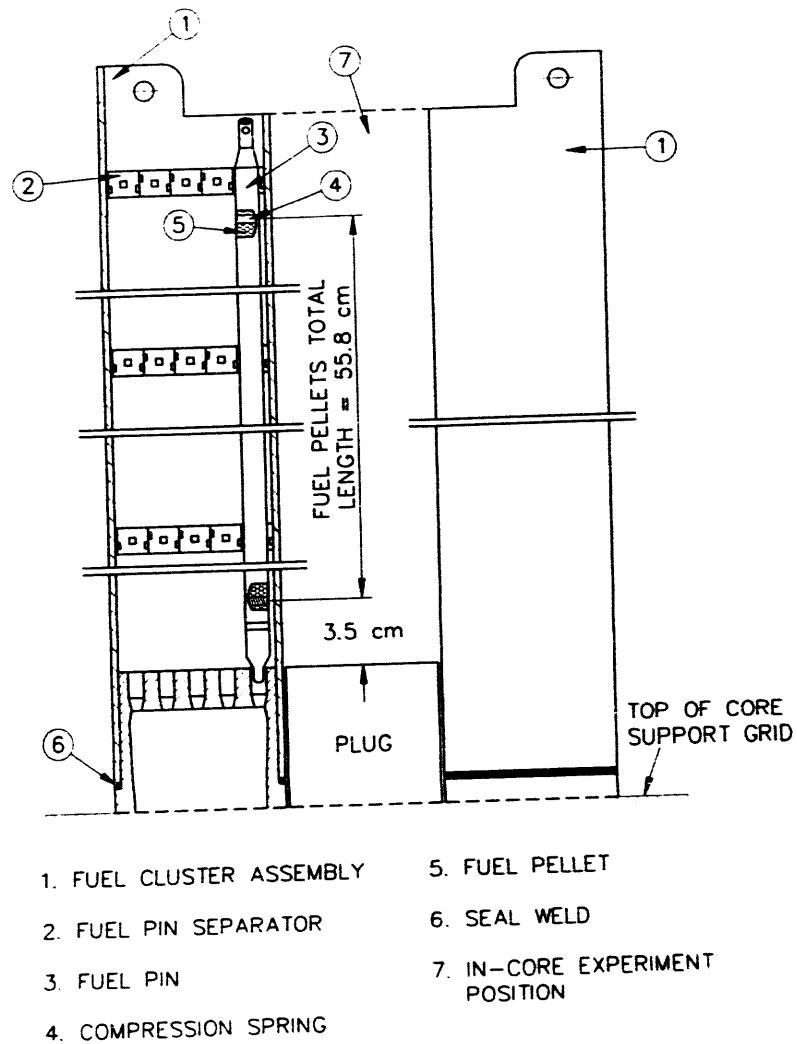

Fig. 4. Axial Detail of SSR Core.

All detectors were counted using a germanium detector and multichannel analyzer system with an energy resolution of 1.8 keV for $E_\gamma = 1332.5$ keV. The reaction rate is given by

$$R = \frac{A_p \cdot A \cdot \lambda \exp(\lambda t_w)}{y \cdot \eta \cdot \iota \cdot p \cdot A_b \cdot m \cdot N_A [1 - \exp(-\lambda t_i)] [1 - \exp(-\lambda t_m)]}$$

where:

A_p = photopeak area,

A = atomic mass of parent nuclide,

λ = daughter disintegration constant,

t_w = cooling time,

y = { fission yield of fission product of interest for fission detectors, / 1.0 for activation detectors,

η = detection efficiency,

ι = emission probability,

p = detector purity,

A_b = isotopic abundance of parent nuclide,

m = detector mass,

N_A = Avogadro's number,

t_i = irradiation (activation) period, and

t_m = measurement period.

The values obtained for the reaction rate were corrected for the neutron self shielding during activation and for gamma-ray self absorption during measurement. A correction was also made for the flux depression in the water due to the presence of the experiment, by the method of [6]. All of the corrections were small (<1.5%). The measured reaction rates are listed in Table 1. The errors associated with the irradiation and counting of the detectors was determined to range between 5 and 7%.

From the values obtained for R_{Au} and $[R_{Au}]_{Cd}$, the thermal neutron flux is

$$\phi_{th} = \frac{R_{Au} - [R_{Au}]_{Cd}}{\sigma_{Au}} = 3.277 \times 10^{13} \text{ n cm}^{-2} \text{ s}^{-1}$$

where $\sigma_{Au} = 98.8$ b for $E_n = 0.0253$ eV,

and where no correction has been made for epithermal neutron capture in the Cd cover. From the Ni reaction rate and the Ni cross section for $E_n = 2.5$ MeV the fast flux is

$$\phi_{Ni} = 8.837 \times 10^{12} \text{ n cm}^{-2} \text{ s}^{-1}.$$

Fluxes Computed with the SAND II Code

We used the SAND II computer code to determine differential and integral neutron fluxes. The input data for the code included the power-normalized saturation activities from the reaction rate measurements and an initial trial neutron spectrum to approximate the true spectrum. Since no suitable measured spectrum was available, we built an input spectrum as follows:

$$\phi(E) \propto f \cdot \frac{E}{(kT)^2} \cdot \exp\left(\frac{-E}{kT}\right) + \frac{\Delta(E/kT)}{E} + C \cdot E^{0.5} \cdot \exp\left(\frac{-E}{1.296}\right)$$

where:

$$\Delta(E/kT) = \begin{cases} 0; & \frac{E}{kT} \leq 3.19 \\ 1 + 1.6 \cdot \left(\frac{E}{kT} - 5\right) \cdot \exp\left(\frac{E}{3kT}\right); & \frac{E}{kT} > 3.19 \end{cases}$$

$f = \phi_{th}/\phi_{epi}$; and E and k are expressed in MeV and MeV K^{-1}, respectively.

The solutions for the differential and integral spectra are shown in Fig. 5. Integration of the SAND II results yields the following fluxes:

$\phi_{total} = 7.384 \times 10^{13}$ n cm^{-2} s^{-1} $(10^{-10} \leq E < 14.0$ MeV)

$\phi_{th} = 4.294 \times 10^{13}$ n cm^{-2} s^{-1} $(10^{-10} \leq E < 1.20 \times 10^{-6}$ MeV)

$\phi_{fast} = 1.324 \times 10^{13}$ n cm^{-2} s^{-1} $(E > 0.1$ MeV).

SPD SILVER REACTION RATE MEASUREMENTS TO DETERMINE THERMAL NEUTRON FLUX DISTRIBUTIONS

Two self-powered neutron detectors (SPDs) with silver emitters were specially designed for neutron flux measurements inside a fuel rod location in a TRIGA fuel cluster or in irradiation channels of the active core [7]. The sensitive portion of the silver emitter is 85 mm in length and 0.5 mm in diameter.

To obtain a neutron flux distribution, the active part of the SPD was positioned to a given level inside a fuel cluster or irradiation channel. After waiting for the silver activity to saturate or decay, depending on whether the flux is increasing or decreasing, a number of readings (in mV) were taken at one minute intervals and averaged to determine the relative flux at that position. For these measurements we tried to wait at least three minutes after moving the detector, and from four to eleven readings were averaged. The distance between two steps was 50 mm in most cases and 100 mm in one case.

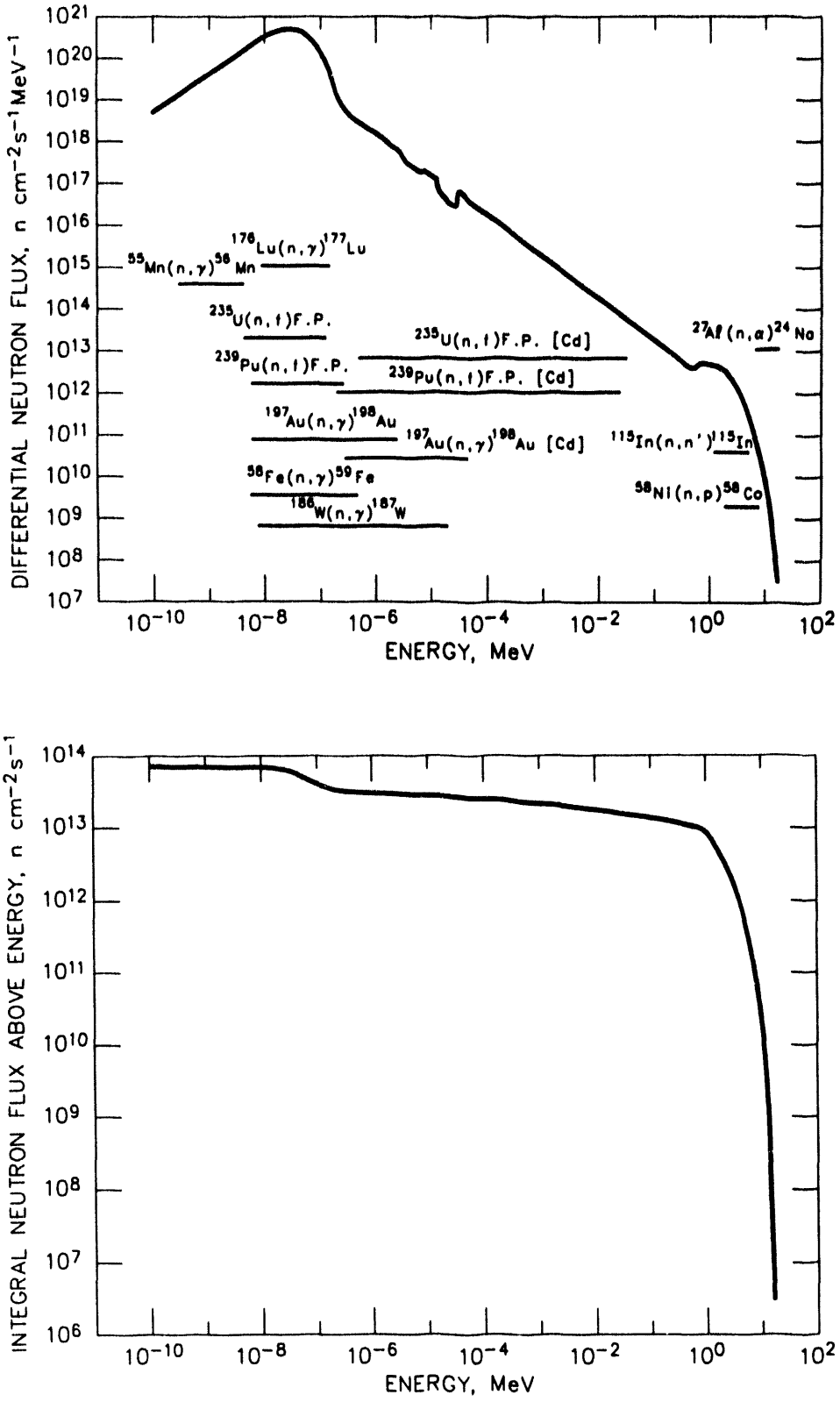

Fig. 5. Differential and Integral Neutron Flux Spectra Measured in the Water-Filled Experiment Position XC1.

At the lowest possible level for the detector in a fuel rod location within a fuel cluster, the middle of the silver emitter was located 50 mm above the bottom of the lowest fuel pellet. At the lowest position of the SPD in the experimental location XC1 with a plug at the bottom, the middle of the silver emitter was located 20 mm above the bottom of the lowest fuel pellet.

After equilibrium is achieved, the SPD output is proportional to the neutron absorption rate in the silver emitter, which is, of course, proportional to the neutron flux. Although neutron absorption in silver is predominantly in the thermal range, silver does have a substantial epithermal resonance. Therefore, a reaction rate distribution measured with the SPD is equal to the distribution of thermal flux only if the flux spectrum is the same at every measurement point. This is generally a good approximation for axial measurements taken within the fuel column height at a given grid position. However, the flux spectrum might vary axially close to partially inserted control rods. Flux spectra are also expected to be very similar near the centers of well-moderated regions, such as water-filled (empty) experiment positions, so detector responses for these regions would represent relative thermal fluxes. However, careful calibrations must be performed before comparisons of thermal fluxes in regions of differing flux spectra (for example, between the center and the edge of an irradiation channel) can be made.

The raw data are given in Table 2, and axial profiles (using power-normalized data) are presented in Figs. 6 and 7. Axial profiles for two different positions of the control rods are compared in the first two figures, highlighting the perturbation effect of the control rod positions on the flux distribution. The axial peak-to-average factor is shown for each curve. The diagrams with the plots show the locations of the SPDs. It should be noted that positions with empty fuel clusters or with plugs are essentially water-filled. In the measurement in the fuel cluster with shims, stainless steel dummy fuel rods filled the 23 positions not occupied by the SPDs.

REFERENCES

1. M. M. Bretscher, J. L. Snelgrove, and M. Ciocanescu, "Analytical Analyses of Startup Measurements Associated with the First Use of LEU Fuel in Romania's 14-MW TRIGA Reactor," these proceedings.

2. I. Gârlea, C. Miron, T. Musat, and C. Roth, "Proposed Procedures for Flux Measurements in the Romanian TRIGA Reactor," Pitesti (1978).

3. W. N. McElroy, S. Berg, and G. Gigas, "Neutron-Flux Spectral Determination by Foil Activation," Nucl. Sci. Eng. 27, 533-541 (1967).

4. Al. Berinde, Reactor Physics, Bucharest (1970).

5. International Atomic Energy Agency, Handbook on Nuclear Activation Data, Technical Report Series No. 273, Vienna (1987).

6. W. Bothe, "Zur Methodik der Neutronensonden," Z. für Physik **120**, 437-449 (1943).

7. R. Baudry, "Mesure continue des flux de neutrons thermiqes par sonde à émetteur β," Commisariat à l'Energie Atomique Report CEA-R-4312/1972.

TABLE 2. AXIAL SILVER REACTION RATE (THERMAL NEUTRON FLUX) DISTRIBUTION DATA

XC1-G7	AXIAL DIM. (cm)	5	10	15	20	25	30	35	40	45	50	55	60	65	ROD POS. (Index)
WITH	POWER (MW)	3.17	3.11	3.14	3.07	3.06	3.03	3.32	3.36	3.08	3.06	3.19	3.24	3.19	BANK=542
EMPTY	SPD 1 (mV)	1.62	1.98	2.18	2.32	2.22	1.88	1.79	1.35	0.92	0.70	0.46	0.25	0.12	
FUEL	POWER (MW)	3.08	3.04	3.12	3.12	3.05	3.05	3.03	3.09	3.07	3.14	3.09	3.10	3.06	ROD 2=900, BANK=100,
CLUSTER	SPD 1 (mV)	1.26	1.61	1.91	2.22	2.38	2.38	2.22	1.98	1.68	1.30	0.85	0.47	0.20	ROD 3=781
E6	AXIAL DIM. (cm)	2	7	12	17	22	27	32	37	42	47	52	57	62	ROD POS. (Index)
WITH PLUG	POWER (MW)	3.17	3.11	3.14	3.07	3.06	3.03	3.32	3.36	3.08	3.06	3.19	3.24	3.19	BANK=542
	SPD 2 (mV)	1.04	1.34	1.59	1.74	1.80	1.71	1.86	1.58	1.22	0.95	0.68	0.40	0.21	
	POWER (MW)	3.08	3.04	3.12	3.12	3.05	3.05	3.03	3.09	3.07	3.14	3.09	3.10	3.06	ROD 2=900, BANK=100,
	SPD 2 (mV)	0.86	1.22	1.48	1.75	1.90	2.00	1.96	1.88	1.68	1.35	0.89	0.55	0.28	ROD 3=781
XC1-G7	AXIAL DIM. (cm)	5	10	15	20	25	30	35	40	45	50	55	60	65	ROD POS. (Index)
+ ROD 2123	POWER (MW)	3.04	3.13	3.13	3.13	3.10	3.16	3.14	3.09	3.14	3.07	3.05	3.06		BANK=535
IN EMPTY	SPD 1 (mV)	1.55	1.93	2.15	2.30	2.26	1.97	1.62	1.23	0.93	0.69	0.44	0.25		
FUEL	POWER (MW)	2.91	3.06	3.07	3.10	3.13	3.08	3.08	3.02	3.05	3.04	3.07	3.05	3.03	ROD 2=900, BANK=100,
CLUSTER	SPD 1 (mV)	1.20	1.61	1.90	2.22	2.44	2.42	2.25	1.93	1.65	1.26	0.79	0.41	0.20	ROD 3=736
F8	AXIAL DIM. (cm)	5	10	15	20	25	30	35	40	45	50	55	60	65	ROD POS. (Index)
LEU FUEL	POWER (MW)	3.04	3.13	3.13	3.13	3.10	3.16	3.14	3.09	3.14	3.07	3.05	3.06		BANK=535
CLUSTER	SPD 2 (mV)	0.61	0.74	0.79	0.78	0.69	0.49	0.36	0.28	0.23	0.17	0.12	0.08		
- ROD 2123	POWER (MW)	2.91	3.06	3.07	3.10	3.13	3.08	3.08	3.02	3.05	3.04	3.07	3.05	3.03	ROD 2=900, BANK=100,
	SPD 2 (mV)	0.45	0.57	0.66	0.74	0.80	0.80	0.79	0.68	0.61	0.45	0.29	0.14	0.07	ROD 3=736
XC1-G7	AXIAL DIM. (cm)	5	15	25	35	45	55	65							ROD POS. (Index)
FUEL	POWER (MW)	4.87	4.84	4.85	4.97	4.99	5.00	5.03							BANK=640
CLUSTER	SPD 1 (mV)	0.69	1.02	1.16	0.97	0.59	0.27	0.10							
WITH SHIMS	SPD 2 (mV)	0.79	1.03	1.15	0.81	0.35	0.16	0.05							ROD 3=736
XC1-G7	AXIAL DIM. (cm)	7	12	17	22	27	32	37	42	47	52	57			ROD POS. (Index)
WITH PLUG	POWER (MW)	4.88	4.88	4.93	4.96	4.93	4.86	4.98	4.97	5	5.06	4.99			BANK=598
	SPD 2 (mV)	2.25	2.81	3.19	3.31	3.14	2.67	2.06	1.55	1.15	0.77	0.45			
XC3-E9	AXIAL DIM. (cm)	7	12	17	22	27	32	37	42	47	52	57			ROD POS. (Index)
WITH PLUG	POWER (MW)	4.91	4.99	5.01	4.86	4.93	5.02	4.88	4.93	4.92	4.93	4.95			BANK=587
	SPD 2 (mV)	1.56	1.91	2.12	2.16	2.16	2.07	1.87	1.57	1.29	0.89	0.51			

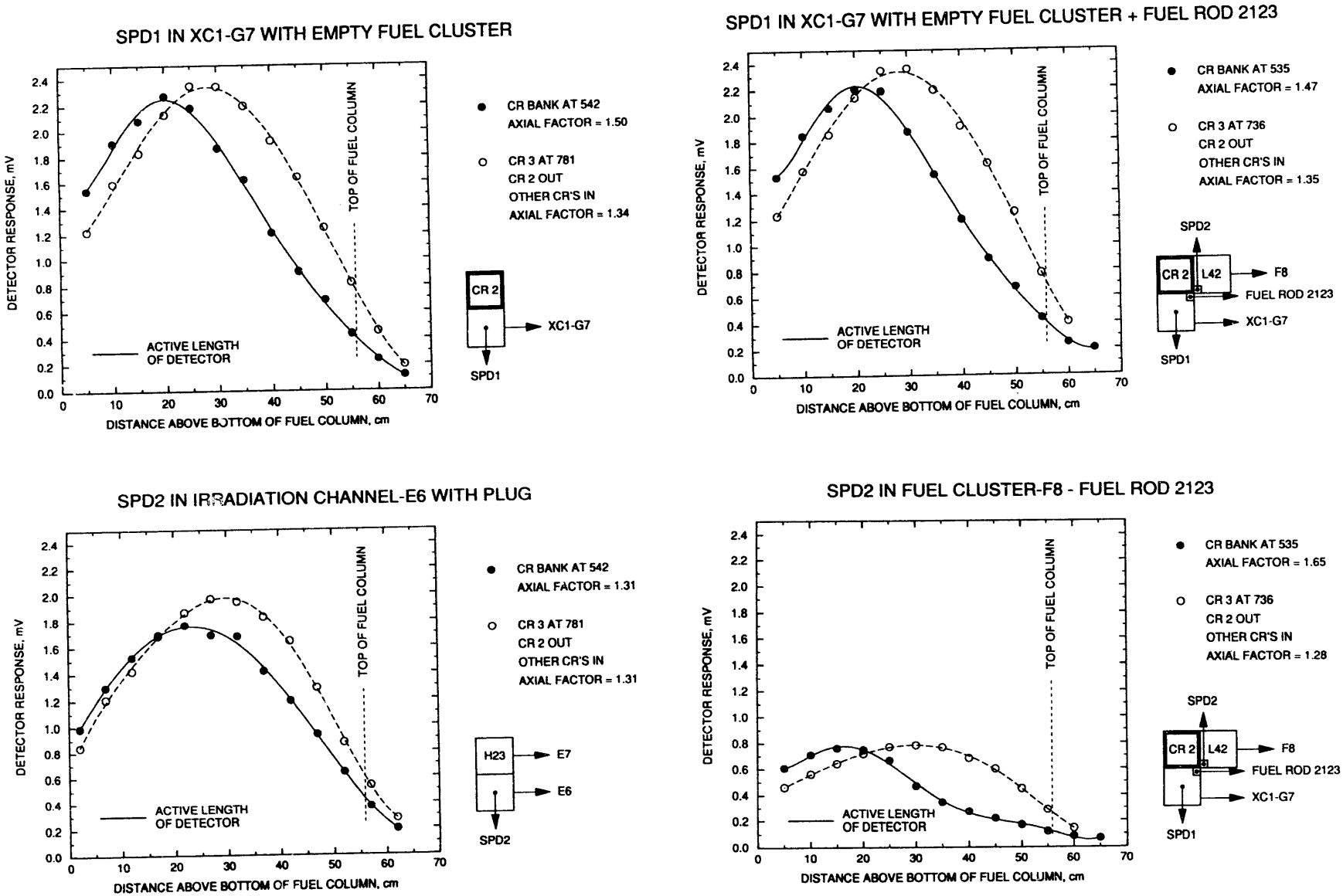

Fig. 6. Axial Distributions of Silver Reaction Rates (Thermal Neutron Fluxes) Measured with SPDs Normalized to 3.0 MW Reactor Power.

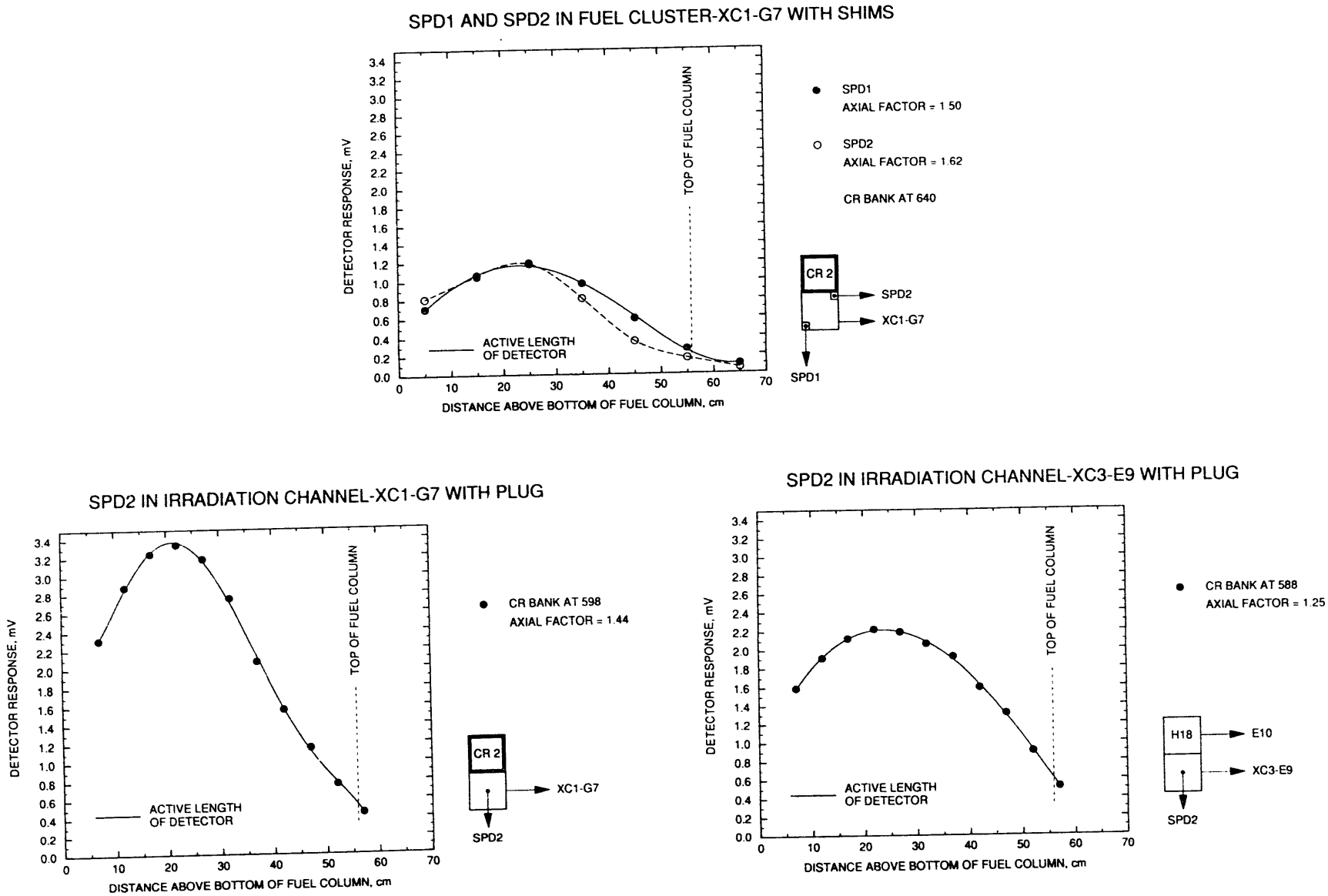

Fig. 7. Axial Distributions of Silver Reaction Rates (Thermal Neutron Fluxes) Measured with SPDs Normalized to 5.0 MW Reactor Power.

PROGRESS OF TRANSIENT IRRADIATION TEST WITH LEU SILICIDE FUEL

H. ICHIKAWA, T. KODAIRA, K. YANAGISAWA AND T. FUJISHIRO

Tokai Research Establishment
Japan Atomic Energy Research Institute
Tokai-mura, Naka-gun, Ibaraki-ken 319-11, Japan

ABSTRACT

Transient irradiation experiments are being progressed in order to study the behavior of low enriched MTR type fuel under transient and/or accidental conditions in the Japan Atomic Energy Research Institute. Up to now, ten experiments have been conducted with fresh silicide fuel mini-plates. The results obtained are summarized as follows:

(1) The maximum fuel surface temperatures were 200℃ to 970℃ with the deposited energy in the fuel mini-plates ranged 62 to 164 cal/g•fuel. The departure from nucleate boiling might occur in every experiments, however, fuel mini-plates remained intact with energy depositions below 82 cal/g•fuel.
(2) With energy dipositions 94 to 97 cal/g•fuel, the fuel mini-plates were damaged with small intergranular cracks despite low fuel plate surface temperature, below 330℃. It is presumed that they were caused by the thermal stress occured during rapid quenching of the fuel mini-plates. No significant dimensional changes observed in these cases.
(3) With energy dipositions above 116 cal/g•fuel, the maximum fuel surface temperatures were beyond 400℃, and the fuel mini-plates were damaged mainly by the melting of the aluminum cladding, accompanying significant dimensional changes.
(4) No fuel fragmentation nor mechanical energy generation was observed even in the experiments in which the maximum fuel temperature exceeded 900℃.

INTRODUCTION

The low enriched, highly dense uranium aluminide/silicide fuels are becoming widely used in research and test reactors. In Japan, the operation of the modified Japan Research Reactor No. 3 (JRR-3M) of the Japan Atomic Energy Research Institute (JAERI) was started in November 1991, using 2.2g/cc dense low enriched (19.75wt%) aluminide fuels. Further, both conversion programs to low enriched silicide fuel core are being successfully progressed on the Japan Material Testing Reactor (JMTR) of JAERI and Kyoto University Research Reactor (KUR).

In order to establish a data base on the behavior of the low enriched plate-type fuels under transient/accidental conditions, the transient irradiation experiments on these fuels are being progressed from December 1990, by the pulse irradiation using the Nuclear Safety Research Reactor (NSRR) of JAERI-Tokai.

The NSRR is a modified TRIGA-ACRP (Annual Core Pulse Reactor) which was built for investigating the nuclear fuel behavior under a reactivity initiated accident (RIA) condition. A positive reactivity of 4.67$ can be inserted to the core in maximum, generating the pulse reactor power of 23,000 MW with a half width of 4.4 msec. The general objectives of the NSRR pulse irradiation tests are to determine threshold energy for fuel failure and to investigate its mechanism and failure consequences under RIA conditions for the Light Water Reactor (LWR) fuels. At present, not only unirradiated LWR fuels but pre-irradiated LWR fuels and fresh plate-type aluminide/silicide fuels are available as test fuels.

We reported the results of first stage experiments with silicide fuel mini-plates at the last RERTR meeting held in Jakarta, Indonesia.[1] After that, another six experiments have been conducted, in which the fuel behavior at relatively low temperature, below 400℃, were studied in detail, trying to simulate the temperature excursion in fuel plates during a transient or RIA conditions of research and test reactors.[2]

TRANSIENT IRRADIATION EXPERIMENT

1. Fuel Mini-plate

The fuel mini-plates used in the transient irradiation experiments have same dimension of 35 mm × 130 mm × 1.27 mm, with fuel core of 25 mm × 70 mm × 0.51 mm. Three kinds of fuel mini-plate with defferent uranium densities are prepared, however, only 4.8g/cc fuel mini-plates have been provided to the experiments, up to now. These fuel mini-plates were fablicated by CERCA, Franse and B&W, USA. The tensile strength of the aluminum cladding are aproximately 230 MPa and 120 MPa for CERCA's plates and B&W's, respectively, and the 0.2% yield strength are 120 MPa and 60 MPa, respectively.

2. Instrumentations and Irradiation Capsules

Five Pt/Pt-13%Rh thermocouples (hereinafter abbreviated T/C's), of which melting point was 1,780℃, were spot welded directly to one side of the surface of each fuel mini-plate at five different locations. After assembling to the supporting device, fuel mini-plate was contained in a irradiation capsule with stagnant water at the room temperature and at one atomospheric pressure. The capsule is a pressure vessel made by the stainless steel. Two capsule pressure sensors and a water level sensor were also installed inside the capsule in order to monitor the pressure pulse and water hammer force caused by the melting and/or fragmentation of fuel mini-plate.

3. Pulse Power History

The deposited energy in fuel mini-plate by pulse irradiation is propotional to the integral value of the reactor pulse power. The

integral value of the reactor power measured by micro fission chamber was used to estimate the deposited energy in each test fuel mini-plate using the power conversion ratio k_g (cal/g•fuel per MW•sec). This ratio was determined through fuel burn-up analysis on irradiated mini-plates at low pulse power, taking the radial and axial power peaking into consideration.

RESULT AND DISCUSSIONS

1. Transient Temperature History

Up to now, ten pulse irradiation tests (#508-1 ~ #508-10) have been conducted. Table 1 shows a summary of fuel behavior derived from in-core measurements and post pulse-irradiation examination (PIE), including the results previously reported [1), 3), 4), 5)] (#508-1, -2, -3 and -4). As shown in this table, four fuel mini-plates were damaged at relatively low fuel surface temperature, below 330℃ (#508-6, -7, -8 and -9).

In Fig. 1, a typical measured transient temperature is shown with the reactor pulse power. It can be seen that the fuel surface temperature increased to 203 ℃, and it once decreased to 194℃ where it remained whithin 10 ms. After that, the fuel surface temperature rose again to the maximum temperature, 244℃. This transient temperature profile indicates that the departure from nucleate boiling (DNB) occured. In all experiments, similar phenomena were observed, and the averaged DNB temperature was 174 ± 6℃. The fuel surface temperature was then quenched to 116℃ in an interval of 0.135 second, and gradually decreased to below 50℃. It is presumed that this rapid quenching from the maximum temperature, 244 ℃ to 116℃ (temperature drop, ΔT=128℃) caused the local thermal stress. Using ΔT, the thermal stress is calculated to be 235 MPa, which is close to the tensile strength value and the yield strength value of cladding mentioned before. The thermal stress estimated using the maximum temperature drop in this study was 394 MPa.

Figure 2 summarizes the relation between the measured peak fuel surface temperature and given deposited energy. It is seen that the irradiated fuel mini-plates kept intact at energy depositions below 82 cal/g•fuel, while they were damaged above 94 cal/g•fuel. It is also seen that the failure mode of fuel mini-plate depended on the fuel surface temperature; at temperatures below 400 ℃, only the local incipient and through-plate crackings were observed. When the temperatures were much higher, large plate deformation occured by softening and melting of aluminum cladding.

2. Metallography, Failure Mode, Mechanism and Dimensional Stability

For metallographic examination, longitudinal and transverse sections were made from near T/Cs and cracks. In Photograph 1, (a) shows an overview of a irradiated fuel mini-plate (#508-8), in which both through-plate cracking and incipient cracking are observed. Both cracks propagated perpendicular to the axial direction. It is seen that the incipient crack was initiated from the aluminum cladding and not from the fuel core from (b). It is also seen from the through-plate crack shown in (c) that the crack propagated intergranulary from outer edge of the

cladding.

Figure 3 shows the failure maps of the fuel mini-plates damaged in pulse irradiation tests from #508-3 to #508-9, in which the deposited energy were 94 to 164 cal/g•fuel. In this figure, relative locations and numbers of cracks, seperations from the fuel core and distribution of the molten aluminum holes are presented.

Dimensional stability of mini-plates under pulse irradiation was also studied using data from PIE and the summary is shown in Table 1. The maximum bowing of each sections cut from mini-plates are all within the range of previously reported. It should be noted that the failures observed below 400℃ in this study were not accompanied by significant changes in the plate dimension, that is, the thermal stress was extremely localized.

CONCLUSIONS

Transient irradiation experiments are being progressed on the low enriched silicide fuel mini-plates by the pulse irradiation. Ten experiments have been conducted with fresh silicide fuel mini-plates cooled by stagnant water at room temperature and at atomospheric pressure. The results obtained are summarized as follows:

(1) The maximum fuel surface temperatures were 200℃ to 970℃ with the deposited energy in the fuel mini-plates ranged 62 to 164 cal/g•fuel. The departure from nucleate boiling might occur in every experiments, however, fuel mini-plates remained intact with energy depositions below 82 cal/g•fuel. Fuel mini-plates were damaged with energy depositions above 94 cal/g•fuel.

(2) With energy dipositions 94 to 97 cal/g•fuel, fuel plates were damaged with small intergranular cracks despite low fuel plate surface temperature, below 330 ℃. These failures might be attributed to the local thermal stress caused by the rapid quenching of fuel mini-plates. The intergranular cracks have propagated from the plate surface to the fuel core. No significant dimensional changes observed in these cases.

(3) With energy dipositions above 116 cal/g•fuel, the maximum fuel surface temperatures were beyond 400℃, and fuel plates were damaged mainly by the melting of the aluminum cladding, accompanying significant dimensional changes.

(4) No fuel fragmentation nor mechanical energy generation was observed even in the experiments in which the maximum fuel temperature exceeded 900 ℃.

The transient irradiation experiments on the low enriched uranium MTR-type fuel are planned to be continuously progressed for several years; the experiments in which more severe conditions will be provided, the experiments using aluminide fuels and pre-irradiated fuel mini-plates, and so on.

ACKNOWLEDGMENT

The authors wish to thank Mr. E. Shirai, Director, Department of Research Reactor and Mr. I. Kobayashi, Director, Department of Fuel Safety Research and Dr. Y. Futamura, Director, JMTR Project for their encouragement and promotion of this work.

REFERENCES

1)H. ICHIKAWA et al., "Behavior of Low Enriched Uranium Silicide Mini-Plates Under Transient Irradiation", Proceedings of 14th International RERTR meeting, to be published.
2)K.YANAGISAWA et al., "Study on Transient Behavior of Low Enriched Uranium Silicide Plate Type Fuel for Research Reactors during RIA Conditions", Journal of Nucl. Sci. & Technol., to be published.
3)K. YANAGISAWA et al., "Technical report: Technical Development on the Silicide Plate-type Fuel Experiment at Nuclear Safety Research Reactor", JAERI-M 91-114 (1991)
4)K. YANAGISAWA, "Post-pulse Detail Metallographic Examinations of Low-enriched Uranium Siliside Plate-Type Miniature Fuel", JAERI-M 91-152 (1991)
5)K. YANAGISAWA et al., "Dimensional Stability of Low Enriched Uranium Silicide Plate-Type Fuel for Research Reactors at Transient Conditions" , Journal of Nucl. Sci. & Technol., 29[3], 233 (1992)
6)K. YANAGISAWA et al., "Study of Transient Behavior of Low Enriched Silicide Fuel Plates by Pulse Irradiation in the NSRR", Proceedings of the 3rd Asian Symposium on Research Reactor, JAERI-M 92-028 (1992)

Table 1 Summary of Transient Irradiation Behavior of Low Enriched Silicide Mini-plate

TEST ID. NO.	#508-1[6]	#508-2[6]	#508-10	#508-7	#508-9	#508-6	#508-8	#508-3[6]	#508-4[6]	#508-5
Deposited Energy (cal/g·fuel)	62	77	82	94	95	96	97	116	154	164
Peak Surface Temperature (℃)										
T/C #1	× [1]	200	216	198	279	270	309	350	971	779
#2	177	179	180	210	315	229	261	305→387	893	689
#3	216	183	227	199	284	202	211	414	652	×
#4	234	178	173	237	285 [4], 305→261	×	244	393	881	918
#5	178	195	204	191	280	205	330	544	305→957	578→665
(#6)	— [2]	—	182	—	282	—	—	—	—	—
(#7)	—	—	173	—	290±14	—	—	—	—	—
Average±Standard Deviation (℃)	201±28	187±10	194±22	207±18	202	227±31	271±48	418±74	871±128	761±117
Max. Temperature Drop ΔT (℃)	128	98	129	122		159	214	440	882	853
Coolant Temperature (℃)										
pre-pulse	20	22	21	24	22	21	25	18	17	22
peak	24	26	28	53	58	43	46	47	35	34
Capsule Pressure (MPa)										
bottom	— [3]	0	0	0	0	0	0	0	0	0
top	—	0	0	0	0	0	0	0	0	0
Water Column Velocity	—	0	0	0	0	0	0	0	0	0
Failure (F) / no Failure (NF)	NF	NF	NF	F	F	F	F	F	F	F
Failure Mode Observed in PIE				Mechanical Cracking due to Thermal Stress					Melting	
				IC × 2 PT × 2	PT × 3	IC × 1 PT × 1	IC × 1 PT × 1	IC × 3	PT × 2 CS CM	IC × 1 PT × 1 CS CM
Max Bowing (mm)	None	None	0.11±0.07	0.12±0.11	—	0.53±0.16	0.14±0.07	1.2 ±0.85	6.4 ±1.8	2.7 ±1.2

Note :
1) × Mulfunction
2) — No thermocouple
3) — Not equipped
4) Two peaks
5) IC:Incipient crack, PT:Through-plate crack, CS:Core seperation, CM:Cladding melt
6) Previously published

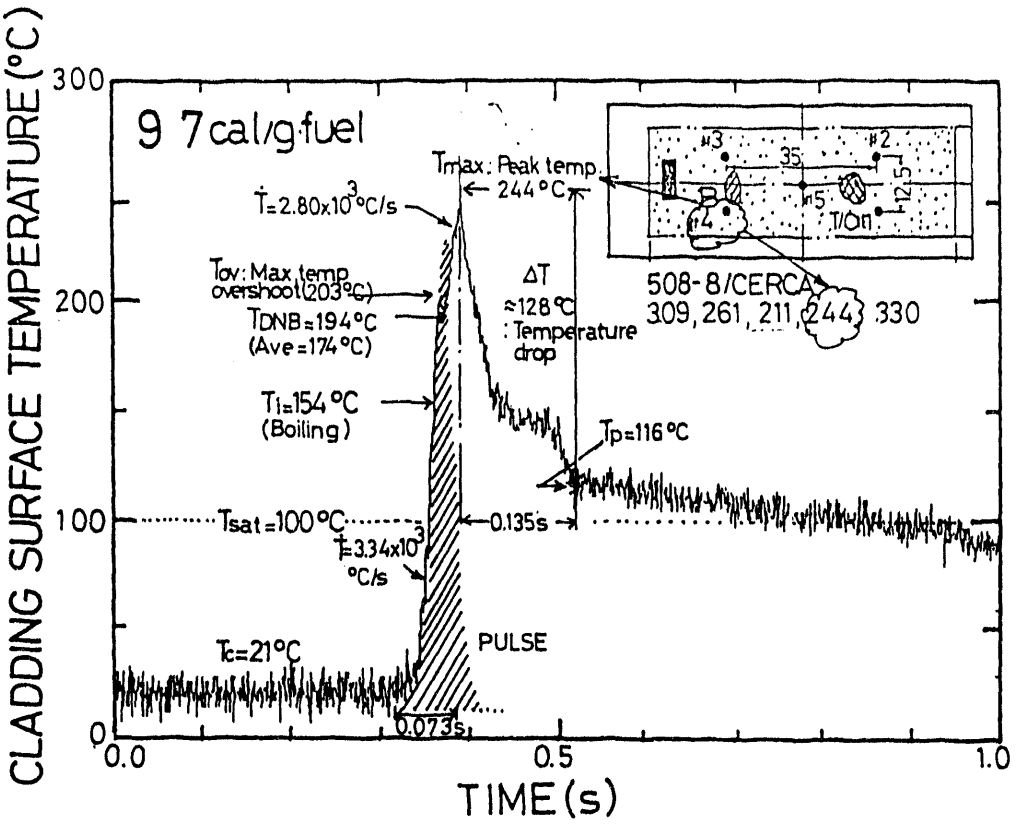

Fig. 1 Typical Surface Temperature Profile of Silicide Mini-plate under Transient Irradiation

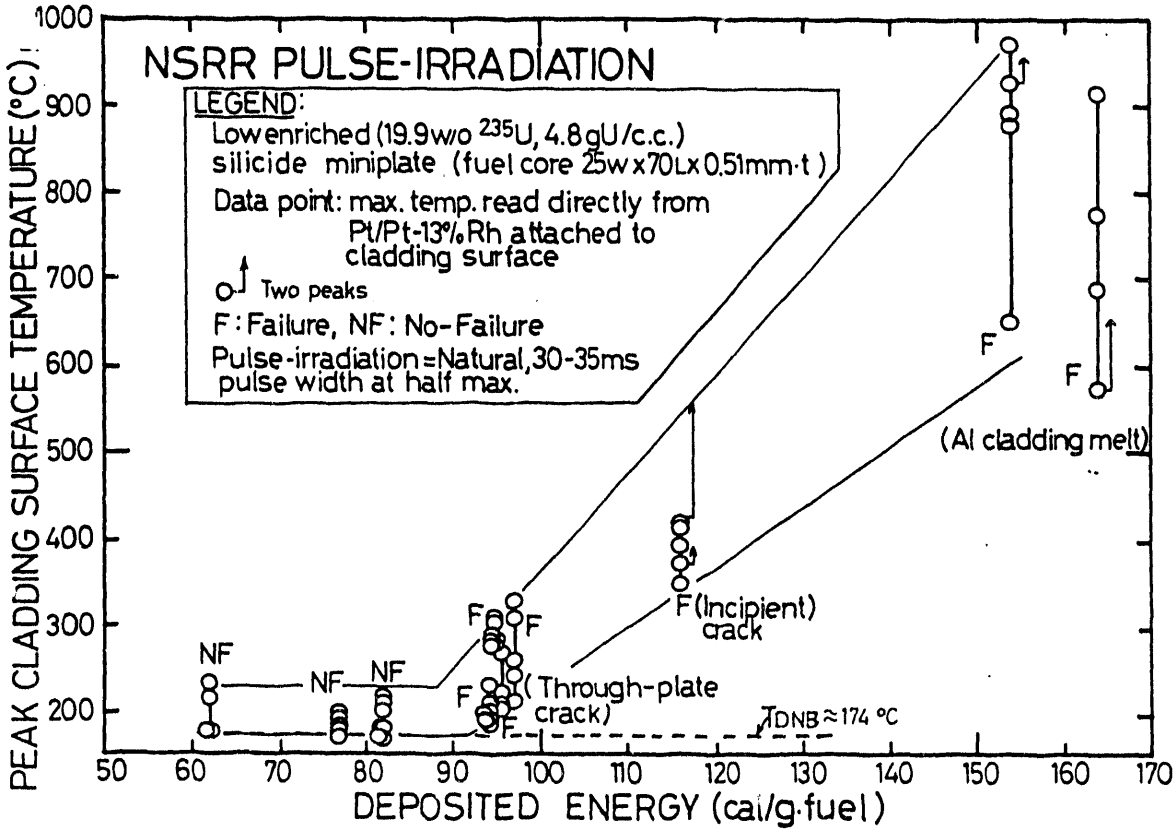

Fig. 2 Fuel Surface Temperature as a Function of Deposited Energy

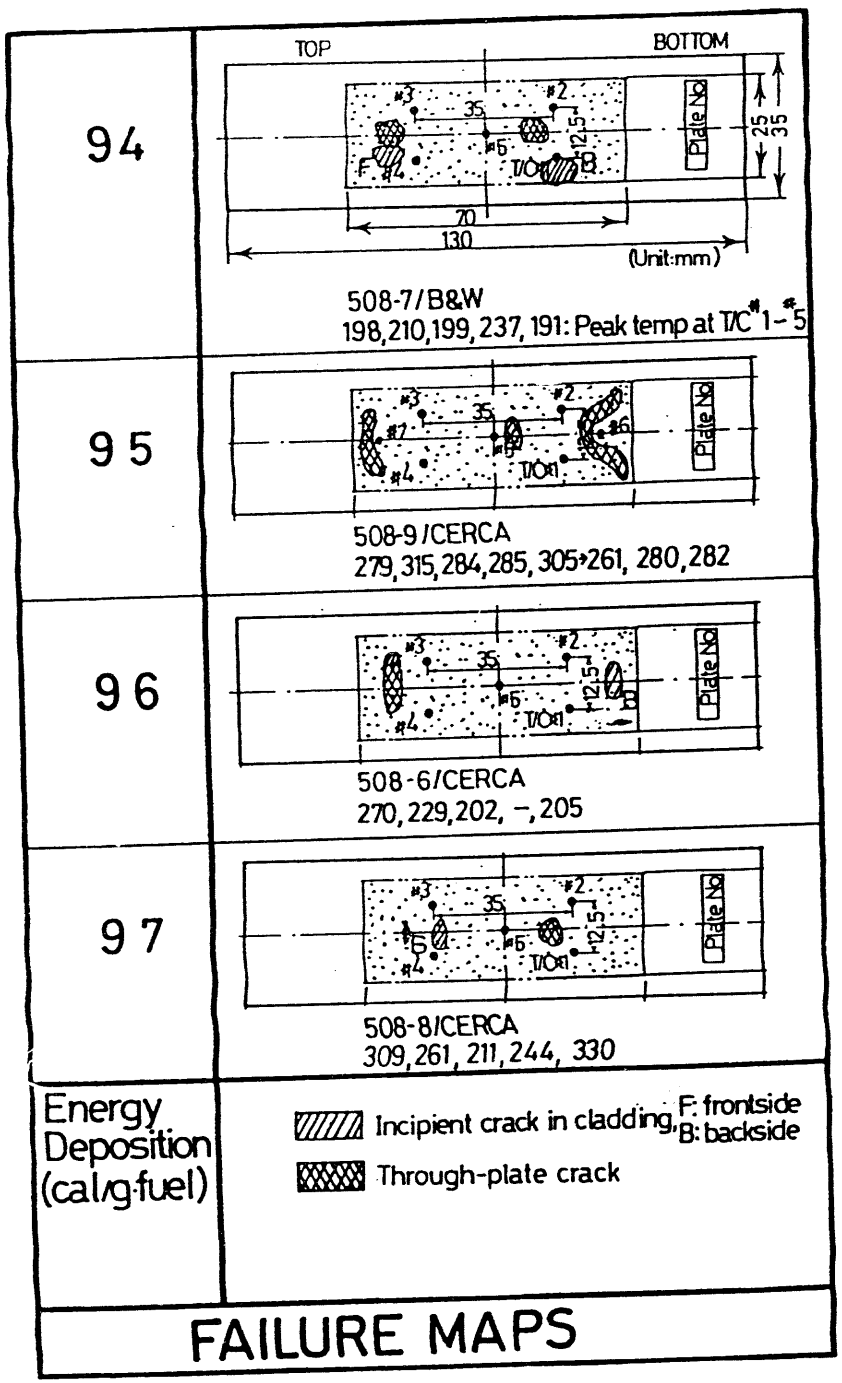

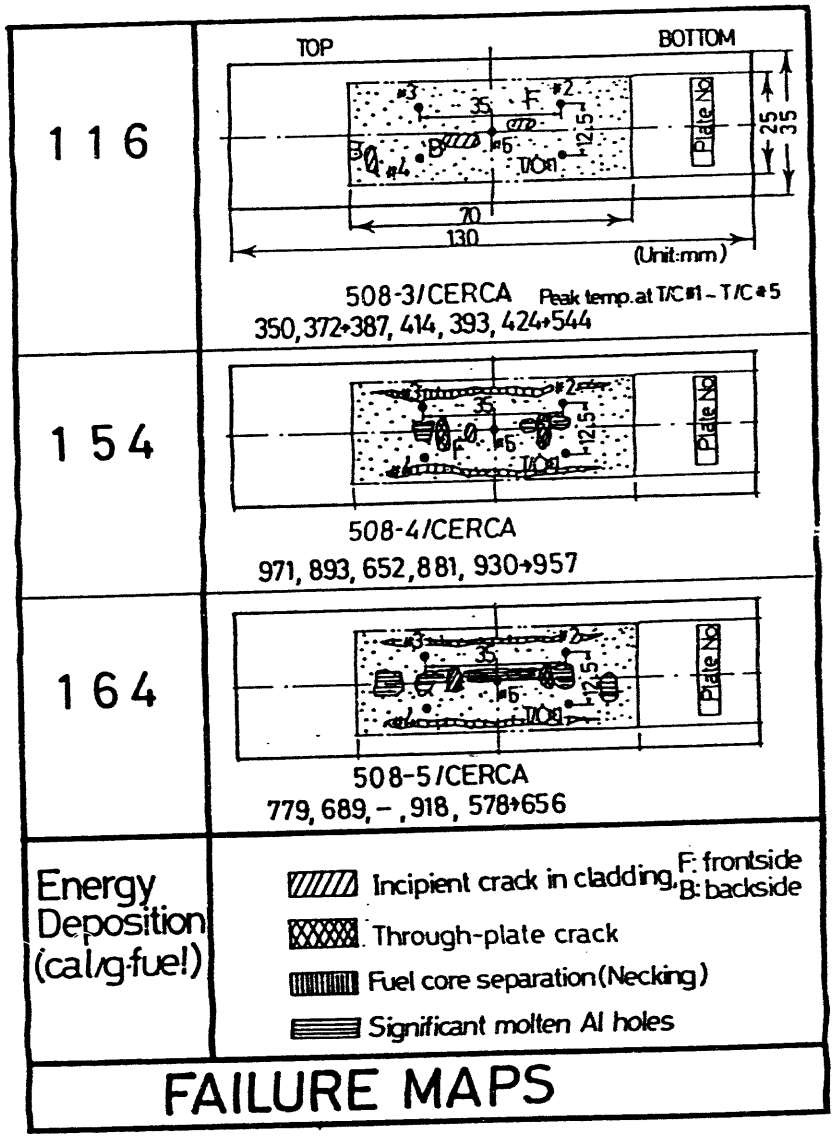

Fig. 3 Failure Map of Seven Mini-Plates as a Function of Deposited Energy

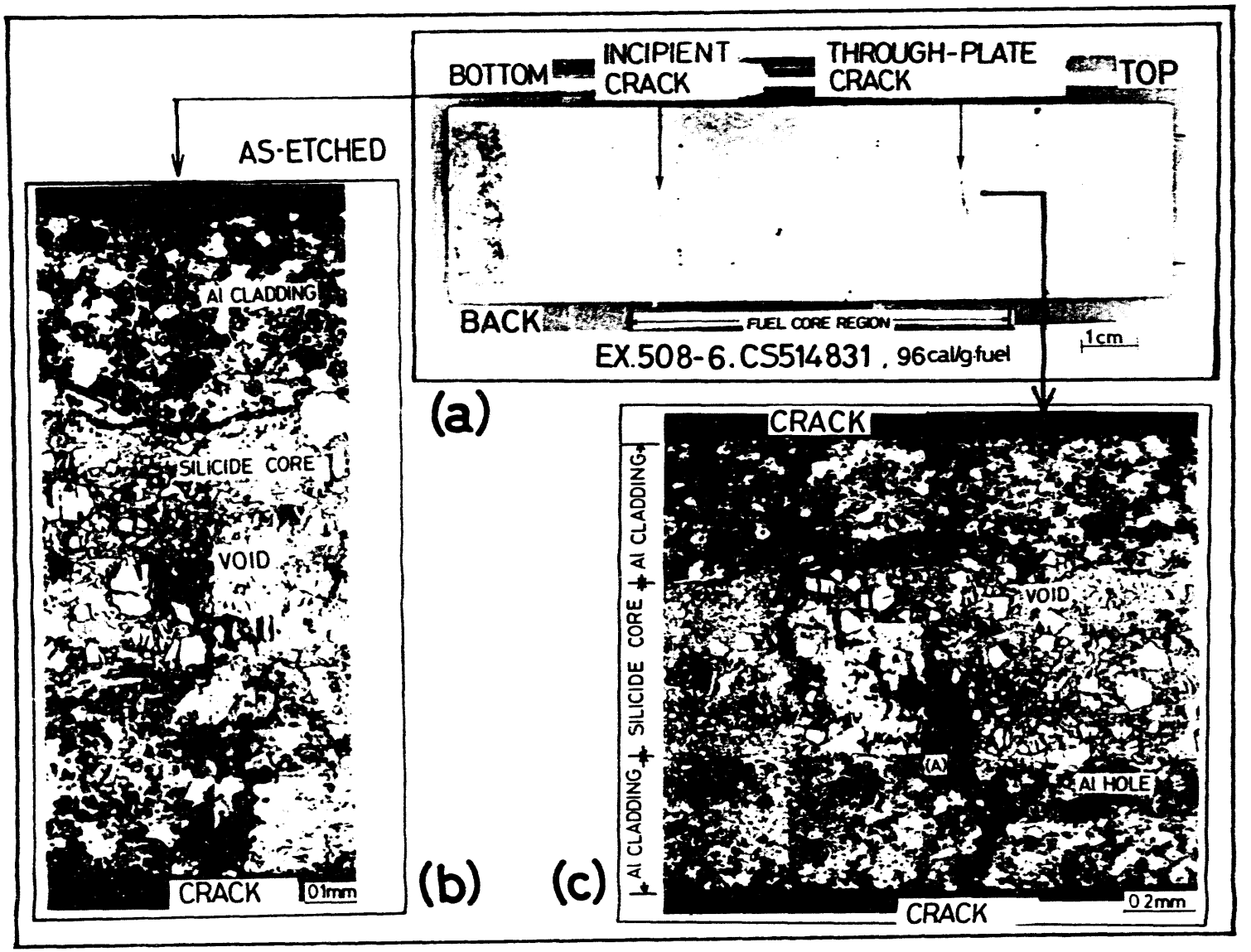

Photograph 1 (a)Overview of the Irradiated Mini-Plate,
(b)the Etched Surface of a Section cut from the Incipient Cracked Area,
(c)the Etched Surface of a Section cut from the Through-Plate Cracked Area

A SWELLING MODEL OF LEU SILICIDE FUEL FOR KMRR

Woan Hwang*, B.G. Kim, K.S. Sim, Y.H. Heo, Ho Chun SUK
Korea Atomic Energy Research Institute
P.O. Box 7, Daeduk-Danji, Daejeon, Korea

ABSTRACT

A lot of efforts have been made internationally to understand the irradiation behavior and the safety characteristics of uranium silicide fuel. One of the important irradiation performance characteristics of the silicide dispersion fuel element is the diametral increase resulting from fuel swelling. This paper represents an attempt to develop the physical model for the swelling, DFSWELL, by modelling the basic irradiation behavior observed from in-reactor experiments. The most important part of developing the swelling model is the identification of the controlling physical processes. The swelling of the silicide fuel is comprised of the volume change due to three major components ; i) the formation of an interfacial layer between the fuel particle and matrix, ii) the accumulation of gas bubble nucleation, iii) the accumulation of solid fission products. In this study, the swelling of the fuel element is quantitatively estimated by considering temperature, fission rate, solid fission product build-up and gas bubble behavior. The DFSWELL model which takes into account the above physical components predicts well the absolute magnitude of silicide fuel swelling in accordance with the power histories in comparison with the experimental data.

INTRODUCTION

In Korea, the Korea Mulipurpose Research Reactor (KMRR) is under construction at KAERI(Korea Atomic Energy Research Institute). The KMRR driver fuel will be made from elements of an extruded uranium silicide dispersion in aluminum, with finned aluminum cladding and aluminum end plugs. The fuel core consists of a dispersion of small particles of a high density uranium silicide compound in a continuous aluminum matrix. The reference fuel material for the KMRR fuel has a nominal composition of 61 wt% U_3Si and 39 wt% Al. We began to develop the fuel performance code to predict the irradiation behavior of U_3Si-Al dispersion fuel elements in research reactors as well as the technique for fabricating the fuel elements.

In reactor irradiation experiments with intermetallic uranium compounds, Hofman showed [1] that an enormous increase in gas bubble growth occurs when a compound becomes amorphous during irradiation. As a result of the interaction of different processes, a material density change so-called fuel swelling, and material phase change, as well as nuclear property changes due to uranium burnup occur.

To develop a comprehensive swelling model, some controlling physical processes on the irradiation behavior of silicide fuel are identified by analyzing the irradiation behaviors reported from the literatures[1-12] in this study. This paper represents an attempt to develop a physical model to efficiently predict the swelling of the silicide fuel according to power history.

PHYSICAL PROCESSES FOR DISPERSION FUEL CORE SWELLING

The most important part of developing a physical model is the identification of the controlling physical processes. So far, some contributing mechanisms [1,4,5,6,11] have been suggested for the swelling of silicide dispersion fuel. However the mechanisms of the swelling behavior for silicide fuel do not fully explain the observed swelling phenomena. Accordingly, it is necessary to extensively identify the controlling processes to develop a comprehensive swelling model. Hence, the limited amount of experimental evidences acquired so far have led to the following conclusive-controlling physical processes :

(i) U_3Si-Al and U_3Si_2-Al are thermodynamically unstable. The type and amount of reaction products (uranium aluminides) formed, obviously varies with concentration and temperature, and can be predicted from the ternary phase diagram. The uranium aluminides UAl_2, UAl_3 and UAl_{4+x} dissolve substantial amounts of silicon at higher temperatures, the solubility is however, in the case of UAl_2 and UAl_3, temperature dependent [2].

(ii) From the result of FZZ-909A experiment, post-irradiation metallography revealed that interfacial layers around reacted silicide particles had reached a thickness of 7.5 μm near the fuel core periphery and 25 μm around particles near the fuel core centre. Again " reacted silicide " particles had coalesced [3].

(iii) The swelling observed in most specimens was clearly associated with a reaction between the fuel particles and the aluminum matrix, the aluminum having reacted with particle surfaces and also penetrated along networks of grain boundaries to attack sub-grains throughout the U_3Si. The end point of such a reaction would occur when all the U_3Si(and the precipitates of U_3Si_2 contained within the U_3Si particles) had been consumed to form $UAl_3Si_{1/3}$. Rates of reaction would be reduced eventually (as observed) due to the impedence, offered to diffusing aluminum atoms, by the $UAl_3Si_{1/3}$ surrounding the U_3Si particles and growing in thickness [4,5].

(iv) The volume change due to uranium burnup will be calculated using the most current uranium-silicon equilibrium phase diagram and measured densities of the phases involved. The amounts of non-gaseous fission products were determined with the aid of published fission yield data for U-235. These contributions to volume change were estimated by evaluating their solubility in the fuel and the tendency to form compounds with each other and with uranium and silicon. These two contributions to swelling, i.e., phase transformation and non-gaseous fission products were combined and yielded as a linear function of fission density. The largest component of the fuel swelling is due to the formation of fission gas bubbles [6].

(v) Nucleation of fission gas bubble in U_3Si fuel was apparently very uniform as compared to the USi*Al fuel. But the fission gas bubble sizes were larger near the fuel core periphery than at the fuel core centre in

both cases [7,8]. It would be considered likely that this result was due to the fact that the local fission rate along the radial direction within the fuel core is different.

(vi) The aluminum having reacted with particle surfaces formed interfacial layers around the silicide particles in the fuel core. The interfacial layers were thinner[3,7,8] near the fuel core periphery than at the fuel core centre. It should be noted that the density of the interfacial layer is lower than that of U_3Si particle.

(vii) The fine particles had essentially completely reacted forming the less dense UAl_3 while only thin interfacial layers formed around the coarser silicide particles. The larger surface area provided by the fine particles undoubtedly led to the increased reaction and contributed significantly to the observed core swelling [9].

(viii) During heat treatment of Al-USiAl particles above a temperature around 200 °C, the aluminum diffuses into the USiAl particles along grain and particle boundaries forming UAl_3 and eventually UAl_3. The aluminum apparently diffuses into the USiAl particles along unstable paths such as subparticle boundaries to form the new Al-U compounds [10].

(ix) Fission gas bubbles have recently been shown to exhibit extremely high growth rates at relatively low temperatures in certain uranium compounds. This accelerated swelling phenomenon occurs only in compounds that undergo a crystalline-to-amorphous transformation, and that it is a manifestation of radiation enhancement of diffusion and plastic flow in amorphous solids [11]. The ion bombardment and in situ TEM experiments of Birtcher et al.[12] on U_3Si underscore the general nature of the effect.

From the foregoing description, the volume changes in irradiated U_3Si-Al were shown to be strongly dependent on temperature and fission rate. The quantitative-amount of swelling for silicide fuel can be estimated as follows by considering temperature, fission rate, solid fission product build-up and gas bubble behavior.

$$\left\{\frac{\Delta V}{V}\right\}_{ts} = \left\{\frac{\Delta V}{V}\right\}_{gb} + \left\{\frac{\Delta V}{V}\right\}_{sp} + \left\{\frac{\Delta V}{V}\right\}_{il}$$

where

$\left\{\frac{\Delta V}{V}\right\}_{ts}$: the total volume change due to the swelling for silicide dispersion fuel

$\left\{\frac{\Delta V}{V}\right\}_{gb}$: the fractional volume change due to the accumulation of gas bubble nucleation and growth

$\left\{\frac{\Delta V}{V}\right\}_{sp}$: the fractional volume changes due to the transformation to a higher silicon phase and the accumulation of solid fission product swelling

$\left\{\frac{\Delta V}{V}\right\}_{il}$: the fractional volume change due to thermal-chemical reaction between fuel particle and matrix

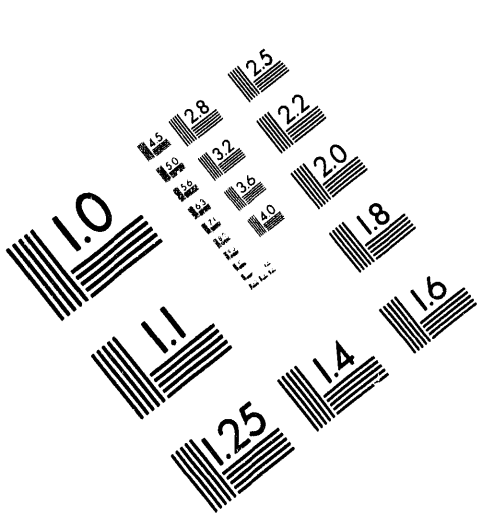

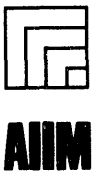

Association for Information and Image Management
1100 Wayne Avenue, Suite 1100
Silver Spring, Maryland 20910
301/587-8202

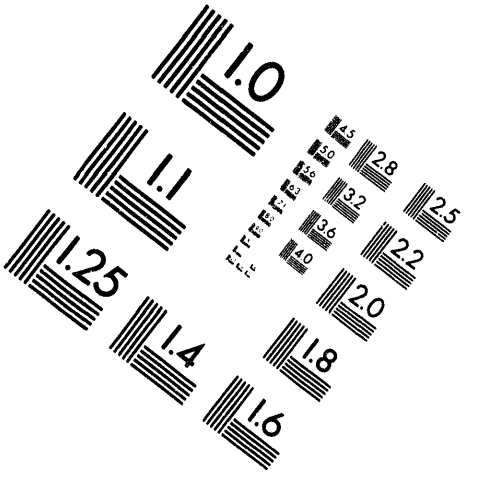

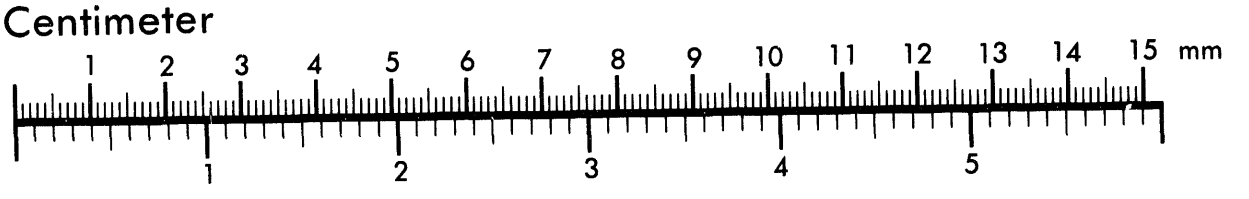

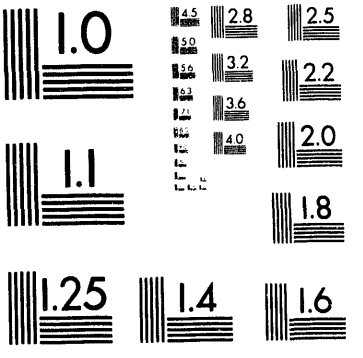

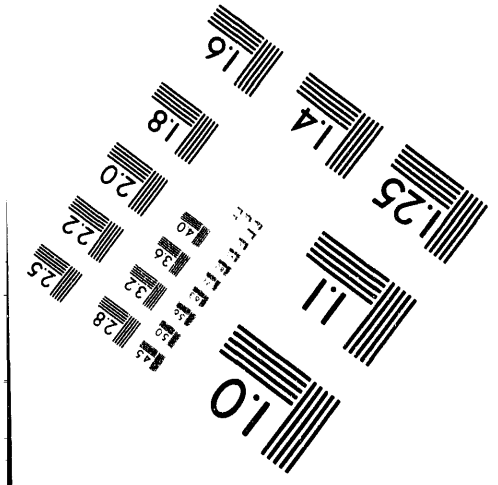

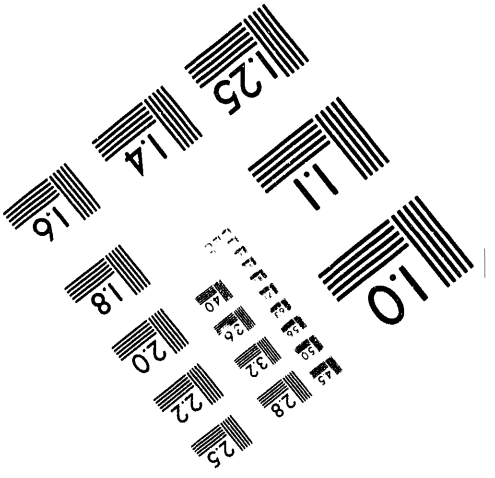

3 of 4

THE MODEL DESCRIPTION

The Modelling of the Volume Change due to the Formation of the Interfacial Layer Between the Fuel Particle and Matrix

As per the foregoing description, the aluminum having reacted with particle surfaces formed interfacial layers around the silicide particles in the fuel core. There are many features for the interfacial layer, however the major characteristics may be explained by the following simple model. The basis reaction between the aluminum matrix and U_3Si particles is[4]

$$U_3Si + 9\ Al \longrightarrow 3\ UAl_3Si_{1/3}. \tag{1}$$

It is inferred that the nine aluminum atoms that react with each U_3Si molecule leave behind in the aluminum matrix nine vacancies. The vacancies are created at the U_3Si/matrix interface and apparently do not migrate away to the free surface, but condense to form pores with volumes which will be assumed to be equal to the sum of the volumes of the vacancies.

If the typical radius of silicide particle is R and the thickness of the interfacial layer is L, the initial volume of the interfacial layer, V_{IL}, is given by

$$V_{IL} = \frac{4}{3} \cdot \pi \cdot (R^3 - r^3_b), \tag{2}$$

where, r_b is $(R - L)$, and V_{IL} is the initial volume of interfacial layer per a silicide particle. On the other hand, the number of silicide particles, N_{SP}, per unit volume of fuel meat, is given by

$$N_{sp} = \frac{\delta_m \cdot F_{sp}}{M_{sp}} \tag{3}$$

where, δ_m is the density of fuel meat, and F_{sp} is weight fraction of U_3Si, and M_{sp} is the weight of a silicide particle. Considering the basis reaction as shown in Eq.(1), the weight of Al required to react with all the U_3Si per unit volume of fuel meat, W_{Al}, is given by

$$W_{Al} = \frac{243}{742} \cdot V_{IL} \cdot \delta_{sp} \cdot N_{sp} \tag{4}$$

where δ_{sp} is the density of U_3Si, 15.58, and 243 is nine times the atomic weight of Al, and 742 is the molecular weight of U_3Si. And the Al-weight per the unit volume of Al-U_3Si, WT_{Al}, is given by

$$WT_{Al} = \delta_m \cdot F_{Al} \tag{5}$$

where, F_{Al} is weight fraction of Al in Al-U_3Si fuel meat. Hence, the increased volume due to the formation of the interfacial layer, for the unit volume of fuel meat, VT_{IL}, is given by

$$VT_{IL} = \frac{(V_{ILT} \times \delta_{sp}) + W_{Al}}{\delta_{il}} + \frac{WT_{Al} - W_{Al}}{\delta_{Al}} + \frac{(M_{sp} - (V_{IL} \cdot \delta_{sp})) \cdot N_{sp}}{\delta_{sp}} + V_{ip} \quad (6)$$

where, $V_{ILT} = V_{IL} \cdot N_{sp}$, δ_{il} is the density of $UAl_3Si_{1/3}$, 6.8,
δ_{sp} is the density of U_3Si, 15.58,
δ_{Al} is the density of Al, 2.7,
V_{ip} is the initial pore volume per unit volume of fuel meat, $(1-(V_{sp} \cdot N_{sp} + VT_{Al}))$,
V_{sp} is the volume of a silicide particle, and
VT_{Al} is the volume of Al-matrix per unit meat volume, WT_{Al}/δ_{Al}.

Also, the unit volume of fuel meat, V_{uc} is given by

$$V_{uc} = V_{sp} \cdot N_{sp} + \frac{WT_{Al}}{\delta_{Al}} + V_{ip} = 1. \quad (7)$$

Therefore the fractional volume increase due to the formation of interfacial layer, for the unit volume of fuel meat, is given by

$$\left(\frac{\Delta V_{uc}}{V_{uc}}\right)_{IL} = \frac{VT_{IL} - V_{uc}}{V_{uc}} = VT_{IL} - 1. \quad (8)$$

The Modelling of the Volume Change due to the Accumulation of Solid Fission Products

The swelling due to solid fission products is caused by the incorporation of solid fission products in the solid lattice and is, therefore, proportional to the number of fissions which have taken place in the fuel.

The volume change for a silicide particle, f_{sp}, due to solid fission is given by

$$f_{sp} = C \cdot 10^{-3} \cdot B_a \quad (9)$$

where, C is a coefficient ranging from 1.26 to 1.86 which was drived from the experimental data[5,12], and B_a is the atomic % burnup. Therefore, the fractional volume change due to the formation of solid fission product, for unit volume of fuel meat, is given by

$$\left(\frac{\Delta V_{uc}}{V_{uc}}\right)_{sp} = \left\{\left(\frac{WT_{Al}}{\delta_{Al}}\right) + V_{ip} + (V_{sp} \cdot N_{sp}) \cdot (1 + f_{sp})\right\} - 1. \quad (10)$$

The Modelling of the Volume Change due to the Accumulation of Gas Bubble Nucleation

In order to estimate the volume change due to the accumulation of gas bubble nucleation, it is necessary to calculate the bubble size distribution formed by the gas atoms produced within the fuel particle. The procedure for calculating the bubble size distribution consists of dividing the bubbles into equal size ranges on a logarithmic scale and averaging properties over the ranges as per Poeppel[13,14].

If n_i is the number of gas atoms in the bubble with the radius, r_i, which is given by the expression[14,15]

$$r_i = \{ (3kT/8\pi\gamma) n_i \}^{1/2}. \tag{11}$$

Hence, the mean radius, $\bar{r}_i$, at a region which is ranged from r_i to r_{i+1} is given by

$$\bar{r}_i = \{ (3kT/8\pi\gamma) ((n_i + n_{i+1})/2) \}^{1/2} \tag{12}$$

where γ is the surface tension of U_3Si, k is the Boltzmann constant, and T is the Kelvin temperature. Since one fission yields 0.310 atoms of Xe and Kr, and 3.1209415×10^{10} fissions per second yield 1 W/sec, hence the number of gas atoms produced within a fuel particle is given by

$$m = 0.310 \cdot C_F \cdot q''' \cdot t \tag{13}$$

where, $C_F = 3.1209415 \times 10^{10}$, t is irradiation time (sec). Based on the bubble size distribution[16], the average number of bubbles per unit fuel particle at a given bubble size range, $\bar{f}_i$, are given by

$$\bar{f}_i \ (n_{i+1} - n_i) =$$

$$0.23\ m \cdot \tau^{-4/5} \int_{n_i}^{n_{i+1}} [\exp(-A(n\tau^{-2/5} - 0.5))][\sinh\{B(n\tau^{-2/5} - 0.5)\}^{1/2}]\ dn. \tag{14}$$

Hence, using $\bar{f}_i$ from Eq. (14), a balance equation can be written as follows

$$m = C_s \sum_{\text{size range}} \bar{f}_i \cdot \frac{(n_i + n_{i+1})}{2} \tag{15}$$

where, C_s is correction coefficient for the concentration per unit fuel particle. Therefore, the equivalent number of bubbles for the median atoms size at given bubble size range is given by

$$f_i = \bar{f}_i \cdot C_s. \tag{16}$$

Eq. (14) can be solved for the bubble size distributions incrementally by using the Gaussian quadrature formula[17]. Finally, the swelling due to

the accumulation of gas bubbles is calculated. The volume increase per fuel particle due to the accumulation of gas bubbles is calculated by considering the bubble size distribution, f_i, using

$$V_b = \frac{4\pi}{3} \sum_{\text{size range}} (\bar{r}_i)^3 f_i \qquad (17)$$

where, V_b is the amount of volume increase due to the formation of fission gas bubbles per unit fuel particle. Therefore, the fractional swelling due to the formation of fission gas bubbles, per unit volume of fuel meat, is given by

$$\left(\frac{\Delta V_{uc}}{V_{uc}}\right)_{bubble} = \frac{((V_{sp} + V_b) \cdot N_{sp} + VT_{Al} + V_{ip}) - V_{uc}}{V_{uc}}$$

$$= ((V_{sp} + V_b) \cdot N_{sp} + VT_{Al} + V_{ip}) - 1 \qquad (18)$$

where, VT_{Al} is the volume of Al-matrix per unit meat volume, WT_{Al} / δ_{Al},
V_{uc} is the unit volume of fuel meat,
V_{sp} is the volume of a fuel particle which is treated as a equivalent sphere of uniform size characterized by a single equivalent radius, and
V_{ip} is the volume of the initial pore per unit fuel meat, $[\ 1 - (V_{sp} \cdot N_{sp} + VT_{Al})\ ]$.

MODEL APPLICATION

To compute the temperature distribution depending on the power history in the fuel element, a program[18] which computes the temperature distribution is adapted. And the present swelling model was incorporated into the program. This incorporated code is referred to as DFSWELL hereafter. DFSWELL code predicts the swelling behavior of silicide fuel by considering the volume change for unit silicide particle and unit volume of the fuel meat, depending on temperature, fission rate, solid fission product build-up and gas bubble behavior. The number of gas atoms produced in a silicide particle and the multi-bubble size distribution depending on the power history were calculated to estimate the volume change of fuel meat due to gas bubble formation and growth. Here, the van der Waals gas law is employed to calculate the bubble size. On the other hand, the behaviours of the interfacial layer and solid fission products were estimated. DFSWELL, incorporating these three mechanisms, was programmed as shown in Fig.1.

COMPARISON WITH EXPERIMENTAL DATA AND DISCUSSION

Experimental data are taken from AECL[7,9] in which the silicide fuels for research reactor were irradiated up to 97.5 atomic % burnup and with the linear powers between 20 kW/m and 110 kW/m, as shown in Fig.2 - 3. The

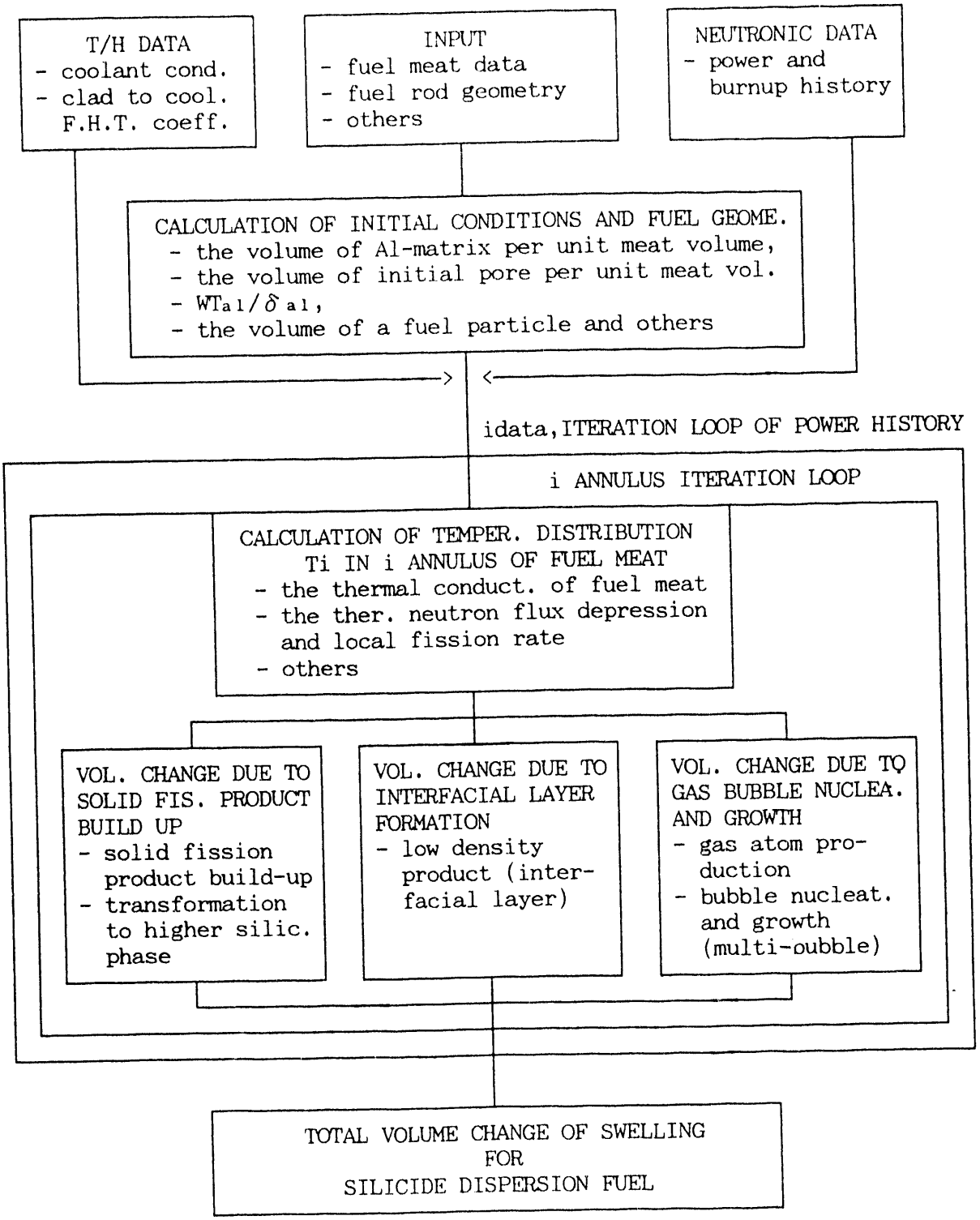

Fig. 1 Calculational procedure of DFSWELL program

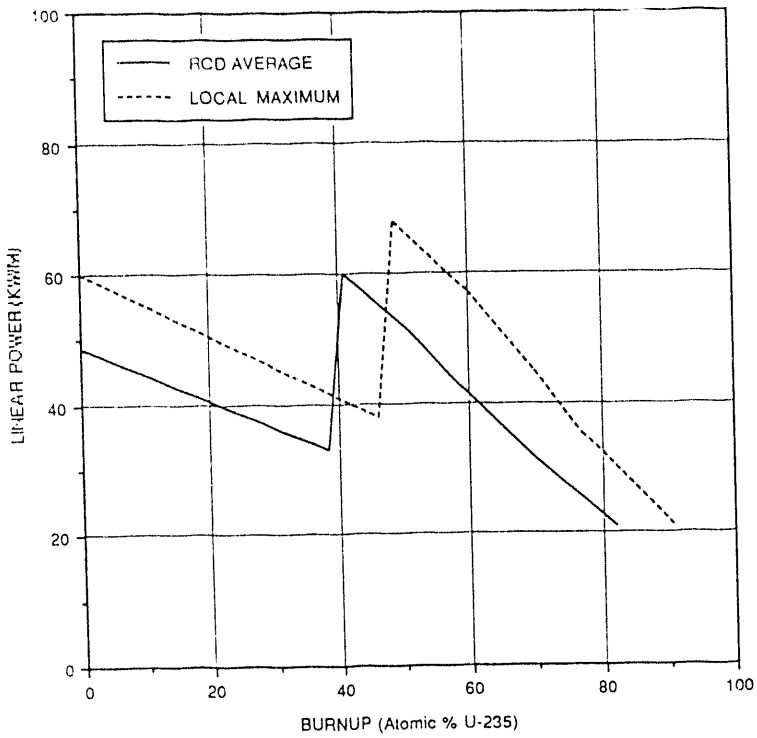

Fig. 2 Typical power history for LEU fuel.

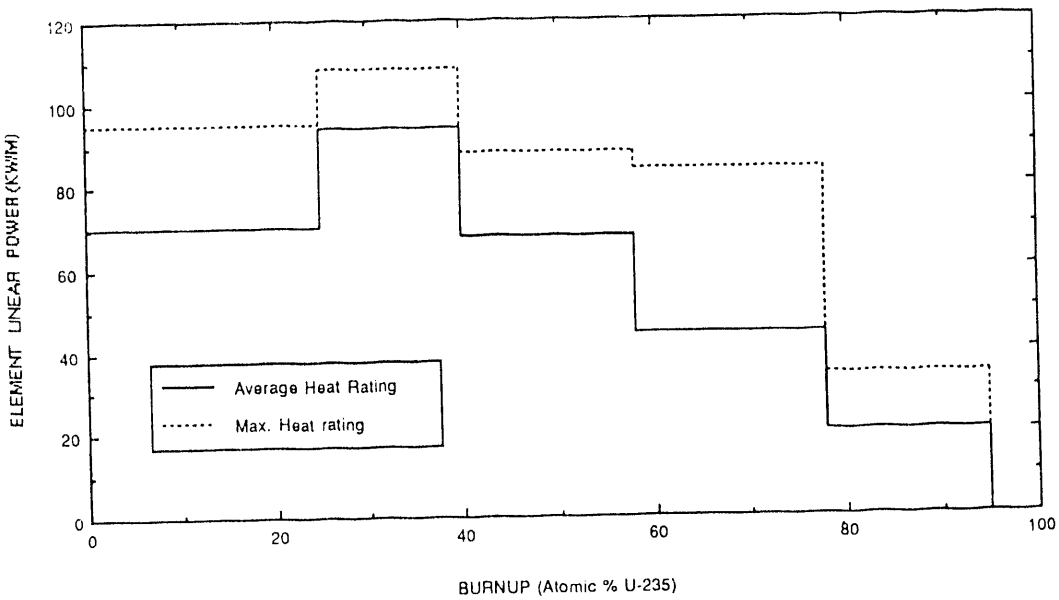

Fig. 3 Power history of mini-elements containing Al-61.5Wt% uranium silicide from experiment EXP-FZZ-918.

irradiation test elements were fabricated into aluminum-clad full-length element about 292 mm long, the fuel core diameter being 5.49 mm and clad wall thickness 0.76 mm. Each element had six cooling fins at 60° C intervals around the cladding, the fin width being 0.76 mm and fin height 1.27 mm. The outside diameter of the cladding was 7.01 mm (exceeding fins).
Fig.4 shows the results of parametric study on the swelling mechanisms for the silicide dispersion fuel. From the result, the volume change due to the accumulation of the solid fission products is proportional to the burnup and its absolute magnitude is relatively less than that of gas bubbles. And, it is apparent that the most dominant parameter of silicide fuel swelling is the volume change due to gas bubble formation and growth.
Fig. 5 shows the calculated fuel swelling versus experimental data. In this Figure, the DFSWELL code predicted well the absolute magnitude of the swelling, in comparison with the wide variety of experimental data.

CONCLUSIONS AND RECOMMENDATIONS

In this study, a comprehensive swelling model for the silicide dispersion fuel has been developed by analyzing the basic irradiation behaviors and some experimental evidences. From the predictions of DFSWELL model and the experimental evidences, it is proposed that the swelling for silicide fuel is comprised of the following three major components ;

$$\left\{\frac{\Delta V}{V}\right\}_{ts} = \left\{\frac{\Delta V}{V}\right\}_{gb} + \left\{\frac{\Delta V}{V}\right\}_{sp} + \left\{\frac{\Delta V}{V}\right\}_{il}.$$

DFSWELL model which takes into account the above three major components on the physical phenomena, predicts well the absolute magnitude of silicide fuel swelling depending on the power histories in comparison with the experimental data. It appears that the most dominant parameter of silicide fuel swelling is the volume change due to gas bubble formation and growth. However, it seems that DFSWELL model tends to overpredict in comparison with experimental results, especially at the region of low burnup. It is therefore recommended that further work for modelling the formation of interfacial layer dependent on the burnup might be required.

REFERENCES

1. Gerard L. Hofman,"Crystal Structure Stability and Fission Gas Swelling in Intermetallic Uranium Compounds", Journal of Nuclear Materials, Vol. 140, pp.256-263, (1986).
2. S. Nazare',"Investigations of Uranium Silicide-based Dispersion Fuels for the Use of Low Enrichment Uranium in Research and Test Reactors", kfk 3372 B, Jun. (1982).
3. J.C. Wood, M.T. Foo, L.C. Berthiaume, L.N. Herbert, J.D. Schaefer and D. Hawley, " Reduced Enrichment Fuels for CANADIAN Research Reactors Fabrication and Performance", Proceeding of the International Meeting on RERTR, ANL, USA,AECL-CRNL, Oct. (1984).

4. J.C. Wood, M.T. Foo, and L.C. Berthiaume," The Development and Testing of Reduced Enrichment Fuels for CANADIAN Research Reactors", Presented at the International Meeting on Research and Test Reactor Core Conversions, ANL, Argonne, Illinois, November(1982)
5. I.J. Hastings and R.L. Stoute,"Temperature-Dependent Swelling in Irradiated U_3Si Fuel Elements", J. Nucl. Mat. Vol.37, p.295-302, (1970).
6. Gerard L. Hofman and Woo-Seog Ryu, "Detailed Analysis of Uranium Siliside Dispersion Fuel Swelling", The Meeting on Reduced Enrichment for Research and Test Reactor, Berlin, Sept. (1989).
7. W. Hwang, D.F. Sears, L.C. Berthiaume and A.K. MacCdrmark, "LEU Fuel Core Swelling Measurements of Fuel Elements in NRU Bays", MEMORANDUM FMB-86-411, CRNL, (1986).
8. L.C. Berthiaum and J.C. Wood, " Hot Cell Examination of Sections of Full-size NRU Rod FL-002 Containing LEU Silicide Dispsion Fuel (EXP-FZZ-913) Cell Job 125", EXP-FZZ-91305, CRNL, (1985).
9. D.F. Sears, L.C. Berthiaume and L.N. Herbert, " Fabrication and Irradiation Testing of LEU Fuels at CRNL Status as of 1987 September", AECL-9632, Sep. (1987).
10. Melville A. Feraday, Moon T. Foo, Ross D. Davidson and John E. Winegar, " The Thermal Stability of Al-USiAl Dispersion Fuels and Al-U Alloys", Nuclear Technology, Vol. 58, Aug (1982).
11. J. Rest, G.L. Hofman, and R.C. Birtcher, " The Effect of Crystal Structure Stability on the Mobility of Gas Bubbles in Intermetallic Uranium Compounds ", 14th International Symposium on Effects of Radiation on Materials, ANL, June, (1988).
12. H.C. Suk, W. Hwang, and K.S.Sim, " KAFEPA : A Computer Code for CANDU -PHWR Fuel Performance Analysis under Reactor Normal Operating Condition", Journal of the Korean Nuclear Society, Vol.19, No.3, (Sep. 1987).
13. J. Brian, O. Knacke, and O. Kubaschewski, " Thermochemical Properties of Inorganic Substances", Springerverlag Publisher, New York (1977).
14. R.B. Poeppel, " An Advanced Gas Release and Swelling Subroutine", ANL, Proceedings of the Conference on Fast Reactor Fuel Element Technology, Session III : Fuel Mechanisms and Properties, New Orleans, Louisiana, April 13-15, (1971).
15. J.W. Harrison, " An Extrapolated Equation of State for Xenon for Use in Fuel Swelling Calculations", Journal of Nuclear Materials, Vol.31, 99-106, (1969).
16. W. Hwang, H.C. Suk, Won Mok Jae, " A Comprehensive Fission Gas Release Model Considering Multiple Bubble Sizes on the Grain Boundary Under Steady-State Conditions," Nuclear Technology Vol. 95, Sep.(1991).
17. Shan S. Kuo, " Computer Applications of Numerical Methods", Addison-Wesley Publishing Company, Massachusetts, Chapter 12 Numerical Integration, p 299-309 (1972).
18. W. Hwang, " A Model for Predicting the Radial Power Profile in CANDU Fuel Pellet", M.S. Thesis, Hanyang University (1987).

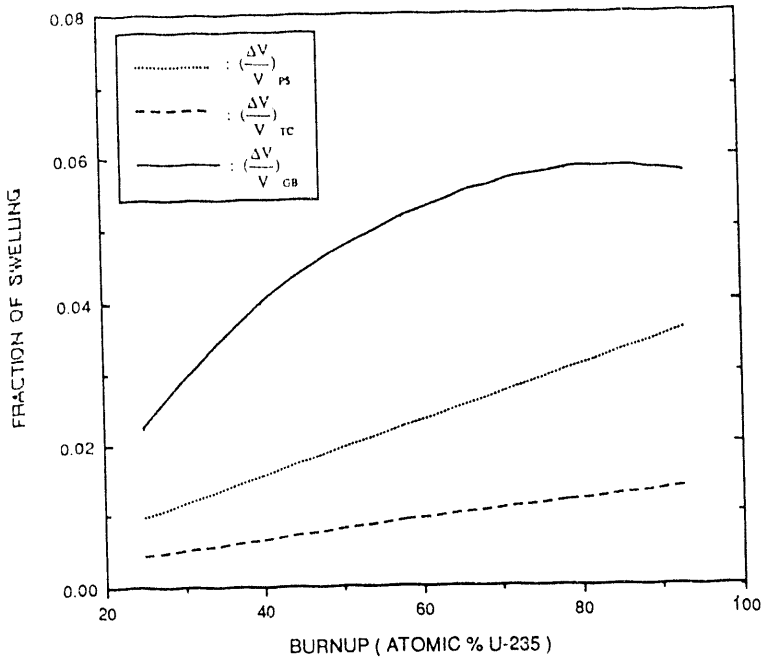

Fig. 4 The results of parametric study on the swelling mechanism for EXP-FZZ-918 fuel rod.

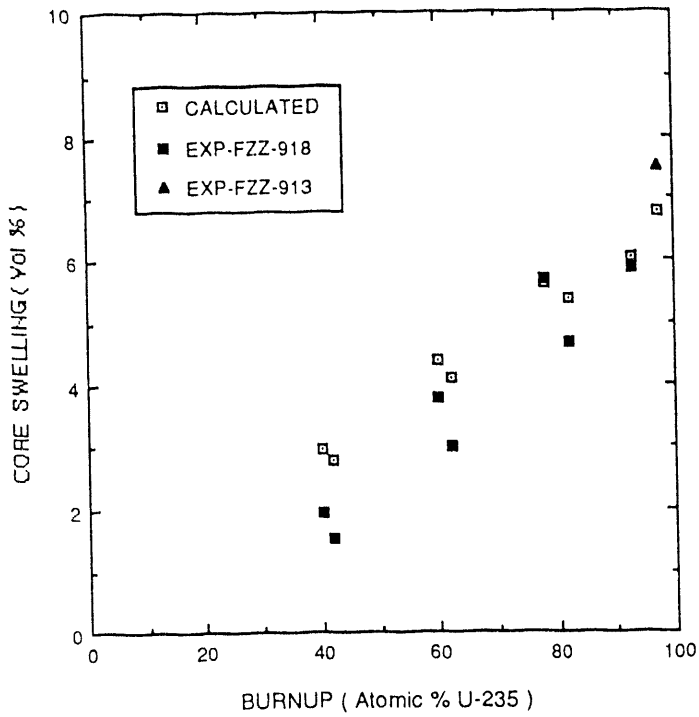

Fig. 5 Comparison of observed swelling of LEU silicide fuel with the calculated swelling using present model.

A NEW SWELLING MODEL AND ITS APPLICATION TO URANIUM SILICIDE RESEARCH REACTOR FUEL

by

Gerard L. Hofman, Jeffrey Rest, and
James L. Snelgrove

Argonne National Laboratory
Argonne, Illinois, USA

ABSTRACT

A new version of the dispersion fuel behavior model currently being incorporated in DART, has been generated. The model's description of fuel swelling - more specifically, the evaluation of fission-gas bubble morphology - is significantly improved. Although some of the assumptions underlying the basic model are derived from systems other than U_3Si_2, it represents a physically realistic interpretation of the observed irradiation behavior of U_3Si_2 over a wide range of fission densities and fission rates.

INTRODUCTION

In order to enhance our understanding of the irradiation behavior of uranium silicide, and thereby improve our confidence in predictions that fall outside areas where actual irradiation testing is feasible, the authors have previously developed a fuel behavior model and implemented it in the DART code.[1]

New data obtained by reanalyzing previous irradiation experiments performed in the Oak Ridge Research Reactor (ORR), and preliminary results from a recent high-flux irradiation experiment in High Flux Isotope Reactor (HFIR), allow us to improve the model. Previous studies had shown that the development of fission-gas bubbles and the swelling behavior of U_3Si_2 depended upon the fission rate.[2] The appearance of fission-gas bubbles resolvable by scanning electron microscopy (SEM) was delayed to a higher fission density in highly-enriched uranium (HEU) silicide compared to low-enriched uranium (LEU) silicide when both were irradiated in a similar flux density in the ORR.

Recent irradiations at a much higher density in the HFIR show a continuation of this trend; however, some shortcomings in the present model became obvious in light of these new data. A more detailed examination of existing SEM results was undertaken to correct this.

EXPERIMENTAL DATA

Several previously obtained scanning electron micrographs were subjected to quantitative image analysis. Fission-gas bubble size distributions were measured, and the volume fraction occupied by gas bubbles was calculated. The bubble volume fractions measured from two LEU and two HEU samples are indicated in Fig. 1. Subtraction of the bubble volume from the total volume change measured by immersion results in the volume change due to solid fission products and very small unresolvable bubbles (the lower line in Fig. 1).

The bubble size distributions are clearly bimodal, as shown for one LEU and one HEU sample in Fig. 2. It has been reported previously[3] that there is a remarkable similarity in bubble morphology between samples that have similar volume increase, albeit at different fission densities. This is even more evident when the measured bubble distributions in Fig. 2 are compared.

The bimodal distributions persist to very high fission densities (as shown in Fig. 3) for HEU at, respectively, 9 and 16 x 10^{27} fissions m^{-3}. The second peak in the distribution shifts to a larger diameter as the bubbles acquire more fission gas. However, the total number of bubbles in the second part of the distribution remains relatively constant for all samples examined (approximately 3 x 10^{18} m^{-3}). We interpret this to mean that the larger bubbles nucleate and grow on a fixed number of sites.

A micrograph from an experiment in which HEU U_3Si_2 was irradiated in the HFIR at a fission rate of ~2 x 10^{22} m^{-3} s^{-1} to a fission density of 20 x 10^{27} m^{-3} is shown in Fig. 4. The fission-gas bubble size, barely visible at this magnification, is clearly smaller for the higher-fission-rate irradiation in the HFIR, and in fact is similar to that for the LEU fuel which attained only 1/3 the fission density of the HEU fuel.

THE MODEL

Current state-of-the-art models for fission-gas behavior in commonly used reactor fuels do not predict a dependence of bubble growth on fission rate, nor do they predict experimentally observable bubbles in bulk crystalline material at typically low research reactor fuel temperatures. Calculations[4] with GRASS-SST[5] have interpreted the swelling as due to the combined effects of a population of bubbles below the limits of experimental re-solution and a distribution of larger, visible bubbles attached to subgrain boundaries. The position of a peak in the bubble distribution is determined by the offset between the growth of the bubbles due to diffusion of gas atoms and shrinkage due to fission-fragment-induced re-solution. Both irradiation-enhanced diffusion and gas-atom resolution have an approximately linear dependence on the fission rate. Therefore, an increase in the rate alone would not significantly affect the position of a bubble peak and thus gas-bubble swelling. Sensitivity studies have also indicated that a large change (hypothetically many orders of magnitude instead of approximately linear) in bubble nucleation rate at higher fission rates would not affect fuel swelling appreciably in these models.

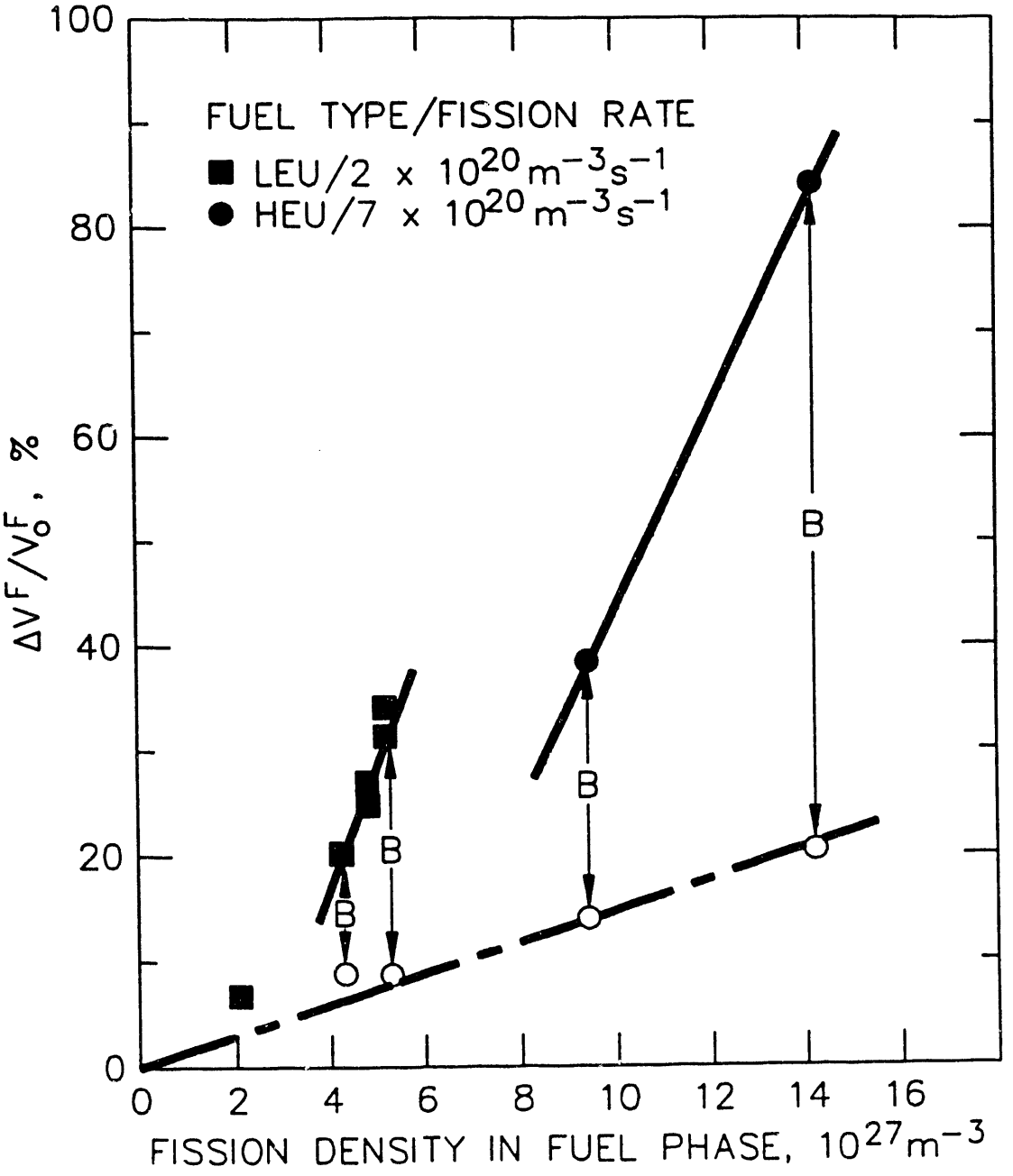

Fig. 1 Total fuel particle swelling and bubble volume fraction, B, of U_3Si_2 of two enrichments (i.e., two different fission rates) dispersed in aluminum, as a function of accumulated fissions in the fuel particles.

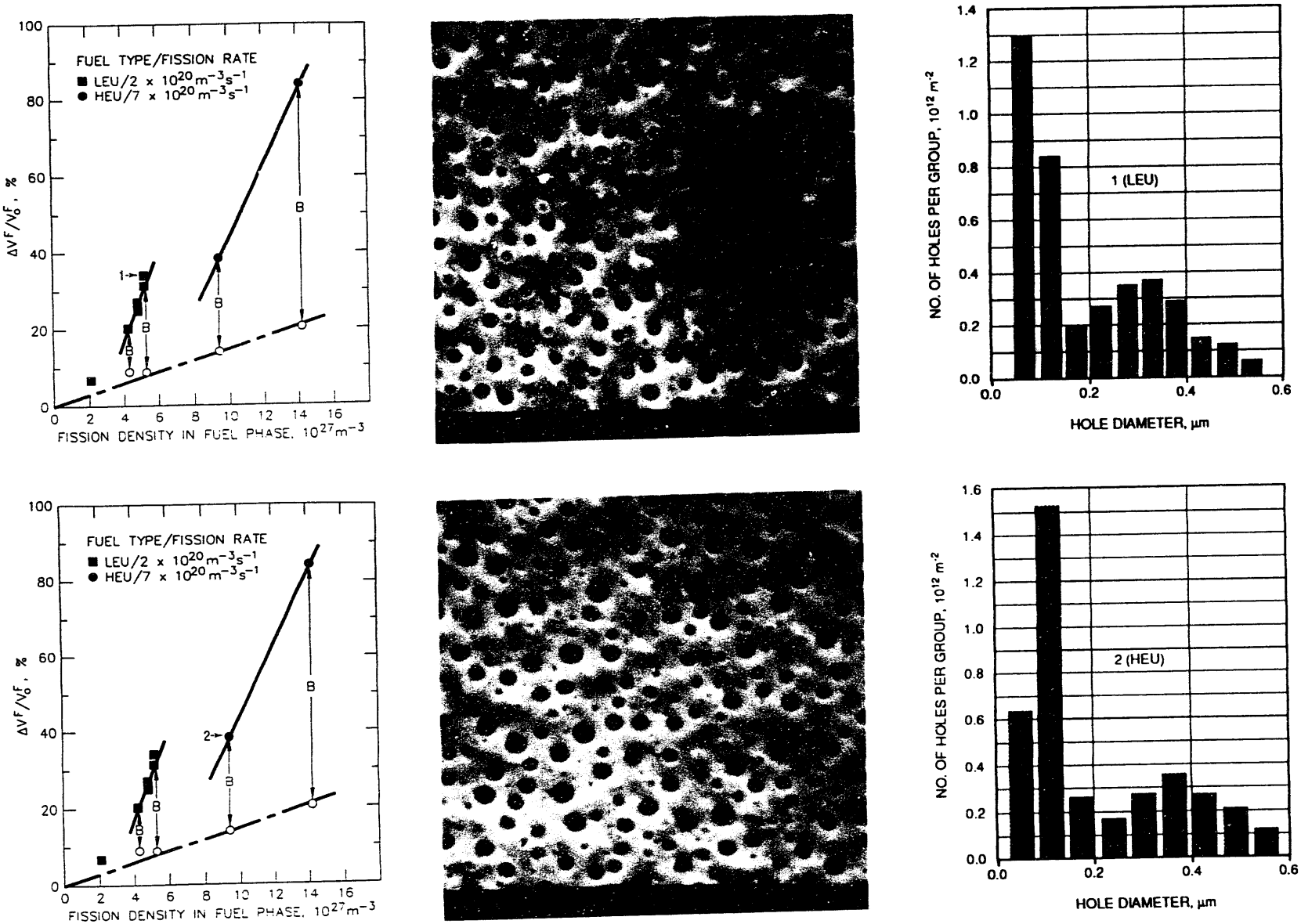

Fig. 2 Swelling and fission-gas bubble distributions of LEU (upper) and HEU (lower) U_3Si_2.

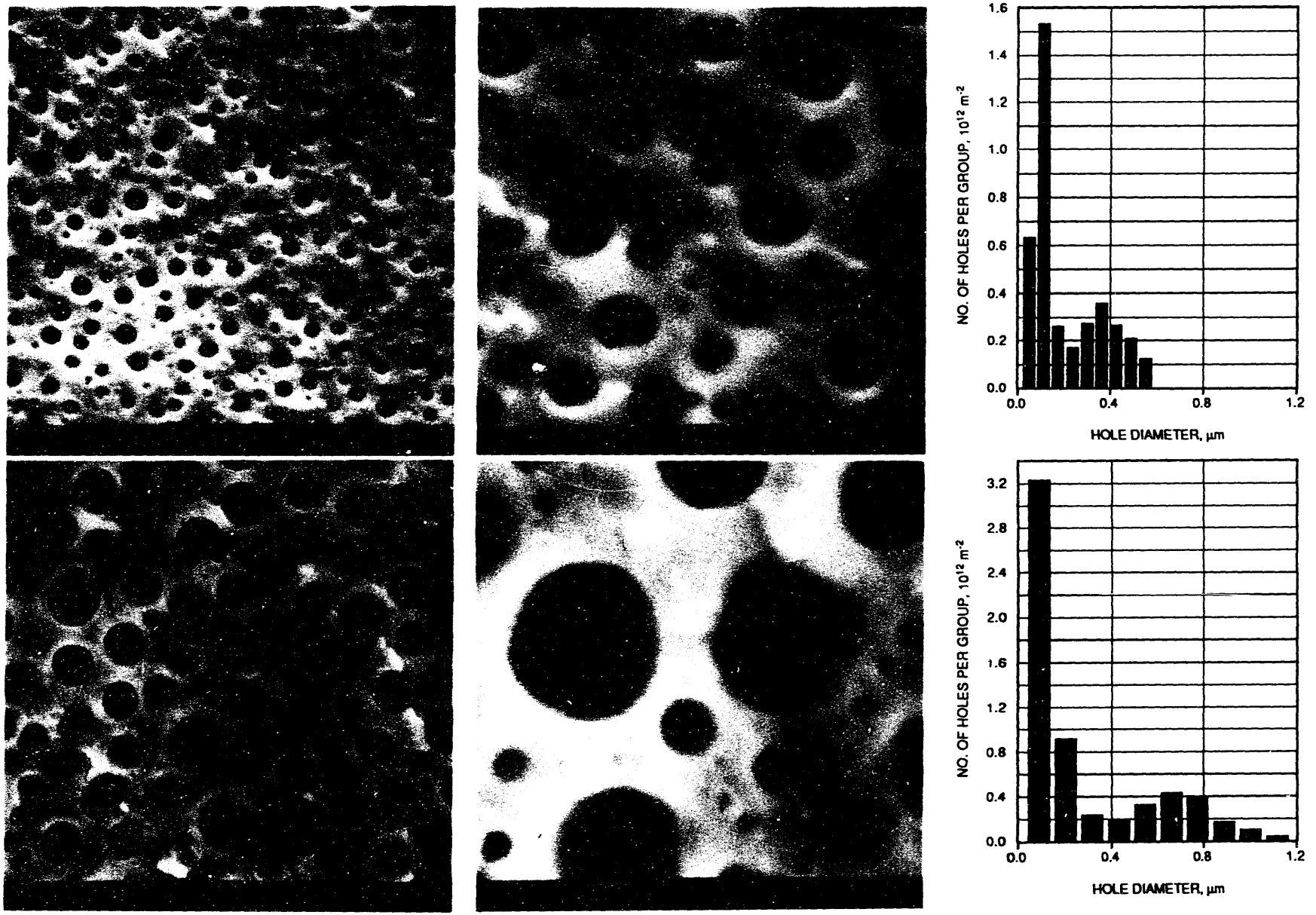

Fig. 3 Fission-gas bubble distributions in HEU U_3Si_2 at 9 x 10^{27} (upper) and 14 x 10^{27} (lower) fiss. m^{-3} and 7 x 10^{20} fiss. m^{-3} s^{-1}.

As mentioned above, a bubble population with bubble diameter large enough to be observed can only be calculated if microstructural features (such as grain boundaries or dislocation networks) are introduced (the original grain size of the fuel is large, i.e., on the order of the fuel particle size). In addition, to provide for an interpretation of the observed rate dependence of swelling, the formation of these defect structures should be a function of fission rate as well as fission density. The formation of such features has been observed in other fuels. Grain "subdivision" was observed by Bleiberg[6] in uranium oxide. He showed that original 10-20 μm grains subdivided into unit sizes of less than 1 μm at ~2 x 10^{27} fissions m^{-3} while retaining their crystalline structure. UO_2 swelling also increased in rate at this point, and the bubble morphology was strikingly similar to that observed in U_3Si_2. One of the present authors (G.L.H.) has also observed transformation of irradiated U_3O_8 to very small grains. Further evidence of this phenomenon has been found in ion bombardment studies on U_3Si above the glass transition temperature.[7] In these studies, recrystallized grain sizes on the order of 100 Å were observed directly in a high-voltage electron microscope. It seems plausible that formation of small grains also occurs in U_3Si_2.

At this time, there is no definitive evidence for such a restructuring of crystalline U_3Si_2 undergoing low-temperature irradiation to high doses. However, preliminary observations indicate that a subgrain-like structure exists in U_3Si_2 above the knee. Detailed examinations of the irradiated material are in progress. These preliminary observations, as well as indirect evidence from the experiments mentioned above, led the authors to speculate that a dense network of grain boundaries forms at a fission density corresponding to the knee in the swelling curve, upon which gas-bubbles nucleate and then grow at an accelerated rate relative to that in the bulk material.

Based on this speculation, the following assumptions were made for the DART model (those critical to the calculation are marked with an asterisk):

1.* Whole bubble destruction is the physically realistic mechanism of gas-atom re-solution from gas bubbles as compared to the previously used "chipping" model. Below a certain critical size, bubbles are completely destroyed when "hit" by a passing fission fragment; above the critical size, the bubbles survive the encounter.

2.* Bubbles on the grain surfaces have a smaller critical size for whole bubble destruction than bubbles in the bulk material due to the strong gas-atom capture strength of the grain surfaces. The following calculations are based on a zero-critical size for grain-boundary bubbles.

3.* Gas atoms diffuse from the bulk to the grain surfaces by athermal (irradiation-enhanced) diffusion.

4. The nucleation factor for bubbles on the grain faces and grain edges is the same as that for bubbles within the grains. (The nucleation factor is the probability that two gas atoms which interact form a stable gas bubble nucleus.)

HFIR-HEU, 90% Bu, 2 x 10^{22} Fiss. m^{-3} s^{-1}

ORR-HEU, 75% Bu, 7 x 10^{20} Fiss. m^{-3} s^{-1}

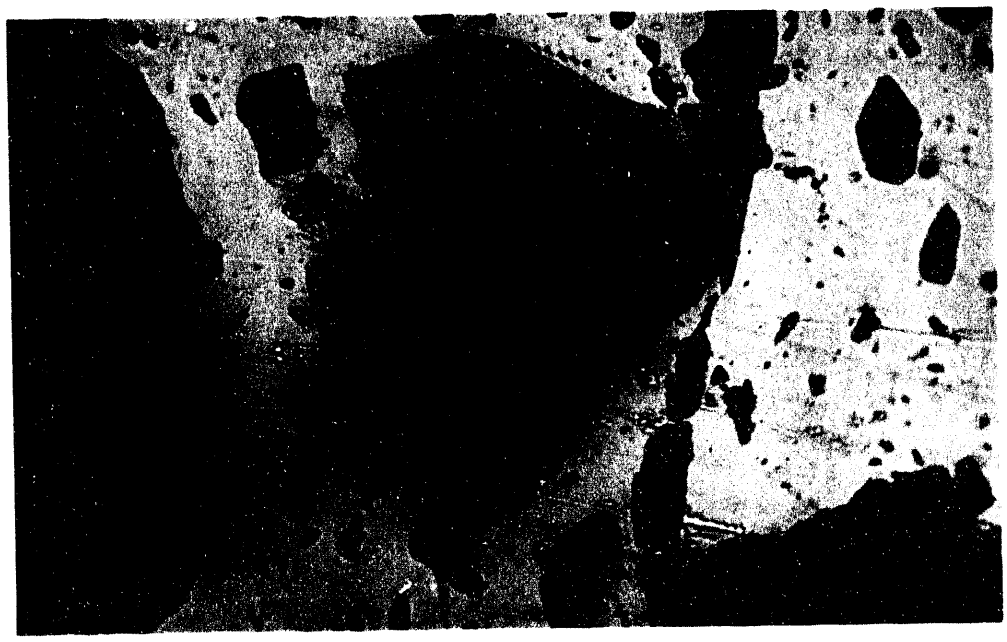

ORR-HEU, 90% Bu, 2 x 10^{20} Fiss. m^{-3} s^{-1}

Fig. 4 Comparison of postirradiation microstructure of HEU U_3Si_2 irradiated in HFIR vs. HEU and LEU U_3Si_2 irradiated in ORR (~500X).

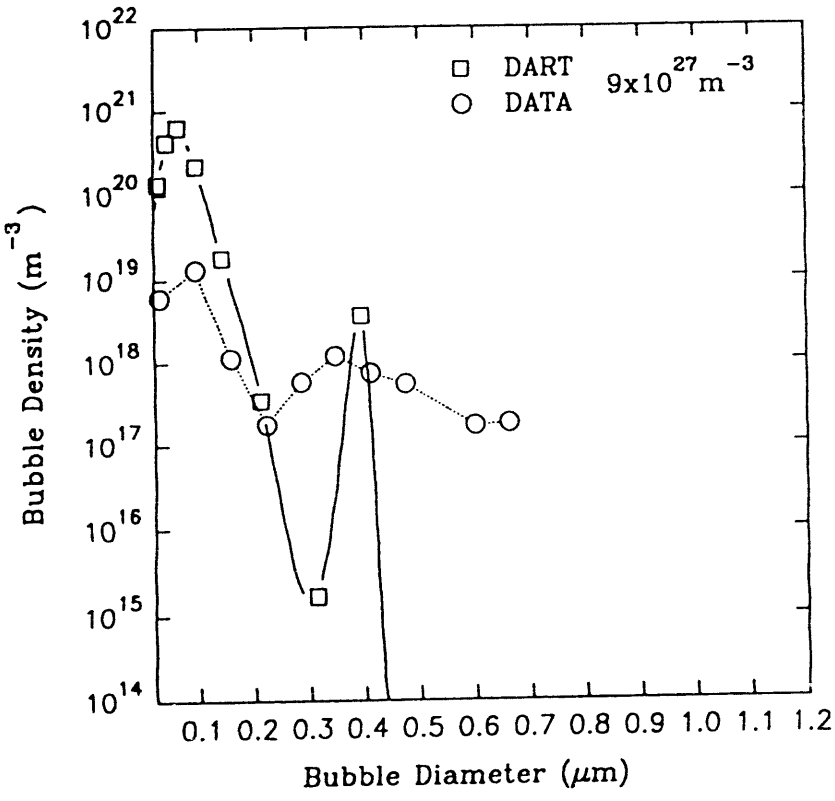

(a)

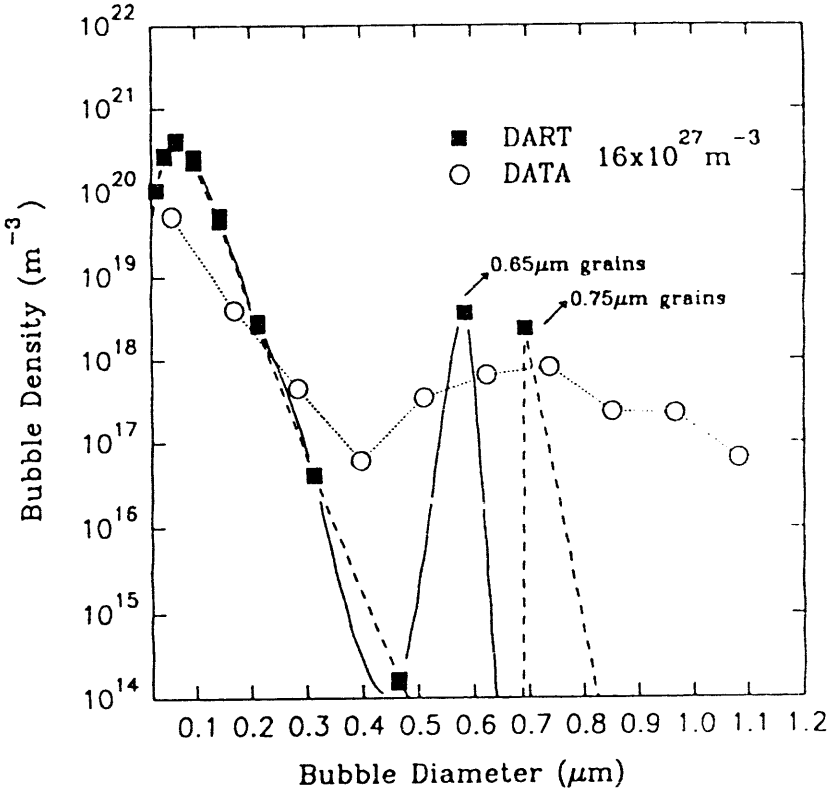

(b)

Fig. 5 Comparison of measured and calculated bubble distributions in U_3Si_2 at 9 x 10^{27} and 16 x 10^{27} fissions m^{-3}. The effects of both fission density and grain size on the position of the second mode of the distribution are evident.

5. The gas-atom diffusivity on grain surfaces is a factor of 10^4 greater than in the bulk material.

6.* Both grain faces and grain edges are included in the calculation. The gas on the grain faces can vent to the grain edges upon bubble interconnection. However, the grain edges form a dead end for the gas. Continued accumulation of gas on the grain edges eventually results in bubble interconnection and enhanced bubble growth.

The results of DART calculations utilizing the above assumptions were not consistent with the recently measured distributions. First, the data show a bi-modal bubble-size-distribution (very evident from the SEM photomicrographs) whereas the calculated distributions did not. (The calculated quantities did show a bi-modal bubble-size-distribution if very small bubbles were included in the plot. However, these small bubbles were well below the limits of experimental resolution.) Second, the calculated distributions were much broader than the measured quantities.

A striking aspect of the observed bubble population is its uniformly distributed, non-interacting nature. This fact, taken together with the inability of DART (using assumptions 1-6 above) to interpret the observations led the authors to modify assumption 6 given above:

6.* The large bubble population inhabits fixed sites. These sites are formed upon grain recrystallization and are associated with nodes formed by the intersection of grain edges within the subgrain boundary structure. Fission-gas which collects along the grain edges vents upon intersection to these nodes where it is trapped. The gas bubbles located at these "dead-end" nodes grow as they continue to collect additional gas.

If the grains are assumed to be cubes and the "dead-end" nodes are taken to be grain corners formed by the intersection of six grain edges, then the number of nodes per cubic centimeter is given by the inverse of the cube of the grain diameter.

Upon grain recrystallization, gas diffuses athermally (irradiation-enhanced diffusion) from the bulk to the grain faces where it accumulates in gas bubbles which grow until grain-face saturation occurs. DART calculates grain-face saturation by fission gas by directly addressing the calculated distribution of fission-gas bubble sizes. Grain-face saturation occurs when the projected areal coverage of the grain-face by these bubbles exceeds the maximum areal coverage. If the gas is assumed to be made of equal-diameter, closely-packed, touching bubbles, the maximum areal coverage per unit area of grain-face is 0.907.

Once formed on the grain edge, the bubbles grow by the accumulation of additional gas arriving from the grain faces. When long-range interconnection of the grain-edge porosity occurs, the gas is vented to the "dead-end" nodes. The DART model for calculating the probability of long-range grain-edge tunnel interconnection is based on the assumption that the long-range interconnection is a function of the swelling of the grain edge bubbles. This assumption is supported by both experiment and theory for oxide fuels. The value of the grain edge bubble fractional swelling at which long-range interconnection takes place if the fuel microstructure and gas bubble morphology are homogeneous is 0.055. To account for local fluctuations in fuel microstructure and gas bubble morphology, the grain-face saturation and the long-range grain-edge interlinkage fractions are assumed to be statistical distributions around average values of these parameters.

The points connected by solid curves in Fig. 5 show the results of DART bubble-size distribution calculations at fission densities of 9 x 10^{27} m^{-3} and 16 x 10^{27} m^{-3} when the "dead-end" nodes are included in the analysis and a recrystallized grain size of 0.65 μm is utilized. Grain recrystallization was taken to occur at a fission density of 2.5 x 10^{27} m^{-3}. Also shown in Fig. 5 are data obtained from SEM micrographs of the irradiated material. The calculated bubble distributions for bubble sizes below 0.4 μm diameter are due to bubbles on the grain faces and the grain edges. The calculated points at bubble diameters of about 0.4 μm [Fig. 5(a)] and 0.6 μm [Fig. 5(b)], respectively, are due to the accumulated gas in the "dead-end" nodes. Currently, DART only calculates the growth of an average-size node and does not account for the experimentally observed distribution of node-bubble sizes. In addition, the observed density of node-bubbles appears to decrease from about 3.6 x 10^{18} m^{-3} at a fission density of 9 x 10^{27} m^{-3} to about 2.4 x 10^{18} m^{-3} at a fission density of 16 x 10^{27} m^{-3}. This phenomenon may be due to smaller node bubbles being consumed by larger node bubbles and is not included in the DART calculations. Consequently, using a 0.65 μm recrystallized grain size, which corresponds to a node density of 3.6 x 10^{18} m^{-3}, the calculated size of the node-bubbles at 16 x 10^{27} m^{-3} will be underpredicted, as seen in Fig. 5(b).

Also shown by the dashed line in Fig. 5(b) are the DART-calculated distributions utilizing a 0.75 μm recrystallized grain size, which corresponds to a node density of 2.4 x 10^{18} m^{-3}. As is shown in Fig. 5(b), a shift in recrystallized grain size from 0.65 μm to 0.75 μm shifts the node-bubble diameter at 16 x 10^{27} m^{-3} from about 0.6 μm to about 0.7 μm. Given the above considerations, the DART calculations shown in Fig. 5 follow the trends of the observed bubble-size distribution in irradiated U_3Si_2 as a function of burnup and, as such, provide plausible physical interpretation of the irradiation behavior. More detailed calculations may be possible when the actual subgrain morphology in the samples can be quantitatively determined.

CONCLUSIONS AND APPLICATION

The current version of DART provides an improved description of the irradiation behavior of U_3Si_2 dispersion fuel. Specifically, the observed fission-gas bubble morphology in samples irradiated in the ORR up to a fission density of 16 x 10^{27} m^{-3} over a fission rate range of 2-7 x 10^{20} m^{-3} s^{-1} can now be more accurately modeled. Recent irradiation experiments with U_3Si_2 in the HFIR at much higher fission rates (up to 2 x 10^{22} $m^{-3}s^{-1}$) afford further validation of the model.

The improvements in the model increase the confidence in predictions of irradiation behavior outside the parameter range for which test results are available. The model can be applied to assess fuel swelling behavior and change in fuel thermal conductivity for both very-high-flux and low-flux reactors.

Because of the more realistic description of fission-gas behavior, the model can be extended to predict off-normal fuel behavior with greater confidence.

REFERENCES

1. J. Rest and G. L. Hofman, "Fundamental Aspects of Inert Gasses in Solids," S.E. Donnelly and J.H. Evans Ed., Plenum Press, 443 (1991).

2. J. Rest and G. L. Hofman, presented at 15th ASTM Symposium on Effects of Radiation on Materials, Nashville, TN (June 17-21, 1990).

3. G. L. Hofman, "The General Evaluation of the Irradiation Behavior of Dispersion Fuels," presented at the 1991 International Meeting on Reduced Enrichment for Research and Test Reactors, Jakarta, Indonesia (November 4-7, 1991).

4. J. Rest et al., "Effects of Radiation on Materials, 14th International Symposium (Vol. II), ASTM STP 1046, N. H. Packan, R. E. Stoller, and A. S. Kumer, Eds., American Society for Testing and Materials, Philadelphia, PA, 789 (1990).

5. J. Rest, "GRASS-SST: A Comprehensive Mechanistic Model for the Prediction of Fission-Gas Behavior in UO_2-Base Fuels During Steady-State and Transient Conditions," NUREG/CR-0202, ANL-78-53, Argonne National Laboratory Report, Argonne, IL (1978).

6. M. L. Bleiberg, R. M. Berman, and B. Lustman, Symposium on Radiation Damage in Solid and Reactor Materials, Proc. Series, IAEA, Venice, 319 (1963).

7. R. C. Birtcher and L. M. Wang, presented at 7th International Conference on Ion Beam Modification of Materials, IBMM90, Knoxville, TN (September 9-14, 1990).

S E S S I O N VI

September 30, 1992

HEU AND LEU FUEL CYCLE

Chairman:

J. Mota
(Euratom Supply Agency, Belgium)

External Research Reactor Fuel Cycle: BACK-END OPTIONS

Gerhard. J. Gruber
NUKEM GmbH
W-8755 Alzenau, Germany

ABSTRACT

The U.S. Deparment of Energy still has not renewed its Off-Site Fuel Policy for the acceptance of spent foreign Research Reactor Fuels.

Two European companies offer reprocessing services under the condition of waste return to the country of origin. Direct disposal of spent RR Fuels is only a very restricted potential national option which has not yet proven its realisation.

Other back-end options are not available for the time being.

INTRODUCTION

NUKEM as an international engineering and trading company is working on nuclear and non-nuclear fields.

Its **Fuel Cycle Services Division**, located in the company's headquarter in Alzenau, has been successfully offering its services on the External Research Reactor (RR) Fuel Cycle for more than **twenty years.**

At the beginning of **1989** - when U.S. Department of Energy (US-DOE) had suspended to accepting foreign RR Fuels - NUKEM started to assist concerned RR operators to close the back-end of their fuel cycles.

Since then NUKEM has helped at least three German reactors to stay **operational** by establishing storage and reprocessing agreements for spent RR Fuels with AEA.

This is an update of the back-end options for the RR Fuel Cycle.

US-DOE (U.S. Department of Energy)

Another year passed by and a new Off-Site Fuel Policy has not yet been announced by the U.S. government. Now it's already **3 years and 9 months** since U.S.-DOE had suspended the acceptance of foreign RR Fuels for reprocessing.

What was the status when NUKEM reported at the meeting in Jakarta last November?

US-DOE had published a proposed **FONSI** ("Finding of No Significant Impact") - including an Environmental Assessment (AE) - in the Federal Register (FR) in May 1991.

This FONSI stated that

a) transportation of spent RR Fuel on the high seas, in U.S. ports and on the highway and

b) reprocessing of the Fuel at the potential sites - which are the Savannah River Site (SRS) and Idaho National Engineering Laboratory (INEL) -

would not significantly affect the quality of the human environment within the meaning of the **National Environmental Policy Act (NEPA) of 1969.**

Also the potential reprocessing impacts at either site would be **insignificant.** And the acceptance of U.S. origin Fuel from abroad serves **non-proliferation interests** by removing **weapon grade** material and is therefore consistent with the Atomic Energy Act.

Major substantial comments on that publication in the FR were received by US-DOE from members of U.S. Congress and environmental groups. Most of the comments were seriously requesting a "full blown" **Environmental Impact Statement (EIS).**

It was up to US-DOE to decide **straight forward** for renewing the reprocessing policy, following up the nuclear non-profileartion aspect.

Or to **perform an EIS** which was predicted to take at least 2 years followed again by the mandatory publication procedure with a lot of uncertainties involved including potential law suits.

What has happened within the US-DOE since Nov. 91 in respect to accepting spent Fuel again?

The subject was obviously given a low priority at US-DOE. No announcement was made about extending its suspended Fuel policy and no decision for an EIS has been taken so far.

In April 1992, Admiral Watkins, the secretary of US-DOE, announced his decision to **phase out** the reprocessing of spent Fuel as soon as possible because the US no longer has the need to reprocess spent Fuel in order to recover the HEU. The cold war was over and President Bush decided to reduce the nuclear weapons stockpile.

That means US-DOE will have to find solutions for **storage** of the Fuel.

This leads to new **questions** for foreign RR operators such as:

- Will US-DOE come into a position to accept spent foreign Fuels for final storage?
- If yes, when and under what conditions?
- How will a possibly new government administration after the election treat that subject?
- What priority will be given to the profileration aspect?

AEA TECHNOLOGY, Great Britain

AEA, as a marketing unit of UKAEA (United Kingdom Atomic Energy Authority) is successfully offering reprocessing services for foreign spent **MTR-HEU-Fuels.**

NUKEM has arranged for two reprocessing contracts and coordinated the relevant shipments to Dounreay in Scotland all within the last year.

These Fuels will be reprocessed in the currently running campaign.

During an international RR operators meeting hosted by AEA in Dounreay in June 1992, AEA offered reprocessing services for **future campaigns.**

Due to the fact that there is no further domestic need for such services in Britain, future campaigns can only be based on a sufficient foreign demand.

To run the plant economically and to keep it operational, AEA needs to reprocess at least **1800 kg total metal per year** over a three years period. This number corresponds to about 500 fuel elements/assemblies.

Relevant contracts for reprocessing do have to contain a **return of waste** clause. Under this clause the waste generated from reprocessing will be returned either in form of "Intermediate Level Residue (ILR)" directly arising from reprocessing or as an equivalent quantity of "High Level Residue (HLR)" if appropriate.

Customers outside EURATOM will need prior **U.S. approval** (so-called MB-10 procedure) for the transfer and retransfer of the U.S. origin material to and from the U.K. But as far as we learned from informal talks the U.S. will not prevent customers from having their spent HEU-Fuels reprocessed in Britain or France.

AEA is also reviewing the possibility of treating spent **LEU-silicide-Fuels** and **TRIGA-($UZrH_x$)-Fuels** as there is currently also no final back-end option available on the market for these types of Fuels.

COGEMA, France

After a period of technical and commercial review COGEMA's option to close the back-end of the Fuel Cycle for MTR-HEU-Fuel became definite within last year.

In **May 1992,** at the occassion of a RR operators meeting in Dresden COGEMA announced officialy its readiness to negotiate reprocessing contracts for MTR-HEU elements individually with interested operators.

The basic conditions were said to be comparable with those of AEA, Dounreay.

That means e. g.:

- return of waste will be mandatory
- recovered uranium cannot be re-enriched and will be returned to the customer for a possible re-use.

But the time prospects are different to AEA's:

Starting in **1994**, COGEMA could accept spent MTR-HEU-Fuels for advance storage. Domestic and foreign Fuel would then be collected to a batch of at least **1000 elements** and reprocessed at a time convenient to COGEMA.

DIRECT DISPOSAL OPTION

Direct Disposal of spent RR Fuels is to be considered as a **national** back-end option for spent HEU-Fuels, at least in Germany.

Germany has an advanced program for Direct Disposal of spen **LWR fuels**.

In 1991 the German Ministry for Research and Developement (BMFT) started to investigate the possibility of whether this route can also be taken for spent **HEU-Fuels**

The concept is based on medium term **dry storage** of the Fuels in casks either on site or in a national repository. Casks are developed and have only to be specially licensed.

Thereafter the Fuel has to be repacked in the **Pilot-Conditioning-Plant** (PKA) and finally disposed under earth.

The **long term behaviour** of the Fuel is still being investigated and the Safeguards questions are under discussion.

OTHER OPTIONS

Russian companies were approached by different parties and through different channels without success.

Even foreign HEU-Fuels of Russian origin are not accepted for reprocessing.

Other options for closing the back-end of the RR Fuel Cycle are **not** known to us.

SUMMARY

The back-end of the RR Fuel Cycle continues to be the cause of great **concern**.

US-DOE still has not announced a new Off-Site Fuel Policy. **AEA** Technology and **COGEMA** offer reprocessing services with the condition of waste-return to the country of origin.

Direct Disposal is a potential option for only a very limited number of countries. Other options are currently not available.

Under these circumstances most of the RR operators worldwide are **without** back-end solution.

NUKEM will continue to watch the development on the Fuel Cycle in order to give best advice and assistance to our customers - as in the past.

THE RE-USE OF HIGHLY ENRICHED URANIUM (HEU) REPROCESSED IN EUROPE

Hans Müller
NUKEM GmbH
W-8755 Alzenau, Germany

ABSTRACT

After the shut-down of the U.S. reprocessing plants for spent research fuel at Savannah River and Idaho Falls research reactor operators outside the US have been facing the dilemma to close their fuel cycle elsewhere. In Europe the British AEA and the French Cogéma have decided to offer reprocessing of spent research reactor fuel in order to close the existing gap.

The re-use of reprocessed HEU in Europe strongly depends on the preparedness of European manufacturers of fuel elements for research reactors to accept the reprocessed uranium as base material for their production.

INTRODUCTION

1. Status of Reprocessing in Europe

AEA, Dounreay having a reprocessing plant available is at the moment reprocessing several hundreds of spent research reactor fuel elements with HEU in a firm campaign. In an early June 1992 symposium at Dounreay AEA offered to potential customers world-wide continuation of reprocessing of spent research reactor fuel for three years at firm conditions and starting in 1993.

The French Cogéma has also announced that they will offer acceptance and reprocessing of spent research reactor fuel containing HEU after 1994 in an already existing reprocessing plant which has to be adapted.

2. The Re-Use of reprocessed HEU

As is known, research reactor fuel with an original U-235 content of 93 % has - after a burn up of 50 % - a final enrichment between 70 to 80 % U-235.

Since U-235 contents between 70 and 80 % are odd ones (Research reactor operators have licensed their fuel either to 19.75 or 90 to 93 % U-235), there is no demand for the direct use of such a fuel. Only DIDO-reactors can utilize these odd U-235 contents in a second fuel cycle.

In consequence thereof the reprocessed HEU - at least what AEA concerns - will be blended down to LEU with a U-235 content of 19.75 % for further use as silicide fuel. This procedure is in line with the implemented US policy of Reducing Enrichment in Research and Test Reactors (RERTR).

3. Comparison of the Specification of so-called "virgin" LEU/HEU with reprocessed HEU

Reprocessed HEU contains increased amounts of U-232 and U-236 in comparison with so-called "virgin" LEU/HEU until now provided to research reactors by the US Department of Energy (DOE). The values of U-232 contained in the spent HEU are in the range of some 10 ppb and U-236 values are in the range of 6 to 12 % depending upon the neutron flux particular to the reactor type. A 19.75 % U-235 enriched uranium obtained by blending of reprocessed HEU will contain values between 1 and 10 ppb for U-232 and a U-236 content of 3 to 4 %.

In papers presented by AEA's Colin McColm at the 14th RERTR meeting in Jakarta in 1991 and at the Uranium Institute Meeting in London on September 10, 1992 AEA clearly declared that AEA has the experience and is licensed to handle the reprocessed HEU and blended HEU for further fuel element production.

For research reactor operators increased U-236 contents should not be a problem since U-236 behaves about in the same manner to that of U-238, i. e. it has a high neutron capture cross section with the resulting parasitic effect on neutrons.

Thus, for the re-use of the LEU obtained by blending of reprocessed HEU it is mandatory that reprocessors of spent research reactor fuels, manufacturers of fresh fuel and the research reactor operators arrive to an agreement about the relevant specifications for this LEU.

At the RERTR meetings in Newport (1990) and Jakarta (1991) I presented proposals to establish common specification of LEU and HEU in the form of metal with the target to standardize and simplify the existing numerous specifications. At the same time I challenged the existing term "virgin" HEU supplied by DOE.

Until then manufacturers of research reactor fuels accepted freshly supplied HEU from DOE as a virgin LEU without checking, for example, transuranic and fission activities.

In connection with the re-use of LEU with U-235 contents of 20 and 35 % from a Zero-Experiment in Europe, NUKEM started to clarify the acceptance of this fuel. We started to look closer to this fuel from its delivery from the US until after its re-availability after termination of the O-Experiment.

In order to allow for a comparison of the so-called "virgin" US HEU I show you as **table 1** the revised DOE specifications Standard Purity for HEU. It shows as typical values for U-234 1.5 % and for U-236 0.54 %. No mention is made to the content of U-232 since in former times nobody showed interest for this content.

TABLE 1

REVISED DOE-SPECIFICATION

IMPURITY	TYPICAL ANALYSIS (PPM)
Al	5.0
B	< 1.0
Be	< 0.15
C	100.0
Ca	< 10.0
Cd	< 0.10
Co	1.0
Cr	10.0
Cu	5.0
Fe	30.0
Li	0.25
Mg	15.0
Mn	5.0
Mo	< 10.0
Na	< 1.0
Ni	15.0
P	< 100.0
Pb	< 5.0
Si	50.0
V	< 1.0
W	100.0
Uranium	99.94 %

GAS ANALYSIS	TYPICAL ANALYSIS (% PPM)
H2	1.09
N2	63.0
O2	31.0

ISOTOPIC ANALYSIS	TYPICAL ANALYSIS
U-234	1.50
U-235	93.15
U-236	0.54
U-238	5.30

As **table 2** I show you again the range of values for U-234 (from 0.5 to 1.14 %) and for U-236 (from 0.01 to 1.57 %) which had determined as former fuel element manufacturer.

Table 3 shows you figures on Plutonium-values which have been found in LEU metal supplied by DOE.

4. Conclusion

As can be easily noted from tables 1 to 3, HEU supplied by DOE never was "virgin". From the values given for U-236 and Plutonium one can come to the conclusion that DOE well used reprocessed uranium in their enrichment process for fresh HEU.

Since we have started in Europe with the reprocessing of spent HEU fuel we have also consequently to deal with the re-introduction of this fuel into the fuel cycle.

We can confirm AEA's figures in the paper "An Assessment of the Use of Recycled Uranium in Low Enriched Research Reactor Fuel" which was presented at the Uranium Institute Annual Symposium on September 11, 1992.

The conclusion of this paper is that the use of recycled uranium to fuel LEU research reactors should therefore be considered as presenting an opportunity to cost effectively utilize an otherwise valueless resource.

Still unclear matters such as specification for the recycled and blended LEU should be solved with the participation of reprocessors, fuel element fabricators and research reactor operators.

NUKEM, being a company active in the external fuel cycle for research and power reactors is ready to assist you in that respect as in the past.

TABLE 2

U-234 AND U-236 VALUES DETECTED BY NUKEM IN FRESH DOE-URANIUM

U-234	min. 0.5 %	max. 1.14 %
U-236	min. 0.01 %	max. 1.57 %

TABLE 3

ANALYTICAL RESULT ON PU DETECTED IN LEU METAL SUPPLIED BY DOE

Pu-238 (Bq/g)	Pu-239 (Bq/g)	Total PU activity (Pu-238 + Pu-239) as Pu-239 (Bq/g)	Total Pu Concentration as PU-239 (ppb)
4.85	5.45	10.3	4.5 +/- 0.5
4.99	5.61	10.6	4.6 +/- 0.5
4.95	5.55	10.5	4.6 +/- 0.5
4.90	5.50	10.4	4.6 +/- 0.5
4.76	5.34	10.1	4.4 +/- 0.5
4.76	5.34	10.1	4.4 +/- 0.5

RECYCLING OF REPROCESSED URANIUM FROM RESEARCH REACTORS

S. Bouchardy and J.F. Pauty
COGEMA, Enrichment Branch
78140 Velizy Villacoublay, France

ABSTRACT

Research reactor fuels were already reprocessed in France in the 1970s, and their reprocessing is expected to resume shortly. The uranium recovered still contains a very high enrichment which should be utilized. The recycling of this reprocessed uranium (RepU) in the form of 19·75% U metal is one attractive method proposed by COGEMA.

This paper reviews the processes for making uranium metal applied at Pierrelatte, either from UF_6 or from recycle materials. It describes the characteristics of the reprocessed uranium and the way in which COGEMA plans to recycle it in its facilities. Problems of radiation protection are discussed, as well as the research and tests under way, which are intended to confirm the feasibility of this solution.

INTRODUCTION

The Pierrelatte facilities were commissioned about thirty years ago to produce highly enriched uranium metal for the French Defence Department. UF_6 is enriched by gaseous diffusion. The metal is prepared by the URE facilities (Recycle and Production Unit). Designed from the outset to recycle fabrication scrap from the Defence Department by nitric dissolution, these facilities are basically ideal for converting the uranyl nitrate produced by reprocessing into uranium metal.

For the past ten years, these facilities also recycle metal from the fabrication scrap received from the CERCA fuel fabrication plant. They also carry out chemical conversions to the chemical forms of the oxide (U_3O_8) or metal for other clients, irrespective of the isotopic uranium content.

These installations were not initially designed to recycle irradiated materials. Problems of radiation protection specific to RepU are currently being examined (see section entitled Evolution of RepU during recycle).

THE URE FACILITY
(Recycle and Production Unit)

Two main process lines, the Dry Process (VS) and Wet Process (VH) are used in different modular facilities designed to operate up to the highest U 235 enrichments, above 93% (Figure 1).

a Dry process

This process leads to the production of the metal from UF_6.

Highly-enriched UF_6 is first reduced in the presence of hydrogen to UF_4. By calcium reduction and remelting, the metal is then cast into 5 kg ingots. The quality of the metal obtained easily meets the standards of fuel fabricators for research reactors.

b Wet process

This process was developed for two purposes:

- to obtain a very pure final product,
- to recycle production scrap from the Defence Department.

The process was also subsequently used to recover material from fuel fabrication scrap.

The scrap, metal U or oxides after possible roasting, or alloys (UAl_x, U_3Si_2) are converted to uranyl nitrate. Other uranium-bearing chemical forms demand more complex treatment. The solution obtained generally undergoes one, or sometimes two purification cycles (TBP solvent treatment).

From uranyl nitrate, the main steps of the process are:

- precipitation in the form of ADU,
- calcination in the form of U_3O_8,
- reduction in the form of UO_2,
- fluoridation to UF_4.

The UF_4 thus produced returns to the dry process for metal production by calcium reduction.

For several years, COGEMA, from its own facilities, has been delivering supplies or material recycle services for research reactors.

REPROCESSED URANIUM

After reprocessing, RepU in the form of uranyl nitrate can be introduced into the wet process, normally after the purification step. However, the chemical impurity content may require a purification cycle.

Reprocessed uranium displays differences from enriched uranium obtained from natural uranium.

From the isotopic standpoint, two artificial radioisotopes are present after irradiation in the reactor, U 236 and U 232.

a Uranium 236

Uranium 236 is a neutron absorbent and may represent a handicap for some users.

However, its presence has no effect for chemical conversion treatments.

b Uranium 232

By contrast, uranium 232, by radioactive filiation, gives Bi 212 and Tl 208, both high-energy gamma emitters which raise specific problems of radiation protection (Figure 2).

U 232 is formed in the reactor in complex ways (Figure 3) requiring detailed modelling to calculate the isotopic distribution.

Pre-irradiation storage time, and initial impurity content (U 236, thorium) are important parameters for the U 232 production rate.

By natural decay, U 235 (93% in fresh metal) and U 234 (more than 1% in fresh metal) produce an accumulation of Pa 231 and Th 230 in the metal. Under irradiation, these two elements yield U 232 (via Pa 232).

Storage time after irradiation is also important for the formation in the reactor of Pu 236, which also yields U 232 by radioactive decay (half-life 2·8 years).

Past reprocessing experience of research reactor fuels and calculations show that the U 232 content can be positioned in the range between 2 and 12 ppb.

c Transuranics and fission products

The uranyl nitrate produced by reprocessing also contains traces of fission products and transuranium elements.

By taking the RepU specifications of electric power reactors as a reference, and assuming that the average value is 50% of the specified limit, the following activities can be considered as representative:

- transuranics: 125 Bq/gU (alpha activity Pu, Am, Np, Cm),
- fission products: 9250 Bq/gU (beta/gamma activity).

d Impurities

Non-radioactive chemical impurities are also present in the nitrate.

The total, normally less than 500 ppm/U, is acceptable. However, a sufficiently high level of impurities may demand a solvent purification step to make the product meet fuel fabrication standards.

RECYCLING PROPOSED

The RepU recovered has considerable residual enrichment, 70 to 80%, which should be utilized.

COGEMA has basically discarded the alternative of fluorination followed by re-enrichment. The high U 236 content of this material would in fact durably pollute the subsequent production of the enrichment cascades.

COGEMA proposes to dilute this material to produce a uranium that can be used in research reactors, with a standard enrichment of 19·75%.

The mixing of R kg of U from RepU with a residual U 235 content of Nr, with D kg U with Nd content yields P kg U product usable at Np content (Np = 19·75%).

The dilution factor f is defined by:

$$f = \frac{P}{R} = \frac{Nr - Nd}{Np - Nd}$$

Thus for 1 kg U/RepU with Nr = 80% diluted with depleted uranium with Nd = 0·30%, we obtain P = 4·098 kg U with Np = 19·75%.

This dilution factor of about 4 commensurately reduces all the contents of potentially problematic elements.

By proceeding with pure dilution nitrate, the U 232, U 236, transuranics and fission products contents are divided by this factor f. The chemical impurity contents are also reduced. The factor varies according to the level of each element present in the dilution uranium.

Dilution with a more enriched uranium yields a larger quantity of product P and hence with higher dilution (Table 1).

Table 1
Dilution factor f

Nd =	Uranium used for dilution depleted U 0·30%	natural U 0·74%	EU 5·0%	MEU 10%
reprocessed U 80%	4·10	4·16	5·08	7·18
reprocessed U 70%	3·58	3·64	4·41	6·15
reprocessed U 60%	3·07	3·11	3·73	5·13

for final product with Np = 19·75%

With 5% uranium, for example, the dilution factor is 5·085. However, an economic approach on an individual case basis should help to decide whether the additional material gained justifies the use of a more costly dilution material.

At all events, it is more interesting to perform this dilution in the reprocessing plant where it raises no problems. The beneficial effect of dilution is advantageous for all the subsequent steps in recycling, beginning with RepU transport, recycling facilities, fuel fabrication plant, storage and handling at the reactor site. The final isotopic adjustment is made at the head end of the metal conversion plant.

EVOLUTION OF RepU DURING RECYCLE

COGEMA has already accumulated considerable experience in recycling reprocessed uranium from nuclear power plant fuels. Conversion of RepU uranyl nitrate from the La Hague plants to UF_4 or U_3O_8 is routine practice at Pierrelatte. COGEMA is thoroughly familiar with developments in the contents of fission products and transuranium elements.

- Virtually 100% of the transuranics accompany the uranium to the oxide and UF_4 steps.
- A maximum of 80% of the fission products are found in the uranium up to UF_4.

The calcium reduction step (which is not carried out on RepU from power reactors) must be subjected to tests. The cautious assumption made today is that there is practically no elimination of transuranium elements in the slag, and that at least 50% of

the fission products should be found in the slag or the offgases from calcium reduction.

The case of U 232 daughters is more complex. Theoretically, perfect separation of the products of the U 232 decay chain should ensure zero activity after complete reprocessing. With the progressive reconstruction of the chain, 90% of the activity of the daughters is again reached after eight years (four half-lives).

In practice, thorium, the first link in the decay chain, may be separated imperfectly, and the time elapsing between reprocessing and refuelling in the reactor could amount to a few years. The presence of a gaseous radionuclide, radon 220, in the chain further complicates the calculations.

Thus it is considered with caution that the gamma emitters bismuth 212 and thallium 208 are at equilibrium with uranium 232.

Table 2 summarizes the changes in RepU through the different steps in recycling.

Table 2
Anticipated changes in characteristics of
RepU in recycling steps

	after reprocessing		after dilution (f = 4)	
	specification	expected values	uranyl nitrate	metal
isotopic content:				
• U 235 (%)	-	60 to 80	19·75	19·75
• U 236 (%)	-	1 to 15	0·25 to 3·75	0·25 to 3·75
• U 234 (%)	-	0·5 to 1·1	0·13 to 0·28	0·13 to 0·28
• U 232 (ppb)	-	2 to 12	0·5 to 3	0·5 to 3
activity:				
• FP (Bq/gU)	18,500	9250	2300	< 1000
• TU (Bq/gU)	250	125	30	30
chemical impurities (ppm)	3000	500	purification possible	fuel standard

RADIATION PROTECTION

The recycling facilities have not secured permanent authorization today to treat products obtained from reprocessing. Safety studies are under way, particularly with respect to radiation protection.

With the anticipated levels of alpha activity and radiation, the first results of these studies show that this treatment is possible, without major changes.

Local shielding will have to be installed at certain workstations and around specific units: column bottoms, annular tanks.

Specific procedures for RepU and complementary instructions will be issued for operating the facilities. The preparation of RepU materials is planned in isolated campaigns. Complete rinsing of the installations at the end of the campaign will help to recover the initial operating conditions.

The presence of transuranium elements and fission products in the effluents must be taken into account. This is a well-known point for the related facilities on the site, which have already routinely converted more than 2000 t of RepU from power reactors.

Technical investigations and supplementary tests are continuing to complete the safety aspects. Particularly examined are developments (migration, possible accumulation) of fission products and transuranium elements. The results of these investigations are not expected to cast doubt on the recyling principle considered.

CONCLUSIONS

The uranyl nitrate produced by the reprocessing of irradiated fuels from research reactors that will be available in a few years can be recycled in metallic form.

After dilution to the standard commercial content (19·75%), COGEMA will produce a uranium metal that can be re-introduced into the fuel cycle of research reactors.

COGEMA is taking measures to be able to meet this demand in the second half of the decade.

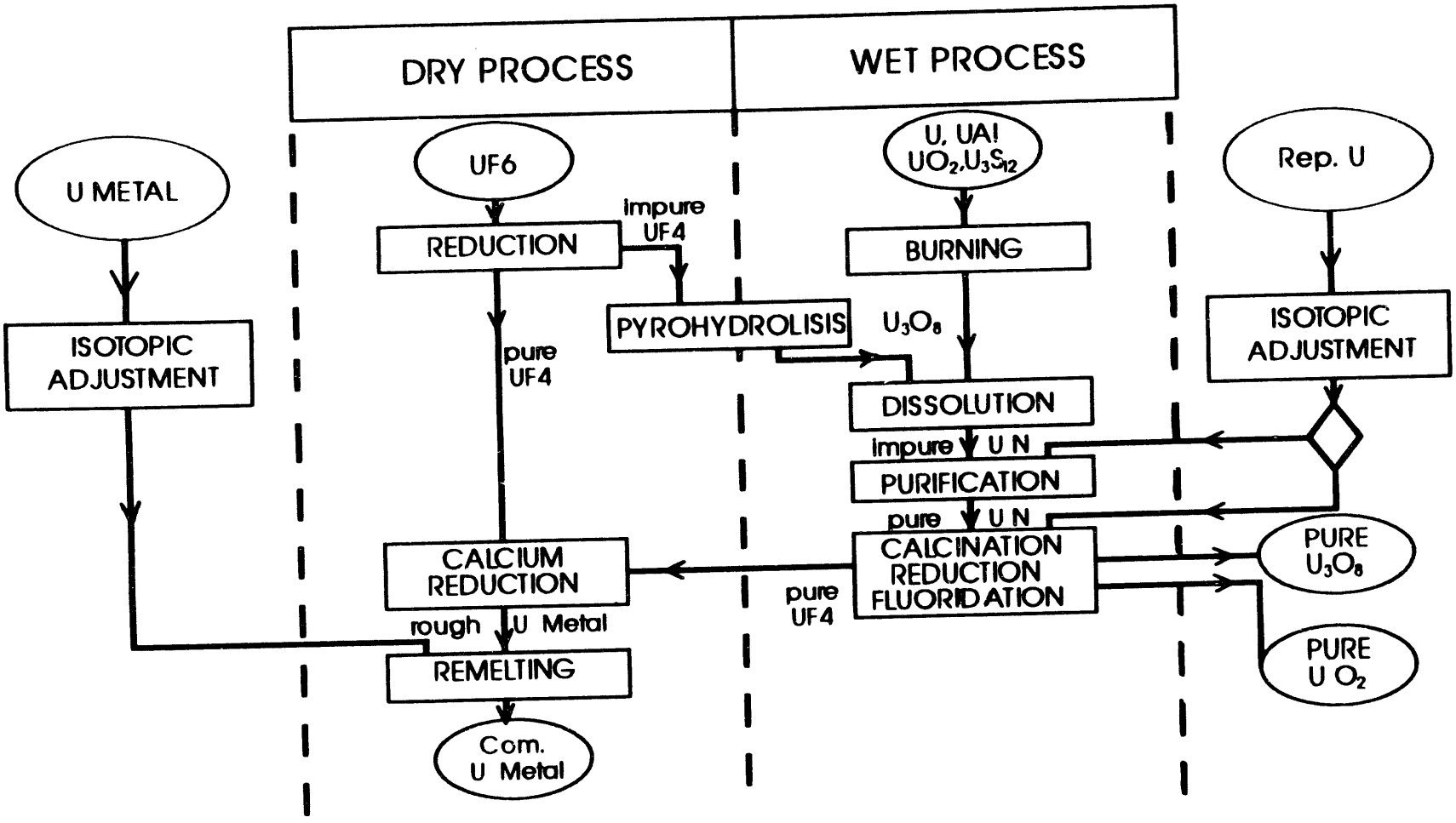

Fig. 1 Uranium Metal Production

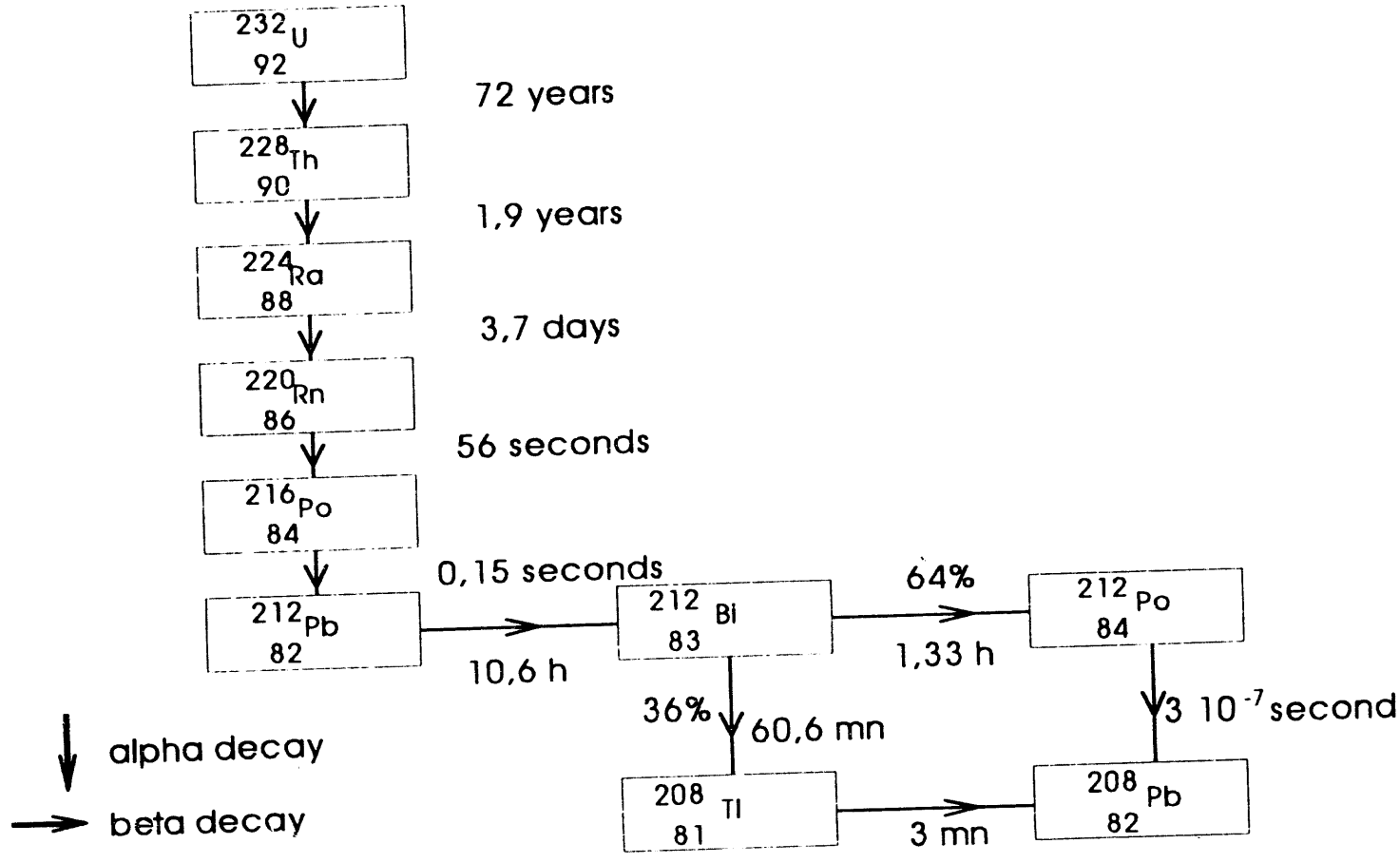

Fig. 2 U_{232} Decay Chain

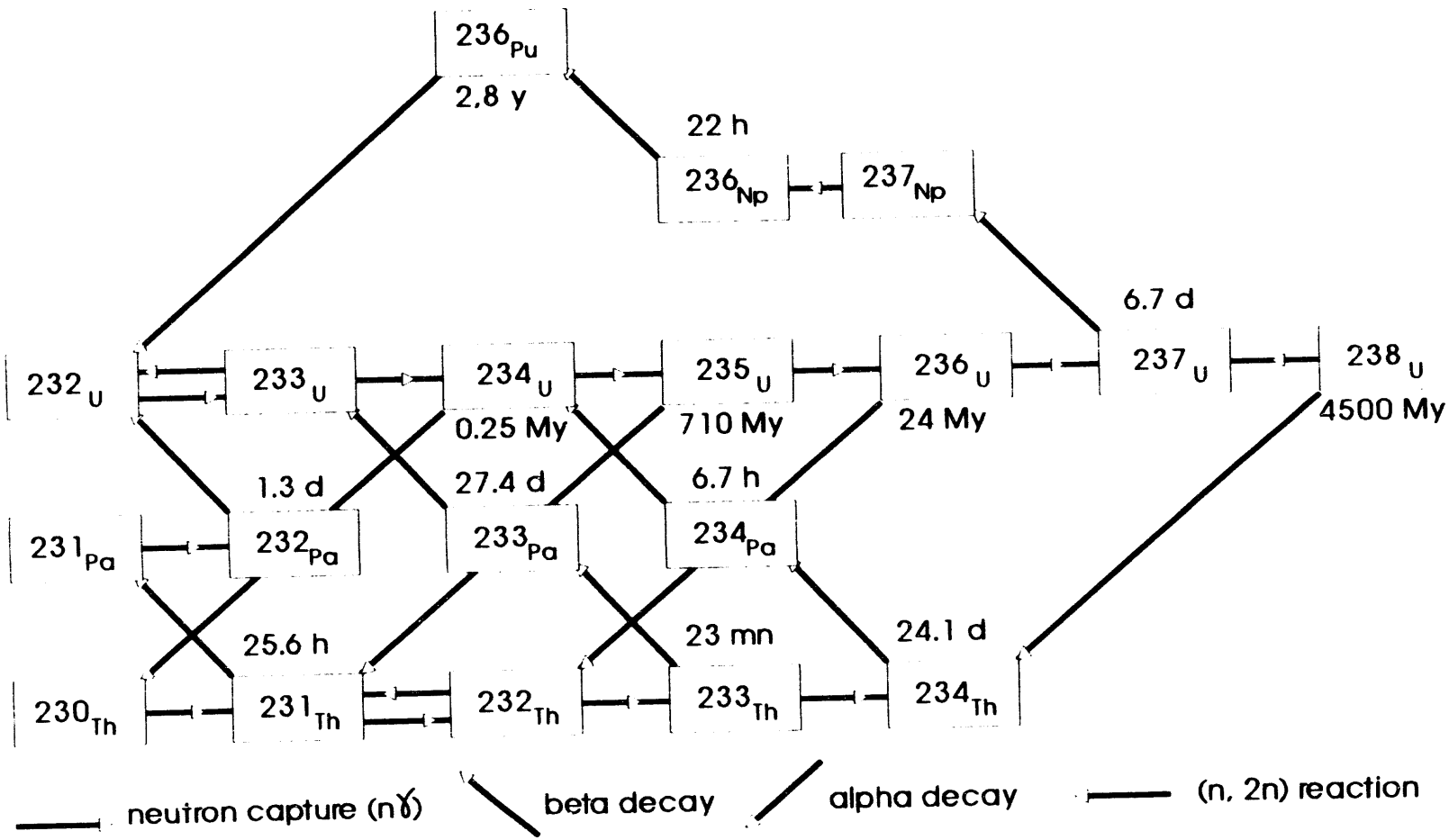

Fig. 3 U_{232} Formation Chain

INTERMEDIATE FUEL ELEMENT STORAGE FACILITY AT REACTOR DR 3

Jens Qvist
Reactor DR 3
Erik Nonbøl
Nuclear Safety Research Dept.
Risø National Laboratory
DK-4000 Roskilde, Denmark

ABSTRACT

In order to cope with delays in the back end of the fuel cycle, a dry vertical storage facility has been constructed at DR 3, a PLUTO type MTR reactor.

The capacity of the facility corresponds to ten years of reactor operation.

The facility consist of four blocks with 12 storage holes each. Each hole houses the equivalent of 9 fuel elements.

Each storage hole is ventilated in order to facilitate monitoring of air humidity and contamination.

Special emphasis is placed on the criticality aspect due to the compact design of the facility.

INTRODUCTION

The main research reactor at Risø National Laboratory is DR 3, a PLUTO type MTR reactor (heavy water moderated and cooled).

Since start of the reactor in early 1961 the back end of the fuel cycle has been based upon reprocessing performed by a number of contractors.

Over the years delays have been experienced for various reasons in the back end of the fuel cycle. In 1991 it became evident, that the then existing delay could be expected to be of longer duration, and that storage capacity for spent fuel would be a problem within few years. Consequently it was decided to extend the intermediate storage capacity at the reactor. This comprises two dry storage facilities and one pool. The latter is used for cutting, storage and transfer to the shipping cask.

Design Principles

From the onset, it was decided that the new facility should be based upon the following principles:

a: Capacity of the facility should correspond to roughly 10 years of reactor operation.

b: Location within the reactor facility area as this is routinely surveyed by the operational staff.

c: Vertical storage which would minimize space demands and ease transfer from the pool.

d: Storage of free cut fuel tubes only in order to reduce the size of the facility.

e: No restrictions regarding burn-up i.e. fuel tubes with maximum fissile content should be accommodated.

f: Long decay time before transfer as this would reduce problems with regard to decay heat removal and minimize health physics risks during handling and storage.

g: Dry storage in order to eliminate corrosion problems and water chemistry control.

h: Requirements for materials in contact with fuel tubes in order to minimize corrosion problems.

i: Ventilation in order to assure drying of the wet tubes from the pool and for monitoring humidity and activity.

Description of the Facility

The adopted principles resulted in a facility comprising four concrete blocks placed vertically under the floor of the active handling bay.

The floor, designed for heavy loads, was cut between the beams resulting in two rectangular holes each accommodating two blocks. These were placed in steel lined holes drilled down into the ground. This design allowed for prefabrication of the blocks, assuring well defined concrete quality and all the holes could be finished before the blocks were placed in the holes. The top face of the blocks is a mild steel plate level with the floor and the top 1.8 m between and around the blocks is filled with heavy concrete while the space between a block and its liner is filled with ordinary concrete.

Each block is an octagonal cylinder 0.88 m across flats and 7.375 m high containing 12 storage holes as shown on Figure 1. The holes are placed in a triangular mesh with a distance of 226 mm between the centerline of the holes. These are made up of mild steel tubes, mild steel being chosen as the best material with regard to contact with concrete. The tubes are mutually supported by spacers assuring correct geometry during construction as well as during concrete pouring. The requirement regarding geometry is that a tube center line should be within +/- 2 mm of correct geometry. The upper part of the holes is stepped and a mild steel plug 755 mm long constitutes shielding upwards.

The bottom of each hole is closed by a disc in the center of which a small steel stud is placed.

Above the plug a space has been arranged for to accommodate seals. This space is closed by a disc with an O-ring that seals against the hole in the top plate.

Inside the holes a stainless steel liner is suspended by means of a ring with a conical seat. The lower part of the liner is positioned radially with respect to the mild steel tube and the liner tube ends 15 mm higher up than the bottom of the mild steel tube.

Ventilation air is thus guided down through the liner tube and up through the gap between the two tubes. An inlet manifold is embedded in the concrete while outlet is via separate tubes in the concrete. These tubes are lead to a common box on one of the flat sides of the block.

Each storage hole houses nine sets of fuel tubes. In order to reduce the load on the tubes and minimize handling, three tubes are stacked on a common post and three posts are stacked one upon the other. The bottom of one post provides radial positioning for the top of the post beneath. The post is made up by a central tube and a perforated bottom disc. The central tube provides radial positioning for the fuel tubes, besides it has a coupling devise for the transfer cask grab.

The post is made of stainless steel and as it, together with the liner made of the same material, are the only components in contact with the fuel tubes, no corrosion problems are to be expected.

Three posts can be accommodated in one storage hole, stacked one upon the other with the lower post resting on the stud in the bottom of the storage hole.

The above design results in a compact storage facility in which an equivalent of 432 fuel elements can be stored in four blocks.

FIG. 1 INTERMEDIATE FUELELEMENT
STORAGEFACILITY AT DR3

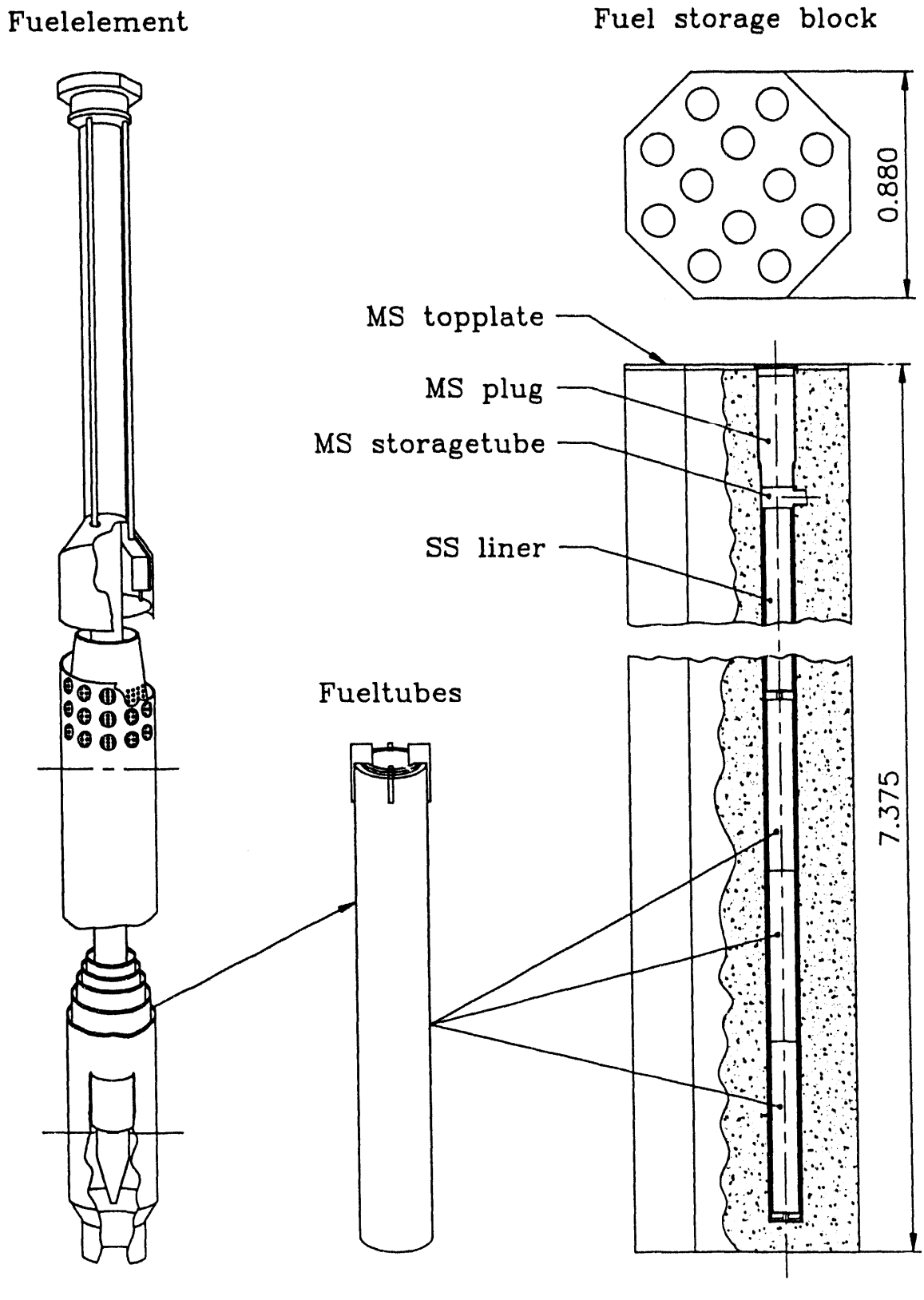

Ventilation and Monitoring

The ventilation system for the four blocks is connected to the existing active handling bay ventilation system with its HEPA filter.

The planned air humidity monitoring system is based upon a single sensor in each of the four common outlet boxes. In case of a steady increase in the reading the individual storage hole outlet tubes will be monitored. If ground water in-leak is found the hole can be emptied and taken out of operation.

Integrity of the cladding of the fuel tubes will be monitored by means of similar procedure for air control.

Construction and Status

Due to the pre-fabrication concept, the construction period at the reactor facility area was very short - about 3 weeks. No major problems were encountered during construction. The facility is now awaiting testing mainly to verify that ventilation flow and humidity control meets specifications.

Control of shielding performance will take place as a part of the loading procedure, when the facility is operational.

Criticality calculations

In order to evaluate the possibility for criticality in the fuel storage the multiplication factor has been calculated for different scenarios as to the content and distribution of the fuel.

For this purpose a two-dimensional code, CCCMO[1], based on collision probability theory has been applied. This code has been verified through several international benchmark problems and it is also used for cross section processing in connection with the 3D-simulator of the DR 3 reactor[2].

Since the program CCCMO is two-dimensional the calculations are made under the assumption of infinite length in the vertical direction. This assumption is also applied to the horizontal plane. Both assumptions make the calculation of the multiplication factor very conservative. The calculations are performed in 76 energy groups with the UKNDL cross section library from 1973 as basis.

If the calculations should have been made for the real geometry Monte-Carlo methods should have been applied. But since the results of the calculations are very far from criticality we

have not found it necessary to make time consuming Monte-Carlo calculations.

Description of the calculations

The calculations are made assuming new LEU fuel elements with a U235 content of 180gr in every storage hole.

The material composition of the mild steel tubes in contact with the concrete is assumed to be 100% Fe.

The composition of the stainless steel is the following:

Fe 74%	Cr 18%	Ni 8%

The concrete has the following material composition (Portland type):

Fe 1.4%	H 1.0%	O 52.9%	Mg 0.2%	Ca 4.4%
Si 33.7%	Na 1.6%	K 1.3%	Al 3.4%	C 0.1%

The geometry applied in the calculations is shown on top of Figure 2 while the real geometry is shown below.

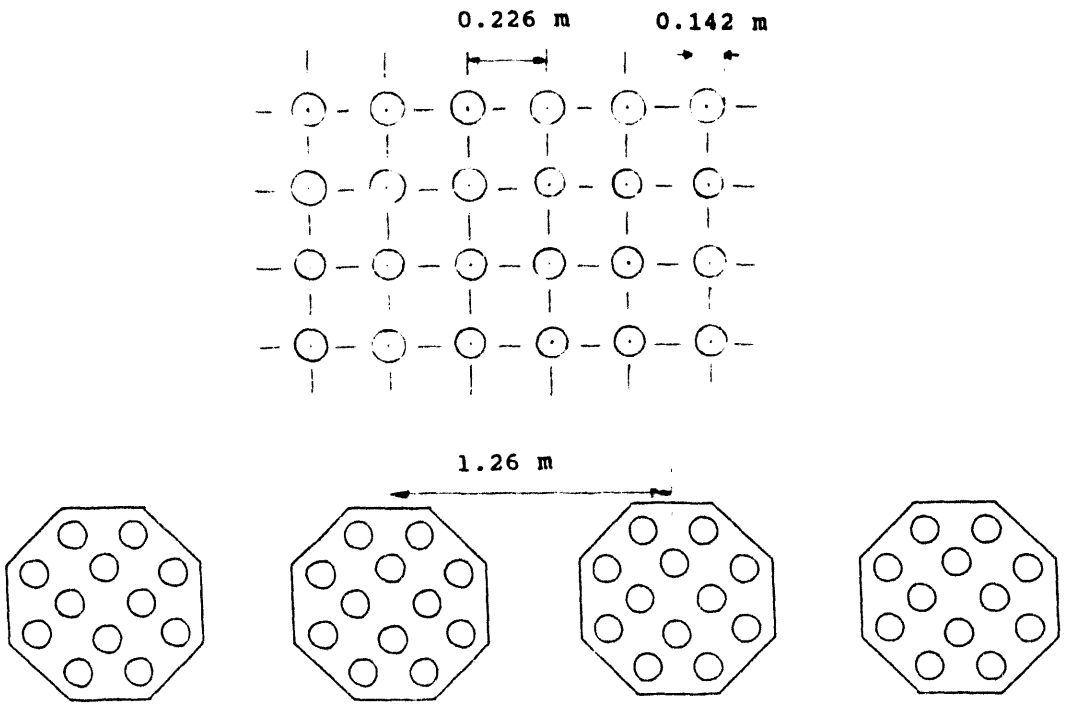

Fig. 2 Horizontal cross section of the fuel storage facility

Parameter studies

Different parameter studies have been performed to take into account uncertainties in material compositions, especially as to the content of hydrogen in the concrete.

Also different accident scenarios have been analyzed, among others flooding of the storage holes by H_2O respectively D_2O, replacement of the steel liners with Al liners, etc.

Table I. Parameter studies of the multiplication factor for intermediate fuel storage

Case	Conditions	k_∞
1	Concrete (1.0%H) + SS + S + Air in fuel,Normal	0.4244
2	Concrete (1.0%H) + SS + S + H_2O in fuel	0.5463
3	Concrete (0.0%H) + SS + S + H_2O in fuel	0.6192
4	Concrete (0.0%H) + SS + S + D_2O in fuel	0.5392
5	Concrete (0.0%H) + Al + Al+ H_2O in fuel	0.7133

Results

Case 1. This calculation represents the most realistic case where the fuel elements are cooled by natural convection. The storage facility is seen to be very subcritical.

Case 2. In this case it is assumed that the space between the concentric fuel rings is flooded by H_2O. The multiplication factor is increased compared with case 1 but still the fuel storage is subcritical.

Case 3. The hydrogen content of the concrete is reduced to 0% resulting in a multiplication factor of 0.6192. The increase in k_∞ compared with case 2 reflects the good moderation effect of the concrete. The storage is super-moderated due to the concrete, thus reducing the hydrogen reduces the absorption and increases the multiplication factor. Subcriticality is still sustained.

Case 4. This scenario is like case 3 but with the space between the fuel rings flooded by D_2O. The reduced multiplication factor is caused by the poor moderation effect of D_2O compared with H_2O.

Case 5. Finally the stainless steel liners are substituted by aluminum liners. The multiplication factor is increased to 0.7133 but still the fuel storage facility is subcritical.

Conclusion

The calculations have shown that even with very conservative assumptions, 180 gram LEU + infinite storage grid, the fuel storage is far from criticality.

If an accident should take place with the fuel storage flooded by water and taking uncertainties in material compositions into account, SS substituted with Al, the facility is still kept subcritical.

In all the considered cases the distance to criticality is so far that even including the normal uncertainties in computer modelling the intermediate fuel storage facility at reactor DR 3 should be well within the nuclear safety limits.

REFERENCES

1. C.F. Højerup, "The Cluster Burnup Program CCCMO and a Comparison of Results with NPD Experiments", Risø-M-1898, 1976.

2. E. Nonbøl, "Development of a Model of the Danish Research Reactor DR 3", Risø-M-2550, 1985.

S E S S I O N VII

September 30, 1992

SAFETY TESTS AND EVALUATIONS

Chairman:

K. Kanda
(KURRI, Japan)

LONG TERM STORAGE/DIRECT DISPOSAL V REPROCESSING - A COMPARISON OF THE COSTS FOR RESEARCH AND TEST REACTOR OPERATORS

C. McColm
AEA Fuel Services

ABSTRACT

Solutions to the back-end closure of the research reactor fuel cycle are being sought worldwide since the decision by US DOE to suspend acceptance of spend fuel from abroad in 1988.

Reprocessing and subsequent credit/re-use of the recovered uranium has been the traditional method adopted as the solution. However, since operators have now been faced with the real costs of reprocessing, subsequent waste treatment and disposal as opposed to the incentive US DOE price of pre 1988, more cost beneficial alternatives are being sought.

One alternative being that of interim storage and possible final disposal in a national repository.

This short paper examines the global costs of the traditional and alternative solutions based on AEA's recent experience of interim storage and extensive experience of reprocessing. The assigned monetary values and assumptions used are meant for comparitory purposes and reflect the most recent data available in the UK and the basic assumption is that the sums involved will be largely representative of the industry worldwide.

MOX STORAGE FACILITY DESCRIPTION

A storage facility has been constructed at Dounreay to store 206 unirradiated MOX fuelled sub-assemblies.

The store is approx 9 m long x 2.75 m wide x 4.1 high and is constructed in reinforced concrete with vertical steel tubes providing sub-assembly location. Wall thickness is 0.4 m to provide shielding for the neutron emissions from plutonium and the γ emissions from plutonium decay products, thus keeping surface dose rates to less than 2.5 μSv/hr.

The facility is licensed by the Nuclear Installations Inspectorate for ten years operation and is seismically qualified to a peak-ground acceleration of .2 g and a "cliff-edge" acceleration of 0.25 g. It has forced cooling to cater for a peak load of 18 kw and is situated in a building with all radiological monitoring, physical security, cranage and support services installed.

Although the store was constructed for short-term (< 10 years), storage of unirradiated fuel, the fact that it is shielded and seismically qualified allows reasonable parallels to be drawn with the requirements for a shielded MTR store.

The principle differences will be the arrangements for loading and unloading of irradiated fuel elements; the practice currently for the MOX assemblies is flaskless transfer, clearly not possible for irradiated MTR elements. It is therefore envisaged that a rotating shield roof for flask mating and indexing of the storage tubes will be required at an additional cost of approximately £250K.

COST COMPARISON - REPROCESSING V INTERIM STORAGE/DISPOSAL

The following analysis determines the per element (see appendix 1 for element description) costs to an operator for the management of spent fuel arisings.

1. Reprocessing:

   a. Reprocessing and waste conditioning

      Using AEA Fuel Services published prices:

      1 element @ 4 kg total metal x £4K/kg total metal

      Reprocessing = £16K/element

   b. Disposal to Repository

      Using latest estimate for Intermediate Level Waste by UK Nirex Ltd:

      20 kg total metal/m^3, 4 kg total metal/element, £18K/m^3 disposal

      Disposal cost/element = 18K/20 x 4 = £3.6K/element

   c. Totals

Total reprocessing/disposal	=	£16K
per fuel element	+	£3.6K
	=	£19.6K

2. Interim Storage/Disposal

   a. Interim Storage

      Using the costs estimated in appendix 2:

      ie Capital Cost of Facility of £1M
         Per annum operating cost of £50K

It is assumed that element production rate is 30/year, the tore can hold 600 elements, earliest disposal is 20 years after irradiation an that reactor life is 20, 30, 40, and 50 years.

Using the above figures the Interim storage costs are therefore:

Reactor Life (yrs)	No of Elements (-)	Required Store Life (YRS)*	Cost/Element (£K)
20	600	40	5.00
30	900	50	3.89
40	1200	60	3.33
50	1500	70	3.00

*Required store life is 20 years more than that of the reactor life as, due to the minimum cooling time for disposal, the store emptying time will be 20 years.

b. Pre-treatment of Elements Prior to Disposal

Pre-treatment is required a) in order that the elements can be dismantled to distribute the 100g fissile material between two waste packages, thus keeping within the 100g/m^3 or 50g/500 ℓ package limits and b) to distribute the fissile material homogeneously within the packages.

Maximum Cost: Very close to reprocessing as the process would essentially be one of distributing the fissile mass homogeneously throughout the 500 ℓ drum ie dissolution, in-drum mixing with a substrate and solidification. This is essentially reprocessing without the separation and removal of uranium. Licensing conditions and capital investment identical to that of a reprocessing plant, ie £16K/element.

Minimum Cost: This would involve the mechanical breakdown of the element, backfilling and sealing of the waste drums.

Estimated cost/element assuming that a shielded cell exists would be approximately £5K/element. Licensing conditions would be similar to that of a PIE facility.

Range of costs ∴ £5K to £16K/element.

c. Disposal to Repository

Using latest estimate by UK Nirex Ltd:-

100g fissile limit/m^3, 100g fissile/element, £18K/m^3 disposal.

Disposal cost/element = £18K

d. Totals

	£K/element
Interim storage	3-5
Pre-treatment for disposal	5-16
Disposal	18
TOTAL	£26K to £39K/element

ADDITIONAL COSTS

Reprocessing : Additional Costs

1a. Transportation of spent fuel: Reactor to reprocessor
2a. Recovery of uranium and blending to 20% for re-use
3a. Transportation of residues: Reprocessor to disposal facility

Reprocessing: Reduction in Costs

1b. Reuse/sale of recovered uranium

Interim Storage/Disposal: Additional Costs

1c. Transportation of spent fuel: Reactor to storage facility
2c. Transportation of elements: Interim storage to disposal facility

Assumptions

(1a + 2a + 3a - 1b) = (1c + 2c)

ie the additional costs associated with each disposal option are similar.

CONCLUSIONS

1. The only currently licensed option for the closure of the Research Reactor Fuel Cycle is reprocessing.

2. Reprocessing, given the assumptions used in this study, represents the most cost effective solution to the fuel cycle closure.

3. Uncertainties regarding the extent of fissile material dispersal in disposal packages make budgeting for post interim storage costs extremely difficult to predict, if not impossible.

4. Interim storage without a fully licensed, approved and costed ultimate disposal route having been established is taking a large risk.

APPENDIX 1

ASSUMPTIONS AND CRITERIA USED IN DETERMINING COMPARATIVE COSTS OF BACK END CLOSURE METHODS

FUEL ELEMENT DESCRIPTION AND STORAGE REQUIREMENTS

1.	Physical:	Length	=	< 1 metre
		Diameter (A/F for square)	=	< 0.15 metre
		Weight (total)	=	4 kg
		Weight (fissile)	=	0.1 kg U235 + Pu
		Weight (uranium)	=	0.15 kg
2.	Neutronic:	Heat output	=	0.030 KW
		Criticality separation	=	0.25 m ctr to ctr
		Shielding requirement	=	0.5 m concrete
3.	Quantity:	30 elements/yr over a minimum of 20 years		

FUEL STORAGE DESCRIPTION AND STORAGE REQUIREMENTS

1. Physical:
   - Minimum 40 year life
   - Capacity of 600 elements
   - Seismic qualification 0.25 g
   - Keff on flooding Keff + 3σ < 0.9
2. Radiological: External surface dose rate 2.5 µSv/hr

DISPOSAL FACILITY CONSTRAINTS

1. Physical:
   - Standard 500 ℓ ILW drums
   - < 30 W heat/package
   - Contents of package grouted
   - Minimum 20 year cooling/decay for MTR fuel
2. Criticality:
   - Less than 50 g fissile material per package
   - Fissile content to be homogeneously distributed within package

APPENDIX 2

SPENT MTR ELEMENT STORAGE - CONSTRUCTION AND OPERATING COSTS

CAPITAL COSTS

Component	Cost (£K)
Design (Civil and Mechanical)	184)
Design (Electrical and Instrument)	)
Civil and Mechanical Installation	)
Electrical and Instrument Installation	364)
Services and Supplies	)
Project Management	)
Seismic Qualifications	)
Consultants	196)
Sundry Inspections	)
Licensing	)
TOTAL	£744 K
Rotating Roof Valve	£250K
TOTALS	~£1M

OPERATING COSTS

Ground Rental)	
Maintenance)	£50K per annum
Surveillance)	

COST MAKE UP OF STORAGE AND REPROCESSING

2 YEARS BUILD STORE	30 ELEMENTS/YR TO STORE OPERATION	30 ELEMENTS/YR TO STORE 0-30 YRS 30 ELEMENTS/YR TO DISPOSAL 20-50YRS	
20 YR Total 1000	(40 x 50) = 2000	(18 x 600) 10800	Total/Cost £13,800K Cost/Element £23 K/EL + £5K-£16K/EL pre treatment = £28K - £39K element
30 YR Total 1000	(50 x 50) = 2500	(18 x 900) 16200	Total/Cost £19,700K Cost/Element £21.9K/EL £26.9K - £37.9K
40 YR Total 1000	(60 x 50) = 3000	(1800 x 1200) 21600	Total/Cost £25,600K Cost/Element £21.3 K/EL £26.3K - £37.3K
50 YR Total 1000	(70 x 50) = 3500	(18 x 1500) 27000	Total/Cost £31,500K Cost/Element £21.0K/EL £26K - £37K
Estimate for Direct Disposal (European Research Reactor)			£35.7J/EL
Reprocessing: (£4K/kg x 4 kg/element) = £16K/element + 18K/m^3/ 20 Kg/m^3 x 4 kg/element = £3.6 u/el			£19.6K/EL

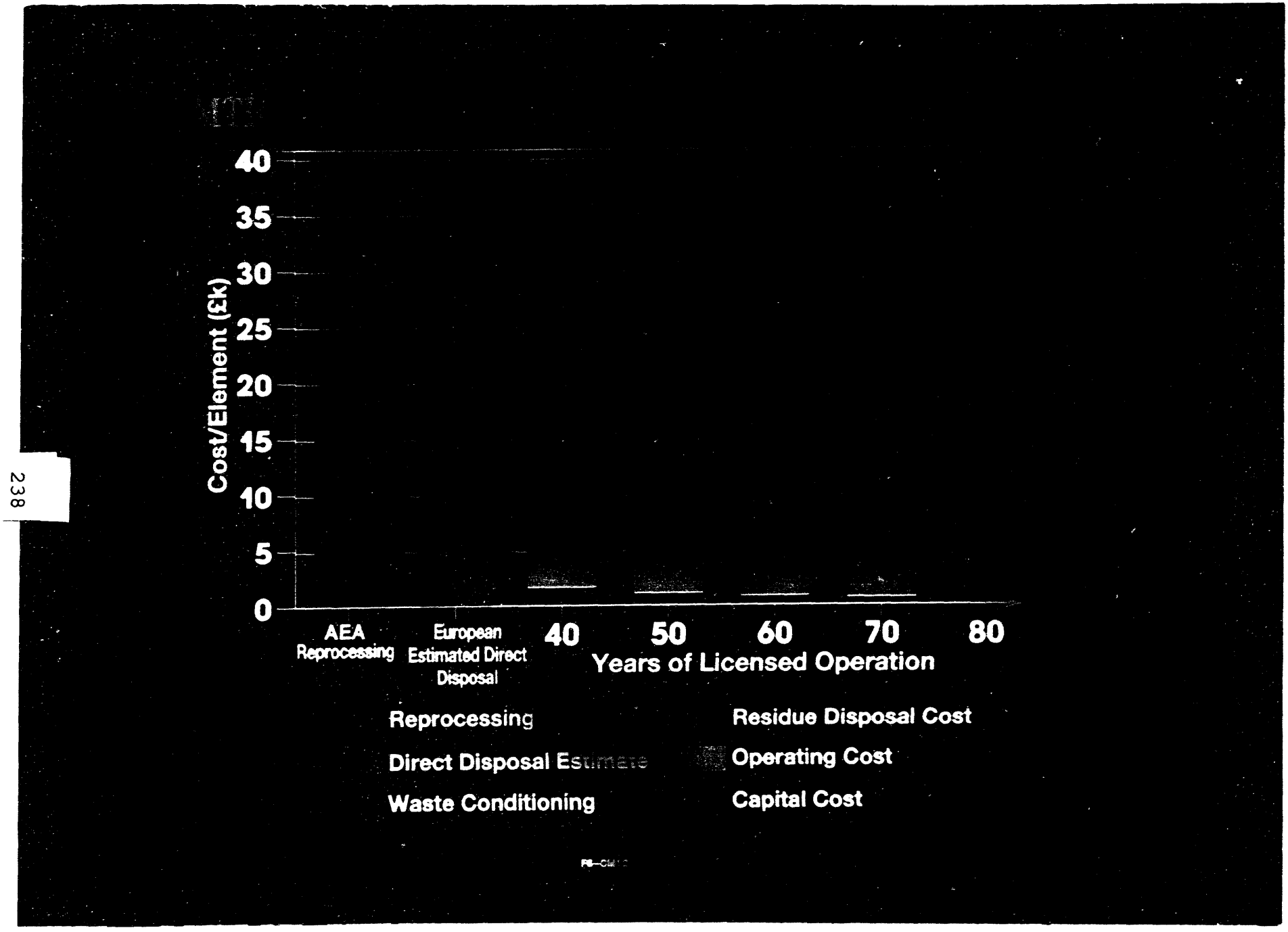
Cost/Element (£k)
40
35
30
25
20
15
10
5
0
AEA Reprocessing
European Estimated Direct Disposal
40
50
60
70
80
Years of Licensed Operation
Reprocessing
Direct Disposal Estimate
Waste Conditioning
Residue Disposal Cost
Operating Cost
Capital Cost

ANALYSES FOR CONVERSION OF THE GEORGIA TECH RESEARCH REACTOR FROM HEU TO LEU FUEL

J.E. Matos, S.C. Mo, and W.L. Woodruff
Argonne National Laboratory
Argonne, Illinois, USA

ABSTRACT

The 5 MW Georgia Tech Research Reactor (GTRR) is a heterogeneous, heavy water moderated and cooled reactor, fueled with highly-enriched uranium aluminum alloy fuel plates. The GTRR is required to convert to low enrichment (LEU) fuel in accordance with USNRC policy. Results of design and safety analyses performed by the RERTR Program at the Argonne National Laboratory for LEU conversion of the GTRR are summarized. Only those parameters which could change as a result of replacing the fuel are addressed. The performance of the reactor and all safety margins with LEU fuel are expected to be about the same as those with the current HEU fuel.

INTRODUCTION

The results of design and safety analyses performed by the RERTR Program at the Argonne National Laboratory for conversion of the Georgia Tech Research Reactor from the use of HEU fuel to the use of LEU fuel are presented. The objectives of this work were to: (1) maintain or improve upon the present reactor performance and margins of safety, (2) maintain as closely as possible the technical specifications and operating procedures of the present HEU core, and (3) utilize a proven fuel assembly design that is economical to manufacture.

The GTRR core contains provisions for up to 19 fuel assemblies spaced 6 inches apart in a triangular array. The fuel is centrally located in a six-foot diameter aluminum vessel which provides a two-foot thick D_2O reflector completely surrounding the core. The vessel is surrounded radially and beneath by an additional two-foot thick graphite reflector. The reactor is controlled by means of four cadmium shim-safety blades that swing downward through the core between adjacent rows of fuel assemblies and one cadmium regulating rod that moves vertically in the radial D_2O reflector. The reactor is equipped with 22 horizontal and 23 vertical experimental facilities for extracting neutron beams and performing irradiations. A shielded room (10 feet by 12 feet inside) for biomedical research is located at the side of the reactor.

The reactor performance objectives and design constraints that were addressed in designing the LEU fuel assembly are discussed in Ref. 1. The LEU fuel assembly has the same overall design as the present HEU fuel assembly, except that it contains 18 fueled plates with LEU U_3Si_2-Al fuel and two non-fueled plates instead of 16 fueled plates with HEU U-Al alloy fuel and 2 non-

fueled plates. Each HEU assembly contains 188 g ^{235}U and each LEU assembly contains 225 g ^{235}U. The LEU core will use the same control system, heat removal system, and auxiliary systems as the current HEU core.

Reactor Models

A detailed Monte Carlo model of the reactor was constructed including all beam tubes, experiment penetrations, the bio-medical facility, shim-safety blades, and regulating rod in order to obtain absolute excess reactivities and shutdown margins for comparison with limits specified in the Technical Specifications. The diffusion theory model did not include the control absorbers or the various experiment facilities. A simplified Monte Carlo model similar to the diffusion model was constructed to verify that the diffusion theory model was correct. Nuclear cross sections in seven energy groups were calculated using standard methods for use in the diffusion theory calculations.

Critical Experiment

In 1974, a critical experiment was built using 9 fresh HEU fuel assemblies. The core was made critical at different shim-safety blade positions with the regulating rod nearly fully-withdrawn and nearly fully-inserted. The excess reactivities calculated for these critical configurations using the detailed Monte Carlo model were -0.91 ± 0.20% Δk/k and -1.22 ± 0.22% Δk/k, respectively. The reactivity bias of about -1.0 ± 0.3% Δk/k in the calculations is attributed to uncertainties in the nuclear cross sections and uncertainties in the reactor materials.

NEUTRONIC PARAMETERS

Excess Reactivity

Calculated excess reactivities (including reactivity bias) for fresh HEU and LEU cores with 17 fuel assemblies are shown in Table 1. The Technical Specifications limit the excess reactivity to a maximum of 11.9% Δk/k. The LEU core is expected to satisfy this requirement.

Table 1. Excess Reactivities of HEU and LEU Cores with 17 Fresh Fuel Assemblies

	Calculated Excess React.[1], % Δk/k (±1σ)	
	Fresh HEU Core	Fresh LEU Core
Detailed Monte Carlo Model	11.7 ± 0.4	9.4 ± 0.4
Simplified Monte Carlo Model[2]	16.8 ± 0.4	14.3 ± 0.4
Diffusion Theory Model[2]	16.6	14.6

[1] The reactivity bias of -1.0 ± 0.3% Δk/k was added to calculated values. [2] Detailed Monte Carlo model without experiment penetrations, shim-safety blades, and regulating rod.

The reactivity effect of replacing all air-filled experiment facilities in the detailed Monte Carlo model with D_2O or graphite was calculated to be 4.5 ± 0.3% Δk/k. Replacing the control absorbers in their fully-withdrawn position with D_2O gave a worth consistent with zero. Thus, the simplified Monte Carlo and diffusion theory models are consistent with the detailed Monte Carlo model if the reactivity worth of the experiment facilities is accounted for.

Fuel Lifetimes

Burnup calculations were run for HEU and LEU cores with 17 fuel assemblies to estimate fuel lifetimes. Reactivity profiles (including the 1% Δk/k reactivity bias) are shown in Fig. 1 over a limited burnup range. The dashed lines show the end-of-cycle excess reactivity range that accounts for reactivity losses due to experiment facilities (4.5 ± 0.3% Δk/k), cold-to-hot swing (~0.3% Δk/k), and control provision (~0.5% Δk/k) that are not included in the diffusion theory model. Reactivity losses due to equilibrium Xe and Sm are included in the curves. The results show that the HEU and LEU cores will have about the same lifetime.

Fig. 1. Burnup Reactivity Profiles

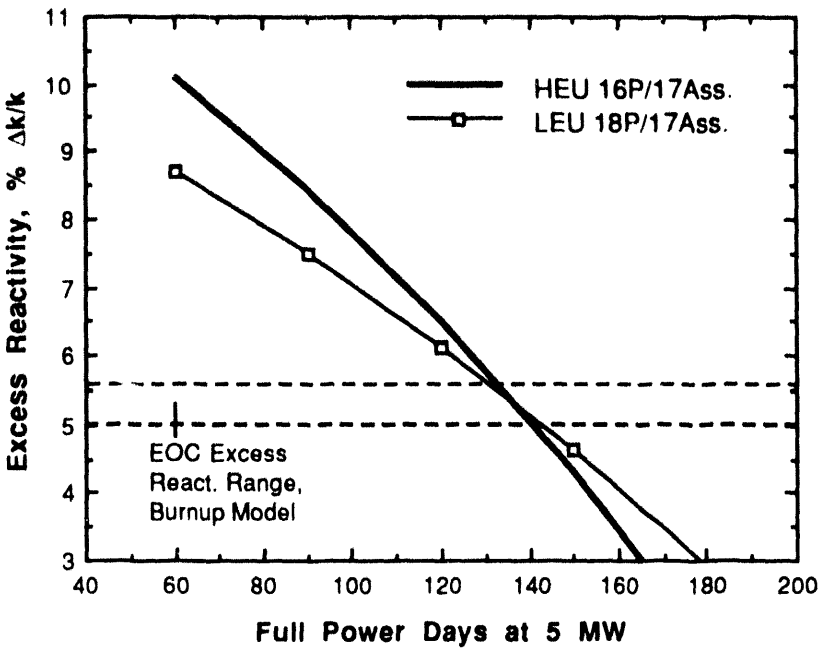

Power Distributions and Power Peaking Factors

Power distributions and nuclear power peaking factors were calculated to be very similar in HEU and LEU cores with 14 and 17 fresh fuel assemblies.

Temperature Coefficients and Kinetics Parameters

Reactivity coefficients for the coolant and the fuel Doppler were computed as functions of temperature for fresh HEU and LEU cores with 14 and 17 fuel assemblies. Also computed were the void coefficient, the whole-reactor isothermal temperature coefficient, and the prompt neutron lifetime. Fresh cores were calculated because they are limiting cores. As fuel burnup increases, the neutron spectrum becomes softer and the reactivity coefficients become more negative. Key temperature coefficients and kinetics parameters are summarized in Table 2.

Table 2. Reactivity Coefficients (% Δk/k/°C at 45°C) and Kinetics Parameters

	HEU		LEU	
	14 Ass.	17 Ass.	14 Ass.	17 Ass.
Coolant	-0.0076	-0.0069	-0.0067	-0.0066
Fuel Doppler	~0.0	~0.0	-0.0017	-0.0020
Whole Reactor Isothermal[1]	-0.0224	-0.0201	-0.0232	-0.0215
Void Coefficient[2]	-0.0383	-0.0392	-0.0333	-0.0350
l_p[3], μs	780	704	745	695
β_{eff}	0.00755[4]	0.00755[4]	0.0075 - 0.0076[5]	

[1] Includes fuel, coolant, inter-assembly water, and reflector. [2] % Δk/k/% Void. Uniform voiding of coolant in all fuel assemblies. [3] Calculated prompt neutron lifetime. [4] Measured effective delayed neutron fraction. [5] Estimated value.

Shutdown Margins

The Technical Specifications require that the reactor have a shutdown margin of at least 1% Δk/k with the most reactive shim-safety blade (blade #3) and the regulating rod fully withdrawn. Shutdown margins calculated using the detailed Monte Carlo model gave - 7.1 ± 0.2% Δk/k for an HEU core and - 8.8 ± 0.2% Δk/k for an LEU core with 17 fresh fuel assemblies. Both cores satisfy the shutdown margin requirement.

In addition to the automatic protective systems, manual scram and reflector drain provide backup methods to shut the reactor down by operator action. Results of Monte Carlo calculations with shim-safety blade positions that would bring the reactor near critical are shown in Table 3. These results show that the top reflector worth of the LEU core is slightly larger than that of the HEU core.

Table 3. Calculated Top Reflector Worths (% Δk/k) of HEU and LEU Cores with17 Fuel Assemblies and Control Blades near CriticalPositions

Top D_2O Reflector	HEU Core	LEU Core
D_2O 1" Above Fuel Meat	- 2.58 ± 0.29 (1σ)	- 2.73 ± 0.31 (1σ)
D_2O 2" Above Fuel Meat	- 2.05 ± 0.28	- 2.42 ± 0.30

THERMAL-HYDRAULIC SAFETY PARAMETERS

Thermal-hydraulic safety limits and safety margins calculated using the PLTEMP code[2] for the LEU core with 14 fuel assemblies were compared with the thermal-hydraulic safety parameters used as bases for the current Technical Specifications. ANL analyses for the LEU core used a combined multiplicative and statistical treatment of a revised set of engineering uncertainty factors. Results for the HEU core obtained using ANL's statistical treatment agree well with the original analyses performed by Georgia Tech. The modified Wheatherhead correlation[3] was used for departure from nucleate boiling (DNB), the Forgan-Whittle correlation[4] was used for flow instability, and the Bergles and Rohsenow correlation[5] was used for onset of nucleate boiling (ONB).

Safety Limits

Calculated reactor power limits based on DNB and flow instability are shown in Table 4 for 14-assembly HEU and LEU cores with the minimum coolant flow of 1625 gpm and with the coolant lowflow limit of 760 gpm. Power limits based on the flow instability criterion are adequate to ensure the safety of the facility. The main reason for differences between the HEU and LEU cores is that the manufacturing specifications for LEU silicide dispersion fuel plates contain a factor of 1.2 for homogeneity of the fuel distribution while the HEU alloy fuel has a corresponding factor of 1.03.

Table 4. Reactor Power Limits (MW) in 14-Assembly Cores Based on DNB and Flow Instability for a Maximum Inlet Temperature of 50.5°C .

Reactor Coolant	GTRR-HEU		ANL-LEU	
Flow, gpm	DNB	Flow Instability	DNB	Flow Instability
760	5.5	5.3	5.3	5.0
1625	11.5	10.6	10.8	10.6

Safety limits for the reactor inlet temperature were calculated at the maximum reactor power of 5.5 MW and the minimum coolant flow of 1625 gpm. The results are shown in Table 5. A safety limit for the reactor outlet temperature was then established by adding the average temperature rise across the core to the limiting inlet temperature. These results show that the HEU and LEU cores have nearly identical safety limits on the reactor inlet and oulet temperatures.

Table 5. Safety Limits on Reactor Inlet and Outlet Temperatures.

	GTRR-HEU	ANL-LEU	
Parameter	DNB	DNB	Flow Instability
Limiting Reactor Inlet Temp., °C	77.8	77.2	76.7
Ave. Coolant Temp. Rise across Core, °C	8.9	9.4	9.4
Limiting Reactor Outlet Temp., °C	86.7	86.6	86.1

Safety System Trip Settings

The safety system trip settings in the current GTRR Technical Specifications for power levels >1 MW and the nominal value for each parameter are shown in Table 6.

Table 6. Current Safety System Trip Settings for Power Levels >1 MW.

Parameter	Trip Setting	Nominal Value
Thermal Power, MW	5.5	5.0
Reactor Coolant Flow, gpm	1625	1800
Reactor Outlet Temperature, °C	59.4	54.4

These settings are based on a criterion that there shall be no incipient boiling during normal operation. The criterion is applied in GTRR by ensuring that the surface temperature at any point on a fuel assembly does not exceed the coolant saturation temperature at that point. This criterion

is conservative because there is an additional margin of ~14°C between the D_2O saturation temperature and the temperature at which onset of nucleate boiling occurs.

Combinations of reactor power, coolant flow rate, and reactor inlet temperature that were calculated to have zero subcooling (fuel surface temperature = coolant saturation temperature) for HEU and LEU cores with 14 fuel assemblies are shown in Table 7. Underlined values for the HEU core correspond with the trip settings shown in Table 6. Corresponding underlined values for the LEU core were determined to be more conservative than those for the HEU core. Thus, the current trip settings for the HEU core can also be used for the LEU core.

Table 7. Parameter Combinations for Zero Subcooling with 14-Assembly Cores

	HEU Core			LEU Core		
Reactor Power, MW	5.5	5.0	5.0	5.6	5.0	5.0
Coolant Flow Rate, gpm	1800	1625	1800	1800	<1625	1800
Reactor Inlet Temp., °C	45.6	45.6	50.5	45.6	45.6	53.3
Temp. Rise Across Core, °C	8.9	8.9	8.9	9.4	9.4	9.4
Reactor outlet Temp., °C	54.4	54.4	59.4	55.0	55.0	62.7

The results in Table 8 show that the degree of subcooling (ΔT_{sub}) at the hottest spot of the limiting fuel assembly under nominal operating conditions is expected to be 6.1°C in the LEU core and 4.4°C in the HEU core. Both of these margins are adequate. Another criterion that is often used in research reactors is that the margin to onset of nucleate boiling (ONB) should be equal to or greater than 1.2. ONB occurs at a temperature of about 118.9°C, which is ~14°C above the D_2O saturation temperature of 104.4°C. The margin to ONB in the LEU core was computed by increasing the reactor power until ONB occured and dividing by the nominal reactor power of 5 MW. These margins are adequate to ensure that the LEU core can be operated safely at a power levels of 1-5 MW.

Table 8. Margins to D_2O Saturation Temperature and ONB for 14-Assembly Cores

Parameter	GTRR-HEU	ANL-LEU
Thermal Power, MW	5.0	5.0
Reactor Coolant Flow, gpm	1800	1800
Reactor Inlet Temp., °C	45.6	45.6
ΔT_{sub}, °C	4.4	6.1
Margin to ONB	-	1.44
Limiting Power Based on ONB, MW	-	7.2

ACCIDENT ANALYSES

A spectrum of accident scenarios was evaluated by Georgia Tech in its safety documentation for 5 MW operation using HEU fuel. These scenarios were thoroughly reviewed and only those that could be affected by changing the fuel assemblies from HEU to LEU were addressed.

Startup Accident

The worst case for a possible startup accident in the current HEU core was determined to result from the simultaneous withdrawal of one shim blade and the regulating rod. Calculations were done using the PARET code[6] for the HEU and LEU cores with 14 fuel assemblies in which reactivity was added at a rate of 0.005 Δk/k per second starting from a power level of 5 MW. Both the HEU and LEU cores were scrammed by the overpower trip at 5.5 MW. A time delay of 100 ms was assumed between introduction of the scram signal and release of the shim-safety blades. Both cores reached a peak power of 5.9 MW at a time of 0.335 s after the transient was initiated. Peak surface cladding temperatures of 80.6°C and 77.8°C were reached in the limiting fuel assembly of the HEU and LEU cores, respectively. The peak power is well below the safety limits of 11.5 MW in the HEU core and 10.6 MW in the LEU core. The peak surface cladding temperatures are far below the solidus temperature of 660°C in the 1100 Al cladding of the HEU core and far below the solidus temperature of 582°C in the 6061 Al cladding of the LEU core. Thus, no damage to the fuel and no release of fission products is expected.

Inadvertent Reactivity Insertions Due to Experiment Failure (with Scram)

The Technical Specifications limit the magnitude of the reactivity worth of each unsecured experiment to 0.4% Δk/k and the reactivity worth of each secured removable experiment to 1.5% Δk/k. The objective of these specifications is to prevent damage to the reactor and to limit radiation dose to personnel and the public in event of experiment failure.

The PARET code was used to calculate the consequences of inadvertent step reactivity insertions of 0.4% Δk/k and 1.5% Δk/k in HEU and LEU cores with 14 fuel assemblies. The model and methods that were used for analysis of the SPERT-II BD-22/24 HEU core[7,8] were also used to analyze the HEU and LEU cores of the GTRR. Temperature coefficients included contributions from only the coolant and the fuel. Calculations were performed with the reactor at nominal operating conditions of 5 MW power, a coolant flow rate of 1800 gpm, and a reactor inlet temperature of 45.6°C. A scram signal was initiated when the reactor power reached the safety system overpower trip setting of 5.5 MW. A time delay of 100 ms was assumed between introduction of the scram signal and release of the shim-safety blades. The results of these calculations are shown in Table 9.

Table 9. Results of Assumed Step Reactivity Insertions Due to Experiment Failure (with Scram)

Parameter	HEU Core		LEU Core	
Step Reactivity Insertion, % Δk/k	0.4	1.5	0.4	1.5
Asymptotic Period, s	0.18	0.05	0.18	0.05
Peak Power, MW	7.4	27.5	7.4	27.2
Peak Surface Cladding Temp., °C	84.4	136.1	81.7	130.6

A positive step reactivity change less than 0.4% Δk/k caused by the ejection or insertion of experiments would result in transient behavior that would not exceed the safety limits for the HEU or LEU cores. The peak power of 7.4 MW in both cores is well below the safety limits of 11.5 MW in the HEU core and 10.6 MW in the LEU core.

Step reactivty insertions of 1.5% Δk/k would result in peak surface cladding temperatures that are far below the solidus temperature of 660°C in the 1100 Al cladding of the HEU core and far below the solidus temperature of 582°C in the 6061 Al cladding of the LEU core. Thus, no damage to the fuel and no release of fission products is expected.

Maximum Positive Reactivity Insertion Without Scram

The Technical Specifications limit the potential reactivity worth of each secured removable experiment to 1.5% Δk/k. The purpose of this analysis is to show that there is a sufficient margin between the maximum allowable reactivity worth of a single experiment and the maximum step reactivity insertion that can be tolerated without fuel damage, assuming failure of reactor scram systems.

Analysis for the current HEU core used SPERT-II experimental data[8] as a basis for estimating the step reactivity insertion that would result in the onset of steam blanketing in the GTRR. In the present analysis, the PARET code was used to compute the step reactivity insertion required to initiate steam blanketing (film boiling) in both the SPERT-II B22/24 core and 14-assembly GTRR cores with HEU and LEU fuel. Key kinetics parameters and results are shown in Table 10. Power peaking factors are similar in the SPERT-II and GTRR cores. The inverse period corresponding to onset of steam blanketing as determined from the SPERT data is about 13 s^{-1}. The PARET code predicts onset of film boiling for a step insertion of $2.0 (1.5% Δk/k) with an inverse period of 12 s^{-1}, in good agreement with experiment.

Table 10. Comparison of Kinetics Parameters and Onset of Steam Blanketing Results

	SPERT-II	14 Assembly GTRR	
	B-22/24	HEU	LEU
Prompt Neutron Generation Time, μs	660	780	745
Beta Effective	0.0075	0.00755	0.00755
Coolant Temperture Coeff., $/°C	-0.00867	-0.00874	-0.00689
Void Coefficient, $/% Void	-0.0729	-0.0509	-0.0442
Doppler Coefficient, $/°C	~0.0	~0.0	-0.00096
Operating Pressure, kPa	122	127	127
Step Reactivity Insertion, $ (% Δk/k)	2.00	1.99	1.95
Inverse Period, s^{-1}	12	19	19
Energy/Plate at t_m, kWs	31.8	31.2	32.0
Peak Cladding Temp at Peak Power, °C	204	218	225
Peak Cladding Temperature at Onset of Steam Blanketing, °C	252	257	257

The same methodology was used to compute GTRR cores with 14 fuel assemblies. The step insertions needed to initiate film boiling (~$2.0) and the peak surface cladding temperatures (250-260°C) at the onset of steam blanketing are nearly the same. At the time of peak power, the energy deposited per plate is about the same in the SPERT and GTRR cores. The peak surface cladding temperature at the time of peak power is about 220°C in the GTRR cores and about 204°C in the SPERT core.

The SPERT-II B22/24 tests[8] indicate that even more extensive film boiling (or steam blanketing) does not result in temperatures that exceed the solidus temperature of the cladding. The most extreme case in the test series with a reactivity insertion of $2.95 (2.2% Δk/k) resulted in a peak surface cladding temperature of 337°C, a temperature far below the solidus temperature of 582°C for 6061 Al cladding. The GTRR SAR also notes that the maximum temperature for large insertions is primarily limited by the energy deposited in the plate with very little effect from the boiling heat transfer.

Since the behavior of the SPERT-II B22/24 and GTRR 14-assembly cores is very similar, a step reactivity insertion greater than 2.2% Δk/k would be required to initiate melting of the GTRR LEU core. The margin of at least 0.7% Δk/k above the maximum allowed reactivity worth of 1.5% Δk/k for a single experiment is sufficient to ensure that the facility is safe in the unlikely event that the maximum allowed reactivity were inserted in a step and the reactor scram system failed to function.

Design Basis Accident

The Design Basis Accident for the HEU core in the GTRR safety documentation is the melting and release of the fission products from one fuel assembly into the containment atmosphere. This accident was assumed to occur during a fuel transfer operation in which an irradiated fuel assembly was being moved from the core to the fuel storage area using a shielded transfer cask. Fuel assemblies are not normally discharged from the reactor until at least 12 hours after reactor shutdown. This ensures that sufficient fission product decay heat has been removed from the assembly and that the surface temperature of the fuel plates will not reach 450°C when the assembly is moved into the cask.

In spite of administrative controls, it is conceivable that a fuel assembly could be withdrawn from the reactor prior to a 12 hour cooldown period. Some or all of the fuel plates within the assembly could then melt and release some of their fission products into the containment atmosphere. In the current GTRR SAR, the source term for evaluating the radiological consequences of this accident was obtained by assuming that an HEU fuel assembly with equilibrium burnup was removed from the core before the 12 hour cooldown period. All of the plates in the fuel assembly melt and the isotopes of iodine, krypton, and xenon were released to the containment. The limiting dose is the thyroid dose from the iodine isotopes.

Since the HEU and LEU cores operate at 5 MW, neutron flux levels and equilibrium concentrations of iodine, xenon, and krypton will be about the same in the two cores. From burnup calculation results shown in Fig. 1, it was concluded that the lifetimes of the HEU and

LEU core will be about the same. As a result, concentrations of the other fission products in the LEU and HEU fuel assemblies will be very similar. The exception is that the LEU assembly will contain larger concentrations of plutonium isotopes. Reference 9 contains a detailed analysis comparing the radiological consequences of a hypothetical accident in a generic 10 MW reactor using HEU and LEU fuels. This analysis concluded that the buildup of plutonium in discharge fuel assemblies with ^{235}U burnup of over 50% does not significantly increase the radiological consequences over those of HEU fuel. Because fission product concentrations in the GTRR HEU and LEU cores are expected to be comparable, the thyroid dose shown in the GTRR SAR for HEU fuel will be the limiting dose for both cores.

COOLING TIME REQUIREMENTS

The primary coolant pumps must be operated for 8 hours following operation at power levels of more than 1 MW to preclude the possibility of fuel plate melting in the event of a loss-of-coolant accident following reactor shutdown. In addition, a minimum cooldown time of twelve hours is required before fuel assemblies are transferred out of the reactor. A limit of 450°C was set in the Technical Specifications as the upper limit for a fuel plate temperature to preclude melting of the plates.

The analysis method followed the superposition technique used in the GTRR safety documentation for the HEU core, with modification of the input parameters appropriate for the LEU fuel assembly design. The most important modification was that the maximum power per fuel plate in the LEU assembly was reduced by a factor of 16/18 since an HEU assembly contains 16 fueled plates and an LEU assembly contains 18 fueled plates. A standard 3-week operating history consisting of 4.3 days at full power of 5 MW and 2.7 days shutdown was used for 14 assembly cores with HEU and LEU fuel.

The results for loss-of-coolant from the reactor vessel after eight hours of cooling gave a maximum plate temperature of 425°C in the HEU core and 400°C in the LEU core. The maximum temperature occurred 45 minutes after loss-of-coolant in the HEU core and 50 minutes after loss-of-coolant in the LEU core. Thus, the current Technical Specification requirements on cooling times are more conservative for the LEU core than for the HEU core.

FUEL HANDLING AND STORAGE

The objective of the Technical Specifications that apply to the handling and storage of fuel assemblies is to prevent inadvertent criticality outside of the reactor vessel and to prevent overheating of irradiated fuel assemblies.

Irradiated fuel assemblies are stored in aluminum racks fastened to the side walls of a light water pool. There is one rack along each of the two walls and each rack can accomodate up to 20

assemblies in a linear array. The center-to-center spacing of the assemblies is six inches and the separation between assemblies is about three inches.

A systematic nuclear criticality assessment[10] been done for infinite-by-infinite arrays of fresh LEU fuel assemblies with ^{235}U contents between 225 and 621 grams using the ORR fuel storage rack spacing specifications[11] of 0.7 inch assembly separation and 6.8 inch row separation. An assembly similar to the GTRR LEU assembly with a ^{235}U content of 225 grams gave a k_{eff} of 0.72, well below the maximum k_{eff} of 0.85 needed to ensure an adequate margin below criticality for storage of irradiated fuel assemblies. The GTRR storage configuration discussed above will have k_{eff} less than 0.72.

Currently, no more than four unirradiated HEU fuel assemblies can be together in any one room outside the reactor, shipping container, or fuel storage racks. Calculations of HEU and LEU cores indicate that a grouping of four LEU assemblies will be less reactive than the same configuration of HEU assemblies. Thus, the current specification will also hold for LEU fuel.

CONCLUSION

Conversion of the GTRR core from HEU to LEU fuel is feasible utilizing an LEU assembly containing 18 DOE standard silicide fuel plates (for university MTR-type reactors) as a replacement for the current HEU assembly with 16 fueled plates. Both HEU and LEU assemblies contain two unfueled outer plates to form an enclosed flow volume. The LEU assemblies would contain 225 g ^{235}U instead of 188 g ^{235}U in the current HEU assemblies.

Calculations shown in Ref.1 indicate that the epithermal flux at the bio-medical facility will be slightly larger in the LEU core. The lifetime of the LEU core is expected to be about the same as that of the HEU core. All safety margins with the LEU fuel are very similar to those with the current HEU fuel and are adequate to ensure the safety of the facility.

REFERENCES

1. R.A. Karam, J.E. Matos, S.C. Mo, and W.L. Woodruff, "Status Report on Conversion of the Georgia Tech Research Reactor to Low Enrichment Fuel," Proc. 1991 International Meeting on Reduced Enrichment for Research and Test Reactors, Jakarta, Indonesia, 4-7 November 1991 (to be published)

2. K. Mishima and T. Shibata, "Thermal-hydraulic Calculations for KUHFR with Reduced Enrichment Uranium Fuel," KURRI-TR-223 (1982), and K. Mishima, K. Kanda, and T. Shibata, "Thermal-hydraulic Analysis for Core Conversion to Use of Low-enriched Uranium Fuels in the KUR," KURRI-TR-258 (1984).

3. R. J. Weatherhead, "Nucleate Boiling Characteristics and the Critical Heat Flux Occurrence in Subcooled Axial-Flow Water Systems," ANL-6674, 1963.

4. R. H. Whittle and R. Forgan, "A Correlation for the Minima in the Pressure Drop Versus Flow-Rate Curves for Subcooled Water Flowing in Narrow Heated Channels," Nuclear Engineering and Design, Vol. 6, (1967) pp. 89-99. "Guidebook on Research Reactor Core Conversion from the Use of Highly Enriched Uranium to the Use of Low Enriched Uranium Fuels", IAEA-TECDOC-233 (1980) pp. 99-106.

5. A.E. Bergles and W.M. Rohsenow, "The Determination of Forced-Convection Surface-Boiling Heat Transfers," Transactions of the ASME 86 (Series C - Journal of Heat Transfer), pp. 365-371 (August 1964).

6. C.F. Obenchain, "PARET - A Program for the Analysis of Reactor Transients," IDO-17282, Idaho National Engineering Laboratory (1969).

7. W. L. Woodruff, "Additional Capabilities and Benchmarking with the SPERT Transients for Heavy Water Applications of the PARET Code," Proc. XIIth International Meeting on Reduced Enrichment for Research and Test Reactors, Berlin, 10.-14. September 1989., Konferenzen des Forschungs-zentrums Jülich(1991).

8. J. E. Grund, "Self-Limiting Excursion Tests of a Highly Enriched Plate-Type D2O-Moderated Reactor, Part I. Initial Test Series", USAEC Report IDO-16891, Phillips Petroleum Co., July 12, 1963.

9. W.L. Woodruff, D.K. Warinner, and J.E. Matos, "A Radiological Consequence Analysis with HEU and LEU Fuels," Proc. 1984 International Meeting on Reduced Enrichment for Research and Test Reactors, Argonne National Laboratory, Argonne, IL, October 15-18, 1984, ANL/RERTR/TM-6, CONF-8410173, pp. 472-490 (July 1985).

10. R.B. Pond and J.E. Matos, "Nuclear Criticality Assessment of LEU and HEU Fuel Element Storage," Proc. 1983 International Meeting on Reduced Enrichment for Research and Test Reactors, Japan Atomic Energy Research Institute, Tokai, Japan, October 24-27, 1983, JAERI-M 84-073, pp. 416-425 (May 1984).

11. J.T. Thomas, "Nuclear Criticality Assessment of Oak Ridge Research Reactor Fuel Element Storage," ORNL/CSD/TM-58, Oak Ridge National Laboratory (1978).

SAFETY ANALYSIS OF THE JMTR WITH LEU FUEL

Yoshihiro Komori, Fumio Sakurai, Etsuo Ishitsuka, Takeshi Sato,
Minoru Saito and Yoshiaki Futamura

Japan Atomic Energy Research Institute
Oarai Research Establishment
Oarai-machi, Ibaraki-ken, Japan

ABSTRACT

The license on the use of the LEU silicide fuel for the JMTR (Japan Materials Testing Reactor) was issued in March of 1992, and the core conversion will be carried out in 1993. The safety analysis for the JMTR LEU core was performed in order to examine validity of the safety design principles. Safety criteria for the abnormal conditions were also reviewed. The result suggests that emergency cooling system and safety protection system need to be upgraded for the primary coolant piping failure. Other postulated abnormal conditions were verified to be safely handled with the present safety system.

INTRODUCTION

The JMTR is a 50MW tank type reactor, moderated and cooled by light water. The primary cooling system is pressurized at about 14 kg/cm^{2}G. The reactor core consists of 22 standard fuel elements, 5 control rods with fuel followers, beryllium and aluminium reflectors with irradiation holes. The operating pattern of the JMTR with the present MEU core follows 26-day operating period including 2-day middle shutdown for refueling. Thermohydraulic data of the JMTR are shown in Table 1.

The core conversion from MEU fuel to LEU fuel will be scheduled to be made in 1993. The U_3Si_2 fuel with 4.8 g/cm^3 of uranium density was selected as the LEU fuel in order to eliminate the middle shutdown for refueling. Burnable absorbers of aluminum sheathed Cd wires are placed in each side plate to adjust the excess reactivity at the beginning of an operating cycle.

For the core conversion, the safety analysis of the JMTR was entirely reviewed and revised based on the latest knowledge such as new DNB correlation[1]. Design Basis Events (DBEs) of the reactor were reconsidered. Selected DBEs were classified into abnormal transients during operation and accidents, and responses of the reactor to these DBEs were analyzed.

Table 1 Thermohydraulic Data of the JMTR

Reactor Type	:	Tank type
Thermal Power	:	50 MW
Primary Coolant		
Coolant	:	Light Water
Pressure	:	13 kg/cm²abs (Cooling Channel Exit)
Temperature	:	49℃(Inlet), 56℃(Outlet) (Maximum)
Flow Rate	:	6000 m³/h
Power Density	:	490 KW/ℓ (Average)
Heat Flux	:	120 W/cm² (Average)

DESIGN BASIS EVENTS AND SAFETY CRITERIA FOR THE SAFETY ANALYSIS

POSTULATED DESIGN BASIS EVENTS

DBEs were postulated and analyzed in order to confirm validity of safety design principles of the JMTR. DBEs are classified into abnormal transients during operation and accidents, as previously described.

Abnormal transients during operation include DBEs which are caused by single failure or malfunction of reactor facilities and components, single operator error, and other disturbances which are anticipated during reactor life time. Accidents include DBEs which result in severer conditions than abnormal transients during operation. The accidents are determined to be less probable than abnormal transients during operation, but have a possibility of radioactive release to the environment.

Various kinds of single failures, malfunctions and disturbances of process variables are postulated and preliminarily analyzed to establish the severest scinario for each DBE. Selected DBEs are listed in Table 2.

SAFETY CRITERIA

For abnormal transient during operation, the core should not exceed the allowable design limits of fuel, and the reactor facility should be able to restore to the normal operation condition. Safety criteria to confirm these are as follows.

(1) Minimum DNBR should be beyond 1.5
(2) Fuel cladding should not fail mechanically
(3) Pressure of the primary cooling system should be less than the maximum operating pressure

For the criterion (1), DNB correlations scheme was selected for the DNB correlation and the allowable minimum DNBR was determined to be 1.5 based on DNB experiment carried out by author et al.[1] To satisfy the criterion(2), maximum temperature of fuel meat should be below blistering temperature, and the thermal stress in the fuel cladding should be below yield stress. The blistering temperature is conservatively determined to be 400 ℃ based on

measured data for silicide fuels.[2] Concerning the criterion(3), no pressure increases are possible due to failures of pressurizing related system in the JMTR. There would be no possibility of significant pressure increase for primary cooling system without boiling of primary coolant. Therefore, the criteria(3) is interpreted to the condition that temperature of primary coolant should be below saturating point.

For accidents, the reactor core should not melt or not be damaged seriously and any secondary damages to cause other abnormal conditions should not occur. Radioactive barrier should be also properly designed. Safety criteria to confirm these are as follows.

(1) Fuel should not cause significant mechanical energy with its failure
(2) Core should not be seriously damaged, and maintain enough coolability
(3) Pressure of the primary cooling system should be less than the maximum operating pressure.
(4) Risk of radiation exposure to the public should not be significant

Criteria (1) and (2) could be satisfied when maximum temperature of fuel meat is below melting point of the fuel cladding. This was experimentally confirmed to be valid in the NSRR. Solidus point of aluminum alloy for the fuel cladding(582℃) is chosen as the melting point. To satisfy the criterion (4), effective radiation dose should be less than 5 mSv.

Table 2 Design Basis Events for the JMTR Safety Analysis

Abnormal Transient during Operation
(1) Reactivity Anomalies
a. Withdrawal of control rods at reactor start-up
b. Withdrawal of a control rod during full power operation
c. Cold water insertion
d. Reactivity insertion by in-core experiments
(2) Decrease in Heat Removal by Reactor Cooling System
a. Primary cooling flow coastdown
b. Secondary cooling flow coastdown
c. Loss of commercial power
d. Depressure of primary coolant
Accident
(1) Reactivity Insertion
a. Reactivity insertion by failure of irradiation facility
(2) Decrease in Heat Removal by Reactor Cooling System
a. Main circulation pump shaft seizure
b. Secondary pump shaft seizure
c. Primary coolant piping failure
d. Flow blockage to fuel coolant channel
(3) Radioactive Release to the Environment
a. Fuel handling accident

ANALYSIS OF PRIMARY COOLANT PIPING FAILURE ACCIDENT

Analytical results for DBEs show that safety criteria are satisfied with present JMTR safety system for all postulated DBEs except for primary coolant piping failure accident. This chapter focuses on analytical result of the piping failure accident and required upgrading of the safety system.

JMTR COOLING SYSTEM

The generated heat in the reactor core is rejected by the primary cooling system, and then transfered into atmosphere through the secondary cooling system. The emergency cooling system is provided to remove core decay heat during emergencies and reactor shutdown. A schematic diagram of the primary and emergency cooling system is shown in Figure 1.

In the primary cooling system, four main circulation pumps energized with commercial power and three heat exchangers are installed in parallel. Three of main circulating pumps are running to maintain the flow rate of 6000 m^3/h during the reactor normal operation.

Emergency cooling system consists of two emergency pumps, syphon break valves, connecting valves and the recirculation system. All these components are energized with the emergency power system whose power is supplied by diesel-engine generators. To assure the required flow after main circulating pumps coastdown without reliance on emergency pump start-up, one emergency pump operates continuously during reactor operation. Connecting valves, syphon break valves and the recirculation system are installed to prevent loss of coolant in primary piping failure accident.

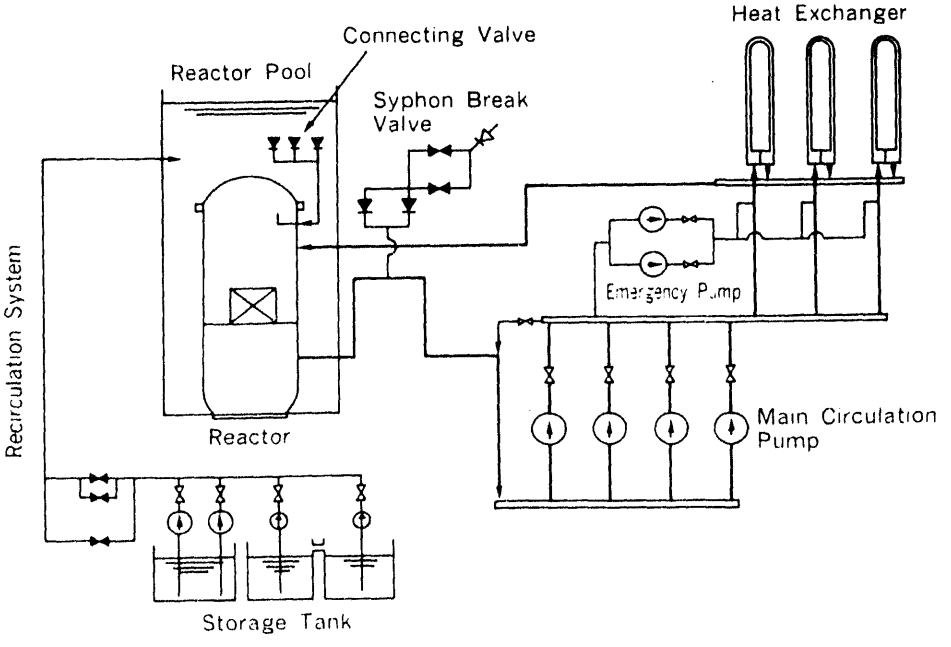

Figure 1 JMTR Cooling System

ANALYTICAL CONDITIONS

The probability of the failure of primary coolant boundary is extremely low since the boundary is constructed of stainless steel, and in-service inspection has been properly conducted. The failure of primary coolant boundary, however, is postulated in order to prove the validity of the reactor safety system design. Principal analytical conditions are as follows.

(1) The location of boundary failure should be apparently the lowest point of the primary cooling system, and this is the header at the inlet of heat exchangers. Preliminary analysis was conducted parametizing the location of the boundary failure, and the header at the inlet of heat exchangers was verified to cause the severest condition.

(2) Referring design philosophy of moderate-energy fluid system in NUREG-800[3], failure area of the header is assumed as Dt/4. (D ; diameter, t ; wall thickness) This is correspondent to the failure area of 29.7 cm^2 for the header (approx. 900mm in diameter) at the inlet of heat exchangers.

(3) When the reactor inlet pressure decreases below 12 kg/cm^2G, reactor shutdown is initiated with a scram signal by the reactor inlet low-pressure. This scram system is composed of two independent channels.

(4) Commercial power is conservatively postulated to be unavailable.

(5) Single failures are postulated for safety actions required for mitigating the consequence of the accident.

ANALYTICAL RESULT WITH PRESENT SAFETY SYSTEM

Analytical result with present safety system is shown in Figure 2. Thermohydraulic transient analysis code, THYDE-P developed by JAERI[4], was used with full plant simulation in the analyses. The primary cooling system pressure rapidly reduces due to the failure, and the pressure loss causes significant reduction in critical heat flux. Minimum DNBR, therefore, quickly reduces to 1.49, so there could be a possibility of departure from nucleate boiling in the hot channel.

The scram signal due to the reactor inlet pressure-low ($12kg/cm^2G$) is activated at 0.1 second after the pipe break, and the scram is initiated with the delay time of 0.4 second. The scram is completed at 0.9 second after the break. The minimum DNBR is recovering beyond 1.5 as the reactor power is decreasing by the scram. Main circulation pumps shut off by the assumption of loss of commercial power, while the emergency pump continues to operate. After the shut off of main circulation pumps, primary coolant flow gradually coasts down in about three seconds and finally stays at about 420 m^3/h by an emergency pump alone. The reduction of the primary coolant flow causes the minimum DNBR to reduce to 1.0, and results in the fuel temperature rise.

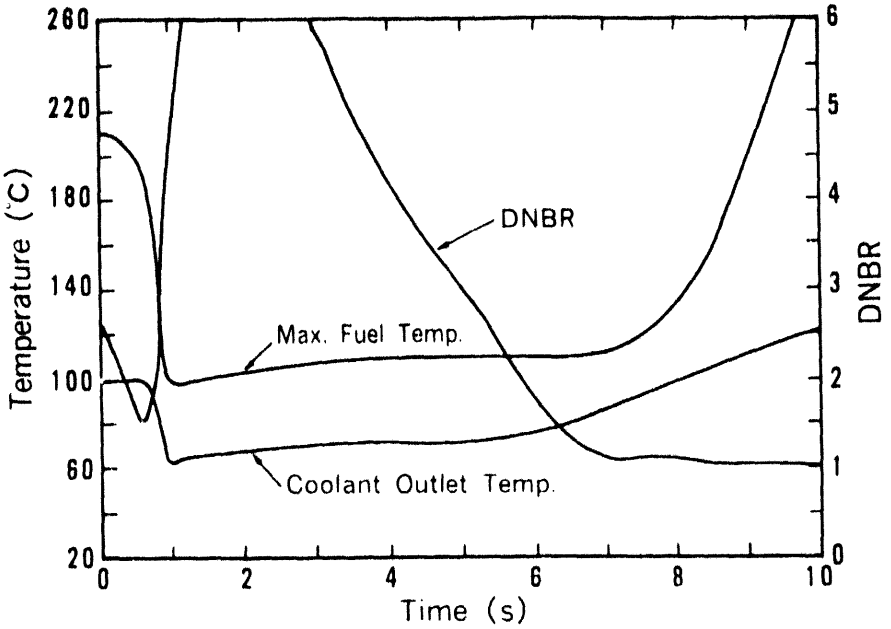

Figure 2 Analytical Result of the Primary Coolant Piping Failure Accident with Present Safety System

REQUIRED UPGRADINGS OF SAFETY SYSTEMS

Thermohydraulic analysis for the primary coolant piping failure indicates that the safety system is required to be upgraded to prevent departure from nucleate boiling, and following two problems should be solved.

a) Sudden pressure drop after the failure
b) Lack of primary coolant flow after main circulating pumps shut off

Since it seems impossible to prevent the system pressure drop due to the break, a realistic solution is to scram the reactor earlier in order to cope with decreasing critical heat flux. The scram signal due to the loss of commercial power was determined to be newly added to the safety protection system, and its delay time for initiating the reactor scram was designed to be within 200 miliseconds, which is approximately half of the present scram.

Problem b) could be solved simply by increasing the primary coolant flow after main circulating pumps shutoff. Required flow rate of primary cooling system is illustrated in Figure 3. The solid line(A) indicates the present primary coolant flow after the failure, and the dashed line is correspondent to the flow rate to maintain minimum DNBR at 1.5. It is apparently seen that present flow rate drops below the required value from about 7seconds after the failure, and primary coolant flow should be maintained at no less than 1300 m^3/h to eliminate potential of the DNB.

Various options were discussed including upgradings of emergency pumps to increase flow rate for decay heat removal. This option, however, would

result in very large modification of the safety system. One of the main circulating pumps was finally determined to continue to operate as the emergency cooling system. This requires very little modification with primary cooling system. Replacement of diesel-engine generators is incorporated with this modification in order to supply the power to the main circulating pump for decay heat removal. The replacement of diesel-engine generators are also supported by the philosophy of preventive maintenance for aging facilities.

Analytical result with the upgraded safety system is illustrated in Figure 4.[5] The minimum DNBR right after the failure is improved up to 1.6. Subsequent decrease of minimum DNBR due to primary coolant flow coastdown is also extensively mitigated, and the fuel temperature rise could be negligible.

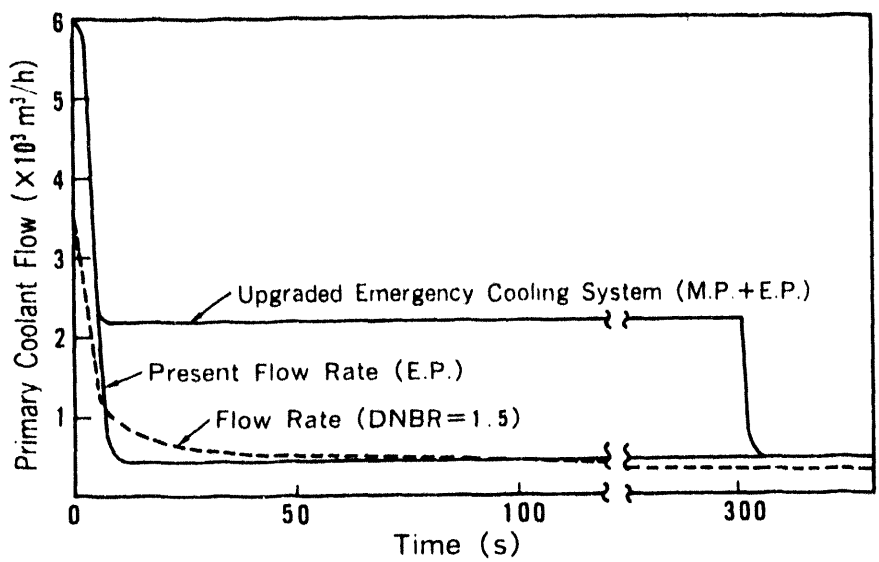

Figure 3 Required Primary Coolant Flow Rate

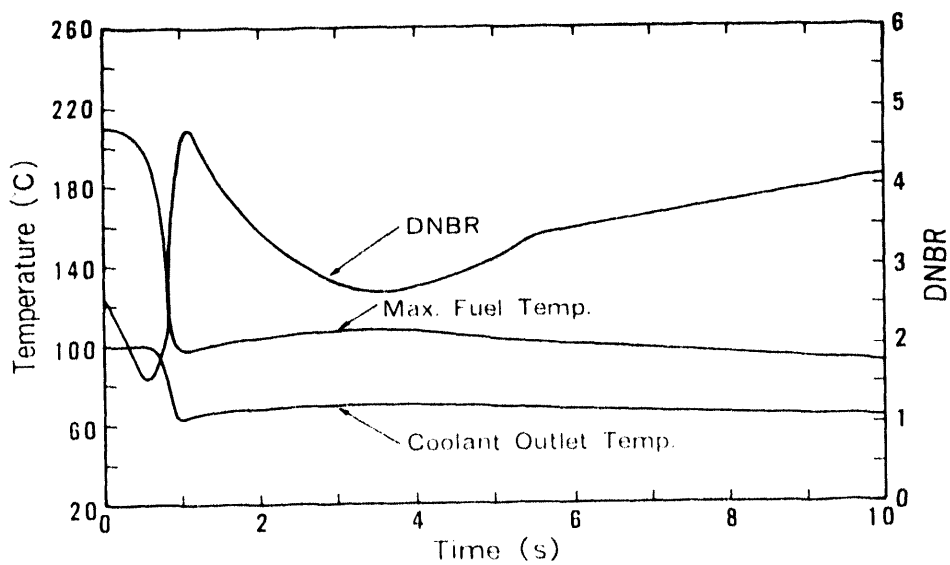

Figyre 4 Analytical Result with Upgraded safety System

CONCLUDING REMARKS

Safety analysis of the JMTR LEU core on the latest knowledges shows that safety criteria are satisfied with the present JMTR safety system for all postulated DBEs except for primary coolant piping failure accident. One of the main circulating pump is going to be modified to continue to operate after the primary coolant piping failure accident in order to maintain required flow rate. The safety protection system and the emergency power system is determined to be upgraded.

REFERENCES

[1] Y.Komori, et al. : Experimental Study on DNB Heat Flux Correlations for the JMTR Safety Analysis, 13th RERTR International Meeting (1990)

[2] U.S.Nuclear Regulatory Commission : Safety Evaluation Report Related to the Evaluation of Low-Enriched Uranium Silicide-Aluminum Dispersion Fuel for Use in Non-Power Reactors, NUREG-1313 (1988)

[3] U.S.Nuclear Regulatory Commission : Standard Review Plan for the Review of Safety Analysis Reports for Nuclear Power Plants, NUREG-800 (1981)

[4] Y.Asahi, et al. : THYDE-W; RCS(Reactor Coolant System) Analysis Code, JAERI-M-90-172 (1990)

[5] Etsuo Ishituka, et al. : Safety Analysis of JMTR LEU Fuel Cores (2) -Thermohydraulic Analysis- (in Japanese), JAERI-M-92-096 (1992)

DOSE ANALYSIS IN SAFETY AND SITE EVALUATION FOR THE JMTR CORE CONVERSION TO LEU FUEL

Noboru Tsuchida, Tadao Shiraishi, Yutaka Takahashi,
Seiji Inada, Kyoshiro Kitano, Minoru Saito
and Yoshiaki Futamura

Japan Atomic Energy Research Institute
Oarai Research Establishment
Oarai-machi, Ibaraki-ken, Japan

ABSTRACT

Dose analyses in the safety evaluation and the site evaluation were performed for the Japan Materials Testing Reactor(JMTR) core conversion from Medium Enrichment Uranium(MEU) fuel to Low Enrichment Uranium(LEU) fuel. In the safety evaluation, the effective dose equivalents for the public surrounding the site were estimated in the design basis accidents with release of radioactive fission products to the environment. In the site evaluation, maximum exposure doses to the public were estimated in major accident and hypothetical accident. It was confirmed that risk of radiation exposure of the public is negligible and the siting is appropriate for the LEU core as for the present MEU core.

INTRODUCTION

The safety and site evaluation was executed for the JMTR core conversion from MEU fuel (UAlx-Al) to LEU fuel (U_3Si_2-Al).

The exposure doses to the public surrounding the site were evaluated for the postulated accidents. Flow blockage to a coolant channel and fuel handling accident were selected as the dose evaluating event among the design basis accidents of the JMTR, because these accidents were possible to release radioactive to the environment.

In the flow blockage to a coolant channel, the influence of the radiation to the public is evaluated on the assumption that two fuel plates formed a coolant channel are damaged due to cooling shortage after operating for 125 days at 50 MW. While in the fuel handling accident, one fuel plate is damaged due to drop a fuel element in handling to take out from the reactor core after a day since the reactor shutdown.

In the site evaluation, the flow blockage to a coolant channel is selected for the major accident and the hypothetical accident which are defined as the siting basis events[1], because it has the possibility of spreading radioactive release. The major accident is the upper limit of accident which is considered to occur from the engineering standpoint. The hypothetical accident is the postulated accident with release of radioactive materials beyond the major accident. It is assumed that 5% of fission products inventory in the

reactor would be released from the fuel for the major accident, and 100% would be released for the hypothetical accident.

METHOD OF DOSE ASSESSMENT

For the evaluation of the off-site radiation exposure in the accidents, the following four exposure pathways are considered:

1. Internal exposure by inhalation of the radioactive that is released to the atmosphere.
2. External gamma-ray exposure from the radioactive cloud that is released to the atmosphere.
3. Direct external gamma-ray exposure from fission products that are released into the reactor building.
4. External skyshine gamma-ray exposure from fission products that are released into the reactor building.

Fig.1 shows the flowchart of dose analyses in the accidents.

In the design basis accidents, the radiation exposures are calculated in effective dose equivalents, and total effective dose equivalent is obtained by summing them.

In the siting basis events, the maximum exposure doses to the thyroid and the whole body are calculated. For the hypothetical accident, a collective dose is also calculated.

Noble gases and iodine of fission products, respectively, mainly contribute to the doses. For this analysis, the release fraction of iodine from damaged silicide fuel was adopted to be 60%. The validity of the value was confirmed by a experiment[2] in the Department of JMTR Project.

FLOW BLOCKAGE TO COOLANT CHANNEL

In the flow blockage to coolant channel, the amount of fission products released to the atmosphere is evaluated by using the release paths model, as shown in Fig.2. The release paths and parameters of fission products in the accident are shown in Fig.3.

In the accident, fission products released into the coolant are transferred to the degas tank and the reactor building through the primary cooling system. For 5 min after the accident initiation, the fission products in the degas tank are discharged from the stack to the atmosphere via the irradiation experiment facilities ventilation system, and the fission products in the reactor building are discharged via the normal ventilation system.

Within 5 min from the accident initiation, fission products in the primary coolant are detected by the fuel failure detection system. When the fission products are detected, the reactor is shut down, at the same time, isolation valves (a), (b), (c) and (d) as shown in Fig.2 are closed and the normal and irradiation experiment facilities ventilation systems are stopped to prevent release of fission products. The emergency ventilation system is always operating under normal and accident conditions using emergency electric source.

It is assumed in the safety analysis that the leakage of the fission products from the primary cooling system to the reactor building continues for long period after 5 min from the accident initiation. Fission products leaked to the reactor building are discharged from the stack to the atmosphere via the emergency ventilation system. In this analysis, the released fission products are conservatively calculated over an infinite

period after occurrence of the accident.

The release mode of fission products to the atmosphere is shown as Fig.4.

FUEL HANDLING ACCIDENT

In the fuel handling accident, the amount of fission products released to the atmosphere is evaluated by using the release path model, as shown in Fig.5.

The fission products are released from the damaged fuel plate into the reactor pool water. The fission products in the water are transferred into the air in the reactor building, and are discharged from the stack to the atmosphere via the normal ventilation system instantaneously.

For this accident, doses by the direct gamma-ray and the skyshine gamma-ray from fission products in the reactor building are negligible, because it is assumed that the fission products in the reactor building is instantaneously released from the stack to the atmosphere.

RESULTS OF RADIATION EXPOSURE

The effective dose equivalent is 1.5×10^{-5} Sv in the flow blockage to a coolant channel and is 6.5×10^{-7} Sv in the fuel handling accident. The results are lower than the dose limit of 5 mSv, which was set up by the Japanese Nuclear Safety Commission for a design basis accident[3].

In the major accident, dose to the thyroid of child is 7.9×10^{-4} Sv (the dose limit of 1.5 Sv) and dose to the whole body is 1.3×10^{-4} Sv (the dose limit of 0.25 Sv). In the hypothetical accident, dose to the thyroid of adult is 9.3×10^{-3} Sv (the dose limit of 3 Sv) and dose to the whole body is 2.5×10^{-3} Sv (the dose limit of 0.25 Sv), and the collective dose is 2,600 man-Sv (the dose limit of 20,000 man-Sv). These dose limits were set up by the Japanese Nuclear Safety Commission for siting basis events[1].

CONCLUSIONS

For the evaluation of off-site radiation exposure in the design basis accidents and the siting basis events of the JMTR with LEU fuel, analytical models of evaluating events, release paths of fission products to the atmosphere, and radiation exposure pathways were considered. In the design basis accidents, the effective dose equivalents were sufficiently low values. In the siting basis events, the maximum doses to the public were very low. It was confirmed that the safety design and siting are appropriate for the LEU core as for the present MEU core.

REFERENCES

1. Atomic Energy Commission, Examination Guide for Reactor Siting and Guidelines for Interpretation in their Application, May 1964, revised by Nuclear Safety Commission, March 1989.
2. to be published.
3. Nuclear Safety Commission, Examination Guide for Safety Evaluation of Light Water Nuclear Power Reactor Facilities, August 1990.

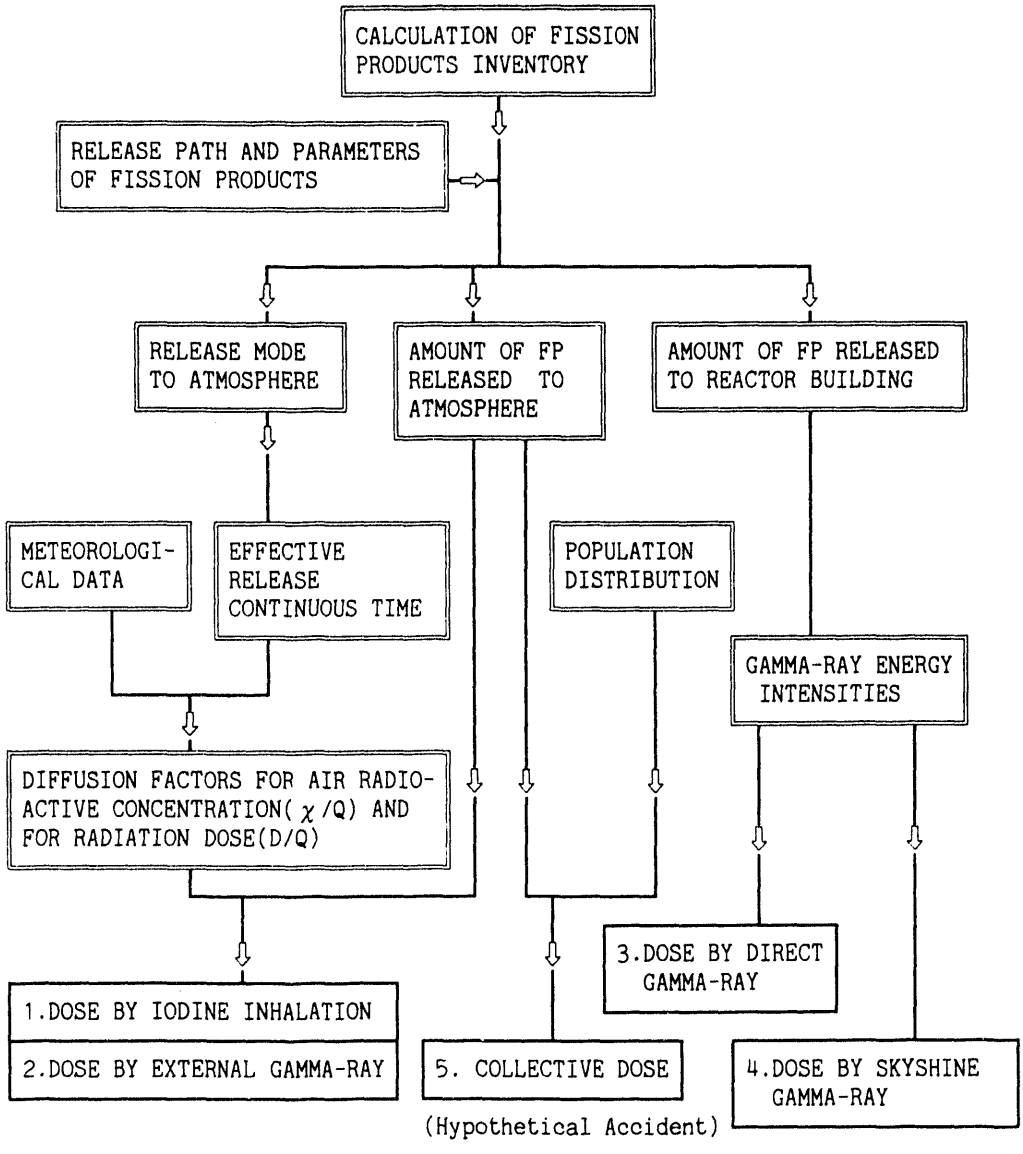

Fig.1 Flowchart of dose analyses in the accident

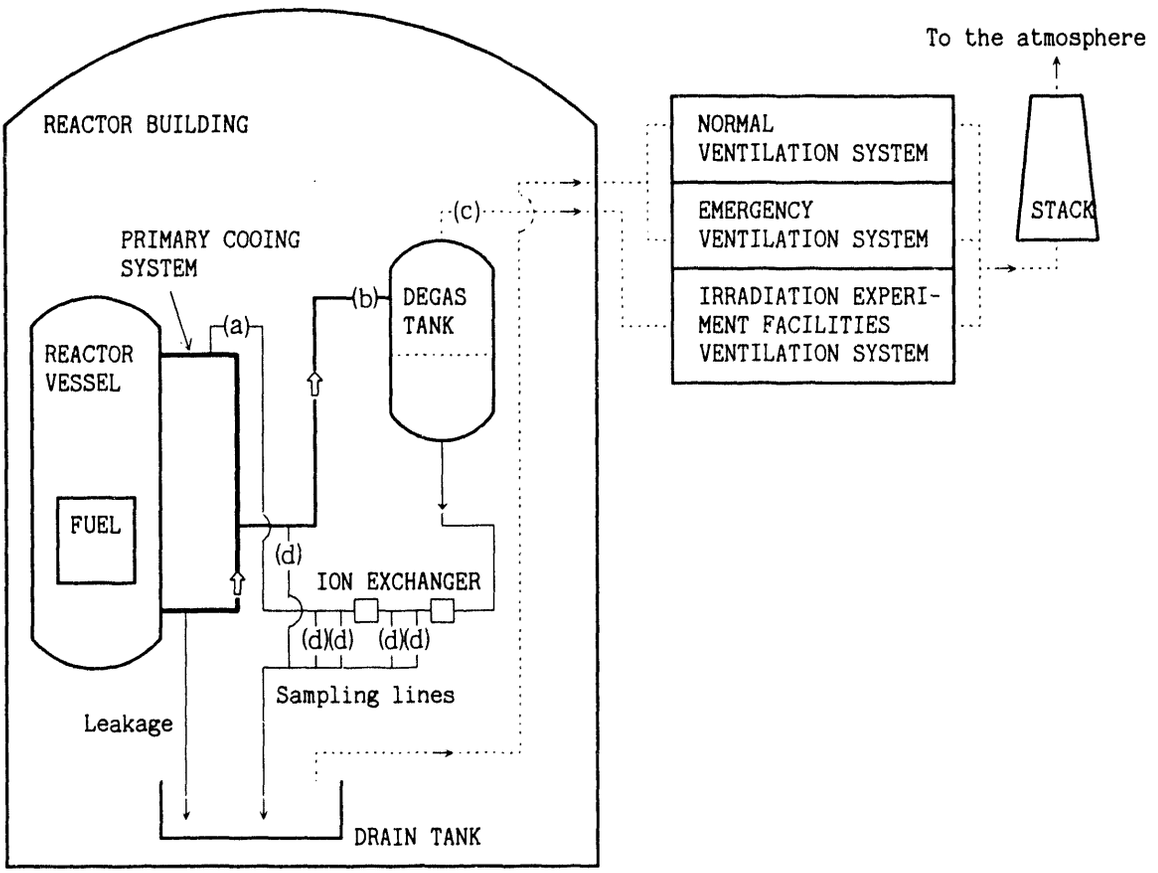

RELEASE PATHS OF FISSION PRODUCTS

RELEASE CONDITIONS OF FISSION PRODUCTS

1) Within 5 min from fuel damage, fission products in the primary coolant are detected by the fuel failure detection system.
2) When fission products are detected in the primary coolant, the reactor is shut down, valves (a), (b), (c) and (d) are closed and the normal and irradiation experiment facilities ventilation systems are stopped automatically.
3) For the safety analyses, it is assumed that release of fission products continues by leakage of the primary coolant after 5 min from the fuel damage.

Fig.2 Release paths and conditions of fission products in the flow blockage to a coolant channel

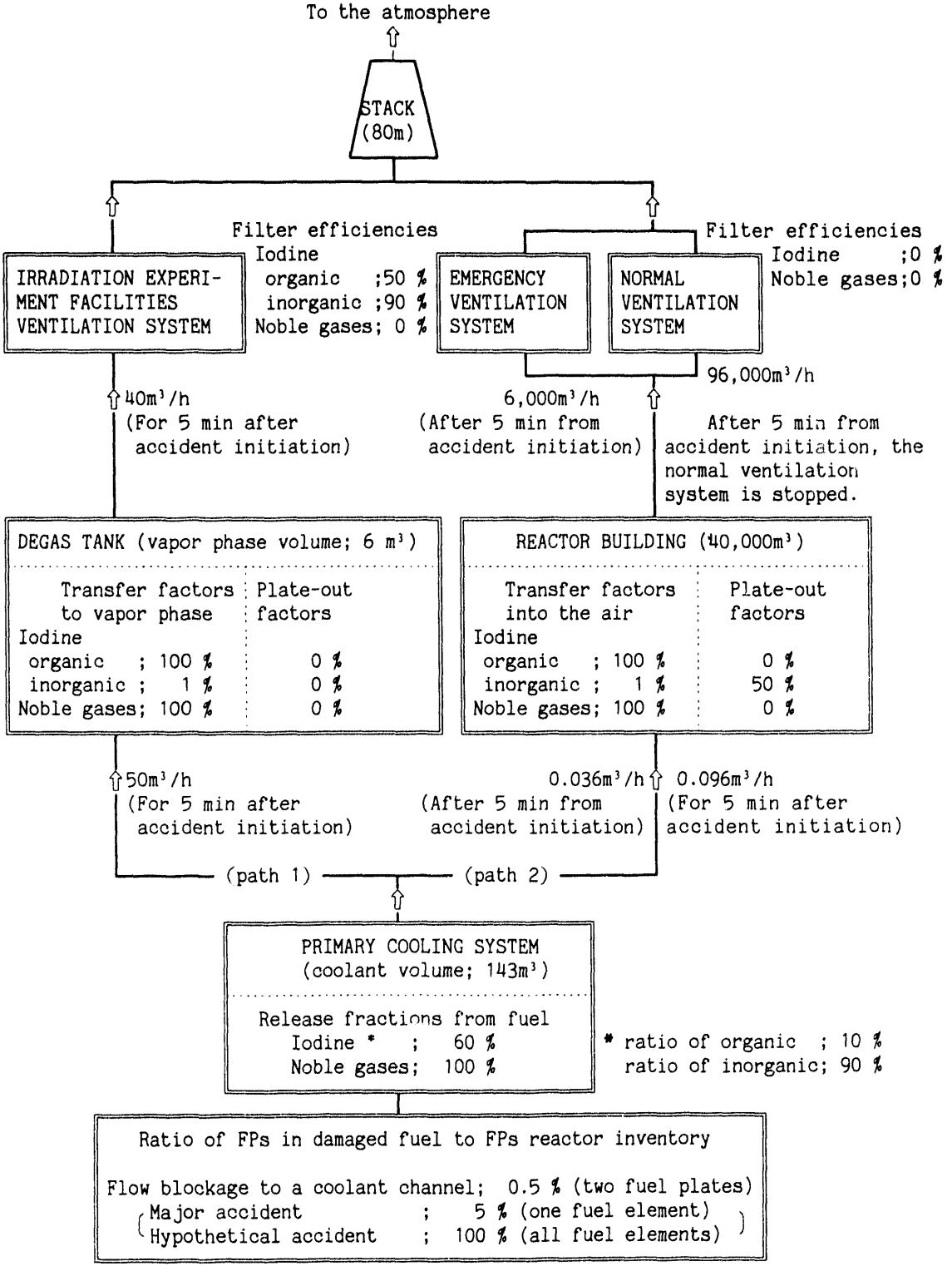

Fig. 3 Release paths and parameters of fission products in the flow blockage to a coolant channel

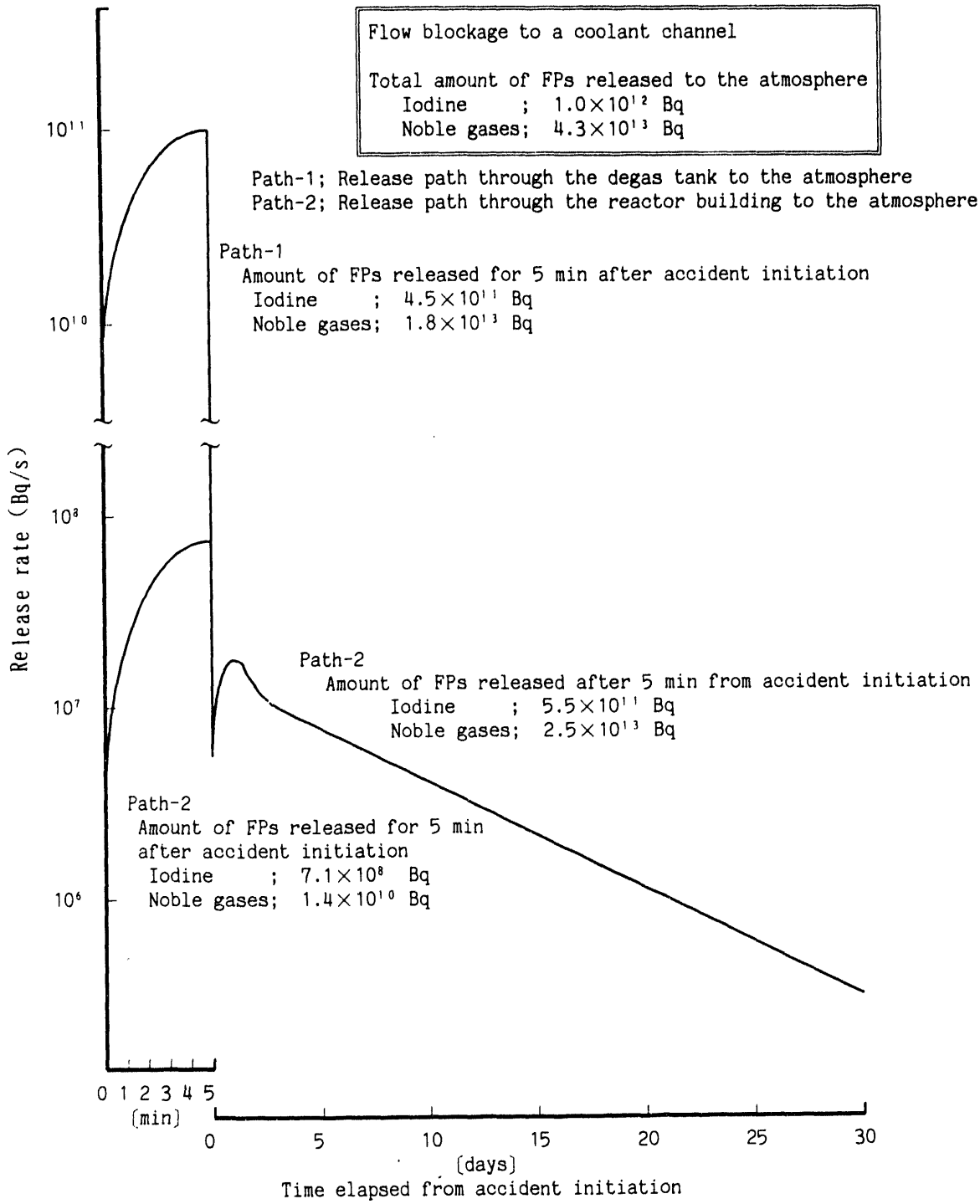

Fig. 4 Change in release rate of FPs to the atmosphere with the time elapsed from accident initiation in the flow blockage to a coolant channel (Release mode)

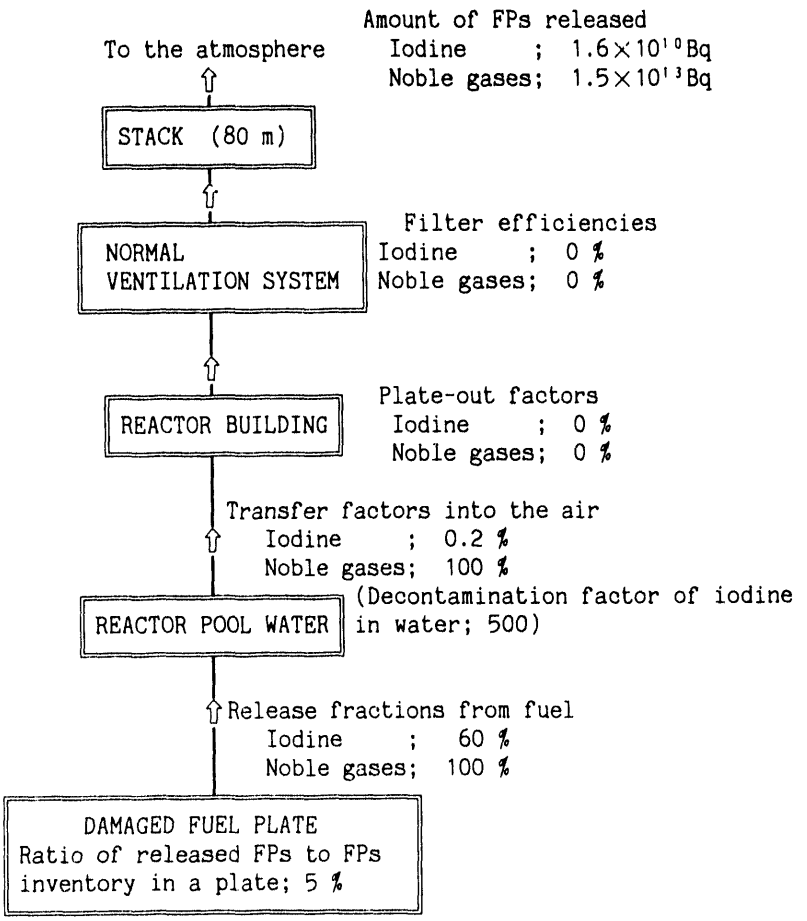

After 1 day from reactor shutdown, a fuel element is dropped in the reactor pool, and one side of a fuel plate is damaged.

Fig. 5 Release path and parameters of fission products in the fuel handling accident

EARLY DETECTION OF COOLANT BOILING IN RESEARCH REACTORS WITH MTR-TYPE FUEL

R. Kozma, E. Türkcan, J.P. Verhoef

Netherlands Energy Research Foundation, Business Unit Nuclear Energy
P.O. Box 1, NL-1775 ZG Petten
The Netherlands

ABSTRACT

In this paper, a reactor core monitoring system having the function of early detection of boiling in the coolant channels of research reactors with MTR-type fuel is introduced. The system is based on the on-line analysis of signals of various ex-core and in-core neutron detectors. Early detection of coolant boiling cannot be accomplished by the evaluation of the DC components of these detectors in a number of practically important cases of boiling anomaly. It is shown that noise component of the available neutron detector signals can be used for the detection of boiling in these cases. Experiments have been carried out at a boiling setup in the research reactor HOR of the Interfaculty Reactor Institute, Technical University Delft, The Netherlands.

INTRODUCTION

Thermohydraulic conditions in the core of research reactors can change significantly due to HEU → LEU conversion. Also, safety margins towards onset of boiling vary. The presence of boiling is undesirable in research reactors, as boiling can easily lead to burnout and consequent melting of the fuel [1]. Coolant boiling has to be prevented by all means, and, in case of occurrence, it has to be detected as early as possible in order to avoid damage of the reactor core. One of the potentially most dangerous events which may lead to coolant boiling is the sudden (partial) blockage of coolant channels. A number of voidage-detection methods is based on monitoring sudden decrease of the neutron flux caused by the negative void effect. Studies performed during the implementation of such a method in the research reactor of the Interfaculty Reactor Institute (IRI), TU Delft, The Netherlands, show that an initial reactivity step of 50 pcm, or 5 % of neutron flux decrease was needed in most cases in order to generate trip conditions [2].

At the first phase of the development of coolant boiling anomaly, the changes in the neutron flux are not strong enough to initiate reactor trip. At certain disadvantageous positions in the core, moreover, coolant boiling may develop and remain undetected even at a very advanced stage. By monitoring the small fluctuations (noise) of the neutron flux around its average value can furnish us with the proper information to detect the anomaly at an early stage. Boiling detection based on neutron noise analysis is introduced in this paper.

Research aiming at studying boiling neutron noise has been conducted for years in IRI in the NIOBE project (Noise Investigations On Boiling Effects) [3]. In this research, physical phenomena related to boiling in research reactors with plate-type fuels have been analysed thoroughly. Presently, a project has started at ECN, Petten, which aims at the implementation of the results obtained at NIOBE for the High Flux Reactor (HFR) in Petten.

HFR uses MTR-type fuel assemblies [4] which are similar to those used at HOR. The fuel assemblies have horizontal cross section 8.1 cm × 7.7 cm and active length of 60 cm both at HFR and HOR. An HFR-assembly contains 23 vertically arranged curved fuel plates, while an assembly in the HOR has 19 flat fuel plates. The uranium is about 93 % enriched in ^{235}U in both reactors at the present. A typical core lattice of HFR is a 9 × 9 array with 33 fuel assemblies, while the HOR has a 7 × 6 array with 25 fuel assemblies. The power of HFR is 45 MW, which is much higher than the power of HOR (2 MW). This higher power at HFR needs more intensive cooling than at HOR. Accordingly, the coolant speed in the fuel assembly is 7 m/s and 0.5 m/s in HFR and HOR, respectively. HOR has narrow coolant channels of width 0.3 cm. The channels of HFR are even narrower (0.255 cm). Boiling in narrow coolant channels has a few special features analysed in detail during the NIOBE experiments. The peculiar character of boiling in narrow channels has important implications on boiling detection methods in reactors with plate-type fuels.

ECN has experience with on-line monitoring of operational parameters of nuclear reactors, including Borssele PWR, and HFR [5]. In the framework of the present investigations the on-line monitoring system of ECN has been connected to the boiling setup in HOR during the experiments from May to July, 1992. The results indicate that it is possible to detect coolant channel boiling/void in NIOBE.

EXPERIMENTS

Experiments have been carried out at the NOIBE boiling setup of IRI. Here, the main properties of this setup are given [6]. NIOBE consists of a simulated MTR-type fuel assembly within a closed coolant loop, a circulation pump, two flowmeters, and a number of thermocouples and in-core detectors. The simulated assembly has an almost square cross-section (dimension: 7.7 cm × 8.1 cm) and an active length of 62.5 cm; it is located next to the core of HOR. The pump and the control valves are found at positions above the pool water level.

The simulated fuel assembly has three electrically heated fuel plates. The heating power can be varied continuously or step-wise by making use of electrical power units at each plate separately. The heating power of a plate can reach a maximum of 7 kW. By varying the heating power of the plates, different levels of coolant boiling can be induced in NIOBE. There are two coolant channels in the simulated assembly between plates no. 1 and 2, and plates no. 2 and 3, respectively. The coolant is pumped through the channels with the circulation pump. The flow rate in each channel can be adjusted by remote controlled valves. Both coolant channels have a rectangular cross-section of dimensions 6.15 cm × 0.5 cm. The total length of a channel is 62.5 cm.

In the experiments, signals of both incore and excore neutron detectors were used. Excore detectors are ionisation chambers located around the reactor core. The incore neutron detectors are self-powered neutron detectors (SPNDs) with Cd-Mg emitters. SPNDs are arranged in strings.

The SPND strings are movable in axial direction. Each string consists of two SPNDs at a fixed distance. In the present experiments, strings no. 1 and no. 4 were used. The axial positions of the lower detectors, SPND 1/L and SPND 4/L, were at 30 cm measured from the bottom of the fuel plates. The distance between the detectors in both of these strings was 10 cm, thus the higher detectors (SPND 1/H and SPND 4/H) were located at elevation of 40 cm. The temperature of the fuel plates and the coolant is measured by chromel-alumel thermocouples. In the experiments, signals of a thermocouple at the outlet of channel 1 (TC_{out}) and of a thermocouple in the third plate ($TC_{3,3}$) have been monitored. In addition, flow signals in both coolant channels (FL/1 and FL/2) and the voltage of the heating applied at plate no. 2 have been available.

Different thermohydraulic states of the coolant can be generated in the coolant channels of the simulated assembly by varying the electrical heating power and the flow rate. In these experiments, void effects in the coolant channels of NIOBE have been simulated by two means: (a) increasing the electrical heating power locally; (b) injecting Nitrogen gas into a coolant channel.

Data Transmission and Signal Processing

Detector signals have been conditioned in order to have values in the range of - 5 V to 5 V. The conditioned signals entered the signal patch panel (SPP) located in the noise measurement room outside the reactor hall of the HOR. No additional signal conditioning (e.g. filtering) took place before the signals entered SPP. Both AC and DC components of the signals have been processed using the micro-processor based signal conditioning unit (SCU) and the data transmission unit. This system can handle up to 16 channels in DC and AC modes and it has been used in earlier experiments on fuel dynamics in HFR [7, 8]. Data have been transmitted to the ECN site located at a distance of 120 km from HOR via synchronous modems by using a common telephone line.

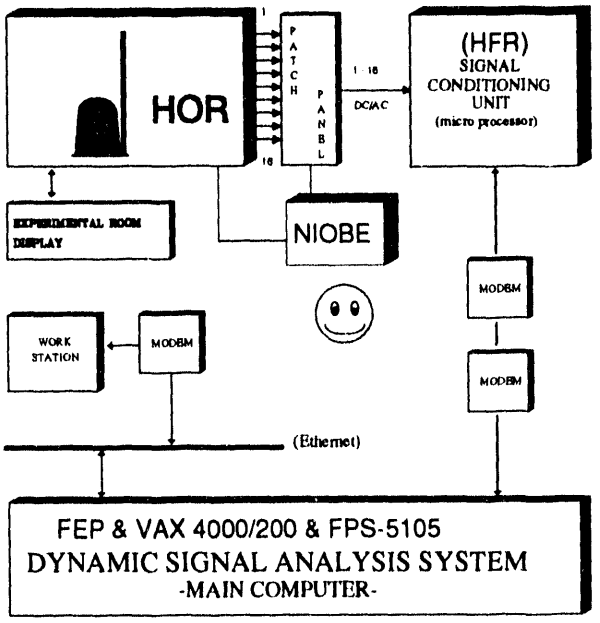

Figure 1: *Schema of Measurement System of the Boiling Experiment*

The signals pass front end processing (FEP) and enter a VAX 4200 computer equipped with an array processor (FPS). The array processor performs FFT analysis and calculates auto- and cross-spectra for prescribed channels. In a typical experiment, FFT analysis is done in every 4 s for a measurement with sampling rate of 32 samples per second. In real-time calculations, the spectra are calculated by exponential averaging. At the same time, the AC/DC signals are stored on disk for further off-line analysis. The AC/DC signals, together with the results of the on-line time- and frequency-domain analysis have been transferred back to the IRI by using another telephone line and two asynchronous modems. The schematic view of the data acquisition system used during the experiments is given in Fig.1. The results of both on-line and off-line analysis of the two types of boiling/void signals will be given in the paper.

DISCUSSION OF EXPERIMENTAL RESULTS

Boiling of the coolant in the channels of NIOBE has been initiated by increasing the electrical heating power at the fuel plates of the simulated assembly in experiment IRI10A. In Figure 2, the heating voltage (DC signal) is displayed vs. time (the duration of each block is 4 s). The experiment starts with stationary thermohydraulic conditions corresponding to coolant state without boiling in the channels; see Figure 2 from 1 to 500 blocks. This is followed by some transients till block no. 1200, after which stationary thermohydraulic state with intensive coolant boiling is maintained till the end of experiment IRI10A. The maximum void fraction in the coolant channels was about 50 % according to numerical calculations. Figures 3 and 4 display DC components of in-core SPND and ex-core neutron detector signals, respectively. The SPND DC signal shows gradually decreasing absolute value in Figure 3 (note: the SPND signals are measured in negative volts). This decrease is in the order of 1.7 %. On the other hand, ex-core detectors do not detect significant DC variations; see Fig. 4.

In experiment IRI12A, no electrical heating has been applied at the fuel plates of NIOBE. Instead, we have injected nitrogen gas into a coolant channel in order to produce void effects. The nitrogen gas passes through the channel in the form of bubbly/slug flow. In Fig. 5, the control signal of the nitrogen flow is shown. After some preliminary attempts, a relatively high void fraction has been established in the channel at block no. approximately 4200. Based on the measured value of the nitrogen flow rate and the measured terminal velocity of bubbles in between the plates, the maximum void fraction value of about 20 % has been found in experiment IRI12A. During the second half of this experiment, the nitrogen flow has been continuously reduced to zero. In the experiment with nitrogen injection, changes of the DC signals due to boiling were insignificant for in-core SPNDs (Fig. 6) and for ex-core neutron detectors as well (Fig. 7).

The analysis of the AC signals of the neutron detectors (i.e. neutron noise analysis) have been carried out by the code FAST, which is a real-time multi-channel time- and frequency-domain code [5]. The real-time power spectra are computed by using exponential averaging and the dynamic behaviour of the signal is identified continuously. In experiment IRI10A, the analysis has been started from the first block with averaging of 300 blocks of data (duration of 1200 s). In every following analysis, this data window has been shifted by 25 blocks (100 s), yielding 77 sets of auto-power spectra (APSDs) for each detector signal and their cross-power spectra (CPSD). In the analysis, signals of 3 SPNDs, 3 ex-core detectors, and 2 thermocouples have been evaluated.

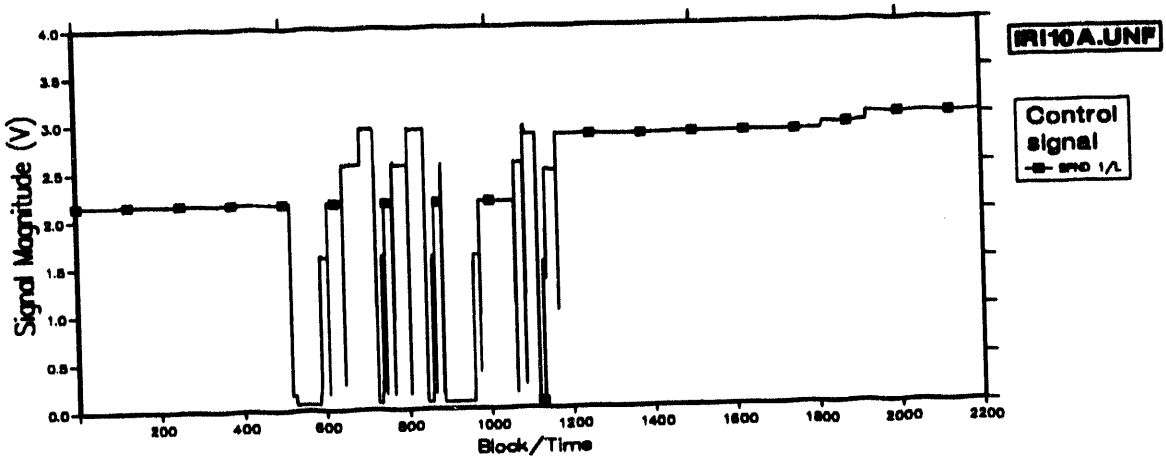

Figure 2: *Control Signal (heating power level) in Experiment IRI10A*

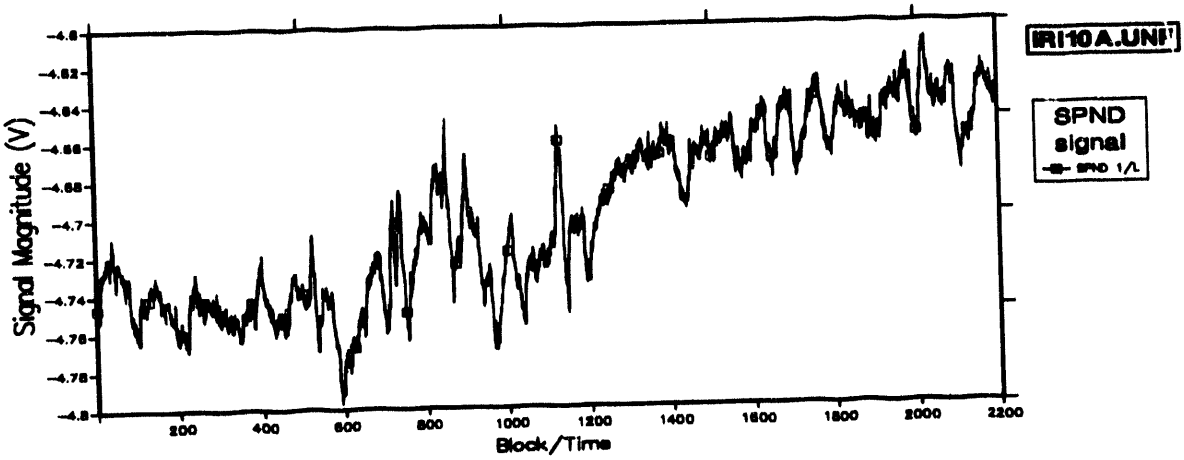

Figure 3: *DC Component of the Signal of SPND 1/L in Experiment IRI10A*

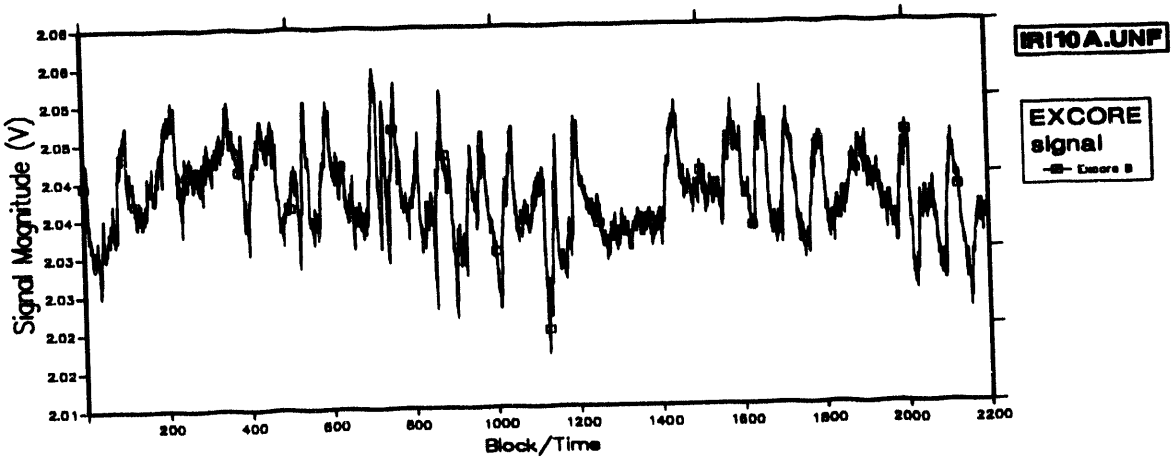

Figure 4: *DC Component of the Signal of Detector EXCORE B in Experiment IRI10A*

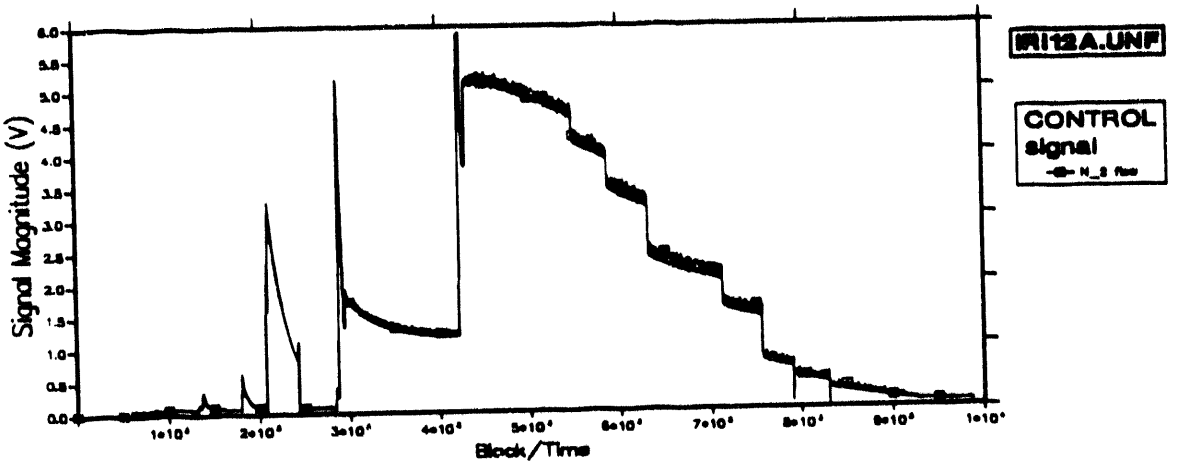

Figure 5: *Control Signal (Nitrogen flow) During Experiment IRI10A*

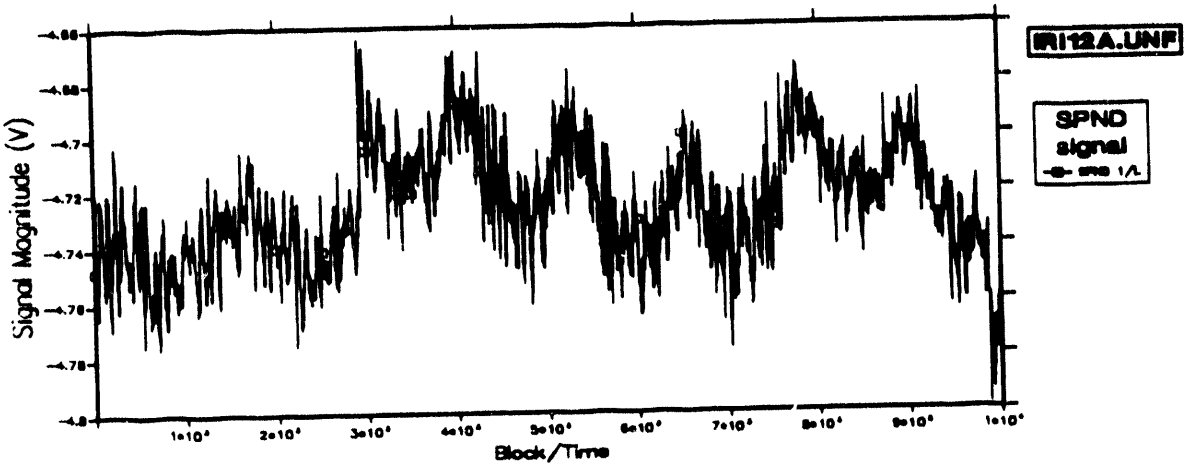

Figure 6: *DC Component of the Signal of SPND 1/L in Experiment IRI12A*

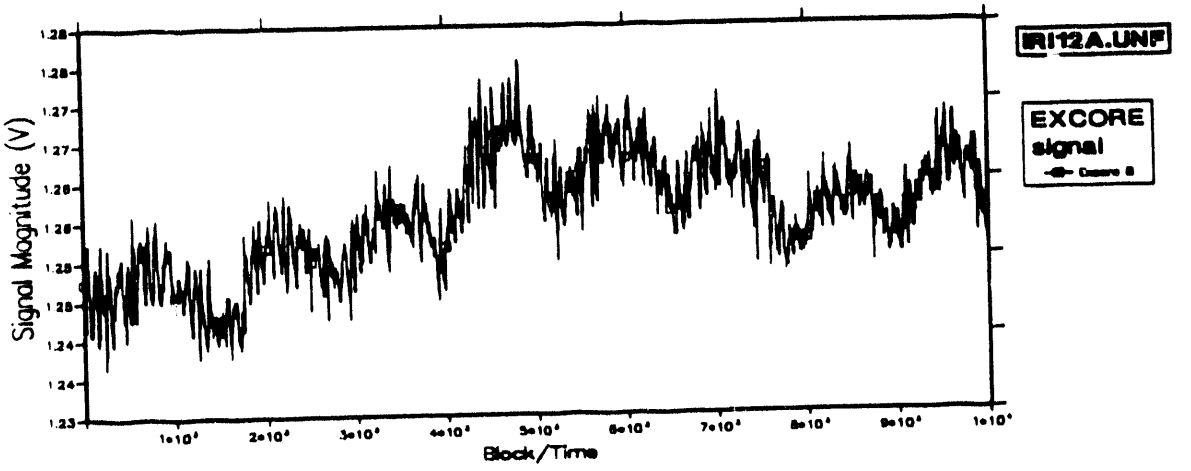

Figure 7: *DC Component of the Signal of detector EXCORE B in Experiment IRI12A*

In experiment IRI12A, AC signals of 5 detectors have been evaluated: two SPNDs, two ex-core neutron detectors and the nitrogen flowmeter. 300 blocks of data have been used for the determination of auto- and cross-spectra starting with the base spectra (blocks 700 to 1000), followed by the analysis of blocks 4600 to 4900 (with the maximum nitrogen flow) and 15 more FFT analyses of length of 300 blocks till block no. 10600 (with zero flow rate of nitrogen).

APSDs of in-core SPND 1/L and ex-core neutron detector B are given in Figs. 8 to 11 for the whole period of experiments IRI10A and IRI12A, respectively. The most important boiling/void effects identified in the experiments are:

- relatively wide spectral changes in the neutron noise at high frequencies,
- spectrum peaks caused by boiling induced mechanical oscillations.

Boiling peaks appear in the corresponding APSDs at about 3 Hz and at its harmonics in Fig. 8 (SPND 1/L). With the development of the boiling, the intensity of this peak ceases and a much wider increase of the noise magnitude appears up to the maximum frequency (16 Hz). Spectral changes measured by ex-core neutron detectors are much less pronounced: the APSDs of the ex-core detectors are dominated by a strong peak between 4 and 7 Hz, which is present in the spectrum independently on the boiling state.

In experiment IRI12A with nitrogen injection, in-core SPNDs indicate continuous spectral change with decreasing void fraction in the coolant channel; see Fig. 10. The pronounced boiling peak at about 2 Hz with a clear phase-shift between noise signals of SPNDs in one string indicate bubble transport in the channel. This effect can be used for the determination of the velocity of bubbles in the channels [6]. The spectra of ex-core detectors are similar to those in experiment IRI10A, i.e. they have a strong peak between 4 and 7 Hz, as it is seen in Fig. 11.

The increase of the neutron noise intensity over a given frequency range is characterized by the normalized root-mean-square (NRMS) neutron noise. The NRMS neutron noise over frequencies f_1 to f_2 is defined as follows:

$$NRMS(\mathbf{r}, f_1, f_2) = \frac{1}{I_N}\sqrt{\int_{f_1}^{f_2} APSD_{NN}(\mathbf{r}, f)df} \qquad (1)$$

Here, I_N is the DC component of the detector signal. NRMS values have been calculated over different frequencies for each ex-core and in-core neutron detectors. All of the neutron detectors show NRMS increase when coolant boiling occurs in NIOBE. The increase in the NRMS depends on several factors, including the location of the detectors with respect to the boiling region and the reactor core, the intensity and type of boiling, the frequency range chosen, etc. The most pronounced increase is detected by the SPNDs at high frequencies. They show an increase of up to 300 % at frequencies between 6 Hz and 16 Hz in experiment IRI10A. A weaker, but statistically significant NRMS increase is detected by ex-core NDs as well (up to about 25 %) over the same frequency interval. The error of the measured NRMS is 0.27 % in these experiments, so boiling anomaly can be detected clearly both by in-core and ex-core detectors.

The above results can be expressed in absolute units as well. The NRMS increase due to boiling is 1.85×10^{-4} in experiment IRI10A, which results in a reactivity change of 0.13 pcm. At the same time, ex-core neutron detectors see a vibration induced peak between 5 Hz and 7 Hz, having a reactivity effect of 0.05 pcm, which is constantly present in the spectra. The bubbling neutron noise

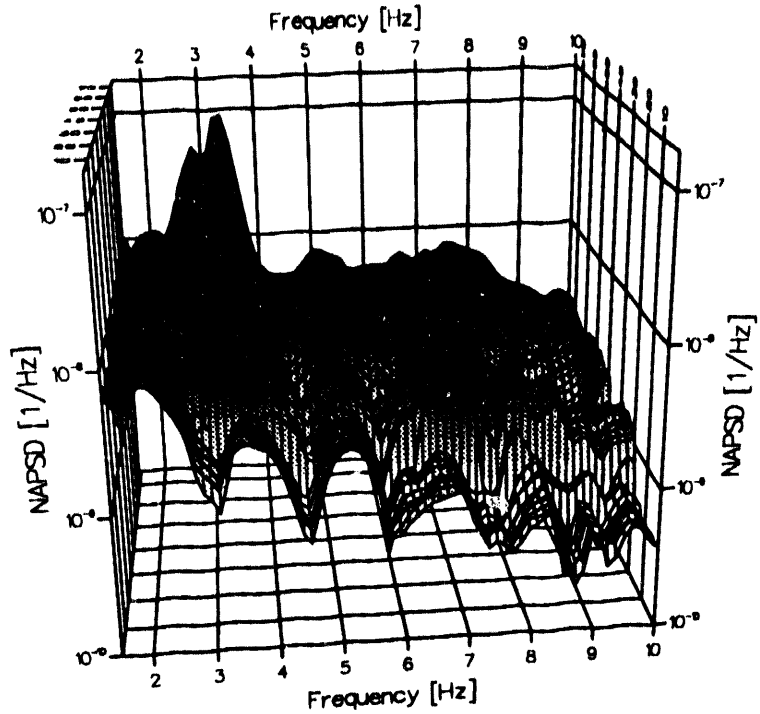

Fig. 8: *NAPSD functions versus time for SPND 1/L in Experiment IR110A, Frequency from 1.5–10.0 Hz.*

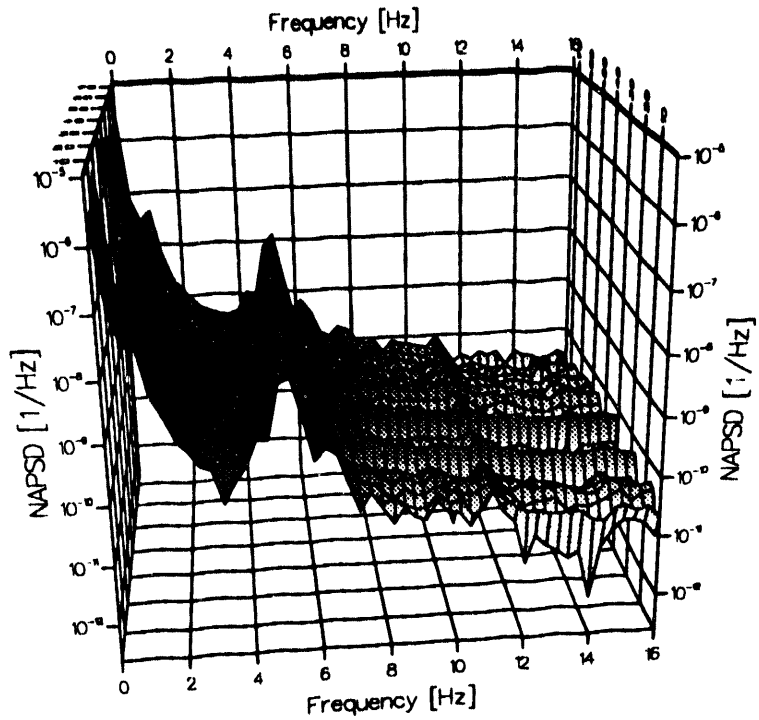

Fig. 9: *NAPSD function versus time for Ex-Core Neutron Detector B in Experiment IR110A.*

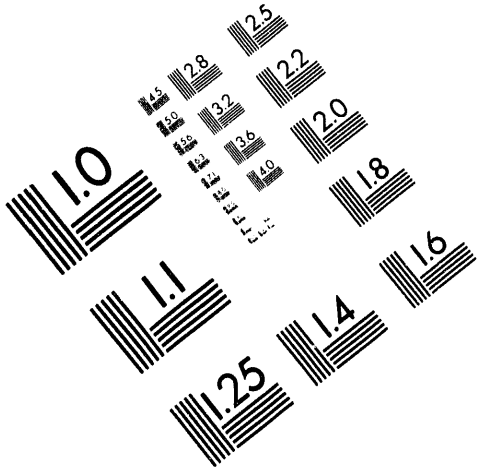

Association for Information and Image Management

1100 Wayne Avenue, Suite 1100
Silver Spring, Maryland 20910

301/587-8202

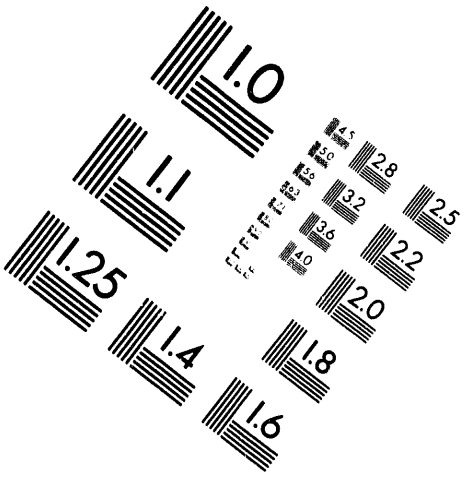

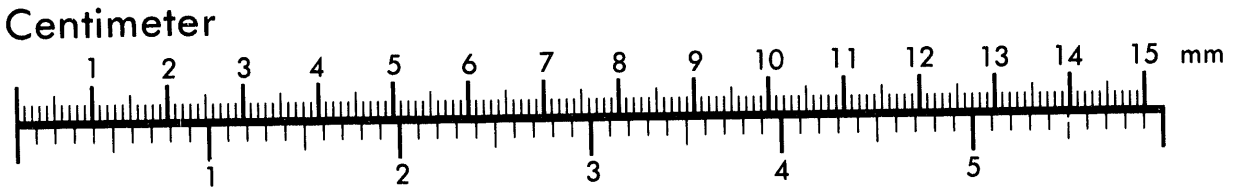

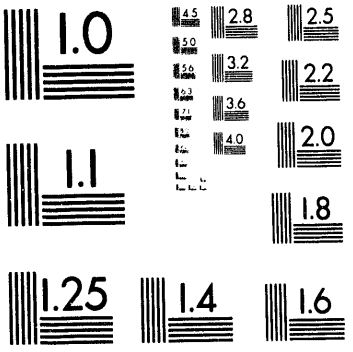

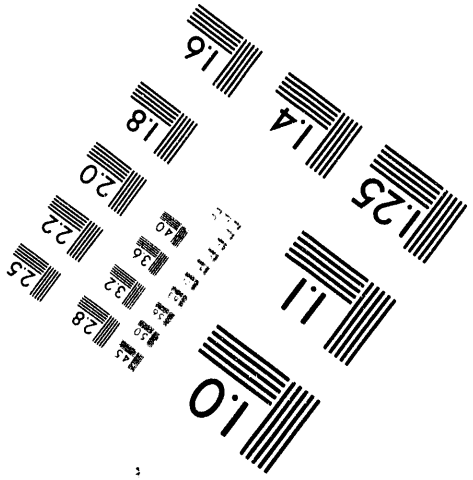

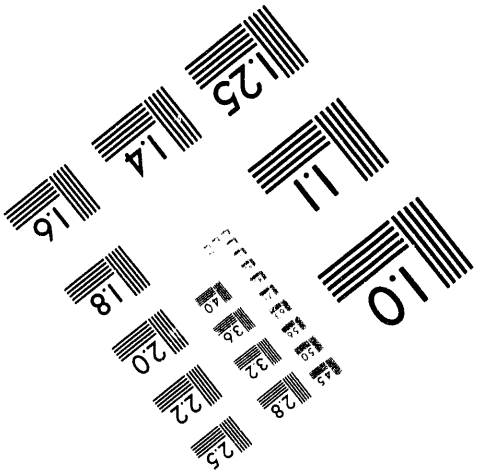

4 of 4

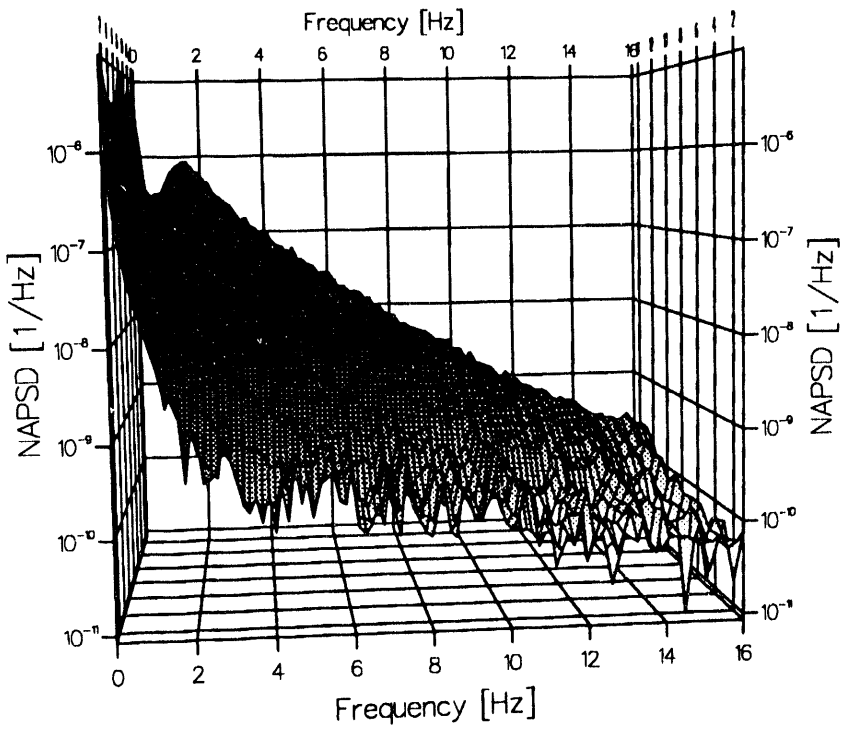

Fig. 10: *NAPSD function versus time for SPND 1/L in Experiment IRI12A.*

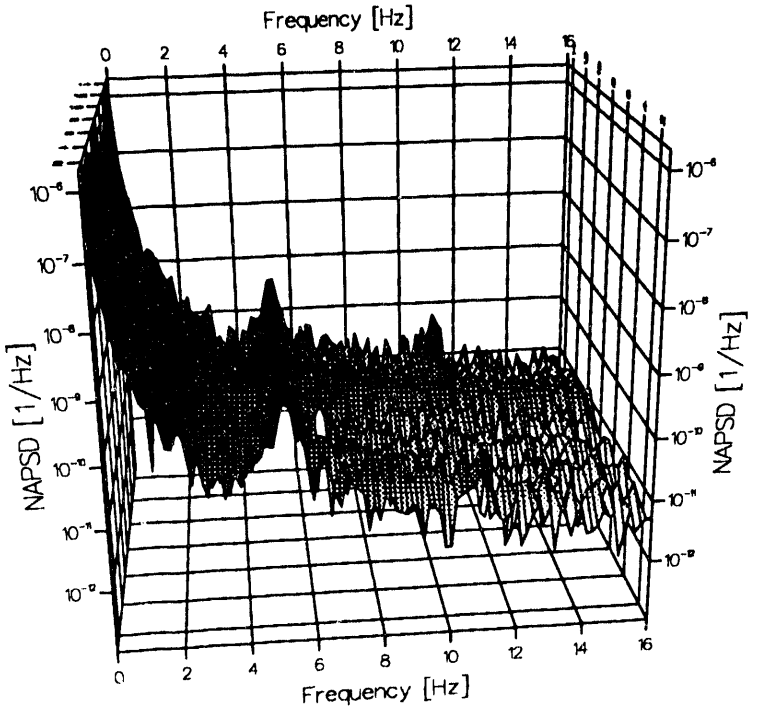

Fig. 11: *NAPSD function versus time for Ex-Core Neutron Detector B in Experiment IRI12A.*

in experiment IRI12A shows an increase of 1.60×10^{-3}, which corresponds to 1.12 pcm reactivity. The void fraction value in the coolant channel (maximum of 20 %) evaluated from this reactivity effect is in good agreement with the actual value determined from the known values of nitrogen flow.

CONCLUDING REMARKS

Results of experiments with coolant boiling in actual reactor environment are presented. Coolant boiling in the channels of a simulated fuel assembly has been detected based on the analysis of neutron noise. The experiments indicate that even very small amount of void can be detected at the early stage of boiling in the coolant channels having a reactivity effect of less than 1 pcm. In the case of HEU → LEU conversion at the HFR, the expected modifications in the neutronic and thermohydraulic characteristics of the core may introduce changes in the properties related to the onset of boiling and bubble detachement criteria. The coolant boiling in these circumstances can be detected at a very early stage by the methodology outlined in this paper.

Although boiling induced variations in the DC component of the neutron detector signals could not produce an unambiguous criterion for boiling detection in the case of low level of boiling (void fraction in two coolant channels below 50 %), but in combination with noise criteria DC analysis can facilitate early identification of coolant boiling in nuclear reactors. In the recent years, also several new methods and algorithms have been developed for the identification of changes in signal patterns either by using DC signals with powerful sequential statistical tests or by applying classical algorithms to identify spectral changes in real-time, or by using neural networks as spectral pattern classifiers.

ACKNOWLEDGEMENTS The authors wish to express their appreciations to the Department of Reactor Physics, IRI, Technical University Delft, for their cooperation in this experiment and to the Reactor Operation Group of HOR for their help in completing the measurements at the HOR. Special thanks are due to dr G.J.H. van Nes for his innovations in the graphical representation of the results.

REFERENCES

1. W.L. Woodruff, *Nuclear Technology*, Vol. 64 (Feb.1984), pp.196-206
2. J.W. De Vries, H. Van Dam,and G. Gysler, *IAEA-SM-310* (1986), pp.546-552
3. J.E. Hoogenboom, B.H. Van Meulenbroek, H. Van Dam, and E.B.J. Kleiss, *Progress in Nuclear Energy* (1985) Vol. 15, pp. 771-779
4. Röttger, A.Tas, P. von der Hardt, W.P.Voorbraak, *High Flux Materials Testing Reactor HFR Petten*, EUR 5700 EN (1986)
5. Türkcan E., W.H.J.Quaadvliet, T.T.J.M.Peeters, and J.P.Verhoef, ECN-RX–91-057 (1991) and SMORN VI, May 12-24 (1991),Gatlinburg, TN, USA, Paper 3.01 (1991)
6. Kozma R. (1992) *Nuclear Reactor Noise Investigations on Boiling Effects in a Simulated MTR-type Fuel Assembly*, Thesis, Delft (1992)
7. Türkcan E., G. Tsotridis, R.L. Moss (1988) *Progress in Nuclear Energy*, Vol.21, pp. 393-403
8. Türkcan E. (1988) *On-line Monitoring of HFR Operation and Fuel Dyn.*, in Proc. European Working Group Irrad. Tech., SCK/CEN Mol, Belgium

A Comparison of WIMS-D4 and WIMS-D4m Generated Cross-section Data with Monte Carlo

W. L. Woodruff, J. R. Deen
Argonne National Laboratory
Argonne, Illinois 60439, USA
and
C. I. Costescu
University of Illinois
Urbana-Champaign, Illinois 61801, USA

ABSTRACT

Cross-section and related data generated by a modified version of the WIMS-D4 code for both plate and rod type research reactor fuel are compared with Monte Carlo data from the VIM code. The modifications include the introduction of a capability for generating broad group microscopic data and to write selected microscopic cross-sections to an ISOTXS file format. The original WIMS-D4 library with H in ZrH, and ^{166}Er and ^{167}Er added gives processed microscopic cross-section data that agree well with VIM ENDF/B-V based data for both plate and TRIGA cells. Additional improvements are in progress including the capability to generate an ENDF/B-V based library

Introduction

The WIMS-D4 code[1] has been modified to improve the performance for research reactor applications and to produce microscopic cross-sections that interface with current codes. This code has been used to generate cross-section data for both pin and plate type research reactor fuels. These data are compared with Monte Carlo data from the continuous energy VIM code.[2]

The Codes and Libraries

The original WIMS-D4 code and library were obtained from the Oak Ridge Radiation Shielding Information Center (RSIC). The library contained 101 isotopes with 69 energy group data. This version of the code uses a single spatial mesh point for each region (fuel, clad, coolant and moderator) with the full 69 energy groups in the initial collision probability solution. This coarse spatial flux is used for the resonance evaluation. These 69 group macroscopic cross-sections are then collapsed over each region to a selected intermediate group structure. These intermediate group data are used to compute a detailed spatial flux, eigenvalue, reaction rates,

and to collapse to the selected broad group structure (usually ~2-8 groups). The code gives macroscopic cross-sections for each region and a set of cell averaged data. The code is capable of treating multicell and cluster models (with rods or plates). The code also uses the 69 group coarse spatial flux to collapse regional microscopic cross-sections to the intermediate group structure

The use of this initial flat flux approximation to obtain broad group microscopic data can give poor results for a thick moderator, the extra region in a super-cell model, and for high absorption regions. The WIMS-D4m version[3] of the code introduces a broad group structure for use in the spatial averaging. The detailed spatial flux in the intermedate group structure is used for this purpose. This step is done for the user requested isotopes after the intermediate group averaging of the microscopic cross-sections. The broad group microscopic cross-sections may be burnup dependent and averaged over multiple sets of edit cells (groups of regions). These microscopic data are written in the binary ISOTXS format[4] in order to be compatible with many of the neutronics codes in the USA .

The original WIMS library has been augmented to include data for hydogen in ZrH and the isotopes ^{166}Er and ^{167}Er for TRIGA reactor applications. This library is based on data generated in the United Kingdom and not ENDF/B data. A comparison of selected data has found that the WIMS data falls somewhat between the ENDF/B versions IV and V data.

The VIM code uses ENDF/B data to provide a continuous energy Monte Carlo solution for generalized geometry neutron eigenvalue and fixed source problems. These VIM data for this study are based on ENDF/B version V data. The VIM results are used here as a standard for comparison of WIMS data. The solutions in each case include 2,000,000 neutron histories to give eigenvalues with standard deviations of $\pm$0.0005. The microscopic cross-section data are tallied to match the broad group structure of the WIMS model and have uncertainies of less than $\pm$0.5% in all cases and less than $\pm$0.1% in most cases.

Plate Type Model

The original IAEA benchmark geometry[5] has been selected as the basis for the plate type reactor comparisons. Many research institutions have experience in computing cross-section data in this three energy group model. The specified models for the standard and control super-cell were used for both the HEU and LEU fuels. The HEU case has the specified loading of 12.17 g ^{235}U/plate with UAl_x-Al fuel. The LEU case uses U_3Si_2-Al in a DOE standard fuel plate with a loading of 12.50 g ^{235}U/ plate. The HEU super-cell WIMS data are compared with the available data from the earlier cases in Table I.

The VIM comparisons for the absorption rates and k-infinity results are shown in Table II. Table III provides a comparison of some of the microscopic data averaged over the unit cell. The agreement for absorption rates is excellent, while the WIMS k-infinity for HEU shows a bias of almost -0.7%. In Table III, the three group spectra show some small differences with the largest for group 1 of the standard HEU cell at -2.2%. The microscopic cross-section data also show some

variations from the VIM data with the largest difference of -5.4% for the resonance group (2) in the LEU standard cell. This suggests that the library data and/or resonance treatment could be improved for WIMS.

Table I. IAEA HEU Benchmark Comparison

		Super-cell Data	
	g	WIMS	EPRI-CELL
U-235 Absorption	1	1.877	1.727
	2	39.36	39.24
	3	427.0	422.8
U-235 Fisson	1	1.602	1.453
	2	25.81	25.99
	3	362.9	360.5
U-238 Absorption	1	0.371	0.345
	2	26.94	27.14
	3	1.805	1.769
U-238 Fission	1	0.195	0.180
	2	0	0
	3	0	0

Table II. Relative Absorption Rates -Plate Cells

	HEU Element				LEU Element			
	Standard		Control		Standard		Control	
Isotope	WIMS	VIM	WIMS	VIM	WIMS	VIM	WIMS	VIM
U-235	0.8587	0.8596	0.8147	0.8146	0.8025	0.8018	0.7768	0.7757
U-238	0.0046	0.0045	0.0032	0.0031	0.0813	0.0837	0.0644	0.0662
Al	0.0452	0.0437	0.0464	0.0457	0.0362	0.0348	0.0382	0.0374
Si	-----	-----	-----	-----	0.0008	0.0008	0.0007	0.0007
O	0.0027	0.0022	0.0029	0.0024	0.0026	0.0022	0.0029	0.0023
H	0.0889	0.0900	0.1329	0.1342	0.0765	0.0770	0.1170	0.1178
k-inf.	1.7352	1.7468	1.6580	1.6678	1.6283	1.6356	1.5858	1.5926
± 1 Sigma		0.0005		0.0005		0.0005		0.0005
Diff., %	-0.664		-0.588		-0.446		-0.427	

TRIGA Models

The TRIGA fuel designs and fuel types are characterized in Table IV with HEU FLIP fuel and two LEU fuels, referred to as 20-20 and 20-30. The single rod element is typical of the standard Mark series design, while the four rod element is typical of conversions where plate type fuel was replaced with TRIGA fuel. The broad group energy structure chosen for this comparison is shown in Table V, and matches as closely as possible the standard seven group set used by General Atomic (GA)[6] for most neutronic analyses.

Table III. Few Group Spectra and Microscopic Cross-sections - Plate Cells

	HEU Element				LEU Element			
	Standard		Control		Standard		Control	
g	WIMS	VIM	WIMS	VIM	WIMS	VIM	WIMS	VIM
Spectra Data								
1	0.5206	0.5322	0.4783	0.4760	0.5393	0.5383	0.4959	0.4946
2	0.2617	0.2583	0.2398	0.2364	0.2630	0.2595	0.2431	0.2394
3	0.2177	0.2095	0.2819	0.2876	0.1978	0.2022	0.2610	0.2660
U-235 Absorption Data								
1	1.868+0	1.739+0	1.869+0	1.741+0	1.870+0	1.740+0	1.869+0	1.741+0
2	3.937+1	3.997+1	4.008+1	4.050+1	3.859+1	3.922+1	3.939+1	3.988+1
3	4.299+2	4.198+2	4.572+2	4.474+2	4.223+2	4.122+2	4.506+2	4.405+2
U-235 Fission Data								
1	1.596+0	1.465+0	1.602+0	1.472+0	1.597+0	1.465+0	1.602+0	1.471+0
2	2.582+1	2.639+1	2.625+1	2.671+1	2.532+1	2.600+1	2.581+1	2.641+1
3	3.654+2	3.579+2	3.889+2	3.817+2	3.588+2	3.514+2	3.833+2	3.758+2
U-238 Absorption Data								
1	3.728-1	3.532-1	3.783-1	3.598-1	3.705-1	3.512-1	3.765-1	3.584-1
2	2.650+1	2.664+1	2.713+1	2.731+1	6.961+0	7.357+0	7.991+0	8.421+0
3	1.817+0	1.763+0	1.919+0	1.865+0	1.788+0	1.735+0	1.894+0	1.839+0
Al Absorption Data								
1	4.550-3	4.292-3	4.712-3	4.531-3	4.539-3	4.280-3	4.698-3	4.512-3
2	1.704-2	1.074-2	1.712-2	1.087-2	1.687-2	1.046-2	1.699-2	1.065-2
3	1.560-1	1.520-1	1.652-1	1.610-2	1.539-1	1.498-1	1.636-1	1.591-1
H Absorption Data								
1	2.074-6	9.382-5	2.040-6	9.221-5	2.082-6	9.405-5	2.046-6	9.246-5
2	1.417-2	1.453-2	1.436-2	1.474-2	1.378-2	1.412-2	1.407-2	1.441-2
3	2.353-1	2.309-1	2.501-1	2.456-1	2.322-1	2.278-1	2.477-1	2.431-1

Table IV. TRIGA Fuel Design Data

Design Parameters	Single Rod	Four Rods
Fuel Element	Hexagonal	Square
Element Geometry	4.250 (hex.)	3.886 (square)
Fuel Rod Pitch, cm	0.635	0.457
Central Zr Rod OD, cm	3.632	3.482
Fuel Pellet OD, cm	3.734	3.584
Fuel Rod OD, cm		

Fuel	Specifications		
FLIP	Er in Pellet, w/o	1.6	1.5
	Fuel Enrichment ^{235}U, w/o	70.0	70.0
	U in Pellet, w/o	8.5	8.5
	^{235}U Loading/rod, g	135.0	126.0
LEU-20	Er in Pellet, w/o	0.50	0.4
(20-20)	Fuel Enrichment ^{235}U, w/o	19.75	19.75
	U in Pellet, w/o	20.0	20.0
	^{235}U Loading/rod, g	98.0	91.0
LEU-30	Er in Pellet, w/o	0.90	0.84
(20-30)	Fuel Enrichment ^{235}U, w/o	19.75	19.75
	U in Pellet, w/o	30.0	30.0
	^{235}U Loading/rod, g	161.0	150.0

Table V. Broad Group Energy Structure -TRIGA

g	Upper Bound of Energy Group, eV WIMS/VIM	GA
1	1.000+7	1.49+7
2	5.000+5	6.08+5
3	9.118+3	9.12+3
4	1.123	1.125
5	0.400	0.420
6	0.140	0.140
7	0.050	0.050

Table VI. Relative Absorption Rates - Single Rod TRIGA

	HEU		LEU 20		LEU 30	
Isotope	WIMS	VIM	WIMS	VIM	WIMS	VIM
U-235	0.6752	0.6787	0.6939	0.6974	0.6754	0.6774
U-238	0.0272	0.0281	0.0925	0.0935	0.1119	0.1132
Er166	0.0101	0.0105	0.0045	0.0046	0.0065	0.0067
Er167	0.1988	0.1986	0.0930	0.0924	0.1263	0.1269
H in ZrH	0.0196	0.0197	0.0271	0.0272	0.0147	0.0148
H in H2O	0.0191	0.0189	0.0254	0.0251	0.0167	0.0162
Zr in ZrH	0.0252	0.0208	0.0278	0.0231	0.0225	0.0182
Fe	0.0145	0.0144	0.0194	0.0192	0.0125	0.0122
Cr	0.0050	0.0051	0.0067	0.0067	0.0043	0.0043
Ni	0.0037	0.0036	0.0049	0.0047	0.0032	0.0031
O	0.0009	0.0007	0.0009	0.0007	0.0009	0.0008
k-inf.	1.3260	1.3400	1.3922	1.4087	1.3383	1.3508
± 1 Sigma		0.0005		0.0005		0.0005
Diff., %	1.045		-1.171		-0.925	

Table VII. Relative Absorption Rates - Four Rod TRIGA

	HEU		LEU 20		LEU 30	
Isotope	WIMS	VIM	WIMS	VIM	WIMS	VIM
U-235	0.6857	0.6872	0.7017	0.7039	0.6857	0.6873
U-238	0.0263	0.0270	0.0890	0.0893	0.1084	0.1088
Er166	0.0093	0.0095	0.0039	0.0039	0.0059	0.0061
Er167	0.1856	0.1844	0.0814	0.0804	0.1162	0.1159
H in ZrH	0.0200	0.0201	0.0286	0.0287	0.0150	0.0151
H in H2O	0.0232	0.0256	0.0303	0.0326	0.0202	0.0222
Zr in ZrH	0.0238	0.0202	0.0277	0.0233	0.0218	0.0176
Fe	0.0154	0.0153	0.0206	0.0203	0.0133	0.0131
Cr	0.0053	0.0054	0.0071	0.0071	0.0046	0.0046
Ni	0.0039	0.0038	0.0052	0.0050	0.0034	0.0033
O	0.0010	0.0008	0.0009	0.0008	0.0010	0.0010
k-inf.	1.3507	1.3616	1.4116	1.4254	1.3622	1.3732
± 1 Sigma		0.0005		0.0005		0.0005
Diff., %	0.801		-0.968		0.801	

The relative absorption rates and k-infinity comparisons are given in Tables VI and VII. The agreement for absorption rates is generally very good with the worst agreement for absorption of Zr in ZrH. The WIMS library has only data for elemental Zr, while VIM has specific data for Zr in ZrH. Although the contribution is small, the addition of these data to the WIMS library would be an improvement. The largest bias is -1.2% for the LEU20 single rod cell. The four rod cell bias is less than 1.0% in all cases. The results for both types of TRIGA cells are very similar.

Tables VIII and IX provide a comparison of the spectra and selected microscopic cross-section data for both types of TRIGA cells. Again these results are very similar for the two cell types. The differences in pitch and rod size are apparently not a factor. The fuel to coolant ratios are very similar for the two cases. One could probably generate one set of microscopic data for use with both cell designs.

The spectra for the TRIGA cases are fairly hard. In this seven group structure, the resonance energy group for ^{238}U is group three. The two highest energy groups contain almost 60% of the neutrons, while the lowest groups (4-7) contain only about 13%. When these percentages are compared with the plate cases in Table III, one sees that the TRIGA spectra are considerably harder. This is largely due to the significant absorption in ^{167}Er over the resonance and lower energy range (see groups 3-7 in Table VIII and IX).

The microscopic cross-section data show more variation for the TRIGA cells with a larger number of energy groups, but the agreement is still fairly good. While the absorption in group 2 shows some significant variations for both ^{235}U and ^{238}U, the overall absorption rates in Tables VI and VII agree very well. The TRIGA cases also show WIMS with a lower resonance absorption for ^{238}U in the LEU fuels. The single rod cases are about 4% lower, while the four rod cells are less than 3% under the VIM values.

Conclusions

The WIMS data for both plate type and TRIGA type cells agree reasonably well with the corresponding VIM Monte Carlo ENDF/B-V data. Given that the cross-section libraries for the two codes are not based on the same evaluations, some differences should be expected. The k-infinities for the super-cells show a negative bias in all of the WIMS cases ranging from -0.4 to -1.2% with the plate cases showing a smaller bias.

The reaction rate data for absorption in the plate cases show excellent agreement. The TRIGA cases also show good agreement with the exception of Zr in ZrH. The WIMS library does not have data for Zr in ZrH corresponding to the VIM data. The absorption rate attributed to Zr is only about 2% of the total for the cell, and thus these differences are not a significant concern. The addition of these data to the WIMS library is still recommended.

Table VIII. Few Group Spectra and Microscopic Cross-sections -Single Rod TRIGA

	HEU		LEU 20		LEU 30	
g	WIMS	VIM	WIMS	VIM	WIMS	VIM
Spectra Data						
1	0.3462	0.3554	0.3274	0.3363	0.3522	0.3687
2	0.2359	0.2323	0.2278	0.2240	0.2483	0.2489
3	0.2900	0.2778	0.2737	0.2681	0.2835	0.2825
4	0.0255	0.0246	0.0272	0.0274	0.0244	0.0251
5	0.0278	0.0299	0.0324	0.0336	0.0256	0.0270
6	0.0430	0.0498	0.0665	0.0675	0.0406	0.0417
7	0.0316	0.0302	0.0450	0.0430	0.0254	0.0245
U-235 Absorption Data						
1	1.361+0	1.332+0	1.363+0	1.333+0	1.363+0	1.333+0
2	2.416+0	2.143+0	2.417+0	2.145+0	1.918+0	2.143+0
3	3.258+1	3.314+1	3.318+1	3.365+1	3.095+1	3.168+1
4	7.541+1	7.481+1	7.881+1	7.992+1	7.589+1	7.709+1
5	2.004+2	1.988+2	2.067+2	2.080+2	1.985+2	1.998+2
6	2.972+2	2.976+2	3.118+2	3.116+2	2.889+2	2.897+2
7	4.502+2	4.604+2	4.985+2	5.094+2	4.255+2	4.355+2
U-235 Fission Data						
1	1.304+0	1.250+0	1.305+0	1.250+0	1.304+0	1.250+0
2	1.863+0	1.660+0	1.864+0	1.661+0	1.863+0	1.660+0
3	2.064+1	2.103+1	2.096+1	2.138+1	1.971+1	2.026+1
4	6.561+1	6.582+1	6.867+1	7.025+1	6.607+1	6.777+1
5	1.640+2	1.640+2	1.692+2	1.714+2	1.624+2	1.646+2
6	2.533+2	2.541+2	2.656+2	2.660+2	2.462+2	2.473+2
7	3.837+2	3.939+2	4.250+2	4.358+2	3.627+2	3.727+2
U-238 Absorption Data						
1	3.809-1	3.774-1	3.785-1	3.751-1	3.764-1	3.735-1
2	3.006-1	2.643-1	3.007-1	2.640-1	3.002-1	2.629-1
3	1.437+1	1.515+1	6.035+0	6.256+0	4.561+0	4.743+0
4	5.492-1	5.447-1	5.710-1	5.708-1	5.521-1	5.530-1
5	8.750-1	8.665-1	9.048-1	9.033-1	8.652-1	8.646-1
6	1.360+0	1.346+0	1.424+0	1.407+0	1.324+0	1.312+0
7	1.809+0	1.832+0	2.002+0	2.025+0	1.711+0	1.734+0
Er167 Absorption Data						
1	8.436-2	8.334-2	8.534-2	8.413-2	8.596-2	8.467-2
2	7.787-1	7.715-1	7.788-1	7.722-1	7.770-1	7.705-1
3	9.315+1	1.057+2	1.086+2	1.217+2	9.161+1	1.055+2
4	2.619+3	2.483+3	3.078+3	3.007+3	2.753+3	2.714+3
5	9.760+2	1.055+3	9.996+2	9.321+2	9.872+2	9.206+2
6	4.563+2	4.342+2	4.752+2	4.516+2	4.451+2	4.243+2
7	4.711+2	4.595+2	5.208+2	5.074+2	4.460+2	4.354+2
H in ZrH Absorption Data						
1	9.645-7	3.444-5	9.714-7	3.447-5	9.754-7	3.447-5
2	3.700-6	1.469-4	3.703-6	1.470-4	3.699-6	1.466-4
3	9.616-3	9.706-3	9.641-3	9.762-3	9.119-3	9.223-3
4	5.972-2	5.925-2	6.229-2	6.254-2	6.011-2	6.043-2
5	1.030-1	1.029-1	1.066-1	1.074-1	1.019-1	1.028-1
6	1.657-1	1.638-1	1.733-1	1.712-1	1.613-1	1.596-1
7	2.237-1	2.252-1	2.473-1	2.489-1	2.117-1	2.131-1
H in H2O Absorption Data						
1	8.837-7	3.145-5	8.871-7	3.141-5	8.917-7	3.143-5
2	3.557-6	1.448-4	3.551-6	1.444-4	3.550-6	1.443-4
3	1.012-2	1.034-2	1.013-2	1.037-2	9.852-3	1.008-2
4	7.255-2	7.200-2	6.946-2	7.008-2	7.255-2	7.297-2
5	1.282-1	1.285-1	1.219-1	1.236-1	1.294-1	1.310-1
6	2.247-1	2.250-1	2.110-1	2.116-1	2.330-1	2.326-1
7	6.117-1	6.076-1	5.615-1	5.570-1	6.371-1	6.332-1
Zr in ZrH Absorption Data						
1	1.320-2	9.994-3	1.314-2	1.003-2	1.310-2	1.004-2
2	8.544-3	1.945-2	8.551-3	1.951-2	8.556-3	1.945-2
3	9.726-2	6.892-2	9.728-2	6.902-2	9.962-2	7.085-2
4	3.304-2	3.232-2	3.449-2	3.412-2	3.325-2	3.296-2
5	5.702-2	5.618-2	5.905-2	5.863-2	5.635-2	5.609-2
6	9.095-2	8.946-2	9.526-2	9.351-2	8.841-2	8.717-2
7	1.215-1	1.230-1	1.346-1	1.360-1	1.147-1	1.164-1

Table IX **Few Group Spectra and Microscopic Cross-sections -Four Rod TRIGA**

	HEU		LEU 20		LEU 30	
g	WIMS	VIM	WIMS	VIM	WIMS	VIM
Spectra Data						
1	0.3440	0.3503	0.3225	0.3297	0.3494	0.3578
2	0.2315	0.2271	0.2226	0.2177	0.2340	0.2391
3	0.2805	0.2735	0.2700	0.2626	0.2811	0.2732
4	0.0259	0.0248	0.0275	0.0262	0.0246	0.0238
5	0.0278	0.0310	0.0334	0.0360	0.0267	0.0288
6	0.0531	0.0559	0.0723	0.0755	0.0443	0.0466
7	0.0362	0.0374	0.0517	0.0523	0.0296	0.0307
U-235 Absorption Data						
1	1.368+0	1.343+0	1.370+0	1.345+0	1.370+0	1.345+0
2	2.422+0	2.152+0	2.424+0	2.153+0	2.420+0	2.151+0
3	3.270+1	3.313+1	3.329+1	3.362+1	3.101+1	3.158+1
4	7.510+1	7.390+1	7.875+1	7.739+1	7.556+1	7.424+1
5	1.985+2	1.941+2	2.057+2	2.017+2	1.964+2	1.918+2
6	2.927+2	2.824+2	3.092+2	3.010+2	2.836+2	2.724+2
7	4.296+2	4.033+2	4.814+2	4.610+2	4.041+2	3.738+2
U-235 Fission Data						
1	1.311+0	1.262+0	1.313+0	1.262+0	1.311+0	1.262+0
2	1.868+0	1.667+0	1.870+0	1.668+0	1.867+0	1.667+0
3	2.062+1	2.101+1	2.102+1	2.136+1	1.974+1	2.021+1
4	6.533+1	6.506+1	6.863+1	6.811+1	6.579+1	6.533+1
5	1.625+2	1.601+2	1.684+2	1.665+2	1.607+2	1.582+2
6	2.494+2	2.411+2	2.635+2	2.570+2	2.416+2	2.325+2
7	3.662+2	3.481+2	4.103+2	3.944+2	3.445+2	3.199+2
U-238 Absorption Data						
1	3.846-1	3.822-1	3.817-1	3.804-1	3.796-1	3.784-1
2	3.013-1	2.655-1	3.015-1	2.647-1	3.009-1	2.638-1
3	1.444+1	1.523+1	6.173+0	6.345+0	4.593+0	4.739+0
4	5.465-1	5.382-1	5.703-1	5.619-1	5.494-1	5.402-1
5	8.672-1	8.466-1	9.012-1	8.827-1	8.566-1	8.361-1
6	1.339+0	1.277+0	1.412+0	1.359+0	1.298+0	1.232+0
7	1.726+0	1.605+0	1.932+0	1.833+0	1.625+0	1.489+0
Er167 Absorption Data						
1	8.420-2	8.370-2	8.547-2	8.448-2	8.601-2	8.506-2
2	7.800-1	7.750-1	7.808-1	7.744-1	7.788-1	7.729-1
3	9.433+1	1.063+2	1.126+2	1.237+2	9.322+1	1.065+2
4	2.643+3	2.487+3	3.111+3	2.916+3	2.776+3	2.600+3
5	9.644+2	1.027+3	9.905+2	1.070+3	9.741+2	1.048+3
6	4.483+2	4.111+2	4.703+2	4.356+2	4.357+2	3.979+2
7	4.496+2	4.027+2	5.027+2	4.592+2	4.235+2	3.738+2
H in ZrH Absorption Data						
1	9.650-7	3.477-5	9.743-7	3.481-5	9.776-7	3.481-5
2	3.710-6	1.474-4	3.716-6	1.474-4	3.711-6	1.471-4
3	9.654-3	9.709-3	9.690-3	9.769-3	9.163-3	9.232-3
4	5.946-2	5.857-2	6.224-2	6.138-2	5.984-2	5.886-2
5	1.021-1	1.006-1	1.062-1	1.049-1	1.009-1	9.928-2
6	1.631-1	1.553-1	1.719-1	1.653-1	1.582-1	1.499-1
7	2.135-1	1.973-1	2.388-1	2.253-1	2.031-1	1.830-1
H in H2O Absorption Data						
1	8.780-7	3.110-5	8.825-7	3.106-5	8.868-7	3.108-5
2	3.550-6	1.440-4	3.547-6	1.441-4	3.547-6	1.437-4
3	1.018-2	1.043-2	1.020-2	1.046-2	9.927-3	1.019-2
4	7.220-2	7.260-2	6.918-2	6.930-2	7.221-2	7.261-2
5	1.277-1	1.311-1	1.217-1	1.246-1	1.290-1	1.324-1
6	2.253-1	2.384-1	2.115-1	2.214-1	2.333-1	2.475-1
7	5.974-1	6.360-1	5.508-1	5.821-1	6.204-1	6.640-1
Zr in ZrH Absorption Data						
1	1.330-2	1.007-2	1.325-2	1.010-2	1.321-2	1.012-2
2	8.560-3	1.956-2	8.571-3	1.954-2	8.575-3	1.952-2
3	9.694-2	6.887-2	9.689-2	6.881-2	9.915-2	7.020-2
4	3.292-2	3.195-2	3.447-2	3.348-2	3.312-2	3.211-2
5	5.657-2	5.480-2	5.886-2	5.725-2	5.587-2	5.420-2
6	8.967-2	8.485-2	9.457-2	9.032-2	8.692-2	8.190-2
7	1.166-1	1.078-1	1.307-1	1.231-1	1.097-1	9.995-2

The WIMS microscopic absorption cross-sections for ^{238}U in the resonance range are lower by more than 5% for the LEU plate cases and by about 4% for the TRIGA cases. The addition of ENDF/B-V data to correspond to that in VIM may resolve some of the differences noted. The overall absorption rate does not seem to be strongly affected by the differences observed in the microscopic data.

This improved version of the WIMS-D4 code gives a respectable set of data with the current library for both plate and rod type fuel. The code provides and option for generating microscopic cross-sections in the ISOTXS format to interface with neutronics codes using this format. The code is also capable of generating macroscopic data averaged over selected regions. Further improvements in the code are in progress including 2D transport and treatments for non-lattice heterogeneities (experiments, control rods, reflectors, etc.). A new all ENDF/B-V library will be generated in the near future with the inclusion of additional desired materials.

References

1. "Documentation for CCC-576/WIMS-D4 Code Package," RSIC Computer Code Collection, Oak Ridge National Laboratory, Dec. 1990

2. R. Bloomquist, "VIM - A Continuous Energy Neutronics and Photon Transport Code," ANS Proceedings of the Topical Meeting on Advances inReactor Computations, Salt Lake City, Utah, pp. 222-224, Mar. 1983

3. WIMS-D4M Manual (to be published)

4. "Standard Interface Files and Procedures for Reactor Physics Codes, Version III," Compiled by B. M. Carmichael, LA-5486-MS, pp. 8-13, Feb. 1974

5. "Research Reactor Core Conversion from the Use of Highly Enriched Uranium to the Use of Low Enriched Uranium Fuels - Guidbook," IAEA-TECDOC-233, pp. 60-71 and pp. 447-628, 1980

6. IAEA-TECDOC-233, p. 264

S E S S I O N VIII

September 30, 1992

CORE CONVERSION STUDIES

Chairman:

G. Thamm
(KFA, Germany)

CORE CONVERSION OF IAN-R1 REACTOR

Arturo Spin Ramírez

Instituto de Asuntos Nucleares

Santafé de Bogotá, Colombia

ABSTRACT

The IAN-R1 reactor has been operating by the Instituto de Asuntos Nucleares since early 1965. The reactor is used for the production of short lived radioisotopes, radiochemistry, neutron activation analysis and training. The power level is 30 kw. The reactor core consists of 16 HEU plate-type fuel elements, that have been in the core for over 27 years. At 1990 the instrumentation was replaced for a new control system with a microprocessor driven digital control console and data acquisition system. Last year it was installed a new radiation monitoring system and control rod drives with stepping motor drives. The future modifications of the reactor will include the core conversion to LEU and finally the increase of the power between 500 kw and 1 Mw.

INTRODUCTION

IAN-R1 reactor is a pool type reactor operating in Santafé de Bogotá since 1965. It is placed at the Instituto de Asuntos Nucleares (IAN) and operating at 30 kw. Given its importance for the application of nuclear technology in Colombia for various purposes (mainly in areas of neutron activation analysis, production of short lived radioisotopes for engineering and industrial application and production of radioactive material for teaching and research purposes) a program of modernization of the reactor began some years ago, with support of IAEA and the U.S.A. Government. Now we have renovated the instrumentation for operation and control to continue with the core conversion and increase of power. The modification in process includes the conversion of the core to low-enriched fuel during the next step

and finally the increase to 500 kw-1 Mw. In all the steps the safety of the facility has been optimized.

CORE CONVERSION

The core and associated experimental facilities of the reactor were designed to meet the requirements for a flexible and safe research and training reactor. The core configuration consists of a 4 by 4 array of fuel elements, plate type, reflected on four sides with graphite and on the top and botton with water. The core contains 13 standard 10-plate fuel elements, 3 rod-well fuel elements and a reflector of 20 graphite elements. The three fuel elements containing rod wells have 6 fuel plates rather than 10 as in the 13 standard elements. FIGURE 1 presents the actual core. All the fuels are HEU-90% enriched.

The plate-type HEU fuel elements will be replaced with TRIGA type 4-rod LEU fuel clusters, designed and fabricated by G.A. with aluminum bottom adapter to fit into the existing IAN-R1 grid plate. The adapter contains four tapped holes into which the fuel rods are threaded. A control/experiment guide tube can also replace one of the fuel rods in a cluster. The guide tube screws into the cluster bottom adapter, just as a fuel rod does. The cluster has a modified top fitting to accept the guide tube.

The first step of conversion to LEU fuel will be a mixed core. For a mixed core of TRIGA fuel and plate-type fuel exists several options like four (4) standard TRIGA type 606 4-rod LEU fuel clusters, containing 12 wt-% U and less than 20% enriched uranium plus two (2) standard TRIGA type 806 3-rod LEU fuel clusters containing 12 wt-% U and less than 20% enriched uranium, plus seven (7) standard HEU 10-plate fuel elements 90 % enriched uranium plus three (3) standard HEU 6-plate fuel elements 90% enriched uranium, or similar with nine (9) TRIGA clusters and four (4) standard HEU 10-plate fuel elements plus three (3) standard HEU 6-plate fuel elements.

Finally, the new TRIGA core will have 8 4-rod LEU TRIGA fuel clusters plus 6 3-rod LEU TRIGA fuel clusters, three of these with one irradiation position. FIGURE 2 presents the IAN-R1 mixed core with nine TRIGA clusters.

The employment of the same actual grid plate for all those configurations is possible. The new core will have three additional in core irradiation places, comparing with the actual core that has only irradiation places in the reflector. This will be a mixed core with nine TRIGA clusters and seven HEU plate type elements during the intermediate step, before the complete core conversion to LEU TRIGA fuel. According to the size of the

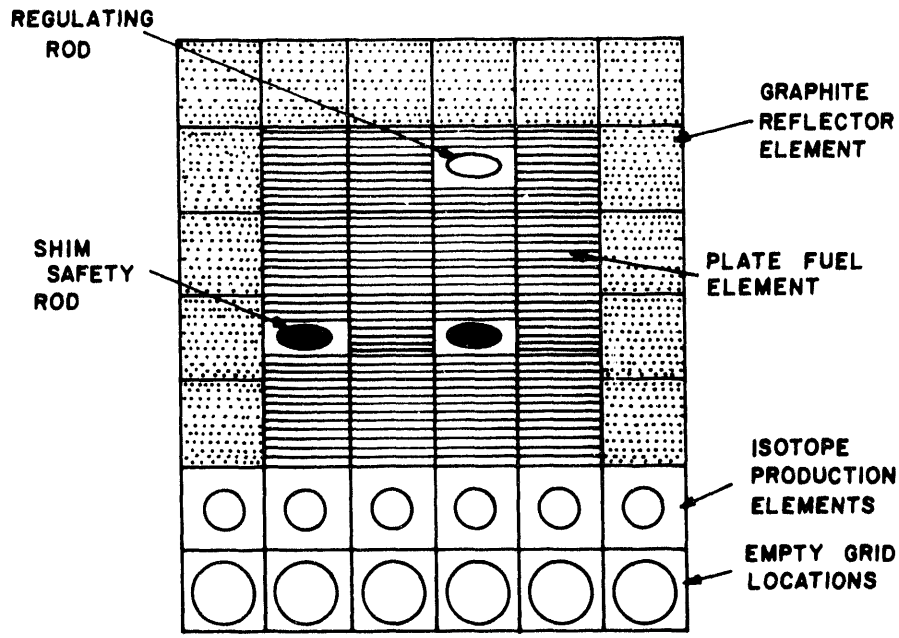

Fig. 1 IAN-R1 HEU Core Configuration.

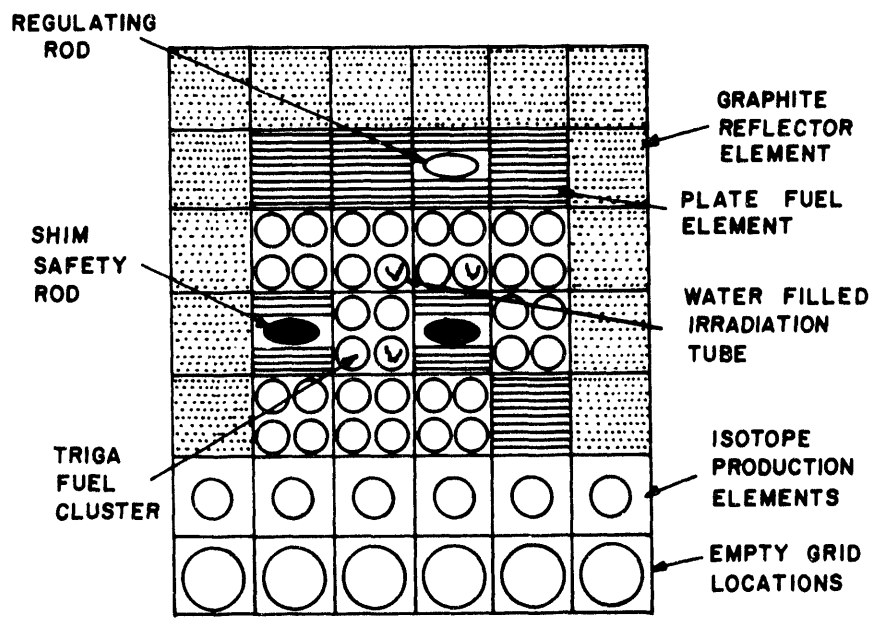

Fig. 2 IAN-R1 Mixed Core With Nine TRIGA Clusters.

grid plate, empty grid locations will permit increase of power during the next step.

For the mixed core of TRIGA fuel and plate type fuel we will mantain the actual excess of reactivity of 0.6 %. The complete TRIGA core will require about 45-50 fuel rods for an operational loading with an excess of reactivity between about 0.6% and 1.5%. This final core, before the increase of power, will have three in core irradiation places and three new control rods.

UPGRADE AND TRAINING

Considering that the IAN-R1 is the only reactor operating in Colombia, all the knowledge that can be possibly acquired in the field of nuclear technology during the process of modernization, will be very useful for the country and will contribute to a better qualified technical staff and for this reason a very well designed training program, with assistance of IAEA is under consideration.

This program includes training in TRIGA core thermohydraulic and neutron calculations and also for a mixed core HEU plate type fuel and TRIGA fuel. This training is divided in three parts: one of these in site with experts, and the other two in a nuclear center and General Atomics TRIGA Group in San Diego, California. Additionally, we will receive assistance of IAEA for the SAR and also for evaluation of the design and construction of a new pool for spent fuel.

The complete program focus on the final increase of power between 500 kW and 1 Mw. During this time an important cooperation plan with G.A. and IAEA will permit us to improve our irradiation facilities for radioisotopes and radiopharmaceutical production, neutron radiography and additional facilities for research with universities.

TECHNICAL CONTRACTUAL CONSIDERATIONS

Even if this project includes IAEA and G.A., some technical compromises of the supplier are under evaluation. One of the most important considerations is the guarantees of operation of the reactor with the mixed core and with the TRIGA core, in equal or better conditions comparing with the actual HEU core. Technical support of G.A. for the SAR in all the cases and participation of G.A. during components installation, startup and testing are included. The testing shall include preoperational

testing, initial startup of the reactor, adjustment of excess reactivity, control rod calibration and operation of the reactor, at its steady-state power level for a continuous period of eight hours. An proper execution of procedures will be defined between IAN and G.A. with assistance of IAEA. Safety procedures and evaluation of the safety will be considered as first priority.

OTHER ACTIVITIES WITH ASSISTANCE OF IAEA AND THE U.S.A. GOVERNMENT

The modernization of the IAN-R1 reactor has included until now, the renewal of the instrumentation for a new control system with microprocessor driven digital control console and data acquisition system, the replacement of the control rod drives and the installation of a new radiation monitoring system. Technical assistance for all these steps has been very useful to the IAN.

CONCLUSION

After the complete process of core conversion to LEU, the IAN-R1 reactor will be in the best conditions to increase its power between 500 kw and 1 Mw. During all this preliminary steps, we have obtained important experience and knowledge that will certainly help us finding better possibilities for the colombian reactor and for the nuclear industry.

STATUS OF THE BER II

A. Axmann, H. Buchholz, C.O. Fischer and H. Krohn
Hahn-Meitner-Institut Berlin

ABSTRACT

The BER II could start the operation with high enriched materials after a shut-down period for upgrading procedures. The application for the use of low enriched fuel was submitted to the authority. Whereas all data for a LEU core are evaluated, HEU-LEU mixed fuel elements are still under investigation. A licencing problem occurs with the open back end of the fuel cycle.

INTRODUCTION

After a long struggle with the local authority the licence for the restart of the BER II with high enriched materials was issued on March 26, 1991. The history of the BER II begins with the construction in 1969-1973 followed by a 12 year period of successful 5 MW operation. The BER II was shut-down in August 1985 in order to start an extensive upgrading program. The main goal was to enhance the neutron flux density at the beam ports by a factor of 8. This was accomplished by a power increase from 5 to 10 MW, by a reduction of the core size and the installation of a beryllium reflector with proper adjustments of the beam tube noses to the maximum of the neutron flux density in the reflector. A cold neutron source was also added.

Restart of the BER II with HEU

After the restart in April 1991, full power of 10 MW was achieved in the first days of 1992. The licence includes the operation of a standard core and a compact core, thus all variations between them are allowed. At first, the standard core was build-up and the typical measurements and calibrations were performed. Then it was decided not to continue with the compact core but first to provide neutrons to the users. A time scale for the BER II is shown in Table 1.

Accompanying the step by step power increase, the cold neutron source was in stand-by operation at 35°C and measurements of essential data, as for instance the moderator chamber temperature, were performed. Finally, the hydrogen in the moderator chamber was cooled down to 25 Kelvin and the routine operation began.

In summary, the restart of the BER II was accomplished without surprising effects. The expected behavior was confirmed and the data of the neutron flux density measurements resulted in great satisfaction. $1.2 \cdot 10^{14}$ n/cm^{2}sec were measured in the maximum of the neutron flux density in the undisturbed reflector for the standard core, Figure 1. Figure 2 shows the fuel arrangement in the standard and compact core.

Time-Scale of BER II	HMI
Construction	1969-1972
Costs total	12 Mio DM
Operation period 5 MW until	August 1985
Start of upgrading	August 1985
Goal: - Power increase 5 to 10 MW - Reduction of grid plate 60 to 42 positions - installation of a beryllium reflector - installation of a cold neutron source	
Restart	April 1991
Full power 10 MW	January 1992
End of start-up procedure	April 1992
Costs of upgrading	150 Mio DM
Application for the use of LEU	April 1992
Accompanying the upgrading: - 3 licences (construction,install. cold neutron source, operation) - 2 public hearings 3 suits	

Table 1: Time scale of the BER II

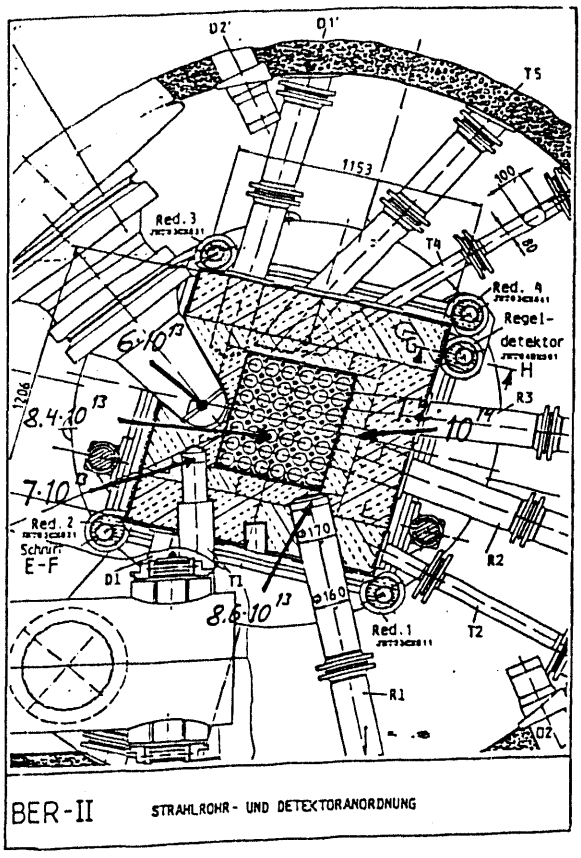

Figure 1: BER II HEU core, neutron flux densities in the core, at the beam holes and at the cold neutron source.

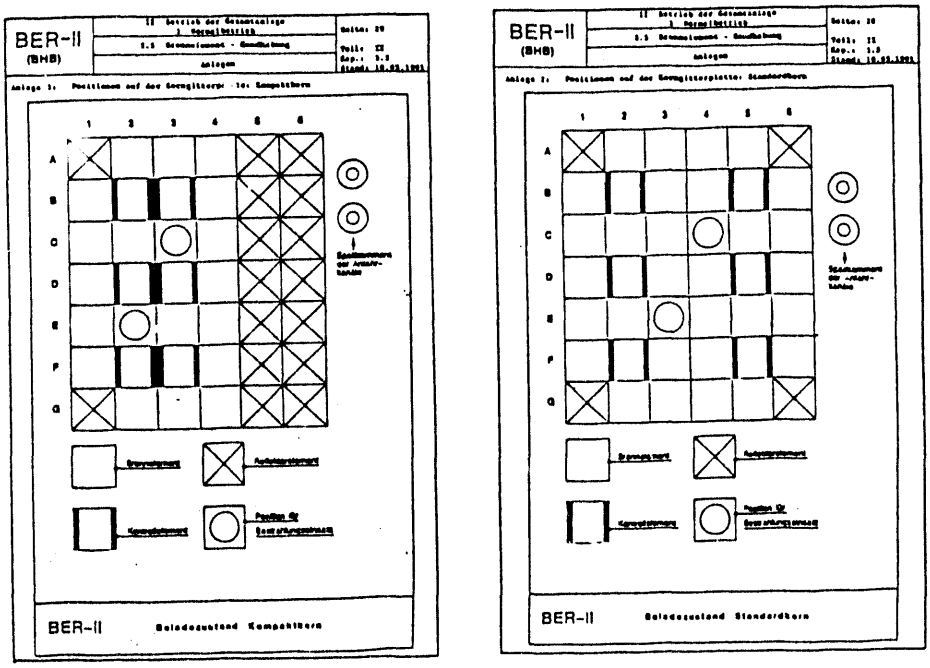

Figure 2: BER II, fuel element arrangements in the compact and standard core.

Parallel to the upgrading program and to the struggle for the licence, the low enriched material was not forgotten and the work to prepare the introduction was promoted. Meanwhile, all data are collected in a report covering all aspects of a safety report. The content of a safety report is regulated by an official guideline. Thus, the fuel element description, their qualification, the head decay generation, credible accidents and fuel element storage have to be examined.

Because of several suits against the upgrading and the operation of the BER II and the cold neutron source, it was decided not to apply for the introduction of low enriched materials before the issue of the operation licence. It could have confused the supreme court to be confronted with an additional parameter. Therefore, the Hahn-Meitner-Institut (HMI) did not apply for the operation of low enriched materials before April 1992.

Application for the use of LEU

Status of investigation and data

The HMI decided not to change the fuel element geometrical size but to increase the weight of U-235 from 180 g in HEU to 323 g in LEU, Table 2. According to the fuel development program this load will require U3Si2-Al. Basic calculations and a conversion study were performed by Interatom (now Siemens). 323 g were found as a compromise. The fuel cycle length was extended as wanted and the core size was conserved in order to supply the beam holes as good as possible.

	HEU	LEU
Material	UAlx	U_3Si_2Al
Overall size	76 x 78 x 873	
No. of plates	23	23
Enrichement	93%	19.75%
U-dens.g/cm^3	0.45	3.7
g U 235	180	323
g U	194	1635

Table 2: Fuel element data

The cycle length was increased from 60 to 85 full-power-days in the case of the standard core and 35 to 60 full-power-days for the compact core. The amount of fuel burn-up was increased also (see Table 3).

compact core	LEU	HEU
number of fuel elements	22,4	22,4
cycle length in MWD	600	350
mean burn up per cycle in %	10	10,5
final burn up in %	60	35
element life time in MWD	3600	1200
standard core		
number of fuel elements	27,4	34,4
cycle length in MWD	850	600
mean burn up per cycle in %	12	12
final burn up in %	70	60
element life time in MWD	5000	3000

Table 3: Characteristic data of LEU and HEU cores

A comparison of the fission product inventories shows only an increase of about 5 % for the core in the case of LEU. But another effect is remarkable. The amount of the actinides is increased up to a factor of 20 (see Table 4). Thus, the decay head will slowly decrease with time. A question of a more political character is the plutonium production rate which increases by a factor of about 20.

An essential question is the transition from a HEU to a LEU core. The idea to replace the HEU core by a fresh LEU core was rejected. Because of the low mean burn-up of a HEU core, one would waste HEU fuel elements before they reach their life time. On the other hand, a reactor operation with reduced power would be necessary as long as the amount of burn-up is low. Therefore several transition cores are planned for the BER II. The first transition core starts with 5 LEU elements. The second core contains 9 LEU elements. The third one contains 14 LEU elements and so on, Figure 3.

	compact core	standard core
	total	
HEU	46.08 MCi	46.96 MCi
LEU	49.12 MCI	48.96 MCi
	fuel element	
HEU	actinides 4.2 E3 Ci	4.8 E3 Ci
	fiss.prod. 2.1 E6 Ci	1,4 E6 Ci
LEU	actinides 8.5 E4 Ci	7.5 E4 Ci
	fiss.prod. 2.1 E6 Ci	1.7 E6 Ci

Table 4: Actinides and fission product inventories

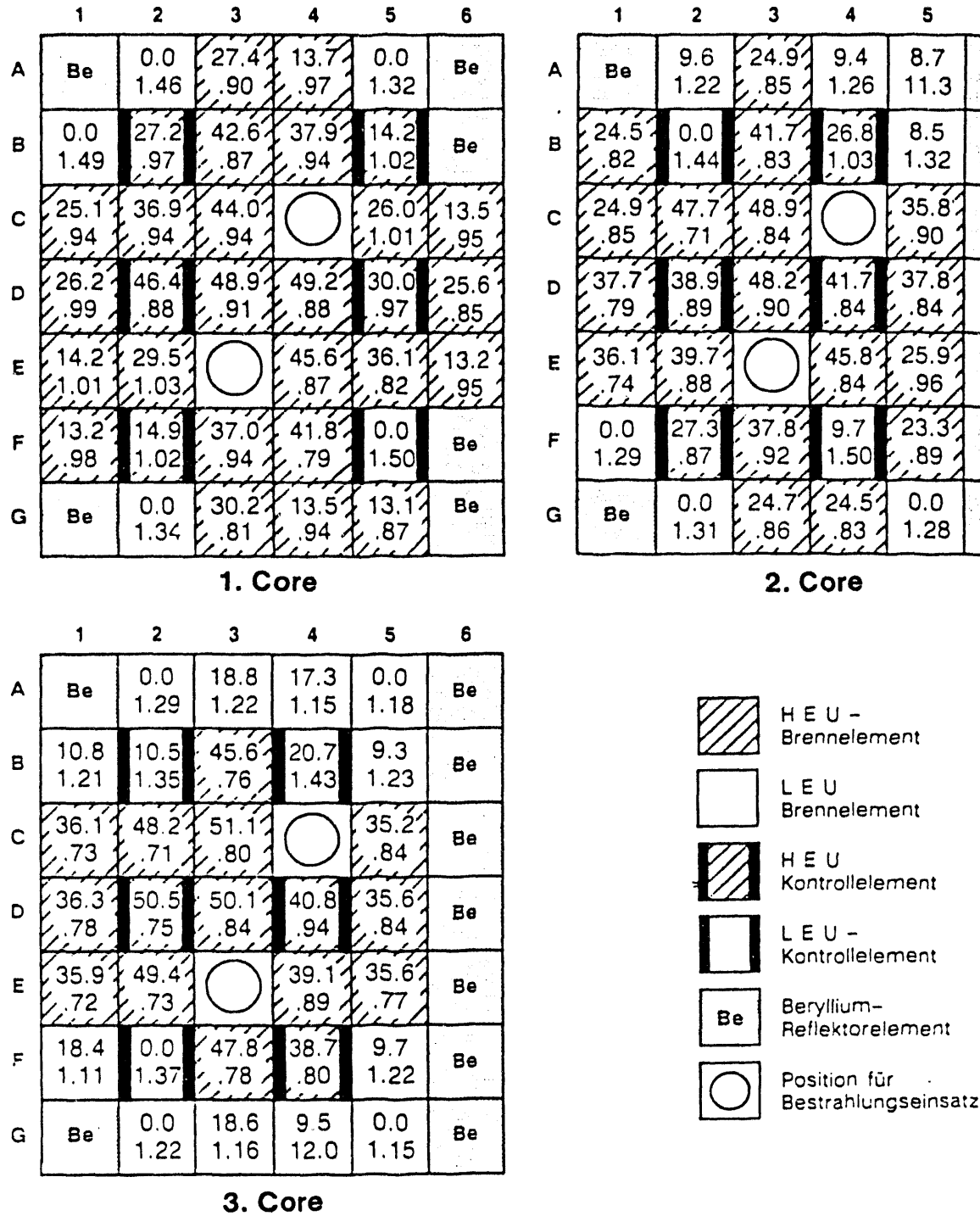

Three HEU-LEU Mixed Cores During HEU-LEU Conversion

Figure 3

After the life time of the transition cores, enough fuel elements of different amounts of burn-up are produced to enable an arrangement of a LEU core for full power operation.

The mixed HEU-LEU cores seem to be a very economic solution. But questions arise concerning the power density distributions. One finds jumps in the power density factors from HEU elements to the neighboring LEU elements because of the difference in the U-235 content. However, this has to be checked very carefully, also for the case of a faulty control rod drive. Each deviation of a control rod from the mean average position of the other rods would increase the difference in the power density factors. Limits have to be evaluated, otherwise the power has to be reduced.

The report describing the operation of a standard and a compact LEU core is completed and represented to the licencing authority. But some questions concerning the operation of a mixed HEU-LEU core under steady-state and transient conditions have to be investigated in more detail.

Licencing procedure

The local authority is already in contact with their technical advisor "Technical Supervisory Association" (TüV) to verify the safety report and the "Nuclear Safety Organisation" (GRS) for questions concerning the safeguards. Then she has to decide whether to issue the licence directly or to ask the public for comments which will be discussed at a public hearing. The scale for such a decision is the amount of gain in reactor safety mainly. There is no question that the introduction of LEU would not reduce the reactor safety. In the case of the BER II the amount of the weight of total U-235 is limited to a certain value which corresponds to the number of storage places. Now for LEU this value has to be increased because of the higher uranium load by a factor of about 2. It is to be decided by the local authority whether this is within public interest. After the licence has been issued it is expected that opponents will bring suit against the authority. The Supreme Court of Administration has then to decide in an accelerated procedure first, whether to stop the execution of the licence and in a second action if the issue of the licence is legal.

Licencing problems

In Germany a licence is issued according to a set of different rules and guidelines. Normally, they are worked out and can be applied only for nuclear power plants. In the case of research reactors there are always problems to apply those regulations. But the local authorities can decide how to interprete the regulations. Essential today is the back end of the fuel cycle for nuclear power plants. But the German authorities feel responsible to the public to include also the research reactors, concerning this question.

Since 1988 the US-DOE refuses to take back the fuel which they had supplied and no other facilities are available. For instance AEA and Cogema are not able to reprocess LEU material from the MTR fuel type at the moment. That means that the back end of the fuel cycle is open. Under these circumstances the local authority will not agree to start with the operation of LEU at the BER II.

It is quite of interest to remember the intention of INFCE to reduce the amount of weapon-grade material in the world. The US-DOE often published their nuclear policy in the Federal Register to support the intention of INFCE. But the realization of the INFCE conclusion is blocked now by the US-DOE policies by not accepting the fuel from the BER II. HEU and LEU materials are both concerned. The back end for the BER II

HEU material is not closed either, and the BER II cannot introduce LEU for the same reason.

Germany had started its own investigation to close the back end of the fuel cycle by developing a program for a long term interim and final storage of research reactor fuel in Germany without the possibility of reprossessing. But the realisation does not only depend on the solution of the technical and financial questions, it depends also on the necessary licences. As long as this procedure is not settled it will not be accepted as an alternative way for the solution of the back end of the LEU fuel cycle.

Time scale

Suppose there would not be any questions concerning the back end of the fuel cycle, then a time scale for the introduction of LEU is of interest. The approval of the technical concept by the TÜV will be expected by April 1993. If a public hearing cannot be avoided, this would take place in the summer of 1993. The licence could be issued by the end of 1993. Without the public hearing the licence could be issued in the summer of 1993. Fresh LEU fuel elements cannot be ordered before the iussue of the licence. The time for fabrication is assumed to be more than 1 year. This sums up to a delivery date late in 1994 and the first LEU core test could be in 1995.

But as long as the back end of the fuel cycle is not closed, the licence for the operation of LEU will not be issued.

Conclusion

The Hahn-Meitner-Institut has not applied for the conversion from HEU to LEU material but for the introduction of an alternative fuel to HEU, which means LEU. If the licence is issued it will decide later, whether it will use HEU or LEU depending on the situation on the site of the supply of fuel or the site of the back end of the fuel cycle. The Hahn-Meitner-Institut would follow the INFCE intention but sees no other way to continue the reactor operation for the users community as long as Germany depends on unforeseen foreign interests.

GREEK RESEARCH REACTOR PERFORMANCE CHARACTERISTICS AFTER ADDITION OF BERYLLIUM REFLECTOR AND LEU FUEL

by

J. R. Deen and James L. Snelgrove

Argonne National Laboratory
Argonne, Illinois, USA

and

C. Papastergiou

National Center for Scientific Research
Athens, Greece

ABSTRACT

The GRR-1 is a 5-MW pool-type, light-water-moderated and-cooled reactor fueled with MTR-type fuel elements. Recently received Be reflector blocks will soon be added to the core to add additional reactivity until fresh LEU fuel arrives. REBUS-3 xy fuel cycle analyses, using burnup dependent cross sections, were performed to assist in fuel management decisions for the water- and Be-reflected HEU nonequilibrium cores. Cross sections generated by EPRI-CELL have been benchmarked to identical VIM Monte Carlo models. The size of the Be-reflected LEU core has been reduced to 30 elements compared to 35 for the HEU water-reflected core, and an equilibrium cycle calculation has been performed.

INTRODUCTION

The Reduced Enrichment Research and Test Reactor (RERTR) Program and the National Center for Scientific Research "Demokritos" initiated a new joint study program in 1991 to investigate the conversion of the Greek Research Reactor (GRR-1) from HEU to LEU fuel. This study is a continuation of a previous joint study[1] completed in 1981. This paper presents the results of modeling the current HEU core operations and the core changes expected upon adding a new Be reflector on two core faces. Since LEU fuel is not expected before August 1993 and fresh HEU fuel supplies are very low, some attention is being devoted to fuel cycle strategies to increase the lifetime of the Be-reflected HEU core. One equilibrium Be-reflected LEU core design will be presented that has fuel cycle characteristics similar to the current HEU core. In addition to providing guidance on fuel management strategies, these preliminary calculations will provide fuel element loadings for use in analyzing the transition to an LEU core.

GRR-1 CORE AND FUEL CHARACTERISTICS

The GRR-1 is a 5-MW pool-type, light-water-moderated and -cooled reactor fueled with MTR-type HEU fuel elements. The core consists of 29 or 30 standard fuel elements and six control fuel elements. Each standard element consists of 18 flat fuel plates, and the control elements have ten fuel plates. A Ag-In-Cd control rod is inserted into the center of each control element. In the future the core will be used for various isotope production projects and Si-doping. The dimensions of the fuel plate and coolant volume of the proposed LEU fuel element are identical to those of the existing HEU design. A comparison of HEU and LEU fuel element characteristics is presented in Table 1.

TABLE 1
STANDARD AND CONTROL FUEL ELEMENT CHARACTERISTICS

DESIGN PARAMETER	STANDARD		CONTROL	
	HEU	LEU	HEU	LEU
Enrichment, wt. %	93	19.75	93	19.75
Fuel Meat Composition	UAl	U_3Si_2	UAl	U_3Si_2
^{235}U/Element, g	180.8	222.2	100.3	123.4
Number of Plates/Element	18	18	10	10
Plate Thickness, cm	0.152	0.152	0.152	0.152
Fuel Meat Thickness, cm	0.050	0.076	0.050	0.076
Clad Thickness, cm	0.051	0.038	0.051	0.038
Water Channel Thickness, cm	0.290	0.290	0.290	0.290

THE FUEL CYCLE ANALYSIS MODEL

The fuel cycle analyses were performed using REBUS-3 with five neutron groups in xy geometry.[2] The increased accuracy that would be gained by the use of three-dimensional analyses would be small for the GRR-1 because of its low discharge fuel burnup. The burnup-dependent microscopic cross sections were obtained from a slab geometry representation of important core materials using EPRI-CELL.[3] Based on previous studies, the side plate was separated from the fuel-clad-moderator zone to provide more accurate reactivity and power peaking predictions from the diffusion theory model. The fuel zone cross sections were found to be in excellent agreement with those obtained from a VIM[4] Monte Carlo calculation of the fuel cells using ENDF/B-IV data.

Modeling of ex-core materials consisted of representing the graphite thermal column and the Pb gamma shield located between the core face and the thermal column. Other ex-core

features, including experiments, beam tubes, and irradiation rigs, were omitted from this model because of insufficient information. We believe this simplified model is sufficiently accurate for this stage of the study.

An estimate of the reactivity bias of the fuel cycle model was obtained from an xyz diffusion theory model of an all-fresh GRR-1 startup core configuration 4B-2. With control rods at their critical positions, k_{eff} was calculated to be 1.010. This overprediction in reactivity is probably caused by inaccuracies in radial and axial ex-core material descriptions as well as by the diffusion model itself. This reactivity bias has been adopted for all fuel cycle analyses. The extrapolation distances for the planar fuel cycle model were obtained from this fresh fuel startup core calculation.

ANALYSES OF THE HEU WATER-REFLECTED CORE

^{235}U loadings for each element in core and in the storage pools were provided by the GRR-1 staff and used to model the actual HEU core fuel cycle beginning on October 26, 1990. The core consisted of 29 HEU standard elements and six control elements arranged as shown in Fig. 1. The GRR-1 ^{235}U loadings were used in conjunction with an EPRI-CELL depletion model of the standard and control elements to obtain a complete set of fuel isotopics for each element in the core.

The operation of the October 26, 1990 core was followed for 6.66 fpd, after which a fresh fuel element was added and the highest burnup fuel element was discharged. This refueled core was depleted for an additional 22.61 fpd and shut down on May 31, 1991. At this point a spent fuel element was added to the core in position D-6 without discharging any fuel. This increased the core size to 30 standard elements and six control elements and the ^{235}U core loading by 126 g. This core configuration has remained unchanged to date. The current operation schedule has been significantly reduced due to the shortage of additional HEU fuel supplies.

The typical operation schedule for a week at the GRR-1 consists of full-power operation for five to six hours per week day; the reactor is shut down at all other times. From the exact shutdown and operation intervals, the core excess reactivity was calculated for June 3-7, 1991 using the REBUS fuel cycle model. The calculated core reactivities at the beginning and end of each irradiation day are compared to hypothetical equilibrium steady-state operation over the same period in Fig. 2. On Monday morning, with ^{135}Xe at its lowest level of the week, the core $k_{eff} = 1.066$. At the end of the day, the core reactivity has fallen to $k = 1.060$ due to the buildup of ^{135}Xe. For the remainder of the week, the core reactivity increases during the day due to the burnout of ^{135}Xe accumulated during the preceding night's shutdown period. During the week the startup excess reactivity decreases each day except Friday, when a slight increase in excess reactivity has been observed at the GRR-1 and predicted using this model. From these results, shown in Fig. 3, one can also note that the GRR-1 never reaches equilibrium ^{135}Xe. The ^{149}Sm concentration changes very little and remains between saturation and equilibrium values during the entire week, as shown in Fig. 4. This operation schedule, with short irradiation intervals and relatively long shutdown periods, maintains poison concentrations low enough to provide the excess reactivity required for continued operation.

HEU Water Reflected GRR-1 Reference Core 4B-13

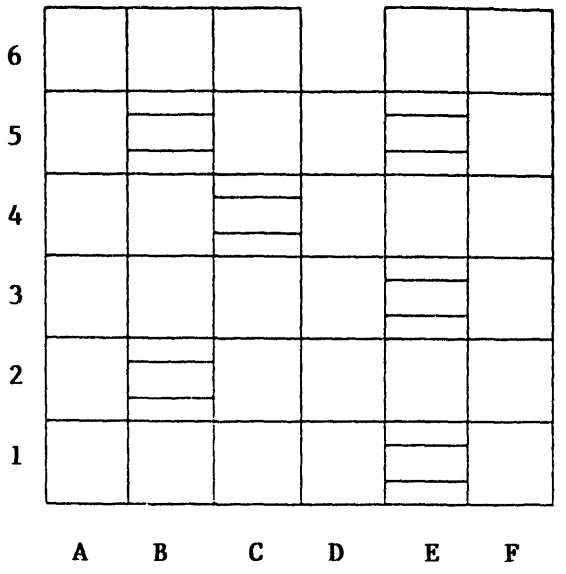

Figure 1

GRR–1 REBUS Reactivity During June 3–7,1991

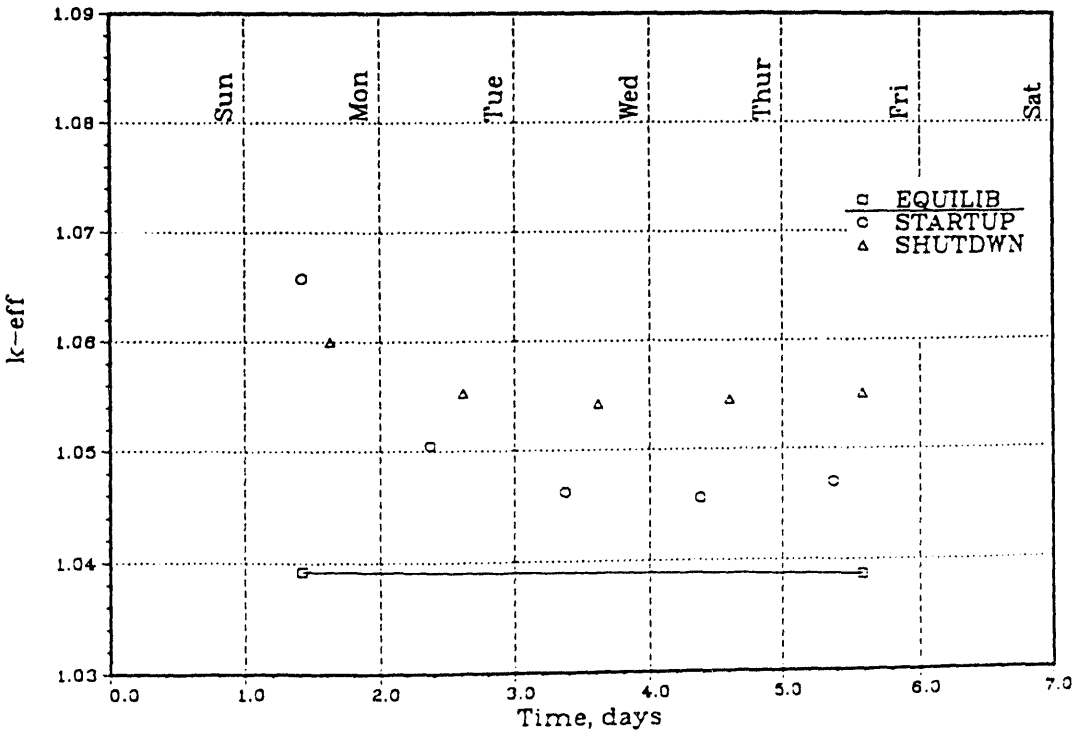

Figure 2

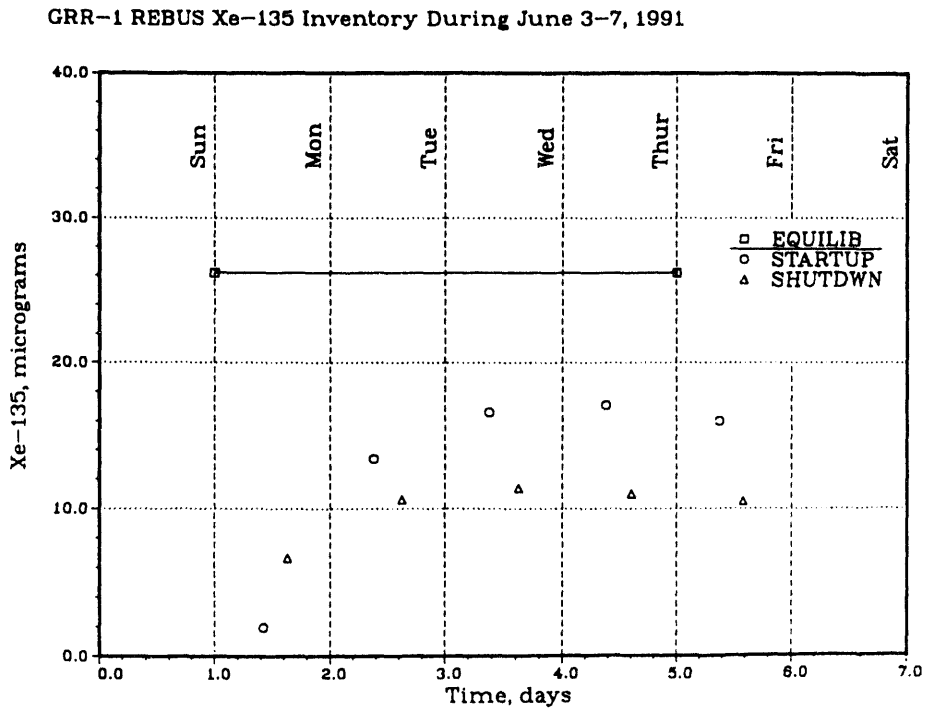

Figure 3

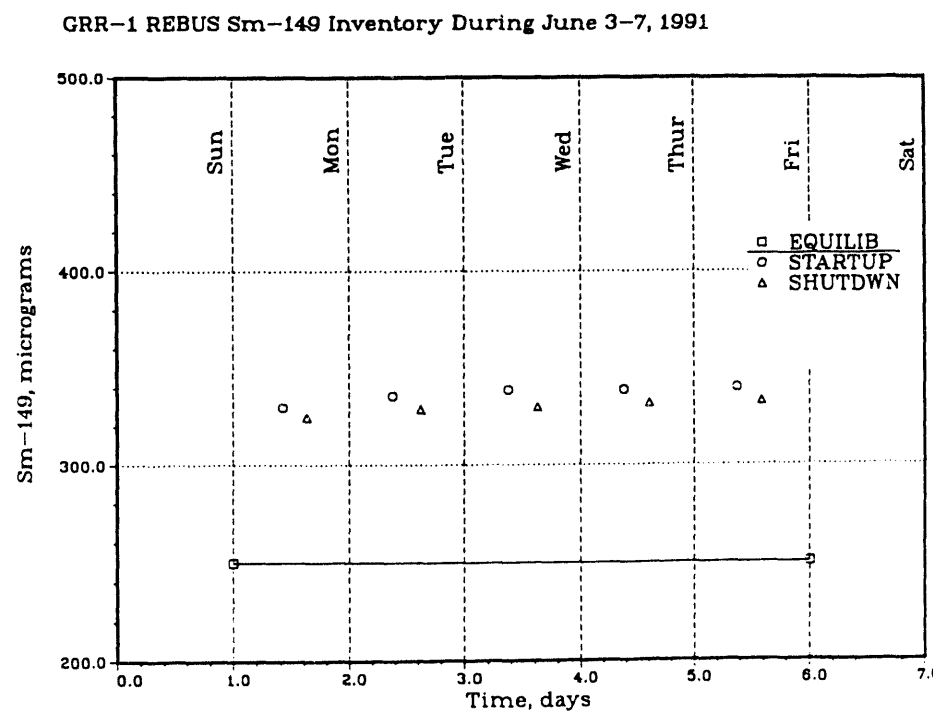

Figure 4

ANALYSES OF THE HEU Be-REFLECTED CORE

The actual depletion of the current water-reflected core has been modeled up to the current time and projected to January 1, 1993, assuming only 50 MWh of operation per week in order to conserve fuel. The Be blocks were received during this past summer and are expected to be positioned as shown in Fig. 5. The core size will be reduced from 30 standard and six control elements to 25 standard and five control elements by removing the highest-burnup elements. This Be-reflected core has an excess reactivity at startup of k_{eff} = 1.0382, which is very close to the beginning of cycle reactivity of an HEU water-reflected equilibrium core. This core loses about 85¢ in reactivity for each 10 fpd of operation. Therefore, the Be-reflected HEU core can be operated on the reduced operation schedule with the remaining fresh HEU fuel inventory until the summer of 1993 when the LEU fuel supplies arrive. If it should be deemed necessary to substitute an additional control element for a standard fuel element, approximately $2 in reactivity would be lost. Other fuel cycle options that might prove necessary would be an increase in core size using previously discharged fuel elements.

ANALYSES OF THE LEU Be-REFLECTED CORE

An equilibrium fuel cycle calculation of a preliminary LEU core configuration, shown in Fig. 6, has been made. One fresh standard element was loaded at the beginning of each cycle, and one control element was loaded at the beginning of each fourth cycle. The total residence time for all fuel was 24 cycles. The cycle length was chosen to be 10.3 days with a core consisting of 24 standard fuel elements and 6 control elements. The smaller LEU core has the same excess reactivity at the beginning and end of the cycle and the same cycle length as the reference water-reflected HEU equilibrium core. The power peaking in the LEU core has increased by 20%, which is inversely proportional to the core size decrease. The equilibrium discharge burnup in the LEU core was reduced to 24%. This core represents an initial attempt to design a replacement LEU core. If the LEU number of elements was reduced by removing one standard element in location C-6 in order to provide an in-core irradiation position, the core reactivity would be reduced by $2.5 for the same cycle length. Another option would be to remove one control element to provide an in-core irradiation position, in which case the reactivity penalty would be decreased.

HEU Be Reflected GRR-1 Core

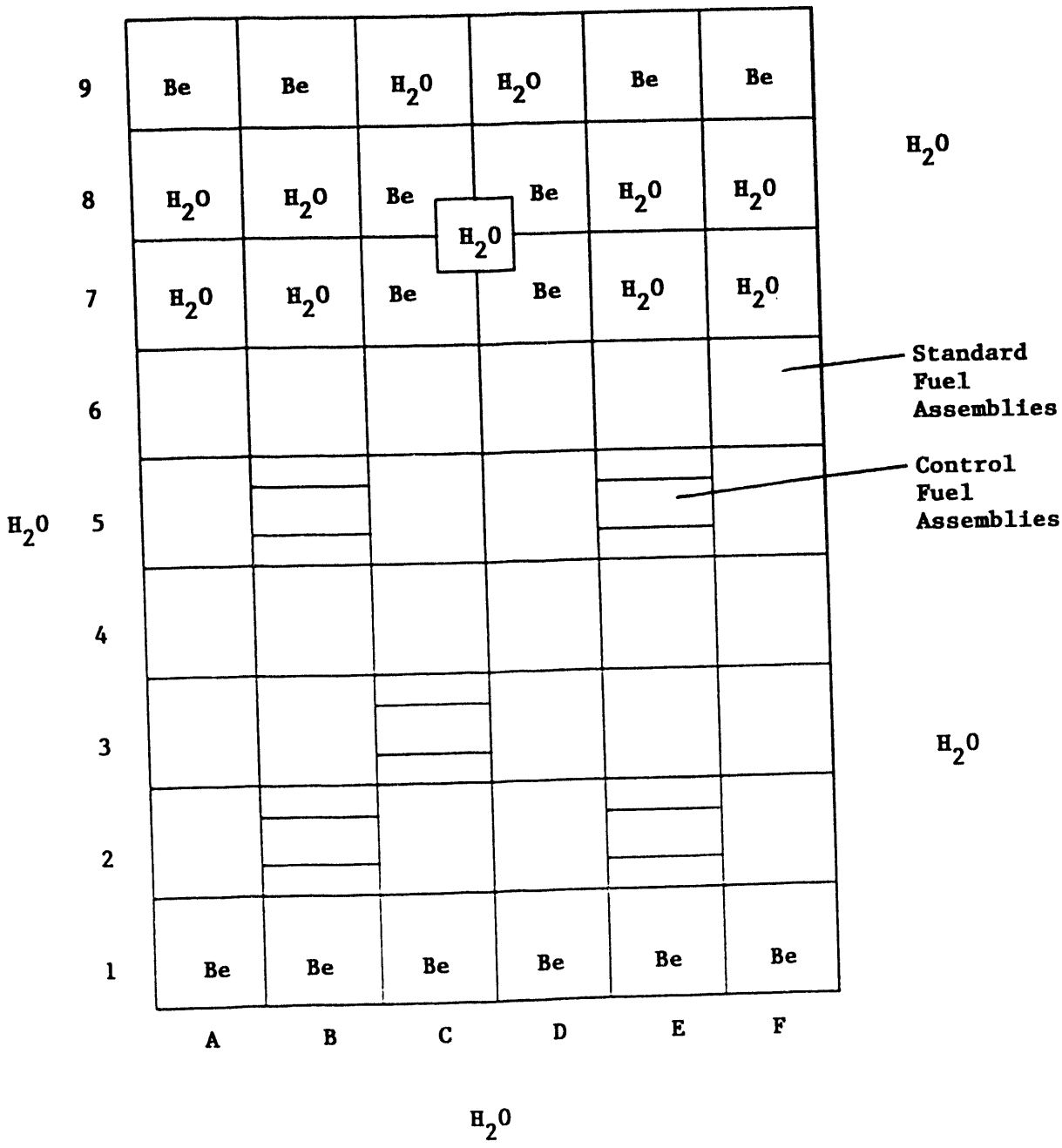

Figure 5 Be Core HEU Configuration with 25 + 5 Elements

LEU Be Reflected GRR-1 Core

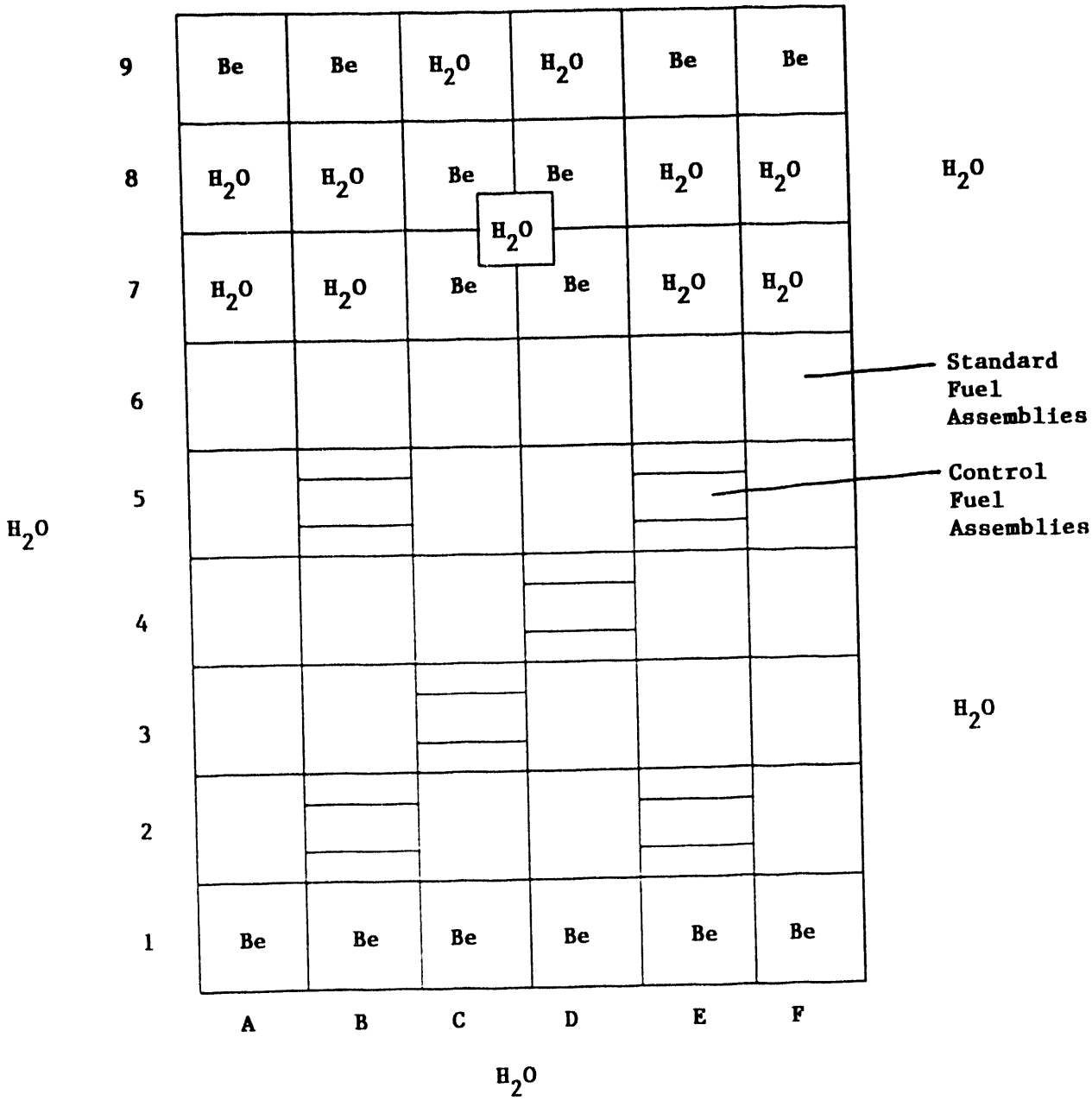

Figure 6. Be Core Configuration With LEU Fuel 24 + 6 Elements

Locations of experimental facilities will significantly affect the final core configuration. The reactivity performance could be increased without a change in core size by replacing one control element with a standard element if the core can be adequately controlled using five control elements.

CONCLUSIONS

The GRR-1 has had to significantly reduce its operation schedule caused by a shortage of fresh HEU fuel. Once all the necessary preparations for installation of the Be reflector for the HEU core have been completed, additional reactivity can be added to extend the core lifetime until LEU fuel arrives next summer. The use of the reactor for isotope production and Si-doping will significantly affect the final decision regarding the most suitable LEU core configuration. The issues of transition from HEU to equilibrium LEU cores by the addition of one element per cycle must also be addressed.

REFERENCES

1. C. Papastergiou and J. Deen, "Neutronic Calculations for the Conversion of the GRR-1 Reactor from HEU Fuel to LEU Fuel," unpublished ANL report, (November, 1981).

2. B. J. Toppel, "A User's Guide for the REBUS-3 Fuel Cycle Analysis Capability," ANL-83-2, (March, 1983).

3. B. A. Zolotar, et al., "EPRI-CELL Code Description," Advanced Recycle Methodology Program System Documentation,", Part II, Chapter 5, (September, 1997).

4. R. N. Blomquist, "VIM - A Continuous Energy Neutronics and Photon Transport Code," pp. 222 - 224, ANS Proceedings of the Topical Meeting on Advances in Reactor Computations, Salt Lake City, Utah, (March 28 - 31, 1983).

S E S S I O N IX

October 1, 1992

UTILIZATION OF CONVERTED REACTORS

Chairman:

J.W. Schreader
(AECL Research, Canada)

HEU AND LEU MTR FUEL ELEMENTS AS TARGET MATERIALS FOR THE PRODUCTION OF FISSION MOLYBDENUM

A. A. Sameh, A. Bertram-Berg, Nuclear Research Center Karlsruhe, Cyclotrone Laboratory, P.O. Box 3640, D-7500 Karlsruhe, GER

Introduction

The processing of irradiated MTR-fuels for the production of fission nuclides for nuclear medicine presents a significantly increasing task in the field of chemical separation technology of high activity levels. By far the most required product is Mo-99, the mother nuclide of Tc-99m which is used in over 90% of the organ function tests in nuclear medicine. Because of the short half life of Mo-99 (66 h) the separation has to be carried out from shortly cooled neutron irradiated U-targets. The needed product purity, the extremly high radiation level, the presence of fission gases like xenon-133 and of volatile toxic isotopes such as iodine-131 and its compounds in kCi-scale require a sophisticated process technology.

An important aspect, which has also be considered in a modern production plant, is the treatment of the process waste streams and the recycling of the uranium, as the accumulation of larger amounts of this sensitive material, especially in case of HEU, cannot be recommended for safeguard and economic reasons. The adaptation of technologies as practised in the reprocessing of mixed oxide fuels from nuclear power stations cannot be generally recommended either for several reasons:

- The expected cooling times of the fuel used for Mo-production are by far less than those of the mixed oxide fuel. This can cause serious problems in offgas treatment and extracting agent degradation.
- High installation and running costs for the relative small scale batches of the Mo-plant
- Spreading of plutonium know how technology.

In this publication data will be presented that show the advances in the KFK-molybdenum production and fuel recycling process, as well as results for the first successful hot runs with LEU-fuel targets of uraniumsilicide in 100 Ci scale. The included fuel recycling conception demonstrates the possibility of avoiding plutonium technology.

These results were obtained by a development program which was started 1987 to solve the problem of the chemical resistency of uraniumsilicide which can be used as a target material with high fuel density for the production of fission molybdenum.

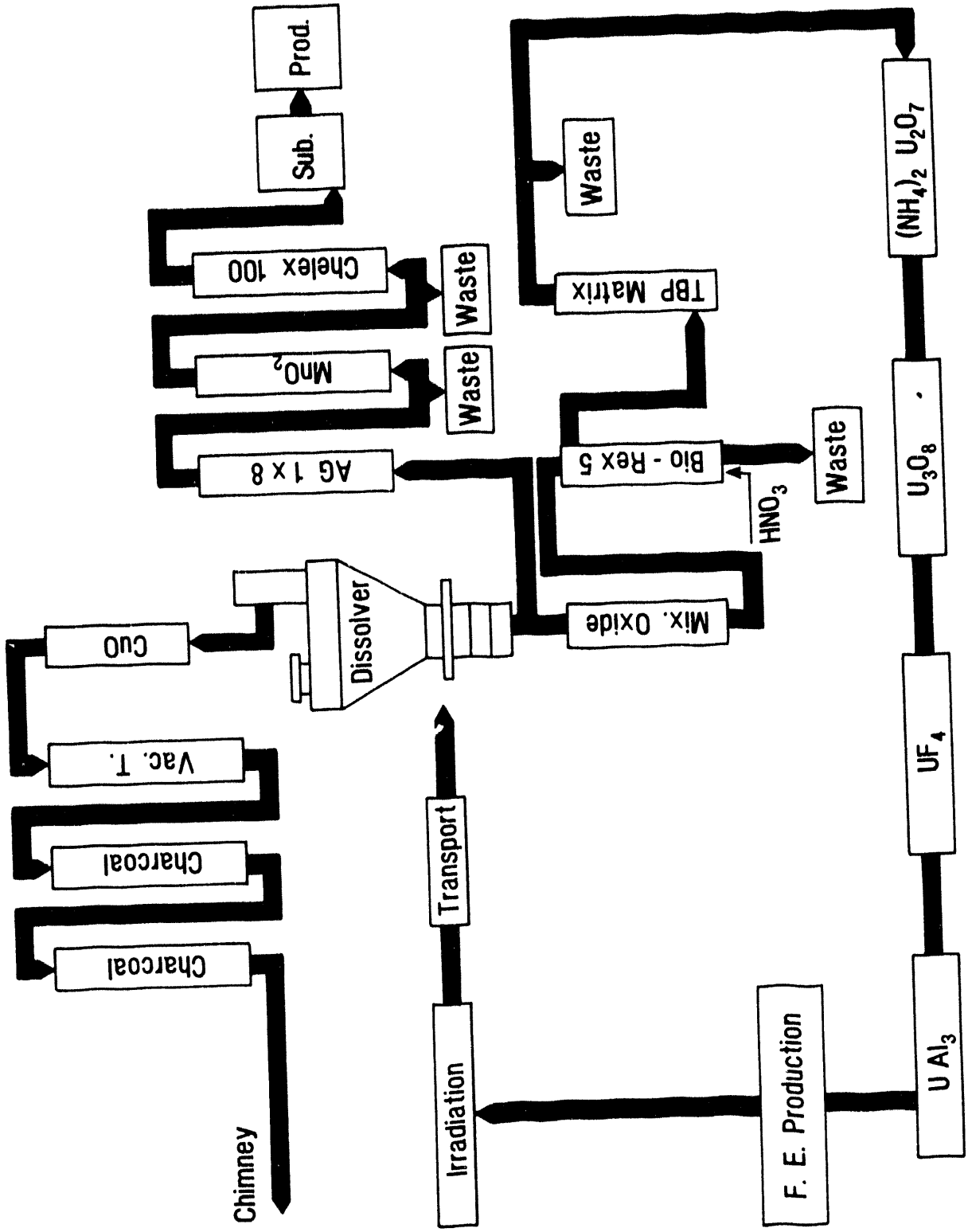

Fig. 1: Scheme of the KfK fission molybdenum production cycle from irradiated UAl_x targets

The achievement of this aim would allow the replacement of HEU by LEU in the Mo-production. An important aspect which had to be taken into account, was, that all modifications in the process could be adopted economically and without significant changes in the installation hard wear for the existing KfK production cycle from UAl_x targets [1], as shown in figure 1.

Another aim of this program was the development and demonstration of an efficient chromatographic system for the selective separation and purification of iodine from the acidic streams of the molybdenum production process. The realization of this aim would have two benefits, higher process economy due to optimizations in the waste treatment costs and additional income from iodine-131 selling.

Production cycle of fission molybdenum

Preparation of the uraniumsilicide alloy

The uraniumsilicide was produced by melting uranium and silicon metal together at 1850°C in an argon gas atmosphere.

According to realistic production conditions the U-metal preparation had to be started from U_3O_8 generated from the calcination of yellowcake, which presents the last chemical step of the uranium purification process.

The uranium oxide was transfered to a nickel crucible and converted to the tetrafluoride by treatment with a gas mixture of hydrogen and hydrogenfluoride in an argon gas atmosphere at 650°C. The reaction was carried out in a nickel oven. The UF_4-powder was then converted to KUF_5 by melting the tetrafluoride with the stochiometric amount of potassiumfluoride in the same oven at 850°C. Due to the high chemical reactivity of this system, the conversion to KUF_5 was carried out in a graphite crucible. The product was powdered and added in small portions to a melting electrolyses bath containing a salt mixture of 50 weight% NaCl and $CaCl_2$, in which the graphite crucible was the anode. A molybdenum sheet was used as the cathode. The process was carried out in an argon gas atmosphere at 800°C. After the electrolysis the uranium carrying cathode was washed in an ultrasonic bath subsequently with ethylalcohol containing few percents of water and cold water to dissolve the salts accompanying the uranium. The dried U-powder was finally melted with silicon to U_3Si_2.

Production and irradiation of the MTR-fuel target

The alloy was transfered into a glove box line in which the U_3Si_2 was grinded in a hard metall swinging mill. Only particles with grain sizes below 40 micro meters were mixed with aluminium powder of the same particle size. Aliquots of this mixture were pressed

at 8 t/cm^2 to rectangles of 40 x 30 mm^2 and 2.5 mm thickness.

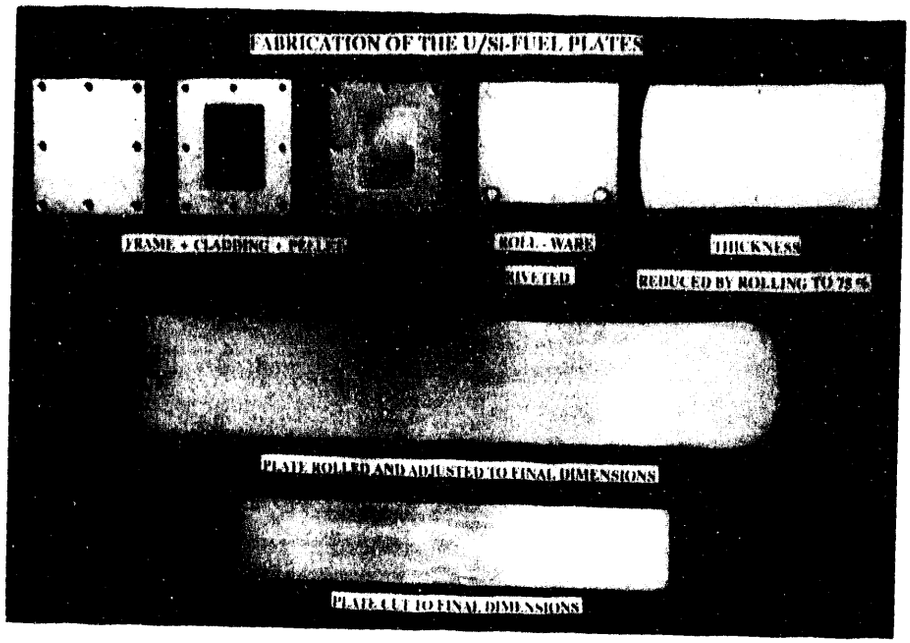

Fig.2: Procedure for the production of the uranium silicide target starting with the pressed rectangle fuel meat

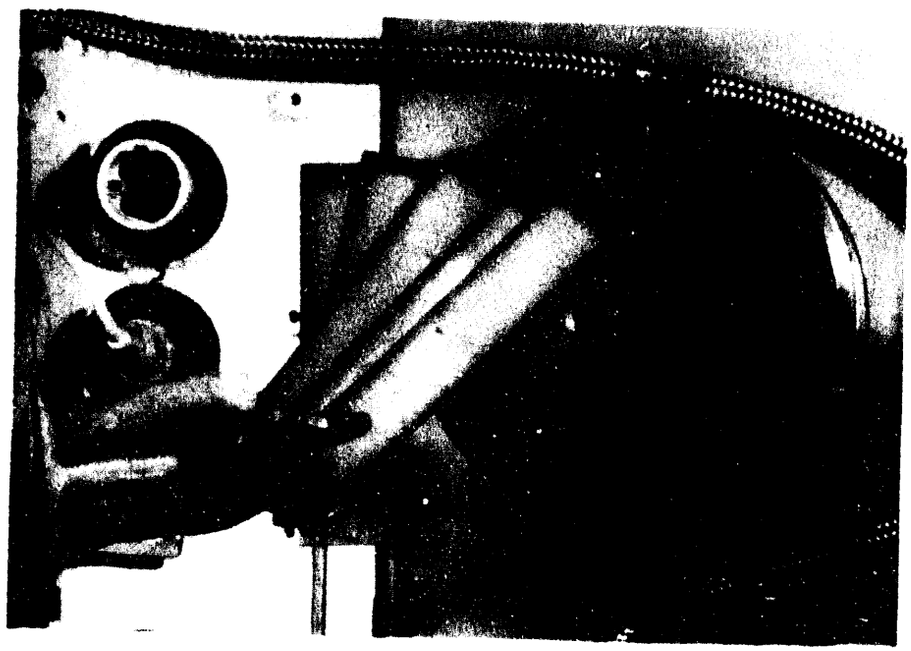

Fig.3: Photograph of five irradiated uranium silicide plates containing LEU after five days of irradiation. The U-enrichment degree was 19,75%, the U-densitiy was 2.3 g/cm^3

Each rectangle was put into a suitable frame of an aluminium-magnesium alloy (AlMg1). Each meat rectangle was then covered with AlMg1 plates, the whole package was riveted and rolled to a final thickness of 1.3 mm. All mentioned steps were carried out in argon atmosphere. Figure 2 shows the described procedure with pictures for the target production.

After passing through the same quality control tests as common MTR-fuel plates, the targets were irradiated for five days in thermal neutron fluxes of approximately $1x10^{14}$ n/sec^1cm^2 in a forced cooled loop. After the plates had been removed from the reactor, they were cooled for 12 hours and then transported to the production plant where they were processed. Figure 3 shows a batch of five irradiated plates before the dissolution.

Chemical process for the molybdenum separation

The Mo-separation is started by an alkaline digestion process in 6 M KOH. During this procedure aluminium and several fission products which are located on the surface of the unsoluble silicide particles are dissolved. These are mainly the alkaline and alkaline earth cations as well as iodine, tellurium and molybdenum. Experiments have shown that only between 10 and 20 % of their content in the target are released that way.

The offgas of the alkaline digestion contains the hydrogen generated from the aluminium dissolution and the magnesium conversion to the hydroxide together with the equivalent amount of the fission noble gases. The major radioactivity of this gas stream is caused by xenon-133. The noble gases leave the dissolver at its upper end driven by nitrogen, which is constantly metered into the dissolver together with the hydrogen. The hydrogen is oxidized to water via a copper oxide oven. The resulting water is condensed. Xenon is collected together with the nitrogen in preevacuated stainless steel tanks and later on pumped to the xenon delay section passing deep bed carbon filters.

The alkaline solution containing molybdenum is sucked out of the dissolver through a stainless steel filter and enters a column filled with the strong basic exchanger AG1X8 (200-400 mesh, BioRad (USA)) which had been transfered into the OH^--form prior to use. The molybdenum is retained quantitatively on the stationary phase.

In comparison with the digestion of UAl_x containing targets in which quantitative conversion is achieved, U_3Si_2 presents an extremly resistent compound. It is, as already mentioned, not significantly reacting with the caustic solution so that approximatly 85% of the generated fission nuclides, including molybdenum still remain in the residue after filtration [2].

For this reason this residue is treated with a mixture of HF, H_2O_2 and KJO_4 at 20°C. After 30 minutes potassium hydroxide is added to the dissolver until a total molarity of approximately 1 M KOH in the whole system is achieved. The solution is boiled for 30

minutes to drive out the H_2O_2 and then cooled to a temperature of 40 °C. This alkaline solution now contains all the molybdenum and the same fission nuclide impurities as in the case of the alkaline digestion solution only in higher content.

The attack of the silicide presented the main task of the investigations. They led to the development of a new process [3] which permits an efficient and quick chemical conversion of the uranium silicide, so that the previously in the crystals of the alloy enclosed fission nuclides are released. It will be described in more detail in the following part of the publication. The description of the whole Mo-production process will be continued afterwards.

Catalytic conversion of the uraniumsilicide alloy

The chemical principle of the newly developed dissolution system which consists of a mixture of HF, H_2O_2, KJ is based on the catalytic oxidation of the uranium to UF_4 by the reaction between the silicide and hydrogen fluoride. Uranium tetrafluoride is forming an unsoluble layer wrapping the uranium silicide particles and prevents, together with the generated hydrogen bubbles, the penetration of HF to the alloy. Beside this, the generated hydrogen bubbles hinder the H_2O_2 to oxidize the U^{+4} to U^{+6} before its decomposition on the surface of the fine residue. Only the presence of iodine eliminates these drawbacks. The hydrogen generated during dissolution is oxidized by the iodine. The formed iodide is immidiately oxidized back by the H_2O_2 to J_2, which is again oxidizing the U^{+4} to U^{+6}. The use of iodine compounds in higher oxidation states such as KJO_4 accelerate in the beginning the uranium oxidation and its conversion. The optimum process conditions were determined in several experiments in which relevant parameters such as the contact time between the solid and aqueous phase, the H_2O_2, the HF, and the catalysator concentrations were varied.

The determination of the conversion yields was carried out in the following way. At the end of each experiment the reaction was stopped by adding a surplus amount of KOH soluuon to the system. The liquid phase was separated by centrifugation. The residue was washed several times with diluted KOH and the liquid phase separated as above mentioned. At last the residue was treated with boiling 3 M HNO_3 for few minutes, which dissolved the formed diuranate precipitate immidiately. The dissolved uranium amount is identical with the converted silicide amount. The uranium concentration was determined via spectral photometry and the converted uranium amount by comparing the uranium amounts before and after treatment with the oxidizing HF mixture. The presence of a dark residue was a clear hint for unconverted silicide crystals. Figure 4 shows the influence of the potassium periodate concentration in the HF/H_2O_2 mixture on the uranium conversion after the treatment of the silicide residue.

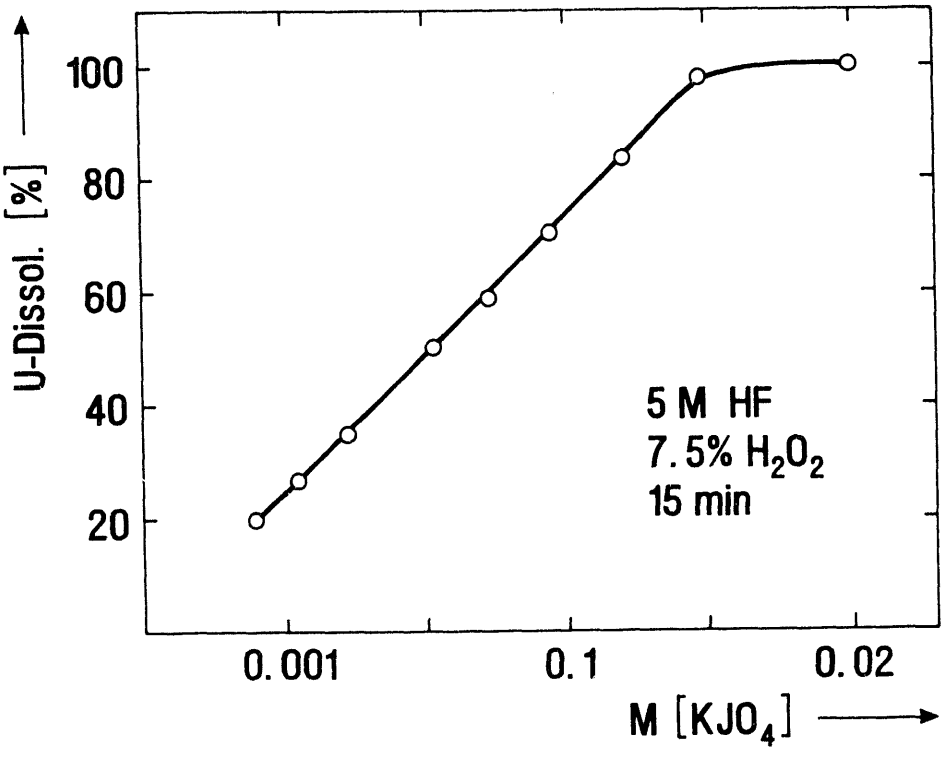

Fig.4: Influence of the KJO_4 concentration on the dissolution yield of U_3Si_2 in a mixture of 5M HF and 7.5 vol% H_2O_2, contact time 15 min, temperature 20°C

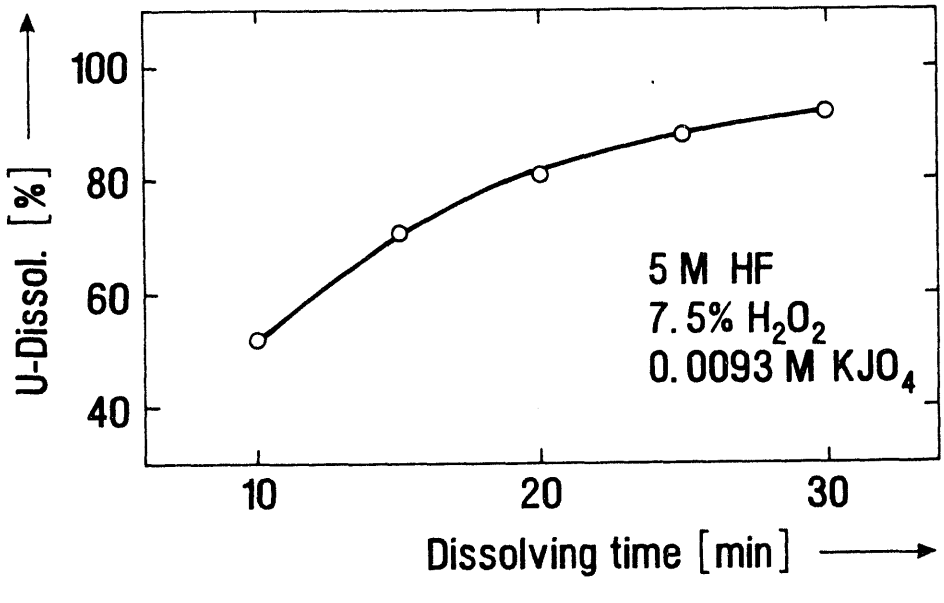

Fig.5: Uranium dissolution yield as a function of the contact time between U_3Si_2 and a solution containing 5M HF, 5 vol% H_2O_2 and 0.0093 M $KJIO_4$ at 20°C

The curve shows the significant influence of the periodat respectively iodine content in liquid mixture for the conversion of the U_3Si_2 residue. It also shows, that under these conditions, a periodat molarity of 0.015 M is already sufficient to complete the conversion.

Another relevant parameter for process operation is the needed contact time between the silicide residue and the aqueous phase to obtain complete conversion of the alloy. For this task several experiments were carried out. To increase the accuracy of the expected data the iodine, respectively jodate content in the solution was lowered to extent the time needed for quantitative conversion. Figure 5 shows the uranium solubility progress as a function of the contact time between U_3Si_2 and a mixture of HF, H_2O_2 and KJO_4.

Continued description of the chemical process for the molybdenum separation

After the igestion of the silicide KOH had been added to precipitate U and most of the fission products. After filtration the alkaline solution is passed through the already partially loaded AG1 column where the molybdenum is retained again. After washing the column subsequently with 3 M KOH and water, the molybdenum is eluted quatitatively with HNO_3 or $HNO_3/NaNO_3$ solution. The choice of the eluent concentration depends on the process conception. In case iodine shall be separated, the acid concentration has to be lowered and the salt content has to be increased. The need for iodine separation in this part of the process can be caused by:

- Waste treatment restrictions against the storage of high iodine activities on organic materials such as the anionic exchanger
- Commercial interest for J-131. In case of the need for high specific activities, the iodine has to be eluted from the fission product batch obtained by the digestion step or from the iodate breakthrough of the first AG1 loading step.

Selective Iodine separation

The eluate of the AG1 column is collected in a stainless, offgas controlled vessel. After adding of a solution of $NaNO_2$ in water, the mixture is passed through a column of a nonpolar macroporous matrix of polystyrenedivinylbenzene such as Lewatit 1023 (product of Bayer Leverkusen, Germany) or the Bio-Beads Adsorbents SM-2, SM-4, SM-16 (Bio-Rad Richmond, California, USA) or the slightly polar macroporous matrix of acrylic ester SM-7 (Bio-Rad). Iodine is retained on these stationary phases quantitatively in form of the element.

The advances of this new development [4] are extremely high efficiency and selctivity for iodine adsorption. Figure 6 shows the iodine retention behaviour on Lewatit 1023 and

SM-7 from a dynamic aqueous phase of 1 M HNO_3 containing preadded $5x10^{-6}$ mol/ml KJ and $5x10^{-6}$ mol/l $NaNO_3$. The iodine determination was carried out by γ-spectroscopy of a I-123 indicator.

The results underline the advantage of SM-7 in comparison with Lewatit 1023 which was, under these conditions, even at low iodine loading degrees not able to retain this element completely.

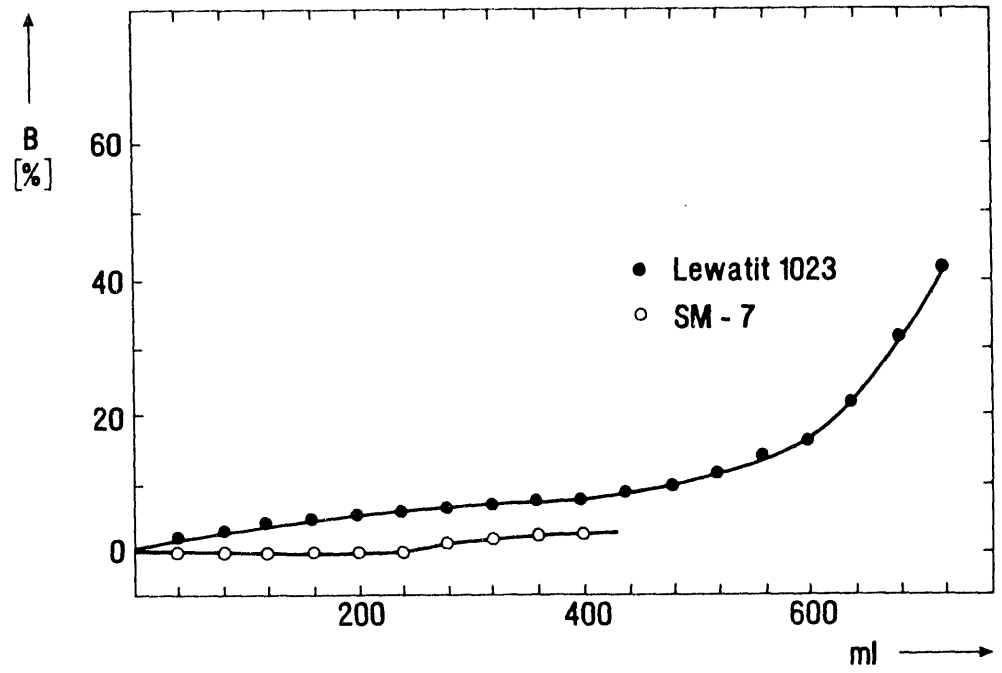

Fig.6: Iodine breakthrough for a Lewatit 1023 and a SM-7 matrix, column inner diameter 9.7 mm , height 100 mm, matrix weight 2 g, particle size 0.2-0.4 mm, loading speed 15 column volumes/h.

In contrary to this, SM-7 retained iodine efficiently. It could not be detected behind the column until 200 ml of the feed solution had passed through the stationary phase. This amount is equivalent to > 80 mg iodine/g matrix.

The mentioned difference between both adsorbers is turning to the opposite if the aqueous solution is contaminated by organic solvents, as in case of nuclear fuel waste streams.

The desorption of iodine from the loaded matrix can be carried out by different organic and inorganic reagents like chloroform, benzen, respectively alkali hydroxides with or without oxidation or reduction agents. Desorption curves with chloroform, 2 M NaOH and 2 M NaOH + 5 vol% H_2O_2 are plotted in figure 7.

The iodine elution with organic diluents can not be recommended in case of high iodine activities beccause of the volatility of the iodine and eventually formed I-organic compounds.

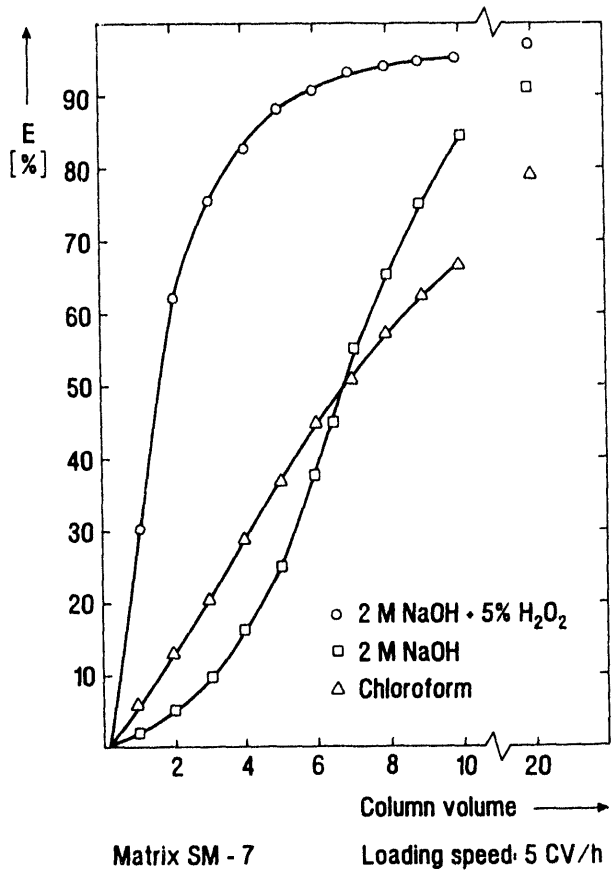

Fig.7: Iodine desorption yield from loaded SM-7 columns, the loading degree of the stationary phase was 80 mg J_2/gSM-7

Mo-adsorption on manganese dioxide and feed adjustment for the chelex-100 column

The iodine free Mo-containing solution running through the J separation column is directly passed through a chromatographic column of manganese dioxide. The material used in these experiments was delivered from Recherche Appliquee du Nord (France) under the trade name of "Manox A". Molybdenum is adsorbed quantitatively on the stationary phase together with the main bulk of the accompanying fission products. Iodine impurities in every oxidation stage as well as anionic species and the alkaline and alkaline earth cations are not retained on the oxide. After washing the oxide with HNO_3 and subsequently with water, the dry column is treated with 10 column volumes of a mixture of ammonia thiocyanate, potassium iodide and sodium sulphite in 2 M sulphuric acid. Suitable concentrations for the added compounds are 0.02 mol/l for SCN^-, 0.04 mol/l for SO_3^{-2} and 0.001 mol/l for the I^-. The feeding of this solution through the column has to be carried out from the bottom to the top. Under these conditions the whole stationary phase including the adsorbed activity is being dissolved. The obtained solution presents the feed of the following chelex-100 column.

The manganese dioxide loading and its complete dissolution combined with the simultaneous adjustment of the feed of the following column is a new process [ ]. It permits:

- Quick and lossfree combination of the AG 1 column with the chelex-100 system which guaratees excellent product purities
- Efficient reduction of the waste ammount generated under the former conditions [1] in which the Molybdenum was eluted with sulphuric acid and subsequently with ammonium hydroxide and sodium sulfate mixtures that had to be adjusted into the suitable feeding conditions of the chelex column later on.
  Additional increase of the molybdenum decontamination from the highly radiotoxic nuclides J-131 and Sr-90

Final chromatographic purifcation of molybdenum on chelex-100

The solution containing the molybdenum, the dissolved manganese and the accompanying fission product impurities are passed through a chelex-100 column. The molybdenum is retained quantitatively on the exchanger as $[Mo(SCN)_6]^{-3}$ [6,7], while the manganese ions and the fission product species are not adsorbed on the column. Chelex-100 is a styrene divinylbenzene copolymer containing iminodiacetat ions which act as chelating groups for metal ions. The advantage of chelex-100 for the purification of molybdenum is based on the capability of the resin to act as anionic or as cationic exchanger in dependence of the pH in the process solution. Under strongly acidic conditions it is an anionic exchanger which is able to adsorb the negatively charged molybdenum-rhodano complexes quantitatively, while they are efficiently desorbed from the stationary phase in strongly basic solutions .

To achieve optimum Mo-retention conditions on chelex the adsorber has to be pretreated with 2 M sulphuric acid containing approximately the same SCN^-, SO_3^{-2} and I^- amounts as in the feed. The preconditioning has to be done just before the molybdenum loading.

The column is subsequently washed with sulphuric acid containing thiocyanate, pure sulphuric acid and water. The molybdenum elution from the column is carried out with 1 M NaOH. To guarantee a product of highest purity the procedure is repeated on a second smaller chelex-100 column of a particle size range between 100-200 mesh.

A significant difference presents the molybdenum elution from this column. It has to be carried out with 6 M ammonium hydroxide in consideration for the final process step, the molybdenum oxide sublimation.

Molybdenum oxide sublimation and product adjustment

The ammonium molybdat eluate is transfered to the sublimation cell. The molybdenum solution is evaporated to a volume of few milliliters and afterwards placed into a platinum crucible. The solution is evaporated on an elecric hot plate and the crucible with the completely dry residue slowly heated up to about 700°C in a quartz glass apparatus

inside a resistance furnace.

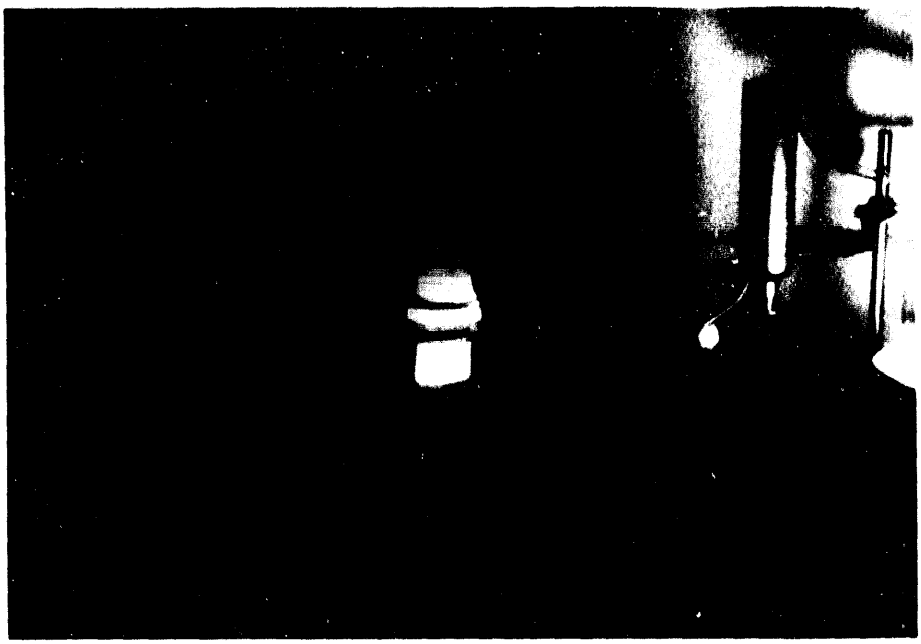

Fig.8: Condensed molybdenum trioxide between the connected quartz sublimation and condensation devices.

At this temperature all organic impurities possibly introduced from the ion exchangers into the product are removed.

Table 1: Quality analysis of the end product in comparison with the impurities tolerated by the european pharmacopoeia

Impurity	^{131}I	^{103}Ru	^{106}Ru	^{95}Zr	^{95}Nb	^{125}Sb	^{137}Cs	α	^{89}Sr and ^{90}Sr, resp.
Limit values according to P.E.	50	50	the rest of emitters together 100 ppm					10^{-3}	0,6 and 0,06, resp.
KfK molybdenum	0,005	0,01	0,0004	-	0,001	0,0005	-	$<2\times10^{-5}$	$<2\times10^{-5}$
	0,006	0,01	0,0003	-	0,0015	0,0006	-	$<2\times10^{-5}$	$<2\times10^{-5}$

Foreign Nuclides Related to ^{99}Mo at Time of Calibration in ppm

The last process is the sublimation of the molybdenum oxide. It is started after a quartz glass condensation device has been placed over the quartz vessel in the furnace and the temperature increased to about 1150°C. The molybdenum volatilization is completed in about 30 minutes. Molybdenum trioxide is condensed, as showed in figure 8, between the upper part of the quartz apparatus located in the furnace and the quartz condensation device.

After removal the platinum crucible with the residue out of the quartz device, the oxide on the quartz glass is dissolved with ammonia vapour. The molybdenum solution is mixed with sodium hydroxide and ammonia is removed by boiling. The solution obtained represents the final product.

TAble 1 its quality analysis in comparison with the impurities tolerated by the european pharmacopoeia.

Uranium recycling

The insoluble residue in the dissolver contains about 99% of the initially irradiated uranium as alkali diuranate together with the insoluble fission product species such as ruthenium, zirconium, niobium, and the lanthanides. Due to the higher U-238 percentage in the low enriched fuel used in the investigation further contaminations through the generated transuranium elements has to be taken into account. Under aspects of economy and safeguard regulations the uranium has to be recycled. As already mentioned, the adaptation of technologies as practised in the reprocessing of mixed oxide fuels from nuclear power stations cannot be recommended, as the short cooling times result in much higher radiation dose concentrations and contamination levels of the uranium by I-131.

According to these considerations a suitable process was developped and successfully demonstrated at KfK [8,9]. It is based on the formation of soluble negatively charged uranyl tricarbonato-complexes $[UO_2(CO_3)_3]^{-4}$. The dissolution can be carried out in hydrogen carbonate, carbonate or in mixed solutions of them. Fast dissolution is achieved in presence of oxidation agents such as hydrogen peroxide at temperatures between 20-40°C. Figure 9 shows the dissolution behaviour of ammonium diuranate as a function of the CO_3^{2-} concentration.

The data show that the maximum uranium solubility in this system is about 48 g/l. For practical conditions the aimed solubility has to be in the range of 40 g/l. The obvious disadvantage of limited solubility in HCO_3^-/CO_3^{-2} media is by far overcompensated through the achieved advances, which are:

High decontamination of the uranium already during dissolution. In comparison with the fuel dissolution in nitric acid, in which nearly the whole the residue is

dissolved, the HCO_3^-/CO_3^{-2} offers a selective dissolution of the uranium. The obtained decontamination factors for uranium from the residue are in the avarage of 100. The high efficiency includes also the decontamination from the generated transuranium elements neptunium und plutonium. Both are completely retained in the residue when the basic solution is boiled for 30 minutes.

Safe processing conditions, as carbonate solutions are absolutely non corrosive and demand only simple offgas treatment outlays because iodine is not volatile in basic media

Quick and economic further chromatographic decontamination of the solution containing uranium on compact, cheap, and radiation resistent inorganic adsorbers

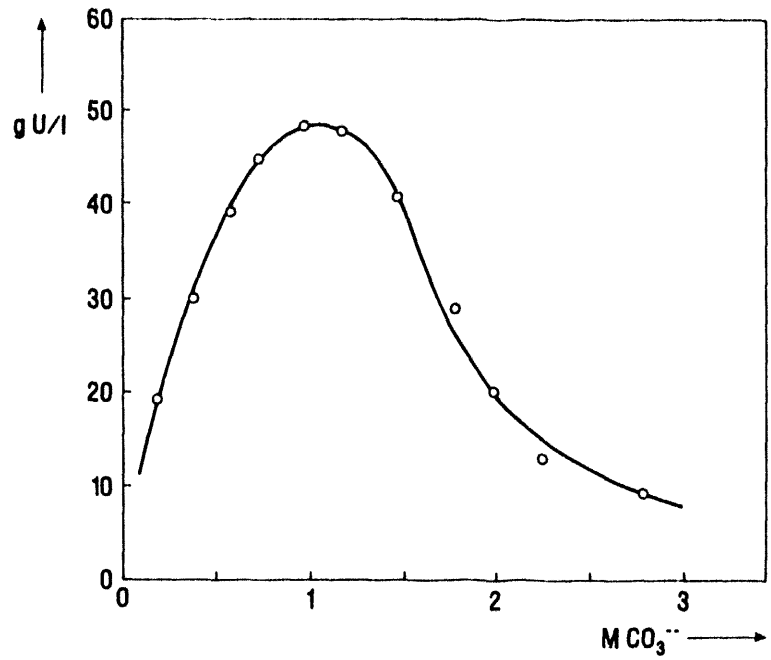

Fig.9: Dissolution behaviour of ammonium diuranate as a function of the CO_3^{2-} concentration

Chromatographic decontamination of the uranium tricarbonate stream

The formation of the uranium tricarbonato complexes is accompanied by the co-formation of soluble fission product carbonate species [10]. Their separation from the fuel stream was the aim of experimental investigations to find out suitable, radiation resistent, inorganic adsorbers which are able to retain as much as possible of them. The investigations were started by static distribution expriments with tracers of relevant fission products on the most promising adsorbers. Figure 10 shows the highest distribution coefficients of cesium, cerium, strontium, and zirconium on their most efficient adsorbers as

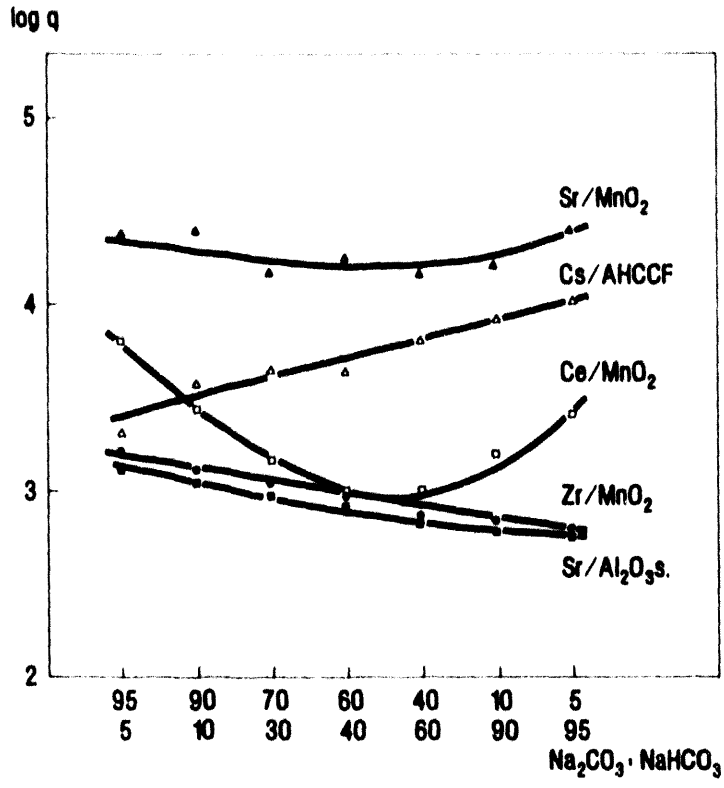

Fig.10: Distribution coefficients of Cs on $(NH_4)_2[CoFe(CN)_6]$, Ce, Sr, Zr on MnO_2 and Sr on Al_2O_3 in different HCO_3^-/CO_3^{-2} ratios, at 1 M total hydrogen carbonate/carbonate molarity

The obtained data show that suitable decontamination results can be achieved, even in solutions containing high carbonate concentrations. They were confirmed in first dynamic experiments. Fission product traces passed through columns of the most promising stationary phases and the breakthrough during loading and washing with 1 M carbonate solutions were determined. The following table lists the determined breakthrough percentage of Ce, Cs, Ru, Sb, Sr and Zr on columns of AHCCF $(NH_4)_2[CoFe(CN)_6]$, acidic Al_2O_3, MnO_2

The data above underline the efficiency of the inorganic exchangers for the fission product separation in this system. Only ruthenium is not completely retained on the named adsorbers. The best Ru-decontamination was achieved through the use of aluminium oxide columns. The detailed breakthrough behaviour of ruthenium on Al_2O_3, AHCCF, MnO_2, and SnO_2 columns during the loading and washing steps is plotted in figure 11. The successful adaptation of these promising systems under real process conditions depends on further informations such as the specific retention capacity of each element in

presence and in absence of uranium under practical loading speeds.

Table 2: Loading solution: 10 ml, washing solution: 15 ml, total HCO_3^-/CO_3^{-2} content: 1 M, column diameter: 9.7 mm, bed volume: 5.5 ml, adsorber weight: 5 g, loading speed: 30 cv/h.

Fiss. Prod.	Ce	Cs	Ru	Sb	Sr	Zr
Al_2O_3	100	60	94	38	100	0
AHCCF	98	100	31	0	0	100
MnO_2	100	7	82	100	100	100
SnO_2	95	0	6	0	100	63

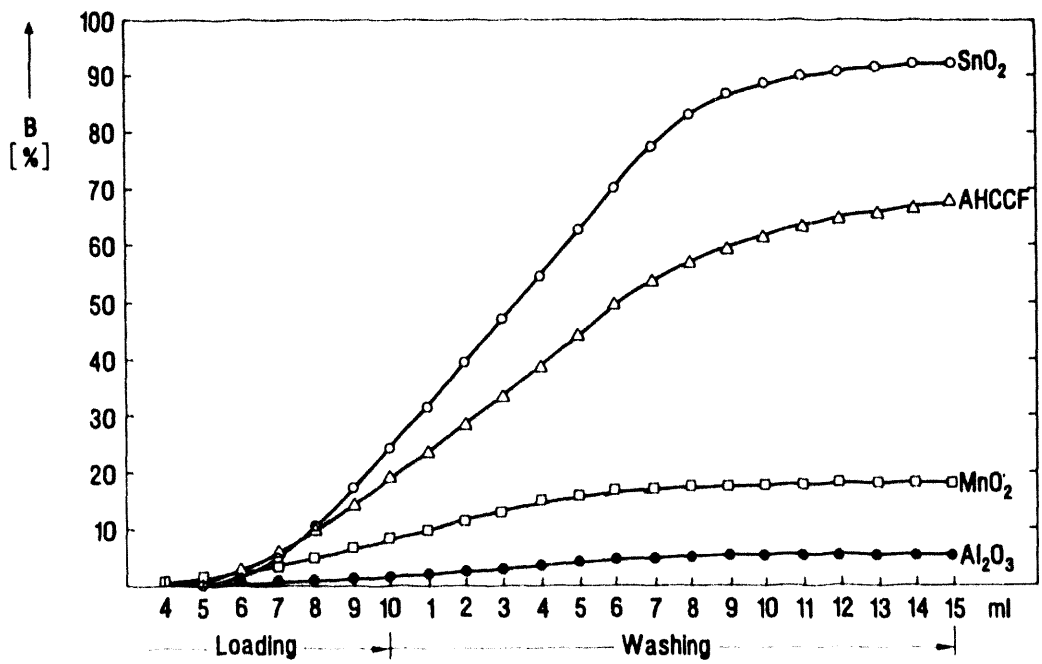

Fig.11: Breakthrough curves of Ru-carbonate species on columns of AHCCF, Al_2O_3, MnO_2, and SnO_2, the loading conditions were similar to those in the table above.

The corresponding data for cerium and zirconium are plotted in figure 12 and 13.

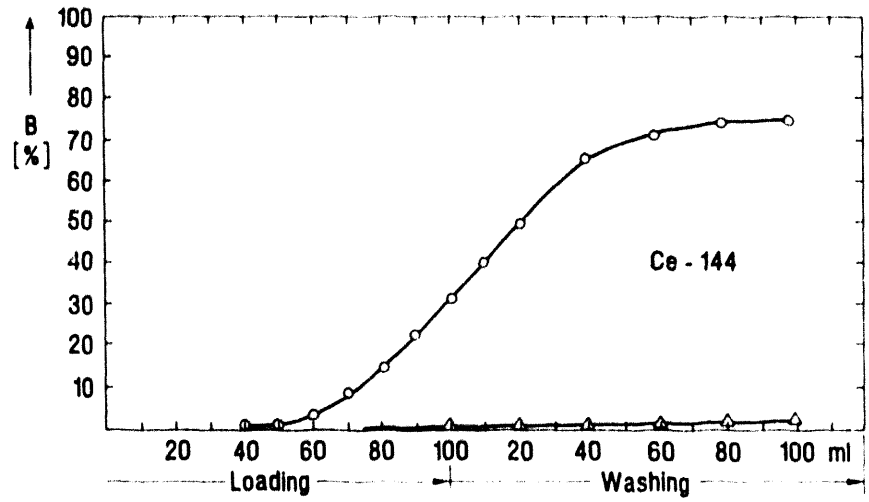

Fig.12: Breakthrough of cerium loaded on a MnO_2 column from hydrogencarbonate/carbonate containing solution, the upper curve is for the uranium free system; loading solution: HCO_3^-/CO_3^{-2}, ratio: 95/5, total molarity 1 M, Ce-concentration: 1 mg/l, U-concentration: 35 g/l, column inner diameter: 9.7 mm, bed volume: 5.5 ml, adsorber weight: 5.0 g MnO_2, loading speed: 30 cv/h

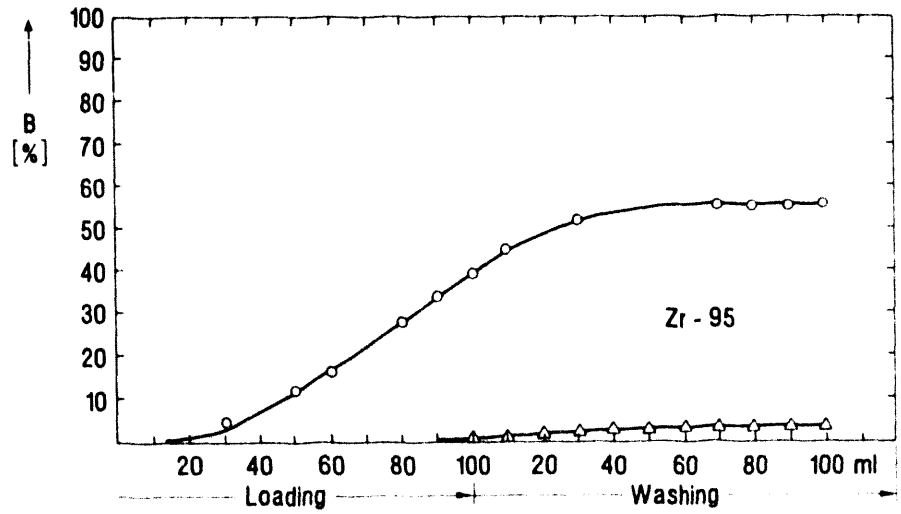

Fig.13: Breakthrough of zirconium loaded on a MnO_2 column from hydrogencarbonate/carbonate containing solution, the upper curve is for the uranium free system; loading solution: HCO_3^-/CO_3^{-2}, ratio: 95/5, total molarity: 1 M, Zr-concetration 1 mg/l, U-concentration: 35 g/l, column inner diameter: 9.7 mm, bed volume: 5.5 ml, adsorber weight: 5.5 g MnO_2, loading speed: 30 cv/h

Both figures underline the high efficiency of MnO_2 as a matrix for the chromatographic separation of cerium and zirconium from hydrogencarbonate/carbonate containing solutions.

An interesting result presents the increase of the fission product retention in presence of uranium. The most probable explanation for this behavior is the decrease in concentration of free HCO_3^-/CO_3^{-2} ions caused by the complex formation with uranium. Higher HCO_3^-/CO_3^{-2} concentrations lead to the formation of stronger negative charged fission product species which are less retained on the adsorber.

Uranium concentration and final purification

The decontaminated fuel solution has to undergo a final purification process in which the alkaline salt content and the still remaining fission product nuclides are eliminated. Best results are achieved by the proved, deeply studied and optimized Purex process [11,12]. It is based on the extraction of uranium from nitric acid solutions in tributyl phosphate.

Optimum process conditions are obtained by the extraction of uranium from approximately 3 M HNO_3 into an organic phase containing 30 vol% TBP in kerosene. The liquid/liquid extraction system is the best solution for middle to large scale batches that can be processed continuously. For the molybdenum targets where batch sizes of only 1 - 2 kg have to be processed, modifications and simplifications are recommended. The most practical solution is achieved by using the solid-bed extraction technique [13]. It is based on the loading of the pure extraction agent, TBP, on a macroporous nonpolar matrix of polystyrene divinylbenzene such as Lewatit 1023 (Bayer Leverkusen,Germany) [14], Bio-Beads SM-2 and SM-4 (Bio-Rad, Richmond, California, USA) or the low to intermediate polar acrylic ester matrix SM-7 (Bio-Rad). The described technique combines the high decontamination efficiency of the TBP/HNO_3-system with the simple handling of chromatography operations. The uranium extraction on the solid bed column cannot be started before the carbonate ions are trapped and the uranium concentraion in the feed of the column is increased to approximately 100 g/l. The high U-concentration is needed to achieve efficient fuel decontamination.

This can be realized by an efficient process variation basing on the quantitative adsorbtion of the uranyl tricarbonate species on the intermediate basic exchanger Bio-Rex5 (Bio-Rad) followed by the concentrated elution of the uranium with 3 M HNO_3 [8]. The uranium elution has to be carried out from the bottom to the top of the column, so that the formation of over pressure in the column from the generated carbon dioxide, can be minimized. The eluate is passed, after the ventilation of the CO_2, directly through the bottom of the solid bed column loaded with the TBP-kerosene mixture. Uranium is retained as a sharp yellow band on the stationary phase, the fission products

leave the column on the top. After the washing of the loaded organic phase the uranium is eluted with 0.02 M HNO_3. Figure 14 shows typical solid bed extraction curves for uranium and the accompanying fission products on a TBP loaded SM-7 column.

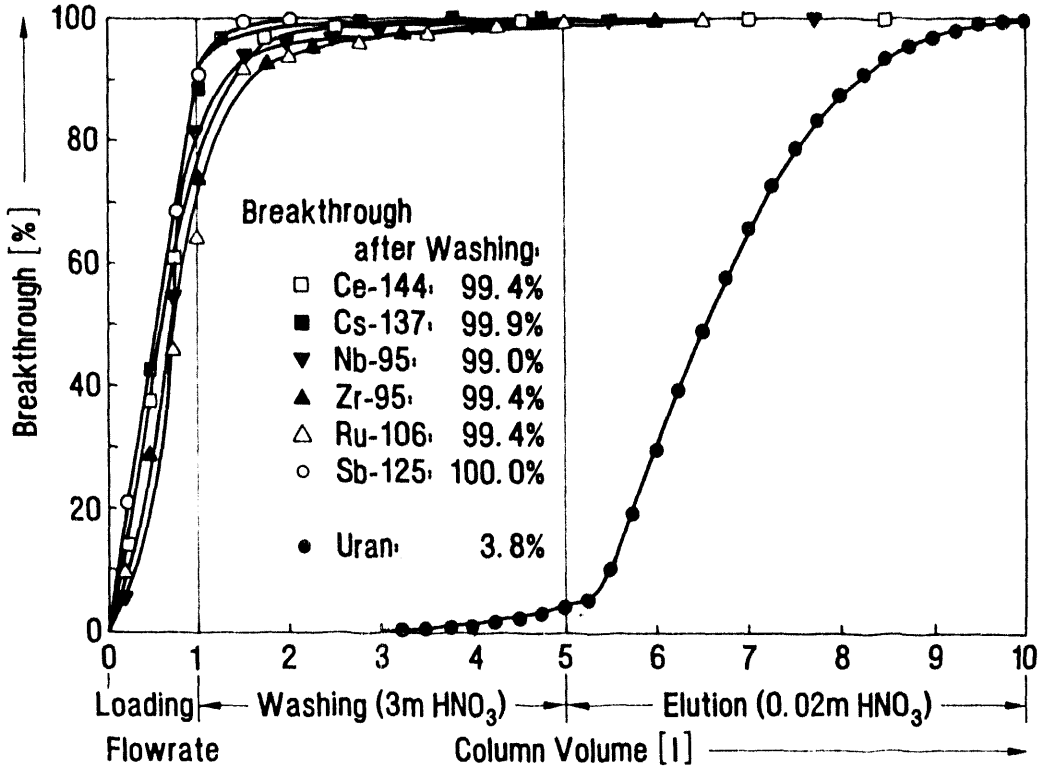

Fig.14: Decontamination of uranium on a TBP loaded SM-7 column.

The uranium breakthrough after washing the stationary phase with three column volumes of 3 M HNO_3 is separately collected and added, after reconcentration, to the next batch.

The uranium eluat is mixed with a solution of higher enriched uranium, so that the enrichment loss through the irradiation is balanced to 19.8% U-235. The mixture is poured into an ammonium hydroxide solution under permanent stirring. After the drying of the precipitate the yellow cake is calcinated at 800°C to U_3O_8 and the cycle is continued as already described. Figure 15 shows the simplified scheme of the developed fission molybdenum production cycle from irradiated uranium silicide targets

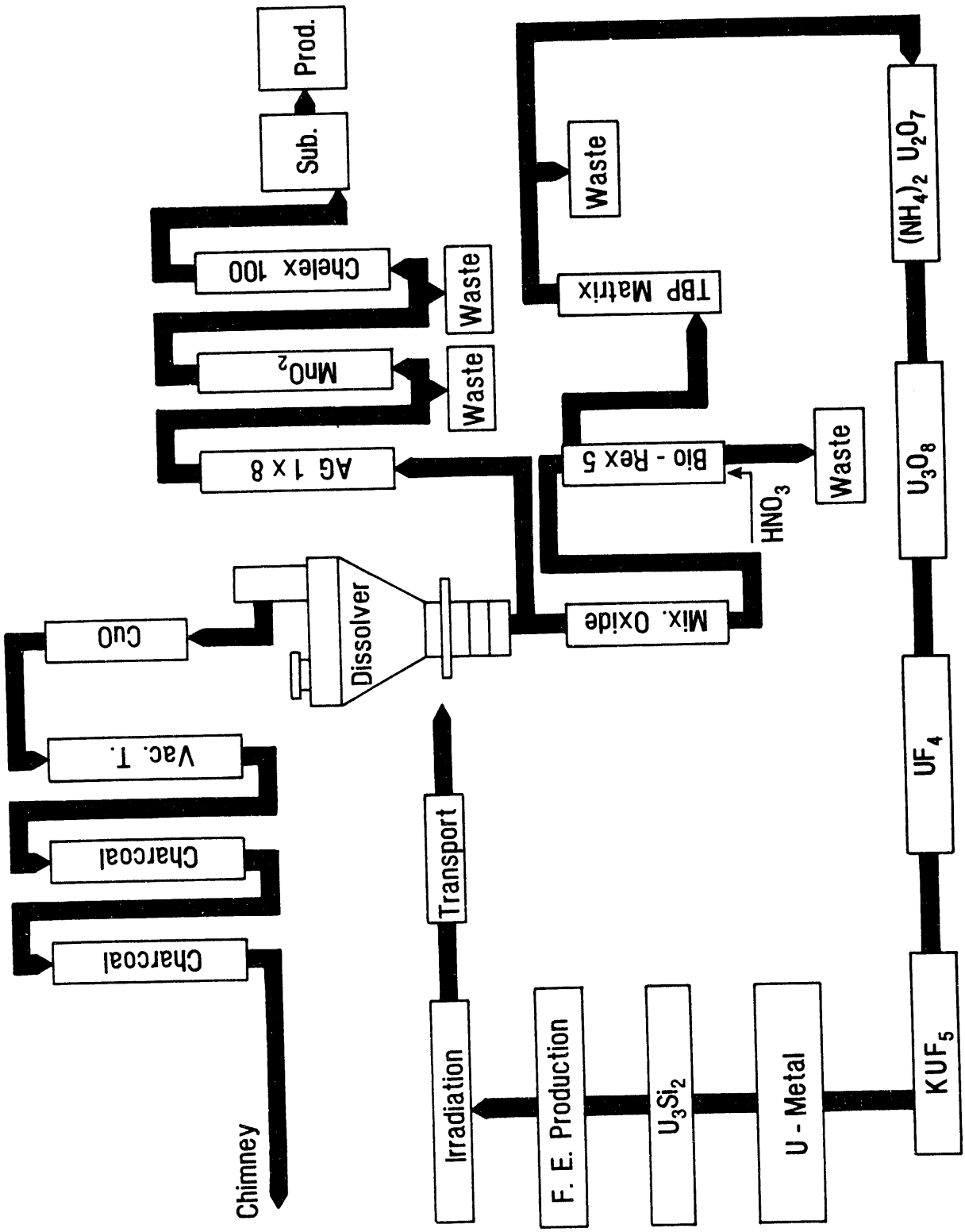

Fig. 15: Fission molybdenum production cycle from irradiated U_3Si_2-targets

[1] A.A. Sameh, H.J. Ache; Radiochim. Acta, No. 41, 1987, p. 65

[2] G.F. VandeGrift, J.D. Kwok, S.L. Marshall, D.R. Vissers, J.E. Matos; International Meeting on Reduced Enrichment for Research and Test Reactors (RERTR), Sept. 28th - Oct. 2nd 1987 in Buenos Aires, Argentine

[3] A.A. Sameh, A. Bertram-Berg; German patent application P4231955.2, Sept. 1992

[4] A.A. Sameh, M. Reich; German patent No. 3904167, April 1990

[5] A.A. Sameh, W. Leifeld; German patent application P4231997.8, Sept. 1992

[6] A.A. Sameh, J. Hoogveldt, J. Reinhardt; German patent 2610948, Sept. 1979, USA patent 4094953, June 1978

[7] A.A. Sameh, J. Hoogveldt, J. Reinhardt; German patent 2758783, November 1980

[8] A.A. Sameh, J. Haag; German patent 3144974, August 1985; USA patent 4460547, July 1984

[9] A.A. Sameh, J. Haag; German patent 3428877, October 1990; USA patent 4694768, August 1987

[10] A.A. Sameh, U. Bendt, W. Rottmann, W. Leifeld, U. Kaminski; International Conference on Nuclear Fuel Reprocessing and Waste Management RECOD 87, 23rd -27 th of August 1987 in Paris, France

[11] R.G. Wymer, B.L. Vondra; Light Water Reactor Fuel Cycle, CRC Press, Inc. Boca Raton, Florida

[12] H.J. Bleyl, D. Ertl, H. Goldacker, G. Petrich, J. Römer, H. Schmieder; Kerntechnik 55, No.1, 1990, p. 21

[13] R. Kroebel, A. Maier; Int. Solv. Extr. Conference in Lyon, France, 1974, 35, p. 2095, France

[14] H. Eschrich, W. Ochsenfeld; Sep. Sci. Technology, 15, 1980, p. 697

Epi-thermal Neutron Spectra from Low and High Enrichment Uranium Fuels at the Georgia Tech Research Reactor for Boron Neutron Capture Therapy

Kathleen A. Klee and Ratib A. Karam
Neely Nuclear Research Center
Georgia Institute of Technology
Atlanta, GA 30332

Boron Neutron Capture Therapy (BNCT) is an alternative treatment modality for highly malignant and invasive cancers such as glioblastoma multiforme. Conventional therapies, such as radiation therapy and surgery, are not effective against glioblastoma multiforme because of the multitude of tiny fingerlets protruding from the tumor mass out into healthy brain tissue. The technique of BNCT is dependent on the preferential loading of a B10-enriched compound into the tumor mass. Utilizing the proper beam of epi-thermal neutrons, the B(n,alpha)Li reaction releases both an alpha particle and a lithium ion, with an average total kinetic energy of 2.33 MeV. These particles have ranges in tissue comparable to the diameter of a cell, approximately 11 microns (1). The dose will be highly localized to the tumor volume, therefore killing the tumor mass while sparing the surrounding healthy brain tissue.

The Georgia Tech Research Reactor (GTRR) is a heavy water moderated and cooled reactor with a maximum power level of 5MW. The GTRR was designed with a bio-medical facility in place adjacent to the reactor. Plate-type high-enriched fuel, with 11.75 grams U-235 per plate, is currently in use. Sometime in the next two years, a switch will be made to low-enriched fuel, along with an increase in plates per fuel element, from 16 to 18 plates. The low-enriched plates will contain 12.5 grams U-235 per plate. The GTRR has provision for up to a 19-element core. The Technical Specifications and Safety Analysis Report, however, limit the size of the smallest core to 14 elements.

Interest in the GTRR as a neutron source for BNCT application continues to be widely expressed by several parties including EG&G, DOE, Neutron Technology, The Australian Nuclear Science and Technology Organization, and others. Recently several groups, including David Nigg and Floyd Wheeler at Idaho National Engineering Laboratory, have collaborated on a conceptual design of a filter to produce a beam of epi-thermal neutrons, near optimum, for BNCT at the GTRR (5). Nigg and Wheeler performed their calculations in two steps. In the first step, the intensity, spectrum, and angular distributions of the neutrons entering the aluminum/D20 filter were determined (Figure 1). In the second step, the neutron flux distribution throughout the entire filter and collimator structure was determined. Two-dimensional, discrete-ordinate models of the structure, utilizing the DORT code

and the BUGLE-80 coupled neutron-gamma cross-section library, were used in both steps. The TORT code was also used in obtaining depth dose results.

Additionally, Argonne National Laboratory, through the efforts of Dr. James Matos and colleagues, have been evaluating the safety implications of the conversion from HEU to LEU fuel. The EPRI-CELL code was used to prepare microscopic cross sections, in seven energy groups, for both HEU and LEU fuel. Three-dimensional reactor calculations were performed using both the VIM code, a continuous energy Monte Carlo code, and the DIF3D diffusion theory code.

In order to provide an independent confirmation of Argonne's and INEL's calculations, MCNP, a continuous energy and space Monte Carlo code, was used to duplicate the as-built Georgia Tech Research Reactor with no approximations. MCNP can be used for both neutron and photon transport. In all calculations, Version IV of MCNP and ENDF/B-IV cross sections were used.

K-eff calculations for 9, 14, and 19 element cores were performed for HEU and LEU fuels. Table 1 summarizes the results. The 9 - element HEU core served as a benchmark for the calculations. The measured k-eff of the 9 - element HEU core, rods fully out, was 1.00. The MCNP value for the as-built core is 1.004 (for 100,000 histories). The agreement is excellent.

TABLE 1 - Selected K-eff for benchmark calculations

Type	Fuel Assembly	Enrichment	Rods (deg)*	K-eff	Histories
w/ports	9	HEU	47	0.894 ± .0076	15000
	9	HEU	0	1.010 ± .0080	15000
	9	HEU	0	1.004 ± .0035	100000
	9	HEU	-	1.015 ± .0074	15000
	14	HEU	47	0.986 ± .0033	100000
	14	HEU	0	1.133 ± .0040	100000
	14	LEU	47	0.975 ± .0035	100000
	14	LEU	0	1.110 ± .0034	100000

* The control rods are fully out at 0 degrees and fully in at 55 degrees.

The 14 - element core is considered the reference core for BNCT applications. It is the smallest core allowed by our license and it provides the most intense beam at 5 MW. The reactivity difference between the HEU and LEU 14 - element cores is approximately 2.0% $\delta k/k$ with the control rods fully out. The reactivity worth of the central fuel element was measured in a 14-element core to be 2.6% $\delta k/k$. The value calculated by MCNP was

2.6 ± 1.0%, another confirmation of the ability of MCNP to predict the GTRR parameters correctly.

The neutron-flux spectra were calculated, for a 14 - element core configuration, at a k-eff of approximately 1.000. The control blades, in both the HEU and LEU models, were rotated and MCNP runs made in order to locate the correct blade positions to maintain a k-eff of 1.000 + 0.05.

TABLE 2 - Blade Position for K-eff of 1.000

Core	Blade Position*	k-eff
HEU	40 degrees	0.997 ± 0.0054
LEU	38 degrees	0.999 ± 0.0056

* Again, blades at 55 degrees are fully in.

The as-built HEU fuel element (16 plates), used in MCNP, is shown in Figure 2. The in-vessel neutron filter composed of 90% by volume aluminum and 10% heavy water is shown in Figure 3. Figure 4 shows a cross sectional view of the core filters and collimators leading to the bio-medical facility. Figure 5 is a detailed view of the aluminum filters outside the reactor vessel.

Figure 6 shows the neutron spectrum obtained with MCNP, for the HEU 14 -element core, at the center of the beam emerging from the collimator in the bio-medical room. This spectrum is compared with the results obtained by Nigg and Wheeler (5). The two spectra compare well. The neutron spectrum obtained using the LEU core is shown with the HEU spectrum in Figure 7. Again the two results compare reasonably well, with even fewer neutrons above 1 MeV, indicating little difference between the HEU and LEU produced spectra.

The Georgia Institute of Technology is pursuing the conversion of the Georgia Tech Research Reactor for use in Boron Neutron Capture Therapy. Within the next two years, GTRR will be converted from HEU to LEU fuel. Epi-thermal beam parameters, for both HEU and LEU fuels, were studied at this time so the conversion can be made with minimal interruption of the project. MCNP was chosen as the Monte Carlo transport code used in all calculations. The input geometry model used thus far was based on the conceptual design of the epi-thermal neutron facility by David W. Nigg and Floyd J. Wheeler at the Idaho National Engineering Laboratory. Using MCNP, various k-eff and reactivity worths, primarily for purposes of confirmation, and neutron-flux spectra were determined. Based on the calculated neutron-flux spectra presented here, the Georgia Tech Research Reactor produces a suitable epi-thermal neutron beam, with either HEU or LEU fuel, for future trials of BNCT, a treatment modality for otherwise untreatable malignancies.

REFERENCES

1. Brownell, G.L. et al. "Boron Neutron Capture Therapy." Modern Trends in Radiotherapy I. New York: Appleton-Century-Crofts, 1967. 132-144.

2. Brugger, R.M. et al. Summarization of Epi-thermal Neutron Beam Parameters. Nuc. Tec. 98:322, June 1992.

3. Freese, Ken E. Private communication. Argonne National Laboratory, 1974.

4. Freese, Ken E. Private Communication. Argonne National Laboratory, 1990.

5. Matos, J.E. et al. "Analyses for Conversion of the Georgia Tech Research Reactor from HEU to LEU Fuel." These proceedings. Argonne National Laboratory, 1992.

6. Nigg, D.W. and F. J. Wheeler, "Conceptual Physics Design of an Epi-Thermal Neutron Facility for Neutron Capture Therapy at the Georgia tech Research Reactor." Trans. ANS 65;146-147. June, 1992.

7. "MCNP-4, Monte Carlo Neutron and Photon Transport Code Systems," Obtained from Radiation Shielding Information Center, Oak Ridge National Laboratory. CCC-200A/B, 1992.

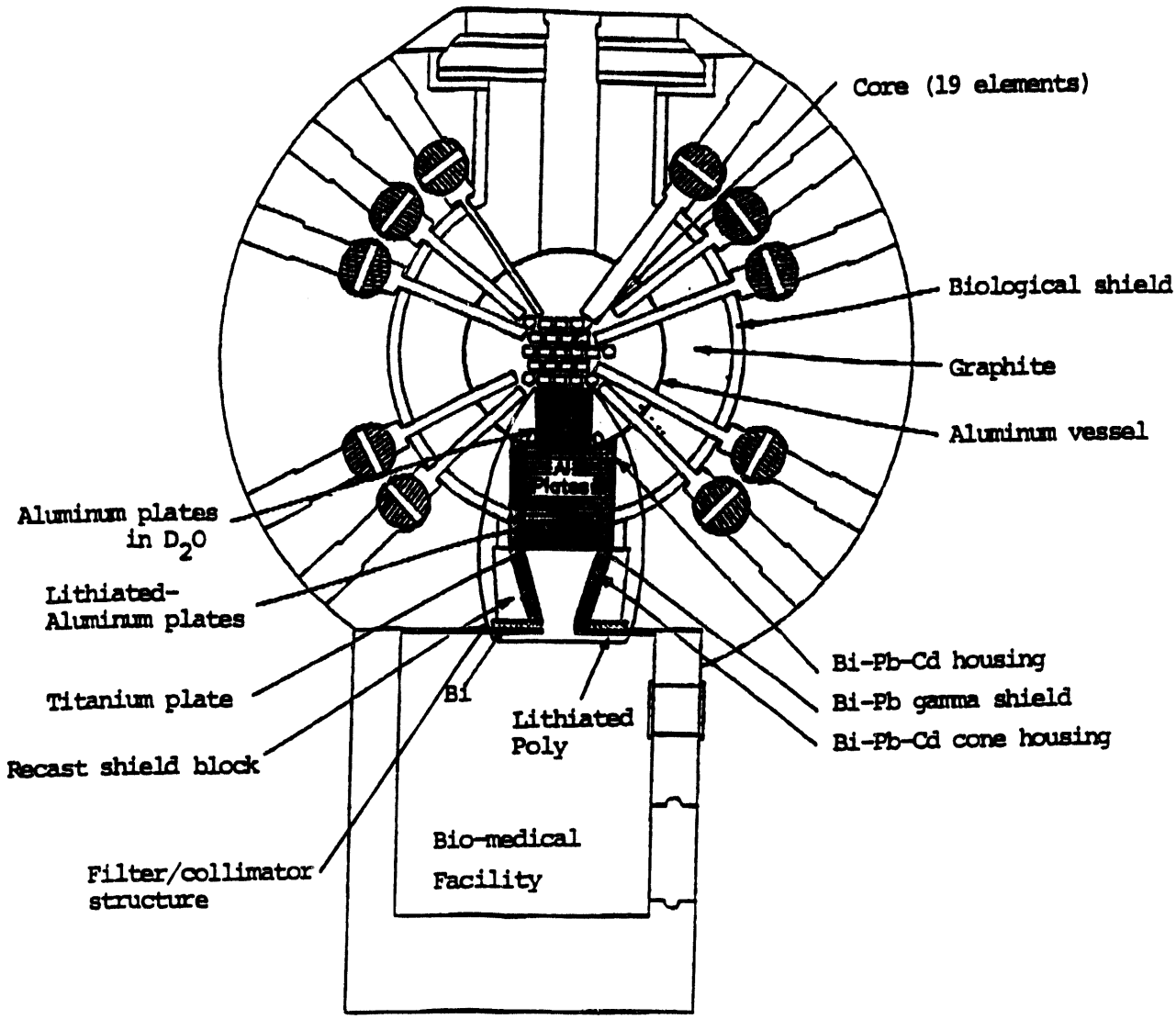

Figure 1. Conceptual design of the bio-medical port filter and collimator structure at the GIRR (Nigg and Wheeler).

Figure 2. As-built HEU fuel element (16 plate).

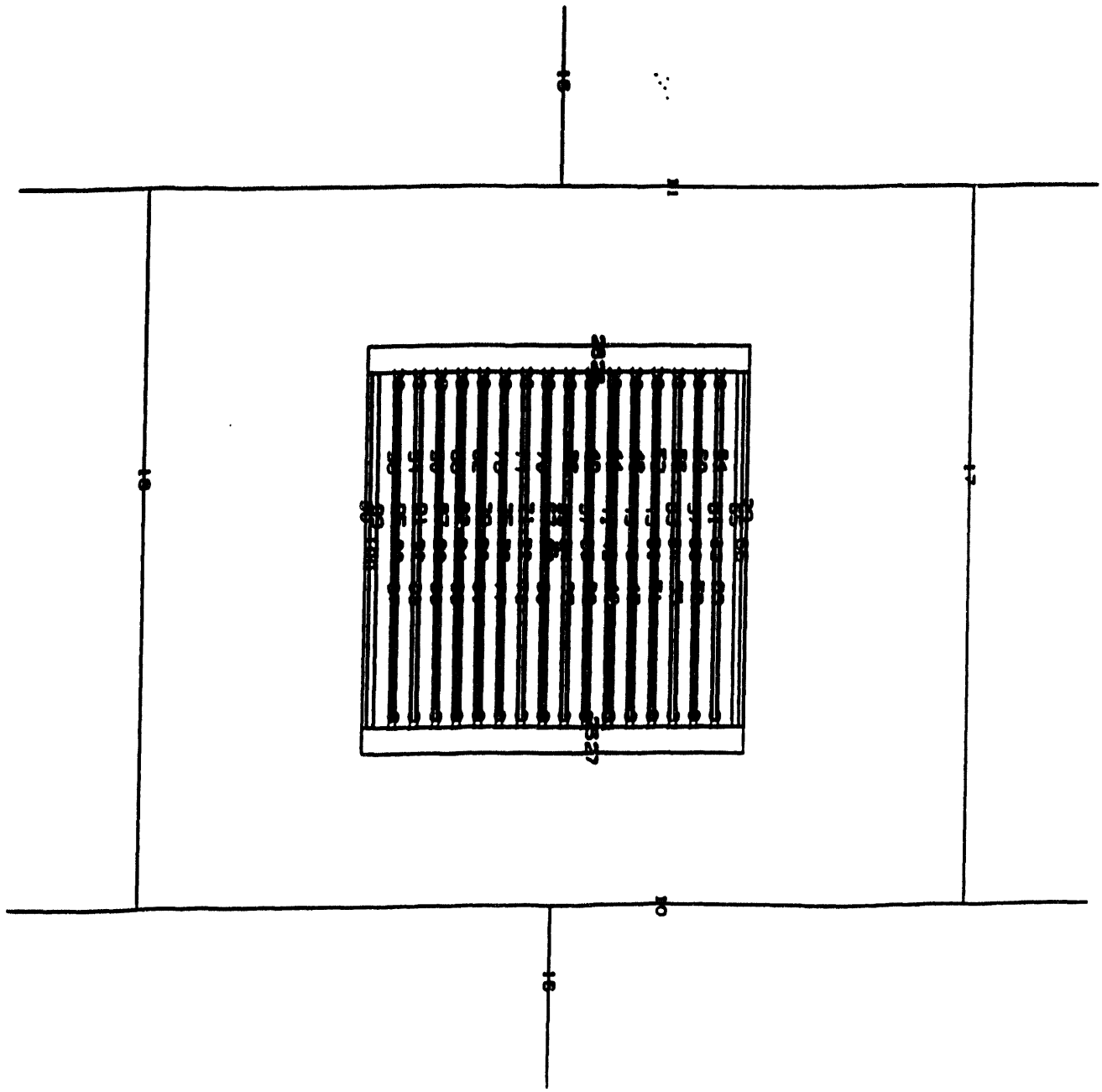

Figure 3. In-vessel neutron filter.

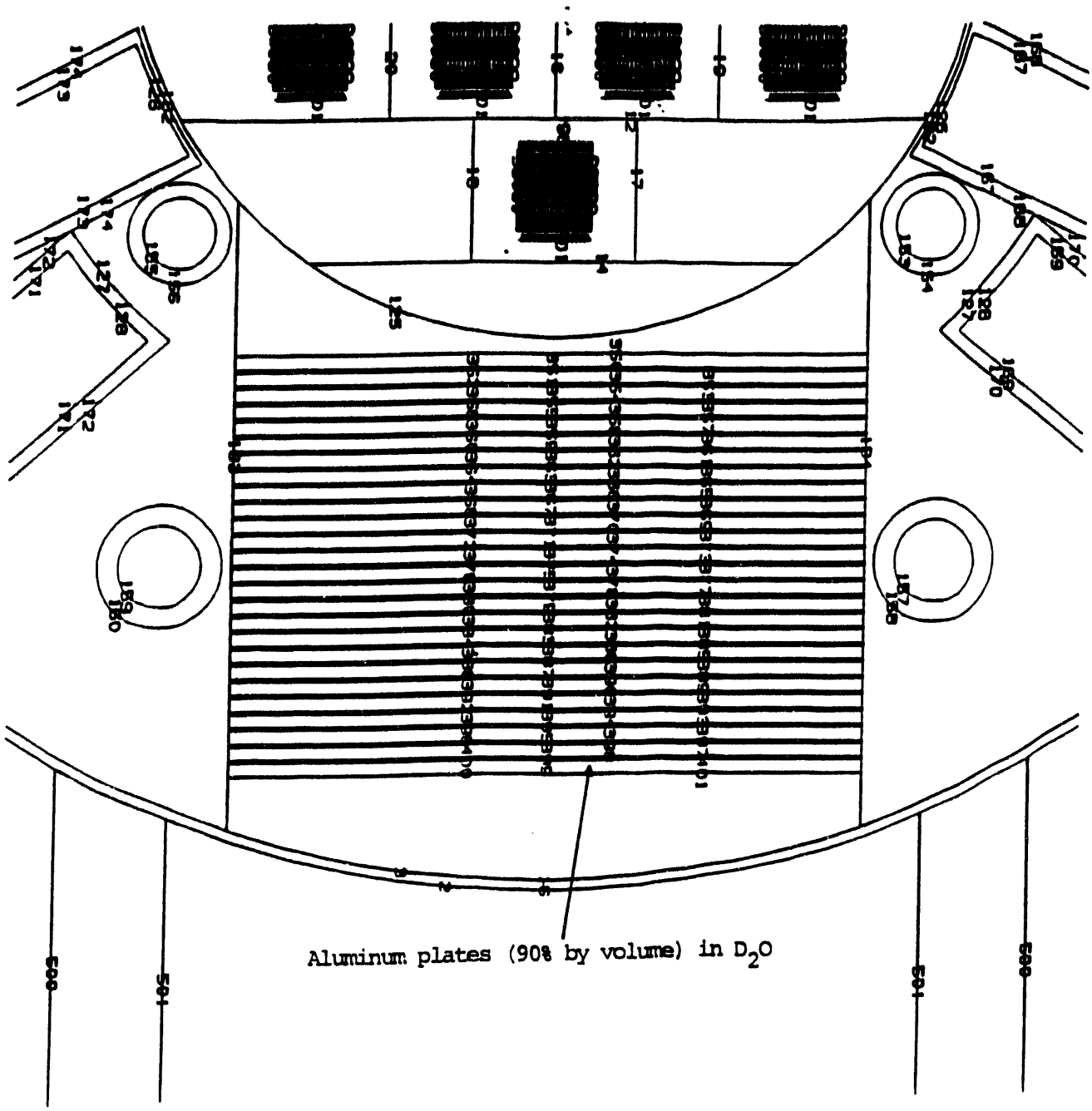

Figure 4. Core filters and collimators leading to the Bio-medical facility.

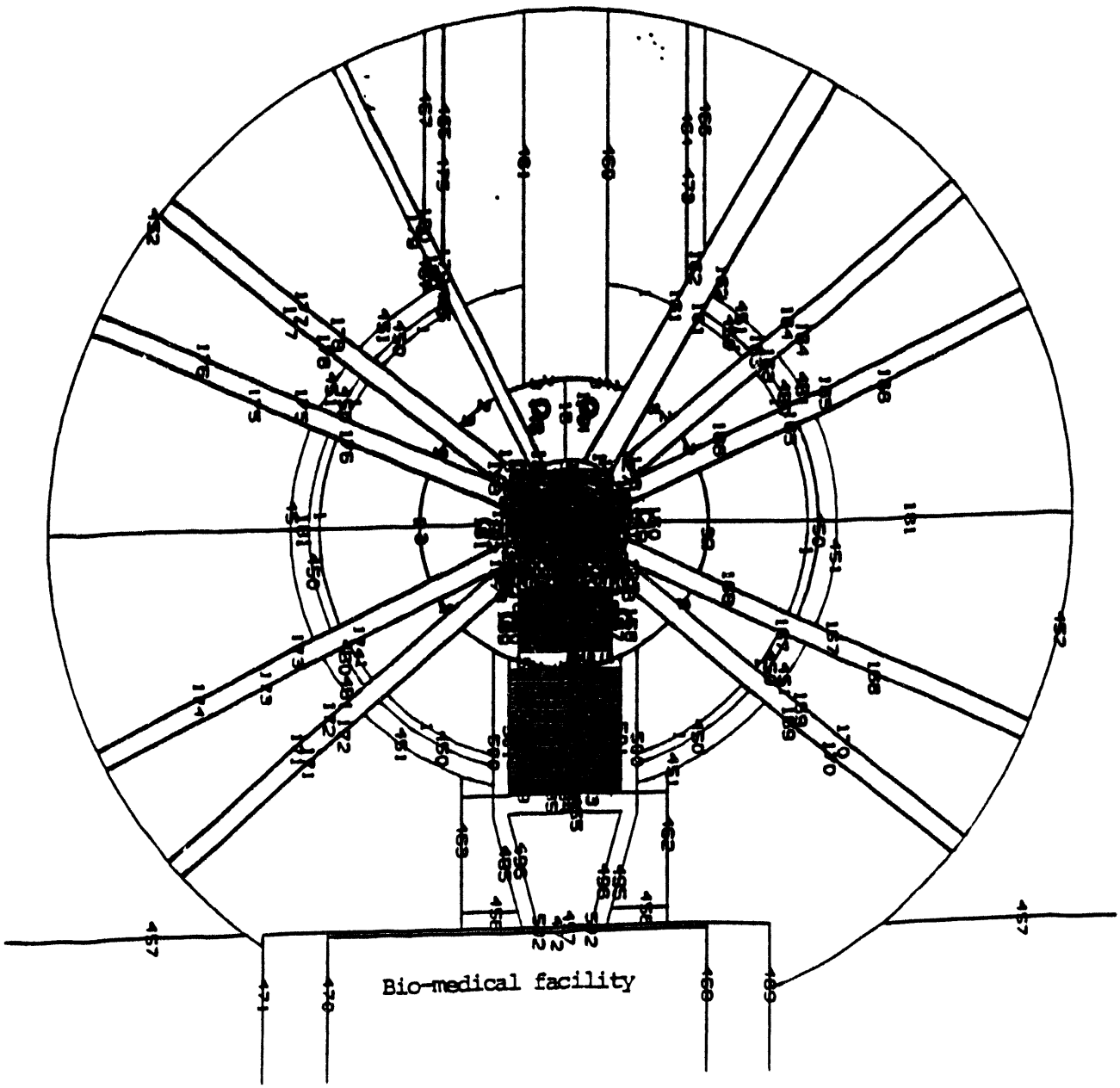

Figure 5. Detailed view of filters and collimators outside the reactor vessel.

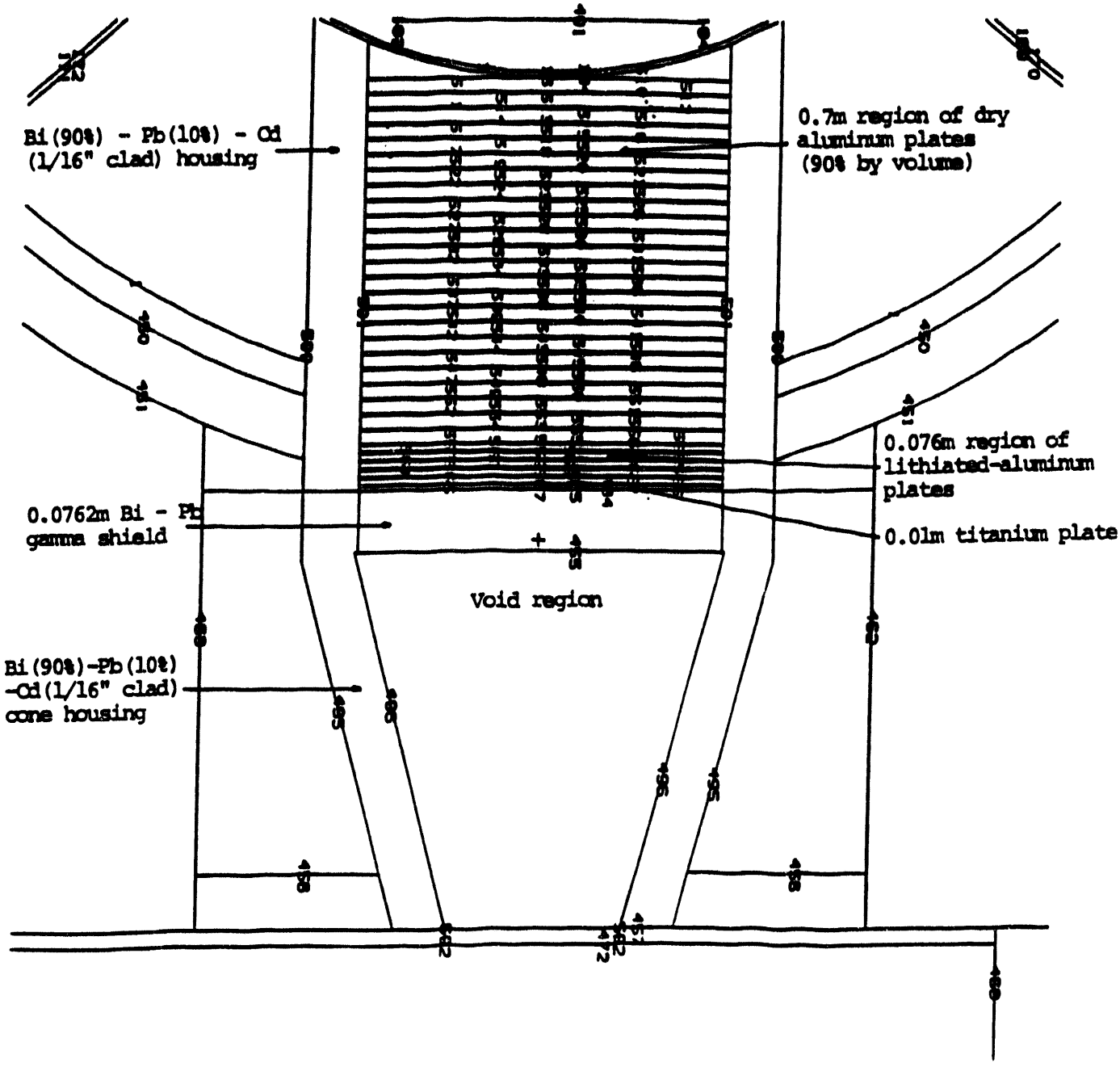

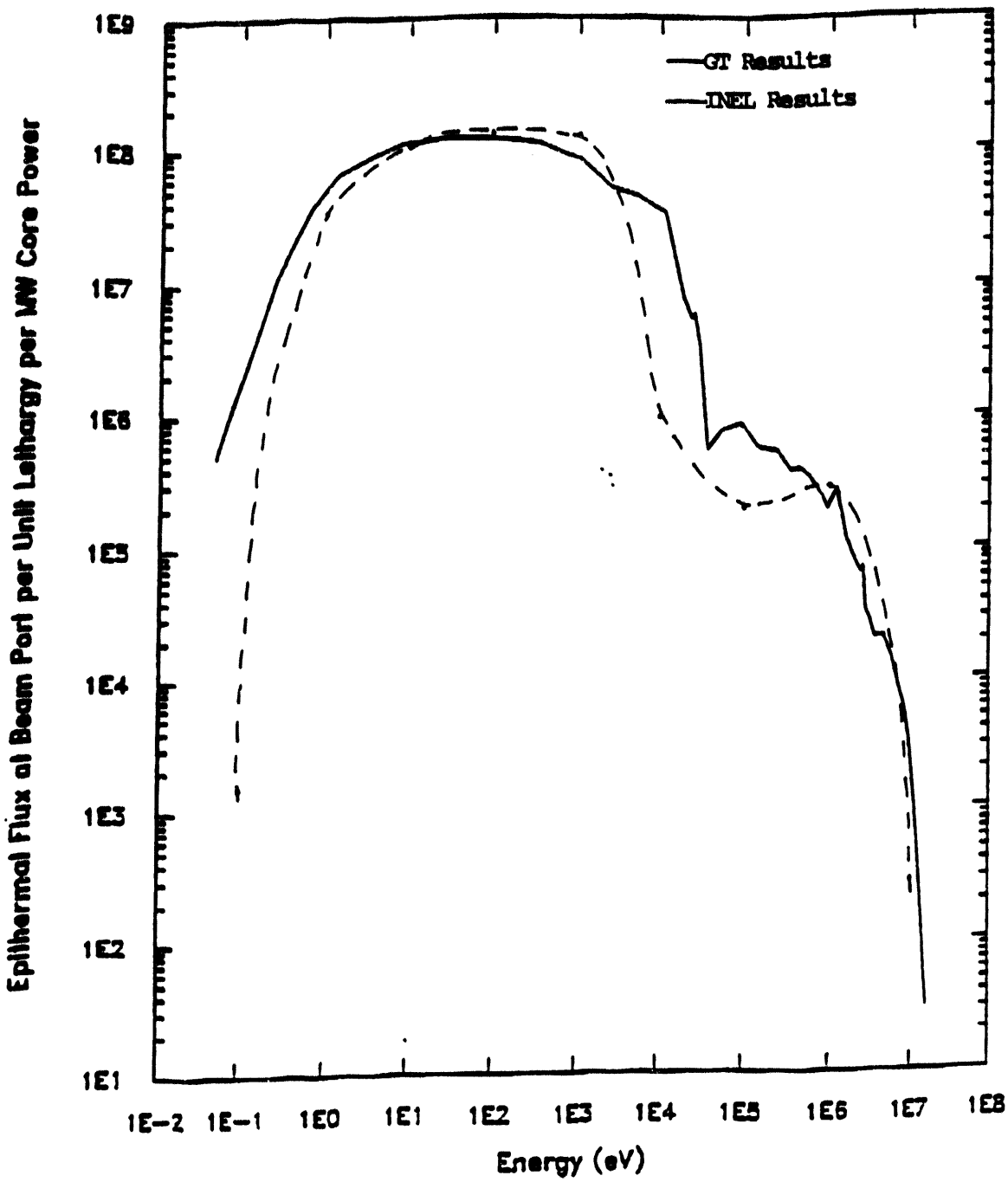

Figure 6. Neutron spectra at the port entrance to the bio-medical facility for a 14 - element HEU core.

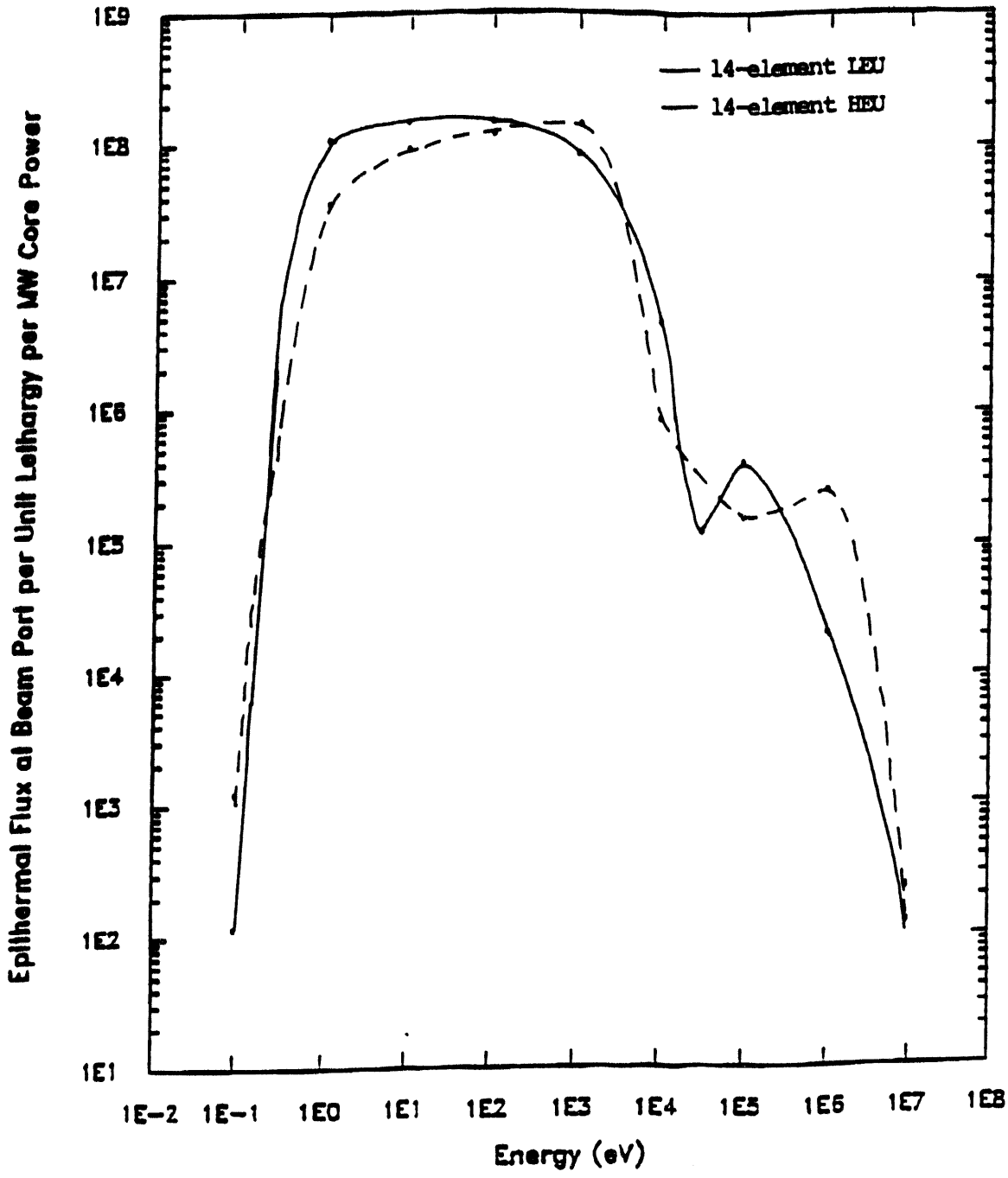

Figure 7. Neutron spectra at the port entrance to the bio-medical facility for both 14 - element LEU and HEU cores.

CONTRIBUTED PAPERS

CHILEAN FUEL ELEMENTS FABRICATION PROGRESS REPORT

J. Baeza, H. Contreras, J. Chávez,
J. Klein, R. Mansilla, J. Marín and R. Medina.
COMISION CHILENA DE ENERGIA NUCLEAR[1]
Amunátegui 95. Casilla 188-D
Santiago, Chile.

ABSTRACT

Due to HEU-LEU core conversion necessity for the Chilean MTR reactors, the Fuel Elements Plant is being implemented to LEU nuclear fuel elements fabrication. A glove box line for powder-compact processing designed at CCHEN, which is supposed to operate under an automatic control system, is at present under initial tests. Results of first natural uranium fuel plates manufacturing runs are shown.

INTRODUCTION

In 1982, a basic research project related to nuclear fuel fabrication started at CCHEN. Research in miniplates and nuclear fuel obtainment were the mayor aims in the early stages of this project. During 1985 some experience was achieved in order to design the **P**lanta de **E**lementos **C**ombustibles[2], **PEC.** One of its first goals was the repair of the 90% enriched uranium-aluminum alloy fuel meat supplied by **JEN**[3] for the Chilean research reactor, **RECH-2**[4]. Both, fuel elements plant and reactor are located in Lo Aguirre Nuclear Center, approximately 30 km. west from Santiago, Chile's capital.

The plant was built during 1986, completed in 1987 and finished the fuel elements overhaul in 1988. The 31 HEU fuel elements were fully disassembled because of mechanical damage caused by an inadequate loading system. A general criteria to reject fuel plates with scratches and dents deeper than 100 μm was used. 29 elements were reassembled after a rigorous dimensional and quality control inspection. A small plate protection was added in order to prevent mechanical damage during charge. The reactor loading system was modified, too. [1]

Due to worldwide HEU-LEU core conversion, LEU nuclear fuel elements for RECH-1 and RECH-2 research reactors are scheduled for future fabrication in Chile. Since then, the plant has been implemented to that objective. The first nuclear fuel elements production programmed by the plant are the U_3O_8-Al plates 66.5 wt%, U_3O_8 (37.5 vol%) (2.6 gm/cm^3 total uranium) for the RECH-2 reactor.

[1] Chilean Commission for Nuclear Energy (CCHEN).
[2] Fuel Elements Plant.
[3] Junta Energía Nuclear (from Spain).
[4] Reactor Experimental de Chile N°2 (Experimental Reactor of Chile).

During an IAEA expert mission in March 1992, the first ten U_3O_8-Al full size fuel plates, using natural uranium, were manufactured to demonstrate the process. Some pitfalls observed during this fabrication process are under corrective improvements at the moment, so that a final manufacturing simulation run should be carried out in the near future.

This report presents the actual status of the LEU plate type fuel element fabrication in Chile, with emphasis on the glove box line completion. Results of the first plate manufacturing process are also briefly reviewed here.

CCHEN LEU FUEL SUPPLY REQUIREMENTS

RECH-1 (La Reina Nuclear Center). This is a 5 MW research reactor used for radioisotope production and material and irradiation tests. It has successfully been in operation with 80% HEU UAlx-alloy type fuel from 1975 to 1988 and 45% MEU fuel since then. It is scheduled to start using LEU fuel elements not until 1997. The uranium density required for this final core conversion must be up to 3.7 gm/cm^3 [2].

RECH-2 (Lo Aguirre Nuclear Center). This is a 10 MW, open pool type research reactor moderated and cooled by light water, planned to be used in irradiation, production and training. Initially it went critical in 1977 and, due to major systems modifications, finally on September 6, 1989, the reactor went critical. Characterization operations are in progress for full exploitation at full power, which is limited now to 2 MW with HEU fuel made in Spain. Future plans intend to convert this reactor to LEU fuel operation at 10 MW. It is programmed using U_3O_8-Al alloy type fuel elements with a density up to 2.6 gm/cm^3 [1].

CCHEN LEU FUEL MANUFACTURING FACILITIES

CONVERSION PLANT. The UF_6-U_3O_8 Conversion Plant will convert ammonium diuranite (ADU) into high-fired U_3O_8 powder, necessary to fulfill the fuel plate manufacturing requirements. The plant is under licensing process and is regularly providing U_3O_8 natural uranium to the Fuel Elements Plant for manufacturing simulation runs.

FUEL FABRICATION PLANT. The Fuel Elements Plant, built in 1986, was first used to overhaul the fuel elements of the RECH-2 reactor. The main steps of that work included structural components manufacturing (side plates, bolts, spacers and holders), overall inspection and measurements, fuel elements disassembling, fuel plates inspection, cleaning, X-ray and flatness checking and fuel elements reassembling.

The manufacturing area is divided into the following six distinguished sectors:

Glove Box Line. In order to fulfill special requirements to manipulate uranium powders, a 5 glove box line was installed. It allows working under safe conditions with a controlled atmosphere, whether humidity or oxygen controlled, depending the fuel type to prepare, U_3O_8-Al or silicides. This line will be explained further in more details.

Machining and Assembling Line. In general, this line includes those conventional machines that can be found in any machine shop, in order to manufacture the structural pieces of the fuel elements. A special mention should be done to the universal (column-and-knee) type milling machine with memory-programmable control system.

Welding station. This station includes a sophisticated arc welding installation with electronic control, specially designed for top quality TIG welding, which is used to seal up the frame-compact-cover set.

Rolling, Straightening and Shearing Station. This station includes an electric furnace, heating by 100% forced convection, for plate annealing between rolling passes, a combined two-high hot and cold / four-high cold reversible laboratory rolling mill, a precision straightening machine for plate trimming and a shearing machine with a maximum cutting thickness of 8 mm.

Surface Treatments Station. This facility has the cells properly equipped for surface pickling and fuel plates and structural components degreasing.

Quality Control Line. This line includes, among any others, a portable X-ray generator, 200 kV, 8 mA, directional, automatic control panel CF5 with microprocessor, an X-ray film viewer, a three axis coordinate measuring machine and all the right equipment to perform the correct QC standards simply and safely.

GLOVE BOX LINE

Due to severe conditions for uranium powder manipulation, special requirements to operate these type of facilities, implies a glove box installation to meet those requirements. Under these considerations, the plant was designed and constructed including the space to perform these activities. Two rooms, one with a 5 glove box line to perform from powder weighing to frame-compact-cover assembling and a second room with a 3 glove box line for silicide powder preparation, were installed. Economical restrictions and Chilean own developments were the mayor reasons to implement both glove box lines with CCHEN own funds.

A Chilean manufacturer built the boxes under CCHEN specifications. Some accessories, like gloves, flanges, air locks, blank covers, sealing caps and waste containers were brought in Argentina and other equipment like balances, filters, manometers, gauges, etc. were imported from other countries.

Glove boxes are interconnected by a transfer duct whose access is controlled by a pneumatic sliding door.

POWDER WEIGHING GLOVE BOX. This first box is equipped only with an electronic balance for powder weighing. It has a serial RS-232 port for weight data acquisition in a host computer, so it is possible to know and track how much uranium and aluminum powder has each compact.

POWDER BLENDING GLOVE BOX. Powders weighted in the first box are transferred to this one which includes a motor-driven stainless steel blender which was designed at the plant to operate at prefixed angles at different speeds. It has six arms to support the blending capsules. Each arm can be adjusted between 0° and 90°. The capsule is firmly attached to the arm by a dynamic system which provides a safety operation. The blender also operates at different speeds that can be controlled from 0 to 200 rpm.

COMPACTING GLOVE BOX. After proper blending operation, the capsules are transferred in an egg shape device to the compacting glove box. Actually, this is a 200 ton. press with a glove box attached to its structure. Initially the matrix was manufactured with an adjustable

compacting die at the plant floor shop. After a few compact operations, decisions were taken in order to have a fixed die. New compacting die tests with natural uranium-aluminum powder showed compacts complying with tighter dimensional tolerances.

COMPACT DIMENSIONING GLOVE BOX. This box includes an electronic gage and another electronic balance. Close to the box, a vacuum furnace, designed and built at the plant, is used for compact degassing. A transfer box is used to transport compacts between the glove box and the furnace.

Once the compacts are pressed, they are arranged in a tray, which holds up to 12 compacts. Then, they are put inside the furnace and degassed for one hour at 540°C in a 10^{-5} mbar vacuum atmosphere. Compacts are left in vacuum inside the furnace until temperature is below 50°C. After degassing, compacts are transferred again to the glove box, where they are weighted and measured. After data recording, compacts are transferred to the last glove box.

COMPACT ASSEMBLING GLOVE BOX. After compact measuring, the same degassing tray is used to transfer compacts to this box. A top cover is placed on frame after the compact is inserted directly into the frame cavity. The "sandwich" assembly is identified by vibratooled numbers.

CONTROL SYSTEM. The control system implemented at the Plant has a platform based in a PLC. The control strategy allows interaction between the different line manufacturing stages and visualization by a mimic panel in real time of the different process variables states. It was design in order to keep up the oxygen and humidity levels within its reference points.

Line safety requirements establish to maintain room pressurized in 15 mm H_2O differential pressure respect glove box interior pressure. Taking up that U_3O_8 must have a humidity control, the system also has different loops to maintain the room pressure in its reference and at the same time provides the automatic mechanisms, controlled by the PLC, for the fire extinguishing system.

In general, the system controls the following parameters: (a) oxygen and humidity levels, (b) room pressure, (c) emergency air extraction and (d) fire control.

RECH-2 FUEL DESIGN

NEUTRONICS AND THERMAL HYDRAULICS [3]. In this section, the most important aspects considered for the conversion of the RECH-2 reactor using low enrichment uranium U_3O_8-Al fuel are presented. After preliminary studies and looking for the reduction of the number of variables, the following dimensions for the fuel plate have been adopted: plate thickness 1.32 mm, meat thickness 0.56 mm, clad thickness 0.38 mm, meat width 62 mm and active length 610 mm. Due to theoretical aspects, manufacturing restrictions and reactor characteristics, the conversion has been restricted to the study of 19, 20 and 21 plates fuel elements with water channel thickness of 2.68, 2.47 and 2.28 mm respectively. The fuel meat density has been varied from 2.3 to 3.0 gm/cm^3 and the meat porosity has been taken as 5%.

Using WIMS[1] and CITATION[2] codes, reactivity/gram of U^{235} as a function of meat uranium density for a 31 fuel elements core configuration has been calculated, Figure 1. This

[1] Spectral Computer Code.
[2] Diffusion Computer Code.

figure shows, for any density, a more efficient use of uranium in the 19 plates fuel element case. Also, it shows that the 21 plates fuel element represents the worst uranium usage.

After detailed neutronics calculations, an element with 20 plates of U_3O_8-Al fuel and uranium density of 2.6 gm/cm^3 has been adopted. This element will contain 217.5 grams of U^{235} with a total uranium inventory of 1,101 grams. Also, a 32 fuel elements core configuration with a flux trap at G5 position has been proposed as reference core, Figure 2. The reactivity excess at beginning of cycle is 10.5 %Δk/k with a control system worth of 14.09 %Δk/k. These values give a reactor shut-down margin of 3.59 %Δk/k. In Figure 3, the reactivity behavior as a function of the total operation time at nominal power is presented.

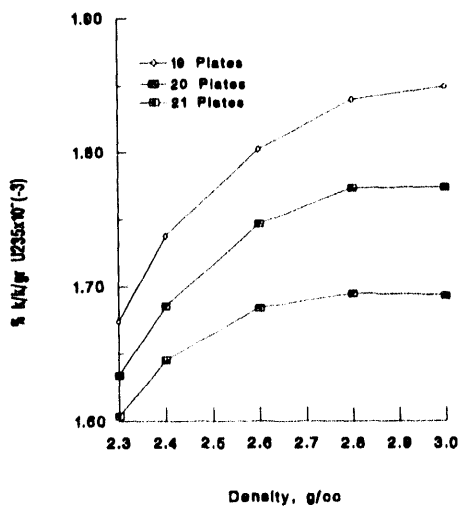

Figure 1. 31 fuel element core configuration reactivity as a function of density.

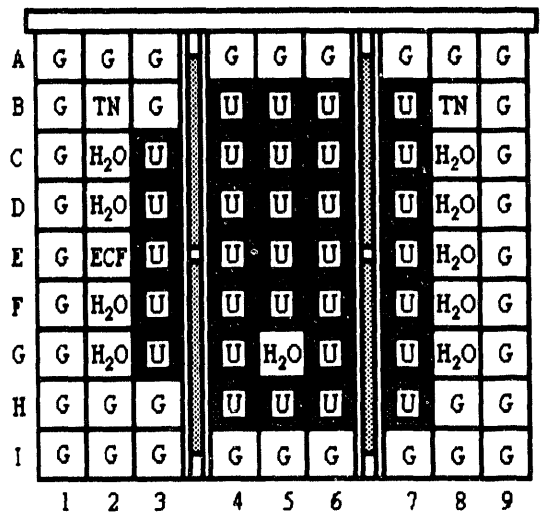

Figure 2. 32 fuel element core configuration with flux trap.

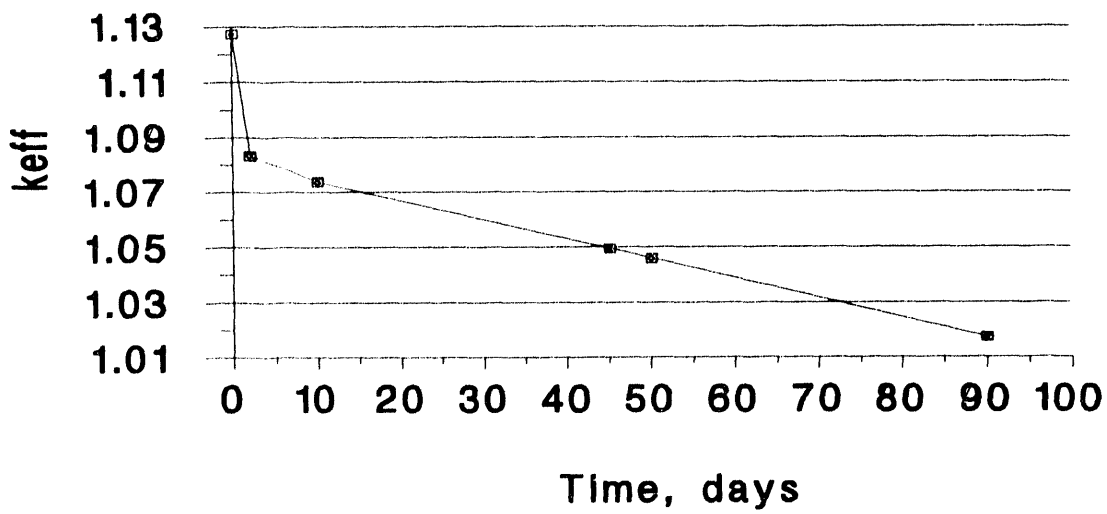

Figure 3. Reactivity Behavior as a Function of the Total Operation Time.

Some thermal hydraulic parameters for the 32 fuel elements core configuration with flux trap have been calculated. These parameters are necessary in order to estimate if the safety margins in critical conditions are acceptable to continue a more detailed study. In general, the more important thermal hydraulic design criteria are imposed by limiting constraints. The nucleate boiling must be avoided in any channel, even in the hottest channel, in order to stay away of the flow instability induced by the partial boiling in the core. This constraint gives a wide enough margin respect to the fuel plate destructive burn-out. To reach the previous goal, the DNB ratio should not be less than 1.5 during steady-state operating conditions and transients.

The TRANSV2[1] computer code was used to perform the thermal hydraulic analysis. The reactor core has been studied through the modeling of: (a) a single channel which represents the average behavior of the core and (b) a hot channel which represents the average channel affected by the nuclear hot channel factors and, due to conservative criteria, by the engineering hot channel factors.

The design nominal power of the RECH-2 reactor is 10 MW. The refrigeration of the core is obtained with a primary coolant circuit which provides a maximum flow rate of 1200 m^3/hr. In the 32 fuel element core it was found that a 73.2% of the nominal flow rate circulate through the inner channels of the fuel elements with an average water velocity of 2.44 m/s. The total pressure drop across the core is 0.138 Kg/cm^2.

With the design data for the proposed fuel element, the hydraulic characteristics of the core, the hot channel factors, the axial power distribution and a coolant inlet temperature of 35°C, it was found that the maximum heat flux for the hottest channel is 65.76 W/cm^2, the maximum temperature is 94.2°C, the ONB ratio is 1.44, the OFI ratio is 2.24 and the DNB ratio is 2.64.

As conclusions, the neutronics and thermal hydraulic analyses recommend for the RECH-2 research reactor a 20 plates fuel element using LEU U_3O_8-Al fuel and the better performance at nominal power of 10 MW is achieved with a 2.6 gm/cm^3 uranium density. This last result confirms the RECH-2 reactor conversion feasibility using U_3O_8-Al fuel.

MANUFACTURING. After neutronics and thermal hydraulic calculations, a fuel element basic engineering design was made. Figure 4 shows schematically the RECH-2 fuel element cross

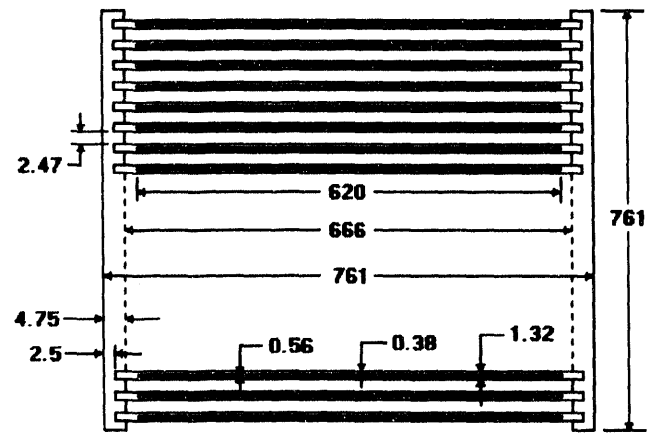

Figure 4. Schematic RECH-2 fuel element cross section design (nominal dimensions in mm).

[1] Thermal Hydraulic Computer Code.

section manufacturing design. From the manufacturing point of view, the most important differences between this design and the actual RECH-2 fuel element (JEN) are the increase in the fuel plates number and the decrease in the fuel plate thickness and water channel gap.

FUEL PLATE MANUFACTURING SIMULATION TEST

In March'92 an IAEA expert, Mr. Rodney Knight [4], worked during three weeks at the plant. During his mission, 10 full natural uranium fuel plates were manufactured. Results of this initial test are shown in this section.

COMPACTS. Using an adjustable compact die assembly, the first 10 compacts were made. Because of this adjustable matrix, some problems were encountered and reflected in compact dimensions differences. Even though, these compacts were used much more to check the other steps of the fuel plate manufacturing process, like "sandwich" welding, hot and cold rolling and X-ray fuel location and distribution examining.

The matrix was modified and is under initial compact fabrication tests at present. Preliminary results show that important improvements were achieved and compacts are now under specifications.

FUEL PLATES. After frame-compact welding, "sandwiches" were put inside the electric furnace for plate annealing. The sequence used for fuel plate hot/cold rolling is shown in Table I.

Table I. Fuel plate rolling sequence (dimensions in mm).

ROLLING TYPE	HOT	HOT	HOT	HOT	HOT	HOT	HOT	HOT	HOT	COLD
INITIAL THICKNESS	11.2	9.52	8.09	5.66	4.53	3.62	2.90	2.32	1.85	1.48
% REDUCTION	15	15	30	20	20	20	20	20	20	7
FINAL THICKNESS	9.52	8.09	5.66	4.53	3.62	2.90	2.32	1.85	1.48	1.35

In this initial test, some examinations were made. Samples of two plates (2 and 9) were cut from six different positions as shown in Figure 5.

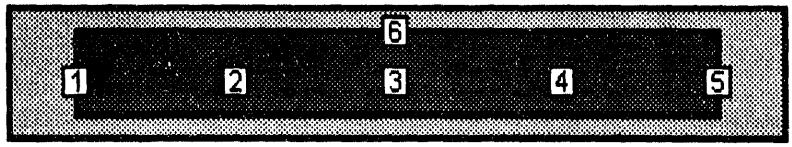

Figure 5. Sample Cuts in 2 Fuel Plates for Metallographic Analyses.

Meat and cladding thickness were determined. Also, meat-clad bonding, stringering, dog boning, fish tail, remote islands and core location and homogeneity were observed and analyzed.

RESULTS. Results of cladding and meat thickness mean values are presented in Table 2. Standard deviation, σn-1, for each case is also shown.

Table II. Cladding and meat thickness (mm).

		PLATE N° 2		PLATE N° 9	
SAMPLE N°	SIDE	$\overline{X}$	σn-1	$\overline{X}$	σn-1
1	CLAD A	0.407	0.020	0.401	0.014
	MEAT	0.533	0.020	0.554	0.037
	CLAD B	0.403	0.012	0.399	0.021
2	CLAD A	0.407	0.014	0.416	0.017
	MEAT	0.522	0.028	0.517	0.018
	CLAD B	0.415	0.020	0.410	0.009
3	CLAD A	0.410	0.020	0.482	0.033
	MEAT	0.524	0.017	0.570	0.029
	CLAD B	0.428	0.012	0.435	0.023
4	CLAD A	0.410	0.018	0.430	0.015
	MEAT	0.533	0.023	0.517	0.021
	CLAD B	0.408	0.019	0.426	0.017
5	CLAD A	0.383	0.013	0.401	0.018
	MEAT	0.577	0.039	0.524	0.040
	CLAD B	0.392	0.022	0.420	0.024

Metallographic cuts, Figures 6 and 7, showed an excellent bonding between clad and meat, and full U_3O_8 particles, with no (shrinkage) comminution and no stringering. Even though some dog boning and fish tail were found, Figures 8 and 9, their extent complied with and actually were below specifications. Finally, fuel plate radiographs showed a good core location and homogeneity and remote islands were not found.

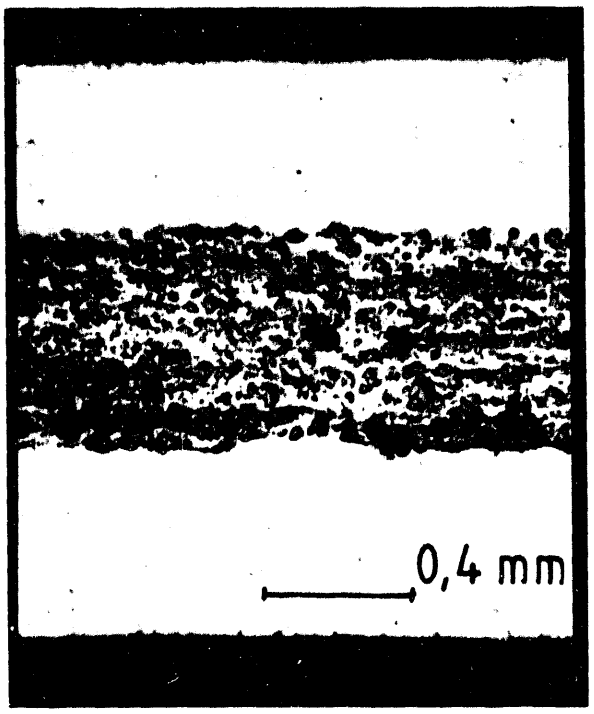

Figure 6. Micrograph (50x) showing clad-meat bonding (Plate 9, sample 3).

Figure 7. Micrograph (200x) showing U_3O_8 particles (Plate 9, sample 3).

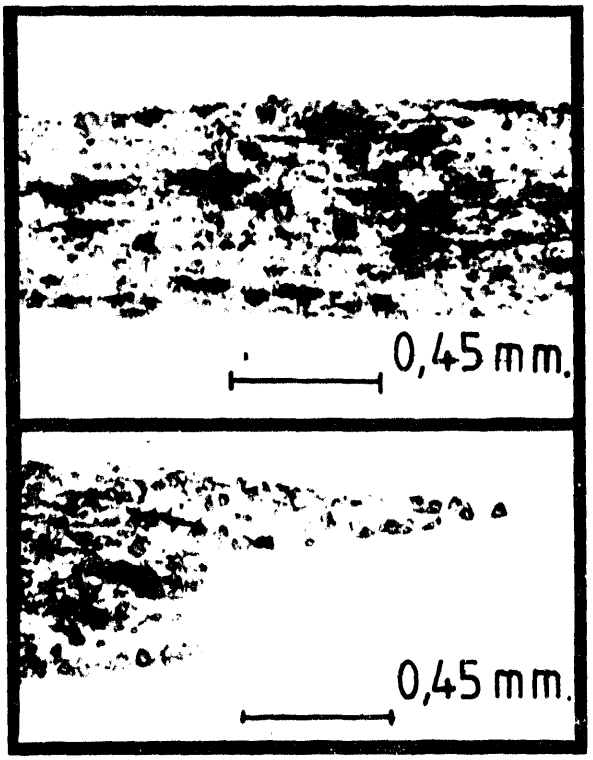

Figure 8. Micrograph (50x) showing dog boning and fish tail effect (Plate 2, sample 5).

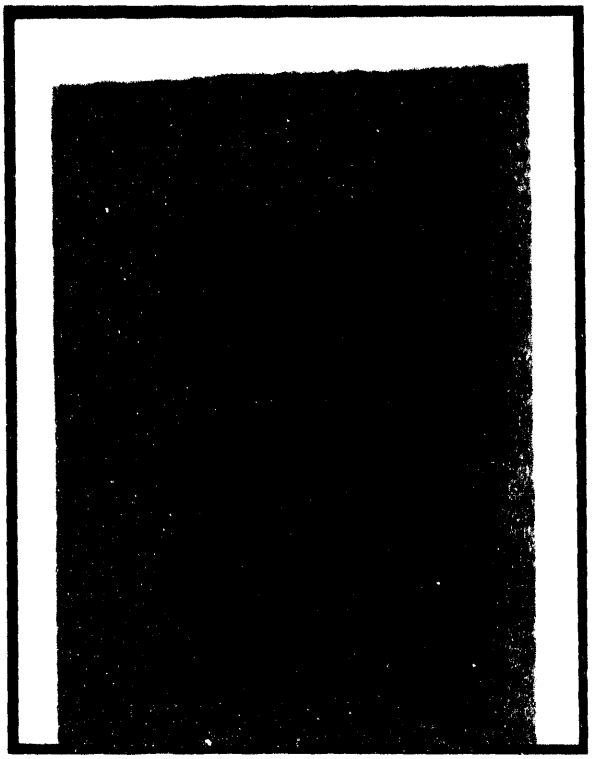

Figure 9. Plate radiograph (partial) showing end core location and homogeneity.

CONCLUSIONS AND FUTURE WORKS

- Initial results in fuel elements fabrication using natural uranium, show that future MTR nuclear fuel elements under Chilean specifications and design should be manufactured at CCHEN.

- The simulated fabrication process to manufacture fuel plates using natural uranium and to assemble fuel elements should continue to May 1993.

- The Fuel Elements Plant is under final tests and licensing and should start in the near future with LEU MTR nuclear fuel fabrication and should satisfy Chilean nuclear fuel necessities.

- Future research and development in silicides is planned to start in 1993 to satisfy next RECH-1 nuclear fuel necessity.

ACKNOWLEDGMENTS

The authors would like to thank the fuel elements plant technicians, N. Salazar, C. Marchant, V. Cepeda and F. Fernández who made contributions and suggestions in many technical details.

REFERENCES

[1] G. Torres, "Puesta en Servicio del Reactor Experimental del CEN Lo Aguirre", Nucleotécnica N° 17, October 1989.

[2] A. Poblete, "Gestión de Combustible 1989-1997 del Reactor RECH-1 de la Reina", Technical Inform N° RLR-06-1990, May 1990.

[3] J. Klein, R. Medina, C. Henríquez y O. Mutis, "Análisis Neutrónico y Termohidraúlico para la Definición del Elemento Combustible de Bajo Enriquecimiento del RECH-2", Technical Inform, Reactor Phisics Division, 1992.

[4] R. Knight, "Fabrication of Fuel Plates Using Either U_3O_8 or U_3Si_2", IAEA Expert Report, April 1992.

LETTER FROM MR. SUN RONGXIAN, NUCLEAR POWER INSTITUTE OF CHINA

Dr. Karsten Haack
Reactor DR3
Risø National Laboratory
Post Box 49
DK 4000, Roskilde, Denmark

September 1, 1992

Dear Dr. Karsten Haack:

Thank you very much for your invitation to the 1992 RERTR International Conference in Roskilde, Denmark. I regret that I will not be able to attend the conference due to a lack of funds.

Nevertheless, as you are aware, I am interested in the conference. I am curious as to the progress being made by my colleagues in each country and would also like to present my own achievements and experiences. Please send me a copy of the papers presented at the conference, an agenda, a list of participants, and the time and location of the 16th RERTR International Conference.

In turn, the following is a brief presentation that I have prepared for you and the other attendants concerning the progress of RERTR in our institute:

The Nuclear Power Institute of China (NPIC) has produced the U_3Si_2-Al dispersion fuel elements for the domestic three MW pool reactor and for the Pakistan Research Reactor (PARR). These fuel elements are in operation at the present time. The original power of PARR is five MW; however, after improvement, the power reached nine MW and the thermal neutron flux rose to 1.4E14 in the core. When the fuel elements were put into the PARR for 10 months, their condition did not change visibly and no contaminants were found in the water system. The power will soon reach 10 MW, the designated new value.

In addition, NPIC has finished another batch of fuel elements for PARR this year. My fellow researchers took part in the production and furthered improved the fabricating process as follows:

1. Dogbone: As mentioned in an earlier paper, we improved the frame construction. As a result, the dogbone was effectively reduced. However, the specification of PARR fuel elements requires a minimum cladding thickness of 0.30 mm; yet, this is difficult. So, we again improved the property of the frame to meet the requirements.

2. White spots: As mentioned above, the improved frame construction can also effectively eliminate stray fuel particles from the compact during assembling and rolling. Six fuel plates out of 670 produced this year have white spots on unpermitted areas; however, five plates out of the six mentioned above were relieved by excavating the fuel particles. In order discover the reason, we carefully analyzed the fabricating process and ultimately found some particles adhering to the

compact surface after degassing. On the average, about 1.2 mg powder was collected from the surface of each compact. By removing the powder and using the improved frame, the white spots were basically eliminated.

3. Blister: There are many factors affecting bonding quality, such as surface treatment and recontamination of the frame and cover, etc. However, we found some small blisters in meat-free areas near the meat. Such a phenomenon depends on the heating schedule. Before the first pass of rolling, if the billet is held in the furnace for enough time and the temperature does not rise during later rolling, this kind of blister will fail to appear.

4. Detecting meat oxidation by NDT: As mentioned in our earlier paper, if the billets were not fully protected from oxidation during the initial heating, the end of the meat would become grayish-black. Now that we can detect the oxidation area, this provides the guidance necessary to the protective effort and insures the quality of fuel plates by using ultrasonic equipment.

NPIC is willing to cooperate with the colleagues in each country on developing new fuel elements and providing U_3Si_2-Al plate-type fuel elements and its manufacturing techniques to the user.

Regards.

Yours Sincerely

Sun Rongxian

Nuclear Materials Department
Nuclear Power Institute of China
Post Box 191-106 Chengdu
61005, China

Final List of Attendees

1992 International Meeting on Reduced Enrichment for Research and Test Reactors

Risø National Laboratory
September 27 - October 1, 1992

Adolph, Eivind (Mr.)
Risø National Laboratory
Post Box 49
DK-4000 Roskilde, Denmark

Phone: 45-46-77-5702
Telex: 43116 RISOE DK
Fax: 45-4235-1173

Akhtar, Khalid (Mr.)
IAEA
Wagramerstrasse 5
Postfach 100
A-1400 Vienna, Austria

Phone: 43-222-2360
Telex: 1-12645
Fax: 43-1-234564

Aldemir, Tunc (Dr.)
The Ohio State University
Department of
Mechanical Engineering
206 West 18th Avenue
Columbus, Ohio 43210

Phone: 1-614-292-4627
Telex: -
Fax: 1-614-292-3163

Ballagny, Alain (Mr.)
French Atomic Energy Commission
DRN/DRE CEN/Saclay
91191 Gif Sur Yvette, France

Phone: 33-1-69-08-4195
Telex: 604641 F ENERG
Fax: 33-1-69-08-8015

Bartoli, Bernard (Mr.)
CEA/CEN Cadarache
13108 Saint Paul Les Durance
Cedex, France

Phone: 33-42-25-7122
Telex: CEACA 440 678 F
Fax: 33-42-25-3553

Beeckmans, Andre (Mr.)
CEN/SCK
200 Boeretang
B-2400 Mol, Belgium

Phone: 32-14-31-1801
Telex: 31922 ATOMOL B
Fax: 32-14-31-5021

Beylot, Jean Pierre (Mr.)
CEA
Direction des Reacteurs Nucl.
Service du Reacteur Osiris
91191 Gif Sur Yvette
Cedex, France

Phone: 33-1-69-08-4042
Telex: -
Fax: 33-1-69-08-6511

Böllerts, Wolfgang (Mr.)
Nissho Iwai Deutschland GmbH
Kreuzstr. 34
D-4000 Düsseldorf 1, Germany

Phone: 49-211-1378-212
Telex: 8582360 (8582367)
Fax: 49-211-1352-49

Bonnery, Christophe (Mr.)
COGEMA/BE
2, rue Paul Dautier
78140 Velizy-Villacoubley
Cedex, France

Phone: 33-1-39-46-9641
Telex: 697 833 f
Fax: 33-1-34-65-1377

Borring, Jan (Mr.)
Fuel Element Manufacture Plant
Risø National Laboratory
Post Box 49
DK-4000 Roskilde, Denmark

Phone: 45-46-77-5738
Telex: 43116A RISOE DK
Fax: 45-42-35-1173

Bouchardy, Serge (Mr.)
COGEMA/BE
2, rue Paul-Dautier
78141 Valizy-Villacoubley
Cedex, France

Phone: -
Telex: 697 833 F
Fax: 33-1-34-65-1377

Buchholz, Heinz (Dr.)
Hahn-Meitner-Institut Berlin GmbH
Postfach 39 01 18
Glienicker Strasse 100
D-1000 Berlin 39, Germany

Phone: 49-30-8008-2743
Telex: 185763
Fax: 49-30-8009-2082

Copeland, George L. (Dr.)
Metals and Ceramics Division
Oak Ridge National Laboratory
Post Box 2008, Bldg 4508, MS-6089
Oak Ridge, Tennessee 37831-6089

Phone: 1-615-574-3909
Telex: 810-572-1076 US DOE OKRE
Fax: 1-615-576-3894

Dagan, Ron (Mr.)
Soreq Nuclear Research Center
Yavne 70600, Israel

Phone: 972-8-43-4719
Telex: -
Fax: 972-8-43-0070

Deen, James R. (Dr.)
RERTR/AP-207
Argonne National Laboratory
9700 S. Cass Avenue
Argonne, Illinois 604239

Phone: 1-708-252-4853
Telex: 6871701 DOE-ANL
Fax: 1-708-252-5161

DeVries, Jacob W. (Mr.)
HOR/IRI
Interuniversitair Reactor Institut
Mekelweg 15 (Post Box 5042)
NL 2629 JB Delft, The Netherlands

Phone: 31-15-78-1402
Telex: 38214 IRI NL
Fax: 31-15-78-6422

Downs, V. Dean (Mr.)
Babcock and Wilcox Company
Naval Nuclear Fuel Division
Post Box 785, Mt. Athos Road
Lynchburg, VA 24505-0785

Phone: 1-804-522-5660
Telex: 901640 B&W NNFD LY
Fax: 1-804-522-5922

Durand, Jean-Pierre (Mr.)
CERCA
Les Berauds
26104 Romans-Sur-Isere, France

Phone: 33-75-05-6061
Telex: FCOMB A 345155F
Fax: 33-75-05-2536

Fanjas, Yves (Mr.)
CERCA
Les Berauds
26104 Romans-Sur-Isere, France

Phone: 33-75-05-6061
Telex: FCOMB A 345155F
Fax: 33-75-05-2536

Floto, Heinz (Mr.)
Risø National Laboratory
Post Box 49
DK-4000 Roskilde, Denmark

Phone: 45-4-677-4355
Telex: 43116A RISOE DK
Fax: 45-4-675-5052

Fukushima, Shonosuke (Mr.)
Nissho Iwai Corporation
4-5, Akasaka 2-Chome
Minato-Ku, Tokyo 107 Japan

Phone: 81-3-588-2794
Telex: 22233
Fax: 81-3-588-4924

Fuse, Peter-Michael (Mr.)
NUKEM GmbH
Postfach 1313
Industriestrasse 13
D-8755 Alzenau, Germany

Phone: 49-6023-911-604
Telex: 4188 233 nuka d
Fax: 49-6023-911-600

Futamura, Yoshiaki (Dr.)
Japan Atomic Energy Research Institute (JAERI)
Tokai-mura, Naka-gun
Ibaraki-ken, Japan 311-13

Phone: 81-292-67-4111, x 4300
Telex: J24596
Fax: 81-292-67-7144

Gevers, Arthur (Dr.)
Comm of the European Communities
Joint Research Center Petten
Post Box 2 1755 ZG Petten
The Netherlands

Phone: 31-2246-5129
Telex: 57211 REACP
Fax: 31-2246-1449

Goutx, Daniel (Mr.)
COGEMA
2, rue Paul Dautier
78141 Valizy-Villacoublay
Cedex, France

Phone: 33-1-39-46-9641
Telex: 697 833 f
Fax: 33-1-34-65-1377

Grønberg, Lisbeth
Risø National Laboratory
Post Box 49
DK-4000 Roskilde, Denmark

Phone: 45-46-77-4608
Telex: 43116A RISOE DK
Fax: 45-42-35-1173

Gruber, Gerhard (Mr.)
MGR MTR Fuel Services
Alzenau Branch
Fuel Cycle Services Div.,
Nukem GmbH
Postfach 1313, Industriestr 13
D-8755 Alzenau, Germany

Phone: 49-6023-500-609
Telex: 4188233 NUKA D
Fax: 49-6023-500-600

Guiheux, Jean Michel
COGEMA/DC
2, rue Paul Dautier
78140 Velizy-Villacoublay
Cedex, France

Phone: 33-1-39-46-9641
Telex: 697 833 f
Fax: 33-1-34-65-1377

Haack, Karsten (Mr.)
Risø National Laboratory
Post Box 49
DK-4000 Roskilde, Denmark

Phone: 45-46-77-4302
Telex: 43116A RISOE DK
Fax: 45-46-75-5052

Håkansson, Rune (Mr.)
Studsvik Nuclear AB
S-61182 Nykoping, Sweden

Phone: 46-155-22260
Telex: 64013 STUDS S
Fax: 46-155-63070

Harbonnier, Gerard (Mr.)
CERCA
Les Berauds
26104 Romans-Sur-Isere
France

Phone: 33-75-05-6061
Telex: FCOMB A 345155F
Fax: 33-75-05-2536

Hassel, Horst W. (Mr.)
NUKEM GmbH
Postfach 1313
D-8755 Alzenau, Germany

Phone: 49-6023-500-380
Telex: 4188233 NUKA D
Fax: 49-6023-500-382

Hofman, Gerard L. (Dr.)
EBR II-ANL West
Argonne National Laboratory
9700 South Cass Avenue
Argonne, Illinois 60439

Phone: 1-708-252-6683
Telex: 6871701 DOE-ANL
Fax: 1-708-252-5161

Hurand, Jean-Pierre (Mr.)
CERCA
Les Berauds
26104 Romans-Sur-Isere, France

Phone: 33-75-05-6061
Telex: FCOMB A 345155F
Fax: 33-75-05-2536

Hwang, Woan (Mr.)
Korea Atomic Energy Res Institute
Daeduk Science Town
Post Box 7
Daejun 305353, Korea

Phone: 82-42-820-2309
Telex: 45553 kaeri k
Fax: 82-42-820-2702

Ichikawa, Hiroki (Mr.)
RES Reactor Tech Dev Div
Dept of Res Reactor Operation
Japan Atomic Energy Res Institute
2-4 Shirane, Shirakata
Tokai-mura, Naka-gun
Ibaraki-ken 319-11 Japan

Phone: 81-292-82-5639
Telex: J24596 JAERI
Fax: 81-292-82-5258

Jensen, Søren E. (Mr.)
Risø National Laboratory
Post Box 49
DK-4000 Roskilde, Denmark

Phone: 45-46-77-4304
Telex: 43116A RISOE DK
Fax: 45-46-77-55052

Jonsson, Erik (Mr.)
Studsvik Nuclear AB
S-611 82 Nykoping Sweden

Phone: 46-155-22260
Telex: 64013 STUDS S
Fax: 46-155-63070

Kampmann, Dan (Mr.)
Danish Nuclear Inspectorate
Datavej 16
3460 Birkerød, Denmark

Phone: 45-45-82-8222
Telex: 2 7410 CFS DK
Fax: 45-45-82-0876

Kanda, Keiji (Dr.)
Kyoto University
Research Reactor Institute
Kumatori-cho, Sennan-gun
Osaka 590-04 Japan

Phone: 81-724-53-2145
Telex: 5397073 KURRIA J
Fax: 81-724-53-0360

Karam, Ratib A. (Dr.)
Neely Nuclear Research Center
Georgia Institute of Technology
Atlanta, Georgia 30332

Phone: 1-404-894-3120
Telex: 542507 GTRIOCAA
Fax: 1-404-853-9325

Kim, Chang Kyu (Mr.)
Korea Atomic Energy Res Institute
Nuclear Materials Development
Department
Daeduk Science Town
Post Box 7
Daejun 305-353, Korea

Phone: 82-42-820-2309
Telex: 45553 kaeri k
Fax: 82-42-820-2702

Kjems, Jørgen (Mr.)
Risø National Laboratory
Post Box 49
DK-4000 Roskilde, Denmark

Phone: 45-46-77-4602
Telex: 43116A RISOE DK
Fax: 45-42-35-1173

Knop, Wolfgang (Mr.)
GKSS Forschungszentrum
Geestacht mbH
Postfach 11 60
2054 Geestacht, Germany

Phone: 49-4152-871-200
Telex: 218712 gkssg d
Fax: 49-4152-871-338

Kobayashi, Keiji (Mr.)
Research Reactor Institute
Kyoto University
Kamatori-cho, Sennan-gun
Osaka 590-04, Japan

Phone: 81-724-52-090
Telex: 5397073 kurriaj
Fax: 81-724-53-0360

Kobayashi, Masaru (Mr.)
PECHINEY, Japan
43'rd Floor, Shinjuku Mitsui
Bldg. 2-1-1 Nishi-Shinjuku
Shinjuku-ku, Tokyo 163, Japan

Phone: 81-333-49-6660
Telex: 232 4895 PECHIJ J
Fax: 81-333-49-6770

Komori, Yoshihiro (Mr.)
Oarai-Machi Establishment
Japan Atomic Energy Res Institute
Oarai-machi, Higashi-Ibaraki-gun
Ibaraki-ken 311-13 Japan

Phone: 81-292-67-4111
Telex: J24596
Fax: 81-292-64-8480

Kozma, R. (Mr.)
ECN Petten
Westerduinweg 3
Post Box 1
1755 ZG Petten, The Netherlands

Phone: 31-2246-4385
Telex: 57211 REACP NL
Fax: 31-2246-3490

Krull, Wilfried (Dr.)
GKSS, Reaktorstrasse 7-9
Forschungszentrum Geestacht
Postfach 1160
2054 Geestacht, Germany

Phone: 49-4152-87-1200
Telex: 218712 GKSS G
Fax: 49-4152-87-1338

Lelievre, Bernard (Dr.)
CERCA
Les Berauds BPN 14
26104 Romans Cedex, France

Phone: 33-75-05-6000
Telex: 345 155 F
Fax: 33-75-65-2536

Listik, Evzen (Mr.)
Nuclear Research Institute
250 68 Rez, Czechoslovakia

Phone: 42-2-685-7831
Telex: -
Fax: 42-2-685-7155

Matos, James (Dr.)
Engineering Physics Div.
Argonne National Laboratory
9700 South Cass Avenue
Argonne, Illinois 60439

Phone: 1-708-252-6758
Telex: 6871701 DOE-ANL
Fax: 1-708-252-5161

McClary, Michael V. (Mr.)
Office of International Affairs
US Department of Energy
IE-13 Forrestal Building
1000 Independence Avenue
Washington, DC 20584

Phone: 1-202-586-6194
Telex: -
Fax: 1-202-586-6789

McColm, Colin (Mr.)
UK Atomic Energy Authority
Dounreay Thurso Caithness
Scotland, United Kingdom

Phone: 44-847-62-121
Telex: 75297 ATOMDY G
Fax: 44-847-80-3049

McDonough, Michael D. (Mr.)
109 Timberline Drive
Conway, South Carolina 27526

Phone: 1-803-347-7699
Telex: -
Fax: 1-803-347-0027

Michaels, Theodore (Mr.)
US Nuclear Regulatory Commission
Mail Stop 11H3
Washington, DC 20555

Phone: 1-301-504-1102
Telex: 908142 NRC-BHD WSH
Fax: 1-301-504-0259

Mota, Jose (Mr.)
Administrator
Euratom Supply Agency
Commission of the
European Communities
Rue De La Loi 200
B-1049 Brussels, Belgium

Phone: 32-2-235-2399
Telex: 21877 COMEU B
Fax: 32-2-235-0527

Müller, Hans (Mr.)
Fuel Cycle Services Division
NUKEM GmbH
Postfach 110080
D-6450 Hanau 11, Germany

Phone: 49-6023-500-604
Telex: 4188233 NUKM D
Fax: 49-6023-500-600

Naccache, Sanir J.P. (Mr.)
Export Director, CERCA
9-11, Rue Georges Enesco
94008 Cretail Cedex, France

Phone: 33-1-43-77-1263
Telex: 264-276
Fax: 33-1-46-98-9265

Nakajima, Teruo (Mr.)
Japan Atomic Energy Research Institute (JAERI)
JRR-4 Operation Division
Tokai-mura, Naka-gun
Ibaraki-ken 319-11, Japan

Phone: 81-292-82-5639
Telex: -
Fax: 81-292-82-5258

Nilsson, Tage M. (Mr.)
Risø National Laboratory
Post Box 49
DK-4000 Roskilde, Denmark

Phone: 45-46-77-5774
Telex: 43116A RISOE DK
Fax: 45-42-35-1173

Nonbøl, Erik (Mr.)
Risø National Laboratory
Post Box 49
DK-4000 Roskilde, Denmark

Phone: 45-46-77-4923
Telex: 43116A RISOE DK
Fax: 45-42-35-1173

Paillere, Jacques (Mr.)
French Atomic Energy Commission
Service Reacteur Osiris
CEN/Saclay
91191 Gif Sur Yvette, France

Phone: 33-1-69-08-4042
Telex: 604641F ENERG
Fax: 33-1-69-08-6511

Palleck, Steve (Mr.)
Senior Fuel Engineer
AECL Research, Chalk River Labs., Chalk River
Ontario KOJ IJO, Canada

Phone: 1-613-584-3311
Telex: -
Fax: 1-613-584-3250

Papastergiou, Constantinos (Mr.)
N.R.C. Demokritos
Greek Atomic Energy Commission
Aghia Paraskevi
Athens, Greece

Phone: 30-1-651-4118
Telex: 216199 ATOM GR
Fax: 30-1-653-3431

Parker, Keith A. (Mr.)
UK Atomic Energy Authority
Commercial Directorate, Rm E443
Cheshire, Warrington, WA3 6AT
England

Phone: 44-925-31-244, x 2631
Telex: 629301 ATOMRY G
Fax: 44-925-25-2631

Pauty, Jean Francois (Mr.)
COGEMA/BE
2, rue Paul Dautier
78140 Velizy-Villacoublay
Cedex, France

Phone: 33-1-39-46-9641
Telex: 697 833 f
Fax: 33-1-34-65-1377

Porte, Philippe (Mr.)
CERCA
9-11 Rue Georges Enesco
94008 Creteil, Cedex, France

Phone: 33-1-43-77-1263
Telex: 264276
Fax: 33-1-46-98-9265

Poupard, Jean-Francois (Mr.)
CERCA
Les Berauds, B P 1114
26104 Romans, Cedex
France

Phone: 33-75-05-6120
Telex: 345155
Fax: 33-75-05-3958

Preble, Harry E. (Mr.)
Babcock and Wilcox
Naval Nuclear Fuel Division
Post Box 785
Mt. Athos Road
Lynchburg, Virginia 24505-0785

Phone: 1-804-522-5660
Telex: 901640 B&W NNFD LY
Fax: 1-804-522-5922

Quinton, Paul (Mr.)
CERCA
9-11 Rue Georges Enesco
94008 Creteil, Cedex, France

Phone: 33-1-43-77-1263
Telex: CERCA 264 276
Fax: 33-1-46-98-9265

Qvist, Jens (Mr.)
Risø National Laboratory
Post Box 49
DK-4000 Roskilde, Denmark

Phone: 45-46-77-4323
Telex: 43116A RISOE DK
Fax: 45-42-35-1173

Raisonnier, Daniele (Mr.)
Transnucleaire, SA
11 bis rue Christophe Colomb
75008 Paris, France

Phone: 33-1-47-20-2608
Telex: 280 992
Fax: 33-1-47-20-2608

Ravenscroft, Norman (Mr.)
Edlow International Company
1815 N. Street, N.W., Suite 910
Washington, DC 20006 USA

Phone: 1-202-833-8237
Telex: 64387
Fax: 1-202-483-4840

Reasor, Nathaniel H. (Mr.)
Babcock and Wilcox
Naval Nuclear Fuel Division
Post Box 785
Lynchburg, Virginia 24505

Phone: 1-804-522-6239
Telex: 901640 B&W NNFD LY
Fax: 1-804-522-5922

Rebreyend, Catherine (Ms.)
CERCA BP 1114
26104 Romans Cedex, France

Phone: 33-75-05-6000
Telex: -
Fax: 33-75-05-2536

Roegler, Hans-Joachim (Mr.)
Siemens AG
Friedrich-Ebert-Str. 76B
Bergisch Gladback 1,
100351 W-5060, Germany

Phone: 49-2204-844-681
Telex: -
Fax: 49-2204-842-207

Romano, Rene (Mr.)
CERCA
Tour Manhattan - Cedex 21
92087 Paris la Defense 2, France

Phone: 33-1-47-52-7888
Telex: -
Fax: 33-1-46-98-9265

Rydin, Roger A. (Dr.)
University of Virginia
Reactor Facility
Charlottesville, Virginia 22901

Phone: 1-804-924-7136
Telex: -
Fax: 1-804-982-5473

Rysavy, Jaroslav (Mr.)
Nuclear Research Institute
250 68 Rez
Czechoslovakia

Phone: 42-2-685-7831
Telex: -
Fax: 42-2-685-7155

Sameh, Abdel H. Ali (Mr.)
Nuclear Research Center Karslsruhe
Postfach 3640
D-7500 Karlsruhe, Germany

Phone: 49-7247-823-436
Telex: -
Fax: 49-7247-825-982

Schmidt, Thomas (Mr.)
Nuclear Cargo & Service GmbH
Rodenbacher Chaussee 6
Postfach 11 00 30
D-6450 Hanau 11
Germany

Phone: 49-6181-582-066
Telex: 4 184 123
Fax: 49-6181-573-692

Schreader, J.W. Jack (Mr.)
Atomic Energy of Canada, Ltd.
Chalk River Nuclear Laboratory
Chalk River, Ontario KOJ 1JO
Canada

Phone: 1-613-584-3311, x 4350
Telex: 053-34555 AECL B CKR
Fax: 1-613-584-3250

Sears, David (Mr.)
Atomic Energy of Canada, Ltd.
Fuel Material Branch
Chalk River Nuclear Laboratory
Chalk River, Ontario
Canada KOJ 1JO

Phone: 1-613-584-3311
Telex: 053-34555 AECL B CKR
Fax: 1-613-584-3250

Singer, Klaus (Mr.)
Risø National Laboratory
Post Box 49
DK-4000 Roskilde, Denmark

Phone: 45-46-77-4607
Telex: 43116A RISOE DK
Fax: 45-42-35-8531

Snelgrove, James L. (Dr.)
Engineering Physics Division
Argonne National Laboratory
9700 South Cass Avenue
Argonne, Illinois 60439

Phone: 1-708-252-6369
Telex: 6871701 DOE-ANL
Fax: 1-708-252-5161

Spin, Arturo (Dr.)
Reactor Coordinator
Instituto de Asuntos Nucleares
Avenida El Dorado, Carrera 50
Post Box 8595
Bogota, Columbia

Phone: 57-1-222-0071
Telex: 42416 IAN BGCO
Fax: 57-1-222-0173

Thamm, Gerd Horst (Mr.)
Z e n t r a l a b l e i t u n g
Forschungsreaktoren
Kernforschungsanlage Juelich GmbH
Postfach 1913 D-5170
Juelich 1, Germany

Phone: 49-2461-61-5055
Telex: 833556-20 KF D
Fax: 49-2461-61-3841

Thom, David (Mr.)
AEA - Fuel Services
Thurso Caithness KW147TZ
Scotland

Phone: 44-847-803-000
Telex: 75297
Fax: 44-847-803-052

Thorlaksen, Bjørn (Mr.)
Danish Nuclear Inspectorate
Datavej 16
3460 Birkerød, Denmark

Phone: 45-45-82-8222
Telex: 2 7410 CFS DK
Fax: 45-45-82-0876

Thurgood, Brian E. (Mr.)
General Atomics, TRIGA Group
3550 General Atomics Court
San Diego, California 92121-1194

Phone: 1-619-455-3580
Telex: -
Fax: 1-619-455-4169

Toft, Palle (Mr.)
Risø National Laboratory
Post Box 49
DK-4000 Roskilde, Denmark

Phone: 45-46-77-5778
Telex: 43116A RISOE DK
Fax: 45-42-35-1173

Travelli, Armando (Dr.)
Engineering Physics Division
Argonne National Laboratory
9700 South Cass Avenue
Argonne, Illinois 60439

Phone: 1-708-252-6363
Telex: 6871701 DOE-ANL
Fax: 1-708-252-5161

Tschiesche, Horst (Mr.)
Nuclear Cargo & Service GmbH
Rodenbacher Chaussee 6
Postfach 11 00 30
D-6450 Hanau 11, Germany

Phone: 49-6181-582-427
Telex: 4184123 TNH D
Fax: 49-6181-357-3692

Tsuchida, Noboru (Mr.)
Japan Atomic Energy Res Institute
Oarai-Machi, Higashi Ibaraki-gun
Ibaraki-ken, Japan

Phone: 81-292-64-8347
Telex: J24596
Fax: 81-292-64-8480

Vanluchene, Patricia (Ms.)
NUKEM GmbH
Postfach 1313
D-8755 Alzenau, Germany

Phone: 49-6023-500-380
Telex: 4188233 NUKA D
Fax: 49-6023-500-382

Wijtsma, Fred J. (Mr.)
Netherlands Energy Research Foundation (ECN)
Post Box 1
1755 ZG Petten, The Netherlands

Phone: 31-2246-4949
Telex: 57211 REACP NL
Fax: 31-2246-1612

Woodruff, William L. (Dr.)
EP Division-RERTR Program-Bldg.207
Argonne National Laboratory
9700 South Cass Avenue
Argonne, Illinois 60439

Phone: 1-708-252-8634
Telex: 6871701 DOE-ANL
Fax: 1-708-252-5161

Xerri, Christophe (Mr.)
Reprocessing Branch
Contracts, Transports,
and Planning Division
COGEMA
2 Rue Paul Dautier, BP4
78141 Velizy-Villacoubley
Cedex, France

Phone: 33-1-39-46-9641
Telex: 697833 COGEM
Fax: 33-1-39-46-5205

DISTRIBUTION FOR ANL/RERTR/TM-19 (CONF-9209266)

Internal:

A. Schriesheim
C. E. Till
P. I. Amundson
D. W. Cissel
W. L. Deitrich
M. H. Derbidge
L. G. LeSage
R. B. Poeppel
R. J. Teunis
A. Travelli (75)
D. C. Wade
All ANL Attendees (15)
TIS Files (1)

External:

ANL East Library

ANL West Library

DOE-OSTI, for distribution per UC-940 (99)

Manager, Chicago Operations Office, DOE

Director, Technology Management Div., DOE-CH

Engineering Physics Division Review Committee:

Robert J. Budnitz, Future Resources Associated
Michael J. Driscoll, Massachusetts Institute of Technology
George H. Gillespie, G.H. Gillespie Associates
W. Reed Johnson, University of Virginia
James E. Leiss, Consultant
Warren F. Miller, Jr., University of California
Gerold Yonas, Sandia National Laboratories

All Non-ANL Attendees and Participants (67)

DATE
FILMED
6/30/94

END